MSN
MICROWAVE SYSTEMS NEWS

The Microwave System Designer's Handbook

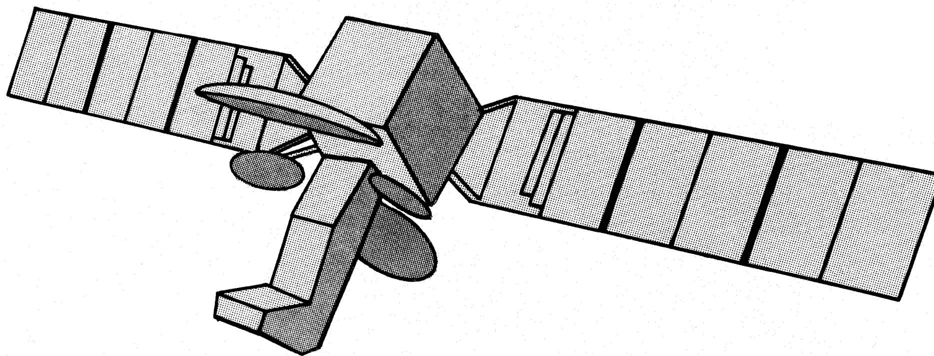

Published by
EW Communications, Inc.
1170 East Meadow Drive, Palo Alto, California 94303
Telephone (415) 494-2800 TWX 910-379-6584 Telex 171433
Bert Berson, Editor, Consulting in Technology, Mountain View, California

The Microwave System Designer's Handbook, First Edition (ISSN 0164-3371) is published in 1983 as Volume 13 Number 12 of **Microwave Systems News.** Copyright 1983 by EW Communications, Inc. Library of Congress Catalog Card Number 80-643290. All rights reserved. Reproduction in whole or in part without written permission of the publisher is prohibited. Send new and old addresses (including mailing label) with zip code numbers to P.O. Box 50249, Palo Alto, CA 94303. Postmaster: Send Form 3579 to EW Communications, Inc., P.O. Box 50249, Palo Alto, CA 94303. Second-class postage paid at Palo Alto, California, and additional mailing offices.

Microwave Systems News is sent free each month to individuals actively engaged in microwave programs and projects. To become a regular subscriber to *MSN*, fill out the application form in the back of this volume. Paid subscription rates for non-qualified recipients are: USA, $35 one year, $58 two years; International and Canada (surface), $52 one year, $93 two years; International and Canada (airmail), $65 one year, $118 two years. Additional copies of *The Microwave System Designer's Handbook* can be obtained by filling out and mailing the order coupon in the back of this volume.

MSN

NOVEMBER 1983 VOL. 13 NO. 12

The Microwave System Designer's Handbook

Inside This Issue

Foreword

7 **Premier Issue Reflects Our Industry's Growth and Diversity**
By Bert Berson, *Consulting in Technology*

8 **Author Biographies**

Commercial Communications

11 **Commercial Communications Applications Show Diversity**
By Alan Walker, *Farinon Div., Harris Corp.*

Military Microwaves

15 **Military Systems Needs Drive Component Demand**
By Kenneth J. Sleger, *Naval Research Laboratory*

22 **Mm-Wave Threats Continue to Grow**
By Alexander E. Braun, *EW Communications, Inc.*

Solid State Devices and Hybrid Technology

32 **Silicon Bipolar Transistors and Integrated Circuits Continue to Grow**
By Craig P. Snapp, *Avantek, Inc.*

43 **Bipolar Matrix**

72 **Gallium Arsenide Growth Diversifies**
By Joseph Barrera, *Harris Microwave Semiconductor Corp.*

89 **GaAs FET Matrix**

104 **Thin Film Processing of Hybrid ICs**
By Ralph Tramposch, *Materials Research Corp.*

Tubes

126 **Tubes Still Vital to Microwave Systems**
By Robert Espinosa, *Varian Associates*

Components

153 **Ferrites Control Microwave Systems**
By Fred J. Rosenbaum, *Central Microwave Co.*

168 **Understanding Filters and Multiplexers**
By Harold L. Schumacher, *Microphase Corp.*

182 **Designing a Synthesized Signal Generator**
By Howard W. Mette, *Gigatronics, Inc.*

194 **Diode Switching**
By Robert V. Garver, *Harry Diamond Laboratories*

207 **YIG-Tuned Oscillator Fundamentals**
By Northe K. Osbrink, *Avantek, Inc.*

226 **Cost-for-Performance Criteria for Mixers**
By Ferenc Marki, *Western Microwave, Inc.*

237 **Antenna Design Tradeoffs Examined**
By J.R. Forrest, *University College London*

Testing

244 **Microwave System Testing**
By Alan W. Carlson, *M/A-Com, Components, Inc.*

258 **Semiconductor Thermal Considerations**
By Bernard S. Siegal, *Sage Enterprises, Inc.*

267 **Testing Oscillators, Amplifiers, and Mixers**
By C.E. Foster, C.E. Krehbiel, and K. Zublin, *Wavetek, Inc.*

Special Section
Millimeter-Wave Technology

278 **Introduction**
By John Kuno, *Hughes Aircraft Co.*

280 **Solid-State Sources Power Millimeter Transmitters**
By R.S. Ying, *Hughes Aircraft Co.*

288 **Specifying Millimeter Converters**
By Jeffrey A. Paul, *Hughes Aircraft Co.*

290 **E-Plane Filters Designed for Millimeter Use**
By D.W. Ball and L.Q. Bui, *Hughes Aircraft Co.*

292 **Index of Advertisers**

About the Cover

Communication . . . a keystone to progress. *The Microwave System Designer's Handbook* meets the needs of design engineers active in the developments of satellite communication as well as the entire spectrum of the dynamic microwave industry.

Cover design by Burt Sakai & Susan Thrasher

Premier Issue Reflects Our Industry's Growth and Diversity

By Bert Berson, *Editor*

The microwave industry is in a period of tremendous change. First, the market is growing at a rate that will force change. Free-world production of microwave equipment is expected to grow from $22 billion in 1980 to $56 billion by 1986. At the same time, U.S. applications of microwave components will swell from $3 billion to around $7 billion.

Within this steady, upward rise, some fields will outstrip the overall market; one of the fastest and most glamorous segments is packaged GaAs FETs, whose sales are expected to soar 27 percent a year.

This growth is causing change, both in the composition of the marketplace and the technologies' growth demand. For instance, the AMRAAM program, which calls for production of 5,000 air-to-air missiles a year, requires advances in production techniques such as automated testing, advances perhaps more significant than those required in designing the seeker.

Similarly, Milstar, the $6- to $10-billion communication satellite program promised for the early 1990s, will place tremendous demands on industry; upwards of 4,000 mobile terminals operating at 44/20 GHz will be purchased at around $1,000,000 each. Such mass production of systems operating at 44 GHz has never been attempted.

While military programs such as AMRAAM and Milstar will fuel industry growth, it is unlikely that defense spending will hold its dominant 63-percent share of the market. Major communications networks from cellular radio to direct-broadcast television to air phones are about to emerge. Again, mass production is the key to realizing the promise of these systems and for the first time this capability is emerging.

Most encouraging is the evolving ability to put entire microwave functions on a single, monolithically fabricated chip of gallium arsenide, or perhaps silicon. Here, commercial markets may switch traditional roles with defense programs to become the technology driver.

Merging of digital and microwave technologies is increasing on several levels. Intelligence about new threats is leading electronic warfare systems designers to turn to digital, microwave memory loops incorporating switches that operate in nanoseconds. Increased threat densities and need for high dynamic ranges has led to development of detector log video amplifiers (DLVAs), which amplify weak signals more than stronger signals.

Monolithics promise to play a substantial role in catalyzing the merger of digital and microwave technologies. With GaAs ICs used at microwave frequencies to perform digital functions beyond silicon's capabilities, we will see direct signal processing at microwaves as dividers, adders, shift registers, A/D and D/A converters, all in GaAs, become available.

Despite the changes occurring in our industry, it has been over 30 years since the MIT Rad Lab's multivolume series provided an introduction to microwave technology. Since that time the industry has been without a basic guide to modern microwave design.

Filling that gap is the purpose of this *Microwave System Designer's Handbook*. A series of articles takes the reader through basic principals in each device and component area crucial to modern systems design. Basic definitions, principals of operation, and guidelines on selecting and specifying are reviewed in each chapter and many survey the state of the art in each field. Detailed surveys of available GaAs FET and bipolar products are included separately.

A pair of overview articles examines trends in military and commercial technology to set the stage for the individual chapters of the Technology section.

A great deal of effort has been put into making the premier issue of the *MSDH* a valuable reference tool. We trust you will find the Handbook as useful as we found it enjoyable to work with the many respected industry authorities who served as contributing editors. In addition, we would like to thank two members of the staff of Consulting in Technology, Mary Bernstein and Adam Bowen, whose support was essential to getting the job done. A special thanks goes to Bill Berridge of Avantek who helped us assemble the oscillator section.

■

Author Biographies

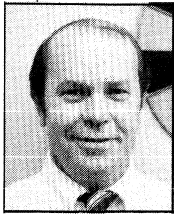

D.W. BALL
"E-Plane Filters Designed for Millimeter Use"

Mr. Ball is the assistant manager of the Solid State Subsystem Department at the Electron Dynamics Division of Hughes Aircraft Company in Torrance, California. He was formerly with Rockwell International's Space and Secure Communications Division. He received a B.S. in Electrical Engineering from West Coast University in Los Angeles, California and currently has 21 credits toward his Master's at California State University at Fullerton.

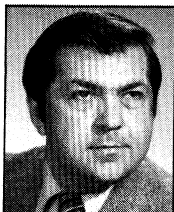

DR. JOSEPH S. BARRERA
"Gallium Arsenide Growth Diversifies"

Dr. Barrera is the director of GaAs Operations for Harris Microwave Semiconductor, Inc., which he co-founded in 1980. Harris Microwave Semiconductor is located in Milpitas, California. He was formerly with Hewlett-Packard's Microwave Semiconductor Division and also with Hewlett-Packard's Corporate Research Center. Dr. Barrera received his B.S. in Electrical Engineering from Harvey Mudd College in Claremont, California. The M.S.E.E. and Ph.D. degrees were obtained in Solid State Electrical Engineering from Carnegie-Mellon University in Pittsburgh, Pennsylvania.

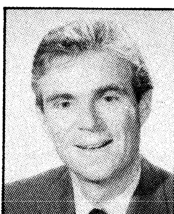

BERT BERSON
Editor of *The Microwave System Designer's Handbook*

Mr. Berson is founder and president of Consulting in Technology, a consulting firm providing guidance and support to the microwave industry. He previously was vice-president of the Microwave Semiconductor Division of Avantek, Inc., Santa Clara, California. Prior to that position, Mr. Berson was manager of Microwave Solid State Device Technology at RCA David Sarnoff Research Center, and senior physicist at General Dynamics. Mr. Berson received his B.S. in Electrical Engineering from City College of New York, and M.S. in Engineering Physics from University of Rochester, Rochester, New York.

ALEXANDER E. BRAUN
"Millimeter-Wave Threats Continue to Grow"

Mr. Braun is the editor of *Microwave Systems News* magazine and the managing editor of *The Microwave System Designer's Handbook*. He has had a long career as a science and industry journalist and has received awards for his writings, which have been read in many countries in several languages. Mr. Braun served on the board of the International Science Writers Association, and is a member of the National Association of Science Writers. He received his B.A. in English from San Jose State University and completed special course work at the University of California, Berkeley.

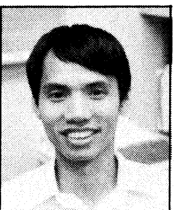

LONG Q. BUI
"E-Plane Filters Designed for Millimeter Use"

Mr. Bui is a staff engineer at the Electron Dynamics Division of Hughes Aircraft Company in Torrance, California. Mr. Bui received his B.S. and M.S. degrees from the University of Texas at Austin.

ALAN W. CARLSON
"Microwave System Testing"

He is presently a vice-president at M/A-Com Components, Inc. in Burlington, Massachusetts, where he is the manager of the Automatic Test Equipment Group. He received his B.S., M.S., and Ph.D. degrees in Electrical Engineering from Massachusetts Institute of Technology, in Cambridge, Massachusetts.

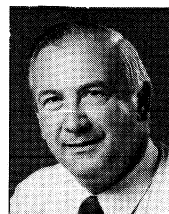

ROBERT ESPINOSA
"Tubes Still Vital to Microwave Systems"

He is currently the director of Technology Development with the Electron Device Group at Varian Associates in Palo Alto, California. Prior to that, he was with Varian's Microwave Tube Division, the Warneke Electron Tube Corporation, Raytheon Corporation, and Watkins-Johnson. Mr. Espinosa received a B.S. in Electrical Engineering from Seattle University, and M.S. in Electrical Engineering from Stanford University.

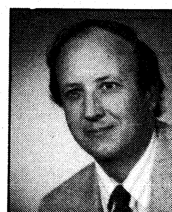

DR. JOHN R. FORREST
"Antenna Design Tradeoffs Examined"

He is currently a professor of Electrical Engineering at University College in London, England. Previously, he was a research associate and lecturer at the Institute for Plasma Research at Stanford University in Stanford, California. Dr. Forrest received his Master's degree from Cambridge University, England and completed research for his doctorate at Oxford University in England.

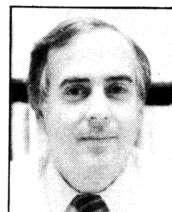

CHARLES E. FOSTER
"Testing Oscillators, Amplifiers, and Mixers"

He is presently the manager of the Microwave Business Unit at Wavetek in San Diego, California. Previously, Mr. Foster was Laser Marketing manager with Hughes Aircraft Company, and held positions at Watkins-Johnson and with the U.S. Navy. He received a B.S. in Electrical Engineering from Clemson University and M.S. degree in Business Administration from Harvard University.

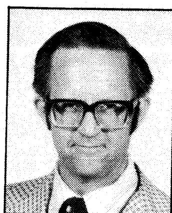

ROBERT V. GARVER
"Diode Switching"

Mr. Garver is supervisory physicist in Microwave/Electromagnetic Effects at Harry Diamond Laboratory in Adelphi, Maryland. Mr. Garver received his B.S. degree in Physics from the University of Maryland, College Park, Maryland. and M.S. in Engineering Administration from George Washington University in Washington, D.C. He is a Fellow of the IEEE.

COURTNEY E. KREHBIEL
"Testing Oscillators, Amplifiers, and Mixers"

He is presently engineering manager of the Microwave Business Unit at Wavetek in San Diego, California. Prior to joining Wavetek, Mr. Krehbiel was with Watkins-Johnson. He received both his B.S. and M.S. in Electrical Engineering from the University of Illinois.

DR. H.J. KUNO
Author of Introduction to Special Section on Millimeter-Wave Technology

He is currently in charge of research, engineering, and manufacturing of solid-state microwave and millimeter-wave devices, products, and subsystems for Hughes Aircraft Company in Torrance, California. Previously, Dr. Kuno was with the RCA David Sarnoff Research Center in Princeton, New Jersey, and with NCR Electronics Division at Hawthorne, California. He received his B.S., M.S., and Ph.D. degrees in Engineering from the University of California at Los Angeles. He is a Fellow of the IEEE.

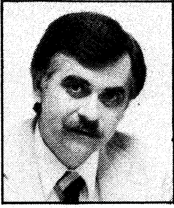

FERENC MARKI
"Cost-for-Performance Criteria for Mixers"

He is currently the manager of the Microwave Integrated Circuit Division at Western Microwave, Inc. in Sunnyvale, California. Previously, Mr. Marki was with Avantek, Inc. and with Watkins-Johnson Solid State Division. He received his B.S. degree from the University of California at Berkeley.

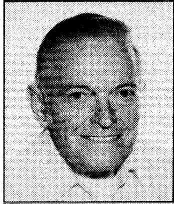

HOWARD W. METTE
"Designing a Synthesized Signal Generator"

Mr. Mette is currently marketing manager for Gigatronics in Pleasant Hill, California. He was previously national sales manager for the Systron Donner Instrument Division in Concord, California. Before that, he was marketing manager for Rutherford Electronics. Mr. Mette attended UCLA.

NORTHE K. OSBRINK
"YIG-Tuned Oscillator Fundamentals"

Mr. Osbrink is the manager of Publications Editing at Avantek. Previously, he worked as a member of the technical staff of the Rockwell International B-1 Division, and as *Electronic Design* magazine's Western editor. He received his B.S. in Electrical Engineering from Northrop University in Inglewood, California.

JEFFREY A. PAUL
"Specifying Millimeter Downconverters"

He currently works as assistant department manager of the Millimeter-Wave/Microwave Circuits Department of the Electron Dynamics Division of Hughes Aircraft Company in Torrance, California. Mr. Paul received his B.S. in Electrical Engineering from Carnegie-Mellon University, and received his Master's from Stanford University.

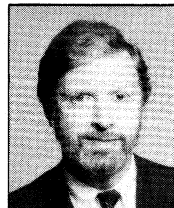

FRED J. ROSENBAUM
"Ferrites Control Microwave Energy"

Dr. Rosenbaum is chief scientist at Central Microwave in St. Louis, Missouri. He was previously Professor of Electrical Engineering at Washington University, St. Louis, where he directed the Microwave Laboratory. Before that, he worked in the Research Division of McDonnell Aircraft Corp. Dr. Rosenbaum received his B.S., M.S., and Ph.D. degrees in Electrical Engineering from the University of Illinois. He is a Fellow of the IEEE.

HAROLD L. SCHUMACHER
"Understanding Filters and Multiplexers"

Mr. Schumacher is department head, Filters and Multiplexers, at Microphase Corporation in Connecticut. Previously, he was chief engineer for Waveline, Inc., Gombos Microwave and RLC Electronics, and a senior engineer for the Electronics Division of ACF Industries. Mr. Schumacher received his B.E. in Electrical Engineering from the Polytechnic Institute of Brooklyn, and studied at its Graduate Electrical Engineering Department.

BERNARD S. SIEGAL
"Semiconductor Thermal Considerations"

He is the founder, president, and chief executive officer of Sage Enterprises, Inc. Previously, Mr. Siegal held positions with Varian Associates, Hewlett-Packard, Microwave Associates, Siliconix, Intersil, ANCON, and Addington Laboratories. In addition, he was consultant to Quanton Science Corporation. Mr. Siegal received his B.S.E.E. from Cornell University, M.S.E.E. from San Jose State University, and his M.B.A. from the University of Santa Clara, California.

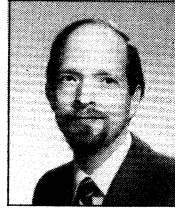

DR. KENNETH J. SLEGER
"Military Systems Needs Drive Component Demands"

He currently works for the Naval Research Laboratory in Washington, D.C., where he is the head of the High Frequency Device Section. Dr. Sleger received his B.S. and M.S. degrees in Electrical Engineering from Case-Western Reserve University, Cleveland, Ohio. He received his doctorate in Electrical Engineering from Carnegie-Mellon University in Pittsburgh.

DR. CRAIG P. SNAPP
"Silicon Bipolar Transistors and Integrated Circuits Continue to Grow"

He is currently working as manager of Silicon Research and Development at Avantek, Inc., in Santa Clara, California. He was previously with the Hewlett-Packard Microwave Semiconductor Division and with the Microwave Institute Foundation of the Royal Institute of Technology in Stockholm, Sweden. Dr. Snapp received his B.S. in Engineering Science from Case-Western Reserve University in Cleveland, Ohio. He received his doctorate degree in Applied Physics from Cornell University in Ithaca, New York.

RALPH F. TRAMPOSCH
"Thin-Film Processing of Hybrid ICs"

Mr. Tramposch is currently sales engineer for Leybold-Heraeus Technologies, Inc., of Enfield, Connecticut. Previously, he held the position of engineering manager for Materials Research Corporation, Orangeburg, New York. Prior to that, he was director of marketing for Ohmtech, Niagara Falls, New York. Mr. Tramposch received a B.S. in Physics from Roanoke College, Salem, Virginia, and his M.S. in Physics from the Rensselaer Polytechnic Institute, Troy, New York.

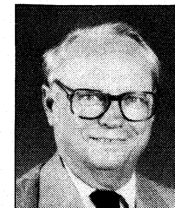

ALAN C. WALKER
"Commercial Communications Applications Show Diversity"

He is currently the manager of Technical Business Development of the Farinon Division of Harris Corporation in San Carlos, California. Previously, Mr. Walker worked with the Vicom Corporation, GTE Lenkurt, and with the Radio Communications Department of Hawaiian Telephone. Mr. Walker received his B.S. in Physics from the University of Hawaii.

ROBERT S. YING
"Solid-State Sources Power Millimeter Transmitters"

He currently works as the manager of the Millimeter-Wave/Microwave Circuits Department at the Electron Dynamics Division of Hughes Aircraft Company in Torrance, California. Mr. Ying received both his B.S. and M.S. in Electrical Engineering from the University of Michigan at Ann Arbor.

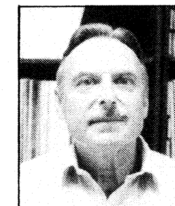

KURT E. ZUBLIN
"Testing Oscillators, Amplifiers, and Mixers"

He is currently senior project engineer within the Microwave Business Unit at Wavetek in San Diego, California. Previously, Mr. Zublin was with Watkins-Johnson, the General Electric Microwave Lab, and with several microwave firms in Europe. He received his degree in Electrical Engineering from the Federal Institute of Technology in Zurich, Switzerland.

Commercial Communications Applications Show Diversity

Commercial communications systems are reviewed in this general survey that sets the stage for the specific technology sections that follow.

By Alan Walker, *Farinon Div., Harris Corporation*

Commercial systems have significantly different requirements from defense systems—differences that should be considered carefully while reading the technical sections in this handbook. For instance, an electronic-warfare suite may demand extremely broad bandwidths, while most commercial systems to date can effectively use narrowband amplifiers and receiver front ends.

Cost is a much stronger driving force in the commercial world than in defense systems. Realizing the huge potential of such commercial communications systems as cellular radio, direct-brodcast television, air-phone networks, and corporate communications networks will depend almost entirely on reducing overall systems costs.

This problem is clearly illustrated in direct-broadcast television. Literally millions of viewers will receive television service through rooftop receivers trained on powerful satellites. Making this service affordable will require delivering terminals that cost perhaps $500 for the entire unit, including antenna, front end, downconverter and amplifiers, IF amplifiers, and indoor tuner. To understand the magnitude of cost reductions required, consider that only recently a pair of GaAs FETs operating at the DBS-TV 12-GHz allocation cost over $500.

Competing technical approaches range from mixer downconverters, to hybrid FET design, to all-monolithic or mixed monolithic and hybrid GaAs and silicon design.

Cellular radio also requires cost-effective solutions. In cellular radio, central base stations receive mobile-phone transmissions from users and relay their signals to other base stations in other cells for retransmission to the receiver. Central to the system is a switch developed by Bell Laboratories that routes signals for upwards of 200 channels between silicon power amplifiers, each handling a single channel and delivering 50 W in relatively high-distortion, Class C operation. Some 5,000 amplifiers have been ordered for Chicago, the first site approved for operation, pending legal arbitration.

Low cost does not mean low technology. Should future generations of cellular radio be able to multiplex signals through a single power amplifier, a much less expensive, more reliable base station could be designed. This would require electronic switching and a "super" multistage bipolar amplifier.

Trials are scheduled for the air phone, which will allow flyers on commercial airlines to place calls through transmissions on 2-MHz bands around 900 MHz. Final allocation is yet to be firmed up. Other applications such as low-power television, multi-point distribution service, automotive collision-avoidance radar, microwave security systems—a vast array of commercial applications—also require cost-effective, microwave solutions.

Included is a listing of many frequency allocations for commercial applications. Terrestrial radio is reviewed in some detail, since it is a market that exists here and now, and represents some growth potential following the AT&T divestitures. The growing use of satellite communications is also described.

For details on operation and performance of microwave components necessary to designing these systems, the reader is referred to the various technical chapters in this handbook.

Band Allocations

Commercial microwave equipment is available in specific frequency assignments ranging between 900 MHz and 40 GHz. The range of these microwave products is quite varied and may consist of fairly low-density applications with only a few voice and/or data circuits to those systems involving up to 6,000 voice channels on a single RF assignment. Users of this equipment may be classified in various groups.

Common-Carrier Classification

- Telephone and telegraph companies;
- Specialized common carriers;
- Limited common carriers; and
- Miscellaneous common carriers.

Private Radio Systems

A variety of applications exist here:

- Public safety services—police, fire, highway maintenance, forestry conservation;
- Special emergency services—medical, disaster relief; and
- Land transportation—motor carriers, railroads, taxicabs, and automobile emergency.

Industrial Radio Services

Many users are setting up their own communications links, augmenting or circumventing conventional telephone long lines. The frequency bands available to these users establish the capacity available and in turn the economic opportunities of these commercial microwave systems. For the common carrier licensees, commonly used frequency allocations are listed in Table I. For private radio systems, somewhat different microwave allocations have been provided; these are listed in Table II.

Terrestrial Links

If we look at the common-carrier microwave applications first, the 2-GHz frequency allocations are suitable for spur routes (side legs to heavier trunk routes), or for intercity trunk radios that tie together smaller communities in less densely settled regions of the United States. We see that

Alan Walker is the technical business development manager of the Farinon Division of the Harris Corporation, San Carlos, Calif.

TABLE I

Common Carrier Frequency Allocations

2 GHz — 2110–2180 MHz, 3.5-MHz bandwidth per channel, typically up to 192 digital voice circuits, or 252 analog circuits

4 GHz — 3700–4200 MHz, 20-MHz bandwidth per channel, provides up to 1,800 FM/FDM circuits, or up to 1,344 digital voice circuits

6 GHz — 5925–6425 MHz, 30-MHz bandwidth per channel, provides up to 2,400 FM/FDM circuits, or up to 2,016 digital voice circuits, or 6,000 single-side-band circuits

11 GHz — 10.7–11.7 GHz, 40-MHz bandwidth per channel, provides up to 2,700 FM/FDM circuits, or up to 2,016 digital voice circuits

18 GHz — 17.7–19.7 GHz, up to 220-MHz bandwidth, provides from 24 to 4,032 digital voice circuits

23 GHz — 21.2–21.8 and 22.4–23.0 GHz, up to 100-MHz bandwidth, principally light density usage

29 GHz — 27.5–29.5 GHz, up to 220-MHz bandwidth

39 GHz — 38.6–40.0 GHz, 50-MHz bandwidth

TABLE II

Private Radio Frequency Allocations

952–962 MHz — channels with 50-kHz, 100-kHz or 200-kHz bandwidths

1850–1990 MHz — channels with 5-MHz and 10-MHz bandwidths (600 FM/FDM circuits or 384 digital voice circuits)

2130–2200 MHz — channels with 800-kHz or 1600-kHz bandwidths (up to 96 FM/FDM circuits)

6525–6725 MHz — channels with 5-MHz and 10-MHz bandwidths (600 FM/FDM circuits or 384 digital voice circuits)

12.2–12.7 GHz — channels with 10-MHz and 20-MHz bandwidths (up to 1200 FM/FDM circuits or 672 digital voice circuits)

18.36–19.04 GHz — up to 288 digital voice circuits

21.8–23.2 GHz — FM video, or up to 3 Mb/sec. of data/voice

38.6–40.0 GHz — FM video, or data

analog radio designs are generally more mature, since that technology has not changed significantly in recent years. These radios have been extended to provide 252 FM/FDM voice circuits within the 3.5-MHz RF channel bandwidth. In contrast, within the last seven years digital microwave designs have advanced from a modest capacity of 48 voice channels using QPSK technology to 192 voice channels using either 16 QAM or 49 QPR modulation techniques.

The 4-GHz microwave band has been the main transcontinental circuit source since the TD-2 radio was introduced back in the 1950s. The original models accommodated only 480 voice channels, but improvements and upgrades have continued until many systems now carry between 1,200 and 1,800 voice circuits per 20-MHz–wide RF channel. Recent digital designs are capable of 90 Mb/sec. in the same 20-MHz bandwidth using 64-state quadrature amplitude modulation.

The 6-GHz microwave band served the rest of the telephone industry for many years, with suppliers such as Motorola, General Electric, Lenkurt, Farinon, Collins, and Raytheon providing equipment for lighter-density applications until the alternative heavy route competitors were authorized by the FCC. Products available now include 2,400-channel FM/FDM systems, up to 6,000-channel single-sideband systems, and 2,016 PCM voice-channel, digital-microwave systems.

At 11 GHz, the microwave route density map is less congested. The fact is directly related to the effect of rain attenuation on path reliability. For the same reliability as 6 GHz, path lengths must be shorter in many areas, and in many instances additional repeater stations must be constructed to overcome the rain outages. The 40-MHz channel bandwidth can support 2,700 FM/FDM circuits, or 2,016 PCM voice-channel, digital-microwave systems. The economics of single-sideband radio design has not proven attractive for this frequency band. Many installations at 11 GHz have resulted from metropolitan congestion at the more desirable frequency allocations of 4 GHz and 6 GHz.

The 18-GHz allocation was originally channelized for 220-MHz bandwidths that would support 274 Mb/sec. (T4 line rate) or 4,032 PCM voice channels using QPSK modulation. Only about six stations in the New York vicinity were installed with this equipment, and it soon became apparent that high-density fiber-optic applications were more attractive economically. In the meantime, light-density applications at 18 GHz appeared on the market, with digital capacities between a single T-1 line and twelve T-1 lines, and over 400 terminals of this are now in the field. Typical applications include high-speed data transmission, or providing 1.544-megabit trunks between digital PBX locations sharing a common processor. The 18-GHz frequency band rechannelization into more usable, narrow band allocations was requested by Farinon in September, 1979. The lack of a rule making this band officially available has inhibited the development of additional products with 672 to 1,344 PCM channels capacity. Some activity is now proposed by the FCC in an attempt to find frequencies for the sharing of the 12.2-12.7 GHz private radio spectrum with direct broadcast satellite systems. FCC Docket 82-334 has received hundreds of comments and reply comments on the proposed relocation of the existing private radio network.

Private Networks

Private radio networks are more complicated to explain than the common-carrier system. The owners of these systems may vary from a small system that needs only a few circuits between plant locations separated by a small distance to that of a major multinational corporation that employs satellite transponders, point-to-point microwave and links, and a communications network spanning more than one continent. (A typical corporate communications network is shown in Figure 2.) These networks can employ TDMA satellite switching, 1.544-megabit conference video circuits, and high-speed digital data routes employing 56-kilobit or higher rates. Standard voice circuits are interconnected

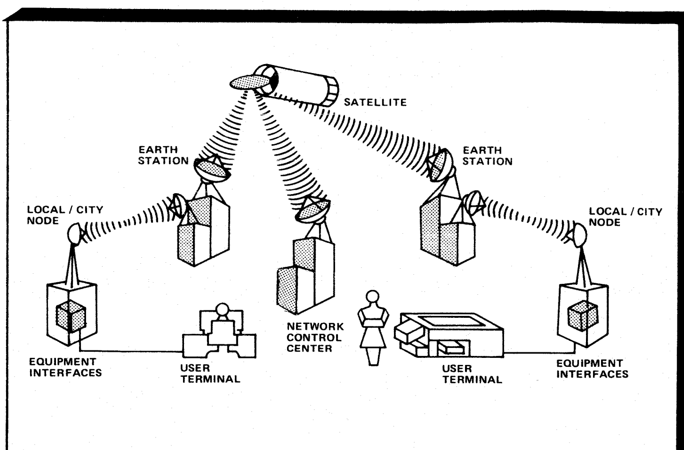

1. Satellite Business Systems will use inexpensive microwave radios to link users to a major Earth terminal site.

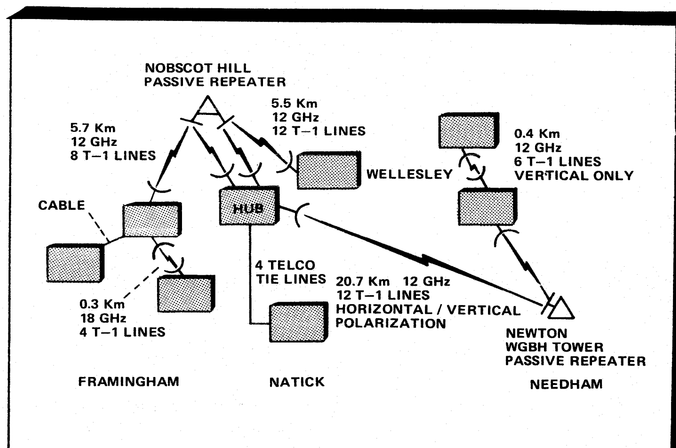

2. Corporate networks are springing up, such as this system installed by Harris/Farinon for Prime Computer.

between different ground stations using the TDMA capability of the system.

Within the private microwave category we find the bulk of the industrial microwave networks that parallel the railroads, the pipelines, and the electric distribution networks, and provide the protection and control of these important utilities. Many of these systems are in excess of 1,000 miles in length and employ analog microwave design with 600-voice-channel capacity, or less. Remodulating repeaters, rather than IF heterodyne designs, are most commonly used, since excellent performance is attainable with loadings of 600 or less circuits, and frequent voice and data drops occur along the network. While many users would rather consider a digital microwave system for new routes today, the capacity of this equipment has only recently attained 384 channels of 64 kilobits each in the 10-MHz bandwidths available. An additional problem exists in that the partial upgrade of an older analog network to a digital system is not easy, since new voice and data channels are required at all of the converted sites, and the interface between the analog and digital portions is difficult at best, even with transmultiplexer technology.

The business grouping within the private microwave category has potential for fast growth, even though this grouping is denied access to the 5- and 10-MHz spectrum. The rapidly increasing costs of telephone and data circuits between plant locations have resulted in a myriad of business microwave networks. The savings that accompany the private ownership of digital PBXs in separate plant facilities, and their interconnection with multiple digital trunks of 1.544-Mb/sec. capacity, enhance the operational flexibility of telephone, data, and computer interconnections in a manner that is very cost effective compared to leased telephone facilities. In many instances we see payback periods as short as two years. The bypass of the telephone network may have an adverse effect on the cost of "plain old telephone service" as these firms adjust to the divestiture of AT&T and the changing communications environment of tomorrow.

Satellite Communications

The move by corporations to satisfy their business communication needs by either leasing transponder time or by signing up for tariff service on satellites represents yet another force aggravating congestion of the frequency bands. (A typical network is shown in Figure 2.)

There are several solutions. Satellite Business Systems, for example, offers tariff service using dedicated satellites operating at the 12-GHz band. These Earth terminals for business use are extremely sophisticated, costing upwards of $300,000 each with complex computer-controlled switching of high data-rate transmissions. Similar high data-rate systems at 4 GHz are offered by various companies.

A less expensive, low-data-rate solution at 4 GHz is offered by Equatorial Communications. Equatorial leases transponder time on existing satellites for such customers as United Press International.These utilize inexpensive 'micro' Earth stations to receive low-power, spread-spectrum transmissions, which allow a significant data rate to be transmitted without exceeding regulations on effective radiated power. Low cost, hybrid FET design and microprocessor control of the terminal make Equatorial's micro-terminals cost-effective.

Commercial communications will continue to move to higher frequencies as witnessed by NASA's Advanced Communication Satellite, which will use 30/20 GHz. Use of 30 GHz for satellite communications has been pioneered by Japan's NHK and the CS-2 satellite. Rain attenuation is a greater factor at 30 GHz than at either 12 or 6 GHz, forcing consideration of multiple, alternate terminals for reception. Japanese efforts include studying the use of 30 GHz for high-definition television, although they have been stymied to date by the need for extremely wide bandwidths.

For the different versions of HDTV these are: Digital HDTV, over 300 MHz; Full HDTV (luminance and color), 30 MHz; and HDTV with luminance only, 20 MHz. This compares with American and Japanese TV which currently require only a 4.2-MHz bandwidth, and voice sent by telephone which needs a 3-kHz bandwidth.

Commercial communications indeed represents a broad and changing field. Technical challenges abound, from developing low-cost satellite Earth terminals to improving transponder linearity. The technical chapters in *The Microwave System Designer's Handbook* provide a basic reference guide to the components that are the building blocks for solving these challenges. ■

Military Systems Needs Drive Component Demands

The requirement for microwave systems to provide battlefield management and force multiplication will determine the trends that component design will follow.

By Dr. Kenneth J. Sleger, *Naval Research Laboratory*

Microwave electronics has played an important role in U.S. military systems beginning with radar applications during the Second World War and progressing in time to other application areas such as electronic warfare, communications, navigation, and missile guidance. This article gives a broad-brush overview of the applications of microwave electronics to modern-day fielded and planned systems. For specific design information, see the individual technical chapters in this handbook.

For the purposes of this discussion, the term microwaves is intended to bracket the electromagnetic spectrum from 1 to 30 GHz. At present this frequency range covers most of the fielded military systems and planned systems concepts. However, factors such as a crowded frequency spectrum, especially under wartime conditions, have focused several advanced systems designs into the millimeter-wave and infrared-optical range above 30 GHz where potential bandwidths are larger and threats fewer. This frequency range will not be covered in this article although it offers certain capabilities limited at microwave frequencies such as covert or cross-talk-free communications and electronic battlefield management under adverse optical visibility. A special section of the handbook examines millimeter technology in a series of complementary articles.

Microwave systems have been cited as a "force multiplier" for the important role they play in sensing and transmitting information and then guiding, controlling, and triggering various munitions carriers.* Such systems extend the analog senses and physical power of military personnel and are acutely necessary in terms of the ever-growing adversary military arsenal. Success in future enemy-provoked wars will depend to a large extent on the use of microwave systems coupled with effective command, control, and communications (C^3), which are considered the brains and nervous systems of any modern military forces. As a result, today's electronic battlefield management emphasizes C^3, electronic warfare, and intelligence systems. Microwave electronics is ultimately linked to the success of virtually all battle-management scenarios by its virtue of direct interface with the real world of analog functions and wide bandwidths.

Applications

The two most important needs of nearly all microwave systems are a high-power source and a very-low-noise sensor. Radar and electronic jammers are common applications of high-power sources while warning and communication receivers dwell on low-noise technology. Most early development of microwave systems usually focuses on these two needs. As the system matures, additional technology is inserted such as signal processing and intelligence for improved C^3. Today's microwave system application areas can be broken down into five distinct areas:

Search and Surveillance

- Detect enemy objects such as enemy planes, ships, submarines, missiles, and missile launches (principally strategic)

Target Acquisition/Fire Control

- Short-range-tracking enemy surveillance for precise identification with ability to fire weapons (tactical)

Communications

- Ground, sea, air, and satellite
- Secure, antijam links

Navigation

- Global strategic positioning to battlefield tactical positioning
- Obstacle avoidance at low altitude without detection

Electronic Warfare

This application area is frequently characterized by these terms and acronyms:

- Electronic Support Measures (ESM)
- Electronic Counter Measures (ECM)
- Electronic Counter-Counter Measures (ECCM)
- Electronic Intelligence (ELINT)
- Passive measures to shield against enemy observation (ESM)
- Warning to detect enemy electronic threat (ESM)
- Active countermeasures to jam enemy systems (ECM)
- Active countermeasures to give deceptive target information (ECM)
- Counter-countermeasures (ECCM)

ELINT is primarily a compendium of previously compiled tactical and strategic information that covers analysis on potential weapon threats and includes intercept and analysis

*For example, see *Spectrum*, Oct. 1982, dealing with military technology.

Dr. Kenneth J. Sleger is head of the high-frequency devices section at the Naval Research Laboratory, Washington, D.C.

Acronyms Used in Table

AIAAM — Advanced Intercept Air-to-Air Missile
AMRAAM — Advanced Medium-Range Air-to-Air Missile
ASPJ — Airborne Self-Protection Jammer
AWACS — Airborne Warning and Control System
IFF — Identification Friend or Foe
JTIDS — Joint Tactical Information Distribution System
MILSTAR — Military Strategic-Tactical and Relay
NTWS — New Threat Warning System

of associated communications traffic. This intelligence acquisition defines the requirements for ESM systems. ESM is primarily passive and confined to identification and location of enemy signals. The importance of electronic warfare cannot be overemphasized. The next major war will highly depend on electronic warfare, either through passive detection or ECM. A close-at-hand example of the power leverage of ECM (or lack of it) can be seen in the Falklands conflict where the French Exocet anti-ship missile drew dramatic attention to the role ECM plays in ships' point defense.

The systems applications of microwaves can be further expanded as shown in the table below. Focus is on modern needs and the perceived technical approach for implementation. Note the importance of radar in virtually all applications areas, though its modern dress is electronically programmable phased arrays with synthetic apertures.

Continued on page 20

Microwave Systems Applications

Search and Surveillance	Target Acquisition Fire Control	Communications	Navigation	Electronic Warfare
Advanced warning AWACS NTWS	*Missile guidance* AIAAM AMRAAM	*Anti-jam* JTIDS IFF	*Global positioning* World navigation	*Jammers* Stand-off Self-protection (ASPJ) Deception
Strategic surveillance Space-based radar	*Remotely piloted vehicles*	*Anti-intercept*	*Low-altitude flight* Obstacle and radar detection avoidance	*Decoys*
Radar echo resolution	*Precision tracking* Multiple, simultaneous targets	*Milstar* Satellite communications worldwide downlink	*Inertial navigation*	*Threat warning* Channelized receivers
	Target recognition	*Fiberoptics links*		*Stealth synergism* Reduced cross-section
	Anti-radiation missile protection			
• Advanced passive and active sensors • Phased-array radar active-aperture arrays • Synthetic-aperture radar • High-probability-of-intercept radar • Small, lightweight transmitters and receivers	• Synthetic-aperture radar • Limited use of active sensors for ARM protection • Netted radar for precision tracking • Electronically agile phased-array radar	• Microwave/fiber-optics interfaces • Spread-spectrum coding • Fast frequency hopping • Small, lightweight transmitters and receivers for satellites • Low-probability-of-intercept radar	• High-resolution radar • Precision-timed, coded radio • Small, lightweight transmitters and receivers for satellites and aircraft	• Programmable high-power broadband amplifiers • High-gain radiators such as lens-fed arrays • Tunable, wide band- • width components • Expendables • Small, lightweight components for aircraft • Wide-bandwidth receiver front ends

Continued from page 17

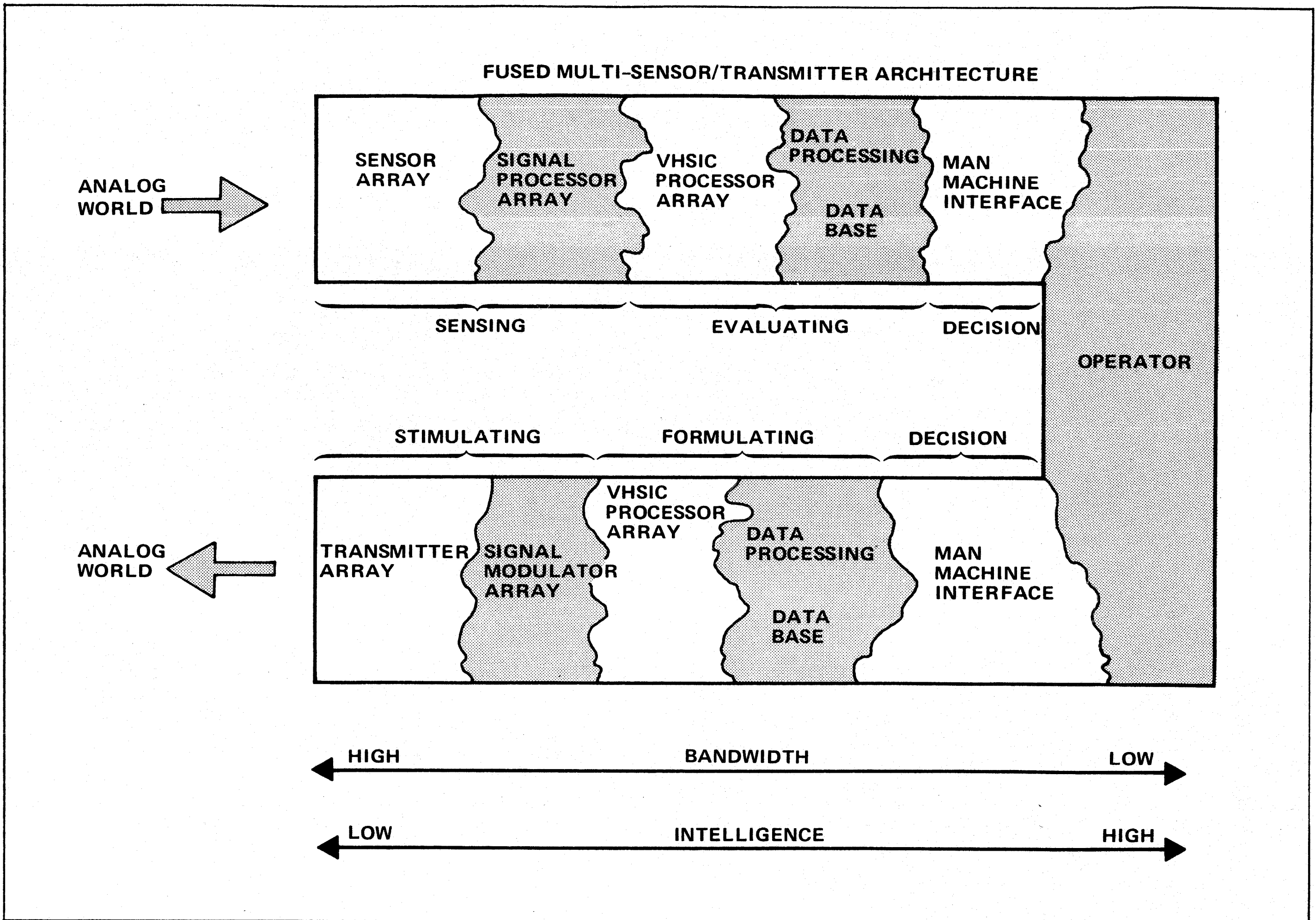

Military systems of the next decade and beyond will require heavy fusion of inputs and outputs between multiple sensors and transmitters in force-multiplying systems. The operator will face massive decision-making tasks, simplified by VHSIC-generation processors and extensive, dynamically configurable data bases. Irregular lines represent data buses of both analog and digital design, as appropriate for greatest throughput, between the various pieces of the architecture puzzle. Using ELINT as an example, such a system might be programmed to recognize, record, and transmit enemy C^3 signals to a distant battle commander, while threats such as approaching gunships would trigger an operator-unassisted request for protective support from nearby surface-to-air missile batteries. The operator, meanwhile, might simply be advised of the actions taken, or called into the loop for a decision on active jamming of missiles launched by the enemy aircraft.

The Future

Future wars will involve the use of sophisticated decoys, false targets, and false information. Thus, microwave technology will require the assistance of microelectronics and computer technology for artifical intelligence or "smart weapons." Such infusion of computer technology will have radical impact on future conflicts and will have the potential to extend C^3 to global, long-range targeting plus tactical warfare. The areas that will be affected are space surveillance, brilliant weapons, stealth technology, and submarine detection, all of which will employ microwave transmitter and sensor devices. It will be necessary to "fuse" these microwave front-end functions to computer or high-speed processing technology such as VHSIC. A new technology thrust, "fusion technology," has emerged to serve this need. The illustration shows a fused system architecture envisioned for the 1990s. The irregular lines represent interface buses between the shown technologies, both analog and digital. Such a fused-system concept will require significant technology insertion by today's standards, even in the microwave area. Higher powers and bandwidths, and smaller size and weight, will be required for many applications forcing the infusion of monolithic and/or miniature hybrid integrated circuits. Still other areas of fusion technology will focus on electronic microwave interfaces to fiberoptics technology for wide bandwidth, cross-talk-free communications and electronic distribution. Finally, the use of microwave directed-energy devices to counter the increasing speed of anti-ship and ballistic missiles, antisatellite applications, and satellite defense applications cannot be neglected. Such fusion of intelligence and microwaves will lead to exciting systems of the future which will further stimulate the talents of systems engineers and designers. ■

Mm-Wave Threats Continue to Grow

A survey of Soviet military developments in the mmw range shows there are reasons to be concerned.

By Alexander E. Braun, *EW Communications, Inc.*

Although the last five years have witnessed remarkable progress in activity in the millimeter-wave region, developments in mm-wave military applications in the United States do not appear to have kept sufficiently abreast of work being carried out elsewhere.*

According to experts in the mm-wave field, the area of growth on which to concentrate for military applications should be principally components. Virtually every component is based on designs created during the 1950s and 1960s. The one exception, in terms of hardware available on the market, is sources. Here, at least, are IMPATTs and some limited Gunn devices at the bottom of the mm-wave frequency spectrum.

The majority of available sources—the backward-wave oscillator, certain vacuum-tube devices, etc.—have been improved, but the basic designs date back 20 or even 30 years. Most of the basic plumbing, in terms of measurement and signal-processing techniques, is relatively old when one considers what is available on the marketplace; thus, whoever builds an mm-wave system using available hardware does it with materials whose basic design is several decades old, again, with the possible exception of some of the sources.

There is very little so-called "new technology" in the mm-wave region that does not use, in one way or another, classic waveguides, hybrids, directional couplers, detectors, attenuators, and so on. The mm-wave market does not seem to offer anything that is at all integrated; for example, it is not possible to get dielectric waveguide components or anything resembling them. Basic isolator and circulator performance is generally poor by microwave standards; because these components are little more than extrapolated microwave designs, it is not surprising that they do not work well at 100 GHz.

The Soviet Threat

Improvements have been developed for transmitters, receivers, and components; however, according to some military experts in and out of the Department of Defense (DOD), not enough is being done, particularly in the European Theater, to counter the threat of the several mm-wave systems developed—and in some cases deployed—by the Soviet Union.

Counters to mm-wave systems operating at a frequency range of 30 GHz and above have yet to be fully developed by the U.S. military largely because, until recently, many of the leading Pentagon planners insisted that there was no significant EHF threat, other than the few signal intelligence systems (SIGINT) said to have been intercepted.

Since a real threat was not encountered—or was too obvious—the DOD has not placed too much priority on requiring its contractors to develop mm-wave systems. Some find the situation analogous to the early days of the involvement in Vietnam back in 1965, when Soviet surface-to-air missiles began downing U.S. aircraft in significant numbers. Only after aircraft-loss rates became unacceptable were electronic countermeasures taken seriously and systems like radar warning receivers and jammers began being designed and produced.

However, the tactical situation is different in the European Theater, where most of the mm-wave requirements are becoming increasingly obvious. And, if they are becoming obvious to some U.S. planners, increased Soviet efforts in the mm-wave region should also be expected.

At present, the United States has a considerable number of weapons and weapon systems that should have something approaching mm-wave-type performance for target designation, identification, and ranging, simply because the optical systems with which those weapons systems are now equipped are not very useful under adverse weather conditions.

If a worst-case situation is assumed (in other words, an attack along the area in northern Europe where NATO and Warsaw Pact forces face each other), it becomes obvious from a cursory survey of weather patterns in the European arena that for approximately 150 days a year, there are conditions (fog, rain, snow, sleet, or any combination of these) which can obscure optical systems (e.g., infrared and laser)—particularly rangefinders, target designators, etc., when they might be needed the most. U.S. tanks in the region (M-1s and M-60s) are equipped with IR systems that run the chance of being partly or totally inoperative a good part of the year. Therefore, there are very serious questions as to how these systems are expected to operate. Mm-wave systems are better at detecting targets through light fog than are IR systems, so it does not require a strategist to see that this is one of the first things to which the technology might be applied.

The alternative has to be examined, particularly when there is strong evidence that the Soviets already have operational, deployed, mm-wave systems which can be used for tactical communications, to aim guns, or to guide missiles. These are not limited to daylight use, like weapons

*The mm-wave region is defined as that section of the spectrum between 30 to 300 GHz, or 1 cm to 1 mm wavelength.

Alexander E. Braun is the Editor of Microwave Systems News *magazine, published by EW Communications, Inc., Palo Alto, Calif.* *The author wishes to express his appreciation to David M. Russell, Associate Editor of* Defense Electronics *magazine, for his assistance.*

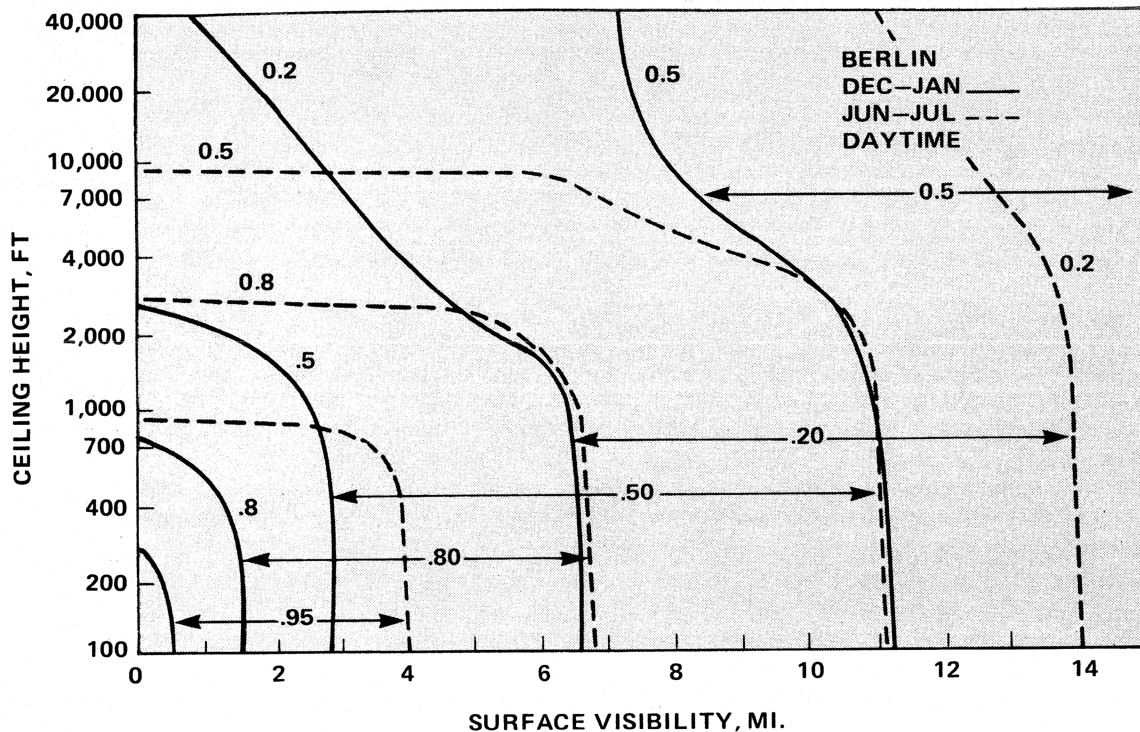

A European weather profile. The probability is that concurrent ceiling and surface visibility values will be equalled or exceeded. This is a winter/summer comparison for the Berlin area.

requiring optical or TV guidance. Millimeter-wave systems are also better at detecting targets through light fog, for instance, than are IR systems.

In the areas of short-range communications, target identification, and others, there is a need to begin using mm-wave systems. The U.S. Army in particular—and to a lesser extent the Navy and the Air Force—have decided that it is necessary to do something, although the programs instituted do not appear to have a very high priority, and the armed forces tend to look toward industry, rather than their own planners, to define problems.

The starting point, therefore, is at the components that must be upgraded. Some work is already proceeding in this direction in places like Lincoln Laboratories, where researchers are looking into GaAs-based integrated mm-wave components. Results so far would appear to be encouraging, but there is nothing in full-scale production yet, nothing that will enable a manufacturer to put systems together—a classical chicken vs. egg syndrome.

The mm-wave parts problem is far from over. Millimeter-wave systems houses such as Honeywell, Hughes, Raytheon, and Westinghouse are beginning to claim having mastered the majority of production bottlenecks, declaring their readiness to meet DOD requirements; however, they have not as yet been given much of an opportunity to prove this—hardly an encouraging sign to the component manufacturers.

The Soviet lead in deploying mm-wave and near mm-wave systems has been met with a slow, initial U.S. effort to catch up. From air defense systems such as the SA-11 and SA-13 surface-to-air missiles to naval systems like the dual frequency Kite Screech shipboard radar, the Soviet Union appears heavily committed to modernizing its defenses with higher-frequency electronics systems.

The Soviets, from what can be gathered from available information, appear to be considerably better than the West in certain areas, particularly filters. While admittedly somewhat limited, they still have some components which appear to provide better performance than those available to the West. The Soviets appear to have gone to the level where they have integrated them, made the systems work, and have deployed them.

Soviet advances in millimeter- and near-millimeter-wave systems have mainly been in the search and fire-control radar areas. In all fairness, however, it should be stated that Soviet radar designers who must only worry about atmospheric propagation have a much simpler life than U.S. designers who are trying to perfect overland look-down systems. Deployment under those circumstances would

understandably come sooner for the Soviets, all other things being equal.

As with most electronic systems, U.S. mm-wave development projects tend to be more complex than Soviet efforts. For example, the U.S. is seriously pursuing autonomous, robotic anti-armor missiles using imaging radar for guidance and target recognition.

In addition to developing the "intelligent" hardware and software that will enable missiles to independently recognize enemy tanks and guide themselves to their targets, clutter-rejection requirements are included. An mm-wave-guided air-to-air or surface-to-air missile does not require the necessary artificial intelligence, nor does it have the clutter problems of a surface seeker.

To shorten the development process of an autonomous anti-tank missile, mm-wave radar may be dropped in favor of a moving target indicator (MTI) radar or an X-band synthetic aperture radar, which has less clutter rejection problems, images well, and sees through poor weather. S-, C-, and K-bands also provide good resolution; so options can accomplish the same feat, and Soviet mm-waves may be more of an apparent threat than at the threshold of a new defense technology gap.

Electronic-warfare systems designers indicate the threat also comes from within: The Soviets are developing an mm-wave challenge, but DOD requirements for countermeasures have not been passed down to contractors.

As always, an important part of the problem is one of budget constraints. With airborne radar warning receivers, for example, the budgetary dilemma often appears in the form of tremendous costs incurred in expanding the existing system's coverage just to the relevant mm-wave frequencies.

Radar Antenna Beamwidth vs. Mm-Wave Frequency

Aperture Size (Meters)	Frequency (GHz) 35	95	140	220
0.01	62.5	23.1	15.6	9.9
0.1	6.3	2.3	1.6	1.0
1.0	0.63	0.23	0.16	0.1

The narrow beams possible with mm-wave radars are less vulnerable to ECM and permit the high resolution useful for target classification and imaging applications.

The Mm-Wave Windows

The frequencies at which all these mm-wave systems operate offer no particular problems; rather, the designers must look to the windows which become available at these frequencies as well as the advantages that they offer.

The standard windows lie in the near-millimeter area, which is down in the 30- to 40-GHz range, and then go through a severe absorption band peaking near 60 GHz then into another hole at about 90 GHz — so that there is another absorption band until another hole is reached at about 140 GHz, and yet another hole at 220 GHz. For both sides of the Iron Curtain, the majority of the concentration going on is on the 90-GHz region for communications and range-finding devices. However, it should be kept in mind that atmospheric attenuation rises rapidly as frequency increases, and the "hole" at 140 GHz could have greater attenuation than at lower frequency "non-hole" regions.

There is also work being conducted by the Soviets around the edge of the absorption bands using what some Pentagon sources describe as "punch-through" communications in which the operational frequency is put somewhere near the edge of an absorption band and power is turned up, resulting in communications with almost no overshoot. A moderate amount of tactical ground-to-air communications is being done this way in the 60- to 80-GHz region where band-edge communication is used; that is, they operate in the edge of absorption bands so that the overshoot is very low, boosting the power only to the required range.

This procedure allows for very secure communications because it is highly directional, due to the high gain achievable from an antenna of a given size. It is also range-limited, making detection impossible by a satellite 100 kilometers up; by the time the signal reaches that level, absorption has attenuated sidelobes to the point where they cannot be found. Reports from certain sources indicate that the Soviets are already experimenting with these systems in their C^3 make-up.

Everything seems to indicate that all this Soviet activity is eliciting little reaction from U.S. military circles. However, it is significant to note that the U.S. Army has slapped the lid on many mm-wave programs, and that obtaining information and clearances to use information coming out of these programs (even though some of it is already in the literature), has become increasingly difficult. In the 1982 Microwave Theory and Techniques Symposium held in Dallas, for example, a number of pages had to be pulled out of the proceedings due to "sensitivity of the subject matter." The same thing happened in the Boston symposium held in 1983, where pages had to be razor-bladed out of the proceedings books prior to the beginning of the conference.

The Design of Mm-Wave Systems

Problems in designing mm-wave systems have centered primarily on power and sources. The sources pursued are often cavity resonating oscillators with diodes, but putting these together in power combiners is not an easy technology because of the excessive heat produced in addition to the problems in miniaturizing mechanical parts.

Adequate sources do exist, although it would seem at times the DOD fails to acknowledge this fact. The decisions of those involved in weapons requirement and procurement in the DOD appear to indicate a belief that mm-wave technology is a long way from the cost-effective, rugged maturity needed to field mass quantities of systems, and that procurement at this point would be premature. Industry often disagrees with this outlook.

Engineers working with millimeter-wave systems have been experimenting with solutions to the source problem for decades (some early aircraft radars developed in Great Britain during World War II operated in the EHF range), but the poor availability of sources has precluded, and/or postponed, widespread acceptance and usage.

Sources for millimeters are now more readily available, both in vacuum-tube and solid-state form. Solid-state

IMPATTs serve low-power applications, with Watts of peak power (and tens of milliwatts average) up to the 300-GHz region. Gunn oscillators can be used up to 100 GHz and slightly beyond, klystrons to 200 GHz, and backward-wave oscillators to over 1000 GHz.

Medium-size tubes, such as the magnetron, have been improved in lifetime and are available to 95 GHz. Extended-interaction oscillators are currently in use close to the 300-GHz range. Gyrotrons and other similar devices consistently achieve megawatts of peak power at efficiencies greater than 30 percent, and hundreds of kilowatts CW at near 50 percent efficiencies.

While solid-state sources provide relatively low power, they have the advantage of being smaller and needing lower voltages and prime powers than do tubes. IMPATT oscillators can be obtained for frequencies from 3 to over 240 GHz with five-percent efficiencies at about 40 GHz and under one percent above 100 GHz.

There are commercially produced Gunns that will go from the microwave region to slightly over 100 GHz, with efficiencies ranging from three percent at 40 GHz to less than one percent at 100 GHz.

Developments in mm-wave radar systems also appear to be very encouraging. The greatest advantage offered by radar systems operating in this region is that the signals are inherently more difficult to intercept—and thus, to jam—because of narrower beamwidths and low sidelobes that well-designed EHF systems have relative to those operating at lower frequencies.

Since aperture or antenna size is the primary variable for determining beamwidth, mm-wave radar beamwidths can be made narrower than those of lower-frequency radars for a given antenna size, therefore providing high-quality azimuthal resolution. This feature makes mm-wave radars inherently better suited to imaging applications, requiring high pulse repetition intervals and narrow beamwidths, normally associated with the EHF region. Antennas for millimeter-wave radar also generally offer higher gain than microwave-frequency systems, because of the relatively larger apertures available.

Radar systems operating in millimeter wavelengths are inherently less susceptible to active ECM than are other sensors operating at lower frequencies, because of their narrower beams and smaller sidelobes. This reduction in susceptibility results not only because narrower beamwidths are more difficult to access, and directional problems put a premium on pointing and stability; but also because achieving the power levels necessary for a successful mm-wave jammer is a challenge.

The mm-wave jammer designer faces the same problems of atmospheric attenuation that the radar designer does, thus limiting active ECM systems primarily to short ranges. Standoff jamming is difficult to accomplish in EHF. Adding to the inherent anti-jam characteristics of mm-waves are the wide bandwidths available that allow use of spread spectrum and frequency agility/hopping ECCM features. This further decreases the power available for active ECM if barrage or follower jamming is to be employed.

The principal atmospheric windows exploited for mm-wave use (35, 94, 140, and 220 GHz) have the corresponding bandwidths available: 16, 23, 26, and 70 GHz.

Atmospheric Attenuation Due to Weather

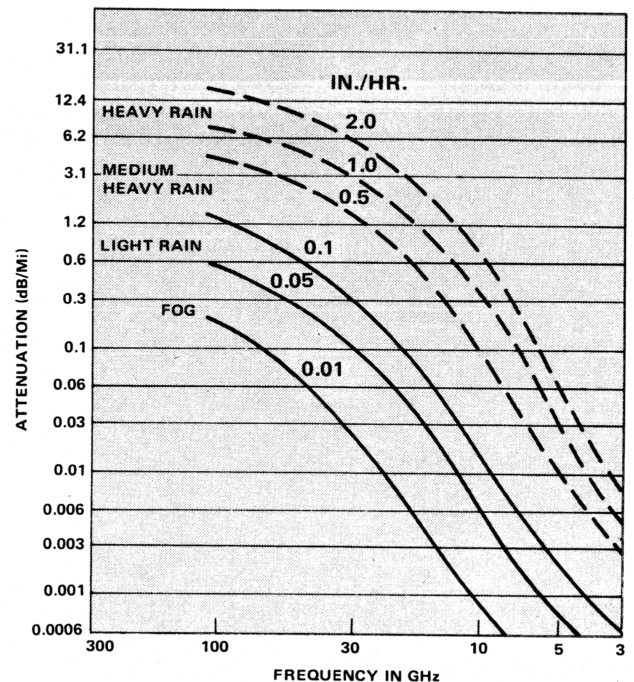

Passive electronic countermeasures (or chaff) are as effective against mm-wave radar as they are against systems operating at lower frequencies. But the traditional medium used to decoy a low-frequency radar, namely, one-half and one-quarter wavelength dipoles made of aluminum or aluminized glass strands, loses its effectiveness if the mm-wave radar to be neutralized operates on a frequency much above 35 GHz. Above that point, the wavelength is so short it requires spectral reflecting particles, or aerosol. Sufficient amounts of testing have been conducted by the DOD and its contractors to determine the types of chaff most effective for radars operating above 35 GHz; so far, however, most requirements handed down for such countermeasures have been in research and development—and not in production.

Particulates that tend to reduce the effectiveness of IR systems, such as sandstorms, smoke, and fog, cause little degradation on mm-wave radar sensors. However, rain, being a natural spectral reflector, inhibits mm-wave penetration of the atmosphere by attenuating and absorbing signal strength, and scattering target-return signal energy, which is then received as noise.

Improving Missile Guidance

Millimeter-wave radars in their current state of development also do not possess an adequate terrain clutter-rejection performance for air-to-surface missile applications. The Wasp missile developed by Hughes, versions of which have been reported to operate at 44 and 94 GHz, as well as systems under development at Raytheon, show promise of overcoming this barrier to acceptance.

For the anti-tank missile role, mm-wave radar as a guidance mechanism from an airborne platform is as yet immature because armored vehicles can often mask themselves in foliage. Martin Marietta/Orlando and Rockwell International are pursuing a solution to that obstacle in the STARTLE program (surveillance and target acquisition for tank location and engagement), which will develop a 94-GHz radar system to be mounted on tanks for locating and targeting enemy tanks.

Missile-guidance requirements make mm-wave radar a logical choice, especially since the missile's slender body cross-section forces the use of a small-diameter antenna. This situation generally requires the use of all-solid-state components and devices, and efforts are underway to develop a TWT of sufficient size and power for mm-wave radar missile guidance. For naval systems requiring sea clutter rejection capabilities such as airborne look-down radars and surface-search shipboard sensors, millimeter waves are well suited.

Countering Mm-Wave Threats

It should be be expected that, as the use of these systems becomes more widespread, countermeasures will follow suit in the shape of jammers and other ECM devices. This is true of any electronics area. All it means is that both sides begin playing the same one-upmanship game each has been playing in every technology since the end of the Second World War. By beginning to encode, and use frequency diversioning and better front-end filters, any number of techniques can be applied to avoid the problem. This is something that has occurred and will continue to occur over the entire spectrum, including optical frequencies, which can also be jammed. This, in turn, will require a redesign of the ECM and ECCM systems.

Clearly, what should be done is to begin seriously considering the possibility of leapfrogging into the next generation, rather than merely fielding systems that are known to work but are also easily neutralized. Plans should be implemented to begin on these second-generation systems in order to have solutions ready that will allow the development of analysis capabilities at those frequencies, as well as jamming capabilities and countermeasure techniques.

Experts appear to agree that countermeasure procedures for these new systems would probably not differ appreciably from those used in normal radar countermeasures at lower frequencies, due particularly to the simplicity of the targeted receivers: Most of them are vulnerable to simple power overload jamming. Thus, the first procedure would be to do a fast-scan technique. Since the passbands are relatively limited, it is not necessary to scan the entire mm-wave region prior to beginning jamming operations.

The next logical step would then be for the other side to encode or to try to use frequency hopping. This could then be countered with broadband noise jamming, duplication of codes, or using a memory loop on an RF signal and sending it out again as a range-gate pull-off technique. In short, using and adapting all the standard procedures which are in use today at lower frequencies.

The challenge to U.S. industry's development of mm-wave radars, for weapons guidance and air search, as well as EW systems, comes not only from the Soviet Union, but from European allies of the U.S. as well. Since adverse weather conditions are far more common in Europe than in the U.S., European defense-electronics industries have been more cognizant of designing all-weather capabilities into their systems. Millimeter-wave systems are better at detecting targets through light fog than are infrared systems, and are not limited to daylight-only use as are such systems as optical and TV-guided weapons.

Unfounded or not, the argument is often heard that because mm-wave components and devices are more difficult to produce than those designed to operate at lower frequencies, costs rise, resulting in the U.S. mm-wave industry almost pricing itself out of the market. Since the U.S. has a far larger force structure and equipment needs than do its European allies, it requires a well-developed defense industrial infrastructure to produce the greater quantities of mm-wave systems.

The complaint is carried further by claims that the European defense establishments do not have the same cost problems as the U.S.

The force structures of West Germany, Great Britain, France, and others, are individually much smaller than those of the U.S., the argument posits; therefore, while the unit cost of any weapon system probably increases with smaller buys, Europe's total potential expenditures are nonetheless smaller, and its defense establishments can thus afford expensive mm-wave systems. This argument conveniently neglects the smaller GNP that is available to support the military establishment.

While it is true that the U.S. millimeter-wave industry has yet to prove it can serially produce complex millimeter-wave defense systems successfully and cheaply, the problem is not so much a lack of production capability as it is the result of a lack of large production orders that could help the mm-wave industry to realize economies of scale. The argument many European countries have leveled at the U.S.—that the U.S. Defense Department is parochial in its purchasing attitude in relation to where it buys its systems (predominantly from U.S. companies)—is probably correct. But, more importantly, U.S. defense planners and funders are even more parochial in the frequency bands in which they will procure weapons systems to operate. The technology either has matured or is on the threshold of being obtained. Pump priming and support are needed now.

Possibly the most ambitious DOD project using the EHF portion of the electromagnetic spectrum is the Milstar satellite program. Using 44-GHz uplinks to the satellites from air, sea, and land terminals, and 20-GHz downlinks, frequency hopping over a 2-GHz range for interception security and anti-jam protection, the system challenges an industry that has little experience in building such high-frequency, high-power systems.

The rapid atmospheric attenuation properties of millimeter waves is also being exploited for intraspace communications use. The 45- to 65-GHz range (and especially 60 GHz) attenuates most rapidly, while the high data rates possible with wideband EHF make millimeter waves particularly useful for satellite communications, where atmospheric attenuation is not a factor.

To protect space communications from terrestrial interception, satellites will use the EHF region to pass data among

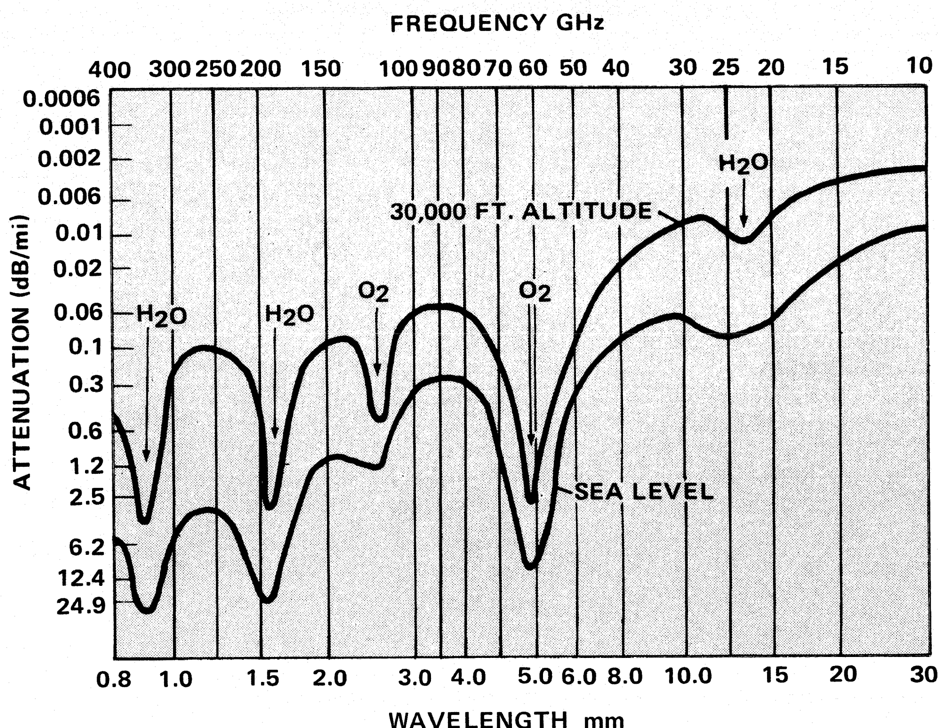

themselves without threat of being received by SIGINT systems based on Earth, since their transmitted signal energy will be uselessly dispersed by traveling partially through the atmosphere. Ship-to-ship communications over short ranges employ the same principle for security.

For land-based military communications, ITT Defense Communications Division, under contract to the U.S. Army CECOM, developed a tunable frequency system called the MISR (mobile intercept resistant radio) operating in the 54- to 58-GHz range that optimizes its frequency for minimal signal overshoot. The signal attenuation that normally frustrates radio designers is exploited by allowing the transmitted signal to travel only the distance desired—to the receiver—and then be rapidly attenuated.

In the short term, at least, the EW and radar communities are concerned with select bands, primarily at 35 and 94 GHz, because of propagation effects. Electronic reconnaissance and SIGINT experts are concerned with the total mm-wave frequency band spread.

MM-Wave Projects Under Development

Mature mm-wave technology is being applied to, or is available for use in, existing systems. For example, satellite communication uplinks at 30 and 44 GHz are possible.

At 35 GHz, the new threat warning receiver, the sense and destroy armor (SADARM) anti-tank submunition, the sensor tank, off-route mine system (STORM) being developed by the Army Armament R&D Command, the U.K.'s Sea Archer shipboard fire control system and Rapier land-based system, the air defense missile system, and the APR-39 radar warning receiver for fixed-wing aircraft or helicopters have been under development for quite some time.

For operation at 94 GHz, quiet radars are being contemplated, as are beam-rider munitions and the infantry man-portable anti-armor assault weapon system (IMAAW) project under development as a possible next-generation light anti-tank missile.

The Air Force has analyzed the feasibility of combining mm-wave and electro-optical sensors in its COSTARS program for target discrimination (real versus decoy), and for search, screening, and pre-classification functions. For advanced weapons delivery, the Air Force is attempting to apply advanced target-acquisition sensors including mm-wave radar and CO_2 laser radar intended to improve day/night and adverse-weather fire control.

The Department of Defense is funding several program elements that seek to develop mm-wave systems and devices, although most are early budgetary line items, indicating the DOD does not plan to field many EHF systems in the near future. For example, DARPA's Defense Research Sciences program element contains provisions for electronic sciences under the Technology Base requests, which will explore new concepts in electronic and optical materials, devices, and device fabrication with the goal of demonstrating their feasibility to provide new technical options for implementing future electronic and optical systems.

Technologies pursued include monolithic microelectronic, microwave, millimeter-wave, and optoelectronic circuits of

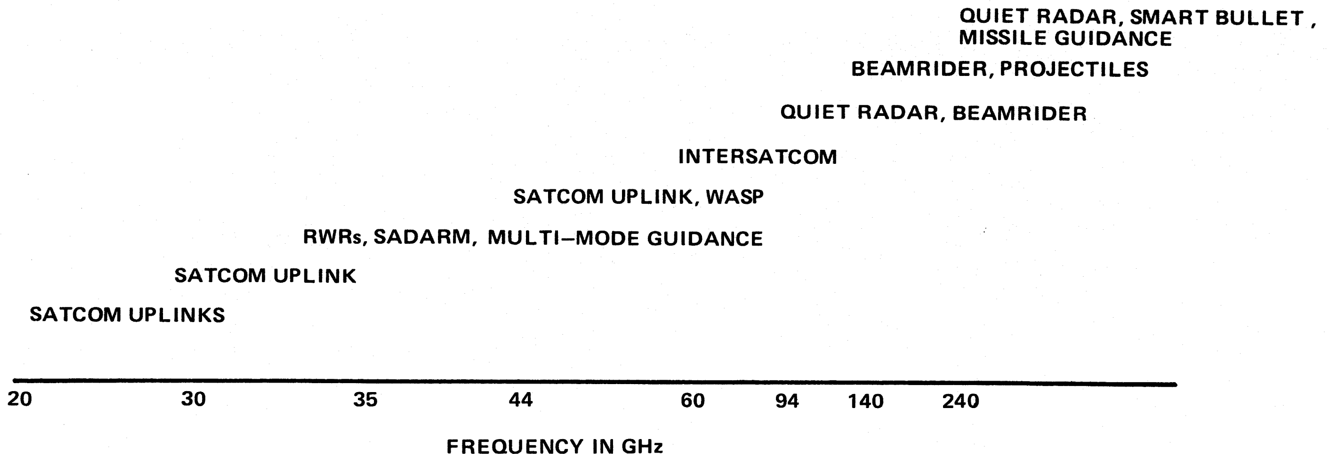

submicron size and made of compound semiconductors or silicon. DARPA's Advanced Indirect Fire System (AIFS) program is developing weapon-technology concepts designed to offset the numerically superior Soviet weapons systems that are expected to be encountered on the modern battlefield. Advanced lock-on-after-launch millimeter-wave and infrared seekers will be developed and demonstrated in both direct- and indirect-fire weapons. Applications will be felt in all three services' artillery, missiles, rockets, and terminally guided submunitions.

The program will address the problems of algorithm development, signal processing speed and capacity, countermeasures, counter-countermeasures, and data bases applicable to mm-wave and IR technologies. Also, the means for incorporating artificial intelligence and knowledge-based systems concepts will be investigated to determine possible performance improvements and the feasibilities of hardware implementation.

The Navy, too, is funding developments in EHF technology (defined by the USN budget as 26 to 140 GHz) to counter the known mm-wave threat and to provide for new communication, radar, and electronic warfare capabilities for smaller and more covert systems.

The Millimeter-Wave Technology project seeks to develop those EHF systems to reduce ECM susceptibility prevalent in the microwave spectrum and increase the effectiveness of surveillance and tracking systems via the greater bandwidths available, while reducing system sizes for aircraft, remotely piloted vehicles, and missile seeker applications.

According to the Navy, areas needing development are high-power, large-bandwidth gyrotrons; monolithic gallium-arsenide receivers; high-burnout diode mixers; protection devices such as field effect transistor switches; and control components—power combiners, circulators, and isolators. isolators.

The Army's efforts in the EHF region focus primarily on developing mm-wave radar guidance for munitions such as SADARM and the Multiple Launch Rocket System. Under the service's Terminally Guided Projectiles program, smart autonomous munitions will be developed for 155-mm artillery, the primary, most numerous weapon in both U.S. and NATO land forces. In FY-1984, the program is scheduled to test candidate IR and mm-wave seekers in helicopter captive flights. Performance will be measured in a variety of topological environments including the U.S., Europe, and the Middle East.

The Army will also begin exploratory development of 94-GHz monolithic transceivers (a receiver/transmitter on a chip) to fit 10-cm terminal guidance submunitions and missile guidance systems.

While this list of mm-wave programs is by no means comprehensive, it is apparent that more effort is needed. Contractors have declared their readiness to go into production of selective mm-wave systems and countermeasures, should they be required.

In developing any new weapons system, a time lag always exists between the threat's initial appearance and the fielding of its counter or counterpart. Yet, the DOD budget is so hard-pressed to procure the weapons systems considered as necessary, even in these lucrative times, that by virtue of diminishing returns on the purchase of hardware, it fills the gaps with obsolete weapons, perpetuating inadequate technologies. At present, it does not appear that this situation will change significantly in the near future. ■

Silicon Bipolar Transistors and Integrated Circuits Continue to Grow

The performance and cost characteristics of the silicon bipolar transistor have established it as the premier microwave device for several different oscillator and small-signal and power amplifier applications.

By Dr. Craig P. Snapp, Avantek, Inc.

The silicon bipolar transistor is now established as the optimum microwave component for a wide variety of small-signal and power amplifier applications up to 6 GHz and for oscillator applications up to 18 GHz. Major advances in process technology have resulted in significant reductions in the cost and improvements in the uniformity of discrete silicon transistors, and have enabled practical monolithic microwave integrated circuits (MMICs) and high-speed digital ICs to become a commercial reality for application at frequencies above 1 GHz. This paper presents a summary overview of the design, general characteristics, and performance of commercial microwave transistors and gives an update on the status of practical silicon monolithic ICs usable at microwave frequencies.

Silicon bipolar process technology has continued to evolve since the first discrete transistors with usable microwave performance became commercially available in the early 1970s. Modern silicon bipolar transistors have been established as the most reliable, cost effective, and easy-to-use component for many important microwave system applications.

Some of the applications that can be successfully addressed by discrete bipolar transistors are represented by the block diagrams shown in Figure 1 of a 3.7–4.2 GHz low-noise TVRO amplifier, a 4 W at 1.7–2.3 GHz linear-power telecommunications amplifier, a 50 W at 900 MHz, CW, cellular radio amplifier and a 2 kW at 1100 MHz, low duty factor, Class-C distance-measuring-equipment (DME) avionics amplifier. Important applications in addition to amplification include wideband and fixed-frequency signal generation at frequencies up to 18 GHz, high-speed current switching, and active mixing. It is now also becoming possible to address a variety of microwave, RF, IF, and LO applications from 100 kHz to over 10 GHz using analog and high-speed digital monolithic ICs fabricated with 10-GHz-F_t bipolar IC processes.

The microwave engineer faced with an appropriate design project can use the overview provided by this article and the referenced papers to obtain a general feeling for the capabilities of silicon bipolar technology before referring to vendor data sheets for guaranteed performance specifications and detailed design information.

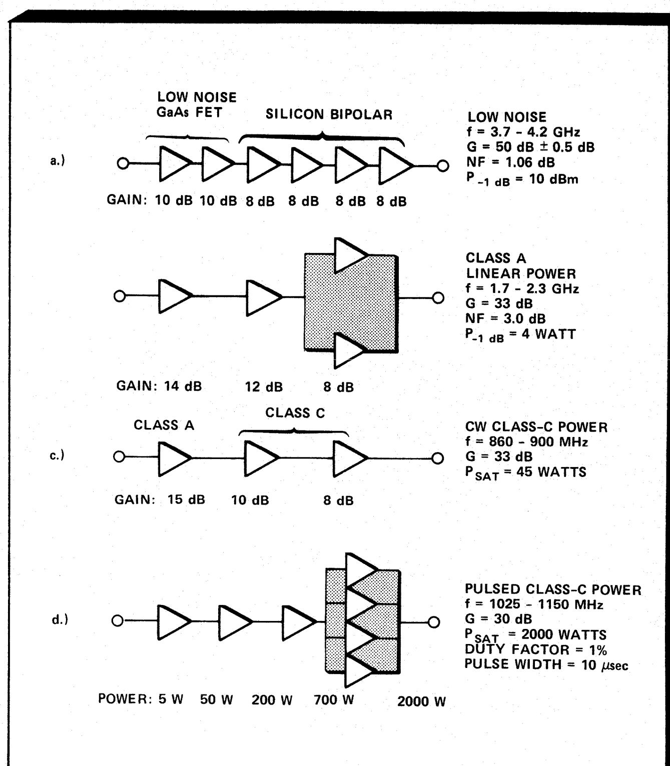

1. Amplifier block diagrams illustrate the wide range of applications that can be succesfully addressed by silicon bipolar transistors.

Transistor Design and Structure

The basic requirements for designing a high-gain, low-noise or power microwave bipolar transistor are well known. The superposition of a small-signal T equivalent circuit over the acutal physical structure of an interdigitated bipolar transistor is shown in Figure 2, which reveals the physical location of the parasitic capacitances and resistances that limit performance. Increases in microwave performance have continued to occur in part through the reduction of these parasitics by scaling of critical lateral geometries to submicron dimensions.

The fundamental time constants that are the ultimate limitation on performance are fixed by the bias conditions and the impurity profile from the surface of the emitter to the collector contact. These time constants determine the frequency (F_t) where the current gain becomes unity. F_{max}, defined as the extrapolated frequency where the maximum available gain (MAG) equals unity, is limited by F_t and

Dr. Craig P. Snapp is manager of Silicon R&D for the Semiconductor Division of Avantek, Inc., Santa Clara, Calif.

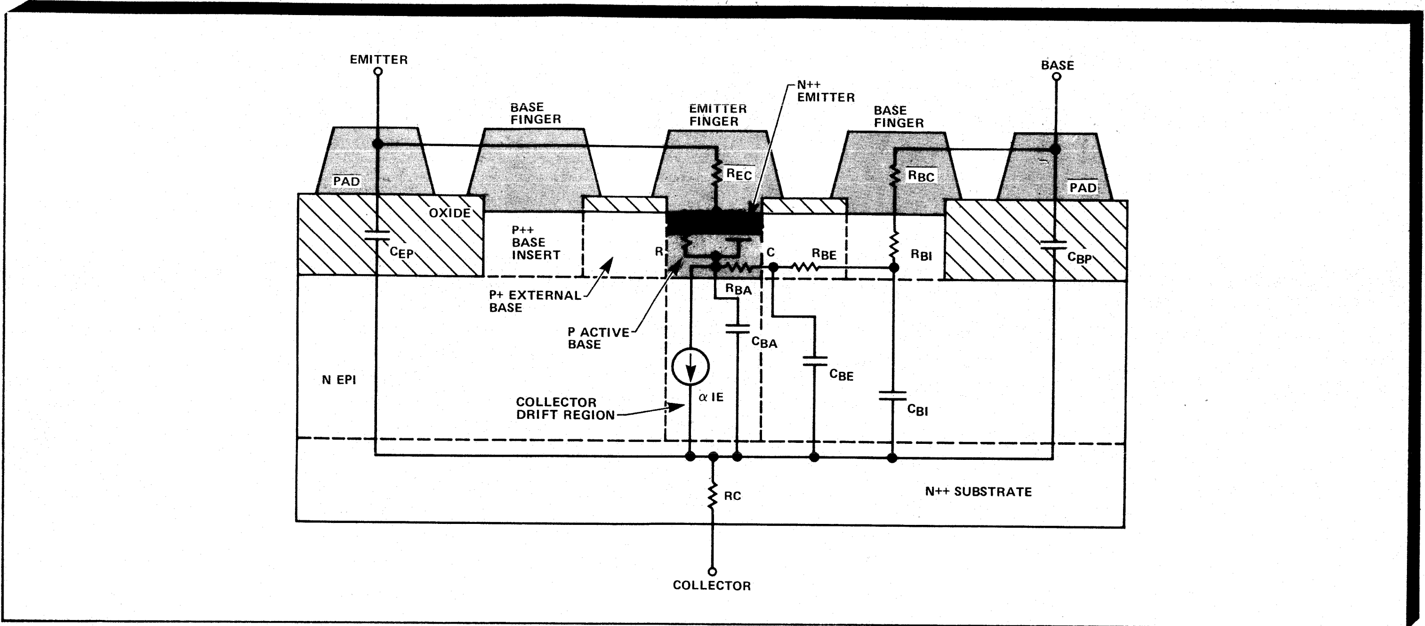

2. Superposition of a small-signal T equivalent circuit over the actual physical structure of an interdigitated bipolar transistor.

parasitics. It can be well approximated by:

$$F_{max} = \sqrt{\frac{F_t}{8\pi R_b C_{cb}}}$$

where R_b is the total base resistance and C_{cb} is the total collector-base capacitance.

Interdigitated emitter structures have been established as a particularly effective design for a wide variety of applications. The performance, design details, and major equivalent-circuit element values of transistors optimized for micropower, low-noise, linear-power, and class-C power are summarized in Tables I, II and III.

The SEM photographs shown in Figure 3 are of actual silicon bipolar transistor chips designed for low-noise, linear-power and class B/C power applications. These interdigitated-structure transistors correspond to types Q3, Q4 and Q5 in the above tables.

The Smith chart shown in Figure 4 of small-signal common-emitter S_{11} and S_{22} versus frequency for Q1, Q2, Q3, Q4 and Q5 transistor chips illustrates the wide range of characteristics that result when bipolar transistors are optimized for different applications. The common-emitter S_{21} gain at 1 GHz versus current of these transistors are shown in Figure 5. The optimum bias current for minimum noise amplification is about 35 percent of the current that results in maximum S_{21} gain. The optimum bias for linear-

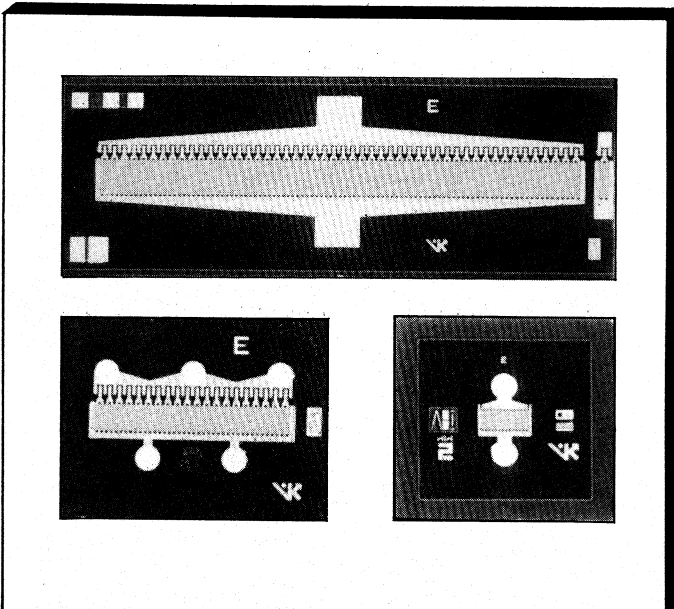

3. SEM photographs of silicon bipolar transistor chips designed for low-noise, linear-power and class B or C power applications.

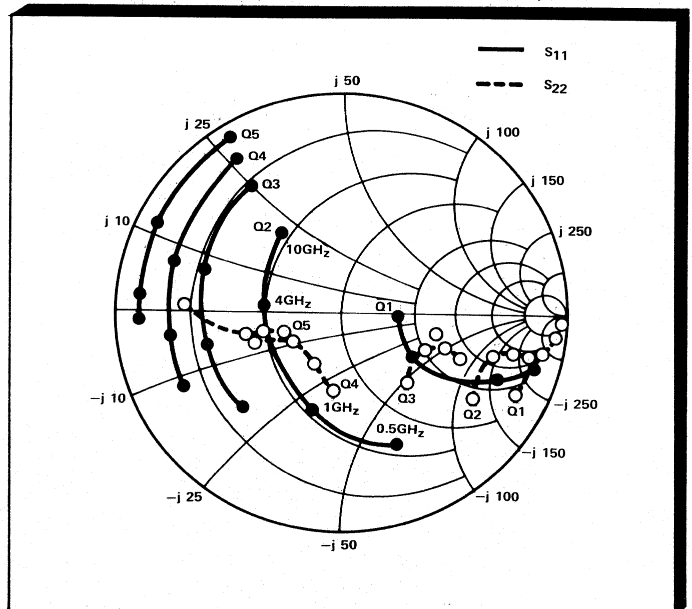

4. Smith chart showing common-emitter S_{11} and S_{22} versus frequency for interdigitated transistor types Q1, Q2, Q3, Q4 and Q5.

TABLE I
Performance Summary of High-Performance Interdigitated Transistors

Transistor Type	Power P W	Gain G_p dB	Eff ηPA %	Min. NF dB	50Ω NF dB	Test G_{nf} dB	F GHz	F_{max} GHz
Q1 micro-power	—	—	—	2.2	5.0	10	2	11
Q2 low-noise	—	—	—	1.8	2.0	12	2	18
Q3 low-noise	—	—	—	1.6	1.7	15	2	21
Q4 linear-power	1	13	40	4.5	6.5	11	2	11
Q5 1 cell class-C	5	11	60	—	—	—	1	7
Q6 12 cell class-C	50	9	50	—	—	—	1	6

TABLE II
Performance Summary of High-Performance Interdigitated Transistors

Transistor Type	Ne	Pe μm	Le μm	Bias V	Bias mA	Die Size mils	θ_{jc} °C/W	Max. ΔT °C	Package
Q1 micro-power	1	4	25	3	2	12 × 12	600	4	70 mil alumina
Q2 low-noise	5	4	25	8	8	12 × 12	400	25	70 mil alumina
Q3 low-noise	14	4	25	8	25	12 × 12	300	60	70 mil alumina
Q4 linear-power	40	6	30	20	125	12 × 15	40	100	200 mil BeO
Q5 1 cell class-C	100	8	50	28	300	14 × 38	9	30	500 mil BeO with internal matching
Q6 12 cell class-C	1200	8	50	28	3600	38 × 168	1.2	60	

Where Ne, Pe, and Le are the number of emitters, the emitter-to-emitter pitch and emitter length respectively.

TABLE III
Key Small-Signal Equivalent Circuit Element Values for High-Performance Interdigitated Transistors

Transistor Type	R_{bal} Ohms	R_e Ohms	C_{te} pF	R_b Ohms	C_{cb} pF	T_b ps	T_d ps	F_t GHz
Q1 micro-power	0	13.3	0.20	85.0	.043	6	7	9.8
Q2 low-noise	0	3.5	1.00	17.0	.081	6	7	9.3
Q3 low-noise	0	1.2	2.70	6.0	.165	6	7	9.0
Q4 linear-power	2.0	0.28	13.3	2.8	.520	7	11	6.8
Q5 1 cell class-C	1.0	0.14	65.0	1.0	2.30	8	26	2.9
Q6 10 cell class-C	0 1	0.012	780.0	0.1	28.0	8	26	2.9

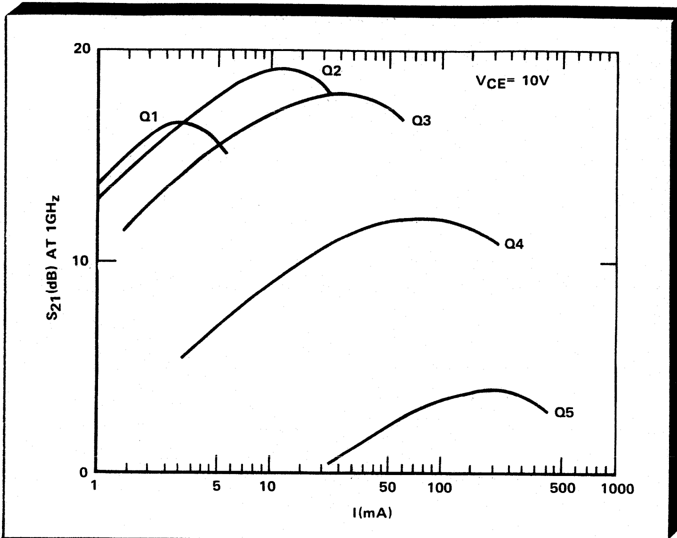

5. Common-emitter S_{21} gain at 1 GHz versus current of transistor Q1, Q2, Q3, Q4 and Q5.

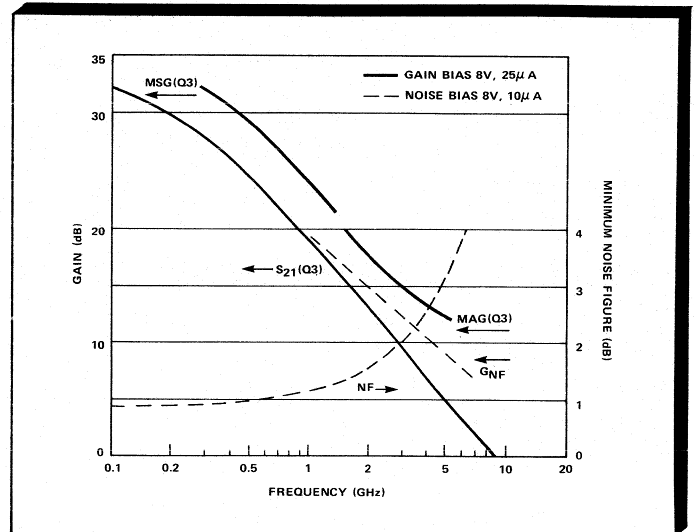

6. Common-emitter S_{21} gain, maximum available gain (MAG), maximum stable gain (MSG), minimum noise figure, and associated gain performance versus frequency of the highest performance commercial low-noise bipolar transistors.

power amplification is at a current where the S_{21} gain is about 0.5 dB less than the peak value.

Low-Noise And High Gain Transistors

Transistors designed for low noise and high gain generally have submicrometer emitter widths and a very small pitch from one emitter strip to the next.[6] The common-emitter S_{21} gain, maximum available gain (MAG) and maximum stable gain (MSG) versus frequency of low-noise transistor chip type Q3 biased at 8 Volts, 25 mA are shown in Figure 6. The high transconductance of bipolar transistors leads to very high S_{21} gains below 4 GHz and makes them ideal for broadband feedback amplifiers.

The noise figure and associated gain performance of the highest performance commercial low-noise bipolar transistors indicates that they should be considered for low-noise front-end and gain stages in amplifiers up to 2 GHz and for low-cost gain stages in low-noise amplifiers with GaAs FET front ends up to 5 GHz. A detailed listing of the small-signal S parameters of a representative transistor designed for low-noise and high-gain amplification is given in Table IV.

The constant noise figure and gain versus source impedance contours at 2 GHz and source reflection coefficient (Γ_0) versus frequency for minimum noise of packaged low-noise transistor type Q3 biased at 8 Volts, 10 mA are shown in Figure 7. The minimum noise figure and maximum available gain (MAG) at 2 GHz were 1.7 and 18 dB, respectively. The design of this transistor resulted in minimum noise figure being achieved with a 50-Ohm input at 1 GHz.

Class A Linear And Class B/C Power Transistors

Well-designed microwave bipolar transistors have been established as reliable and efficient components for CW and pulsed power amplification. Bipolar transistors designed for power amplification have large emitter areas distributed in a multicell configuration, require epitaxial layer specifications that result in high breakdown voltages, and have emitter ballasting resistors to prevent hot spots due to current hogging. Significant attention must be payed to packaging and die-attach uniformity in order to obtain the low thermal

TABLE IV
Common-Emitter S Parameters of Low-Noise Transistor Chip (Q3) Biased at 8 Volts, 10 mA. Emitter and Base Bonding Wire Inductances were 0.15 and 0.3 nH, Respectively.

Freq. GHz	S_{11}		S_{21}		S_{12}		S_{22}	
	mag.	ang.	dB	ang.	dB	ang.	mag.	ang.
0.1	.59	- 55	32	155	−42	70	.90	−15
0.5	.62	−140	25	110	−35	48	.57	−22
1.0	.63	−165	19	95	−32	55	.49	−18
2.0	.65	180	13	80	−28	66	.46	−17
4.0	.65	160	7	65	−22	72	.46	−21
6.0	.67	150	4	50	−19	73	.46	−29
10.0	.72	125	0	25	−15	70	.47	−48

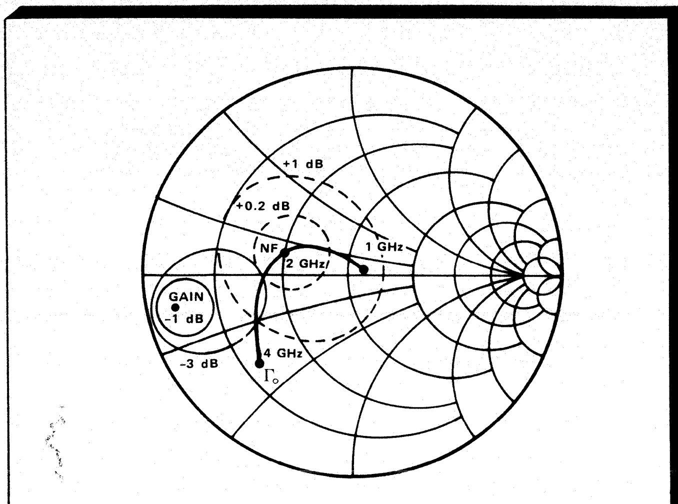

7. Constant noise figure and gain versus source impedance contours at 2 GHz and source reflection coefficient (Γ_0) versus frequency for minimum noise of packaged low-noise transistor type Q3 biased at 8 Volts, 10 mA.

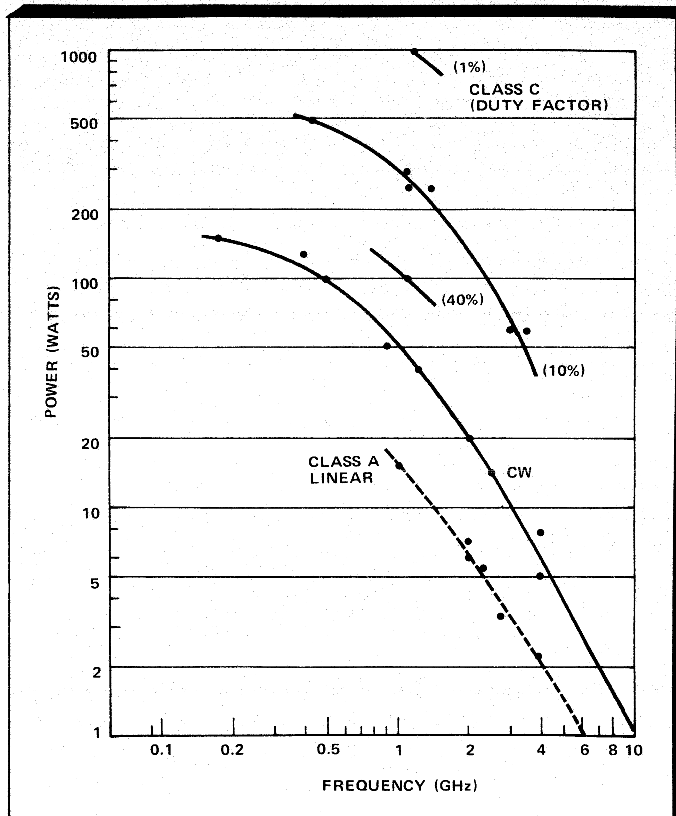

8. Plot of the performance specifications of the highest performance commercial common-emitter Class A and common-base Class C power bipolar transistors versus frequency.

resistance required for reliable operation. Large power transistors also require input LCL matching and in some cases output matching inside the packages in order to increase the chip impedances to practical levels.

The current-controlled nature of bipolar transistors and their very uniform exponential threshold characteristic allows them to be used effectively in large-signal class B or C modes as well as the linear class A bias configuration. The maximum CW power that can be obtained from transistors designed for class C operation is about three times the P_{-1dB} that can be easily obtained from higher gain linear power transistors. Practical power-added efficiencies as high as 60 percent can be achieved in class C operation compared to only 40 percent in class A operation. The Class C mode is also attractive for pulsed power applications since greater than an order of magnitude more peak power can be obtained from transistors designed for low duty-factor operation.

The small-signal common-emitter S parameters of a representative high-performance linear-power transistor capable of delivering 1 W at the 1-dB gain compression point are listed in Table V.

The plot of the performance specifications of the highest performance commercial common-emitter Class A and common-base Class C power bipolar transistors versus frequency shown in Figure 8 indicates that their use for practical power applications extends to frequencies as high as 5 GHz.

Oscillator Transistors

Bipolar transistors are ideal for fixed-frequency or wideband oscillator applications. They have inherently low 1/f noise at low frequencies compared to GaAs FETs, which leads to low phase noise near the carrier when used as

TABLE V
Common-Emitter S Parameters of 1 W Linear-Power Transistor Chip (Q4) Biased at 20 Volts, 125 mA. Emitter and Base Bonding Wire Inductances Were 0.1 and 0.2 nH, Respectively.

Freq. GHz	S_{11}		S_{21}		S_{12}		S_{22}	
	mag.	ang.	dB	ang.	dB	ang.	mag.	ang.
0.1	.57	- 89	28	148	-32	60	.87	- 37
0.5	.81	-155	19	104	-27	32	.39	- 97
1.0	.83	-171	13	90	-27	34	.28	-122
2.0	.84	176	8	77	-25	45	.22	-140
4.0	.84	163	2	59	-21	55	.26	-147
6.0	.84	157	-1	45	-18	55	.29	-150

oscillators.[14] They can be easily tuned over more than two octaves in YIG oscillators since they can have a very wide negative resistance bandwidth in the common-base configuration.[15]

Packaged common-base or common-collector transistors can be used for narrowband signal generation to over 10 GHz. The common-collector configuration is attractive for very stable cavity-tuned oscillators since the thermal resistance of chips mounted in common-collector packages is significantly lower than chips mounted in common-base packages. Unpackaged chips can be used for fundamental signal generation to over 13 GHz in YIG-tuned or varactor-tuned circuits.[16] The use of doubling-circuit techniques has enabled tuning from 6.9 to 19.2 GHz using hyperabrupt varactors.[17]

The oscillator power performance versus frequency of packaged silicon bipolar transistors and YIG and varactor tuned oscillators is shown in Figure 9. The small-signal S parameters of high F_{max} transistor Q3 are listed in Tables VI and VII for the unpackaged common-base and common-collector configurations, respectively.

Reliability

The increasing complexity of microwave systems and the need to reduce system lifecycle cost requires that microwave circuit designers carefully select components and choose

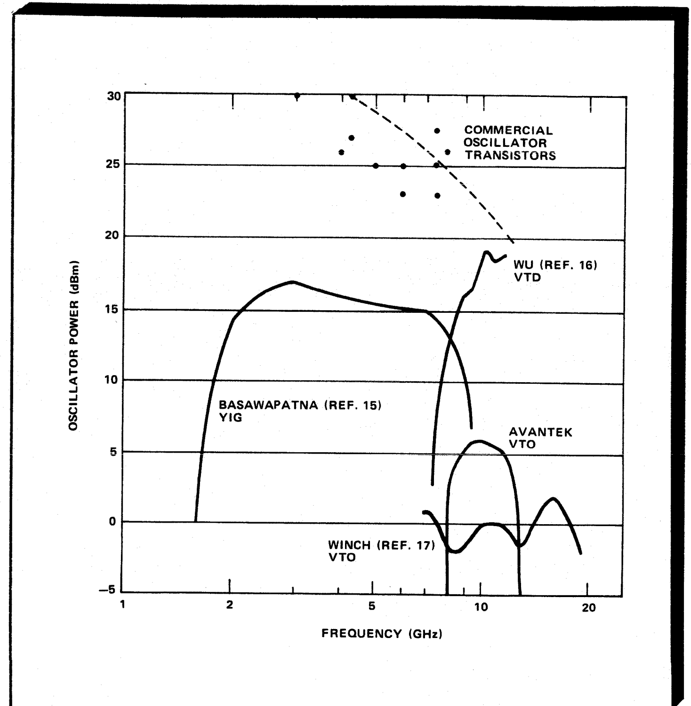

9. Oscillator power performance versus frequency of silicon bipolar transistors.

TABLE VI
Common-base S Parameters of Transistor Chip (Q3) Biased at 10 Volts, 25 mA With 0.3 nH of Base and Emitter Bonding Wire Inductance

Freq. GHz	S_{11} mag.	S_{11} ang.	S_{21} dB	S_{21} ang.	S_{12} dB	S_{12} ang.	S_{22} mag.	S_{22} ang.
1.0	.95	174	5.7	- 12	-47	144	1.00	- 6
2.0	.97	168	5.7	- 25	-35	153	1.02	- 12
4.0	1.08	153	5.8	- 53	-23	147	1.07	- 27
6.0	1.22	133	5.6	- 86	-16	132	1.10	- 46
10.0	1.20	90	2.8	-165	- 9	92	.91	- 89
12.0	1.06	74	1.0	160	- 7.3	76	.74	-105
14.0	.93	63	-0.4	130	- 6.6	65	.62	-117
16.0	.83	56	-1.2	105	- 6	57	.54	-127

TABLE VII
Common-Collector S Parameters of Transistor Chip (Q3) Biased at 10 Volts, 25 mA With 0.2 nH of Emitter and Base Wire Inductance

Freq. GHz	S_{11} mag.	S_{11} ang.	S_{21} dB	S_{21} ang.	S_{12} dB	S_{12} ang.	S_{22} mag.	S_{22} ang.
1.0	.96	- 18	5.5	-11	-14	70	.90	163
2.0	.91	- 35	5.0	-21	- 8	59	.85	147
4.0	.77	- 65	3.5	-37	- 4	37	.72	120
6.0	.64	- 89	2.0	-48	- 2	20	.59	99
10.0	.48	-128	-0.6	-60	- 0.7	- 6	.41	67
12.0	.44	-144	-1.6	-64	- 0.5	-16	.34	54

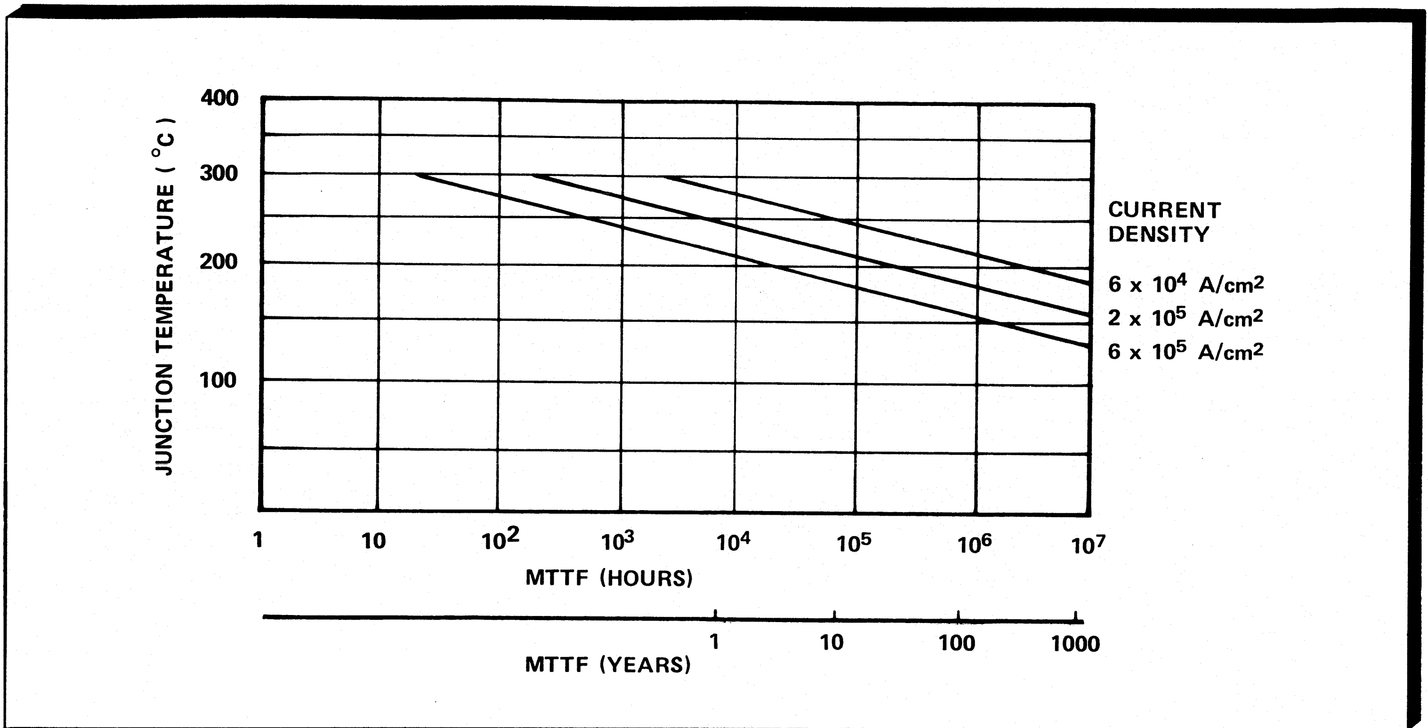

10. Junction temperature versus median time to failure (MTTF) with emitter metal current density as a parameter.

operating conditions that ensure reliable operation. Achieving the ultimate reliability with silicon bipolar transistors and ICs requires that they be well designed, fabricated and assembled with excellent workmanship, and operated at conditions that ensure an adequate median time to failure (MTTF). Bias and large-signal operating conditions must be chosen to avoid junction breakdown and the contact metal migration that is usually the ultimate limitation on reliability.

The MTTF due to current density induced metal migration in contact fingers can be approximated by:

$$\mathrm{MTTF} = \frac{CA\exp(\phi/kT)}{J^2}$$

where C is a constant dependent on the properties of the conductor, A is the cross-section area of the conductor, ϕ is the activation energy of migration, T is the conductor temperature and J is the current density. The activation energy for gold metal migration is between 1.5 and 1.8 eV.

A typical plot of junction temperature versus MTTF with emitter metal current density as a parameter is shown in Figure 10 for a modern Ti/Pt/Au or TiW/Au metal system. Knowledge of the relationship between MTTF and junction temperature or current density can be used along with detailed vendor reliability data to make the optimum tradeoff between reliability and operating conditions for specific applications.

Monolithic Microwave And High-Speed Digital ICs

Ten-GHz-F_t silicon bipolar MMICs are becoming commercially available that should be cost effective for a number of microwave, RF, IF, and LO applications from 100 kHz to 6 GHz for amplifiers and to over 10 GHz for oscillators. In addition to lower cost, they will enable significant reductions

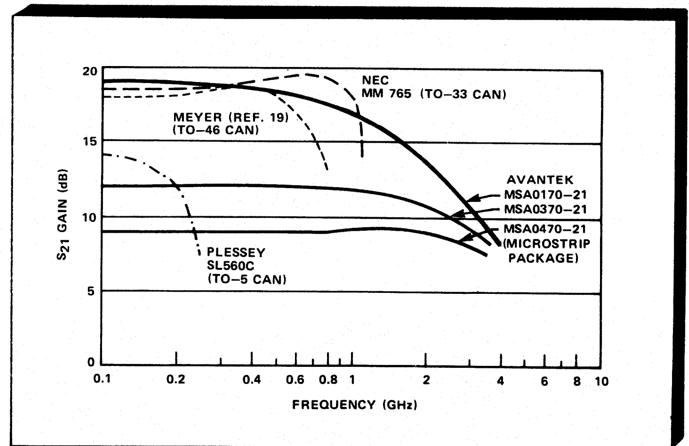

11. S_{21} gain versus frequency of cascadable (VSWR < 2:1) monolithic silicon bipolar IC amplifiers that are usable from VHF to microwave frequencies.

in component size and improvements in uniformity, ruggedness, reliability, and group delay when packaged in small microstrip packages or when used as building-block cells in hybrid MIC supercomponents.[18-23]

The S_{21} gain versus frequency performance of cascadable (VSWR 2:1) monolithic silicon bipolar IC amplifiers that are usable from VHF to microwave frequencies is shown in Figure 11. Commercial products are available in both microstrip packages and TO cans. Microwave circuit designers, who will continue to use discrete bipolar and GaAs FETs in miniature hybrid MICs for the highest performance applications, can now add the silicon bipolar MMIC amplifier to their stable of practical semiconductor components.

As with MMICs, silicon bipolar technology should not be ruled out for high-speed digital applications. Recent

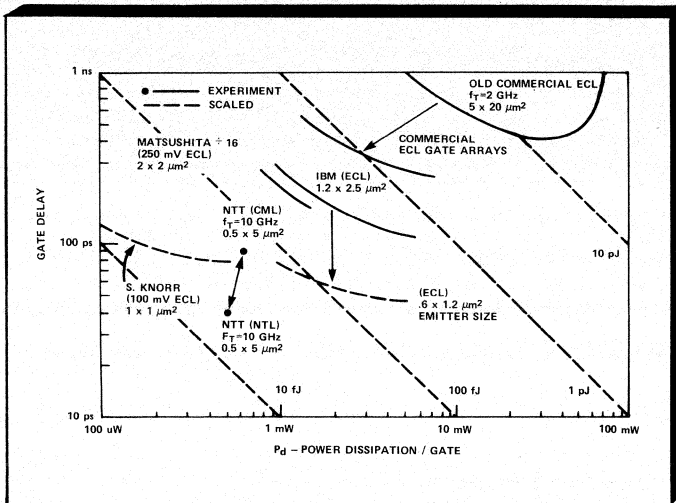

12. Propagation delay versus power dissipation per gate illustrates the evolution of silicon ECL/CML logic to lower power and higher speed. Practical high-speed prescalers have been developed that can operate at clock frequencies up to 5.5 GHz.

results[24-28] demonstrate that the gate speed and power performance of supposedly "mature" ECL/CML has been undergoing significant improvements with reductions of emitter area and advances in isolation technology. The plot of propagation delay versus power dissipation per gate shown in Figure 12 illustrates the evolution of silicon ECL/CML logic to gate delays well below 100 psec. at gate powers less than 1 mW. Practical ECL/CML dividers have been developed that can operate with good sensitivity at clock frequencies up to 5.5 GHz.[29] These results are comparable to the fastest reported GaAs dividers. High-speed commercial ECL prescalers such as the AEG-Telefunken U622BS can operate up to 2.3 GHz with low power and jitter. Scaled ECL/CML[30,31] is also a serious candidate for LSI-complexity digital circuits requiring clock frequencies above 1 GHz. ■

References

1. H.F. Cooke, "Microwave Transistors: Theory and Design," *Proc. IEEE*, Vol. 59, pp. 1163-1181, August 1971.
2. J.S. Lamming, "Microwave Transistors," in *Microwave Devices*, ed. by M.J. Howes and D.V. Morgan, John Wiley and Sons, New York, NY, 1976.
3. C.P. Snapp, "Bipolars Quietly Dominate," *Microwave Systems News*, pp. 45-67, November 1979.
4. *Microwave Transistors*, ed. by E.D. Graham and C.W. Gwyn, Artech House, Dedham, MA, 1975.
5. *Low-Noise Microwave Transistors and Amplifiers*, ed. by H. Fukui, IEEE Press and John Wiley and Sons, New York, NY, 1981.
6. T.H. Hsu and C.P. Snapp, "Low Noise Microwave Bipolar Transistor with Sub-Half-Micrometer Emitter Width," *IEEE Trans. on Electron Devices*, Vol. ED-25, pp. 723-730, June 1978.
7. J.T.C. Chen and C.P. Snapp, "Bipolar Microwave Linear Power Transistor Design," *IEEE Trans. on Microwave Theory and Techniques*, Vol. MTT-27, pp. 423-430, May 1979.
8. G.W. Schreyer, "Circuit Device Interface Techniques for a 5 Watt, 5 GHz Bipolar Microwave Power Transistor," *IEEE Int. Solid-State Circuits Conf. Digest*, pp. 170-171, February 1977.
9. L.B. Max, "Balanced Transistors: A New Option for RF Design," *Microwaves*, pp. 42-46, June 1977.
10. H.T. Yuan, et al, "A 2-Watt X-Band Silicon Power Transistor," *IEEE Trans. on Electron Devices*, Vol. ED-25, pp. 731-736, June 1978.
11. R. Allison, "Silicon Bipolar Microwave Power Transistors," *IEEE Trans. on Microwave Theory and Techniques*, Vol. MTT-27, pp. 415-422, May 1979.
12. R. Basset and M.D. McCombs, "Production Bipolars Edge Out FETs at 4 GHz," *Microwaves*, pp. 43-49, February 1981.
13. W.E. Poole, "S-Band Transistors for Radar Applications," *Microwave Journal*, pp. 85-90, March 1983.
14. J.H. Lepoff and P. Ramratan, "FET vs. Bipolar: Which Oscillator is Quieter?" *Microwaves*, pp. 82-83, November 1980.
15. G.R. Basawapatna and R.B. Stancliff, "A Unified Approach to the Design of Wide-Band Microwave Solid-State Oscillators," *IEEE Trans. On Microwave Theory and Technique*, Vol. MTT-27, pp. 379-385, May 1979.
16. Y.S. Wu, et al, "X-Band Varactor-Tuned Bipolar Transistor oscillator," *IEEE Int. Solid-State Circuits Conf. Digest*, pp. 162-163, February 1979.
17. R.G. Winch, "Wide-Band Varactor-Tuned Oscillators," *IEEE Journal of Solid-State Circuits*, Vol. SC-17, pp. 1214-1219. December 1982.
18. C.P. Snapp, "Advanced Silicon Bipolar Technology Yields Usable Monolithic RF and Microwave ICs," *Microwave Journal*, August 1983.
19. J. Addis, "Design and Process Innovation Converge in 1 GHz Oscilloscope," *Electronics*, pp. 131-138, June 21, 1979.
20. R.G. Meyer and R.A. Blauschild, "A 4-Terminal Wide-Band Monolithic Amplifier," *IEEE Journal of Solid State Circuits*, SC-16, pp. 634-638, December 1981.
21. J.F. Kukielka and C.P. Snapp, "Wideband Monolithic Cascadable Feedback Amplifiers Using Silicon Bipolar Technology," *IEEE Microwave and Millimeter-Wave Monolithic Circuits Sym.*, June 1982.
22. C.P. Snapp, et al, "Practical Silicon MMICs Challenge Hybrids," *Microwaves & RF*, pp. 93-99, November 1982.
23. V. Biancomano, "The Message is Clear: RF Chips Mix Density, High Performance," *Electronic Design*, pp. 107-114, April 14, 1983.
24. J.B. Hughes, et al, "A Versatile ECL Multiplexer IC for the Gbit/s Range," *IEEE Journal of Solid State Circuits*, SC-14, pp. 812-817, October 1979.
25. A. Akazawa, et al, "Low Power 1 GHz Frequency Synthesizer LSI's," *IEEE Journal of Solid State Circuits*, SC-18, pp. 115-121, February 1983.
26. T. Takemoto, et al, "A Vertically Isolated Self-Aligned Transistor — VIST," *IEEE Trans. on Electron Devices*, Vol. ED-29, pp. 1761-1765, November 1982.
27. T. Sakai, et al, "A 3 nsec 1-kbit RAM Using Super Self-Aligned Process Technology," *IEEE Journal of Solid State Circuits*, SC-16, pp. 424-429, October 1981.
28. K. Ooami, et al, "A 3.5 ns 4 Kb ECL RAM," *IEEE Int. Solid-State Circuits Conf. Digest*, pp. 114-115, February 1983.
29. T. Sakai, et al, "Gigabit Logic Bipolar Technology: Advanced Super Self-Aligned Process Technology," *Electronics Letters*, Vol. 19, pp. 283-284, April 14, 1983.
30. D.D. Tang, et al, "1.25 Micrometer Deep-Groove-Isolated ECL Circuits," *IEEE Int. Solid-State Circuits Conf. Digest*, pp. 242-243, February 1982.
31. S.G. Knorr, "The Potential of Bipolar Devices in LSI Gigabit Logic," *IEEE Circuits and Systems Magazine*, Vol. 3, pp. 2-6, January 1981.

Bipolar Matrix

Significant Applications Niche Occupied by Bipolar Transistors

This first edition of *The Microwave System Designer's Handbook* presents the industry's most comprehensive bipolar transistor matrix to date. As was the case in 1982 when *Microwave Systems News* magazine put together its first GaAs FET Matrix (updated elsewhere in the *MSDH*), this project involved a massive investment of time and effort on the part of the *MSDH* editorial staff to obtain the most accurate, up-to-date information possible from the majority of foreign and domestic manufacturers working in this area.

For several applications in the small-signal and power amplifier areas, the silicon bipolar transistor has emerged as the most practical microwave component available. Beyond this, advances in manufacturing technology have reduced the cost and improved the reproducibility of many of these devices. The growing importance of bipolar transistors is also being felt as a result of the burgeoning mobile pager and cellular radio markets, where these devices are expected to make a significant impact.

The matrix of bipolar devices which follows is meant to be a practical tool to help the reader determine which products could best suit his particular needs and applications. It is—by no means—meant to be a user's only tool, however, as a final determination of device choice requires the careful examination and comparison of manufacturers' technical data sheets. It is hoped that this matrix will aid in that decision process by helping the user narrow down his choices to a more easily manageable number.

When using this matrix, please note that whenever a particular manufacturer's specifications have been received in a format that differs from that of the matrix, these differences have been noted in the same line as the manufacturer's name.

Because of the enormous amount of data received and processed from so many different sources in the production of this matrix, the publisher cannot assume any liability for any errors or omissions which may be present.

The device manufacturers listed in the bipolar transistor matrix may be contacted through marketing personnel at the addresses and telephone numbers listed below.

Acrian, Inc. .... (408) 996-8522
10060 Bubb Rd., Cupertino, CA 95014

Avantek, Inc. .... (408) 727-0700
3175 Bowers Ave., Santa Clara, CA 95051

Fujitsu Microelectronics, Inc. .... (408) 980-8585
Microwave and Optoelectronics Div.,
3080 Oakmead Village Dr., Santa Clara, CA 95051

Hewlett-Packard Co. .... (408) 263-7500
350 West Trimble Rd., San Jose, CA 95131

International Microwave Devices, Inc. .... (201) 231-1990
51 Chubb Wy., Somerville, NJ 08876

Microwave Semiconductor Corp. (MSC) .... (201) 469-3311
100 School House Rd., Somerset, NJ 08873

Motorola, Inc. .... (602) 244-3641
5005 East McDowell Rd., Phoenix, AZ 85008

NEC/California Eastern Laboratories, Inc. .... (408) 988-3500
3005 Democracy Wy., Santa Clara, CA 95050

Toshiba Corp. .... Tel: Tokyo 501-5411
1-6 Uchisawi Ai-Cho 1-Chome, Chiyoda-Ku, Tokyo, Japan

Internally Matched Pulsed Power Bipolar Transistors (Class C)

Part Number	Package Type or Chip	Package Configuration	Manufacturer's Remarks	Input or Input/Output Matched	V_{CC}	C_{CB} at V_{CC}	Designed Operating Frequency Range
ACRIAN							
DME150	—	Flange	—	Input/Output	50	N/A	1025-1150
DME250	—	Flange	—	Input/Output	50	N/A	1025-1150
DME375	—	Flange	—	Input	50	75pF	1025-1150
DME375A	—	Flange	—	Input/Output	50	N/A	1025-1150
DME500	—	Flange	—	Input/Output	50	N/A	1025-1150
TPR175	—	Flange	—	Input	50	30pF	1030-1090
TPR400	—	Flange	—	Input/Output	50	75pF	1030-1090
TPR400A	—	Flange	—	Input/Output	50	N/A	1030-1090
TPR500	—	Flange	—	Input/Output	50	N/A	1030-1090
TPR500A	—	Flange	—	Input/Output	50	N/A	1030-1090
UDR450	—	Flange	—	Input/Output	40	N/A	400-450
CDR150	—	Flange	—	Input	50	50pF	750-900
CDR400	—	Flange	—	Input/Output	50	N/A	750-900
LDR10SB	—	Flange	—	Input/Output	36	N/A	1200-1400
LDR40SB	—	Flange	—	Input/Output	36	N/A	1200-1400
LDR55LA	—	Flange	—	Input/Output	28	N/A	1200-1400
LDR100SB	—	Flange	—	Input/Output	36	N/A	1200-1400
LDR75LB	—	Flange	—	Input/Output	35	N/A	1200-1400
LDR125MC	—	Flange	—	Input/Output	41	N/A	1200-1400
0912-7	—	Flange	—	Input	50	10pF	900-1200
0912-25	—	Flange	—	Input	50	25pF	900-1200
TAN15	—	Flange	—	Input	50	12pF	960-1215
TAN75	—	Flange	—	Input/Output	50	N/A	960-1215
TAN150	—	Flange	—	Input/Output	50	N/A	960-1215
TAN150H	—	Flange	—	Input/Output	50	N/A	960-1215
TAN250A	—	Flange	—	Input/Output	50	N/A	960-1215
JTDA50	—	Flange	—	Input/Output	40	N/A	960-1215
JTDA100	—	Flange	—	Input/Output	40	N/A	960-1215
JTDA150	—	Flange	—	Input/Output	40	N/A	960-1215
JTDB25	—	Flange	—	Input/Output	36	N/A	960-1215
JTDB50	—	Flange	—	Input/Output	36	N/A	960-1215
JTDB75	—	Flange	—	Input/Output	36	N/A	960-1215
JTDB100	—	Flange	—	Input/Output	36	N/A	960-1215
DMEG70	—	Flange	—	Input/Output	50	N/A	960-1215
DMEG250	—	Flange	—	Input/Output	50	N/A	960-1215
DME2	—	Stud	—	Input	35	4pF	1025-1150
DME10	—	Pill	—	Input	50	7pF	1025-1150
DME40L	—	Flange	—	Input	28	20pF	1025-1150
DME75	—	Pill	—	Input	50	15pF	1025-1150
INTERNATIONAL MICROWAVE DEVICES							
3135-3	MF-4	.400 Herm Common Base	—	Input/Output	28V	—	3.1 to 3.5GHz
3135-6	MF-4	.400 Herm Common Base	—	Input/Output	28V	—	3.1 to 3.5GHz
3135-10	MF-3	.400 Herm Common Base	Under Development	Input/Output	28V	—	3.1 to 3.5GHz
3135-25	MF-3	.400 Herm Common Base	Under Development	Input/Output	28V	—	3.1 to 3.5GHz
2731-3	MF-4	.400 Herm Common Base	—	Input/Output	28V	—	2.7-3.1GHz
2731-6	MF-4	.400 Herm Common Base	—	Input/Output	28V	—	2.7-3.1GHz
2731-10	MF-3	.400 Herm Common Base	Under Development	Input/Output	28V	—	2.7-3.1GHz
2731-25	MF-3	.400 Herm Common Base	Under Development	Input/Output	28V	—	2.7-3.1GHz
MICROWAVE SEMICONDUCTOR							
AM0405-100	Hermetic	AMPAC™ C/S042	Geometry: Au Metal, Site Ballasted Overlay	In/Out Matched	28V	—	400-450MHz
AM0405-400	Hermetic	AMPAC™ C/S640	Geometry: Au Metal, Site Ballasted Overlay	In/Out Matched	40V	—	400-450MHz
AM1214-300	Hermetic	AMPAC™ C/S038	Geometry: Au Metal, Site Ballasted Overlay	In/Out Matched	50V	—	1235-1365MHz
AM1416-200	Hermetic	AMPAC™ C/S042	Geometry: Au Metal, Site Ballasted Overlay	In/Out Matched	50V	—	1400-1550MHz
AM81718-60	Hermetic	AMPAC™ C/S036	Geometry: Au Metal, Site Ballasted Overlay	In/Out Matched	35V	—	1700-1800MHz
AM82325-40	Hermetic	AMPAC™ C/S036	Geometry: Au Metal, Site Ballasted Overlay	In/Out Matched	40V	—	2300-2500MHz
AM82731-45	Hermetic	AMPAC™ C/S036	Geometry: Au Metal, Site Ballasted Overlay	In/Out Matched	40V	—	2700-3100MHz
AM82931-55	Hermetic	AMPAC™ C/S036	Geometry: Au Metal, Site Ballasted Overlay	In/Out Matched	42V	—	2900-3100MHz
AM83135-50	Hermetic	AMPAC™ C/S064	Geometry: Au Metal, Site Ballasted Overlay	In/Out Matched	42V	—	3100-3500MHz
—	—	—	—	—	—	—	—
MSC81600M	Hermetic	BIGPAC C/S038	Geometry: Au Metal, Site Ballasted Overlay	In/Out Match	50V	—	1090MHz
MSC81550M	Hermetic	BIGPAC C/S038	Geometry: Au Metal, Site Ballasted Overlay	In/Out Match	50V	—	1025-1150MHz
MOTOROLA							
MRF1002MA	—	Micro 280 Stud	—	Input	35	2.5	960-1215
MRF1002MB	—	Micro 280 Pill	—	Input	35	2.5	960-1215

		Center Design Frequency				Absolute Maximum Ratings						Price Quantity	
Peak P_{out}	Gain	Peak Collector Efficiency	Peak Power Added Efficiency	Duty Factor	Pulse Width	V_{CBO}	V_{CEO}	V_{EBO}	I_C	Pt.	Rth.	1-100	1000
150	7[8]	40	—	1	10	55	—	4	15	500	0.35	—	—
250	5[8]	40	—	1	10	55	—	4	20	850	0.2	—	—
375	7	40	—	1	10	55	—	4	30	1160	0.15	—	—
375	6[4]	40	—	1	10	55	—	4	30	1160	0.15	—	—
500	6	35	—	1	10	55	—	3[5]	40	1700	0.1	—	—
175	8[5]	40	—	1	10	55	—	3[5]	10	400	0.4	—	—
400	7[3]	40	—	1	10	55	—	4	30	1160	0.15	—	—
400	6[7]	40	—	1	10	55	—	4	30	1160	0.15	—	—
500	7[7]	40	—	1	10	55	—	3[5]	40	1700	0.1	—	—
500	5[2]	35	—	1	10	55	—	3[5]	40	1700	0.1	—	—
450	8	60	—	2	60	70	—	4	40	875	0.2	—	—
150	7	45	—	2	20	55	—	3.5	10	400	0.4	—	—
400	7	45	—	2	20	55	—	3.5	40	1700	0.1	—	—
10	7	40	—	1	10	50	—	3[5]	1	56	3.1	—	—
40	7	40	—	1	10	50	—	3[5]	3	140	1.25	—	—
55	6.6	40	—	10	1000	50	—	3[5]	10	175	1.0	—	—
100	7	40	—	1	10	50	—	3[5]	10	340	0.5	—	—
75	6.6	40	—	10	350	50	—	3[5]	8	225	0.78	—	—
125	7	40	—	10	50	50	—	3[5]	10	437	0.4	—	—
—	—	—	—	—	—	—	—	—	—	—	—	—	—
—	—	—	—	—	—	—	—	—	—	—	—	—	—
15	7.7	40	—	5	20	50	—	4	2	116	1.5	—	—
75	7.9	40	—	5	20	50	—	4	9	290	0.6	—	—
150	7.0	40	—	5	20	50	—	4	—	—	—	—	—
150	7.0	40	—	5	20	50	—	4	18	580	0.3	—	—
250	6.2	40	—	5	20	50	—	4	30	875	0.2	—	—
50	7.0	40	—	20	10	50	—	3.5	5	218	0.8	—	—
100	7.0	40	—	20	10	50	—	3.5	8	335	0.52	—	—
150	7.0	40	—	20	10	50	—	3.5	—	—	—	—	—
25	7.0	40	—	40	10	50	—	3[5]	5	97	1.8	—	—
50	7.0	40	—	40	10	50	—	3[5]	6.5	145	1.2	—	—
75	7.0	40	—	40	10	50	—	3.5	8	225	0.78	—	—
100	7.0	40	—	40	10	50	—	3[5]	10	233	0.75	—	—
70	6[7]	35	—	5	10	55	—	4	15	250	0.7	—	—
250	6[2]	35	—	5	10	55	—	4	30	875	0.2	—	—
1.5	8[7]	35	—	1	10	55	—	3[5]	0.25	17.5	10	—	—
10	8[2]	35	—	1	10	55	—	3[5]	1	58	3	—	—
40	—	—	—	1	10	55	—	3[5]	—	—	—	—	—
75	7[6]	35	—	1	10	55	—	3[5]	7	270	0.65	—	—
3.0W	6dB	30%	—	20%	250µsec	40V	—	3.0V	—	—	12° C/W	—	—
6.0W	6dB	30%	—	10%	100µsec	45V	—	3.0V	—	—	9° C/W	—	—
10	5dB	30%	—	10%	100µsec	45V	—	3.0V	—	—	5.5° C/W	—	—
25	4.5dB	30%	—	10%	100µsec	45V	—	3.0V	—	—	3° C/W	—	—
3	6dB	30%	—	20%	250µsec	40V	—	3.0V	—	—	12° C/W	—	—
6	6dB	30%	—	10%	100µsec	45V	—	3.0V	—	—	9° C/W	—	—
10	5.5dB	30%	—	10%	100µsec	45V	—	3.0V	—	—	5.5° C/W	—	—
25	5dB	30%	—	10%	100µsec	45V	—	3.0V	—	—	3° C/W	—	—
100W	8.0dB	60%	—	10%	1000µsec	60V	—	3.5V	—	—	1.0° C/W	—	—
400W	7.5dB	55%	—	2%	70µsec	65V	—	3.5V	—	—	0.08° C/W	—	—
270W	6.3dB	40%	—	4%	50µsec	65V	—	3.5V	—	—	0.12° C/W	—	—
180W	6.5dB	40%	—	10%	10µsec	65V	—	3.5V	—	—	0.11° C/W	—	—
60W	6.6dB	40%	—	10%	10µsec	35V	—	3.5V	—	—	0.25° C/W	—	—
40W	6.0dB	35%	—	20%	10µsec	50V	—	3.5V	—	—	0.9° C/W	—	—
45W	5.7dB	30%	—	10%	100µsec	50V	—	3.5V	—	—	1.2° C/W	—	—
55W	5.9dB	30%	—	10%	50µsec	50V	—	3.5V	—	—	0.5° C/W	—	—
50W	5.2dB	30%	—	10%	10µsec	50V	—	3.5V	—	—	0.4° C/W	—	—
—	—	—	—	—	—	—	—	—	—	—	—	—	—
600W	6.0dB	35%	—	1%	10µsec	65V	—	3.5V	—	—	0.09° C/W	—	—
550W	5.6dB	35%	—	1%	10µsec	65V	—	3.5V	—	—	0.09° C/W	—	—
2.0	12.0	45	44	1.0%	10µsec	50V	20	3.5V	.25	7.0	25	32.43	—
2.0	12.0	45	44	1.0%	10µsec	50V	20	3.5V	.25	7.0	25	31.28	—

Internally Matched Pulsed Power Bipolar Transistors (Class C)

Part Number	Package Type or Chip	Package Configuration	Manufacturer's Remarks	Input or Input/Output Matched	V_{CC}	C_{CB} at V_{CC}	Designed Operating Frequency Range
MRF1004MA	—	Micro 280 Stud	—	Input	35	3.3	960-1215
MRF1004MB	—	Micro 280 Pill	—	Input	35	3.3	960-1215
MRF1008MA	—	Micro 280 Stud	—	Input	35	3.5	960-1215
MRF1008MB	—	Micro 280 Pill	—	Input	35	3.5	960-1215
MRF1015MA	—	Micro 280 Stud	—	Input	50	5.0	960-1215
MRF1015MB	—	Micro 280 Pill	—	Input	50	5.0	960-1215
MRF1035MA	—	Micro 280 Stud	—	Input	50	10	960-1215
MRF1035MB	—	Micro 280 Pill	—	Input	50	10	960-1215
MRF1090MA	—	Micro 280 Stud	—	Input	50	12	960-1215
MRF1090MB	—	Micro 280 Pill	—	Input	50	12	960-1215
MRF1150M	—	Micro 400 Flange	—	Input/Output	50	—	1020-1150
MRF1150MA	—	Micro 280 Stud	—	Input	50	25	960-1215
MRF1150MB	—	Micro 280 Pill	—	Input	50	25	960-1215
MRF1250M	—	Micro 400 Flange	—	Input/Output	50	—	1020-1150
MRF1325M	—	Micro 400 Flange	—	Input/Output	50	—	1020-1150
NEC CORPORATION							
NEM1700 Series							
NEM1704B-20	94	Ceramic Flange-Hermetic	Internally Matched	—	20	—	1.5-1.7GHz
NEM1706B-20	94	Ceramic Flange-Hermetic	Internally Matched	—	20	—	1.5-1.7GHz
NEM1710B-20	94	Ceramic Flange-Hermetic	Internally Matched	—	20	—	1.5-1.7GHz
NEM1715B-20	94	Ceramic Flange-Hermetic	Internally Matched	—	20	—	1.5-1.7GHz
NEM1725B-20	94	Ceramic Flange-Hermetic	Internally Matched	—	20	—	1.5-1.7GHz
NEM2000 Series							
NEM2010B-20	94	Ceramic Flange-Hermetic	Internally Matched	—	20	—	1.7-2.0GHz
NEM2310B-20	94	Ceramic Flange-Hermetic	Internally Matched	—	20	—	1.7-2.0GHz
NEM2700 Series							
NEM2701B-20	94	Ceramic Flange-Hermetic	Internally Matched	—	20	—	2.3-2.7GHz
NEM2703B-20	94	Ceramic Flange-Hermetic	Internally Matched	—	20	—	2.3-2.7GHz
NEM2705B-20	94	Ceramic Flange-Hermetic	Internally Matched	—	20	—	2.3-2.7GHz
NEM2708B-20	94	Ceramic Flange-Hermetic	Internally Matched	—	20	—	2.3-2.7GHz
NEM3500 Series							
NEM3501B-20	94	Ceramic Flange-Hermetic	Internally Matched	—	20	—	3.1-3.5GHz
NEM3503B-20	94	Ceramic Flange-Hermetic	Internally Matched	—	20	—	3.1-3.5GHz
NEM3505B-20	94	Ceramic Flange-Hermetic	Internally Matched	—	20	—	3.1-3.5GHz
NEM3508B-20	94	Ceramic Flange-Hermetic	Internally Matched	—	20	—	3.1-3.5GHz
NEM2300 Series							
NEM2305B-20	94	Ceramic Flange-Hermetic	Internally Matched	—	20	—	2.0-2.3GHz
NEM2310B-20	94	Ceramic Flange-Hermetic	Internally Matched	—	20	—	2.0-2.3GHz

Internally Matched CW Power Bipolar Transistors (Class C)

Part Number	Package Type or Chip	Package Configuration	Manufacturer's Remarks	V_{CC}	C_{CB} at V_{CC}	Designed Operating Frequency Range
ACRIAN						
2001	—	Flange	Frequency range in MHz; in Max. Ratings, Rth. is θ jc.	28V	4pF@28V	2000MHz
2003	—	Flange	—	28V	5.0pF@28V	2000MHz
2005	—	Flange	—	28V	7.5pF@28V	2000MHz
2010	—	Flange	—	28V	13.0pF@28V	2000MHz
2010M	—	Flange	—	28V	17.0pF@28V	2000MHz
2015M	—	Flange	—	28V	22.0pF@28V	2000MHz
2301	—	Flange	—	20V	4.0pF@28V	1700-2300MHz
2304	—	Flange	—	20V	7.0pF@28V	1700-2300MHz

Center Design Frequency						Absolute Maximum Ratings						Price Quantity	
Peak P_{out}	Gain	Peak Collector Efficiency	Peak Power Added Efficiency	Duty Factor	Pulse Width	V_{CBO}	V_{CEO}	V_{EBO}	I_C	Pt.	Rth.	1-100	1000
4.0	11.0	45	43	1.0%	10µsec	50V	20	3.5V	.25	7.0	25	31.05	
4.0	11.0	45	43	1.0%	10µsec	50V	20	3.5V	.25	7.0	25	30.01	—
8.0	12.0	45	44	1.0%	10µsec	50V	20	3.5V	.5	11.6	15	32.89	—
8.0	12.0	45	44	1.0%	10µsec	50V	20	3.5V	.5	11.6	15	33.92	—
15.0	12.5	35	34	1.0%	10µsec	60V	—	4.0V	1.0	17.5	10	31.05	—
15.0	12.5	35	34	1.0%	10µsec	60V	—	4.0V	1.0	17.5	10	30.50	—
35.	12.4	34	33	1.0%	10µsec	60V	—	4.0V	2.0	35	5	43.70	—
35.	12.4	34	33	1.0%	10µsec	60V	—	4.0V	2.0	35	5	41.63	—
90	10.8	40	39	1.0%	10µsec	70V	—	4.0V	6.0	290	.6	45.31	—
90	10.8	40	39	1.0%	10µsec	70V	—	4.0V	6.0	290	.6	42.43	—
150	8.7	35	33	1.0%	10µsec	70V	—	4.0V	12	583	.3	CF	—
150	9.8	40	38	1.0%	10µsec	70V	—	4.0V	12	583	.3	51.75	—
150	9.8	40	38	1.0%	10µsec	70V	—	4.0V	12	583	.3	50.60	—
250	7.2	35	33	1.0%	10µsec	70V	—	4.0V	24	1166	.15	133.00	—
325	7.2	35	33	1.0%	10µsec	70V	—	4.0V	24	1166	.15	147.00	—
Typical, W		Typical							A	W			
4.5	9.5	55	—	—	—	45	45	3.0	0.7	11	15	—	—
6.8	8.3	55	—	—	—	45	45	3.0	1.2	16	11	—	—
11	8.5	55	—	—	—	45	45	3.0	1.8	31	5.5	—	—
17	8.5	55	—	—	—	45	45	3.0	2.6	38	4.5	—	—
28	8.5	55	—	—	—	45	45	3.0	3.6	62	2.3	—	—
—	—	—	—	—	—	—	—	—	—	—	—	—	—
10.5	7.2	45	—	—	—	45	45	3.0	2.7	31.8	5.5	—	—
14.8	6.7	45	—	—	—	45	45	3.0	4.5	39	4.5	—	—
—	—	—	—	—	—	—	—	—	—	—	—	—	—
1.6	9.0	43	—	—	—	45	45	3.0	0.6	10.9	16	—	—
3.5	8.5	43	—	—	—	45	45	3.0	1.2	17.5	10	—	—
5.6	7.5	43	—	—	—	45	45	3.0	2.4	29.2	6.0	—	—
10.0	7.0	43	—	—	—	45	45	3.0	3.6	38.9	4.5	—	—
—	—	—	—	—	—	—	—	—	—	—	—	—	—
1.6	9.0	36	—	—	—	45	45	3.0	0.6	10.9	16	—	—
3.5	7.5	36	—	—	—	45	45	3.0	1.2	17.5	10	—	—
5.6	6.5	34	—	—	—	45	45	3.0	2.4	29.2	6.0	—	—
7.9	5.0	33	—	—	—	45	45	3.0	3.6	38.9	4.5	—	—
5.6	7.5	50	—	—	—	45	45	3.0	2.4	29.2	6.0	—	—
11.0	7.5	50	—	—	—	45	45	3.0	3.6	38.9	4.5	—	—

Center Design Frequency					Absolute Maximum Ratings						Price Quantity	
P_{out}	Gain	Collector Efficiency	Power Added Efficiency	Note If Input or Input/Output Matched	V_{CBO}	V_{CEO}	V_{EBO}	I_C	Pt.	Rth.	1-100	1000
1	9	40	—	—	50	—	3.5	—	—	28	—	—
3	8	40	—	—	50	—	3.5	—	—	15	—	—
5	8	40	—	—	50	—	3.5	—	—	8.5	—	—
10	7	40	—	—	50	—	3.5	—	—	6.0	—	—
10	7	40	—	—	50	—	3.5	—	—	6.0	—	—
15	6	40	—	—	50	—	3.5	—	—	3.5	—	—
1.5	8	43	—	—	46	—	3.5	—	—	3.5	—	—
4	8	43	—	—	46	—	3.5	—	—	17	—	—

Internally Matched CW Power Bipolar Transistors (Class C)

Part Number	Package Type or Chip	Package Configuration	Manufacturer's Remarks	V_{CC}	C_{CB} at V_{CC}	Designed Operating Frequency Range
2307	—	Flange	—	20V	10.0pF@28V	1700-2300MHz
3001	—	Flange	—	28V	4.0pF@28V	3000MHz
3003	—	Flange	—	28V	7.0pF@28V	3000MHz
3005	—	Flange	—	28V	10.0pF@28V	3000MHz
0915-40	—	Flange	—	28V	Internal Shunt L	900-1500MHz
2023-1.5	—	Flange	—	24V	3.5@24V	2000-2300MHz
2023-1.5T	—	Flange	—	24V	3.5@24V	2000-2300MHz
2023-3	—	Flange	—	24V	5.0@24V	2000-2300MHz
2023-3T	—	Flange	—	24V	5.0@24V	2000-2300MHz
2023-6	—	Flange	—	24V	—	2000-2300MHz
2023-12	—	Flange	—	24V	—	2000-2300MHz
2023-16	—	—	—	24V	—	2000-2300MHz
2223-9	—	—	—	24V	—	2200-2300MHz
1014-2	—	—	—	28V	4.5pF@28V	1000-1400MHz
1014-6	—	—	—	28V	8.0pF@28V	1000-1400MHz
1014-12	—	—	—	28V	12.0pF@28V	1000-1400MHz
1417-2	—	—	—	24V	4.5pF@28V	1400-1700MHz
1417-6	—	—	—	24V	8.0pF@28V	1400-1700MHz
1417-12	—	—	—	24V	12.0pF@28V	1400-1700MHz
1417-20	—	—	—	24V	—	1400-1700MHz
1618-4	—	—	—	28V	6.0pF@28V	1600-1800MHz
1618-12	—	—	—	28V	12.0pF@28V	1600-1800MHz
1618-25	—	—	—	28V	—	1600-1800MHz
1618-35	—	—	—	28V	—	1600-1800MHz
1720-2	—	—	—	28V	4.5pF@28V	1700-2000MHz
1720-5	—	—	—	28V	8.0pF@28V	1700-2000MHz
1720-9	—	—	—	28V	12.0pF@28V	1700-2000MHz
1720-20	—	—	—	28V	—	1700-2000MHz
1821-3	—	—	—	24V	5.0pF@24V	1800-2100MHz
1821-6	—	—	—	24V	8.0pF@24V	1800-2100MHz
1821-10	—	—	—	24V	—	1800-2100MHz
1821-18	—	—	—	24V	—	1800-2100MHz
INTERNATIONAL MICROWAVE DEVICES						
1416-1	MF-4	.400 Hermetic Common Base	50Ω In 50Ω Out	24V	—	1.4-1.6GHz
1416-3	MF-4	.400 Hermetic Common Base	50Ω In 50Ω Out	24V	—	1.4-1.6GHz
1416-6	MF-4	.400 Hermetic Common Base	50Ω In 50Ω Out	24V	—	1.4-1.6GHz
1416-12	MF-3	.400 Hermetic Common Base		24V	—	1.4-1.6GHz
1416-20	MF-3	.400 Hermetic Common Base		24V	—	1.4-1.6GHz
1618-1	MF-4	.400 Hermetic Common Base	50Ω In 50Ω Out	24V	—	1.6-1.8GHz
1618-3	MF-4	.400 Hermetic Common Base	50Ω In 50Ω Out	24V	—	1.6-1.8GHz
1618-6	MF-4	.400 Hermetic Common Base	50Ω In 50Ω Out	24V	—	1.6-1.8GHz
1618-12	MF-3	.400 Hermetic Common Base		24V	—	1.6-1.8GHz
1618-20	MF-3	.400 Hermetic Common Base		24V	—	1.6-1.8GHz
1252MR	MF-3	.400 Hermetic Common Base		24V	—	1.6-1.7GHz
1272MR	MF-3	.400 Hermetic Common Base		24V	—	1.6-1.7GHz
993303	MF-3	.400 Hermetic Common Base		27V	—	1.6-1.7GHz
1720-1	MF-4	.400 Hermetic Common Base	50Ω In 50Ω Out	24V	—	1.7-2.0GHz
1720-3	MF-4	.400 Hermetic Common Base	50Ω In 50Ω Out	24V	—	1.7-2.0GHz
1720-6	MF-4	.400 Hermetic Common Base	50Ω In 50Ω Out	24V	—	1.7-2.0GHz
1720-12	MF-3	.400 Hermetic Common Base		24V	—	1.7-2.0GHz
1720-20	MF-3	.400 Hermetic Common Base		24V	—	1.7-2.0GHz
1821-1	MF-4	.400 Hermetic Common Base	50Ω In 50Ω Out	24V	—	1.8-2.1GHz
1821-3	MF-4	.400 Hermetic Common Base	50Ω In 50Ω Out	24V	—	1.8-2.1GHz
1821-6	MF-4	.400 Hermetic Common Base	50Ω in 50Ω Out	24V	—	1.8-2.1GHz
1821-10	MF-3	.400 Hermetic Common Base		24V	—	1.8-2.1GHz
1821-18	MF-3	.400 Hermetic Common Base		24V	—	1.8-2.1GHz
1922-1	MF-4	.400 Hermetic Common Base	50Ω In 50Ω Out	24V	—	1.9-2.2GHz
1922-3	MF-4	.400 Hermetic Common Base	50Ω In 50Ω Out	24V	—	1.9-2.2GHz
1922-6	MF-4	.400 Hermetic Common Base	50Ω In 50Ω Out	24V	—	1.9-2.2GHz
1922-10	MF-3	.400 Hermetic Common Base		24V	—	1.9-2.2GHz
1922-18	MF-3	.400 Hermetic Common Base		24V	—	1.9-2.2GHz
2023-1	MF-4	.400 Hermetic Common Base	50Ω In 50Ω Out	24V	—	2-2.3GHz
2023-3	MF-4	.400 Hermetic Common Base	50Ω In 50Ω Out	24V	—	2-2.3GHz
2023-6	MF-4	.400 Hermetic Common Base	50Ω In 50Ω Out	24V	—	2-2.3GHz
2023-10	MF-3	.400 Hermetic Common Base		24V	—	2-2.3GHz
2023-16	MF-3	.400 Hermetic Common Base		24V	—	2-2.3GHz
2223-4	MF-4	.400 Hermetic Common Base	50Ω In 50Ω Out	24V	—	2.2-2.3GHz
2223-6	MF-4	.400 Hermetic Common Base	50Ω In 50Ω Out	24V	—	2.2-2.3GHz
2223-12	MF-4	.400 Hermetic Common Base		24V	—	2.2-2.3GHz
2223-18	MF-3	.400 Hermetic Common Base		24V	—	2.2-2.3GHz
2327-1	MF-4	.400 Hermetic Common Base	50Ω In 50Ω Out	24V	—	2.3-2.7GHz
2327-3	MF-4	.400 Hermetic Common Base	50Ω In 50Ω Out	24V	—	2.3-2.7GHz
2327-5	MF-4	.400 Hermetic Common Base	50Ω In 50Ω Out	24V	—	2.3-2.7GHz
2327-10	MF-3	.400 Hermetic Common Base	—	24V	—	2.3-2.7GHz

Center Design Frequency					Absolute Maximum Ratings						Price Quantity	
P_{out}	Gain	Collector Efficiency	Power Added Efficiency	Note If Input or Input/Output Matched	V_{CBO}	V_{CEO}	V_{EBO}	I_C	Pt.	Rth.	1-100	1000
7	8	40	—	—	46	—	3.5	—	—	8.5	—	—
1	7	30	—	—	50	—	3.5	—	—	35	—	—
3	6	30	—	—	50	—	3.5	—	—	17	—	—
5	5	30	—	—	50	—	3.5	—	—	8.5	—	—
40	7	40	—	—	50	—	3.5	—	—	1.3	—	—
1.5	8	35	—	—	42	—	3.5	—	—	30	—	—
1.5	8	35	—	—	42	—	3.5	—	—	30	—	—
3	8	35	—	—	42	—	3.5	—	—	16	—	—
3	8	35	—	—	42	—	3.5	—	—	16	—	—
6	7	35	—	—	42	—	3.5	—	—	8	—	—
12	7	35	—	—	42	—	3.5	—	—	4.5	—	—
16	6.5	35	—	Input/Output Matched	50	—	3.5	—	—	3.0	—	—
9	7.7	45	—	Input/Output Matched	45	—	3.5	—	—	6.0	—	—
2	6.0	40	—	Input Matched	50	—	3.5	—	—	15.0	—	—
6	6.8	40	—	Input Matched	50	—	3.5	—	—	8.0	—	—
12	6.8	40	—	Input Matched	50	—	3.5	—	—	4.5	—	—
2	8	40	—	Input Matched	50	—	3.5	—	—	15.0	—	—
6	7.2	40	—	Input Matched	50	—	3.5	—	—	8.0	—	—
12	7.0	40	—	Input Matched	50	—	3.5	—	—	4.5	—	—
20	7.0	35	—	Input/Output Matched	50	—	3.5	—	—	2.5	—	—
4	8.0	40	—	—	50	—	3.5	—	—	12°	—	—
12	7.5	40	—	—	50	—	3.5	—	—	5.0	—	—
25	7.0	35	—	—	50	—	3.5	—	—	2.5	—	—
35	7	35	—	—	50	—	3.5	—	—	1.3	—	—
2	7.5	35	—	—	50	—	3.5	—	—	15.0	—	—
5	6.5	35	—	—	50	—	3.5	—	—	8.0	—	—
9	6.5	35	—	—	50	—	3.5	—	—	9.0	—	—
20	6	32	—	—	50	—	3.5	—	—	2.5	—	—
3	7.5	40	—	—	50	—	3.5	—	—	17.0	—	—
6	7.5	40	—	—	50	—	3.5	—	—	9.0	—	—
10	7.0	35	—	—	50	—	3.5	—	—	5.0	—	—
18	6.5	35	—	—	50	—	3.5	—	—	3.0	—	—
1.5	8.7dB	50	—	Input/Output	40	—	3.5	200mA	—	22°C/W	—	—
3	7.8	50	—	Input/Output	40	—	3.5	700	—	15°C/W	—	—
6	7.8	50	—	Input/Output	40	—	3.5	1A	—	9°C/W	—	—
12	7.8	45	—	Input/Output	40	—	3.5	1.5A	—	5.5°	—	—
20	6.5	45	—	Input/Output	40	—	3.5	2A	—	3.5°	—	—
1	7	50	—	Input/Output	40	—	3.5	200	—	22°	—	—
3	7.8	50	—	Input/Output	40	—	3.5	700	—	15°	—	—
6	7.8	45	—	Input/Output	40	—	3.5	1.0A	—	9°	—	—
12	7.4	45	—	Input/Output	40	—	3.5	1.5A	—	5.5°	—	—
20	6.5	45	—	Input/Output	40	—	3.5	2A	—	3.5°	—	—
12	10dB	45	—	Input/Output	40	—	3.5	1.5A	—	5.5°	—	—
25	8dB	40	—	Input/Output	40	—	3.5	2A	—	3.5°	—	—
34	7.7	40	—	Input/Output	45	—	3.5	2.5A	—	3°	—	—
1	7	50	—	Input/Output	40	—	3.5	200	—	22°	—	—
3	7.8	50	—	Input/Output	40	—	3.5	700	—	15°	—	—
6	7.8	45	—	Input/Output	40	—	3.5	1A	—	9°	—	—
12	7.4	40	—	Input/Output	40	—	3.5	1.5A	—	5.5°	—	—
20	6.5dB	40	—	Input/Output	40	—	3.5	2A	—	3.5°	—	—
1.5	7	45	—	Input/Output	40	—	3.5	200	—	22°	—	—
3	7.8	45	—	Input/Output	40	—	3.5	700	—	15°	—	—
6	7.8dB	45	—	Input/Output	40	—	3.5	1A	—	9°	—	—
10	6.6	40	—	Input/Output	40	—	3.5	1.5A	—	5.5°	—	—
18	6	40	—	Input/Output	40	—	3.5	2A	—	3.5°	—	—
1	7	45	—	Input/Output	40	—	3.5	200mA	—	22°	—	—
3	7.8	45	—	Input/Output	40	—	3.5	700	—	15°	—	—
6	7.8	45	—	Input/Output	40	—	3.5	1A	—	9°	—	—
10	6.6	40	—	Input/Output	40	—	3.5	1.5A	—	5.5°	—	—
18	6	40	—	Input/Output	40	—	3.5	2A	—	3.5°	—	—
1	7	45	—	Input/Output	40	—	3.5	200	—	22°	—	—
3	7.8	45	—	Input/Output	40	—	3.5	700	—	15°	—	—
6	7.8	40	—	Input/Output	40	—	3.5	1A	—	9°	—	—
10	6.6	40	—	Input/Output	40	—	3.5	1.5A	—	5.5°	—	—
16	6dB	40	—	Input/Output	40	—	3.5	2A	—	3.5°	—	—
4	9	45	—	Input/Output	40	—	3.5	700	—	15°	—	—
6	7.8	40	—	Input/Output	40	—	3.5	1A	—	9°	—	—
12	7.4	40	—	Input/Output	40	—	3.5	1.5A	—	5.5°	—	—
18	6	40	—	Input/Output	40	—	3.5	2A	—	3.5°	—	—
1	6	40	—	Input/Output	40	—	3.0	200	—	22°	—	—
2.5	7	40	—	Input/Output	40	—	3.0	700	—	15°	—	—
5	7	35	—	Input/Output	40	—	3.0	1A	—	9°	—	—
9	4.8dB	30	—	Input/Output	40	—	3.0	1.5A	—	5.5°	—	—

Internally Matched CW Power Bipolar Transistors (Class C)

Part Number	Package Type or Chip	Package Configuration	Manufacturer's Remarks	V_{CC}	C_{CB} at V_{CC}	Designed Operating Frequency Range
2327-15	MF-3	.400 Hermetic Common Base	—	24V	—	2.3-2.7GHz
3135-3	MF-4	.400 Hermetic Common Base	—	28V	—	3.1-3.5GHz
1214-20	MF-3	.400 Hermetic Common Base	—	24V	—	1.2-1.4GHz
1214-30	MF-3	.400 Hermetic Common Base	—	28V	—	1.2-1.4GHz
MSC						
AM80610-50	Hermetic	AMPAC™ C/S 042	Geometry: Aμ Metal, Site Ballasted Overlay	28.0V	—	750-960MHz
AM81416-20	Hermetic	AMPAC™ C/S 036	Geometry: Aμ Metal, Site Ballasted Overlay	20.0V	—	1400-1600MHz
AM81618-20	Hermetic	AMPAC™ C/S 036	Geometry: Aμ Metal, Site Ballasted Overlay	20.0V	—	1600-1800MHz
AM81719-50	Hermetic	AMPAC™ C/S 036	Geometry: Aμ Metal, Site Ballasted Overlay	28.0V	—	1750-1850MHz
AM81720-20	Hermetic	AMPAC™ C/S 036	Geometry: Aμ Metal, Site Ballasted Overlay	24.0V	—	1700-2000MHz
AM81821-18	Hermetic	AMPAC™ C/S 036	Geometry: Aμ Metal, Site Ballasted Overlay	24.0V	—	1800-2100MHz
AM81922-18	Hermetic	AMPAC™ C/S 036	Geometry: Aμ Metal, Site Ballasted Overlay	24.0V	—	1900-2200MHz
AM82023-16	Hermetic	AMPAC™ C/S 036	Geometry: Aμ Metal, Site Ballasted Overlay	24.0V	—	2000-2300MHz
AM82327-15	Hermetic	AMPAC™ C/S 036	Geometry: Aμ Metal, Site Ballasted Overlay	24.0V	—	2300-2700MHz
MOTOROLA						
MRF2001	—	Micro-230 Flange	—	28V	2.5	1.0 to 2.3
MRF2001B	—	Micro-230 Pill	—	28V	2.5	1.0 to 2.3
MRF2001M	—	Micro-290 Flange	—	24V	4.0	1.7 to 2.3
MRF2003	—	Micro-230 Flange	—	28V	4.0	1.0 to 2.3
MRF2003B	—	Micro-230 Pill	—	28V	4.0	1.0 to 2.3
MRF2003M	—	Micro-290 Flange	—	24V	4.0	1.7 to 2.3
MRF2005	—	Micro-230 Flange	—	28V	7.5	1.0 to 2.3
MRF2005B	—	Micro-230 Pill	—	28V	7.5	1.0 to 2.3
MRF2005M	—	Micro-290 Flange	—	24V	7.5	1.7 to 2.3
MRF2010	—	Micro-230 Flange	—	28V	12.0	1.0 to 2.3
MRF2010B	—	Micro-230 Pill	—	28V	12.0	1.0 to 2.3
MRF2010M	—	Micro-290 Flange	—	24V	14.0	1.7 to 2.3
MRF2016M	—	Micro-290 Flange	—	24V	20.0	1.7 to 2.3
NEC CORPORATION					C_{CB} @ V_{CB}	Test Frequency
NEM0800 Series-7V						
NEM080390-07	90	Ceramic Flange	—	7.2V	8@10V	860MHz
NEM080391-07	91	Ceramic Flangeless	—	7.2V	8@10V	860MHz
NEM080590-07	90	Ceramic Flange	—	7.2V	16@10V	860MHz
NEM080591-07	91	Ceramic Flangeless	—	7.2V	16@10V	860MHz
NEM0500 Series-12V						
NEM052092-12	92	Ceramic Flangeless	—	12.6V	30@10V	500MHz
NEM054029-12	29	Ceramic Flange	—	12.6V	60@10V	500MHz
NEM056029-12	29	Ceramic Flange	—	13.5V	120@10V	500MHz
NEM0800 Series-12V						
NEM080481E-12	81	Ceramic Flange	—	13.5V	7.5@10V	860MHz
NEM081081E-12	81	Ceramic Flange	—	13.5V	15@10V	860MHz
NEM081081B-12	81	Ceramic Flange	—	13.5V	15@10V	860MHz
NEM082081B-12	81	Ceramic Flange	—	13.5V	35@10V	860MHz
NEM084081B-12	81	Ceramic Flange	—	13.5V	70@10V	860MHz
NEM085081B-12	81	Ceramic Flange	—	13.5V	70@10V	860MHz
NEM0800 Series-24/28V						
NEM081568-24	68	Ceramic Flange	—	24V	24@28V	860MHz
NEM085068-28	68	Ceramic Flange	—	28V	40@28V	860MHz
NEM0900 Series-28V						
NEM092081B-28	81	Ceramic Flange	—	25V	25@28V	900MHz
NEM094081B-28	81	Ceramic Flange	—	25V	50@28V	900MHz
NEM096081B-28	81	Ceramic Flange	—	25V	80@28V	900MHz
NEM0500 Series-28V						
NEM054029-28	29	Ceramic Flange	—	28V	42@28V	400MHz
NEM056029-28	29	Ceramic Flange	—	28V	84@28V	400MHz
NEM050029-28	29	Ceramic Flange	—	28V	130@28V	400MHz
NE0200 Series-7V						
NE020214-07	14	TO-39 Metal Can	—	7.2V	17@10V	175MHz
NE020620-07	20	—	—	7.2V	12@10V	175MHz
NE020790-07	90	Ceramic Flange	—	7.2V	12@10V	175MHz
NE020791-07	91	Ceramic Flangless	—	7.2V	12@10V	175MHz

Center Design Frequency				Note If Input or Input/Output Matched	Absolute Maximum Ratings						Price Quantity	
P_{out}	Gain	Collector Efficiency	Power Added Efficiency		V_{CBO}	V_{CEO}	V_{EBO}	I_C	Pt.	Rth.	1-100	1000
15	4.8dB	30	—	Input/Output	40	—	3.0	2.0A	—	3.5°	—	—
2.5	5.5dB	30	—	Input/Output	40	—	3.0	500mA	—	12°	—	—
20	7dB	45	—	Input/Output	45	—	3.5	2.0A	—	3.5	—	—
30	8dB	45	—	Input/Output	45	—	3.5	2.0A	—	3.0	—	—
50.0W	8.5dB	50%	—	In/Out Matched	50V	—	3.5V	—	—	4.0°C/W	—	—
17.6W	6.4dB	45%	—	In/Out Matched	40V	—	3.5V	—	—	3.5°C/W	—	—
16.0W	6.0dB	45%	—	In/Out Matched	40V	—	3.5V	—	—	3.5°C/W	—	—
50.0W	6.5dB	45%	—	In/Out Matched	55V	—	3.5V	—	—	1.5°C/W	—	—
20.0W	6.4dB	42%	—	In/Out Matched	45V	—	3.5V	—	—	3.5°C/W	—	—
18.0W	6.0dB	40%	—	In/Out Matched	45V	—	3.5V	—	—	3.5°C/W	—	—
18.0W	6.0dB	40%	—	In/Out Matched	45V	—	3.5V	—	—	3.5°C/W	—	—
16.0W	6.0dB	40%	—	In/Out Matched	45V	—	3.5V	—	—	3.0°C/W	—	—
15.0W	4.0dB	30%	—	In/Out Matched	40V	—	3.5V	—	—	3.0°C/W	—	—
1.0	10.0	35	33	Input	45	20	4.0	.250	7.0	25	41.74	—
1.0	10.0	35	33	Input	45	20	4.0	.250	7.0	25	39.67	—
1.0	9.5	40	38	Input	45	20	4.0	.25	7.0	25	66.24	—
3.0	8.9	35	33	Input	45	20	3.5	.5	11.6	15	43.81	—
3.0	8.9	35	33	Input	45	20	3.5	.5	11.6	15	41.74	—
3.0	8.5	40	37	Input	45	20	3.5	.5	11	16	66.24	—
5.0	9.0	35	33	Input	45	20	3.5	1.0	25	7.0	54.97	—
5.0	9.0	35	33	Input	45	20	3.5	1.0	25	7.0	48.18	—
5.0	8.0	40	37	Input	45	20	3.5	1.0	22	8.0	76.82	—
10.0	7.0	35	33	Input	45	20	3.5	2.0	35	5.0	56.00	—
10.0	7.0	35	33	Input	45	20	3.5	2.0	35	5.0	53.82	—
10.0	8.0	40	37	Input	45	20	3.5	2.0	35	5.0	101.43	—
16.0	7.0	40	37	Input	45	20	3.5	3.0	50	3.5	105.83	—
Watts								Amps	Watts			
3.5	—	70	—	—	25	12	2.0	1.5	17.5	10	—	—
3.5	—	70	—	—	25	12	2.0	1.5	17.5	10	—	—
5.5	—	80	—	—	25	12	2.0	3.0	35	5.0	—	—
5.5	—	80	—	—	25	12	2.0	3.0	35	5.0	—	—
15	—	65	—	—	35	18	3.0	4.0	43	4.0	—	—
42	—	65	—	—	35	18	3.0	10	100	1.8	—	—
66	—	60	—	—	35	18	3.0	20	175	1.0	—	—
4.5	—	60	—	—	35	18	3.0	1.5	17.5	10	—	—
12.5	—	65	—	—	35	18	3.0	3.0	33	5.3	—	—
10	—	55	—	—	35	18	3.0	3.0	33	5.3	—	—
23	—	50	—	—	35	16	3.0	7.5	80	2.2	—	—
37	—	48	—	—	35	16	3.0	15	146	1.2	—	—
56	—	50	—	—	35	18	3.0	12	170	1.05	—	—
16	—	50	—	—	50	32	3.0	12	100	1.75	—	—
52	—	50	—	—	50	32	3.0	15	160	1.09	—	—
20	—	60	—	—	55	30	3.0	3	50	3.5	—	—
40	—	60	—	—	55	30	3.0	6	120	1.46	—	—
60	—	55	—	—	55	30	3.0	9	170	1.05	—	—
40	—	65	—	—	55	32	3.0	6	88	2.0	—	—
63	—	62	—	—	55	32	3.0	12	160	1.1	—	—
100	—	60	—	—	55	32	3.0	15	200	0.9	—	—
2.0	—	70	—	Unmatched	25	12	2.5	0.75	7.5	20	—	—
6.3	—	70	—	Unmatched	25	12	2.5	1.5	17	8.8	—	—
7.1	—	70	—	Unmatched	25	12	2.5	1.5	17	8.8	—	—
7.1	—	70	—	Unmatched	25	12	2.5	1.5	17	8.8	—	—

Internally Matched CW Power Bipolar Transistors (Class C)

Part Number	Package Type or Chip	Package Configuration	Manufacturer's Remarks	V_{CC}	C_{CB} at V_{CC}	Designed Operating Frequency Range
NE0200 Series-12V						
NE020200-12	Chip	Chip	—	13.5V	7@10V	175MHz
NE020214-12	14	TO-39 Metal Can	—	13.5V	7@10V	175MHz
NE020320-12	20	Stripline Stud	—	13.5V	7@10V	175MHz
NE020390-12	90	Ceramic Flange	—	13.5V	6@10V	175MHz
NE020391-12	91	Ceramic Flangless	—	13.5V	6@10V	175MHz
NE021020-12	20	Stripline Stud	—	13.5V	12@10V	175MHz
NE021090-12	90	Ceramic Flange	—	13.5V	12@10V	175MHz
NE021091-12	91	Ceramic Flangeless	—	13.5V	12@10V	175MHz
NE022025-12	25	Stripline Stud	—	13.5V	25@10V	175MHz
NE022090-12	90	Ceramic Flange	—	13.5V	25@10V	175MHz
NE022091-12	91	Ceramic Flangless	—	13.5V	25@10V	175MHz
NE022526-12	26	Stripline Stud	—	13.5V	25@10V	175MHz
NE024090-12	90	Ceramic Flange	—	13.5V	60@10V	175MHz
NE024091-12	91	Ceramic Flangless	—	13.5V	60@10V	175MHz
NE028029-12	29	Ceramic Flange (Jϕ)	—	13.5V	120@10V	175MHz
NE0200-28V Series						
NE0320-28	20	Stripline Plastic	—	28V	5@28V	175MHz
NE021020-28	20	Stripline Plastic	—	28V	10@28V	175MHz
NE022025-28	25	Stripline Plastic	—	28V	20@28V	175MHz
NE024027-28	27	Stripline Stud	—	28V	42@28V	175MHz
NE028029-28	29	Ceramic Flange (Jϕ)	—	28V	84@28V	175MHz
NEM020029-28	29	Ceramic Flange (Jϕ)	—	28V	130@28V	175MHz
NE0500-28V Series						
NE050320-28	20	Stripline Stud	—	28V	5@28V	400MHz
NE051020-28	20	Stripline Stud	—	28V	10@28V	400MHz
NE052025-28	25	Stripline Stud	—	28V	20@28V	400MHz
NE0800-12V Series						
NE080120-12	20	Stripline Stud	—	13.5V	2.5@10V	860MHz
NE080420-12	20	Stripline Stud	—	13.5V	7.5@10V	860MHz
NE080190-12	90	Ceramic Flange	—	13.5V	2.3@10V	860MHz
NE080191-12	91	Ceramic Flangeless	—	13.5V	2.3@10V	860MHz
NE080490-12	90	Ceramic Flange	—	13.5V	7.0@10V	860MHz
NE080491-12	91	Ceramic Flangeless	—	13.5V	7.0@10V	860MHz
NE081090-12	90	Ceramic Flange	—	13.5V	14@10V	860MHz
NE081091-12	91	Ceramic Flangeless	—	13.5V	14@10V	860MHz
NEL0800 Series-25V						
NEL080120-24	20	Stripline Stud	—	25V	3.5@28V	900MHz
NEL080220-24	20	Stripline Stud	—	25V	6.0@28V	900MHz
NEL080525-24	25	Stripline Stud	—	25V	12.0@28V	900MHz
NE0500-7V Series						
NE050220-07	20	Stripline Stud	—	7.2V	4@10V	500MHz
NE050290-07	90	Ceramic Flange	—	7.2V	4@10V	500MHz
NE050291-07	91	Ceramic Flangeless	—	7.2V	4@10V	500MHz
NE050490-07	90	Ceramic Flange	—	7.2V	8@10V	500MHz
NE050491-07	91	Ceramic Flangeless	—	7.2V	8@10V	500MHz
NE050690-07	90	Ceramic Flange	—	7.2V	16@10V	500MHz
NE050691-07	91	Ceramic Flangeless	—	7.2V	16@10V	500MHz
NE0500 12V-Series						
NE050200-12	Chip	Chip	—	12.6V	2.5@10V	500MHz
NE050214-12	14/14E[6]	—	—	12.6V	2.5@10V	500MHz
NE050320-12	20	Stripline Stud	—	12.6V	6@10V	500MHz
NE050390-12	90	Ceramic Flange	—	12.6V	6@10V	500MHz
NE050391-12	91	Ceramic Flangeless	—	12.6V	6@10V	500MHz
NE051025-12	25	Stripline Stud	—	12.6V	17@10V	500MHz
NE051090-12	90	Ceramic Flange	—	12.6V	11@10V	500MHz
NE051091-12	91	Ceramic Flangeless	—	12.6V	11@10V	500MHz
NE051525-12	25	Stripline Stud	—	12.6V	24@10V	500MHz
NE052090-12	90	Ceramic Flange	—	12.6V	24@10V	500MHz
NE052091-12	91	Ceramic Flangeless	—	12.6V	30@10V	500MHz
NE1000 Series						
NE1005E-20	21	Stripline Stud	—	18	5.3	1.0GHz
NE1010E-20	21	Stripline Stud	—	18	10.5	1.0GHz
NEM1020B-20	94	Ceramic Flange-Hermetic	Internally Matched	20	—	0.8-1.0GHz
NEM1040B-20	94	Ceramic Flange-Hermetic	Internally Matched	20	—	0.8-1.0GHz
NE3000 Series						
NE300100	Chip	Chip	—	20	2.6	1.0-3.0GHz
NE3001B-20	53B	Ceramic Flange-Hermetic	—	20	2.6	1.7-3.5GHz
NE300157B-20	57B	Ceramic Flangless-Hermetic	—	20	2.6	1.7-3.5GHz
NEM3001B-20	94	Ceramic Flange-Hermetic	Internally Matched	20	—	2.7-3.0GHz

Center Design Frequency				Note If Input or Input/Output Matched	Absolute Maximum Ratings						Price Quantity	
P_{out}	Gain	Collector Efficiency	Power Added Efficiency		V_{CBO}	V_{CEO}	V_{EBO}	I_C	Pt.	Rth.	1-100	1000
2.5	—	70	—	Unmatched	38	18	3.0	0.75	7.5	20	—	—
2.8	—	70	—	Unmatched	38	18	3.0	0.75	7.5	20	—	—
3.5	—	65	—	Unmatched	38	18	3.0	0.75	10	15	—	—
3.2	—	60	—	Unmatched	38	18	3.0	0.75	10	15	—	—
3.2	—	60	—	Unmatched	38	18	3.0	0.75	10	15	—	—
8.2	—	65	—	Unmatched	38	18	3.0	1.5	17	8.8	—	—
8.9	—	65	—	Unmatched	38	18	3.0	1.5	17	8.8	—	—
8.9	—	65	—	Unmatched	38	18	3.0	1.5	17	8.8	—	—
20	—	65	—	Unmatched	38	18	3.0	3.0	34	4.4	—	—
20	—	65	—	Unmatched	38	18	3.0	3.0	34	4.4	—	—
20	—	65	—	Unmatched	38	18	3.0	3.0	34	4.4	—	—
20	—	54	—	Unmatched	38	18	3.0	3.0	40	4.4	—	—
40	—	70	—	Unmatched	35	18	3.0	10	70	2.5	—	—
40	—	70	—	Unmatched	35	18	3.0	10	70	2.5	—	—
83W	—	60	—	Unmatched	35	18	3.0	20.0	175	1.0	—	—
5.0W	—	50	—	Unmatched	55	32	3.0	0.75	13	13.5	—	—
14W	—	65	—	Unmatched	55	32	3.0	1.5	22	8.0	—	—
22W	—	70	—	Unmatched	55	32	3.0	3.0	42	4.2	—	—
40W	—	70	—	Unmatched	55	32	3.0	6.0	88	2.0	—	—
84W	—	65	—	Unmatched	55	32	3.0	12	160	1.1	—	—
112W	—	70	—	Unmatched	55	32	3.0	15	200	0.9	—	—
4.0	.10	60	—	Unmatched	55	32	3.0	0.75	13	13.5	—	—
10.7	.63	65	—	Unmatched	55	32	3.0	1.5	22	8.0	—	—
22.4	3.16	70	—	Unmatched	55	32	3.0	3.0	42	4.2	—	—
1.0	.1	60	—	Unmatched	35	18	3.0	0.5	8.3	21	—	—
4.0	1.0	70	—	Unmatched	35	18	3.0	1.5	17.5	10	—	—
1.3	.1	60	—	Unmatched	35	18	3.0	0.25	8.3	21	—	—
1.3	.1	60	—	Unmatched	35	18	3.0	0.25	8.3	21	—	—
5.0	.89	65	—	Unmatched	35	18	3.0	1.5	17.5	10	—	—
5.0	.89	65	—	Unmatched	35	18	3.0	1.5	17.5	10	—	—
11.2	4.0	70	—	Unmatched	35	18	3.0	3.0	35	5	—	—
11.2	4.0	70	—	Unmatched	35	18	3.0	3.0	35	5	—	—
2.4	.5	60	—	Unmatched	50	30	3.0	1.0	12	15	—	—
5.4	1.25	70	—	Unmatched	50	30	3.0	2.0	17.5	10	—	—
10.7	2.5	65	—	Unmatched	50	30	3.0	4.0	32	5.5	—	—
1.4	.13	60	—	Unmatched	25	12	2.0	0.75	8.75	20	—	—
1.4	.13	60	—	Unmatched	25	12	2.0	0.75	8.75	20	—	—
1.4	.13	60	—	Unmatched	25	12	2.0	0.75	8.75	20	—	—
4	.9	65	—	Unmatched	25	12	2.0	1.5	17.5	10	—	—
4	.9	65	—	Unmatched	25	12	2.0	1.5	17.5	10	—	—
7	2.5	65	—	Unmatched	25	12	2.0	3.0	35	5	—	—
7	2.5	65	—	Unmatched	25	12	2.0	3.0	35	5	—	—
1.4	.25	80	—	Unmatched	35	18	3.0	0.4	7.0	—	—	—
1.4	.25	80	—	Unmatched	35	18	3.0	0.4	7.0	—	—	—
3.2	.32	60	—	Unmatched	38	18	3.0	0.75	10	15	—	—
35	.32	60	—	Unmatched	38	18	3.0	0.75	10	15	—	—
3.5	.32	60	—	Unmatched	38	18	3.0	0.75	10	15	—	—
8.9	2.5	70	—	Unmatched	38	18	3.0	2.2	25	6.0	—	—
8.9	2.0	75	—	Unmatched	35	18	3.0	2.0	20	8.8	—	—
8.9	2.0	75	—	Unmatched	35	18	3.0	2.0	20	8.8	—	—
15.8	6.3	75	—	Unmatched	38	18	3.0	3.0	34	4.4	—	—
15	4.0	65	—	Unmatched	35	18	3.0	4.0	43	4.0	—	—
15	4.0	65	—	Unmatched	35	18	3.0	4.0	43	4.0	—	—
6.0	4.8	70	—	—	45	45	3.0	1.0	11	16	—	—
11.2	4.5	70	—	—	45	45	3.0	2.0	22	8.0	—	—
20.0	6.0	50	—	—	45	45	3.0	3.6	35	5.0	—	—
40.0	6.0	50	—	—	45	45	3.0	7.2	80	2.2	—	—
—	—	—	—	—	—	—	—	—	—	—	—	—
1.6	9.0	35	—	—	45	45	3.0	0.6	10.9	16	—	—
1.6	9.0	35	—	—	45	45	3.0	0.6	10.9	16	—	—
1.6	9.0	35	—	—	45	45	3.0	0.6	10.9	16	—	—
1.6	9.0	37	—	—	45	45	3.0	0.6	10.9	16	—	—

Internally Matched CW Power Bipolar Transistors (Class C)

Part Number	Package Type or Chip	Package Configuration	Manufacturer's Remarks	V_{CC}	C_{CB} at V_{CC}		Designed Operating Frequency Range
NE300300	Chip	Chip	—	—	20	4.2	1.0-3.0GHz
NE3003B-20	53B	Ceramic Flange-Hermetic	—	—	20	4.2	1.7-3.5GHz
NE300357B-20	57B	Ceramic Flangless-Hermatic	—	—	20	4.2	1.7-3.5GHz
NEM3003B-20	94	Ceramic Flange-Hermetic	Internally Matched	—	20	—	2.7-3.0GHz
NE3005B-20	53B	Ceramic Flange-Hermetic	—	—	20	7.4	1.7-3.5GHz
NE300557B-20	57B	Ceramic Flangless-Hermetic	—	—	20	7.4	1.7-3.5GHz
NEM3005B-20	94	Ceramic Flange-Hermetic	Internally Matched	—	20	—	2.7-3.0GHz
NEM3008B-20	94	Ceramic Flange-Hermetic	Internally Matched	—	20	—	2.7-3.0GHz
NE4200 Series							
NE420100	Chip	Chip	—	—	20	3.3	2.0-4.4GHz
NE4201B-20	53B	Ceramic Flange-Hermetic	—	—	20	3.3	3.0-4.4GHz
NE420157B-20	57B	Ceramic Flangeless-Hermetic	—	—	20	3.3	3.0-4.4GHz
NEM4201B-20	94	Ceramic Flange-Hermetic	Internally Matched	—	20	—	3.7-4.2GHz
NE4203B-20	53B	Ceramic Flange-Hermetic	—	—	20	4.2	3.7-4.2GHz
NE420357B-20	57B	Ceramic Flangless-Hermetic	—	—	20	4.2	3.7-4.2GHz
NEM4203B-20	94	Ceramic Flange-Hermetic	Internally Matched	—	20	—	3.7-4.2GHz
NEM4205B-20	94	Ceramic Flange-Hermetic	Internally Matched	—	20	—	3.7-4.2GHz
TOSHIBA							Design Frequency
S2746	Package	10mm² Hermetic, Flange	—	28V	—	—	1.64GHz
S2747	Package	10mm² Hermetic, Flange	—	28V	—	—	1.64GHz
S2749	Package	10mm² Hermetic, Flange	—	28V	—	—	3.0GHz
S2745	Package	5.8mm Hermetic, Flange	—	—	—	—	—
S2527	Package	5.8mm Hermetic, Flange	—	—	—	—	—
S2528	Package	5.8mm Hermetic, Flange	—	—	—	—	—

Internally Matched Linear Power Bipolar Transistors (Class A)

Part Number	Package Type or Chip	Package Configuration	Manufacturer's Remarks	I_C	V_{CE}	Peak Ft.	C_{CB} at V_{CE}	1 GHz		
								S_{21} Gain	MAG	MSG (If k<1)
ACRIAN										
10AM05	—	—	—	1.0	20	2.5	16pF @ 28V	—	—	—
10AM11	—	—	—	1.8	20	2.5	32pF @ 28V	—	—	—
10AM20	—	—	—	2.75	20	2.5	47pF @ 28V	—	—	—
23AM01.5	—	—	—	0.28	20	3.0	5.6pF @ 28V	—	—	—
23AM03	—	—	—	0.55	20	3.0	8.5pF @ 28V	—	—	—
23AM03T	—	—	—	0.55	20	3.0	8.5pF @ 28V	—	—	—
23AM06	—	—	—	1.1	20	3.0	15pF @ 28V	—	—	—
23AM06T	—	—	—	1.1	20	3.5	15pF @ 28V	—	—	—
AVANTEK										
AT-64023	230mil Flange stripline, BeOFlange		Ballasted, Input Matched New Product Replaces AT-7510	1.0 mA	15V	7GHz	0.8pF	11.5dB	—	—
INTERNATIONAL MICROWAVE DEVICES										
1416-1L	MF-4	.400 Herm Common Emitter	—	240mA	20V	—	—	—	—	—
1618-1L	MF-4	.400 Herm Common Emitter	—	240mA	20V	—	—	—	—	—
1720-1L	MF-4	.400 Herm Common Emitter	—	240mA	20V	—	—	—	—	—
1821-1L	MF-4	.400 Herm Common Emitter	—	240mA	20V	—	—	—	—	—
1922-1L	MF-4	.400 Herm Common Emitter	—	240mA	20V	—	—	—	—	—
2023-1L	MF-4	.400 Herm Common Emitter	—	240mA	20V	—	—	—	—	—

Center Design Frequency					Absolute Maximum Ratings						Price Quantity	
P_{out}	Gain	Collector Efficiency	Power Added Efficiency	Note If Input or Input/Output Matched	V_{CBO}	V_{CEO}	V_{EBO}	I_C	Pt.	Rth.	1-100	1000
3.2	8.0	32	—	—	45	45	3.0	1.2	17.5	10	—	—
3.2	8.0	32	—	—	45	45	3.0	1.2	17.5	10	—	—
3.2	8.0	32	—	—	45	45	3.0	1.2	17.5	10	—	—
3.5	8.5	37	—	—	45	45	3.0	1.2	17.5	10	—	—
5.0	6.0	28	—	—	45	45	3.0	2.4	29.2	6.0	—	—
5.0	6.0	28	—	—	45	45	3.0	2.4	29.2	6.0	—	—
5.6	6.5	36	—	—	45	45	3.0	2.4	29.2	6.0	—	—
8.9	6.5	35	—	—	45	45	3.0	3.6	38.9	4.5	—	—
1.6	8.0	30	—	—	45	45	3.0	0.6	11	16	—	—
1.6	8.0	30	—	—	45	45	3.0	0.6	11	16	—	—
1.6	8.0	30	—	—	45	45	3.0	0.6	11	16	—	—
1.6	8.0	30	—	—	45	45	3.0	0.6	11	16	—	—
3.2	5.0	30	—	—	45	45	3.0	1.2	17	10	—	—
3.2	5.0	30	—	—	45	45	3.0	1.2	17	10	—	—
3.2	5.0	30	—	—	45	45	3.0	1.2	17	10	—	—
5.0	4.0	25	—	—	45	45	3.0	2.4	29	6.0	—	—
	dB									°C/W		
14	9	52	45	Input/Output Matched	50	20	3.5	3.5	32	5.5	—	—
28	9	52	45	Input/Output Matched	50	20	3.5	7.0	58	3.0	—	—
12	5.4	33	23	Input/Output Matched	50	20	3.5	3.5	32	5.5	—	—
4.4	9.4	45	40	Unmatched	50	20	3.5	1.0	13	13	—	—
1.2	8.0	30	25	Unmatched	50	20	3.5	0.5	5.0	35	—	—
3.6	8.0	35	29	Unmatched	50	20	3.5	1.0	12	15	—	—

1 GHz				Center Design Frequency					Associated Power Added Efficiency	Note if Input or Input/Output Matched	Absolute Maximum Ratings					
P-1 dB	G-1 dB	Power Added Efficiency	Designed Operating Frequency Range	S_{21} Gain	MAG	MSG (if k<1)	P-1 dB	G-1 dB			V_{CBO}	V_{CEO}	V_{EBO}	I_C	Pt.	Rth.
5.0	10.8	—	1.0GHz	—	—	—	—	—	—	Input Matched	65	32	3.5	3.0	25	5
11.0	9.0	—	1.0GHz	—	—	—	—	—	—	Input Matched	65	32	3.5	4.0	41	3
20.0	7.0	—	1.0GHz	—	—	—	—	—	—	Input Matched	65	35	3.5	5.5	63	2
—	—	—	2.3GHz	—	—	—	1.5	7.0	—	Input Matched	45	22	3.5	0.93	7	17
—	—	—	2.3GHz	—	—	—	3.0	6.5	—	Input Matched	45	22	3.5	1.8	14	9
—	—	—	2.3GHz	—	—	—	3.0	6.5	—	Input Matched	45	22	3.5	1.8	14	9
—	—	—	2.3GHz	—	—	—	6.0	6.0	—	Input Matched	45	22	3.5	2.8	21	5
—	—	—	2.3GHz	—	—	—	6.0	6.0	—	Input Matched	45	22	3.5	2.8	21	5
29dBm	15dB	45%	4GHz	3.5dB	9dB	—	27dBm	7dB	30%	Input	25V	18V	2V	150mA	2.25W	40° C/W
—	—	—	1.4-1.6GHz	—	—	—	1W	7dB	—	I/O	40V	20	3.5	180	1	22°
—	—	—	1.6-1.8GHz	—	—	—	1W	7dB	—	I/O	40V	20	3.5	180	1	22°
—	—	—	1.7-2.0GHz	—	—	—	1W	7dB	—	I/O	40V	20	3.5	180	1	22°
—	—	—	1.8-2.1GHz	—	—	—	1W	7dB	—	I/O	40V	20	3.5	180	1	22°
—	—	—	1.9-2.2GHz	—	—	—	1W	7dB	—	I/O	40V	20	3.5	180	1	22°
—	—	—	2.0-2.3GHz	—	—	—	1W	7dB	—	I/O	40V	20	3.5	180	1	22°

Monolithic MMIC Broadband Cascadable Bipolar Amplifiers

Part Number	Package Type or Chip	Package Configuration	Manufacturer's Remarks	Bias Voltage	Operating Bias Current Range (mA)	Test Bias Current (mA)	Required External Passive Components
ACRIAN							
MPA-101	—	—	12 dB gain @ 0.2 GHz	10.0V	100	—	D.C. Block
MPA-201	—	—	12 dB gain @ 0.2 GHz	12.5V	250	—	D.C. Block
MPA-202	—	—	10 dB gain @ 0.2 GHz	15.0V	350	—	D.C. Blocks
PDA-201	—	—	25 dB gain @ 0.2 GHz	15.0V	200	—	External matching circuit
AVANTEK				– 21, – 22 models			
MSA-0170	70 mil	stripline	All MTTFs are for 1.10^6 hrs	5 V	13-25	17	Blocking caps, bias resistor or choke
MSA-0135	micro X	stripline	Low cost, new product	5	13-25	17	Blocking caps, bias resistor or choke
MSA-0270	70 mil	stripline	—	5	18-40	25	Blocking caps, bias resistor or choke
MSA-0235	micro X	stripline	Low cost, new product	5	18-40	25	Blocking caps, bias resistor or choke
MSA-0370	70 mil	stripline	—	5	20-45	35	Blocking caps, bias resistor or choke
MSA-0335	micro X	stripline	Low cost, new product	5	20-45	35	Blocking caps, bias resistor or choke
MSA-0470	70 mil	stripline	New product	6	25-90	50	Blocking caps, bias resistor or choke
MSA-0435	micro X	stripline	Low cost, new product	6	25-90	50	Blocking caps, bias resistor or choke
MSA-0420	200 mil	BeO disk	New product	6.5	25-120	90	Blocking caps, bias resistor or choke
NEC CORPORATION							
MM76515	15	Chip or TO-33	1200 MHz	10V	40-60	45	None
MM76612	12	Chip or TO-72	1200 MHz	5V	15-25	20	None

Oscillator Bipolar Transistors

Part Number	Package Type or Chip	Package Configuration	Manufacturer's Remarks	I_C	V_{CE}	Peak Ft.	C_{CB} at V_{CB}	Test Frequency
ACRIAN								
UMIL 40 FT	LO6	Gemini	Military	3.5	28	4 GHz	3 pF	400
UMIL 20 FT	LO6	Gemini	Military	2.5	28	4 GHz	2 pF	400
VMIL 20 FT	.380 SOE	—	Military and F.M. Broadcast Applications	1.2	28	Calculated 2.8GHz	2 pF	175
VMIL 40 FT	.380 SOE	—	Military and F.M. Broadcast Applications	2.4	28	Calculated 2.8GHz	4 pF	175
VMIL 60 FT	.500 SOE	—	Military and F.M. Broadcast Applications	3.6	28	Calculated 2.8	6 pF	175
VMIL 80 FT	.500 J0	—	Military and F.M. Broadcast Applications	4.8	28	Calculated 2.8	8 pF	175
VMIL 120 FT	J07	—	Military and F.M. Broadcast Applications	7.2	28	Calculated 2.8	12 pF	175
FUJITSU								
FJ7201	BB, CC	Common Collector	—	150	18	4.5GHz	4.0	2.3
INTERNATIONAL MICROWAVE DEVICES								
101	MF-1	Common Base Coax	—	250	20V	—	3 @ 28	2.0
102	MF-1	Common Emitter Coax	—	250	20V	—	3 @ 28	2.0
201	MF-1	Common Base Coax	—	250	20V	—	3.5 @ 20	3.0
202	MF-1	Common Emitter Coax	—	250	20V	—	3.5 @ 20	3.0
301	MF-1	Common Base Coax	—	150 mA	20V	3.5GHz	2.5 @ 20	3.0
302	MF-1	Common Emitter Coax	—	150 mA	20	3.5GHz	2.5 @ 20	3.0
401	MF-1	Common Base Coax	—	150 mA	20	4.5GHz	2.5 @ 20	4.3
402	MF-1	Common Emitter Coax	—	150 mA	20	4.5GHz	2.5 @ 20	4.3
418	MF-6	Common Base Coax	—	150 mA	20	5 GHz	2.5 @ 20	5
419	MF-6	Common Emitter Coax	—	150 mA	20	5 GHz	2.5 @ 20	5
518	MF-6	Common Base Coax	—	100	20	5 GHz	1.8 @ 20	5
519	MF-6	Common Emitter Coax	—	100	20	5 GHz	1.8 @ 20	5
205	MF-2	Common Collector .250 PLG Herm	—	200	24	3 GHz	—	2.3
305	MF-2	Common Collector .250 PLG Herm	—	150	24	3.5GHz	—	2.3
405	MF-2	Common Collector .250 PLG Herm	—	400	24	4.5GHz	—	2.3

S_{21} Gain at 100 MHz	F-1 dB (Frequency Where Gain Is Down 1 dB)	F-2 dB (Frequency Where Gain is Down 2 dB)	.5 GHz				F_{swr} (Frequency Where VSWR = 2:1)		Rth. (Thermal Resistance From Chip to Case)	Case Temperature For Projected MTTF > 1x10^{6} Hours
			NF	P-1 dB	IP3	Group Delay	Input	Output		
—	250 MHz	500 MHz	6.5	+22 dBm	+38 dBm	—	.5 GHz	.5 GHz	—	—
—	200 MHz	500 MHz	7.0	+28 dBm	+43 dBm	—	.5 GHz	.5 GHz	—	—
—	200 MHz	400 MHz	8.2	+32 dBm	+50 dBm	—	.2 GHz	.2 GHz	—	—
				@ 100 MHz			.1 GHz	.1 GHz	—	—
				+27 dB						
										– 21, 22 models
19 dB	.7 GHz	1.5 GHz	5 dB	1.5 dBm	15 dBm	150 ps	3 GHz	3 GHz	120 C/W	140
19 dB	.5 GHz	1.5 GHz	5 dB	1.5 dBm	15 dBm	150 ps	3.0 GHz	3.0 GHz	130 C/W	135
12.5 dB	1.9 GHz	3.0 GHz	6 dB	4.0 dBm	17 dBm	150 ps	3.0 GHz	3.0 GHz	120 C/W	135
12.5 dB	1.7 GHz	3.0 GHz	6 dB	4.0 dBm	17 dBm	150 ps	3.0 GHz	3.0 GHz	130 C/W	130
12.0 dB	2.0 GHz	3.0 GHz	6 dB	10 dBm	23 dBm	150 ps	3.0 GHz	3.0 GHz	120 C/W	130
12.0 dB	1.8 GHz	3.0 GHz	6 dB	10 dBm	23 dBm	150 ps	3.0 GHz	3.0 GHz	130 C/W	125
8.5 dB	2.5 GHz	3.5 GHz	6.5 dB	17 dBm	30 dBm	150 ps	2.5 GHz	2.0 GHz	165 C/W	100
8.5 dB	2.0 GHz	3.0 GHz	6.5 dB	17 dBm	30 dBm	150 ps	2.5 GHz	2.0 GHz	175 C/W	95
9 dB	2.5 GHz	3.5 GHz	6.5 dB	17 dBm	30 dBm	150 ps	2.5 GHz	2.0 GHz	85 C/W	100
19 dB	—	—	5.1 dB	10.0 dBm	—	—	—	—	—	—
19 dB	—	—	5.0 dB	5 dBm	—	—	—	—	—	—

Power Output	Maximum Usable Frequency	Absolute Maximum Ratings						Price Quantity	
		V_{CBO}	V_{CEO}	V_{EBO}	I_C	Pt.	Rth.	1-100	1000
—	500 MHz	30	65	—	8A	—	2.2	—	—
—	500 MHz	45	80	—	4A	—	2.2	—	—
20W	175 MHz	60 Volts	80 Volts	Not applicable	2A	40W	4.4	—	—
40W	175 MHz	60 Volts	80 Volts	Not applicable	4A	80W	2.2	—	—
60W	175 MHz	60 Volts	80 Volts	Not applicable	6A	120W	1.5	—	—
80W	175 MHz	60 Volts	80 Volts	Not applicable	8A	160W	1.1	—	—
120W	175 MHz	60 Volts	80 Volts	Not applicable	12A	240W	.73	—	—
29.5dBm	4.5 GHz	35	22	3	0.5	6W	15	—	—
1.3	2 GHz	50	—	3.5V	300mA	—	30° C/W	—	—
1.3	2 GHz	50	—	3.5V	300mA	—	30° C/W	—	—
1.2	3 GHz	45	—	3.5V	300mA	—	30° C/W	—	—
1.2	3 GHz	45	—	3.5V	300mA	—	30° C/W	—	—
.6	3.5 GHz	45	—	3.5V	200mA	—	30° C/W	—	—
.6	3.5 GHz	45	—	3.5V	200mA	—	35° C/W	—	—
.4	4.5 GHz	40	—	3.5V	200mA	—	25° C/W	—	—
.4	4.5 GHz	40	—	3.5V	200mA	—	25° C/W	—	—
.2	5 GHz	40	—	3.5V	200mA	—	25° C/W	—	—
.2	5 GHz	40	—	3.5V	200mA	—	25° C/W	—	—
.1	5 GHz	40	—	3.5V	100mA	—	45° C/W	—	—
.1	5 GHz	40	—	3.5V	100mA	—	45° C/W		
1	2.7 GHz	45	—	3.5V	300mA	—	17° C/W	—	—
.6	3.5 GHz	45	—	3.5V	200mA	—	35° C/W	—	—
2	4.3 GHz	40	—	3.5V	500mA	—	10° C/W	—	—

Oscillator Bipolar Transistors

Part Number	Package Type or Chip	Package Configuration	Manufacturer's Remarks	I_C	V_{CE}	Peak Ft.	C_{CB} at V_{CB}	Test Frequency
516	MF-8	Common Collector Micro Stripline	—	100	20	5 GHz	—	5
416	MF-8	Common Collector Micro Stripline	—	200	20	5 GHz	—	5
517	MF-7	Common Collector Micro Stripline	—	100	20	5 GHz	—	5
417	MF-7	Common Collector Micro Stripline	—	200	20	5 GHz	—	5
919	MF-6	Common Emitter Coax	—	200	20	7.5GHz	—	7
999001	MF- 9	.200 SOE Common Base	—	150 mA	20	3.5GHz	3pF @ 20V	2.3
999002	MF- 9	.200 SOE Common Emitter	—	150 mA	20	3.5GHz	3pF @ 20V	2.3
914001	MF-14	.280 SOE Common Emitter	Gain, in dB 10	—	—	2 GHz	3.5pF @ 20V	1
2001	MF- 2	.250 FLG. Hermetic Common Base	For Class C 10	—	—	3 GHz	3pF @ 28V	2
2003	MF- 2	.250 FLG. Hermetic Common Base	Unmatched 10.5	—	—	3 GHz	4.5pF @ 28	2
2005	MF- 2	.250 FLG. Hermetic Common Base	Bipolars 9.8	—	—	3 GHz	7pF @ 28	2
2010	MF- 2	.250 FLG. Hermetic Common Base	9.0	—	—	3 GHz	11pF @ 28	2
2301	MF- 2	.250 FLG. Hermetic Common Base	10	—	—	3 GHz	3pF @ 22	2.3
2302	MF- 2	.250 FLG. Hermetic Common Base	9.5	—	—	3 GHz	3pF @ 22	2.3
2304	MF- 2	.250 FLG. Hermetic Common Base	8.5	—	—	3 GHz	5pF @ 22	2.3
2307	MF- 2	.250 FLG. Hermetic Common Base	8.2	—	—	3 GHz	8pF @ 22	2.3
3000	MF- 2	.250 FLG. Hermetic Common Base	7	—	—	3.5GHz	2.5pF @ 28	3
3001	MF- 2	.250 FLG. Hermetic Common Base	7	—	—	3.5GHz	3pF @ 28V	3
3003	MF- 2	.250 FLG. Hermetic Common Base	5	—	—	3.5GHz	4.5pF @ 28	3
3005	MF- 2	.250 FLG. Hermetic Common Base	5	—	—	3.5GHz	7pF @ 28	3
4000	MF- 2	.250 FLG. Hermetic Common Base	5	—	—	4.5GHz	25pF @ 28	4
4001	MF- 2	.250 FLG. Hermetic Common Base	5	—	—	4.5GHz	3pF @ 28	4
MOTOROLA								
MRF905	TO-46	Metal Can	—	100	10	2.5	3.0 @ 20	1.68
BFW92A	Plastic Macro-T	T-Pack	—	35	10	4.5	.5 @ 10	2.205
MRF534	TO-18	Metal Can (PNP)	—	20	10	5.5	.7 @ 5	2.200
MRF911	Plastic Macro-X	SOE	—	30	12	5.0	.6 @ 10	1.030
MRF1015MA	—	Micro 280 Stud	—	400	21	—	5.0 @ 21	1.500
MRF1150MA	—	Micro 280 Stud	Pulsed Power Oscillator	4000	50	—	25 @ 50	1.090
MICROWAVE SEMICONDUCTOR								
MSC85470	Hermetic	Coax C/S 077	Geometry: Site Ballasted Overlay	—	21V	—	2.5 @ 28V	2000MHz
MSC85920	Hermetic	Coax C/S 077	—	—	28V	—	3.0 @ 28V	2000MHz
MSC85853	Hermetic	Coax C/S 077	—	—	21V	—	25 @ 28V	3000MHz
MSC85854	Hermetic	Coax C/S 077	—	—	21V	—	3.5 @ 28V	3000MHz
MSC85204	Hermetic	Stripac™ C/S 091	Geometry: All Metal, Site Ballasted Overlay	—	21V	—	4.0 @ 28V	2700 MHz
MSC85205	Hermetic	Stripac™ C/S 091	—	—	21V	—	7.0 @ 28V	2700MHz
MSC85206	Hermetic	Stripac™ C/S 091	—	—	21V	—	10.0 @ 28V	2700MHz
MSC85221	Hermetic	Stripac™ C/S 091	—	—	21V	—	3.5 @ 28V	4300MHz
NEC CORPORATION								
NE21987	87	Ceramic Flangless-Hermetic	—	20	8	8.0	.4 @ 10V	6.0
NE243 Series								
NE243187	87	Ceramic Flangless- Hermetic	—	80	12	8.5	.65 @ 10V	7.5
NE243188	88	Ceramic Flange-Hermetic	—	80	12	8.5	.65 @ 10V	7.5
NE243287	87	Ceramic Flange-Hermetic	—	120	12	8.5	.95 @ 10V	7.5
NE243288	88	Ceramic Flange-Hermetic	—	120	12	8.5	.95 @ 10V	7.5
NE243499	99	Ceramic Flange-Hermetic	—	200	12	8.5	2.9 @ 10V	7.5
NE33387	87	Ceramic Flange-Hermetic	—	100	6	4.5	1.5 @ 10V	4.0
NE56787	87	Ceramic Flange-Hermetic	—	30	10	6.7	.18 @ 10V	7.5
NE56887	87	Ceramic Flange-Hermetic	—	80	10	4.2	.55 @ 10V	6.0
NE56987	87	Ceramic Flange-Hermetic	—	150	12	—	1.5 @ 10V	6.0
NE575 Series								
NE57510	10	TO-46 Metal Can	—	100	10	2.0	3.0 @ 10V	1.7

Power Output	Maximum Usable Frequency	Absolute Maximum Ratings						Price Quantity	
		V_{CBO}	V_{CEO}	V_{EBO}	I_C	Pt.	Rth.	1-100	1000
.1	5 GHz	40	—	3.5V	100mA	—	40° C/W	—	—
.2	5 GHz	40	—	3.5V	200mA	—	25° C/W	—	
.1	5 GHz	40	—	3.5V	100mA	—	40° C/W	—	—
.2	5 GHz	40	—	3.5V	200mA	—	25° C/W	—	—
.1	7.5 GHz	40	—	3.5V	200mA	—	25° C/W	—	—
.6	3 GHz	45	20	3.5V	200mA	—	25° C/W	—	—
.6	3 GHz	45	20	3.5V	200mA	—	25° C/W	—	—
1	1.5 GHz	45	—	3.5V	200mA	—	25° C/W	—	—
1	2.3 GHz	45	—	3.5V	200mA	—	25° C/W	—	—
3	2.3 GHz	45	—	3.5V	400mA	—	17° C/W	—	—
5	2.3 GHz	45	—	3.5V	700mA	—	8.5° C/W	—	—
10	2.3 GHz	45	—	3.5V	1.5A	—	5° C/W	—	—
1	2.7 GHz	40	—	3.5V	300mA	—	35° C/W	—	
1.75	2.7 GHz	40	—	3.5V	300mA	—	35° C/W	—	—
3.5	2.7 GHz	40	—	3.5V	600mA	—	17° C/W	—	—
6.5	2.7 GHz	40	—	3.5V	1.2A	—	8.5° C/W	—	—
.5	3.5 GHz	45	—	3.5V	100mA	—	45° C/W	—	—
1	3.5 GHz	45	—	3.5V	200mA	—	25° C/W	—	—
2.5	3.5 GHz	45	—	3.5V	400mA	—	17° C/W	—	—
4.5	3.5 GHz	45	—	3.5V	700mA	—	8.5° C/W	—	—
.5	4.3 GHz	45	—	3.5V	100mA	—	45° C/W	—	—
1	4.3 GHz	45	—	3.5V	200mA	—	25° C/W	—	—
.5	—	35	20	3.5	150	2.5	40	2.55	—
.004	2205 to 2235	25	15	3.5	35	.18	250	1.15	—
.01	2200 to 2300	15	10	4.5	30	.3	583	2.07	—
.01	1030 to 1190	20	12	30	40	.4	250	1.74	—
3.0	—	60	—	4.0	1.0	17.5	10	31.05	—
75.0	—	70	—	4.0	12.0	583	.3	51.75	—
0.6W	—	50V	—	3.5V	—	—	35° C/W	—	—
1.3W	—	50V	—	3.5V	—	—	30° C/W	—	—
0.6W	—	45V	—	3.5V	—	—	35° C/W	—	—
1.1W	—	45V	—	3.5V	—	—	30° C/W	—	—
0.8W	—	40V	—	3.5V	—	—	25° C/W	—	—
1.6W	—	40V	—	3.5V	—	—	12.5°C/W	—	—
2.0W	—	40V	—	3.5V	—	—	8.5°C/W	—	—
0.3W	—	40V	—	3.5V	—	—	25° C/W	—	—
0.1W	—	20	10	1.5	80	0.7	70	—	—
0.15W	—	25	16	1.5V	110	2.75	45	—	—
0.15W	—	25	16	1.5V	110	2.75	45	—	—
0.32W	—	25	16	1.5V	220	5.5	30	—	—
0.32W	—	25	16	1.5V	220	5.5	30	—	—
0.63W	—	25	16	1.5V	440	9.7	18	—	—
0.4W	—	28	14	3.0V	200	5.0	35	—	—
.141W	—	25	12	2.0V	40	0.6	40	—	—
0.2W	—	25	15	1.5V	150	1.5	40	—	—
0.30W	—	25	15	2.0V	300	4.5	35	—	—
0.7W	—	40	20	3.0V	250	4.4	40	—	—

Oscillator Bipolar Transistors

Part Number	Package Type or Chip	Package Configuration	Manufacturer's Remarks	I_C	V_{CE}	Peak Ft.	C_{CB} at V_{CB}	Test Frequency
NE57520	20	Stripline Stud	—	100	10	2.0	4.0 @ 10V	1.7
NE643 Series								
NE64310	10	TO-46 Metal Can	—	70	10	2.0	2.0 @ 10V	2.0
NE64320	20	Stripline Stud	—	70	10	2.0	2.5 @ 10V	2.0
NE64587	87	Ceramic Flange-Hermetic	—	7	8	8.5	0.2 @ 10V	6.0
NE77310	10	TO-46 Metal Can	—	100	10	2.5	2.8 @ 10V	2.3
NEX2300 Series								
NEX2301	87	Ceramic Flange-Hermetic	—	—	—	—	2.5 @ 20V	2.3
NEX2301	64, 65	Ceramic Flange or Flangless-Hermetic	—	—	—	—	2.5 @ 20V	2.3
NEX2302	64, 65	Ceramic Flange or Flangless-Hermetic	—	—	—	—	3.7 @ 20V	2.3
NEX2303	64, 65	Ceramic Flange or Flangless-Hermetic	—	—	—	—	6.2 @ 20V	2.3

Unmatched Linear Power Bipolar Transistor (Class A)

Part Number	Package Type or Chip	Package Configuration	Manufacturer's Remarks	I_c	V_{CE}	Peak Ft.	C_{CB} at V_{CE}	1 GHz	
								S_{21} Gain	MAG
ACRIAN									
UTV-005	—	¼″ stud	Notes:	220mA	20V	2.4	3@20	—	—
UTV-010	—	¼″ stud	1. Selection includes	440mA	20V	2.4	7@20	—	—
UTV-020	—	¼″ stud	matched and balanced	440mA	25V	2.4	6@25	—	—
UTV-040	—	¼″ stud	transistors	650mA	25V	2.4	12@25	—	—
UTV-080	—	4-lead balanced	2. Figures in 4GHz block	850x2	26.5V	1.4	15@26.5	—	—
UTV-120	—	8-lead balanced	are 2-GHz ratings	1000x2	26.5V	1.4	23@26.5	—	—
UTVA PM10	—	Module	3. 1.5-30MHz linear	1600mA	26.5V	—	—	—	—
UTVA PM20	—	Module	devices:	3400mA	26.5V	—	—	—	—
UTVA PM30	—	Module	I_c is max Amps;	—	—	—	—	—	—
UTVA PM60	—	Module	V_{CE} is V_{CC} Volts;	—	—	—	—	—	—
10A015	—	—	Peak Ft. is P_{out} Watts	220mA	20V	3.0	3.8pF@28V	—	—
10A030	—	—	C_{CB} is pF	440mA	20V	3.0	6.4pF@28V	—	—
10A045	—	—	4. 1-5-30MHz linear	660mA	20V	3.0	8.9pF@28V	—	—
10A060	—	—	devices are rated for	880mA	20V	3.0	10.8pF@28V	—	—
10A022	—	—	the following electrical	300mA	20V	2.2	5.0pF@28V	—	—
20A015	—	—	characteristics, not max	220mA	20V	3.0	4.2pF@28V	—	—
20A030	—	—	ratings, in far right	440mA	20V	3.0	6.8pF@28V	—	—
20A045	—	—	columns:	660mA	20V	3.0	10.0pF@28V	—	—
20A060	—	—	for V_{CBO}, read BV_{CES}	880mA	20V	3.0	12pF@28V	—	—
			for V_{CEO}, read BV_{CEO}						
			for V_{EBO}, read BV_{EBO}.						
S15-12	G04	380 SOE flange	1.5-30MHz linear	4A	12V	15	60	—	—
S25-12	G04	380 SOE flange	1.5-30MHz linear	8A	12V	25	120	—	—
S50-12	H03	500 SOE flange	1.5-30MHz linear	13A	12V	50	200	—	—
S70-12	H03	500 SOE flange	1.5-30MHz linear	22A	12V	70	400	—	—
S100-12	H03	500 SOE flange	1.5-30MHz linear	50A	12V	100	400	—	—
S15-28	G04	380 SOE flange	1.5-30MHz linear	2A	28V	15	20	—	—
S30-28	G04	380 SOE flange	1.5-30MHz linear	4A	28V	30	40	—	—
H50-28	H03	500 SOE flange	1.5-30MHz linear	10A	28V	50	135	—	—
H100-28	H03	500 SOE flange	1.5-30MHz linear	20A	28V	100	270	—	—
S175-28	H03	500 SOE flange	1.5-30MHz linear	30A	28V	175	400	—	—
S25-50	H03	500 SOE flange	1.5-30MHz linear	5A	50V	25	55	—	—
H100-50	H03	500 SOE flange	1.5-30MHz linear	10A	50V	100	95	—	—
H175-50	H03	500 SOE flange	1.5-30MHz linear	20A	5V	175	180	—	—
S200-50	H03	500 SOE flange	1.5-30MHz linear	30A	50V	200	300	—	—
S250-50	J11	Flange	1.5-30MHz linear	30A	50V	250	300	—	—
BP8-12	TO-220	—	C_{CB} is C_{OB}	2.5A	12.5V	.7GHz	24pF@12.5V	—	—
BP15-12	TO-220	—	—	4.0A	12.5V	.7GHz	65pF@12.5V	—	—
BP30-12	TO-220	—	—	8.0A	12.5V	.7GHz	110pF@12.5V	—	—
BP30-12L	TO-220	—	—	8.0A	12.5V	.7GHz	110pF@12.5V	—	—
CP5-12	TO-220	—	—	2.0A	12.5V	1.5GHz	15pF@12.5V	—	—
CP10-12	TO-220	—	—	2.5A	12.5V	1.5GHz	25pF@12.5V	—	—
CMP18-12	TO-220	—	—	5.0A	12.5V	1.5GHz	50pF@12.5V	—	—
UMOB55	H04	6 lead flange	—	9.0A	12.5V	1.5GHz	—	—	—
8MOB15E	C05	6 lead flange	—	8.5A	12.5V	2.5GHz	—	—	—
8MOB25	C05	6 lead flange	—	12.0A	12.5V	2.5GHz	—	—	—
9BSE2	E04	Stud	—	.75A	12.5V	2.5GHz	5pF@12.5V	—	—
9BSE10	C05	6 lead flange	—	3.0A	12.5V	2.5GHz	9pF@12.5V	—	—
9BSE35	C05	6 lead flange	—	6.0A	12.5V	2.5GHz	36pF@12.5V	—	—
9BSE55	C11	6 lead flange	—	18A	12.5V	2.5GHz	50pF@12.5V	—	—
FM150	H13	½″ offset flange	—	—	28V	0.7GHz	105pF@28V	—	—
FM175	TRB60	6 lead flange	—	—	28V	0.7GHz	105pF@28V	—	—

Power Output	Maximum Usable Frequency	Absolute Maximum Ratings V_{CBO}	V_{CEO}	V_{EBO}	I_C	Pt.	Rth.	Price Quantity 1-100	1000
0.7W	—	40	20	3.0V	250	7.5	20	—	—
0.3W	—	40	20	3.0V	150	2.0	70	—	—
0.5W	—	40	20	3.0V	150	4.3	40	—	—
0.11W	—	25	12	3.0V	65	400	75	—	—
1.2W	—	35	18	3.0V	450	4.4	40	—	—
1.3W	—	45	20	3.0V	600	7.0	25	—	—
1.6W	—	45	20	3.0V	600	11	16	—	—
2.0W	—	45	20	3.0V	1100	18	10	—	—
3.2W	—	45	20	3.0V	2000	29	60	—	—

1 GHz				4 GHz						Absolute Maximum Ratings						Price Quantity	
MSG (if k<1)	P-1dB	G-1dB	Power Added Efficiency	S_{21} Gain	MAG	MSG (if k<1)	P-1dB	G-1dB	Power Added Efficiency	V_{CBO}	V_{CEO}	V_{EBO}	I_C	Pt.	Rth.	1-100	1000
—	—	—	—	—	—	—	—	—	—	45	25	3.5	0.75A	8.8W	20	—	—
—	—	—	—	—	—	—	—	—	—	45	25	3.5	1.5A	17W	10	—	—
—	—	—	—	—	—	—	—	—	—	45	25	4	1.5A	19W	9	—	—
—	—	—	—	—	—	—	—	—	—	45	25	4	2.5A	30W	5	—	—
—	—	—	—	—	—	—	—	—	—	45	28	4	6A	75W	2.3	—	—
—	—	—	—	—	—	—	—	—	—	45	28	4	7A	80W	2.2	—	—
—	—	—	—	—	—	—	—	—	—	—	—	—	—	—	—	—	—
—	—	—	—	—	—	—	—	—	—	—	—	—	—	—	—	—	—
—	—	—	—	—	—	—	—	—	—	—	—	—	—	—	—	—	—
—	1.5	9.0	—	—	—	—	—	—	—	—	—	—	—	—	—	—	—
—	3.0	8.5	—	—	—	—	—	—	—	45	24	3.5	0.75A	6	16	—	—
—	4.5	8.0	—	—	—	—	—	—	—	45	24	3.5	1.5A	12W	8.5	—	—
—	6.0	8.0	—	—	—	—	—	—	—	45	24	3.5	2.25A	17W	7.0	—	—
—	—	—	—	—	—	—	—	—	—	45	24	3.5	3.0A	21W	6.0	—	—
—	—	—	—	—	—	—	—	—	—	45	24	3.5	1.125A	9W	12	—	—
—	—	—	—	—	—	—	1.5	6.0	—	45	24	3.5	0.75A	6W	16	—	—
—	—	—	—	—	—	—	3.0	6.0	—	45	24	3.5	1.5A	12W	8.5	—	—
—	—	—	—	—	—	—	4.5	5.5	—	45	24	3.5	2.25A	17W	7.0	—	—
—	—	—	—	—	—	—	6.0	5.0	—	45	24	3.5	3.0A	21W	6.0	—	—
—	—	—	—	—	—	—	—	—	—	36	18	4	—	—	—	—	—
—	—	—	—	—	—	—	—	—	—	36	18	4	—	—	—	—	—
—	—	—	—	—	—	—	—	—	—	36	16	3.5	—	—	—	—	—
—	—	—	—	—	—	—	—	—	—	36	16	4	—	—	—	—	—
—	—	—	—	—	—	—	—	—	—	36	16	4	—	—	—	—	—
—	—	—	—	—	—	—	—	—	—	60	33	4	—	—	—	—	—
—	—	—	—	—	—	—	—	—	—	60	33	4	—	—	—	—	—
—	—	—	—	—	—	—	—	—	—	70	33	4	—	—	—	—	—
—	—	—	—	—	—	—	—	—	—	70	33	4	—	—	—	—	—
—	—	—	—	—	—	—	—	—	—	60	33	3.5	—	—	—	—	—
—	—	—	—	—	—	—	—	—	—	110	65	4	—	—	—	—	—
—	—	—	—	—	—	—	—	—	—	110	64	4	—	—	—	—	—
—	—	—	—	—	—	—	—	—	—	110	64	4	—	—	—	—	—
—	—	—	—	—	—	—	—	—	—	110	65	4	—	—	—	—	—
—	—	—	—	—	—	—	—	—	—	110	53	4	—	—	—	—	—
—	—	—	—	—	—	—	—	—	—	36	18	4	2.5	25	—	—	—
—	—	—	—	—	—	—	—	—	—	36	18	4	4.0	30	—	—	—
—	—	—	—	—	—	—	—	—	—	36	18	4	8.0	65	—	—	—
—	—	—	—	—	—	—	—	—	—	36	18	4	8.0	65	—	—	—
—	—	—	—	—	—	—	—	—	—	36	18	4	2.0	18	—	—	—
—	—	—	—	—	—	—	—	—	—	36	18	4	2.5	35	—	—	—
—	—	—	—	—	—	—	—	—	—	36	16	4	5.0	67	—	—	—
—	—	—	—	—	—	—	—	—	—	36	16	4	9.0	125	—	—	—
—	—	—	—	—	—	—	—	—	—	36	16	4	8.5	75	3	—	—
—	—	—	—	—	—	—	—	—	—	36	16	4	12	75	3	—	—
—	—	—	—	—	—	—	—	—	—	45	27	3.5	.75	8	—	—	—
—	—	—	—	—	—	—	—	—	—	50	28	4.0	3	27	—	—	—
—	—	—	—	—	—	—	—	—	—	50	30	4	6	100	—	—	—
—	—	—	—	—	—	—	—	—	—	45	26	4	16	145	—	—	—
—	—	—	—	—	—	—	—	—	—	60	25	4	16	165	1	—	—
—	—	—	—	—	—	—	—	—	—	65	33	4	16	190	0.9	—	—

Unmatched Linear Power Bipolar Transistor (Class A)

Part Number	Package Type or Chip	Package Configuration	Manufacturer's Remarks	I_C	V_{CE}	Peak Ft.	C_{CB} at V_{CE}	1 GHz S_{21} Gain	1 GHz MAG
VTV-075	H07	6 lead flange	—	1.2A	25V	1.3GHz	35pF@25V	—	—
VTV-150	H07	6 lead flange	—	2.4A	25V	1.25GHz	68pF@25V	—	—
VTV-300	H07	6 lead flange	—	5A	25V	1.05GHz	135pF@25V	—	—
AVANTEK									
AT-42035	Micro-x	Stripline	High gain	35	8	9GHz	.30 pF	17dB	21
AT-42070	70 mil	Stripline	High gain	35	8	9GHz	.25	18	—
AT-42010	100 mil	Stripline	High gain, new product	35	8	9GHz	.30 pF	17	—
AT-64020	200 mil	BeO disc	Ballasted, new product	110	10	7GHz	.8 pF	12	—
AT-52670	70 mil	Stripline	Ballasted, new product	45	10	7GHz	.45 pF	16	—
AT-52620	200 mil	BeO disc	Ballasted, new product	45	10	7GHz	.5 pF	16	—
FUJITSU									
FJ9203	BB, CC, DD	Common emitter	Peak Ft. in GHz; figures in 4GHz block are 2-3 GHz ratings	60	18	4.0GHz	2.5 (max)	12.5	20
FJ9208	BB, CC, DD	Common emitter	—	100	18	4.0GHz	2.5 (max)	11.5	20
FJ9215	BB, CC, DD	Common emitter	—	220	18	4.0GHz	3.5 (max)	9.5	17
FJ9225	BB, CC, DD	Common emitter	—	380	18	4.0GHz	5 (max)	6.2	15.5
FJ9235	BB, CC	Common emitter	—	700	18	3.6GHz	9 (max)	1.4	—
HEWLETT-PACKARD									
HXTR-3002	Chip	—	Linear power transistor chip with large bonding pads	30mA	18V	—	—	14.0	—
HXTR-5001	Chip	—	Linear power transistor chip	30mA	18V	—	—	15.0	—
HXTR-5002	Chip	—	Linear power transistor	110mA	18V	—	—	13.7	—
HXTR-3102	85 mil	Common emitter	Low cost general purpose linear power transistor	30mA	15V	—	—	12.7	—
HXTR-5101	100 mil	Common emitter	Linear power transistor	30mA	18V	—	—	5.1	—
HXTR-5102	200 mil (bar)	Common emitter	Linear power transistor	110mA	18V	—	—	11.8	—
HXTR-5103	200 mil	Common emitter	Linear power transistor	30mA	18V	—	—	13.8	—
HXTR-5104	200 mil	Common emitter	Linear power transistor	110mA	18V	—	—	11.5	—
INTERNATIONAL MICROWAVE DEVICES									
995002	MF-5	.250 4L isolated stud hermetic	2GHz .5W 8dB gain	120	20	3GHz	—	—	—
995003	MF-5	.250 4L isolated stud hermetic	2GHz 1.0W 7dB gain	220	18	3GHz	—	—	—
995004	MF-5	.250 4L isolated stud hermetic	2GHz 1.5W 6dB gain	360	18	3GHz	—	—	—
604HA	MF-2	.250 flange hermetic	2GHz .5W 8db gain	120	20	3GHz	—	—	—
604HB	MF-2	.250 flange hermetic	2GHz 1.0W 7dB gain	220	18	3GHz	—	—	—
604HC	MF-2	.250 flange hermetic	2GHz 1.5W 6dB gain	360	18	3GHz	—	—	—
NEC CORPORATION									
NEL0800 Series		—	Figures in 4GHz block are 2-3GHz ratings; P-1dB in Watts	—	—	—	—	—	—
NE080120	20	Stripline stud	—	200mA	24V	—	2.0	—	—
NE080220	20	Stripline stud	—	400mA	24V	—	4.0	—	—
NE080525	25	Stripline stud	—	600mA	24V	—	8.0	—	—
NEL2301 Series		—	—	—	—	—	—	—	—
NEL230100	Chip	Chip	—	200mA	15V	2.4	—	—	—
NEL230120	20	Stripline stud	—	200mA	15V	2.4	1.2	—	—
NEL230153	53E	Ceramic flange	Hermetic	200mA	15V	2.4	1.2	—	—
NEL230157	57E	Ceramic flangeless	Hermetic	200mA	15V	2.4	1.2	—	—
NEL230197	97	Ceramic stud	Hermetic	200mA	15V	2.4	1.2	—	—
NEL2302 Series		—	—	—	—	—	—	—	—
NEL230200	Chip	Chip	—	350mA	15V	2.4	2.4	—	—
NEL230220	20	Stripline stud	—	350mA	15V	2.4	2.4	—	—
NEL230253	53E	Ceramic flange	Hermetic	350mA	15V	2.4	2.4	—	—
NEL230257	57E	Ceramic flangeless	Hermetic	350mA	15V	2.4	2.4	—	—
NEL230297	97	Ceramic stud	Hermetic	350mA	15V	2.4	2.4	—	—
NEL2303 Series		—	—	—	—	—	—	—	—
NEL230320	20	Stripline stud	—	600mA	15V	2.4	5.0	—	—
NEL230353	53E	Ceramic flange	Hermetic	600mA	15V	2.4	5.0	—	—
NEL230357	57E	Ceramic flangeless	Hermetic	600mA	15V	2.4	5.0	—	—
NEL230397	97	Ceramic stud	Hermetic	600mA	15V	2.4	5.0	—	—
NEL1300 Series		—	—	—	—	—	—	—	—
NEL130681-12	81	Ceramic flange	—	—	—	1.3GHz Band	—	—	—
NEL132081-12	81	Ceramic flange	—	—	—	1.3GHz Band	—	—	—
TOSHIBA									
S8807	Package	5.8mm Hermetic, flange	—	0.15A	12V	4.0GHz	6.0pF	3.5dB	12dB

1 GHz				4 GHz						Absolute Maximum Ratings						Price Quantity	
MSG (if k<1)	P-1dB	G-1dB	Power Added Efficiency	S_{21} Gain	MAG	MSG (if k<1)	P-1dB	G-1dB	Power Added Efficiency	V_{CBO}	V_{CEO}	V_{EBO}	I_C	Pt.	Rth.	1-100	1000
—	—	—	—	—	—	—	—	—	—	45	28	4	4	53	3.3	—	—
—	—	—	—	—	—	—	—	—	—	45	28	4	8	97	1.8	—	—
—	—	—	—	—	—	—	—	—	—	45	28	4	14	146	1.2	—	—
—	20dBm	19	40%	5dB	10.5	—	19dBm	9.5	35%	20	12	1.5	80mA	600mW	275°C/W	—	—
23	20dBm	19	40%	6dB	11	—	19dBm	9.5	35%	20	12	1.5	80mA	600mW	275°C/W	—	—
23	20dBm	19	40%	6dB	11	—	19dBm	9.5	35%	20	12	1.5	80mA	600mW	275°C/W	—	—
19	29dBm	14	40%	0.0	7	—	26dBm	5.5	30%	25	18	2.0	150mA	2500mW	150°C/W	—	—
23	22.5dBm	15	40%	4dB	9	—	22dBm	7.5	30%	20	12	1.5	100mA	900mW	275°C/W	—	—
23	22.5dBm	15	40%	4dB	9	—	22dBm	7.5	30%	20	12	1.5	100mA	1100mW	200°C/W	—	—
—	—	—	—	5.5	12	—	2.5	10	—	30	20	3.5	.15	2.5	35	—	—
—	—	—	—	5.5	11.7	—	28.5	9.5	—	35	22	3.5	.25	3.0	25	—	—
—	—	—	—	1.7	10.2	—	31.8	8.0	—	35	22	3.5	.50	6.0	12	—	—
—	—	—	—	−2.3	7.2	—	34	6.0	—	35	22	3.5	.80	10	8	—	—
—	—	—	—	−6.0	6.5	—	35.5	5.5	—	35	22	3.0	1.5	22	7	—	—
17.2	22.0	18.0	29%	—	—	—	—	—	—	45V	27V	4V	100mA	1.4W	—	—	—
19.0	23.0	—	—	5.8	8.5	—	22.0	8.0	—	45V	27V	4V	100mA	1.4W	—	—	—
29.0	—	—	—	2.1	10.0	—	27.5	7.5	—	45V	27V	4V	250mA	4W	—	—	—
17.0	21.0	11.5	—	2.7	10.0	—	20.5	6.0	—	35V	25V	3.5V	100mA	700mW	—	5.00	4.40
18.5	23.0	16.0	—	3.5	8.0	—	22.0	7.5	—	45V	27V	4V	100mA	1.1W	—	—	—
18.0	29.0	14.0	—	2.8	8.0	—	27.5	7.0	—	45V	27V	4V	250mA	4W	—	—	—
18.5	23.0	15.5	—	3.7	8.0	—	22.0	6.5	—	45V	27V	4V	100mA	1.4W	—	—	—
16.5	28.5	14.0	—	0.9	8.5	—	27.5	4.0	—	45V	27V	4V	250mA	4W	—	—	—
—	—	—	—	—	—	—	—	—	—	45	20	3.5	120	.5	35°C/W	—	—
—	—	—	—	—	—	—	—	—	—	45	20	3.5	220	1.0	17°C/W	—	—
—	—	—	—	—	—	—	—	—	—	45	20	3.5	360	1.5	8.5°C/W	—	—
—	—	—	—	—	—	—	—	—	—	45	20	3.5	120	.5	35°C/W	—	—
—	—	—	—	—	—	—	—	—	—	45	20	3.5	220	1.0	17°C/W	—	—
—	—	—	—	—	—	—	—	—	—	45	20	3.5	360	1.5	8.5°C/W	—	—
—	—	—	—	—	—	—	—	—	—	—	—	—	—	—	—	—	—
—	1.2	11	—	—	—	—	—	—	—	50	30	3.0	1A	12W	15	—	—
—	2.4	9.8	—	—	—	—	—	—	—	50	30	3.0	2A	17.5W	10	—	—
—	4.8	10.8	—	—	—	—	—	—	—	50	30	3.0	4A	32W	55	—	—
—	—	—	—	—	—	—	—	—	—	—	—	—	—	—	—	—	—
—	—	—	—	—	—	—	1.1	7.5	—	45	20	3.0	0.6A	11W	16	—	—
—	—	—	—	—	—	—	1.1	6.0	—	45	20	3.0	0.6A	11W	16	—	—
—	—	—	—	—	—	—	1.1	7.5	—	45	20	3.0	0.6A	11W	16	—	—
—	—	—	—	—	—	—	1.1	7.5	—	45	20	3.0	0.6A	11W	16	—	—
—	—	—	—	—	—	—	1.1	7.5	—	45	20	3.0	0.6A	11W	16	—	—
—	—	—	—	—	—	—	—	—	—	—	—	—	—	—	—	—	—
—	—	—	—	—	—	—	1.9	6.5	—	45	20	3.0	1.1A	18W	10	—	—
—	—	—	—	—	—	—	1.9	5.0	—	45	20	3.0	1.1A	18W	10	—	—
—	—	—	—	—	—	—	1.9	6.5	—	45	20	3.0	1.1A	18W	10	—	—
—	—	—	—	—	—	—	1.9	6.5	—	45	20	3.0	1.1A	18W	10	—	—
—	—	—	—	—	—	—	1.9	6.5	—	45	20	3.0	1.1A	18W	10	—	—
—	—	—	—	—	—	—	—	—	—	—	—	—	—	—	—	—	—
—	—	—	—	—	—	—	2.8	4.5	—	45	20	3.0	2.0A	29W	6.0	—	—
—	—	—	—	—	—	—	2.8	6.0	—	45	20	3.0	2.0A	29W	6.0	—	—
—	—	—	—	—	—	—	2.8	6.0	—	45	20	3.0	2.0A	29W	6.0	—	—
—	—	—	—	—	—	—	2.8	6.0	—	45	20	3.0	2.0A	29W	6.0	—	—
—	—	—	—	—	—	—	—	—	—	—	—	—	—	—	—	—	—
—	1.0	7.5	—	—	—	—	—	—	—	35	18	3	2A	19.5W	9	—	—
—	1.0	6.0	—	—	—	—	—	—	—	35	18	3	6A	50W	3.5	—	—
—	9	—	25%	—	—	—	—	—	—	50V	20V	3.5V	0.3A	12W	15°C/W	—	—

Low Noise and High Gain Bipolar Transistor (typical performance)

Part Number	Package Type or Chip	Package Configuration	Manufacturer's Remarks	I_C	V_{CE}	Minimum Noise Operation: 0.1 GHz NF dB	0.1 GHz G_A dB	1 GHz NF dB	1 GHz G_A dB	2 GHz NF dB	2 GHz G_A dB	4 GHz NF dB	4 GHz G_A dB	NF with 50 Ω Input/Output and S_{21} at 1 GHz
AVANTEK						@ 0.5 GHz								
AT-41435-3	micro X	stripline	Low noise, Low cost	10mA	8V	—	—	1.3	19.0	1.6	14.0	3.0	10.0	1.3/17
AT-41470	70 mil	stripline	Very low noise, High gain	10	8	—	—	1.3	19.0	1.6	14.0	3.0	10.5	1.3/17
AT-41410	100 mil	stripline	Very low noise, High gain	10	8	—	—	1.3	19.0	1.6	14.0	3.0	10.0	1.3/17
AT-60570	70 mil	stripline	High S21 gain New product replaces AT-4680	4	8	—	—	1.1	19.5	1.4	14	2.7	10	/18
AT-60510	100 mil	stripline	High S21 gain New product replaces AT-4880	4	8	—	—	1.1	19.5	1.4	14	2.7	9.5	/18
AT-42072	TO-72	can	New product	15	8	1.5	21	1.7	15	3.0	8.0	—	—	—
AT-41472	TO-72	can	New product replaces AT-0045	10	8	1.2	22	1.5	17	3.0	9.0	—	—	—
AT-100535	micro X	stripline	General purpose, Low cost New product	5	10	—	—	2.4	13	3.6	9.0	8	—	—
AT-41435-5	micro X	stripline	High gain, low cost	10	8	—	—	—	—	—	—	3.1	10.0	—
AT-100570	70 mil	stripline	General purpose New product	5	10	—	—	2.4	13	3.6	9.0	—	—	—
AT-100510	100 mil	stripline	General purpose New product replaces AT-1825	5	10	—	—	2.4	13	3.6	9.0	—	—	—
AT-100572	TO-72	can	General purpose New product replaces AT-0025	5	10	2.0	15	2.5	10	—	—	—	—	—
AT-101670	70 mil	stripline	General purpose New product replaces AT-2615	10	10	—	—	—	—	3.5	8.5	4.5	6.0	—
AT-101610	100 mil	stripline	General purpose New product replaces At-2815	10	10	—	—	—	—	3.5	8.5	4.5	6.5	—
AT-101672	TO-72	can	General purpose New product replaces AT-0017	10	10	2.3	13	2.8	11	—	—	—	—	—
AT-101635	micro X	stripline	General purpose, Low cost New product replaces AT-00135	10	10	2.2	14	2.6	13	3.5	8.0	—	—	—
FUJITSU						@ 0.1 GHz								
FJ001A	TO-33	Combined emitter	General Purpose to 1GHZ	5	10	1.3	20	2.5	12	—	—	—	—	1.5/6.8dB
FJ001B	TO-72	Combined emitter	General Purpose to 1GHZ	5	10	1.3	20	2.5	12	—	—	—	—	1.5/6.8dB
FJ101	E	Combined emitter	Low Noise/Switching	5	6	—	—	3	13	—	—	—	—	—
FJ201	E, F	Combined emitter	Low Noise	3	6	—	—	2.8	13	4	8	—	—	—
FJ401	E, F, J	Combined emitter	Low Noise	3	8	—	—	—	—	—	—	3.5	6	—
FJ402	E, F, J	Combined emitter	Low Noise	3	8	—	—	—	—	—	—	2.7	8	—
FJ451	LE, J, E, X	Combined emitter	High Gain-Low Cost	5	12	—	—	—	—	—	—	4	7.5	—
FJ901	E, F, M, R	Combined emitter	Dual Switching Transistors	—	—	—	—	—	—	—	—	—	—	—
FJ951	E, DD	Combined emitter	General Purpose to 2 GHZ	—	—	—	—	—	—	—	—	—	—	—
FJ952	E, DD	Combined emitter	General Purpose to 2 GHZ	35	6	—	—	—	—	—	—	—	—	—
HEWLETT-PACKARD														
HXTR-2001	CHIP	—	General purpose transistor chip	7mA	10V	—	—	1.4	16.0	2.2	12.0	4.2	4.0	—
HXTR-3001	CHIP	—	General purpose transistor chip with large binding pads	7mA	10V	—	—	1.7	12.0	2.3	12.0	4.3	4.0	—
HXTR-6001	CHIP	—	Low noise transistor chip	4mA	10V	—	—	1.2	16.5	1.6	13.5	2.7	9.2	—
HXTR-7011	CHIP	—	Low noise transistor chip with large binding pads	10mA	10V	—	—	1.2	18.0	1.7	13.0	2.8	8.2	—
HXTR-2101	100 mil	Combined emitter	General purpose transistor	—	—	—	—	—	—	—	—	—	—	—
HXTR-2102	70 mil	Combined emitter	General purpose transistor	—	—	—	—	—	—	—	—	—	—	—
HXTR-3101	85 mil	Combined emitter	Low cost general purpose transistor	10mA	10V	—	—	1.8	15.5	—	—	—	—	—
HXTR-3103 (2N6838)	85 mil	Combined emitter	General purpose transistor	10mA	10V	—	—	1.7	16.0	2.3	11.0	4.2	8.5	2.1
HXTR-6101 (2N6617)	70 mil	Combined emitter	Low noise transistor	4mA	10V	—	—	1.4	17.5	1.8	13.2	2.8	7.5	—
HXTR-6102 (2N6742)	70 mil	Combined emitter	Low noise transistor	4mA	10V	—	—	1.2	17.5	1.6	13.2	2.5	7.5	—

Maximum Gain Operation								Peak S_{21} Gain at 1 GHz	F_{max} Extro-polated to MAG = 0 dB	Absolute Maximum Ratings						Price Quantity	
				1 GHz		4 GHz											
I_C	V_{CE}	Peak Ft.	C_{CB} at V_{CE}	MAG	MSG (if k < 1)	MAG	MSG (if k < 1)			V_{CBO}	V_{CEO}	V_{EBO}	I_C	Pt.	Rth.	1-100	1000
25	8	9GHz	0.2 pf	—	23	11	—	18 dB	15GHz	20	12	1.5	65mA	500mW	300°	—	—
25	8	9GHz	0.2	—	24	13	—	18 dB	20GHz	20	12	1.5	65mA	500mW	300°	—	—
25	8	9GHz	0.2	—	24	—	13	18 dB	15GHz	20	12	1.5	65mA	500mW	300°	—	—
10	8	9GHz	0.5	—	22	—	13	19 dB	20GHz	20	12	1.5	35mA	150mW	300°	—	—
10	8	9GHz	0.5	—	22	—	13	19 dB	15GHz	20	12	1.5	35mA	150mW	300°	—	—
35	8	9GHz	—	15	—	—	6	12 dB	8GHz	20	12	1.5	80mA	350mW	150°	—	—
25	8	9GHz	0.2	16	—	—	7	13 dB	10GHz	20	12	1.5	65mA	350mW	150°	—	—
15	10	6GHz	—	17	—	6	—	14 dB	8GHz	20	12	1.5	50mA	350mW	300°	—	—
25	8	8GHz	0.18	—	23	11.0	—	18 dB	12GHz	20	12	1.5	65mA	500mW	300°	—	—
15	10	6GHz	—	17	—	6	—	14 dB	8GHz	20	12	1.5	50mA	350mW	300°	—	—
15	10	6GHz	—	17	—	6	—	14 dB	8GHz	20	12	1.5	50mA	350mW	300°	—	—
15	10	6GHz	—	10	—	—	—	9 dB	6GHz	20	12	1.5	50mA	350mW	300°	—	—
35	10	6GHz	1.0	18	—	7	—	12 dB	10GHz	20	12	1.5	100mA	500mW	200°	—	—
35	10	6GHz	1.0	18	—	7	—	12dB	10GHz	20	12	1.5	100mA	500mW	200°	—	—
15	10	6GHz	0.8	9	—	—	—	7 dB	4GHz	20	12	1.5	100mA	300mW	200°	—	—
35	10	6GHz	0.8	17	—	7	—	12 dB	10GHz	20	12	1.5	100mA	300mW	200°	—	—
50	15	3.5	1.2	9	—	—	—	—	8	30	18	3	150	800	—	—	—
10	10	2.5	1.2	8	—	—	—	—	8	30	18	3	150	250	—	—	—
10	6	3	0.7	13	—	—	—	—	5	20	10	3	70	200	—	—	—
20	6	5.0	0.6	16	—	—	—	—	8.5	20	10	—	70	200	—	—	—
10	8	7.5	0.25	—	—	8.5	—	—	11	20	13	3	30	200	—	—	—
—	8	7	0.15	—	—	11	—	—	15	20	13	3	20	200	—	—	—
20	12	6.2	0.20	—	—	10.5	—	—	14	25	17	3	40	400	—	—	—
15	6	8.0	0.45	17.5	—	—	—	—	—	16	8	3	30	250	—	—	—
40	6	5.2	0.70	12	—	—	—	—	4	20	10	3	90	900	—	—	—
35	6	7.0	0.80	17	—	—	—	—	9	20	10	3	70	200	—	—	—
25mA	15V	—	—	24.0	—	—	—	—	7.5GHz	30V	20V	1.5V	70mA	900mW	—	—	—
15mA	15V	—	—	—	23.0	9.0	—	—	6.5GHz	30V	20V	1.5V	70mA	900mW	—	—	—
4mA	10V	—	—	—	—	12.5	—	—	10.0GHz	35V	20V	1.5V	20mA	300mW	—	—	—
10mA	10V	—	—	—	22.0	—	10.5	—	8.0GHz	30V	18V	1.5V	65mA	600mW	—	$6.35	5.30
25mA	15V	—	—	—	21.0	—	10.0	—	6.5GHz	30V	20V	1.5V	70mA	900mW	—	18.50	13.50
25mA	15V	—	—	—	21.5	—	11.0	—	10.0GHz	30V	20V	1.5V	70mA	900mW	—	—	—
15mA	10V	—	—	20.0	—	—	10.0	—	7.5GHz	30V	18V	1.5V	50mA	600mW	—	4.15	3.50
15mA	10V	7.0GHz	0.33 pf	20.0	—	—	—	—	8.5GHZ	30V	18V	1.5V	50mA	600mW	—	7.70	5.90
4mA	10V	—	—	—	—	12.5	—	—	9.0GHz	35V	20V	1.5V	20mA	300mW	—	—	—
4mA	10V	—	—	—	—	12.5	—	—	9.0GHz	35V	20V	1.5V	20mA	300mW	—	—	—

Low Noise and High Gain Bipolar Transistor (typical performance)

Part Number	Package Type or Chip	Package Configuration	Manufacturer's Remarks	I_C	V_{CE}	Minimum Noise Operation								NF with 50 Ω Input/Output and S_{21} at 1 GHz
						0.1 GHz		1		2		4		
						NF dB	G_A dB	NF dB	G_A dB	NF dB	G_A dB	NF dB	G_A dB	
HXTR-6103 (2N6618)	100 mil	Combined emitter	Low noise transistor	3mA	10V	—	—	1.6	16.0	1.8	12.0	2.7	8.0	—
HXTR-6104 (2N6743)	100 mil	Combined emitter	Low noise transistor	3mA	10V	—	—	1.3	16.5	1.5	12.5	2.5	8.0	—
HXTR-6105	100 mil	Combined emitter	Low noise transistor	15mA	15V	—	—	1.6	14.0	2.1	11.0	3.8	9.0	—
HXTR-6106	70 mil	Combined emitter	Low noise transistor	10mA	15V	—	—	1.7	14.5	2.3	10.5	4.0	8.0	—
HXTR-3615	85 mil	Combined emitter	Low cost low noise transistor	10mA	10V	—	—	1.3	16.6	2.0	12.0	3.5	7.0	1.6
HXTR-3645	85 mil	Combined emitter	Low cost high performance transistor	10mA	10V	—	—	1.2	17.5	1.7	13.0	—	—	1.3
HXTR-3675	85 mil	Combined emitter	Low cost high performance transistor	10mA	10V	—	—	1.2	17.7	1.7	13.0	2.8	8.6	1.3
HXTR-7011	100 mil	Combined emitter	Low noise high performance transistor	10mA	10V	—	—	—	—	—	—	—	—	—
MOTOROLA														
MRF901	Plastic Macro-X	SOE	—	5.0	6.0	1.6	23.0	2.0	12.0	2.7	7.0	—	—	—
2N6603	100 Mil Ceramic	SOE	—	5.0	10.0	1.6	23.0	2.0	12.0	2.7	7.0	—	—	—
MRF904	TO-72	Metal can	—	5.0	6.0	1.2	18.0	2.4	8.0	—	—	—	—	—
BFR96	Plastic Macro-T	T-pack	—	10.0	10.	1.8	18.0	3.2	6.0	—	—	—	—	—
BFR91	Plastic Macro-T	T-pack	—	2.0	5.0	1.8	18.0	2.5	8.0	4.0	4.0	—	—	—
MRF911	Plastic Macro-X	SOE	—	5.0	10.0	1.8	19.0	2.5	10.0	4.0	5.0	—	—	—
2N6604	100 Mil Ceramic	SOE	—	5	10	1.7	20	2.8	11.0	4.0	7.0	—	—	—
MRF914	TO-72	Metal can	—	5	10	1.7	20	2.5	7.0	—	—	—	—	—
MRF511	Plastic Macro-X	SOE	—	5	6	0.6	27	1.5	12	2.8	8.0	—	—	—
MRF512	100 Mil Ceramic	SOE	—	5	6	0.6	27	1.5	12	2.5	8.0	—	—	—
MRF513	70 Mil Ceramic	SOE	—	5	6	0.6	27	1.5	12	2.5	8.0	—	—	—
MRF580	Plastic Macro-T	T-Pack	—	50.0	10.0	1.2	21	3.0	9.0	—	—	—	—	—
MRF581	Plastic Macro-X	SOE	—	50.0	10.0	1.2	23	2.9	9.0	—	—	—	—	—
MM4049	TO-72	Metal can	PNP	3.0	5.0	2.5	17.0	3.5	6.0	—	—	—	—	—
MRF534	TO-18	Metal can	PNP	3.0	5.0	3.0	17.0	4.6	6.0	—	—	—	—	—
MRF536	Plastic Macro-X	SOE	PNP	3.0	5.0	2.5	18.0	4.6	7.0	—	—	—	—	—
MRF961	Plastic Macro-X	SOE	—	10.	10.	7.8	19.0	3.2	9.0	—	—	—	—	—
MRF962	100 Mil Ceramic	SOE	—	10.	10.	1.8	21.0	3.2	11.0	—	—	—	—	—
MRF965	TO-46	Metal can	—	10.	10.	1.8	18.0	3.2	6.0	—	—	—	—	—
NEC CORPORATION						@ 0.5 GHz								
NE021 Series		—	—	—	—	—	—	—	—	—	—	—	—	—
NE02103	03	Ceramic Stripline-Hermetic	—	5mA	10	—	—	—	—	2.7	8.5	—	—	—
NE02107	07	Ceramic Stripline-Hermetic		5mA	10	—	—	—	—	2.7	8.5	—	—	—
NE02108	08	Ceramic Stripline-Hermetic	—	5mA	10	—	—	—	—	2.7	8.5	—	—	—
NE219 Series		Ceramic Stripline-Hermetic	—	—	—	—	—	—	—	—	—	—	—	—
NE21903	03	Ceramic Stripline-Hermetic	—	5mA	8	—	—	—	—	2.2	8.0	—	—	—
NE21908	08	Ceramic Stripline-Hermetic	—	5mA	8	—	—	—	—	2.2	8.0	—	—	—
NE327 Series		Ceramic Stripline-Hermetic	—	—	—	—	—	—	—	—	—	—	—	—
NE32702	02	Ceramic Stripline-Hermetic	—	3mA	5	—	—	3.4	8.0	—	—	—	—	—
NE32708	08	Ceramic Stripline-Hermetic	—	3mA	5	—	—	3.4	8.0	—	—	—	—	—
NE416 Series		Ceramic Stripline-Hermetic	—	—	—	—	—	—	—	—	—	—	—	—
NE41603	03	Ceramic Stripline-Hermetic	—	5mA	10	—	—	3.5	8.0	—	—	—	—	—
NE41607	07	Ceramic Stripline-Hermetic	—	5mA	10	—	—	3.5	8.0	—	—	—	—	—
NE56708	08	Ceramic Stripline-Hermetic	—	—	—	—	—	—	—	—	—	—	—	—
NE578 Series		Ceramic Stripline-Hermetic	—	—	—	—	—	—	—	—	—	—	—	—
NE57803	03	Ceramic Stripline-Hermetic	—	3mA	8	—	—	—	—	—	—	4.3	4.0	—
NE57807	07	Ceramic Stripline-Hermetic	—	3mA	8	—	—	—	—	—	—	5.0	4.0	—
NE57808	08	Ceramic Stripline-Hermetic	—	3mA	8	—	—	—	—	—	—	4.3	4.0	—
NE644 Series		—	—	—	—	—	—	—	—	—	—	—	—	—
NE64408	08	Ceramic Stripline-Hermetic	—	5mA	6	—	—	—	—	—	—	2.7	8.5	—
NE64480	80	Ceramic Stripline-Hermetic	—	5mA	6	—	—	—	—	—	—	2.7	8.5	—

				Maximum Gain Operation				Peak S_{21} Gain at 1 GHz	F_{max} Extro-polated to MAG = 0 dB	Absolute Maximum Ratings						Price Quantity	
				1 GHz		4 GHz											
I_c	V_{CE}	Peak Ft.	C_{CB} at V_{CE}	MAG	MSG (if k<1)	MAG	MSG (if k<1)			V_{CBO}	V_{CEO}	V_{EBO}	I_c	Pt.	Rth.	1-100	1000
3mA	10V	—	—	—	—	10.0	—	—	8.0GHz	35V	20V	1.5V	20mA	300mW	—	—	—
3mA	10V	—	—	—	—	10.0	—	—	8.0GHz	35V	20V	1.5V	20mA	300mW	—	—	—
—	—	—	—	—	—	—	—	—	6.5GHz	30V	20V	1.5V	70mA	900mW	—	—	—
—	—	—	—	—	—	—	—	—	6.5GHz	30V	20V	1.5V	70mA	900mW	—	—	—
10mA	10V	5.06GHz	0.3 pf	—	21.0	—	10.0	—	6.0GHz	25V	16V	1.5V	55mA	500mW	—	5.20	4.20
10mA	10V	6.0GHz	0.27 pf	—	21.0	—	—	—	6.5GHz	30V	18V	1.5V	65mA	600mW	—	6.60	5.20
10mA	10V	6.0GHz	0.27 pf	—	21.5	—	9.0	—	7.0GHz	30V	18V	1.5V	65mA	600mW	—	8.40	7.15
10mA	10V	6.0GHz	0.29 pf	—	21.5	—	9.0	—	7.5GHz	30V	18V	1.5V	65mA	600mW	—	39.00	30.50
15	10	4.5	.4@10	14	—	2.5	—	—	5.5	25	15	3.0	30.	375	333	1.50	—
15	10	5.7	.4@10	17	—	3.5	—	14.0	7.5	25	15	3.0	30	400	187	9.75	—
15	10	4.1	.4@10	10	—	—	—	7.5	3.5	25	15	3.0	30	200	875	2.30	—
50	10	4.5	1.2@10	9	—	—	—	8.0	3.0	20	15	3.0	100	500	100	1.76	—
30	5	5.0	.7@10	10	—	—	—	10	3.0	15	12	3.0	35	180	500	1.54	—
30	10	5.0	.6@10	13	—	3.0	—	11.0	6.0	20	12	3.0	40	400	250	1.74	—
30	10	5.6	.5@10	16	—	4.0	—	14.0	6.0	25	15	3.0	50	500	150	9.75	—
20	10	4.5	.7@10	10	—	—	—	6.8	4.0	20	12	3.0	40	200	625	2.55	—
50	8	8.0	.7@6	16	—	4.0	—	13.	7.0	20	10	3.0	70	500	100	1.85	—
50	8	8.0	.7@6	18	—	6.0	—	14.	9.0	20	10	3.0	70	750	133	12.10	—
50	8	8.0	.7@6	18	—	6.0	—	14.	9.0	20	10	3.0	70	750	133	6.13	—
75	10	5.0	1.4@10	10	—	—	—	7.5	3.0	36	18	2.5	200	2500	40	2.30	—
75	10.0	5.0	1.4@10	12.5	—	—	—	7.5	5.5	36	18	2.5	200	2500	40	2.45	—
15	5	5.5	.7@5	—	—	—	—	—	—	15	10	4.5	30	200	875	3.45	—
15	5	5.5	.7@5	—	—	—	—	—	—	15	10	4.5	30	300	583	2.07	—
15	5	6.5	.7@5	10.0	—	—	—	—	—	15	10	4.5	30	300	416	1.30	—
50	10	4.5	1.2@10	13.5	—	—	—	9.0	4.5	20	15	3.0	100	500	100	2.30	—
50	10	4.5	1.2@10	14.5	—	3.8	—	11.0	6.0	20	15	3.0	100	750	133	10.35	—
50	10	4.5	1.6@10	9.0	—	—	—	8.0	3.0	20	15	3.0	100	750	133	2.55	—
—	—	—	@ V_{CB}	—	—	—	—	—	—	—	—	—	—	—	—	—	—
20mA	10	4.5GHz	0.6@10v	18	—	—	—	—	—	25	12	3.0	70mA	580mW	70	—	—
20mA	10	4.5GHz	0.6@10v	18	—	—	—	—	—	25	12	3.0	70mA	350mW	90	—	—
20mA	10	4.5GHz	0.6@10v	18	—	—	—	—	—	25	12	3.0	70mA	350mW	90	—	—
—	—	—	—	—	—	—	—	—	—	—	—	—	—	—	—	—	—
20mA	8	8.0GHz	0.4@8v	18.4	—	—	—	—	—	20	10	1.5	80mA	580mW	70	—	—
20mA	8	8.0GHz	0.4@10v	18.4	—	—	—	—	—	20	10	1.5	80mA	580mW	90	—	—
—	—	—	—	—	—	—	—	—	—	—	—	—	—	—	—	—	—
15mA	5	3.0GHz	0.9@5v	13	—	—	—	—	—	20	12	3.0	50mA	300mW	50	—	—
15mA	5	3.0GHz	0.9@5v	13	—	—	—	—	—	20	12	3.0	50mA	300mW	50	—	—
—	—	—	—	—	—	—	—	—	—	—	—	—	—	—	—	—	—
30mA	10	3.5GHz	1.0@10v	14	—	—	—	—	—	30	18	3.0	100mA	580mW	50	—	—
30mA	10	3.5GHz	1.0@10v	14	—	—	—	—	—	30	18	3.0	100mA	580mW	50	—	—
30mA	10	8.0GHz	0.18@10v	—	—	10.5	—	—	—	25	12	2.0	40mA	600mW	50	—	—
—	—	—	—	—	—	—	—	—	—	—	—	—	—	—	—	—	—
10mA	8	6.0GHz	0.4@8v	—	—	7.4	—	—	—	25	11	3.0	50mA	250mW	95	—	—
10mA	8	6.0GHz	0.4@8v	—	—	7.4	—	—	—	25	11	3.0	50mA	250mW	110	—	—
10mA	8	6.0GHz	0.4@8v	—	—	7.4	—	—	—	25	11	3.0	50mA	250mW	110	—	—
—	—	—	—	—	—	—	—	—	—	—	—	—	—	—	—	—	—
10mA	6	10.0GHz	0.2@10v	12	—	—	—	—	—	20	10	1.5	30mA	260mW	130	—	—
10mA	6	10.0GHz	0.2@10v	12	—	—	—	—	—	20	10	1.5	30mA	260mW	120	—	—

Low Noise and High Gain Bipolar Transistor (typical performance)

Part Number	Package Type or Chip	Package Configuration	Manufacturer's Remarks	I_C	V_{CE}	Minimum Noise Operation								NF with 50 Ω Input/Output and S_{21} at 1 GHz
						0.1 GHz		1		2		4		
						NF dB	G_A dB	NF dB	G_A dB	NF dB	G_A dB	NF dB	G_A dB	
NE645 Series		Ceramic Stripline-Hermetic	—	—	—	—	—	—	—	—	—	—	—	—
NE64508	08	Ceramic Stripline-Hermetic	—	7mA	8	—	—	—	—	1.6	12.0	—	—	—
NE64580	80	Ceramic Stripline-Hermetic	—	7mA	8	—	—	—	—	1.6	12.0	—	—	—
NE98108	08	Ceramic Stripline-Hermetic	—	5mA	6	3.0	7.0	—	—	—	—	—	—	—
NE98203	03	Ceramic Stripline-Hermetic	—	5mA	6	3.0	6.0	—	—	—	—	—	—	—
NE021 Series		—	Low cost	—	—	@ 0.5 GHz		—	—	—	—	—	—	—
NE02112	12	TO-72 metal can	—	3mA	10	1.5	10	—	—	—	—	—	—	—
NE02132	32	TO-92	—	3mA	10	1.5	10	—	—	—	—	—	—	—
NE02133	33	SOT23	—	3mA	10	1.5	11	—	—	—	—	—	—	—
NE02135	35	Micro X	—	3mA	10	—	—	—	—	2.0	—	—	—	—
NE02137	37	Stripline Plastic	—	3mA	10	—	—	1.8	12	—	—	—	—	—
NE219 Series		—	Low cost	—	—	—	—	—	—	—	—	—	—	—
NE21912	12	TO-72 metal can	—	5mA	8	—	—	1.3	10	—	—	—	—	—
NE21935	35	Micro X	—	5mA	8	—	—	—	—	2.2	9	—	—	—
NE21937[2]	37	Stripline Plastic	—	5mA	8	—	—	1.2	12	—	—	—	—	—
NE416 Series		—	Low Cost	—	—	—	—	—	—	—	—	—	—	—
NE41612	12	TO-72 metal can	—	25mA	5	2.3	14	—	—	—	—	—	—	—
NE41632	32	TO-92	—	30mA	10	2.4	14	—		—	—	—	—	—
NE41635	35	Micro X	—	5mA	10	1.5	15	—	—	—	—	—	—	—
NE46734	34	SOT-89	—	30mA	10	2.4	—	—	—	—	—	—	—	—
NE57835	35	Micro X	—	3mA	8	—	—	—	—	2.4	11	—	—	—
NE593 PNP Series		—	Low cost	—	—	—	—	—	—	—	—	—	—	—
NE59312	12	TO-72 metal can	—	3mA	−10	2.4	8.5	—	—	—	—	—	—	—
NE59335	35	Micro X	—	3mA	−10	2.4	8.5	—	—	—	—	—	—	—
NE64535	35	Micro X	Low cost	7mA	8	—	—	—	—	1.6	11	—	—	—
NE66912	12	TO-72 metal can	—	2mA	6	3.0	9	—	—	—	—	—	—	—
NE68337	37	Stripline Plastic	—	.25mA	1	—	9	—	—	—	—	—	—	—
NE71111	11	TO-18-metal can	—	—	—	—	—	—	—	—	—	—	—	—
NE734	Series	—	Low cost	—	—	—	—	—	—	—	—	—	—	—
NE73412	12	TO-72 metal can	—	3mA	10	3.0	15	—	—	—	—	—	—	—
NE73432	32	TO-92	—	3mA	10	3.0	15	—	—	—	—	—	—	—
NE73433	33	SOT23	—	3mA	10	3.0	15	—	—	—	—	—	—	—
NE73435	35	Micro X	—	3mA	10	2.1	16	—	—	—	—	—	—	—
NE73437	37	Stripline Plastic	—	3mA	10	2.3	15	—	—	—	—	—	—	—
NE74014	14	TO-39-metal can	All leads isolated from case	50mA	15	3.5	18	—	—	—	—	—	—	—
NE741 Series		—	Low cost	—	—	—	—	—	—	—	—	—	—	—
NE74113	13	TO-39 metal can	Collector is connected to case	30mA	15	3.0[6]	12	—	—	—	—	—	—	—
NE74114	14	TO-39 metal can	—	30mA	15	3.0[6]	12	—	—	—	—	—	—	—
NE856 Series		—	Low cost	—	—	—	—	—	—	—	—	—	—	—
NE85632	32	TO-92	—	40mA	10	—	—	1.8	9	—	—	—	—	—
NE85633	33	SOT 23	—	7mA	10	—	—	1.1	9	—	—	—	—	—
NE85634	34	SOT-89	—	40mA	10	—	—	1.8	11	—	—	—	—	—
NE85637	37	Stripline Plastic	—	7mA	10	—	—	1.1	12	—	—	—	—	—

Maximum Gain Operation								Peak S_{21} Gain at 1 GHz	F_{max} Extro-polated to MAG = 0 dB	Absolute Maximum Ratings						Price Quantity	
				1 GHz		4 GHz											
I_C	V_{CE}	Peak Ft.	C_{CB} at V_{CE}	MAG	MSG (If k<1)	MAG	MSG (If k<1)			V_{CBO}	V_{CEO}	V_{EBO}	I_C	Pt.	Rth.	1-100	1000
10mA	8	8.5GHz	0.2@10v	11	—	—	—	—	—	25	12	1.5	65mA	400mW	85	—	—
10mA	8	8.5GHz	0.2@10v	11	—	—	—	—	—	25	12	1.5	65mA	400mW	75	—	—
10mA	6	7.0GHz	0.35@6v	10	—	—	—	—	—	10	6	3	30mA	150mW	110	—	—
30mA	6	7.0GHz	0.6@6v	9.5	—	—	—	—	—	20	8	3	80mA	500mW	70	—	—
—	—	—	@ V_{CB}	—	—	—	—	—	—	—	—	—	—	—	—	—	—
20mA	10	4.5GHz	0.6@10v	12.5	—	—	—	—	—	25	12	3.0	70mA	0.35 watts	500	—	—
20mA	10	4.5GHz	0.6@10v	11.5	—	—	—	—	—	25	12	3.0	70mA	0.25 watts	500	—	—
20mA	10	4.5GHz	0.6@10v	14	—	—	—	—	—	25	12	3.0	70mA	0.15 watts	500	—	—
20mA	10	4.5GHz	0.6@10v	18	—	—	—	—	—	25	12	3.0	70mA	0.29 watts	120	—	—
20mA	10	4.5GHz	0.75@10v	14	—	—	—	—	—	25	12	3.0	70mA	0.25 watts	500	—	—
—	—	—	—	—	—	—	—	—	—	—	—	—	—	—	—	—	—
20mA	8	8GHz	0.4@8.0v	16.4	—	—	—	—	—	20	10	1.5	80mA	0.6 watts	90	—	—
20mA	8	8GHz	0.4@8.0v	18.4	—	—	—	—	—	20	10	1.5	80mA	0.58 watts	80	—	—
20mA	8	8GHz	0.70@8.0v	16.0	—	—	—	—	—	20	10	1.5	80mA	0.25 watts	500	—	—
—	—	—	—	—	—	—	—	—	—	—	—	—	—	—	—	—	—
25mA	5	2.7GHz	1.3@5v	10.0	—	—	—	—	—	35	18	3.0	100mA	0.5 watts	50	—	—
50mA	10	3.5GHz	1.0@10v	—	—	—	—	—	—	35	18	3.0	100mA	0.6 watts	208	—	—
30mA	10	3.5GHz	1.0@10v	14.0	—	—	—	—	—	35	18	3.0	100mA	0.6 watts	140	—	—
—	—	4.0GHz	1.1@10v	—	—	—	—	—	—	35	18	3.0	150mA	2.0 watts	62.5	—	—
10mA	8	6.0GHz	0.3@8v	12.0	—	—	—	—	—	20	11	3.0	30mA	0.25 watts	140	—	—
—	—	—	—	—	—	—	—	—	—	—	—	—	—	—	—	—	—
10mA	−10	2.5GHz	0.9@−10v	7.0	—	—	—	—	—	−20	−12	−3.0	−30mA	0.25 watts	300	—	—
−10mA	−10	2.5GHz	0.9@−10v	7.0	—	—	—	—	—	−20	−12	−3.0	−30mA	0.25 watts	130	—	—
10mA	8	8.5GHz	0.2@10v	—	—	10.0	—	—	—	25	12	1.5	65mA	0.4	85	—	—
10mA	10	1GHz	0.6@6v	—	—	—	—	—	—	45	25	4.0	30mA	0.25 watts	300	—	—
0.5mA	10	4.0GHz	02@5v	14.5	—	—	—	—	—	15	8	2.0	5.0mA	0.05 watts	2500	—	—
−10mA	−10	1.0GHz	2.5@−10v	—	—	—	—	—	—	−50	−40	−5.0	−100mA	0.3 watts	150	—	—
—	—	—	—	—	—	—	—	—	—	—	—	—	—	—	—	—	—
10mA	10	2.0GHz	1.1@10v	8	—	—	—	—	—	30	14	3.0	50mA	0.25 watts	120	—	—
10mA	10	2.0GHz	0.75@10v	9	—	—	—	—	—	30	14	3.0	50mA	0.25 watts	500	—	—
10mA	10	2.0GHz	1.0@10v	12	—	—	—	—	—	30	14	3.0	50mA	0.20 watts	500	—	—
10mA	10	3.0GHz	0.55@10v	13.3	—	—	—	—	—	30	14	3.0	50mA	0.25 watts	130	—	—
10mA	10	3.0GHz	0.55@10v	11.0	—	—	—	—	—	30	14	3.0	50mA	0.25 watts	500	—	—
50mA	15	2.0GHz	2.0@15v	6	—	—	—	—	—	45	25	3.0	300mA	5.0 watts	30	—	—
—	—	—	—	—	—	—	—	—	—	—	—	—	—	—	—	—	—
50mA	15	1.7GHz	2.0@15v	1.7	—	—	—	—	—	45	25	3.0	300mA	5.0 watts	35	—	—
50mA	15	1.7GHz	2.0@15v	17	—	—	—	—	—	45	25	3.0	300mA	5.0 watts	35	—	—
—	—	—	—	—	—	—	—	—	—	—	—	—	—	—	—	—	—
20mA	10	6.5GHz	0.65@10v	11	—	—	—	—	—	20	12	3.0	100mA	0.6 watts	500	—	—
20mA	10	7.0GHz	0.65@10v	13	—	—	—	—	—	20	12	3.0	100mA	0.2 watts	—	—	—
20mA	10	6.5GHz	1.0@10v	—	—	—	—	—	—	20	12	3.0	100mA	2.0 watts	312.5	—	—
20mA	10	7.0GHz	0.675@10v	15	—	—	—	—	—	20	12	3.0	100mA	0.2 watts	500	—	—

Low Noise and High Gain Bipolar Transistor (typical performance)

Part Number	Package Type or Chip	Package Configuration	Manufacturer's Remarks	Minimum Noise Operation I_C	V_{CE}	0.1 GHz NF	0.1 GHz G_A	1 NF	1 G_A	2 NF	2 G_A	4 NF	4 G_A	NF with 50 Ω Input/Output and S_{21} at 1 GHz
NE87112	12	TO-72 metal can	—	2mA	6	—	—	4.2	10	—	—	—	—	—
NE889 PNP Series		—	Low cost	—	—	—	—	—	—	—	—	—	—	—
NE88912	12	TO-72 metal can	—	−3mA	−10	—	—	4.5	8	—	—	—	—	—
NE88935	35	Micro X	—	−3	−10	—	—	4.2	10	—	—	—	—	—
NE99532	32	TO-92	—	—	—	—	—	—	—	—	—	—	—	—
NE02100	CHIP	CHIP	All are small signal	3mA	10	—	—	1.8	—	—	—	—	—	—
NE21900	CHIP	CHIP	—	5mA	8	—	—	—	—	2.5	—	—	—	—
NE22100	CHIP	CHIP	—	—	—	—	—	—	—	—	—	—	—	—
NE24300	CHIP	CHIP	—	—	—	—	—	—	—	—	—	—	—	—
NE24600	CHIP	CHIP	—	18mA	15	—	—	4.0	—	—	—	—	—	—
NE32700	CHIP	CHIP	—	3mA	5	1.0	—	—	—	—	—	—	—	—
NE33300	CHIP	CHIP	—	—	—	—	—	—	—	—	—	—	—	—
NE41600	CHIP	CHIP	—	2mA	5	1.0 (Rg = 200Ω)				—	—	—	—	—
NE49300	CHIP	CHIP	—	—	—	—	—	—	—	—	—	—	—	—
NE49400	CHIP	CHIP	—	—	—	—	—	—	—	—	—	—	—	—
NE56700	CHIP	CHIP	—	—	—	—	—	—	—	—	—	—	—	—
NE56800	CHIP	CHIP	MAG@2GHz is 14.0 dB	—	—	—	—	—	—	—	—	—	—	—
NE56900	CHIP	CHIP	MAG@2GHz is 13.0 dB	—	—	—	—	—	—	—	—	—	—	—
NE57500	CHIP	CHIP	—	—	—	—	—	—	—	—	—	—	—	—
NE57800	CHIP	CHIP	—	3mA	8	—	—		—	2.5	—	—	—	—
NE59300	CHIP	CHIP	—	3mA	−10	3.0	—	—	—	—	—	—	—	—
NE59500	CHIP	CHIP	—	—	—	—	—	—	—	—	—	—	—	—
NE64300	CHIP	CHIP	—	—	—	—	—	—	—	—	—	—	—	—
NE64400	CHIP	CHIP	—	5mA	6	—	—	—	—	—	—	2.7	—	—
NE64500	CHIP	CHIP	—	7mA	8	—	—	1.6	—	—	—	—	—	—
NE66900	CHIP	CHIP	—	2mA	6	3.0	—	—	—	—	—	—	—	—
NE71100	CHIP	CHIP	MAG@500 MHz is 9dB	—	—	—	—	—	—	—	—	—	—	—
NE73400	CHIP	CHIP	—	3mA	10	3.0	—	—	—	—	—	—	—	—
NE74000	CHIP	CHIP	—	50mA	15	3.5	—	—	—	—	—	—	—	—
NE74100	CHIP	CHIP	MAG@200 MHz is 17dB	10mA	15	2.7	—	—	—	—	—	—	—	—
NE77300	CHIP	CHIP	—	10mA	10	2.3 (Rg = 50Ω)				—	—	—	—	—
NE85600	CHIP	CHIP	—	7mA	10	—	—	1.1	—	—	—	—	—	—
NE87100	CHIP	CHIP	—	2mA	6	3.0	—	—	—	—	—	—	—	—
NE88900	CHIP	CHIP	—	3mA	−10	2.5	—	—	—	—	—	—	—	—
NE90100	CHIP	CHIP	—	—	—	—	—	—	—	—	—	—	—	—
NE98100	CHIP	CHIP	—	5mA	6	3.0	—	—	—	—	—	—	—	—
NE98200	CHIP	CHIP	—	—	—	—	—	—	—	—	—	—	—	—
NE99900	CHIP	CHIP	—	—	—	—	—	—	—	—	—	—	—	—
TOSHIBA														
2SA1245	Package	TO-236 MOD.	Rth. in °C/mW	−3	−5	—	—	3.0	—	—	—	—	—	—
2SA1161	Package	TO-92 (E-CNT.)	—	−3	−5	—	—	3.0	—	—	—	—	—	—
2SC2498	Package	TO-92 (E-CNT.)	—	5	10	—	—	4.0	—	—	—	—	—	—
2SC2499	Package	TO-92 (E-CNT.)	—	3	10	—	—	2.5	—	—	—	—	—	—
2SC2548	Package	TO-92 (E-CNT.)	—	5	5	—	—	3.5	—	—	—	—	—	—
2SC2644	Package	TO-92 (E-CNT.)	—	10	10	—	—	3.0	—	—	—	—	—	—
2SC2753	Package	TO-92 (E-CNT.)	—	5	10	—	—	1.7	—	—	—	—	—	—
2SC2876	Package	ϕ3.8mm Mold Micro-X	—	10	5	—	—	2.3	—	—	—	—	—	—
2SC3011	Package	TO-236 MOD.	—	5	5	—	—	2.3	—	—	—	—	—	—
2SC3098	Package	TO-236 MOD.	—	5	10	—	—	3.0	—	—	—	—	—	—
2SC3099	Package	TO-236 MOD.	—	3	10	—	—	2.5	—	—	—	—	—	—
2SC3268	Package	SOT-89 MOD.	—	5	10	—	—	2.0	—	—	—	—	—	—
2SC3301	Package	SOT-89 MOD.	—	10	5	—	—	2.3	—	—	—	—	—	—
2SC3302	Package	ϕ3.8mm Mold Micro-X	—	5	10	—	—	1.7	—	—	—	—	—	—
2SC3429	Package	TO-236 MOD.	—	5	10	—	—	1.7	—	—	—	—	—	—
2SC3445	Package	TO-236 MOD.	—	10	5	—	—	2.3	—	—	—	—	—	—
2SC3547	Package	TO-236 MOD.	—	5	10	—	—	2.0	—	—	—	—	—	—
2SC3548	Package	ϕ3.8mm Mold Micro-X	—	5	10	—	—	2.0	—	—	—	—	—	—

Maximum Gain Operation								Peak S_{21} Gain at 1 GHz	F_{max} Extro-polated to MAG = 0 dB	Absolute Maximum Ratings						Price Quantity	
				1 GHz		4 GHz											
I_C	V_{CE}	Peak Ft.	C_{CB} at V_{CE}	MAG	MSG (if k<1)	MAG	MSG (if k<1)			V_{CBO}	V_{CEO}	V_{EBO}	I_C	Pt.	Rth.	1-100	1000
6mA	6	2.0GHz	0.5@6v	8	—	—	—	—	—	45	25	4.0	30mA	0.25 watts	300	—	—
—	—	—	—	—	—	—	—	—	—	—	—	—	—	—	—	—	—
– 20mA	– 10	4.0GHz	1.0@-5v	9.0	—	—	—	—	—	– 20	– 12	– 3.0	– 50mA	0.3 watts	80	—	—
– 20mA	– 10	4.0GHz	1.0@ – 5v	12	—	—	—	—	—	– 20	– 12	– 3.0	– 50mA	0.25 watts	130	—	—
50mA	10	2.5GHz	1.0@10v	15	—	—	—	—	—	35	18	3.0	150mA	0.6 watts	208	—	—
20mA	10	4.5GHz	0.6@10v	18.0	—	—	—	—	—	25	12	3.0	70mA	—	—	—	—
20mA	8	8.0GHz	0.4@8v	12.6	—	—	—	—	—	20	10	1.5	80mA	—	—	—	—
80mA	10	3.2GHz	2@10v	9.0	—	—	—	—	—	35	18	3.0	250mA	7 watts	—	—	—
—	—	—	—	—	—	—	—	—	—	25	15	2.0	300mA	2.75 watts	—	—	—
100mA	15	4.5GHz	1.8@10v	11	—	—	—	—	—	30	20	3.0	250mA	5 watts	—	—	—
15mA	5	3.0GHz	0.9@5v	13	—	—	—	—	—	20	12	3.0	50mA	—	—	—	—
100mA	6	4.0GHz	1.5@10v	16.0	—	4.0	—	—	—	28	14	3.0	200mA	5 watts	—	—	—
30mA	10	3.5GHz	1.0@10v	14.0	—	—	—	—	—	35	18	3.0	100mA	—	—	—	—
—	—	.27GHz	3.2@10v	—	—	—	—	—	—	60	40	8.0	100mA	—	—	—	—
—	—	.28GHz	7.5@ – 10v	—	—	—	—	—	—	– 60	– 40	– 8.0	200mA	—	—	—	—
30mA	10	7.5GHz	0.44@10v	—	—	—	10.5	—	—	25	12	2.0	60mA	0.6 watts	—	—	—
80mA	10	4.2GHz	0.55@10v	—	—	—	—	—	—	25	15	1.5	150mA	1.5 watts	—	—	—
—	12	4.0GHz	—	—	—	—	—	—	—	25	15	2.0	300mA	4.5 watts	—	—	—
100mA	10	2.0GHz	3.0@10v	8.8	—	—	—	—	—	40	20	3.0	250mA	—	—	—	—
10mA	8	6.0GHz	0.4@8v	—	—	—	7.4	—	—	25	11	3.0	50mA	0.25 watts	—	—	—
10mA	– 10	2.0GHz	0.9@ – 10v	7	—	—	—	—	—	– 20	– 12	– 3.0	30mA	0.25 watts	—	—	—
60mA	10	4.0GHz	1.5@10v	—	—	—	4.0	—	—	20	15	3.0	100mA	—	—	—	—
60mA	10	2.0GHz	2.0@10v	11	—	—	—	—	—	40	20	3.0	150mA	—	—	—	—
10mA	6	10.0GHz	0.2@10v	12	—	—	12	—	—	20	10	3.0	30mA	0.25 watts	—	—	—
10mA	8	8.5GHz	0.2@10v	—	—	—	11	—	—	25	12	3.0	65mA	0.4 watts	—	—	—
6mA	10	1.0GHz	0.6@6v	—	—	—	—	—	—	40	25	4.0	30mA	—	—	—	—
10mA	– 10	1.0GHz	2.5@ – 10v	—	—	—	—	—	—	– 50	– 40	– 5.0	100mA	0.3 watts	—	—	—
10mA	10	2.0GHz	1.0@10v	8	—	—	—	—	—	30	14	3.0	50mA	0.25 watts	—	—	—
50mA	15	2.2GHz	2.0@15v	6	—	—	—	—	—	45	25	3.0	300mA	—	—	—	—
50mA	15	1.7GHz	2.0@15v	—	—	—	—	—	—	45	25	3.0	300mA	0.005 watts	—	—	—
100mA	10	2.5GHz	2.8@15v	10.5	—	—	—	—	—	35	18	3.0	450mA	—	—	—	—
20mA	10	7.0GHz	0.65@10v	15	—	—	—	—	—	20	12	3.0	10mA	—	—	—	—
6mA	6	2.0GHz	0.5@6v	8	—	—	—	—	—	45	25	4.0	30mA	0.25 watts	—	—	—
20mA	– 10	4.0GHz	1.2@ – 5v	12	—	—	—	—	—	– 20	12	– 3.0	50mA	0.3 watts	—	—	—
70mA	– 15	2.5GHz	2.5@ – 10v	—	—	—	—	—	—	– 40	– 25	– 3.0	200mA	0.8 watts	—	—	—
10mA	6	7.0GHz	0.35@6v	16	—	—	—	—	—	10	6	3.0	30mA	—	—	—	—
30mA	6	7.0GHz	0.6@6v	15	—	—	—	—	—	20	8.0	3.0	80mA	—	—	—	—
—	—	8.0GHz	0.4@ – 5v	—	—	—	—	—	—	– 15	– 10	– 3.0	50mA	0.6 watts	—	—	—
—	—	—	—	—	—	—	—	—	—	– 15V	– 8V	– 2V	– 30mA	150mW	666	—	—
—	—	—	—	—	—	—	—	—	—	– 15V	– 8V	– 2V	– 30mA	200mW	500	—	—
—	—	—	—	—	—	—	—	—	—	30V	20V	3V	50mA	300mW	333	—	—
—	—	—	—	—	—	—	—	—	—	20V	20V	3V	30mA	300mW	333	—	—
—	—	—	—	—	—	—	—	—	—	20V	10V	3V	30mA	250mW	400	—	—
—	—	—	—	—	—	—	—	—	—	25V	12V	3V	120mA	500mW	200	—	—
—	—	—	—	—	—	—	—	—	—	17V	12V	3V	70mA	300mW	333	—	—
—	—	—	—	—	—	—	—	—	—	15V	7.5V	3V	80mA	200mW	500	—	—
—	—	—	—	—	—	—	—	—	—	20V	7V	3V	30mA	150mW	666	—	—
—	—	—	—	—	—	—	—	—	—	30V	20V	3V	50mA	150mW	666	—	—
—	—	—	—	—	—	—	—	—	—	20V	20V	3V	30mA	150mW	666	—	—
—	—	—	—	—	—	—	—	—	—	17V	12V	3V	70mA	800mW	125	—	—
—	—	—	—	—	—	—	—	—	—	15V	7.5V	3V	80mA	800mW	125	—	—
—	—	—	—	—	—	—	—	—	—	17V	12V	3V	70mA	200mW	500	—	—
—	—	—	—	—	—	—	—	—	—	17V	12V	3V	70mA	150mW	666	—	—
—	—	—	—	—	—	—	—	—	—	15V	7.5V	3V	80mA	150mW	666	—	—
—	—	—	—	—	—	—	—	—	—	20V	15V	3V	30mA	150mW	666	—	—
—	—	—	—	—	—	—	—	—	—	20V	15V	3V	30mA	200mW	500	—	—

Gallium Arsenide Growth Diversifies

Status of GaAs from discretes to monolithics is reviewed with an eye on future prospects.

By Joseph Barrera, *Harris Microwave Semiconductor Corp.*

The GaAs microwave device field has been going strong for over 20 years. Clearly, the largest impact has been made by the GaAs field-effect transistor. The GaAs FET is the basis for a mature discrete device business and is about to create a similarly dynamic market for monolithic integrated circuits, both digital and microwave. It is difficult to suggest, however, that the discrete FET area is so mature that no progress is being made in performance or that all desired types of small-signal, low-noise, or power devices have been made. On the contrary, the technology has moved, and continues to move; so rapidly that often manufacturers are hesitant to stop development and offer a particular device for sale for fear that it will quickly be come obsolete. The user may also share in this concern. Laboratory results still outpace the commercial state of the art (although less so at lower frequencies) and emphasis has clearly shifted to obtaining high power and high gain at frequencies to 44 GHz and over 60 GHz, respectively.

GaAs integrated circuits are the focus of current development. The laboratory work over approximately the past eight years has established a rather sound base of fundamental processing, modeling, and circuit-design technology. The broad array of microwave and digital circuits that have recently been reported show a growing sophistication, complexity and uniqueness in their make-up. There also appears to be greater interest in the practical concerns of yields, repeatable performance and test capability. Commercial digital ICs for microwave systems applications will become available in 1984 and, although standard microwave ICs will likely not be commercially available for several years, they will start to have a real impact on military systems in the near future.

Discrete FET Section Content

The discrete FET section contains five subsections. The first is a short primer on the reasons why FETs work well at high speeds and relates some practical information on typical chip dimensions and types of design layouts for both small-signal and power devices. An attempt is made to relate the concerns chip designers have in deciding on a particular approach and how these decisions may affect the user. A simple and a more detailed equivalent circuit for modeling FETs are also presented. A table of circuit element values is given to help a user get started in modeling a FET of interest and reasons are given for the merits of doing so.

The second subsection gives a detailed discussion of the pros and cons of using chip FETs versus packaged FETs. Various trade-offs are given and examples are shown of typical packages used commercially. The following subsection presents detailed data and discussions of the present commercial state of the art for low-noise, small-signal FETs and power FETs. The emphasis is on available devices and, in the case of low noise, on the range of performance to be expected. The data are presented graphically for easy reference use and are current. The various categories of different FET gate lengths and styles of power FET products are explained. A short presentation is also given on the practicality of specialty FETs like dual-gate devices and FETs used as oscillators, along with a discussion of the positive and negative aspects.

The fourth subsection examines the future performance expectations for commercial low-noise and power FETs. A graphical comparison of calculated 0.25-micron–gate FET noise figure versus frequency and existing laboratory data are presented which show how closely theory and actual results agree. A hopefully pragmatic prediction of future commercial power FET performance versus frequency is also presented. The last subsection includes some practical circuit considerations, particularly concerning FET biasing approaches and the behavior of FETs under large-signal drive conditions.

Integrated Circuits Section Content

All the sections are meant to be a status report on discrete FETs with a collection of pros and cons regarding practical considerations. The data are useful for updating performance for the experienced user, and may help the novice in getting started using FETs.

Two major subsections are included which cover monolithic microwave integrated circuits (MMICs) and digital integrated circuits (DIGICs). The first subsection discusses the MMIC concept and the benefits expected over hybrid MICs. This is followed by a qualitative status report on MMIC progress and gives a modern example of a wideband distributed amplifier. The DIGIC subsection relates the potential microwave system applications of certain GaAs digital ICs and points out the important performance promise they offer. A qualitative status report on DIGICs is given along with a specific example of the use of a GaAs shift register in certain signal identification and processing systems. An example of an expected commercial GaAs DIGIC device is also shown. Finally, a general prognosis for the commercialization of DIGICs and MMICs is ventured.

Discrete FETs

General Description of FETs

• *Working Principles:* The concept of the field-effect transistor has been in existence for many years. In 1965, Mead[1] proposed the specific use of GaAs semiconductor and a

Dr. Joseph S. Barrera is the director of GaAs operations for Harris Microwave Semiconductor, Inc., Milpitas, Calif.

Schottky barrier gate to construct a FET with the potential for high-frequency operation. Subsequent work by Turner and Wilson[2] and many other researchers in the late '60s and early '70s has since led to the modern GaAs FET with gate lengths from 1.0 μm down to submicrometer lengths less than 0.25 μm.

GaAs is an excellent choice for building a microwave transistor for the simple reason that electrons in N-type GaAs channels can be coaxed from point A to point B at very high velocities. With velocity magnitudes of 1×10^7cm/sec. and greater, the intrinsic transit times across gate-channel interaction spaces of 1 μm or less (1×10^{-4}cm) are of the order 10^{-12} sec. to 10^{-11} sec. Response to signals impressed upon the gate can thus be expected well into the millimeter-wave range. Two other ingredients make GaAs ideal for microwave FETs. Electron mobility is high enough (~5000 cm^2/VS) to ensure low parasitic resistance values, and the threshold electric field for producing saturated electron velocities is low enough (~4000 V/cm) so that only one Volt or so is necessary to achieve saturated current levels. Relative to Si, GaAs has about four times higher electron mobility and about five times lower threshold field for velocity saturation. Finally, the fact that GaAs substrates can be made semi-insulating (resistivity $>10^6\Omega$/cm), allows devices to be fabricated with large-area bonding pads without creating intolerable parasitics.

Key to good FET performance is the ratio of g_m/C_{gs} or transconductance divided by gate-to-source capacitance. The higher the value the higher the maximum operating frequency and the power gain, and the lower the noise figure. In turn, the intrinsic ratio is highest for the highest saturated electron velocity and the shortest gate length. Subject mainly to breakdown voltage constraints, FETs are designed with the highest doping level and the shortest gate lengths possible and with gate widths as required for the power levels needed.

• *Physical Description of Chips.* All FET chips or dice in common possess source, drain, and gate terminals for connection to external circuits. These terminals allow bias voltages, loading structures, and signals to be applied. Figure 1 shows a very simple FET chip schematic with the three terminals or bonding pads outlined and with various key dimensions called out. A common confusion is the nomenclature used to describe the gate dimensions. Contrary to first expectation is the fact that the narrow gate dimension (0.25 to 1μm) is the gate length. The gate width is then obviously the dimension used for describing the total active width of the FET structure. For the device shown, the gate finger width and the total gate width are identical. Many FET layouts use multiple gate fingers and the total gate width is then simply the sum of the individual gate finger widths.

Generally, low-noise- or gain-style FETs have total gate widths of 200 to 400 μm and X and Y dimensions of 250 to 500 μm (10 to 20 mils). Power FET chips have varying widths depending on the desired output level. Commercial power FETs typically yield from 250 to 500 mW of 1-dB-gain compressed power per 1000 μm or 1 mm of gate width. The largest chips available unpackaged are typically under 2 W and are thus under 4 to 6 mm of gate width. The X and Y dimensions for 0.5 to 1.5 W chips range from 500 to 1000 μm (20 to 40 mils).

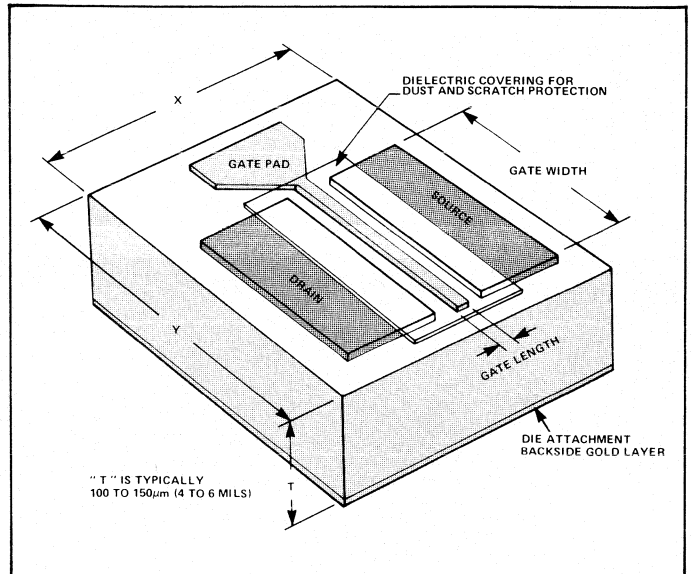

1. The ubiquitous GaAs FET has a simple physical structure, although the use of the terms gate length and width are reversed from what is intuitive.

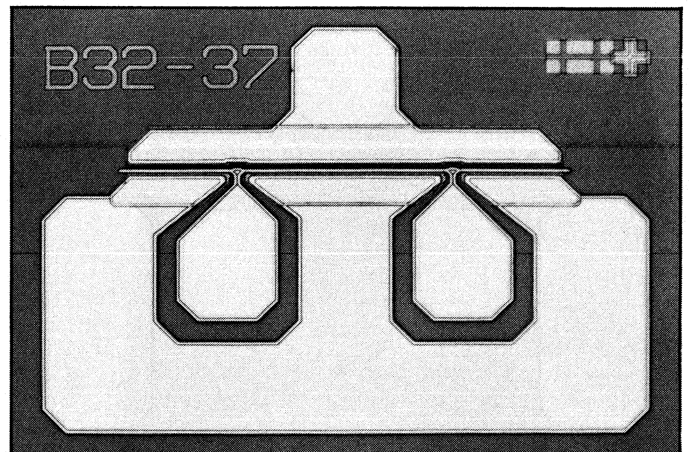

2. Typical is this π-gate layout for a 300-micron gate-width device. Note that it is important to minimize resistance of the gates' parasitic input resistance (Courtesy of Harris Microwave Semiconductor).

Most low-noise– and lower-power–style FETs have π-gate layouts. Figure 2 shows a photomicrograph of such a device with 300 μm gate width and with X and Y dimensions of 400 μm and 550 μm (16 by 22 mils). Such a layout has a wrap-around source connection and a dual feed π-gate. Since the gate metal finger represents a parasitic input resistance, it is important to minimize the resistor value. The π structure shown is equivalent to end-feeding the input signal to four 75-μm–wide gate fingers in parallel. Accordingly, there is an attendant four-fold reduction in parasitic resistance over one signal feed to the end of a single 300 μm finger. The π layout can be extended to much wider FETs and to multiple feeds with the advantage of uniformly applying the input signal. The disadvantage is the increasing X to Y aspect ratio which makes die separation from the wafer more difficult and increases the breakage

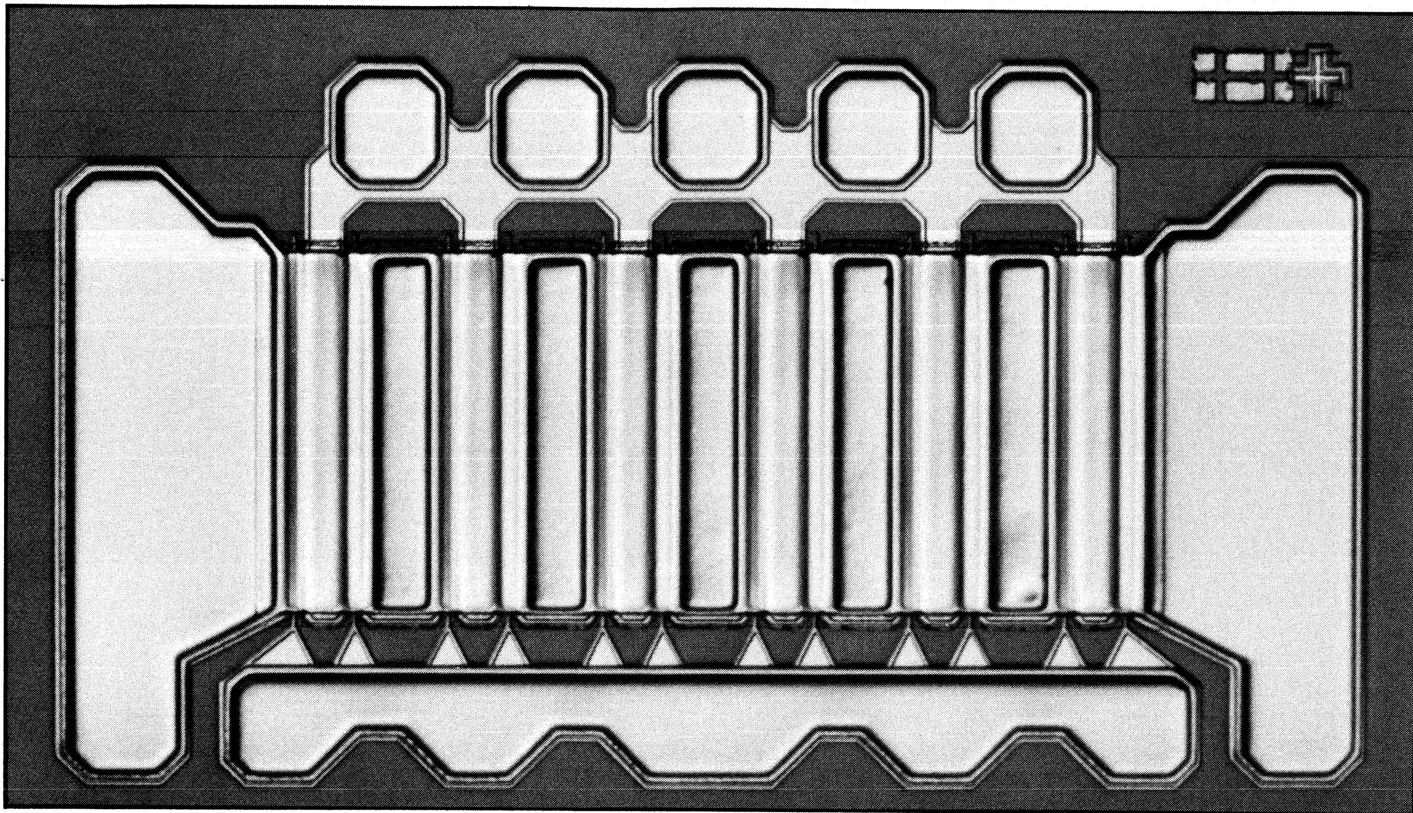

3. A dozen fingers are used in this commercial device, which is an example of an end-fed gate design (Courtesy of Harris Microwave Semiconductor).

possibility in handling intrinsically fragile (easy to cleave) GaAs dice.

Power FET structures generally are designed with fork-like or end-fed gates with multiple fingers. Early power devices were often constructed with tens of gate fingers considerably under 100 μm in width. Modern commercial power FETs have fewer fingers with various widths depending on the gate metal cross section. The larger the gate cross-sectional area, the wider the gate finger can be without creating an unacceptable parasitic effect. Figure 3 shows an end-fed, gate-style commercial power FET with better than 1 W nominal 1-dB-gain compressed-power output. The structure utilizes twelve 0.5 μm long by 200 μm wide gate fingers with large cross-sectional area created with a T-shaped configuration. The chip size is 500 μm $\times$ 800 μm (20 $\times$ 32 mils).

The end-fed, gate-style FET design invariably causes the isolation of either the intermediate drain or source contacts. The solutions for connecting the isolated contacts are to stitch bond wires, create bridge-metal connectors or to create "backside vias" which ground the contacts through a metal-filled hole through the substrate. The wire-stitching technique is the least preferable from an assembly time, labor, and reliability standpoint and does not keep the on-chip inductance low. The via approach is difficult to process but does an excellent job in keeping inductance low. The device in Figure 3 utilizes a plated gold air bridge for source interconnects and does a very good job in minimizing source inductance. A few commercial FETs have the isolated source contacts plated up and are then compression bonded upside-down to a carrier.

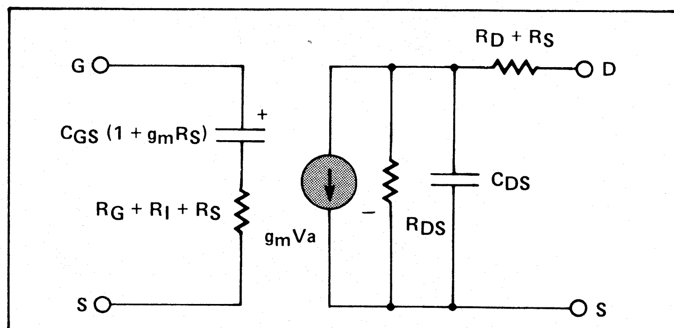

4. A basic equivalent circuit such as this can be used with a conventional Smith chart to produce a first-order approximation for a circuit design.

This technique does a good job of lowering inductance and improving thermal resistance but precludes users from doing their own chip mounting and from inspecting the device in its circuit mounting.

- *Equivalent Circuits.* Most commercial-FET data sheets include the small-signal scattering or S-parameters at various bias levels for characterizing a particular device as a two-port. These data are very useful in doing computer-aided circuit design, but do not allow as much flexibility as a detailed equivalent circuit of a device would.

Simple, unilateral, equivalent circuits which characterize the FET as a series RC input and a shunt RC output with an ideal shunt-voltage–dependent current source are especially useful for simple narrowband amplifier designs. A Smith

Table I.

Symbol	Chip Equivalent Circuit Element	"First Guess" Value
g_{mo}	Intrinsic Transconductance	10^{-1} mS/μm
τ	" Delay Time	4 ps
C_{GS}	" Gate-to-Source Capacitance	7×10^{-4} pF/μm
C_{GD}	" Gate-to-Drain Capacitance	1×10^{-4} pF/μm
C_{SC}	" Space Charge (Dipole) Capacitance	1×10^{-4} pF/μm
C_{DS}	" Drain-to-Source Capacitance	3×10^{-4} pF/μm
R_I	" Undepleted Channel Resistance	2 Ω
R_{DS}	" Drain-to-Source Resistance	400 Ω
R_{SC}	" Space Charge (Dipole) Resistance	-10^2 to 10^4 Ω
R_D	Extrinsic Drain Resistance	3 Ω
R_G	" Gate Resistance	1.5 Ω
R_S	" Source Resistance	3 Ω
C_{GN}	" Gate Excess Capacitance	0.25 pF
L_S	" Source Inductance	0.04 nH
L_G	" Gate Inductance	0.04 nH
L_D	" Drain Inductance	0.04 nH

chart, ruler, and pencil will go a long way in getting a good first-order design when using such an equivalent circuit as shown schematically in Figure 4.

Much more detailed equivalent circuits can be constructed as shown schematically in Figure 5 for a FET physical cross-section. Values for the elements of such a circuit are obtained for a particular FET by using measured DC data and a set of accurate S-parameter measurements for a particular bias condition and for various measurement frequencies. An "educated guess" is made of the intrinsic and extrinsic elements, and S-parameters are calculated as a function of frequency. The procedure is iterated until there is juxtaposition of calculated and measured S parameters. Obviously, a program like COMPACT™ and one's own computer are very useful ingredients.

A collection of first-guess element values and the definitions of the various elements are given in Table I for getting started on a detailed equivalent circuit. The values are intermediate between low-noise and power-style devices and those elements that are gate-width dependent are expressed on a per micrometer basis, except for the R_S, R_I, R_D, and R_G elements. External bonding-wire inductances should be added as appropriate.

The value of such wizardry is that once a fairly unique equivalent circuit is obtained, it can be used for extending the S parameters to lower or higher frequencies, for scaling the parameters when a pair of FETs are combined, for obtaining the S parameters when large signal drive or different bias values are applied (and the intrinsic elements are adjusted according to simple semiconductor equations), or

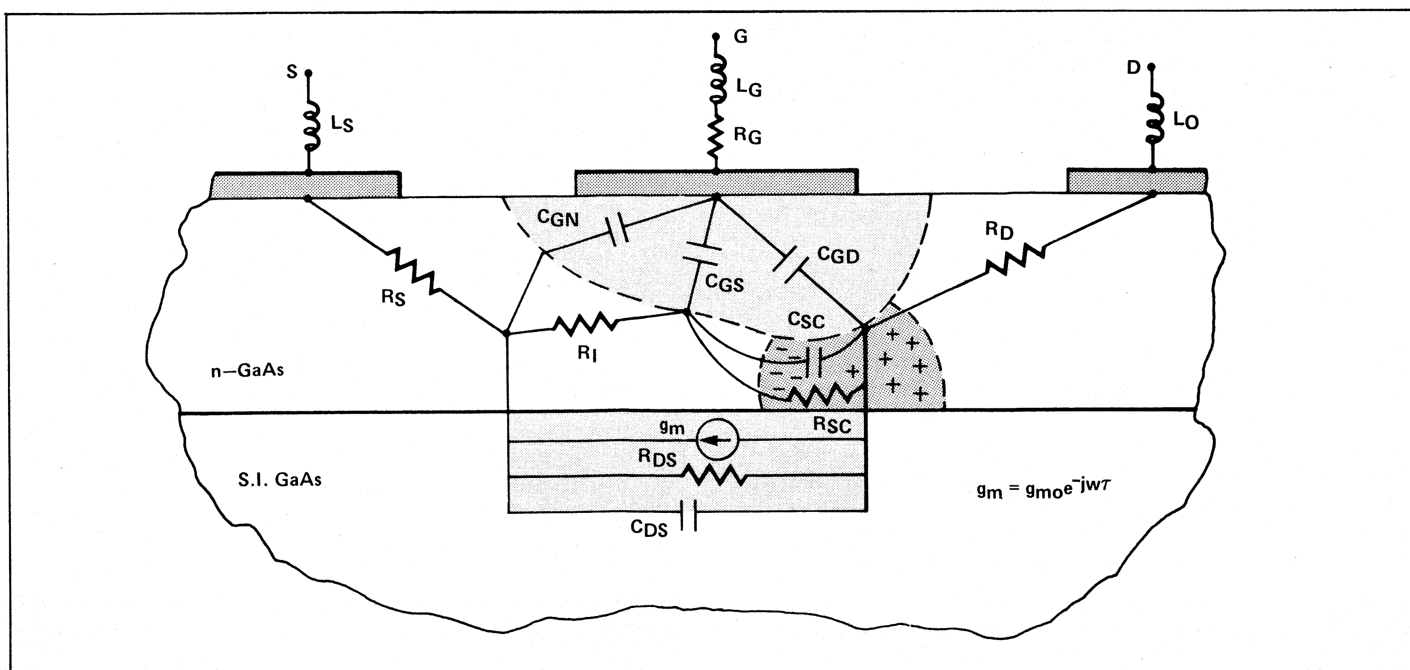

5. Much more detailed equivalent circuits can be generated, and values determined for individual FETs, using accurate S-parameter measurements.

to calculate the S-parameter sensitivities to various externally applied parasitics such as bonding wires or packages. For a finely tuned equivalent, noise generators can be added so that measured spot-frequency noise figures can be matched by calculation. It is then possible to calculate a wideband amplifier result including noise behavior and even large-signal behavior before building a single circuit module.

Chips versus Packaged FETs

• *FET Chip Use Considerations.* The use of FETs in chip form by a manufacturer usually implies a need for small circuit size, optimum performance, and wideband designs. From an equipment and capabilities standpoint it also implies that certain commitments have been made over those for packaged FET use. Often an incoming inspection of vendor devices is made for visual quality using medium-to–high power (1000X) microscopes. A DC IV probing setup is useful and necessary for checking characteristics of incoming devices or checking for changes after a particular assembly operation. An understanding of static-discharge control is necessary for the proper storage, handling, and assembly of chip FETs to avoid charge damage. Finally, die-attach and wire-bonding machines are obviously required along with operators capable of tweezer or collet handling of the fragile dice. Once committed, the chip user has the flexibility of designing circuits with tuning or matching elements immediately next to the device for minimum circuit losses and without fighting the extra parasitics that are introduced by a package. Chip use allows the creation of very compact gain stages, freedom to utilize self-biasing schemes, and the ability to experiment with various parasitic and feedback connections around the chip for achieving optimum wideband performance.

• *Packages and Packaged-FET Considerations.* There are very sound reasons for using FETs in packaged form aside from equipment and chip-handling constraints. Typically, a manufacturer uses packaged FETs for relatively narrowband communications circuits for both low-noise receivers and for transmitters. Softboard matching circuits are often used, and cost pressures require a minimum of tuning and assembly labor. These reasons need not be the only considerations, however. The general advantage of packaged-FET use is that packages are simply easier to handle, to store safely, and to mount in a circuit. The package's ruggedness allows for higher yield in circuit manufacture and does not require critical wire bonding techniques. A hermetic environment is also provided for the chip by a package enclosure. This often allows the overall circuit to be assembled without expensive welded seals. Perhaps the most important advantages are the capabilities to screen packaged parts for critical microwave performance parameters such as noise figure and gain, and for extremely rigorous reliability testing on critical programs. These latter benefits are just not practically realizable for chip parts since their screening must be done on a statistical basis rather than on the exact part to be used in a circuit. Finally, packages are simply the most practical way to use large power FETs. For power levels above about 1 W, large chips or multiple chips are used, and prematching or full matching to 50-Ohm levels is accomplished right next to the chip terminals using distributed- or lumped-circuit sections and many wire bonds within the package interior.

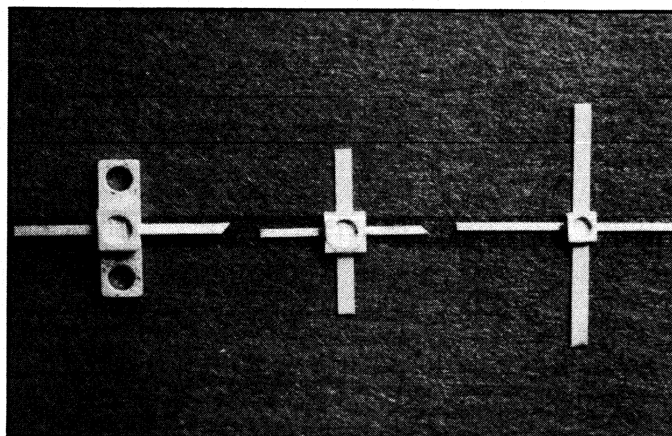

6. Packaging has a substantial impact on GaAs FET performance and reliability. These are typical, hermetic packages.

The device manufacturer is best suited to handle the larger chips and to achieve the necessary connections for performance at a particular power level and frequency band.

Most FET packages are combinations of metal and ceramic, usually aluminum oxide, with the gate and drain leads embedded through the ceramic for isolation and with the source leads made common and intended for RF grounding. A metal lid is normally used with a solder seal to complete the package make-up. For small-signal and lower-power FETs where dissipated power levels are considerably below 1 W, an all-ceramic body and metal leaded package is often used. The most common sizes are nominally 100 mil and 70 mil square. Figure 6 shows an array of such packages in addition to examples of metal-bottom, flange-style packages. For medium-to-1 or -2–W power FETs, the gold-plated OFHC copper-base packages allow low-thermal–resistance mountings for the larger FET chips. Usually such packages range from 100 to 300 mils in the narrow dimension and are mounted to circuit bases with two screws on approximately 250- to 500-mil centers. Multi-Watt, internally matched power FETs require considerably larger copper-based packages. These are needed to house the two large FET chips normally used and for both input and output circuit sections. Overall size is typically 500 mils × 1000 mils with about 700-mil mounting centers. Figure 7 shows an unlidded multi-Watt FET package and an opened commercial device with the circuit elements visible. Such devices are, in effect, mini-amplifiers tuned to particular telecommunications bands with reasonably good VSWR matches.

Aside from the packaged FET's reduced flexibility in circuit usage relative to chip FETs (as described earlier), the only real disadvantage is a somewhat-diminished frequency response. The low-impedance stripline nature of most packages and the typical geometrical layouts cause fairly significant capacitive parasitics to exist on the input and output and from input to output. Source inductance parasitic is also created by the RF current path from chip to true RF ground. These effects typically start causing minor gain degradation at frequencies around 8 to 10 GHz. A few innovative microstrip-style packages have been designed for good results to 18 GHz, but in general, up to X band is the usual range to be considered for packaged FETs.

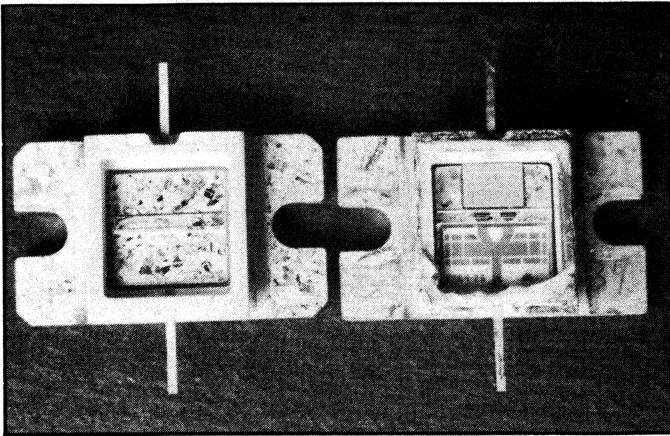

7. Multiwatt FETs are, in effect, amplifiers in themselves, with matching circuitry tuned to the intended bands to provide good impedance matching.

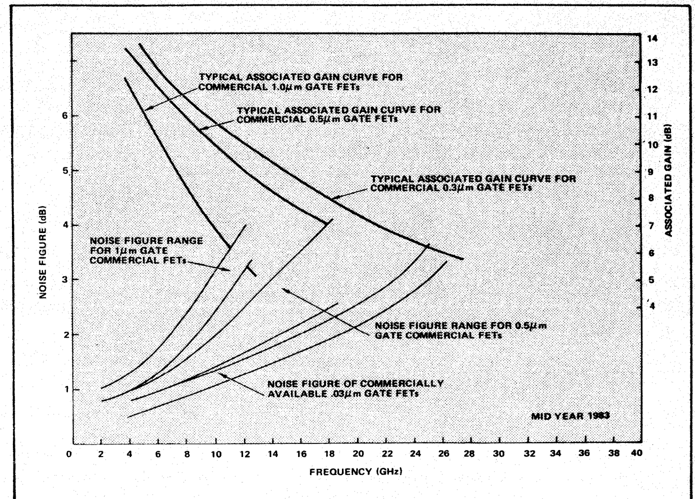

8. Gain and noise figure vary with gate length, here shown for 1.0-micron, 0.5-micron and the newer 0.3-micron devices as well as, not surprisingly, price.

Commercial and Laboratory Device Performance

• *Low Noise/Gain Style Small-Signal FETs.* One of the simplest expressions for the noise figure of a GaAs FET can be derived from the original work by Fukui[3] as

$$F_{MIN} = 1 + K f L_g \sqrt{g_{mo}(R_g + R_s)}$$

where f is frequency in GHz, L_g the gate length in micrometers, g_{mo} the intrinsic transconductance in Siemens and R_g and R_s the gate and source parasitic resistances in Ohms, respectively. The one adjustable parameter, K, is about 0.27 for good devices. The equation is a good guide to building low-noise FETs. The shorter the gate and the lower the parasitics, the lower the noise. The dependent parameter g_{mo} should not be minimized, however. By rewriting the above equation as

$$F_{MIN} = 1 + K^1 f C_{gs} \sqrt{\frac{R_g + R_s}{g_m}}$$

with $K^1 = 0.016$ and C_{gs} the gate-to-source capacitance, it is seen that once again maximizing the g_m/C_{gs} ratio always results in the best performance.

A consequence of the above reasoning is that manufacturers have been steadily pursuing technology to fabricate shorter-gate-length FETs while keeping parasitics to a minimum. Progress has been steady, and today's commercial- and laboratory-device noise figures are approaching very closely the theoretical expectations. The frequencies for which useful associated gains are obtained are pushing into the 30- to 40-GHz range with recent work producing a 60 GHz result.[4]

Figure 8 presents the noise figure versus frequency layout of modern commercial FET chips with typical associated gains. Ranges of data-sheet-typical values are shown for 1.0-μm, 0.5-μm and recent 0.3-μm gate-length devices. Clearly, the lowest values represent the premium devices. There is a fairly general strategy by vendors to offer premium units and utility units which make up the upper part of the ranges. The latter units are often binned devices (from wafer qualification schemes) of identical designs to premium units or they are less-complex, more-easily manufactured devices. The associated-gain data are generally less variable from run to run than the noise-figure data and, consequently, all units offer a good value from a gain-per-stage vantage point. Since only the first or the combined first and second devices in a low-noise amplifier determine the amplifier noise figure, the premium device and the utility gain stage concept is a reasonable one.

• *Power FETs.* In recent years much of the development scramble has involved the achievement of commercial power FETs with as much power at as high a frequency as possible. Much of the driving force is the desire to have solid-state amplifier replacements for larger, heavier, and inconvenient power-supply tube amplifiers for transmitters in telecommunications, radars, and phased arrays. Much progress has been made, but it has been difficult.

Some of the technical issues have been discussed earlier: for example, large chip size, gate finger-width effects, and gain reducing source inductance layout effects. There are several primary problems whose present solutions have led to the existing commercial state of the art. Achieving more power simply requires more total gate width. Indeed, power level can almost be independently obtained by building very wide-gate FETs. The problem is to maintain usable gain at the frequency of interest while achieving the right output power. This gain/gate-width scaling problem has led to clever chip layouts with efforts concentrated on signal phasing, optimum gate lengths and gate finger widths, and source inductance minimization with plated air-bridge and substrate via-hole techniques. Newly stated, the task now is: What maximum gate width chip does one dare make for a given frequency of interest before going to circuit-paralleled multiple chips to obtain higher power?

As gate widths increase, the input and output impedances get lower and lower with the input match becoming the most difficult. A 2400-μm-wide FET has an approximately

Continued on page 82

Continued from page 79

2 Siemens real part impedance, a 4800-μm FET about 1 Siemens, and so on. A circuit designer using a large power FET chip must resonate the input and output capacitances and then transform the real values to 50Ω. There is obviously a practical limit to how large a capacitance and transformation ratio may be obtained for a desired bandwidth. By utilizing high-dielectric substrates and/or lumped capacitive elements, a designer can more easily obtain matches, but at the expense of bandwidth. Again, the task for solving the problem of impedance matching of large-total-gate-width FETs is to determine what maximum size cell should be used and how to combine cells efficiently to achieve the desired results.

Some of the answers to the questions posed can be obtained by examining the array of commercially available power FETs. Figure 9 shows the 1-dB–gain compressed-power levels versus frequency for available devices with gains of at least 4 to 5 dB at the frequency listed. There are four categories shown. First, single, unmounted chips are available which give up to 2 W (33 dBm) output level up to about 8 GHz. Then the fight to maintain gain results in smaller cells and less power with about 1 W at 14 to 15 GHz, and a few hundred milliwatts available at around 18 GHz. Substrate via-hole devices have exhibited near-1–W levels at 18 GHz, but are generally not readily available from vendors. The curve for packaged—but not internally matched—devices maps onto the single chip curve with the exception of 2.8 W being available up to about 7 GHz, and with power fall-off versus frequency shifted by about 2 GHz due to the package parasitics.

The largest gate-width chips used up through C band are found to be around 6000 μm arranged in two to four cells on a single die. In the high X-band region, a typically 3000-μm gate-width chip is found, and the Ku-band devices (where most development work is presently centered) are being manufactured with from 600 to as high as 2400 μm gate widths. These "optimum" cell sizes are very close to values predicted several years earlier by various researchers[5] although progress is pushing toward greater widths.

The third locus of values in Figure 9 is for a collection of recently available devices with input and output matching on low parasitic carriers, or in packages with prematching of the chip inputs. The relative increase in power level over the other two previously discussed curves is due to prematching and chip combining, or to full matching of single chips on low-parasitic carriers.

The fourth category is represented by a collection of narrowband power-FET modules over the frequency range of about 3.5 to 8.5 GHz. All of the most popular telecommunciations bands are represented, particularly the 3.7- to 4.2- and 5.9- to 6.4-GHz bands. The modules are all multi-Watt, internally matched, multiple-FET structures. The most recently available devices provide 6 W of 1-dB-gain compressed power with associated gains of around 6 dB. These modules make use of multicell layouts on a single die with impedance transformation often attempted at the cell level where magnitudes are higher. Eventually, the total chip input impedance is matched with a several-section, low-pass, filter-type transformer using lumped element, high-dielectric capacitors and wire-bond inductors. The outputs use wire-bond inductors and distributed lines. The commercial unit

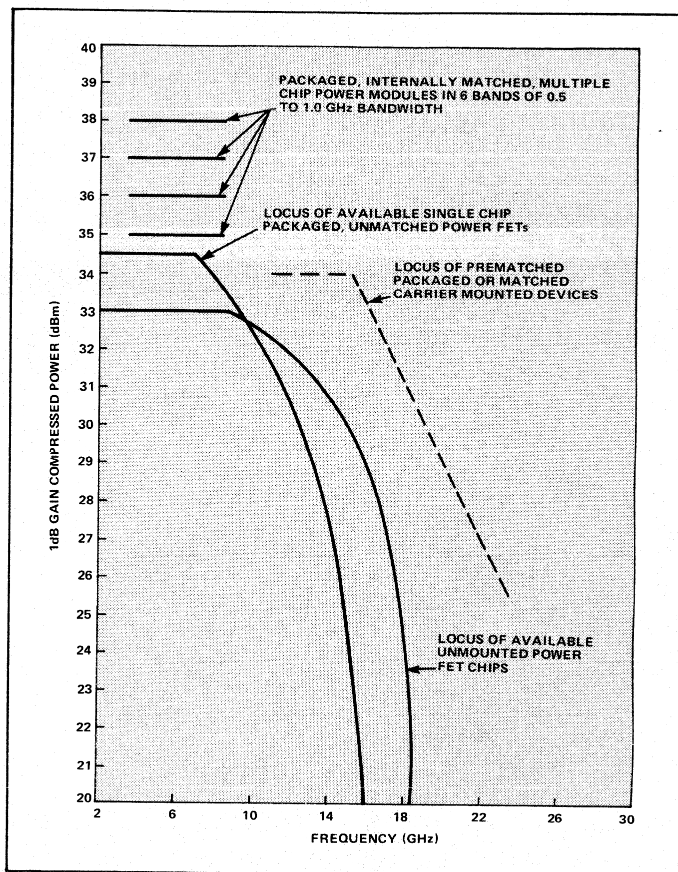

9. Prematching and low-parasitic carriers can significantly increase power.

shown earlier in Figure 7, for example, is a 3-W module using 10 mm of total gate width from two 5-mm gate-width chips. The first capacitor section nearest to the chip inputs uses approximately $E_T = 200$ material to get high enough capacitance for matching.

The near-50–Ohm match provided by the multi-Watt FET module allows quick insertion in amplifiers for a wide variety of narrowband uses. As work on cell optimization continues and cell combining and matching techniques improve, it is expected that higher power, higher frequency, and wider bandwidth modules will become available.

- *Specialty FETs.* Most FETs used in circuits today are involved with low noise amplification, intermediate gain stages, and output driver or output power stages. Although this situation is not likely to change considerably, it must be noted that all electrical engineering circuit functions can be accomplished with FET structures. In particular, the dual-gate FET has been shown capable of a surprising number of specialty tasks. The literature over the past 10 years has presented data for dual-gate FETs used as enhanced-gain amplifiers, switches, resonated switches, broadband attenuators, AM modulators, multipliers, mixers, mixers with gain, self-oscillating mixers, limiters, and phase shifters. Why then aren't dual-gate FETs exceedingly common circuit elements? Perhaps because the dual-gate FET is so versatile it is difficult for a vendor to offer a device that has been truly optimized for a particular use. As discussed earlier, there are many parameters involved in optimizing a single-gate FET. The

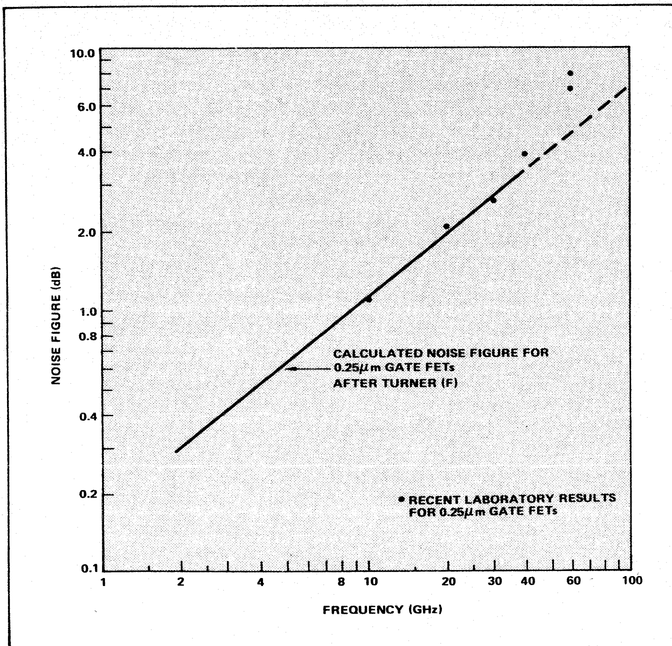

10. Results for submicron gates are closely following projections by Turner, et al, providing commercial devices with performance through 26 GHz and laboratory devices that match theory up to 40 GHz, although deviations occur in the singular result at 60 GHz.

problem becomes increasingly difficult when a second gate and another active region are added, not to mention another terminal with its own considerations of RF termination. There are about a half-dozen commercial dual-gate FETs available today. Most of these devices will do a good job in the various uses listed above, but because of small volume usage and because alternative passive schemes have been available, manufacturers have not made dual-gate–FET development a high priority. A strong potential area for dual-gate usage is in monolithic microwave circuit integration where multi-function chips may be needed. Already, multiple-gate FETs are in common use in digital IC development.

The use of FETs as oscillators is an area where progress is being made. The same devices used for amplification are also useful as oscillators and special designs are not usually needed. Those FETs with high transconductance per unit of gate width and large-cross-section gates with high gate-current capability are to be preferred, but only from a performance and reliability standpoint. Generally, FETs have been used in very wideband sweeper circuits from C to K band where FM noise levels are not as critical as for local oscillators. The prevalent concern is that near-carrier noise is just too high for FETs as compared to Gunn-device oscillators, due mainly to upconverted low frequency 1/f noise. It is indeed true that the typical near-carrier FM noise level of FET oscillators is higher than for Gunn oscillators for the same loaded Q factors. With the use of high-dielectric resonators, however, the FET oscillator's FM noise can be easily reduced to Gunn levels. Overall oscillator efficiency is considerably higher for the FET oscillator, even when only lightly loaded with a very high-Q resonator. The power-added efficiency for the FET as a power amplifier is usually 20 percent and higher, and it is not difficult to construct the FET oscillator to achieve the desired power output and FM noise level while still maintaining an overall efficiency greater than the few percent typical of Gunn oscillators. Researchers are continuing studies which may lead to a better understanding and perhaps control of the source of the 1/f noise.

Although researchers are involved with many different forms of field-effect structures like multi-drain FETs, combined MIS/Schottky-gate FETs and lossy-gate FETs, there is not an obvious special direction of work which is destined to result in commercial offerings. Outside of the intended scope of this writing yet worthy of note is the research taking place on heterojunction AlGaAs/ GaAs FET structures. The present combined efforts may well lead to higher-frequency, lower-noise discrete FETs and faster integrated circuits.

● *Expected FET Performance and Limitations.* It is always risky to make predictions of where a technology like microwave GaAs devices is heading. It is hoped that the present foresight will be outdistanced by stronger-than–anticipated evolutionary events and perhaps unforeseen revolutionary findings. The risk of prediction is lessened by the fact that commercial FETs are established entities and the technology in general is quite mature.

Considering the low-noise area, it is clear that tremendous strides have been made in past years and thus it becomes more difficult to expect large continued improvements. Figure 10 relates to the situation and shows the result of calculated noise figure versus frequency by Turner, et al[6] for a 0.25-μm–gate FET. In the few years since the calculation was done, 0.25-μm FETs have become a reality and available commercial versions through 26 GHz match the calculated data almost exactly (compare Figure 8). Just as impressive are recent laboratory results which match the calculation through about 40 GHz. The record-high–frequency result at 60 GHz[5] shows several dB deviation, but from the extrapolated portion of the theoretical curve.

Given the difficulty of the 0.25-μm gate technology and of attempts to go beyond, it would seem that the noise figures for frequencies up to about 40 GHz, and certainly for the 4- to 20-GHz range, are already at or near expected minimums and will not likely show dramatic improvement. From the commercial standpoint, the establishment of solid devices will occur for the 26-GHz region on up through 40 GHz; and as demand requires, possibly up through 80 GHz. Beyond the 80-GHz region many questions arise that relate to the intrinsic electron transfer mechanism and RF hysteresis effects. These conditions may limit the usefulness of GaAs FETs to operation below 80 to 100 GHz. If 0.1-μm gate-length structures become viable, then the possibilities for enhanced performance from electron overshoot and ballistic motion (higher resulting electron velocities) could exist, especially if one considers AlGaAs/GaAs heterostructures.

Power FETs have also benefited from advancements in technology such as routine 0.5-μm–gate manufacture, air bridges, and backside vias. The better understanding of cell scaling, gate finger-width effects, and chip combining and matching techniques has led to commercial devices with up to 6 W output power for frequencies between 3 and 8 GHz.

A prediction for future commercial power FET devices is given in Figure 11. The bases for the predictions primarily are: the continued demand for more tube replacement power, especially at key military and telecommunication frequencies;

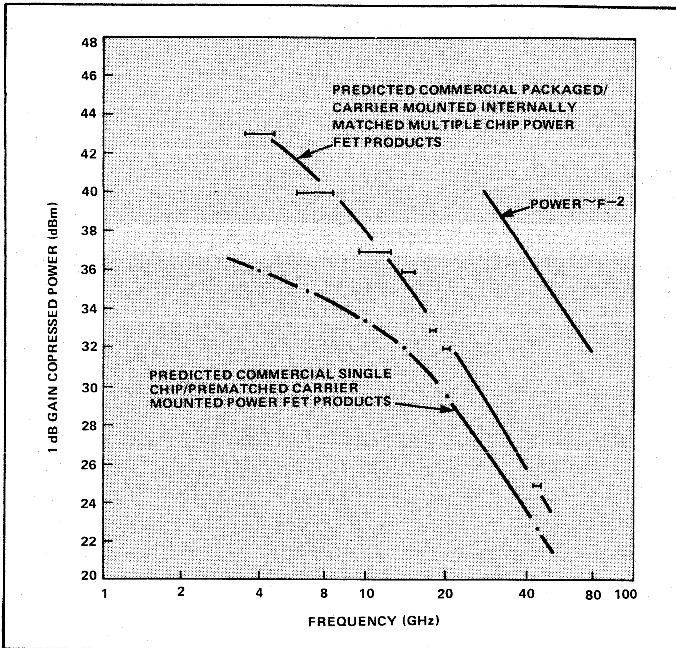

11. Look for commercial power FETs to improve dramatically since laboratory devices are outperforming them by a factor of two to three.

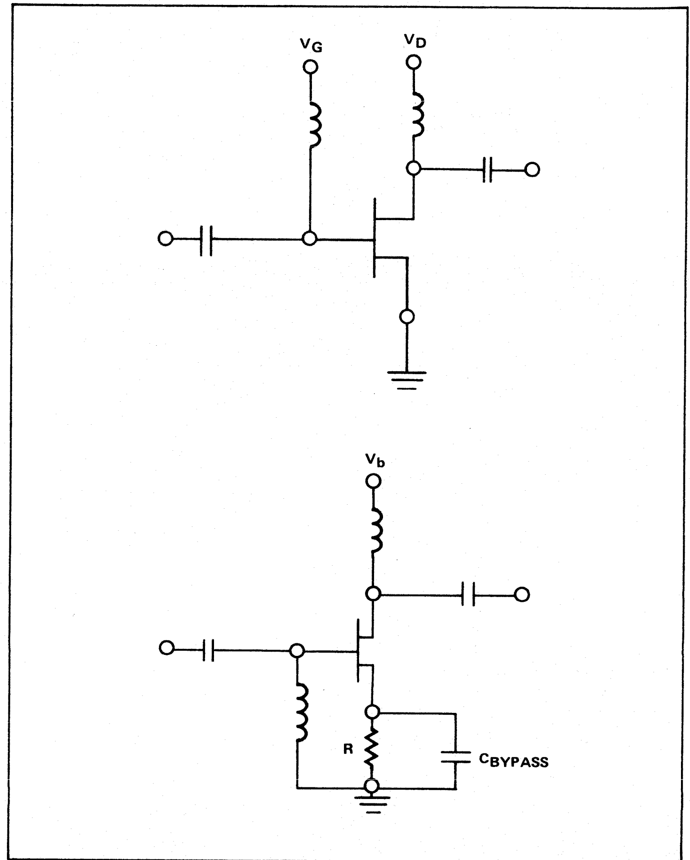

12. Two alternate methods of biasing the FET are (a) intended to provide flexibility and good performance by using two bias supplies, and (b) the 'self bias' approach used when cost dictates a single supply.

the fact that improvements are still to be made on the cell layout, scaling, and combining techniques; and that the laboratory power FET figure of merit of about 1 W/mm is about two to more than three times that for typical commercial devices.

Obtaining designs for the highest output power per millimeter of FET gate width does not always mesh with the requirements of the amplifier designer or the device manufacturer. Power is obviously obtained from the RF voltage and current product, and one might expect that high-drain-voltage, low-current devices and high-saturation–current, moderate-drain–voltage devices could be made equivalently. There are trade-offs, however, which involve reliability, manufacturing yield, chip handling, and efficiency which tend to force the commercial designs in particular directions. Most circuit designers prefer high-voltage (>10 V) and low-current devices whereas drain voltages of 8 to 10 V are much more justifiable when reliability and other parameter optimizations are considered.

Overall—considering the laboratory achievements and the prognosis for efficiency, scaling, and combining improvements—it is expected that 0.6 to 0.8 W/mm will become more common for commercial devices up through about 20 GHz and that substantial single-chip and combined-chip power will be obtained up through the 44-GHz range.

Circuit and Design Considerations

• *Bias Technique.* The most-straightforward way to bias FETs and maintain the highest flexibility in achieving good performance is to provide two bias supplies as shown in Figure 12a. The circuit designer, however, is very often constrained by system and cost requirements to use only a single supply. What is then most commonly used is the "self-bias" technique as shown in Figure 12b. Here, the desired gate voltage is obtained by choosing the resistor value and I_{DS} value such that $-I_{DS}R$ appears at the gate terminal. An RF bypass capacitor is then used to maintain a good RF source grounding. This information is well known, but it is useful to restate it relative to two noteworthy situations. Higher power, single chips are becoming more available and bias currents are correspondingly getting higher so that a 1-W or 2-W device may require 1/3 to over 1/2 Ampere. The dropping resistor for gate bias will be around 4 to 5 Ohms and would dissipate from 1/2 to over 1 Watt. This is not a desperate situation, but when there is a DC input power budget and a tough thermal environment one must consider alternative bias schemes.

The second concern involves the use of devices which employ backside, substrate via-hole grounding. In this case, the source areas on the top of the chip are intimately connected to the backside of the chip, which invariably is attached to RF ground, thus precluding the use of a self-biasing scheme. One could consider mounting the chip on a thin dielectric such as BeO, but then most of the via-hole low inductance benefit would be lost when bonding over to the required bypass capacitor. In those situations where self-biasing resistors and a single bias supply must be used, one must reject via-hole devices, carrier-mounted devices, and packaged devices. Those devices with ample use of plated air-bridge interconnect technology offer the best alternative.

• *Large Signal Considerations.* As discussed in an earlier section, one must have some knowledge of the change in

device output impedance or, equivalently, the required change in output load impedance as input-signal drive brings a device into compression. Ordinarily, designers use large-signal tuner measurements or formal load-pull techniques to painstakingly obtain the data versus power level, frequency, and gain level. Recently, Cripps[7] presented a simple but effective technique for constructing power load-pull contours with a convenient mathematical formulation. The technique is recommended, although the derivation and discussion are not presented here. Suffice to say that one needs only to know the bias voltage and current; then the desired power level and contours can be constructed which compare very well with measurement.

Linearity in power FETs is a very complex issue which cannot be properly covered in this writing. An excellent account and bibliography on linearity and other FET-circuit concerns is given by Schlosser and Sokolov[8] and is highly recommended. Some points worthy of note are that:

- not just the FET alone but the output match directly affect linearity;
- the FET is not a natural third-order device and intercept data are not always very useful in characterizing devices;
- gate bias impedance can affect linearity under high drive and must be properly tailored; and
- backing off on power can result in more rapid improvement in linearity than for TWTs since the carrier-to-intermod (C/I) slope is often greater than 2:1.

More theoretical work coupled with actual measurement is needed to understand the optimization for power and linearity combined. Presently, measurements must be performed on a given device and particular design to really know the resulting amplifier capabilities.

GaAs Integrated Circuits

Monolithic Microwave Integrated Circuits (MMICs)

- *Concept of MMICs.* The integration of many different circuit elements on a chip is certainly not a new concept. We live in an LSI and VLSI world of Si ICs where integration is taken very seriously. Why apply the concept to the microwave world when hybrid ICs (MICs) are doing just fine? The answer really depends on just a few key factors. Volume usage is one important element, as is the technical ability to get a certain task accomplished. MICs are indeed cost-effective for the volumes and applications they are used for, but very few—if any—circuits get shipped as product without some detailed human attention, otherwise known as "tweaking." If significant product volumes ($>10^4$ units/year) are involved and costs are to be minimized, then different techniques must be used and the labor content must be kept to a minimum. The MMIC concept holds the hope that once properly designed, circuits can be manufactured with high reproducibility and with very little technical labor involved in final assembly. For low-volume products, the issue for MMICs is not so clear. Some tasks must use the MMIC approach because of a size requirement, a level of integration requirement, or the fact that wire bonds and discrete elements just will not do the job that is required. Overall, the litany of positive expectations for MMICs includes low cost, improved reproducibility and reliability, small size and weight, broad bandwidth capability, multi-function-on-a-chip capability, few parts per system and fewer interconnects.

The primary driving forces for MMIC development have been the need for compact military T/R phased-array modules, for EW work where various gain stages are needed in volume, and from the commercial world where direct broadcast satellite (DBS) TV receivers would be used in high volume (10^5 to 10^6/year).

- *MMIC Status.* For frequencies of 1 GHz and up, the commercial status of MMIC is simple to describe. At the time of this writing, there are no commercial MMICs available. This is not to say that development of MMICs is not a high priority. Virtually every GaAs laboratory in the world has an ongoing MMIC development program.[9] Many labs have been doing MMIC work for 10 years or more, and the number and variety of various circuits created has been very impressive. Early MMICs were not "pure," in that wire bonds were still incorporated for interconnects on the chip, layouts tended to be straight carryovers of the circuit done by chip and wire and alumina, and complexity was not very high. What became obvious from the early work was that much new ground needed to be covered. Modeling of discrete FETs had to be modified when the same discrete design was embedded in a sea of GaAs and connected by transmission lines instead of wire bonds. Modeling and experiments on GaAs transmission lines, various types of inductors, interdigitated and overlay capacitors, and various coupling structures had to be done almost from scratch.

Considerable progress has been made. Layouts are much more compact, modeling is quite refined, and the basic active and passive elements form blocks from which multi-function circuits or multi-stage amplifiers can be designed and fabricated with reasonable success. Low-noise MMIC stages are starting to have noise figures approaching discrete values, and power amplifier stages have been built with excellent power outputs in the several-Watt range and over wide bandwidths. A 3-W MMIC circuit operating over the 8- to 12-GHz range was reported recently.[10] Perhaps the most revealing measure of progress in MMIC development is that creative use of the medium is taking place. Rather than just replicating MIC circuits, researchers are taking advantage of the precision layout capability of the lithographic process to design feedback amplifiers and switches and phase shifters that could not be built with hybrid techniques. The control of circuit elements and minimization of parasitics, especially at frequencies in X band and above, allow unique circuits to be built with extremely wide bandwidths. An outstanding example of the MMIC approach to creating circuits which likely could not be built in any other way has recently been given.[11] A photomicrograph of the circuit is shown in Figure 13. The distributed traveling-wave amplifier circuit shown has about 4 dB gain over the 2- to 10-GHz range and with 200 to 300 mW of output power.

Performance feasibility has certainly been demonstrated for GaAs MMICs. There yet remain to be answered the questions of performance reproducibility, yield, cost, and reliability. Given the volume demand for phased-array modules, wideband gain stages, and commercial TV receivers (DBS), the issues will likely be favorably settled. Cost can be advantageous relative to MICs if the volume is high enough to warrant the design, layout, mask levels, and GaAs fabrication

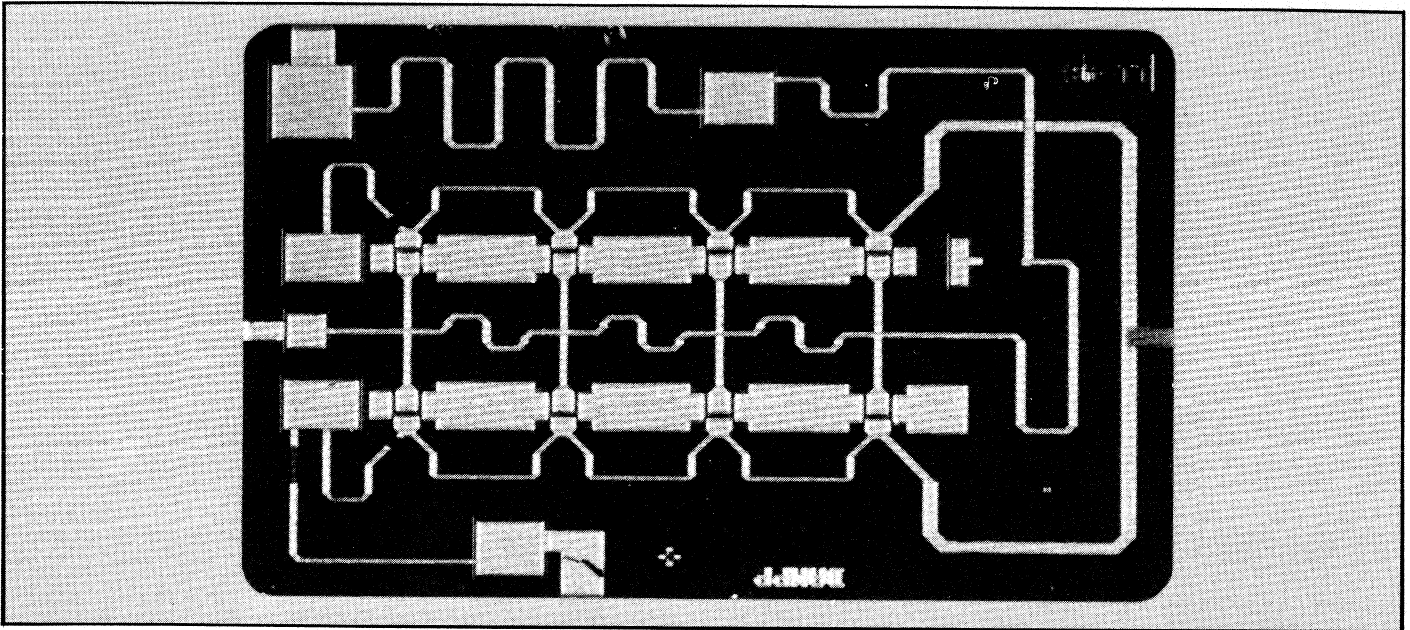

13. This is a distributed, traveling-wave amplifier, which provides 4 dB gain with 200 to 300 mW power across 2 to 20 GHz (Courtesy of Raytheon Corporation).

investment along with an implied reproducibility of circuit performance and simple, rapid testing schemes. The stage has been set; the next two to three years will result in MMICs finding their proper niche.

Digital Integrated Circuits (DIGICs) for Microwave Application

• *Digital/Microwave Applications.* At first, it seems somewhat strange to discuss digital circuits and microwave systems in the same context. In actuality, there has been for many years a strong connection between certain classes of digital circuits and microwave systems. The areas of frequency synthesis, counting and controlling, multiplexing and demultiplexing, and signal processing have generally made use of microwave mixers and detectors and other microwave components directly in conjunction with digital devices such as fixed dividers, variable modulus dividers, shift registers, and memories.

GaAs DIGICs of SSI and MSI complexity can continue this digital/microwave relationship which has existed with high-speed, Si ECL circuits. The GaAs advantage is to provide the same function as Si and perhaps new functions with solid 1-GHz performance over temperature and up to perhaps 10 GHz. Certainly, the 1- to 4-GHz range will be covered with GaAs circuits that make use of existing materials and 1-μm processing technology. The prognosis for enhanced performance is quite good with the pending development of self-aligned 1 μm and submicron gate processing and improved material quality and uniformity.

• *DIGIC Status.* In similar fashion to MMIC development, there has been a tremendous amount of GaAs DIGIC development over the past 5 to 10 years in laboratories all over the world. The examples of DIGIC devices range from an SSI complexity, 10-GHz, divide-by-2 circuit to more recent attempts to construct LSI 1-kbit static memories. Typically, researchers are trading off power and speed, circuit complexity, many different logic families (buffered FET logic, Schottky diode FET logic, enhancement-depletion mode logic, etc.), and different processing approaches to obtain good yields and performance. A major issue is the absolute FET pinchoff- or threshold-voltage level and its variation. Control of the parameter is critical for digital circuit design and for the noise margin available. Bipolar Si threshold voltage depends only weakly on parameters such as doping and geometry variation, whereas GaAs FETs are highly sensitive. The consequence is that zero-Volt or even 1-V threshold values for GaAs FETs are difficult to control. For a 20- to 30-millivolt tolerance on threshold voltage around a 0- to 1-V level, it effectively requires controlling active layer doping and thickness to a few percent and less than 100 Å, respectively. From a practical viewpoint the 1.5- to 2-V pinch-off voltage range will result in realistic circuits for the short term. For the expense in power, reasonable-yield circuits will be made with useful fan-out levels and gate propagation delays of about 100 psec.

The general use of GaAs ICs for microwave and signal processing work should be for frequency prescaling, counting, and controlling. A fast-to-slow, serial-to-parallel function is where the GaAs speed advantage is best used. Practical GaAs DIGICs should have the capability for providing input and output levels that directly interface with Si ECL circuits. This will provide systems designers with a high degree of flexibility while allowing higher input or clock frequencies. An excellent example of a DIGIC building block for many different system applications is a universal shift register. Such a device can be used to take a single (serial) high-speed signal or bit stream and feed out the data in several parallel bit streams. This demultiplexing function can be reversed so that a parallel-to-serial or multiplexing function is accomplished. The device may also be used as a hold register so that the data that are "shifted" into another identical register may be transferred in a time period less than a clock period, and be

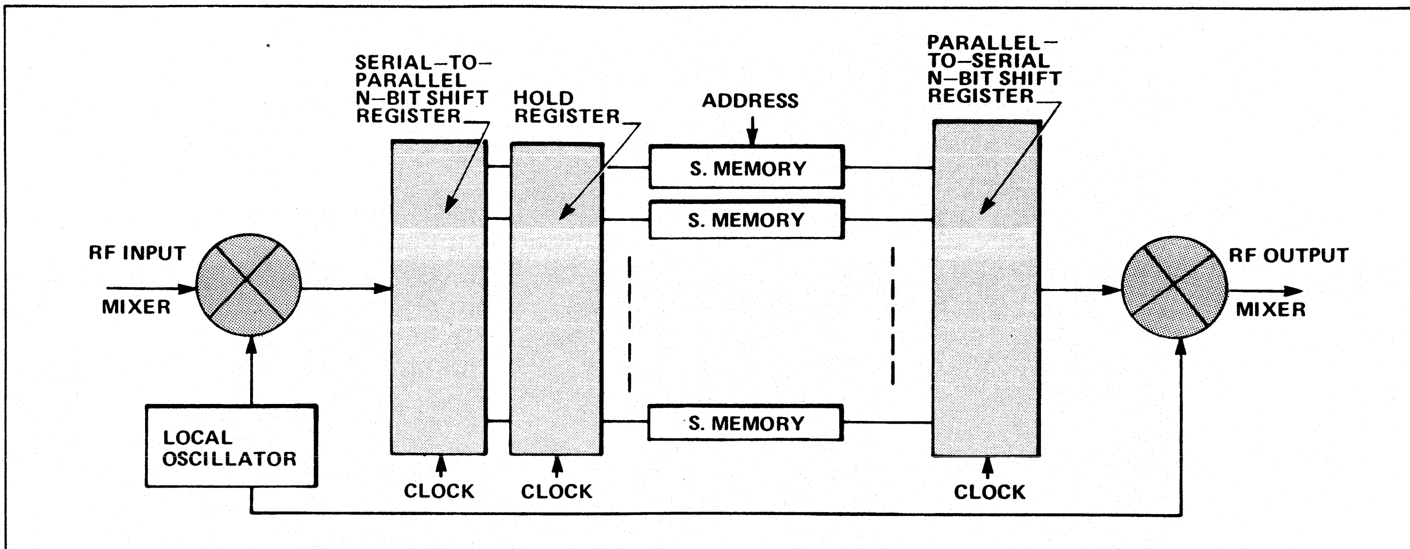

14. A simple digital/RF memory module could take this form.

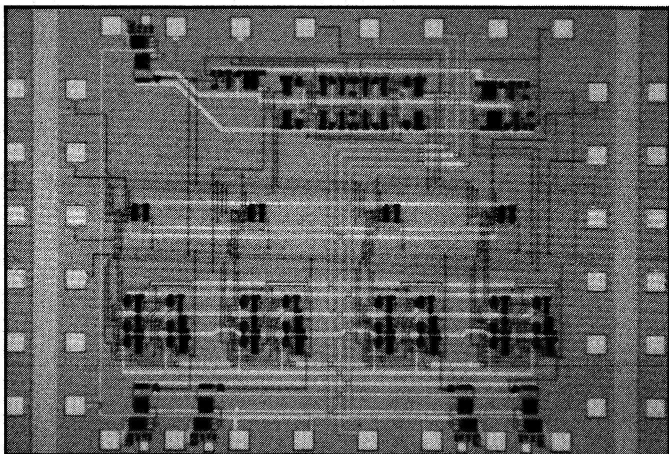

15. This GaAs 4-bit universal shift register will be commercially available (Courtesy of Harris Microwave Semiconductor).

held. These stored data can be further transferred to larger and slower Si registers (memory) at a more relaxed time of N × clock period, where N is the number of bits the GaAs DIGIC can handle (typically 4, 8, 16, and so on).

Digital RF memories and ECM repeater memories presently use the techniques described above using high-speed Si ECL circuits with basic clock rates of 200 to just under 400 MHz. An MSI GaAs universal shift register will allow these systems to perform at basic clock rates of 4 to 8 times those of Si circuits. A schematic of a simple digital RF memory module is shown in Figure 14. A photomicrograph of a GaAs 4-bit universal shift register (to become commercially available) is shown in Figure 15.

Commercial Expectations for GaAs ICs

At the time of this writing, there are no gigahertz, commercial GaAs MMIC or DIGIC products available. In the MMIC arena, production devices will be made in the next two to three years, although it is not clear that "catalog" MMIC products will become available. The more custom nature and the primarily military usage of MMICs may keep the devices that are eventually brought to production internal to those companies doing the work. On the other hand, one can see the utility of compact, wideband and low-cost generic MMIC amplifiers and other microwave components for laboratory and commercial use. Perhaps these also will come about.

The commercial GaAs DIGIC area will definitely be established by the availability of catalog devices. The Si world has set the basis for very useful circuits for high-speed signal processing, logic, and memory. Many of these same functions will be accomplished at much higher speeds by GaAs DIGICs. The level of complexity possible, the power dissipation, the speed advantage and, most importantly, the cost will sort out which GaAs devices make sense relative to comparable Si devices. Finally, not all requirements for fast GaAs DIGICs can be covered by catalog products. There will likely be a product area where a GaAs-cell–array approach is taken in order to quickly create circuits of a more custom nature. ■

References

1. C.A. Mead, *Proc. IEEE*, 54:307, Feb. 1966.
2. J.A. Turner and B.L.H. Wilson, *Proc.* 1968 *Symp. on GaAs*, Paper 30, p. 195.
3. B.S. Hewitt, et al, *Electronics Letters*, 12, 1976, p. 309.
4. E.T. Watkins, 1983 *MTT-Symposium Digest*, Paper D. 7 p. 145, Boston, 1983.
5. J.V. DiLorenzo, *Microwave Journal*, Feb. 1978, p. 39.
6. J.A. Turner, et al, "The Noise and Gain Performance of Submicron Gate Length GaAs FETs," *GaAs FET Principles and Technology*, Artech House 1982, p. 151.
7. S.C. Cripps, *MTT-Symposium Digest*, Paper G-7, Boston 1983, p. 221.
8. W.O. Schlosser, and V. Sokolov, "Circuit Aspects of Power GaAs FETs," *GaAs FET Principles and Technology*, Artech House, 1982, p. 477.
9. D.R. Ch'en, "GaAs MMICs: When Will They Be Ready For Systems Implementation?" *Microwave Systems News*, July 1983, p. 105.
10. R.G. Freitag, et al, *Monolithic Circuits Symposium Digest*, Boston 1983, p. 62.
11. Y. Ayasli, et al, *Monolithic Circuits Symposium Digest*, Boston 1983, p. 67.

GaAs FET Matrix

Emphasis Shifts to Higher Frequencies as GaAs FET Technology Continues Forward

The field of gallium arsenide FETs (field-effect transistors) continues expanding, and is now clearly the basis for a mature discrete device market. The prices of many GaAs FET devices continue to drop, due to lower-cost packages and increased production and reproducibility. The emphasis in this area has shifted to obtaining higher power and gain at frequencies above 40 GHz.

The first GaAs FET matrix presented in the October 1982 issue of *MSN* was very well-received, and generated a great deal of interest in the industry at large. This positive reaction to that first matrix was the deciding factor in the determination to revise and update that data for inclusion in *The Microwave System Designer's Handbook*. The time and effort were obviously well spent.

The data presented here are the best and most complete that were obtainable from those manufacturers which were able to participate in this year's GaAs FET Matrix. Again, as with the Bipolar Matrix making its debut in the *MSDH*, the editorial staff is providing this matrix as a service to the reader, and no liability for errors or omissions is assumed.

The information is being presented in the same format as the 1982 matrix, which was found to be clear and concise. In those cases where a particular FET manufacturer's device specifications were received in a different format or broken down into slightly different parameters from those used in the matrix, this fact has been noted in the appropriate column of the matrix, to the right of the manufacturer's name.

The *MSDH* staff hopes that this new edition of the GaAs FET Matrix will be as useful as last year's was in helping the reader simplify the decision process concerning device choice for his particular applications.

The device manufacturers listed in the GaAs FET Matrix may be contacted through marketing personnel at the addresses and telephone numbers listed below.

Alpha Industries, Inc. .... (617) 935-5150
20 Sylvan Rd., Woburn, MA 01801

Amperex Electronic Corp. .... (516) 931-6200
230 Duffy Ave., Hicksville, NY 11802

Avantek, Inc. .... (408) 727-0700
3175 Bowers Ave., Santa Clara, CA 95051

Dexcel, Inc. .... (408) 727-9801
2285-C Martin Ave., Santa Clara, CA 95050

Fujitsu Microelectronics, Inc. .... (408) 980-8585
Microwave and Optoelectronics Div.
3080 Oakmead Village Dr., Santa Clara, CA 95051

M/A-Com Gallium Arsenide Products, Inc. .. (617) 272-3000
South Ave., Burlington, MA 01803

Microwave Semiconductor Corp. (MSC) .... (201) 469-3311
100 School House Rd., Somerset, NJ 08873

Mitsubishi Electronics America, Inc. .... (408) 740-5900
1230 Oakmead Pkwy., Sunnyvale, CA 94086

Motorola, Inc. .... (602) 244-3641
5005 East McDowell Rd., Phoenix, AZ 85008

NEC/California Eastern Laboratories, Inc. ... (408) 988-3500
3005 Democracy Wy., Santa Clara, CA 95050

Plessey Semiconductors .... (714) 951-5212
Optoelectronics and Microwave Div.
3 Watney, Irvine, CA 92714;

Raytheon Co. .... (617) 393-7300
Special Microwave Devices Operation
Bearfoot Rd., Northborough, MA 01532

Texas Instruments, Inc. .... (214) 995-6531
P.O. Box 225012, Mail Station 12, Dallas, TX 75265

Thomson-CSF Semiconductor Div. .... (213) 887-1010
P.O. Box 1454, Canoga Park, CA 91304

Toshiba Corp. .... Tel: Tokyo 501-5411
1-6 Uchisawi Ai-Cho 1-Chome, Chiyoda-Ku, Tokyo, Japan

Varian, Solid State Microwave Div. .... (408) 988-1331
3251 Olcott St., Santa Clara, CA 95050

GaAs FET Matrix

Low-Noise GaAs FETs

FREQUENCY (GHz)

Part Number	Gate Length μm	f_{MAX} GHz	2			4			6			8			10			12			18		
			NF	G_A	MAG	NF	G_A	MAG	NF	G_A	MAG	NF	G_A	MAG	NF	G_A	MAG	NF	G_A	MAG	NF	G_A	MAG
ALPHA INDUSTRIES, INC.																							
ALF 1000	1.0	60	0.7	15	20	1.3	12.5	16	—	—	—	2.3	10.5	11	—	—	—	—	—	—	—	—	—
ALF 1003	1.0	60	0.7	15	20	1.3	12.5	16	—	—	—	2.3	9.5	11	—	—	—	—	—	—	—	—	—
ALF 1020	1.0	60	0.9	14.0	18	1.6	11.5	15	—	—	—	2.6	9.0	10	—	—	—	—	—	—	—	—	—
ALF 1023	1.0	60	0.9	13.5	18	1.6	11.0	15	—	—	—	2.6	8.5	10	—	—	—	—	—	—	—	—	—
ALF 3000	0.5	70	—	—	—	0.9	13.0	17	—	—	—	1.5	11.0	14	—	—	—	2.1	8.5	9	2.8	6.0	6.5
ALF 3003	0.5	70	—	—	—	0.9	13.0	17	—	—	—	1.5	10.5	14	—	—	—	2.2	8.0	9	—	—	—
ALF 3300	0.5	75	—	—	—	0.8	13.5	18	—	—	—	1.4	11.5	15	—	—	—	1.9	9.0	9.5	2.5	6.5	—
ALF 3303	0.5	75	—	—	—	0.8	13.5	18	—	—	—	1.4	11.0	15	—	—	—	2.1	8.5	9.5	—	—	—
AMPEREX ELECTRONIC CORP.																							
CFX13	0.5	—	—	—	—	—	—	—	—	—	—	—	—	—	2.2	8.0	10.5	2.5	7.5	9.0	—	—	—
CFX14	0.5	—	—	—	—	—	—	—	—	—	—	—	—	—	—	—	—	2.3	8.2	10.0	2.7	6.0	8.0
AVANTEK, INC.																							
AT-8111 (AT-11000)	0.5	30	0.7	18	—	0.9	13	—	1.2	11	—	1.4	9	11	—	—	—	—	—	—	—	—	—
AT-8110 (AT-11070)	0.5	30	0.7	18	—	0.9	13	16	1.3	10	12	1.5	8	10	—	—	—	—	—	—	—	—	—
AT-8251 (AT-12500)	0.5	40	0.7	18	—	0.9	14	—	1.2	12	—	1.4	10	—	1.6	9.5	11	1.8	8.5	9	—	—	—
AT-8250 (AT-12570-1)	0.5	40	0.7	18	—	0.9	14	—	1.3	11	—	1.5	9	13	1.7	8.5	11	1.9	7.5	—	—	—	—
AT-12570-5	0.5	40	0.7	18	—	1.0	13	—	1.5	10	—	1.7	8	13	2.0	7.5	11	2.4	6.5	—	—	—	—
AT-12535	0.5	40	0.7	18	—	1.0	13	—	1.5	10	—	1.7	8	13	2.0	7.5	11	2.4	6.5	—	—	—	—
AT-10650-1	0.5	45	0.7	18	—	0.9	14	—	1.1	13	—	1.4	12	—	1.5	11	12	1.6	9.5	10.5	2.4	6	7
AT-10650-3	0.5	45	0.7	18	—	0.9	14	—	1.1	13	—	1.5	12	—	1.7	11	12	1.8	9.5	10.5	—	—	—
AT-10650-5	0.5	45	0.7	18	—	1.0	13	—	1.2	12	—	1.6	11	—	1.8	10	12	2.0	8.5	10.5	—	—	—
AT-10635	0.5	45	—	—	—	—	—	—	—	—	—	—	—	—	—	—	—	2.5	7.5	11.0	—	—	—
AT-8040	0.5	75	—	—	—	—	—	—	1.7	13	(15)*	—	—	—	—	—	—	2.4	9	(12)*	—	—	—
DEXCEL, INC.																							
DXL-2501A	1.0	—	—	—	—	1.4	13	16	—	—	—	2.2	9	11	—	—	—	—	—	7.5	—	—	—
DXL-2501A-P70	1.0	—	0.5	20	24	1.4	13	16	—	—	—	2.2	9	11	—	—	—	—	—	—	—	—	—
DXL-2502A	0.7	—	—	—	—	1.3	13	17	—	—	—	2.2	10	12	—	—	—	3.2	7	10	—	—	—
DXL-2502-A-P70	0.7	—	—	—	—	1.3	13	17	—	—	—	2.2	10	12	—	—	—	—	—	—	—	—	—
DXL-2503A	0.5	—	—	—	—	1.0	14	18	—	—	—	1.8	11	14	—	—	—	2.8	8.5	12	4.0	6	9
DXL-2503A-P70	0.7	—	—	—	—	1.0	14	18	—	—	—	1.8	11	14	—	—	—	2.8	8.5	11	—	—	—
DXL-2608A	0.6	—	—	—	—	—	—	—	—	—	—	3.0	8	11	—	—	—	—	—	—	—	—	—
DXL-2608A-P70	0.6	—	—	—	—	—	—	—	—	—	—	—	—	—	—	—	—	—	—	—	—	—	—
DXL-1503A	0.5	—	—	—	—	0.8	13	16	—	—	—	1.4	9	13	—	—	—	1.8	8	11	3.5	6	7
DXL-1503A-P70	0.5	—	—	—	—	0.8	13	16	—	—	—	1.4	9	13	—	—	—	1.8	7	10	—	—	—
DXL-0503A	.025	—	—	—	—	0.6	15	18	—	—	—	—	—	—	—	—	—	1.5	10	13	2.3	8.5	11
DXL-0503A-P70	.025	—	—	—	—	0.6	15	18	—	—	—	—	—	—	—	—	—	1.5	10	13	—	—	—
FUJITSU MICROELECTRONICS, INC.																							
FSC07FA	—	—	—	—	—	—	—	—	—	—	—	—	—	—	—	—	—	—	—	—	—	—	—
FSX100FA	—	—	—	—	—	—	—	—	—	—	—	—	—	—	—	—	—	—	—	—	—	—	—
MICROWAVE SEMICONDUCTOR CORP.																							
CFY-10	1.0	—	—	—	—	—	—	—	1.6	10.0	13.0	—	—	—	—	—	—	—	—	—	—	—	—
CFY-13	1.0	—	1.0	13.5	22.0	1.5	12.0	16.0	2.0	10.0	12.5	2.5	9.0	10.0	—	—	—	3.6	6.0	6.5	—	—	—

P_o dBm	f GHz	Max Ratings R_{TH} °C/W	T_J	V_{DS}	V_{GS}	V_{DS} nom volts	I_{DSS} nom mA	V_P nom volts	Package Type	Mfgr.'s Remarks	Price Quantity 1-100	1000
12	4	170	—	5V	−10V	3.5	55	2.5	Chip	Recessed gate structures,	$18.50	—
12	4	170	—	5V	−10V	3.5	55	2.5	Hermetic 70 mil square	broadband and low noise	22.00	—
12	4	170	—	5V	−10V	3.5	55	2.5	Chip	performance for both	12.00	—
12	4	170	—	5V	−10V	3.5	55	2.5	Hermetic 70 mil square	amplifiers and oscillators	15.50	—
10	12	180	—	5V	−6V	3.5	50	2.0	Chip	in commercial and military	26.00	—
10	12	180	—	5V	−6V	3.5	50	2.0	Hermetic 70 mil square	applications.	29.50	—
10	12	180	—	5V	−6V	3.5	50	2.0	Chip	—	37.50	—
10	12	180	—	5V	−6V	3.5	50	2.0	Hermetic 70 mil square	—	42.00	—
13	10	200	175	5	−6	3	35	—	FO-92	Avail as chip CFX13X	64.00	—
13	10	200	175	5	−6	3	35	—	FO-92	Avail as chip CFX14X	68.00	—
+21	4	100	175	—	—	3	120	−1.5	—	—	—	—
+21	4	250	175	—	—	3	120	−1.5	—	—	—	—
+20	4	160	175	—	—	3	100	−1.5	—	—	—	—
+20	4	300	175	—	—	3	100	−1.5	—	—	—	—
+20	4	300	175	—	—	3	100	−1.5	—	—	—	—
+20	4	300	175	—	—	3	100	−1.5	—	—	—	—
+18	12	300	175	—	—	3	50	−1.5	—	—	—	—
+18	12	300	175	—	—	3	50	−1.5	—	—	—	—
+18	12	300	175	—	—	3	50	−1.5	—	—	—	—
17	12	200	175	7	−5	3	50	−2	Micro-x	Low cost	19.75	16.00
8	12	250	150	5	−4	3	40	−2	50 mil stripline	Usable in Ku-band	110.00	84.00
+18	8	100	175	10	—	6	70	−2	Chip form	3.5V, 15mA for NF OPT, or 6V, 0.5 I_{DSS} for power	—	—
+17	8	200	175	10	—	6	70	−2	P70-Hermetic	—	—	—
+10	12	180	175	10	—	4	40	−2	Chip form	Good wideband gain performance thru 15 GHz. Designed for X-band performance	—	—
+10	12	300	175	10	—	4	40	−2	P70-Hermetic	—	—	—
+12	18	180	175	10	—	4	60	−2	Chip form	Super gain performance thru 18 GHz good for 20-21 GHz. Designed for maximum gain @ 18 GHz	—	—
+12	12	300	175	10	—	4	60	−2	P70-Hermetic	2501, 2502, 2503 have been qualified for and used in "Hi-Rel" programs.	—	—
+21	8	70	175	10	—	6	175	−3	Chip form	Designed for high trans-conductance for feedback applications	—	—
+21	8	170	175	10	—	6	175	−3	P70-Hermetic	—	—	—
+10	8	180	175	10	—	3	30	−1	Chip form	Designed for low noise performance	—	—
+10	8	300	175	10	—	3	30	−1	P70-Hermetic	—	—	—
+10	12	190	175	6	—	3	40	−1	Chip form	Ultra low noise. Super high gain at 20-22 GHz.	—	—
+10	12	310	175	6	—	3	40	−1	P70 Hermetic	12 GHz LNA application.	—	—
—	4.0	—	+175	8.0	−5.0	3.0	10	−1.5	FA	Low cost	—	—
12	12	—	+175	12	−5.0	5.0	45	−2.5	FA	Gain stage	—	—
—	—	—	—	—	—	—	—	—	—	New release	—	—
13.4	4.0	—	—	5.0	±5	4	60	−2.5	Cerec	—	14.50	—

Low-Noise GaAs FETs

FREQUENCY (GHz)

Part Number	Gate length µm	f_{MAX} GHz	2			4			6			8			10			12			18		
			NF	G_A	MAG	NF	G_A	MAG	NF	G_A	MAG	NF	G_A	MAG	NF	G_A	MAG	NF	G_A	MAG	NF	G_A	MAG
CFY-14	1.0	—	1.1	12.0	30.0	1.7	10.5	14.0	2.2	8.5	10.0	3.0	7.0	8.0	—	—	—	—	—	—	—	—	—
CFY-11	1.0	—	1.0	13.5	22.0	1.5	12.0	16.0	2.0	10.0	12.5	2.5	9.0	10.0	—	—	—	3.6	6.0	6.5	—	—	—
CFY-12	1.0	—	1.1	12.0	20.0	1.7	10.5	14.0	2.2	8.5	10.0	3.0	7.0	8.0	—	—	—	—	—	—	—	—	—
CFY-15	0.5	—	—	—	—	—	—	—	—	—	—	—	—	—	—	—	—	2.2	9.0	12.0	—	—	—
MITSUBISHI ELECTRONIC AMERICA, INC.																							
CERAMIC PACKAGE																							
MGF 1202	.8	55	—	—	—	1.4	11	16	—	—	—	—	—	—	—	—	—	—	—	—	—	—	—
MGF 1203	.5	90	—	—	—	.8	14	18	—	—	—	—	—	—	—	—	—	—	—	—	—	—	—
MGF 1402	.8	70	—	—	—	1.1	13	18	—	—	—	—	—	—	—	—	—	—	—	—	—	—	—
MGF 1403-11-09	.5	90	—	—	—	.8	14	18	—	—	—	—	—	—	—	—	—	—	—	—	—	—	—
MGF 1403-61-20	.5	90	—	—	—	—	—	—	—	—	—	—	—	—	—	—	—	1.9	11	14	—	—	—
MGF 1403-61-23	.5	90	—	—	—	—	—	—	—	—	—	—	—	—	—	—	—	2.1	11	14	—	—	—
MGF 1404-11-07	.3	100	—	—	—	.6	15	18	—	—	—	—	—	—	—	—	—	—	—	—	—	—	—
MGF 1404-61-16	.3	100	—	—	—	—	—	—	—	—	—	—	—	—	—	—	—	1.5	12	15	—	—	—
MGF 1404-61-17	.3	100	—	—	—	—	—	—	—	—	—	—	—	—	—	—	—	1.6	12	15	—	—	—
MGF 1412-11-08	.7	80	—	—	—	.7	13	18	—	—	—	—	—	—	—	—	—	—	—	—	—	—	—
MGF 1412-11-09	.7	80	—	—	—	.8	13	18	—	—	—	—	—	—	—	—	—	—	—	—	—	—	—
MGF 1412-11-10	.7	80	—	—	—	.9	13	18	—	—	—	—	—	—	—	—	—	—	—	—	—	—	—
CHIPS																							
MGFC 1402-(*)	.8	70	—	—	—	1.1	13	18	—	—	—	—	—	—	—	—	—	—	—	—	—	—	—
MGFC1403-(*)-09	.5	90	—	—	—	.8	14	18	—	—	—	—	—	—	—	—	—	—	—	—	—	—	—
MGFC1403-(*)-19	.5	90	—	—	—	—	—	—	—	—	—	—	—	—	—	—	—	1.9	11	14	—	—	—
MGFC1403-(*)-21	.5	90	—	—	—	—	—	—	—	—	—	—	—	—	—	—	—	2.1	11	14	—	—	—
MGFC1403-(*)-23	.5	90	—	—	—	—	—	—	—	—	—	—	—	—	—	—	—	2.2	11	14	—	—	—
MGFC1404-(*)-07	.3	100	—	—	—	.6	15	18	—	—	—	—	—	—	—	—	—	—	—	—	—	—	—
MGFC1404-(*)-18	.3	100	—	—	—	—	—	—	—	—	—	—	—	—	—	—	—	1.6	12	15	—	—	—
MGFC1412-(*)-09	.7	80	—	—	—	0.9	13	18	—	—	—	—	—	—	—	—	—	—	—	—	—	—	—
MGFC1412-(*)-10	.7	80	—	—	—	1.0	13	18	—	—	—	—	—	—	—	—	—	—	—	—	—	—	—
NEC CORPORATION/ CAL EASTERN LABS, INC.																							
NE67300	0.25	100	0.3	18.0	19.5	0.4	14.5	17.0	0.7	13.0	16.5	1.0	11.5	16.0	1.2	10.5	12.5	1.4	10.0	11.0	2.1	8.0	8.5
NE67383	0.25	100	0.3	18.0	19.5	0.4	14.5	17.0	0.7	13.0	16.5	1.0	11.5	16.0	1.2	10.5	12.5	1.6	10.0	11.0	2.1	8.0	8.5
NE71000	0.25	100	0.4	18.0	19.5	0.6	14.5	17.0	0.8	13.0	16.5	1.1	11.5	16.0	1.3	10.5	12.5	1.6	10.0	11.0	2.3	8.0	8.5
NE71083	0.25	100	0.4	18.0	19.5	0.6	14.5	17.0	0.8	13.0	16.5	1.1	11.5	16.0	1.3	10.5	12.5	1.7	10.0	11.0	2.3	8.0	8.5
NE13700	0.5	80	0.6	17.0	19.0	0.7	14.0	17.0	1.0	12.5	17.0	1.2	11.0	15.0	1.5	10.0	12.0	1.7	9.0	11.0	2.3	5.0	6.0
NE13783	0.5	80	0.6	17.0	19.0	0.8	14.0	17.0	1.0	12.5	17.0	1.2	11.0	15.0	1.5	10.0	12.0	1.9	9.0	11.0	2.3	5.0	6.0
NE70000	0.5	80	0.7	17.0	19.0	0.7	14.0	17.0	1.1	12.5	17.0	1.3	11.0	15.0	1.6	10.0	12.0	2.0	9.0	11.0	—	—	—
NE70083	0.5	80	0.7	17.0	19.0	0.7	14.0	17.0	1.1	12.5	17.0	1.3	11.0	16.0	1.6	10.0	12.0	2.2	9.0	11.0	—	—	—
NE21800	1.0	60	0.8	15.0	19.0	1.0	12.0	17.0	1.3	11.0	13.0	1.7	10.5	12.0	2.2	9.0	9.5	2.4	7.5	9.5	—	—	—
NE21889	1.0	60	0.8	15.0	19.0	1.0	12.0	17.0	1.3	11.0	13.0	1.7	10.5	12.0	2.2	9.0	9.5	2.8	7.5	9.5	—	—	—
NE72000	1.0	60	1.0	13.0	19.0	1.3	10.0	16.0	1.6	8.5	13.0	2.1	7.0	12.0	2.6	6.0	9.0	—	—	—	—	—	—
NE72089	1.0	60	1.0	13.0	19.0	1.3	10.0	16.0	1.6	8.5	13.0	2.1	7.0	12.0	2.6	6.0	9.0	—	—	—	—	—	—
NE24400	1.0	55	1.0	14.0	22.0	1.3	13.5	17.0	1.7	11.5	13.0	2.0	10.5	12.0	2.6	9.5	10.5	2.6	7.0	10.0	—	—	—
NE24483	1.0	55	1.0	14.0	22.0	1.3	13.0	17.0	1.7	11.5	13.0	2.0	10.0	11.0	2.6	9.5	10.5	3.0	6.5	9.0	—	—	—
NE38800	0.5	80	1.0	14.5	20.0	1.2	14.0	18.0	1.7	12.0	16.0	1.7	12.0	14.0	2.6	9.5	13.0	2.1	9.5	12.0	4.0	6.0	7.5
NE38883	0.5	80	1.0	14.5	20.0	1.2	14.0	18.0	1.7	12.0	16.0	1.7	12.0	13.0	2.6	9.5	13.0	2.6	8.0	11.0	—	—	—
NE46383	1.0	45	—	—	—	1.7	17.0	18.0	—	—	—	3.0	12.0	14.0	—	—	—	4.0	9.0	10.0	—	—	—
PLESSEY SEMICONDUCTORS																							
GAT 1/010 in P101 package	4		2.5	—	12	Maximum recommended frequency is 1.5 GHz									—	—	—	—	—	—	—	—	—
GAT 4 P107 package	1	85	—	—	—	—	—	—	—	—	—	2.1	7	11	—	—	—	—	—	—	—	—	—
GAT 6 P100 chip	0.5	—	—	—	—	1	15	19	—	—	—	1.5	11.5	15	—	—	—	2.2	9.5	13	3.5	7	—
RAYTHEON CO.																							
RLK 048	0.5	80	—	—	—	—	—	—	1.0	12	16	1.2	11	15	1.7	10.5	12	1.9	9.5	10	2.5	7.0	8.0
RLX 835	1.0	50	—	—	—	1.5	13	16	2.0	11	14	2.5	9.0	12	3.0	7.0	10	3.5	5.0	8.0	—	—	—
THOMSON-CSF																							
TC 1100	1	—	—	—	—	1.5	12	15	—	—	—	—	—	—	—	—	—	—	—	—	—	—	—
TC 1101	1	—	—	—	—	1.5	12	15	—	—	—	—	—	—	—	—	—	—	—	—	—	—	—

P_O dBm	f GHz	Max Ratings R_{TH} °C/W	T_J	V_{DS}	V_{GS}	V_{DS} nom volts	I_{DSS} nom mA	V_P nom volts	Package Type	Mfgr.'s Remarks	Price Quantity 1-100	1000
13.4	4.0	—	—	5.0	±5	4	60	−2.5	Cerec	—	13.80	—
13.4	4.0	200	—	5.0	±5	4	60	−2.5	Metal ceramic	—	—	—
13.4	4.0	200	—	5.0	±5	4	60	−2.5	Metal ceramic	—	—	—
—	—	—	—	—	—	—	—	—	Metal ceramic	—	—	—
—	—	—	150	8	−6	3	70	−2	70 mil. ceramic stripline	—	7.45	—
—	—	—	—	6	−6	3	50	−2	70 mil. ceramic stripline	—	20.70	—
—	—	—	—	8	−6	3	70	−2	70 mil. metal-ceramic stripline	—	10.95	—
—	—	—	—	6	−6	3	50	−2	70 mil. metal-ceramic stripline	—	26.00	—
—	—	—	—	6	−6	3	50	−2	70 mil. metal-ceramic stripline	—	32.50	—
—	—	—	—	6	−6	3	50	−2	70 mil. metal-ceramic stripline	—	26.00	—
—	—	—	—	6	−6	3	40	−2	70 mil. metal-ceramic stripline	—	52.00	—
—	—	—	—	6	−6	3	40	−2	70 mil. metal-ceramic stripline	—	65.00	—
—	—	—	—	6	−6	3	40	−2	70 mil. metal-ceramic stripline	—	48.60	—
—	—	—	—	8	−6	3	70	−2	70 mil. metal-ceramic stripline	—	27.25	—
—	—	—	—	8	−6	3	70	−2	70 mil. metal-ceramic stripline	—	21.80	—
—	—	—	—	8	−6	3	70	−2	70 mil. metal-ceramic stripline	—	16.40	—
—	—	—	—	8	−6	3	70	−2	.015″ x .018″ x .005″	(*) Chips are available in	8.80	—
—	—	—	—	6	−6	3	50	−2	.020″ x .014″ x .005″	three visual inspection	20.80	—
—	—	—	—	6	−6	3	50	−2	.020″ x .014″ x .005″	grades as follows;	31.20	—
—	—	—	—	6	−6	3	50	−2	.020″ x .014″ x .005″	A (−11 or −61) space	25.30	—
—	—	—	—	6	−6	3	50	−2	.020″ x .014″ x .005″	grade	20.80	—
—	—	—	—	6	−6	3	40	−2	.020″ x .014″ x .005″	B (−12 or −62) mil std 883	43.40	—
—	—	—	—	6	−6	3	40	−2	.020″ x .014″ x .005″	C (−13 or −63)	43.40	—
—	—	—	—	8	−6	3	70	−2	.015″ x .018″ x .005″	commercial	17.50	—
—	—	—	—	8	−6	3	70	−2	.015″ x .018″ x .005″		12.45	—
14.5	12.0	190	175	5.0	−6.0	3.0	50	−1.1	Chip	—	—	—
14.5	12.0	450	175	5.0	−6.0	3.0	50	−1.1	Ceramic, hermetic	—	—	—
14.5	12.0	190	175	5.0	−6.0	3.0	50	−1.1	Chip	—	—	—
14.5	12.0	450	175	5.0	−6.0	3.0	50	−1.1	Ceramic, hermetic	—	—	—
15.0	12.0	170	175	5.0	−6.0	3.0	50	−1.1	Chip	—	—	—
15.0	12.0	450	175	5.0	−6.0	3.0	50	−1.1	Ceramic, hermetic	—	—	—
15.0	12.0	170	175	5.0	−6.0	3.0	50	−1.1	Chip	—	—	—
15.0	12.0	450	175	5.0	−6.0	3.0	50	−1.1	Hermetic, ceramic	—	—	—
17.0	4.0	170	175	5.0	−6.0	3.0	60	−2.0	Chip	—	—	—
17.0	4.0	400	175	5.0	−6.0	3.0	60	−2.0	Hermetic, ceramic	—	—	—
17.0	4.0	170	175	5.0	−6.0	3.0	60	−2.0	Chip	—	—	—
17.0	4.0	400	175	5.0	−6.0	3.0	60	−2.0	Hermetic, ceramic	—	—	—
10.0	4.0	170	175	5.0	−10.0	3.0	60	−2.5	Chip	—	—	—
10.0	4.0	400	175	5.0	−10.0	3.0	60	−2.5	Hermetic, ceramic	—	—	—
10.0	4.0	170	175	5.0	−8.0	3.0	60	−2.0	Chip	—	—	—
10.0	4.0	400	175	5.0	−8.0	3.0	60	−2.0	Hermetic, ceramic	—	—	—
10.0	4.0	400	175	8.0	−8.0	4.0	60	−3.0	Hermetic, ceramic	Dual gate FET in cascode configuration for high gain	—	—
—	—	—	—	—	—	—	—	—	P101 package	Max. recommended freq. 1.5 GHz	—	—
—	—	—	—	—	—	—	—	—	P107 package	—	—	—
—	—	—	—	—	—	—	—	—	P100 chip	—	—	—
8	12	200	175°	8.0	−6.0	4	40	1.5	.070″ square	Prices are for packaged devices	60.00	—
10	12	200	175°	10.0	−7.0	5	40	1.5	.070″ square, .10″ sq.	Price for quantities above 100 to be negotiated	20.00	—
15	4	180	170	7	−6	3	75	−3	BMH 83	—	—	—
18	4	100	170	7	−6	3	150	−3	BMH 83	Low 3rd order intermodulation		—

GaAs FET Matrix

Low-Noise GaAs FETs

FREQUENCY (GHz)

Part Number	Gate length µm	f_{MAX} GHz	2			4			6			8			10			12			18		
			NF	G_A	MAG	NF	G_A	MAG	NF	G_A	MAG	NF	G_A	MAG	NF	G_A	MAG	NF	G_A	MAG	NF	G_A	MAG
TC 1400	0.5	—	—	—	—	—	—	—	—	—	—	—	—	—	2.5	8.5	11	—	—	—	—	—	—
TOSHIBA CORP.																							
S8831	0.5	—	—	—	—	1.1	13	18	—	—	—	1.8	10	13	—	—	—	—	—	—	—	—	—
JS8831-AS	0.5	—	—	—	—	1.1	13	18	—	—	—	2.3	10	13	—	—	—	—	—	—	—	—	—
S8804-AS	0.5	—	—	—	—	—	—	—	—	—	—	1.4	11	14	—	—	—	2.2	8.5	10	—	—	—
JS8804-AS	0.5	—	—	—	—	—	—	—	—	—	—	1.4	11	14	—	—	—	2.2	8.5	10	—	—	—
JS8818-AS	0.3	—	—	—	—	—	—	—	—	—	—	—	—	—	—	—	—	1.5	10.0	11	2.1	7.5	9.0
JS8819-AS	0.5	—	—	—	—	—	—	—	—	—	—	1.2	11	15	—	—	—	1.8	9	10	—	—	—
JS8819-AS	0.5	—	—	—	—	—	—	—	—	—	—	1.2	11	15	—	—	—	1.8	9	10	—	—	—
JS8830-AS	0.25	—	—	—	—	—	—	—	—	—	—	—	—	—	—	—	—	—	—	—	2.0	8	9.5
VARIAN ASSOCIATES																							
VSF9320	.5X240	—	—	—	—	.8	13	15	—	—	—	—	—	—	1.7	9.5	12	—	—	—	2.5	7	8.0
VSF9321	.5X240	—	—	—	—	.8	13	15	—	—	—	—	—	—	1.7	9.5	12	—	—	—	2.5	7	8.0
VSF9330	.5X240	—	—	—	—	.8	13	15	—	—	—	—	—	—	1.7	9.5	12	—	—	—	2.5	7	8.0
VSF9331	.5X240	—	—	—	—	.8	13	15	—	—	—	—	—	—	1.6	10.5	12	—	—	—	2.5	7	8.0
VSF9340	.5X285	—	—	—	—	.7	14	16	—	—	—	—	—	—	1.6	10.5	12	—	—	—	2.5	7	8.0
VSF9341	.5X285	—	—	—	—	.7	14	16	—	—	—	—	—	—	1.6	10.5	12	—	—	—	2.5	7	8.0
VSF9345	.5X285	—	—	—	—	.7	14	16	—	—	—	—	—	—	1.6	10.5	12	—	—	—	2.5	7	8.0
VSF9346	.5X285	—	—	—	—	.7	14	16	—	—	—	—	—	—	1.6	10.5	12	—	—	—	2.5	7	8.0

Dual-Gate GaAs FETs

FREQUENCY (GHz)

Part Number	Gate length µm	f_{MAX} GHz	AGC dB	2			4			6			8			10			12			18		
				NF	G_A	MAG	NF	G_A	MAG	NF	G_A	MAG	NF	G_A	MAG	NF	G_A	MAG	NF	G_A	MAG	NF	G_A	MAG
AVANTEK, INC.																								
AT-11200	500	21	50(1)	—	—	—	—	—	—	—	—	—	—	—	—	—	—	—	5.5	15	(16)(2)	6.0	11	(12)2
AT-12000	250	30	50(1)	—	—	—	—	—	—	—	—	—	—	—	—	—	—	—	4.5	15.5	(18)(2)	5.0	13	(16)2
DEXCEL, INC.																								
DXL-2704A	0.5	—	3.5	—	—	—	2	16	20	—	—	—	—	—	—	14	—	—	—	—	—	—	—	—
DXL-2704A-P70	—	—	—	—	—	—	—	—	—	—	—	—	—	—	—	—	—	—	—	—	—	—	—	—
DXL-2704A-P70B	—	—	—	—	—	—	—	—	—	—	—	—	—	—	—	—	—	—	—	—	—	—	—	—
MITSUBISHI ELECT. AMERICA, INC.																								
MGF-1100	1.0	35	12	1.5	14	16	2.5	9	12	—	—	—	—	—	—	—	—	—	—	—	—	—	—	—
MOTOROLA, INC.																								
MRF 966	1.0	6.0	37	2.2	13.2	14	—	—	—	—	—	—	—	—	—	—	—	—	—	—	—	—	—	—
MRF 967	1.0	6.0	37	2.2	11.5	11.5	—	—	—	—	—	—	—	—	—	—	—	—	—	—	—	—	—	—
NEC CORPORATION/ CAL EASTERN LABS, INC.																								
NE46300	1.0	45	—	1.2	22.0	—	1.5	19.0	20.0	2.0	18.0	19.0	2.7	16.5	18.0	3.4	14.5	16.0	3.7	13.0	13.5	—	—	—
NE46385	1.0	45	—	1.2	22.0	—	1.7	17.0	18.0	2.3	16.0	17.0	3.0	15.0	17.0	3.8	13.0	15.0	4.1	9.0	11.0	—	—	—
NE46383	—	—	—	—	—	—	—	—	—	—	—	—	—	—	—	—	—	—	—	—	—	—	—	—
NE41137	—	—	—	1.3	20.0	—	—	—	—	—	—	—	—	—	—	—	—	—	—	—	—	—	—	—
PLESSEY SEMICONDUCTORS, INC.																								
DUGAT 10/000	1	60	30	—	—	—	1.5	21	22	—	—	—	2.8	16	17	—	—	—	3.6	13	14	—	—	—
RAYTHEON CO.																								
RDX 832	1	50	30	—	—	—	—	—	—	—	—	—	—	—	—	4	10	12	—	—	—	—	—	—
TEXAS INSTRUMENTS																								
53000	2.5	2.5	55	—	12	—	—	—	—	—	—	—	—	—	—	—	—	—	—	—	—	—	—	—
53030	2.5	3.0	50	—	16	—	—	—	—	—	—	—	—	—	—	—	—	—	—	—	—	—	—	—

P_O dBm	f GHz	Max Ratings R_{TH} °C/W	T_J	V_{DS}	V_{GS}	V_{DS} nom volts	I_{DSS} nom mA	V_P nom volts	Package Type	Mfgr.'s Remarks	Price Quantity 1-100	1000
13	10	200	170	5	−6	3	60	−3	BMH 83	—	—	—
10	8	450	175	5	−6	3	50	−1	Stripline 70 mil.	—	—	—
10	8	200	175	5	−6	3	50	−1	Chip form	—	—	—
10	12	450	175	5	−6	3	50	−1	Stripline 70 mil.	—	—	—
10	12	200	175	5	−6	3	50	−1	Chip form	—	—	—
10	12	200	175	5	−6	3	50	−1	Chip form	—	—	—
10	12	450	175	5	−6	3	50	−1	Stripline 70 mil.	—	—	—
10	12	200	175	5	−6	3	50	−1.0	Chip form	—	—	—
8	18	250	175	4	−5	3	50	−1.0	Chip form	—	—	—
+15	8	271	+180	+5	−5	3	35	−2.5	Chip	R_{TH} is for chip alone	—	—
+15	8	—	+180	+5	−5	3	35	−2.5	.070 package	—	—	—
+15	8	217	+180	+5	−5	3	35	−2.5	Chip	—	—	—
+15	8	—	+180	+5	−5	3	35	−2.5	.070 package	—	—	—
+17	8	182	+180	+5	−5	3	45	−1.5	Chip	[RF data not applicable for packaged FETs at above 12 GHz]	—	—
+17	8	—	+180	+5	−5	3	45	−1.5	.070 package		—	—
+17	8	182	+180	+5	−5	3	45	−1.5	Chip		—	—
+17	8	—	+180	+5	−5	3	45	−1.5	.070 package		—	—

P_O dBm	f GHz	Max Ratings R_{TH} °C/W	T_J	V_{DS}	V_{GS}	V_{DS} nom volts	I_{DSS} nom mA	V_P nom volts	Package Type	Mfgr.'s Remarks	Price Quantity 1-100	1000
16	12	150	300	8	−5	6	80	−2	15x17 mil chip	(1) AGC: 4 GHz, V_{GS2} = O_V to −2V	115	100
13	12	250	300	8	−5	6	40	−2	11x15 mil chip	(2) (MAG) — max, stable gain: 10 $\log_{10}\|S_{21}/S_{12}\|$, dB	98	84
+10	8	150	175	10	—	4v	60	−3	—	Cascode configuration yields 16 dB gain at 13 GHz	—	—
—	—	—	—	—	—	—	—	—	P70-Hermetic	P70-3 terminal hermetic package with cascode bonding configuration	—	—
—	—	—	—	—	—	—	—	—	P70B-Hermetic	P70B-4 terminal hermetic package	—	—
+17	2	—	150	8	−6	3	30	−1.5	70 mil ceramic	—	Contact factory	—
+10	1.0	285	125	10	−8	5	50	−2.5	Plastic Macro-X	AGC: 1 GHz. Low cost.	3.55	—
+10	1.0	285	125	10	−8	5	50	−2.5	70 mil ceramic	AGC: 1 GHz. Hermetic	11.33	—
10.0	4.0	170	175	8.0	−8	4.0	60.0	−3.0	Chip	Space qualified	—	—
10.0	4.0	400	175	8.0	−8	4.0	60.0	−3.0	Ceramic, Hermetic	—	—	—
10.0	4.0	400	175	8.0	−8	4.0	60.0	−3.0	Ceramic, Hermetic	Cascoded configuration for high gain	—	—
—	—	500	125	10.0	−4.5	5.0	40.0	−3.0	—	Low-cost plastic package	—	—
—	—	—	—	—	—	—	—	—	P100 chip	—	—	—
15	10	130	175	10	−8	4	50	−3	Available on Carrier	Price is for packaged devices. Price for quantities above 100 to be negotiated.	$60.00	—
—	—	—	—	12V	4V	8	50	2.0	Plastic Cross Pack	—	—	<$1
—	—	—	—	12V	4V	8	70	2.0	Plastic Cross Pack	—	—	—

Power GaAs FETs

	FREQUENCY (GHz)														
	2			4			6			8			10		
Part Number	Power-Out 1-dB Compression W	Max Gain dB	η	Power-Out 1-dB Compression W	Max Gain dB	η	Power-Out 1-dB Compression W	Max Gain dB	η	Power-Out 1-dB Compression W	Max Gain dB	η	Power-Out 1-dB Compression W	Max Gain dB	η
ALPHA INDUSTRIES INC.															
APX 5000	—	—	—	—	—	—	—	—	—	—	—	—	.1	7	—
APX 5050	—	—	—	—	—	—	—	—	—	—	—	—	.1	7	—
APX 6000	—	—	—	—	—	—	—	—	—	—	—	—	.25	7	—
APX 6050	—	—	—	—	—	—	—	—	—	—	—	—	.25	7	—
AMPEREX ELEC. CORP.															
CFX21	—	—	—	—	—	—	—	—	—	.08	10.0	—	.06	7.5	—
CFX30	—	—	—	—	—	—	—	—	—	.10	8	—	.10	7	—
CFX31	—	—	—	—	—	—	—	—	—	.25	8	—	.25	7	—
CFX32	—	—	—	—	—	—	—	—	—	.50	7	—	—	—	—
CFX33	—	—	—	—	—	—	—	—	—	1.0	6	—	—	—	—
FLM6472-3B	—	—	—	—	—	—	—	—	—	—	—	—	—	—	—
FLM7177-3B	—	—	—	—	—	—	—	—	—	—	—	—	—	—	—
FLM7785-3B	—	—	—	—	—	—	—	—	—	—	—	—	—	—	—
FLM3742-5	—	—	—	—	—	—	—	—	—	—	—	—	—	—	—
FLM4450-5	—	—	—	—	—	—	—	—	—	—	—	—	—	—	—
FLM5964-5	—	—	—	—	—	—	—	—	—	—	—	—	—	—	—
FLM6472-5	—	—	—	—	—	—	—	—	—	—	—	—	—	—	—
FLM7177-5	—	—	—	—	—	—	—	—	—	—	—	—	—	—	—
FLM7785-4	—	—	—	—	—	—	—	—	—	—	—	—	—	—	—
FLM3742-6	—	—	—	—	—	—	—	—	—	—	—	—	—	—	—
FLM4450-6	—	—	—	—	—	—	—	—	—	—	—	—	—	—	—
FLM5964-6	—	—	—	—	—	—	—	—	—	—	—	—	—	—	—
FLM6472-6	—	—	—	—	—	—	—	—	—	—	—	—	—	—	—
FLM7177-6	—	—	—	—	—	—	—	—	—	—	—	—	—	—	—
FLM7785-6	—	—	—	—	—	—	—	—	—	—	—	—	—	—	—
FLX06MH-12	—	—	—	—	—	—	—	—	—	—	—	—	—	—	—
FLX12MH-12	—	—	—	—	—	—	—	—	—	—	—	—	—	—	—
FLK06MH-14	—	—	—	—	—	—	—	—	—	—	—	—	—	—	—
FLK12MH-14	—	—	—	—	—	—	—	—	—	—	—	—	—	—	—
FLS31MM	3.2	10	—	2.5	6.5	28	—	—	—	—	—	—	—	—	—
FLS50MM	—	—	—	4.0	5.5	32	—	—	—	—	—	—	—	—	—
FLC08ME	—	—	—	.63	9.0	35	1.26	7.5	35	—	—	—	—	—	—
FLC15ME	—	—		1.26	7.5	35	—	—	—	—	—	—	—	—	—
FLC30ME	—	—	—	2.5	6.5	35	—	—	—	—	—	—	—	—	—
FLC081WF	—	—	—	—	—	—	—	—	—	.56	6.5	27	—	—	—
FLC151WF	—	—	—	—	—	—	—	—	—	1.12	5.5	22	—	—	—
FLX03MB	—	—	—	—	—	—	—	—	—	—	—	—	—	—	—
FLX06MB	—	—	—	—	—	—	—	—	—	—	—	—	—	—	—
FLX12MB	—	—	—	—	—	—	—	—	—	—	—	—	—	—	—
FLX03WG	—	—	—	—	—	—	—	—	—	—	—	—	—	—	—
FLX06WG	—	—	—	—	—	—	—	—	—	—	—	—	—	—	—
FLK03WG	—	—	—	—	—	—	—	—	—	—	—	—	—	—	—
FLK06WG	—	—	—	—	—	—	—	—	—	—	—	—	—	—	—
AVANTEK, INC.															
AT-8161 (AT-11600)	—	—	—	0.4	12	33	0.4	10.5	30	0.4	9	28	0.4	7.5	24
AT-8160 (AT-11611)	—	—	—	0.4	11	32	0.4	9.5	27	0.3	8	23	—	—	—
AT-11671	—	—	—	0.4	11	32	0.4	9.5	27	0.3	8	23	—	—	—
AT-8151 (AT-11500)	—	—	—	0.8	12	33	0.7	10	28	0.6	8	24	0.6	7	20
AT-8150 (AT-11511)	—	—	—	0.8	11	33	0.7	9	27	0.6	7	22	—	—	—
AT-11571	—	—	—	0.8	11	33	0.7	9	27	0.6	7	22	—	—	—
AT-8141 (AT-11400)	—	—	—	1.6	9	30	1.4	7	26	1.2	6	21	—	—	—
AT-8140 (AT-11411)	—	—	—	1.4	9	27	1.2	6.5	21	1.0	.5	15	—	—	—
IM-2935-3	—	—	—	—	—	—	—	—	—	—	—	—	—	—	—
IM-3742-3	—	—	—	3.2	12	32	—	—	—	—	—	—	—	—	—
IM-4450-3	—	—	—	—	—	—	—	—	—	—	—	—	—	—	—
IM-5764-3	—	—	—	—	—	—	3.2	10	31	—	—	—	—	—	—
IM-6171-3	—	—	—	—	—	—	3.2	10	31	—	—	—	—	—	—
IM-9178-3	—	—	—	—	—	—	—	—	—	3.2	9	30	—	—	—
IM-9984-3	—	—	—	—	—	—	—	—	—	3.2	9	30	—	—	—
IM-3742-6	—	—	—	6.3	9	27	—	—	—	—	—	—	—	—	—
IM-5464-6	—	—	—	—	—	—	6.3	8	25	—	—	—	—	—	—

12 GHz Power-Out 1-dB Compression W	12 GHz Max Gain dB	12 GHz η	18 GHz Power-Out 1-dB Compression W	18 GHz Max Gain dB	18 GHz η	P_O dBm	f GHz	Max Ratings R_{TH} °C/W	Max Ratings T_J	Max Ratings V_{DS}	Max Ratings V_{GS}	V_{DS} nom volts	I_{DSS} nom mA	V_P nom volts	Package Type	Price Quantity 1-100	Price Quantity 1000
—	—	—	—	—	—	20	10	110	—	12	−8	10	80	−4	Chip	$32.00	—
—	—	—	—	—	—	20	10	110	—	12	−8	10	80	−4	100 mil flange pkg.	47.00	—
—	—	—	—	—	—	24	10	60	—	12	−8	10	160	−4	Chip	43.50	—
—	—	—	—	—	—	24	10	60	—	12	−8	10	160	−4	100 mil flange pkg.	58.50	—
—	—	—	—	—	—	18	11	200	175	8	−6	6	40	—	FO-92	78	—
—	—	—	—	—	—	24	10.7	100	175	12	−10	8	100	—	FO-85	138	—
—	—	—	—	—	—	27	8.5	60	175	12	−10	8	250	—	FO-85	152	—
—	—	—	—	—	—	30	8.5	30	175	12	−10	8	500	—	FO-85	216	—
—	—	—	—	—	—	20	10.7	100	175	12	−10	8	60	—	FO-85	124	—
—	—	—	—	—	—	36	7.2	7	175	15	−5	10	2200	−3.0	IM	—	—
—	—	—	—	—	—	36	7.7	7	175	15	−5	10	2200	−3.0	IM	—	—
—	—	—	—	—	—	36	8.5	7	175	15	−5	10	2200	−3.0	IM	—	—
—	—	—	—	—	—	37	4.2	5.7	175	15	−5	10	3200	−4.0	IM	—	—
—	—	—	—	—	—	37	5.0	5.7	175	15	−5	10	3200	−4.0	IM	—	—
—	—	—	—	—	—	37	6.4	5.7	175	15	−5	10	3200	−4.0	IM	—	—
—	—	—	—	—	—	37	7.2	5.7	175	15	−5	10	3200	−4.0	IM	—	—
—	—	—	—	—	—	37	7.7	5.7	175	15	−5	10	3200	−4.0	IM	—	—
—	—	—	—	—	—	37	8.5	5.7	175	15	−5	10	3200	−4.0	IM	—	—
—	—	—	—	—	—	38	4.2	4.0	175	15	−5	10	4400	−3.0	IM	—	—
—	—	—	—	—	—	38	5.0	4.0	175	15	−5	10	4400	−3.0	IM	—	—
—	—	—	—	—	—	38	6.4	4.0	175	15	−5	10	4400	−3.0	IM	—	—
—	—	—	—	—	—	38	7.2	4.0	175	15	−5	10	4400	−3.0	IM	—	—
—	—	—	—	—	—	38	7.7	4.0	175	15	−5	10	4400	−3.0	IM	—	—
—	—	—	—	—	—	38	8.5	4.0	175	15	−5	10	4400	−3.0	IM	—	—
—	—	—	—	—	—	29	12.5	30	175	15	−5	10	600	−4.0	MH	—	—
—	—	—	—	—	—	31.5	12.5	17	175	15	−5	10	1200	−4.0	MH	—	—
—	—	—	—	—	—	29	14.5	30	175	15	−5	10	600	−4.0	MH	—	—
—	—	—	—	—	—	31.5	14.5	17	175	15	−5	10	1200	−4.0	MH	—	—
—	—	—	—	—	—	34	4	13	175	15	−5	10	1400	−4.0	ME/MM	—	—
—	—	—	—	—	—	36	4	10	175	15	−5	10	1800	−4.0	ME/MM	—	—
—	—	—	—	—	—	28	4	50	175	15	−5	8.5	350	−3.5	ME	—	—
—	—	—	—	—	—	31.0	4	25	175	15	−5	8.5	700	−3.5	ME	—	—
—	—	—	—	—	—	34.0	4	13	175	15	−5	8.5	1400	−3.5	ME	—	—
—	—	—	—	—	—	28.5	8	45	175	15	−5	10	400	−4.0	WF	—	—
—	—	—	—	—	—	30.5	8	23	175	15	−5	10	800	−4.0	WF	—	—
.25	8	13	—	—	—	24	12	60	175	15	−5	10	300	−4.0	MB	—	—
.50	7	12	—	—	—	27	12	30	175	15	−5	10	600	−4.0	MB	—	—
1.12	5.5	12	—	—	—	30.5	12	17	175	15	−5	10	1200	−4.0	MB	—	—
.40	7.5	22	—	—	—	26	12	40	175	15	−5	10	300	−3.0	WG	—	—
.80	6.5	21	—	—	—	29	12	20	175	15	−5	10	600	−3.0	WG	—	—
—	—	—	.40	6.5	21	26	14.5	40	175	15	−5	10	300	−3.0	WG	—	—
—	—	—	.80	5.5	19	29	14.5	20	175	15	−5	10	600	−3.0	WG	—	—
0.4	6	19	—	—	—	+26	4	66	175	+14	−7	9	250	−3	—	—	—
—	—	—	—	—	—	+26	4	70	175	+14	−7	9	250	−3	—	—	—
—	—	—	—	—	—	+26	4	70	175	+14	−7	9	250	−3	—	—	—
0.5	6	17	—	—	—	+29	4	32	175	+14	−7	9	500	−3	—	—	—
—	—	—	—	—	—	+29	4	35	175	+14	−7	9	500	−3	—	—	—
—	—	—	—	—	—	+29	4	35	175	+14	−7	9	500	−3	—	—	—
—	—	—	—	—	—	+32	4	23	175	+14	−7	9	1000	−3	—	—	—
—	—	—	—	—	—	+32	4	27	175	+14	−7	9	1000	−3	—	—	—
—	—	—	—	—	—	+35	2.9-3.5	7.5	175	+14	−7	9	2400	−3	—	—	—
—	—	—	—	—	—	+35	3.7-4.2	7.5	175	+14	−7	9	2400	−3	—	—	—
—	—	—	—	—	—	+35	4.4-5.0	7.5	175	+14	−7	9	2400	−3	—	—	—
—	—	—	—	—	—	+35	5.9-6.4	7.5	175	+14	−7	9	2400	−3	—	—	—
—	—	—	—	—	—	+35	6.4-7.1	7.5	175	+14	−7	9	2400	−3	—	—	—
—	—	—	—	—	—	+35	7.1-7.8	7.5	175	+14	−7	9	2400	−3	—	—	—
—	—	—	—	—	—	+35	7.9-8.4	7.5	175	+14	−7	9	2400	−3	—	—	—
—	—	—	—	—	—	+38	3.7-4.2	4	175	+14	−7	9	4500	−3	—	—	—
—	—	—	—	—	—	+38	3.7-4.2	4	175	+14	−7	9	4500	−3	—	—	—

Power GaAs FETs

FREQUENCY (GHz)

Part Number	2 Power-Out 1-dB Compression W	2 Max Gain dB	2 η	4 Power-Out 1-dB Compression W	4 Max Gain dB	4 η	6 Power-Out 1-dB Compression W	6 Max Gain dB	6 η	8 Power-Out 1-dB Compression W	8 Max Gain dB	8 η	10 Power-Out 1-dB Compression W	10 Max Gain dB	10 η
DEXCEL, INC.															
DXL-3501A	—	—	—	.20	12	—	—	—	—	.20	8	—	—	—	—
DXL-3501A-P70	—	—	—	.20	12	—	—	—	—	.20	8	—	—	—	—
DXL-3501A-P100F	—	—	—	.20	12	—	—	—	—	.20	8	—	—	—	—
DXL-3503A	—	—	—	—	—	—	—	—	—	—	—	—	—	—	—
DXL-3503A-P70	—	—	—	—	—	—	—	—	—	—	—	—	—	—	—
DXL-3504A	—	—	—	—	—	—	—	—	—	—	—	—	—	—	—
DXL-3504A-P70	—	—	—	—	—	—	—	—	—	—	—	—	—	—	—
DXL-3504A-P100F	—	—	—	—	—	—	—	—	—	—	—	—	—	—	—
DXL-3605A	—	—	—	—	—	—	—	—	—	—	—	—	—	—	—
DXL-3605A-P100F	—	—	—	—	—	—	—	—	—	—	—	—	—	—	—
DXL-3608A	—	—	—	—	—	—	—	—	—	.25	8	—	—	—	
DXL-3608A-P100F	—	—	—	—	—	—	—	—	—	.25	8	—	—	—	
DXL-3610A	—	—	—	—	—	—	—	—	—	—	—	—	—	—	—
DXL-3610A-P100F	—	—	—	—	—	—	—	—	—	—	—	—	—	—	—
DXL-3615A	—	—	—	.40	11	—	—	—	—	.32	8	—	—	—	—
DXL-3615A-P100F	—	—	—	.40	11	—	—	—	—	—	—	—	—	—	—
DXL-3630A	—	—	—	.62	11	—	—	—	—	.62	8	—	—	—	—
DXL-3630A-P100F	—	—	—	.62	11	—	—	—	—	.62	8	—	—	—	—
DXL-3640A	—	—	—	1.3	9	—	1.1	7	—	1.0	5	—	—	—	—
DXL-3640A-P100F	—	—	—	1.3	9	—	1.1	7	—	1.0	5	—	—	—	—
DXL-3680-4	—	—	—	2.2	9.5	—	—	—	—	—	—	—	—	—	—
DXL-3680-6	—	—	—	—	—	—	2.0	6.5	—	—	—	—	—	—	—
DXL-36120-4	—	—	—	3.5	9	—	—	—	—	—	—	—	—	—	—
DXL-36120-6	—	—	—	—	—	—	3.0	6	—	—	—	—	—	—	—
DXL-36160-4	—	—	—	4.0	9	—	—	—	—	—	—	—	—	—	—
DXL-36160-6	—	—	—	—	—	—	3.5	6	—	—	—	—	—	—	—
FUJITSU MICROELECT. INC.															
FSX100FA	—	—	—	—	—	—	—	—	—	.025	12	—	—	—	—
FSX51WF	—	—	—	.06	14	—	—	—	—	.06	10	—	—	—	—
FSX52WF	—	—	—	.20	14	—	—	—	—	.20	10	—	—	—	—
FSX53WF	—	—	—	.40	12.5	—	—	—	—	.40	8.5	—	—	—	—
FLSO9MM	.80	13	—	.63	9	32	—	—	—	—	—	—	—	—	—
FLS16MM	1.4	11	—	1.26	7.5	29	—	—	—	—	—	—	—	—	—
FLC301MG-4	—	—	—	—	—	—	—	—	—	—	—	—	—	—	—
FLC301MG-6	—	—	—	—	—	—	—	—	—	—	—	—	—	—	—
FLC301MG-8	—	—	—	—	—	—	—	—	—	—	—	—	—	—	—
FLM3742-3	—	—	—	—	—	—	—	—	—	—	—	—	—	—	—
FLM4450-3	—	—	—	—	—	—	—	—	—	—	—	—	—	—	—
FLM5964-3	—	—	—	—	—	—	—	—	—	—	—	—	—	—	—
FLM5964-3B	—	—	—	—	—	—	—	—	—	—	—	—	—	—	—
M/A-COM, INC.															
MA-4F101	—	—	—	—	—	—	—	—	—	—	—	—	—	—	—
MA-4F102	—	—	—	—	—	—	—	—	—	—	—	—	—	—	—
MA-4F103	—	—	—	—	—	—	—	—	—	—	—	—	—	—	—
MA-4F100-500	—	—	—	—	—	—	—	—	—	—	—	—	—	—	—
MA-4F1001	—	—	—	—	—	—	—	—	—	—	—	—	—	—	—
MA-4F010	—	—	—	—	—	—	—	—	—	—	—	—	—	—	—
MA-4F020	—	—	—	—	—	—	—	—	—	—	—	—	—	—	—
MA-4F001-500	—	—	—	—	—	—	—	—	—	—	—	—	—	—	—
MICROWAVE SEMICOND. CORP.															
MSC 88000	—	—	—	0.06	12	40	0.06	10.5	30	0.05	8	25	0.05	8	22
MSC 88001	—	—	—	0.28	10	40	0.27	8	30	0.26	7.2	25	0.24	7	22
MSC 88002	—	—	—	0.54	10	40	0.53	8	30	0.52	6.7	25	.5	6.5	22
MSC 88004	—	—	—	1.0	9	40	0.97	8	30	0.94	6.5	25	.9	6.0	22
MSC 88008	—	—	—	2.0	10	40	1.8	8	30	1.6	7.0	25	1.4	6.5	22
MSC 88012	—	—	—	4.0	8	40	3.5	7.5	30	—	—	—	—	—	—
MSC 88100	—	—	—	—	—	—	—	—	—	0.07	9.5	30	0.07	8	26
MSC 88101	—	—	—	—	—	—	—	—	—	0.25	8.5	30	0.25	7	26

12 Power-Out 1-dB Compression W	12 Max Gain dB	12 η	18 Power-Out 1-dB Compression W	18 Max Gain dB	18 η	P_O dBm	f GHz	Max Ratings R_{TH} °C/W	Max Ratings T_J	Max Ratings V_{DS}	Max Ratings V_{GS}	V_{DS} nom volts	I_{DSS} nom mA	V_P nom volts	Package Type	Price Quantity 1-100	Price Quantity 1000
.16	5	—	—	—	—	+22	12	100	175	12	—	8	130	−4	Chip form	—	—
.16	5	—	.030	5	—	+23	8	200	175	12	—	8	130	−4	P70-Hermetic, 70 mil	—	—
.050	7	—	—	—	—	+22	12	105	175	12	—	8	150	−4	P100-Hermetic, 100 mil	—	—
—	—	—	.090	5	—	+15	18	180	175	12	—	6	90	−4	Chip form	—	—
.10	7	—	—	—	—	+15	12	300	175	12	—	—	90	−5	P70-Hermetic, 70 mil	—	—
.10	7	—	—	—	—	+19	18	180	175	12	—	6	110	−5	Chip form	—	—
.10	7	—	—	—	—	+20	12	300	175	12	—	6	110	−5	P70-Hermetic, 70 mil	—	—
.13	7	—	.125	4.5	—	+20	16	185	175	12	—	6	110	−5	P100-Hermetic, 100 mil	—	—
.13	7	—	—	—	—	+21	18	100	175	12	—	6	140	−5	Chip form	—	—
.20	7	—	—	—	—	+22	12	105	175	12	—	6	150	−5	P100-Hermetic, 100 mil	—	—
.20	7	—	—	—	—	+23	12	70	175	20	—	8	200	−4	Chip form	—	—
.20	7	—	—	—	—	+24	8	75	175	20	—	8	220	−4	P100-Hermetic, 100 mil	—	—
.20	7	—	.200	4	—	+23	18	50	175	12	—	6	280	−5	Chip form	—	—
.40	5	—	—	—	—	+23	12	55	175	12	—	6	300	−5	P100-Hermetic, 100 mil	—	—
—	—	—	—	—	—	+25	8	40	175	20	—	8	450	−5	Chip form	—	—
—	—	—	—	—	—	+27	4	45	175	20	—	8	500	−5	P100-Hermetic, 100 mil	—	—
.40	4	—	—	—	—	+26	12	35	175	20	—	9	400	−4	Chip form	—	—
—	—	—	—	—	—	+28	8	40	175	20	—	9	450	−4	P100-Hermetic, 100 mil	—	—
—	—	—	—	—	—	+32	4	20	175	20	—	9	800	−4	Chip form	—	—
—	—	—	—	—	—	+31	6	20	175	20	—	9	900	−4	P100-Hermetic, 100 mil	—	—
—	—	—	—	—	—	+33.5	4	10	175	20	—	9	2000	−4	P300F-Hermetic, 300 mil	—	—
—	—	—	—	—	—	+33	6.4	10	175	20	—	9	2000	−4	P300F-Hermetic, 300 mil	—	—
—	—	—	—	—	—	+35.6	4.0	6.5	175	20	—	9	2000	−4	P300F-Hermetic, 300 mil	—	—
—	—	—	—	—	—	+35	6.4	6.5	175	20	—	9	3000	−4	P300F-Hermetic, 300 mil	—	—
—	—	—	—	—	—	+36	4.0	6	175	20	—	9	3600	−4	P500F-Hermetic, 500 mil	—	—
—	—	—	—	—	—	+35.5	6.4	6	175	20	—	9	3600	−4	P500F-Hermetic, 500 mil	—	—
.016	9.0	—	—	—	—	12	12	250	+175	12	−5	8	60	−2.5	FA	—	—
.05	6	—	—	—	—	18	8	150	175	12	−5	8	60	−2.5	WF/W	—	—
.13	6	—	—	—	—	23	8	100	175	12	−5	8	150	−4.0	WF/W	—	—
.25	5.0	—	—	—	—	25	8	50	175	12	−5	8	300	−4.0	WF/W	—	—
—	—	—	—	—	—	28	4	50	175	15	−5	10	350	−4.0	ME/MM	—	—
—	—	—	—	—	—	31	4	25	175	15	−5	10	700	−4.0	ME/MM	—	—
—	—	—	—	—	—	33	4.2	10	175	15	−5	10	1600	−4.0	MG	—	—
—	—	—	—	—	—	33	7.2	10	175	15	−5	10	1600	−4.0	MG	—	—
—	—	—	—	—	—	33	8.5	10	175	15	−5	10	1600	−4.0	MG	—	—
—	—	—	—	—	—	35	4.2	8	175	15	−5	10	1800	−4.0	IM	—	—
—	—	—	—	—	—	35	5.0	8	175	15	−5	10	1800	−4.0	IM	—	—
—	—	—	—	—	—	35	6.4	8	175	15	−5	10	1800	−4.0	IM	—	—
—	—	—	—	—	—	36	6.4	7	175	15	−5	10	2200	−3.0	IM	—	—
—	—	—	—	—	—	—	8	—	175	12	10	—	330	6.0	Hermetic, metal-ceramic	—	—
—	—	—	—	—	—	—	10	—	175	12	10	—	330	6.0	Hermetic, metal-ceramic	—	—
—	—	—	—	—	—	—	8	—	175	12	10	—	660	6.0	Hermetic, metal-ceramic	—	—
—	—	—	—	—	—	—	10	—	175	12	10	—	330	6.0	Chip	—	—
—	—	—	—	—	—	—	10	—	175	10	8	8	80	5.5	Hermetic, metal-ceramic	—	—
—	—	—	—	—	—	—	10	—	175	10	8	8	80	5.5	Hermetic, metal-ceramic	—	—
—	—	—	—	—	—	—	10	—	175	10	8	8	80	5.5	Hermetic, metal-ceramic	—	—
—	—	—	—	—	—	—	12	—	175	10	8	8	80	5.5	Chip	—	—
.04	6.5	20	—	—	—	20	6	60	175	10	−8	8	90	5	Hermetic	—	—
.22	6.0	20	—	—	—	24	6	50	175	10	−8	8	150	6	Hermetic	—	—
.5	5.5	20	—	—	—	27	6	35	175	10	−8	9	300	6	Hermetic	—	—
.88	5.0	20	—	—	—	30	6	20	175	10	−8	9	700	6	Hermetic	—	—
—	—	—	—	—	—	33	6	10	175	10	−8	9	1400	4	Hermetic	—	—
0.07	7.0	22	—	—	—	—	—	—	—	—	—	—	—	—	No data available for this model number		
0.25	6.5	22	—	—	—	18	12	60	175	10	−8	8	90	5	Chip carrier	—	—
0.5	6.0	22	—	—	—	24	12	50	175	10	−8	8	150	6	Chip carrier	—	—

Power GaAs FETs

FREQUENCY (GHz)

Part Number	2 Power-Out 1-dB Compression W	2 Max Gain dB	2 η	4 Power-Out 1-dB Compression W	4 Max Gain dB	4 η	6 Power-Out 1-dB Compression W	6 Max Gain dB	6 η	8 Power-Out 1-dB Compression W	8 Max Gain dB	8 η	10 1-dB Compression W	10 Max Gain dB	10 η
MSC 88102	—	—	—	—	—	—	—	—	—	0.5	8	30	0.5	6.5	26
MSC 88104	—	—	—	—	—	—	—	—	—	1.0	7	30	1.0	6.5	26
MSC 88199	—	—	—	—	—	—	—	—	—	—	—	—	—	—	—
MSC 88200	—	—	—	—	—	—	—	—	—	—	—	—	—	—	—
MSC 88201	—	—	—	—	—	—	—	—	—	—	—	—	—	—	—
MSC 88202	—	—	—	—	—	—	—	—	—	—	—	—	—	—	—
MSC 88204	—	—	—	—	—	—	—	—	—	—	—	—	—	—	—
MSC 88300	—	—	—	—	—	—	—	—	—	—	—	—	—	—	—
MSC 88302	—	—	—	—	—	—	—	—	—	—	—	—	—	—	—
MPF-5964-6	—	—	—	—	—	—	5.6	7	25	—	—	—	—	—	—
MPF-6471-3	—	—	—	—	—	—	—	—	—	—	—	—	—	—	—
MITSUBISHI ELECT. AMERICA, INC.															
MGF-1801	—	—	—	—	—	—	—	—	—	0.2	9	25	—	—	—
MGF-1802	—	—	—	—	—	—	—	—	—	0.2	9	25	—	—	—
MGF-2116	—	—	—	—	—	—	—	—	—	—	—	—	—	—	—
MGF-2117	—	—	—	—	—	—	—	—	—	—	—	—	—	—	—
MGF-2124	—	—	—	—	—	—	—	—	—	—	—	—	—	—	—
MGF-2124F	—	—	—	—	—	—	—	—	—	—	—	—	—	—	—
MGF-2124G	—	—	—	—	—	—	—	—	—	—	—	—	—	—	—
MGF-2148	—	—	—	—	—	—	—	—	—	—	—	—	—	—	—
MGF2148F	—	—	—	—	—	—	—	—	—	—	—	—	—	—	—
MGF-2148G	—	—	—	—	—	—	—	—	—	—	—	—	—	—	—
MGF-2172	—	—	—	—	—	—	—	—	—	2.5	5.5	20	—	—	—
MGF-2205	—	—	—	—	—	—	—	—	—	—	—	—	—	—	—
MGF-2206	—	—	—	—	—	—	3.5	6	25	—	—	—	—	—	—
MGFC34M	—	—	—	—	—	—	5.5	4.5	20	—	—	—	—	—	—
MGFX34M	—	—	—	—	—	—	2.3	4.5	25	—	—	—	—	—	—
NEC CORPORATION/ CAL EASTERN LABS, INC.	dBm			dBm			dBm			dBm			dBm		
NE694 Series	20	15	40	20	13	40	20	11	35	19	9.8	30	19	9.5	30
NE69400	—	—	—	—	—	—	—	—	—	—	—	—	—	—	—
NE69489	—	—	—	—	—	—	—	—	—	—	—	—	—	—	—
NE695 Series	22	14	40	22	11	40	22	9	35	22	6	30	—	—	—
NE69500	—	—	—	—	—	—	—	—	—	—	—	—	—	—	—
NE69589	—	—	—	—	—	—	—	—	—	—	—	—	—	—	—
NE8000 Series	23	7	34	23	6	34	23	5	30	—	—	—	—	—	—
NE800000	—	—	—	—	—	—	—	—	—	—	—	—	—	—	—
NE800075	—	—	—	—	—	—	—	—	—	—	—	—	—	—	—
NE8001 Series	26	7	34	26	6	34	26	5	30	—	—	—	—	—	—
NE800100	—	—	—	—	—	—	—	—	—	—	—	—	—	—	—
NE800196	—	—	—	—	—	—	—	—	—	—	—	—	—	—	—
NE800199	—	—	—	—	—	—	—	—	—	—	—	—	—	—	—
NE8002 Series	29	7	34	29	6	34	29	5	30	—	—	—	—	—	—
NE800200	—	—	—	—	—	—	—	—	—	—	—	—	—	—	—
NE800296	—	—	—	—	—	—	—	—	—	—	—	—	—	—	—
NE800299	—	—	—	—	—	—	—	—	—	—	—	—	—	—	—
NE8004 Series	32	7	34	32	6	34	32	5	30	—	—	—	—	—	—
NE800400	—	—	—	—	—	—	—	—	—	—	—	—	—	—	—
NE800495	—	—	—	—	—	—	—	—	—	—	—	—	—	—	—
NE8008 Series	35.5	7	34	35.5	6	34	35	5	30	—	—	—	—	—	—
NE800898	—	—	—	—	—	—	—	—	—	—	—	—	—	—	—
NE9000 Series	—	—	—	—	—	—	—	—	—	—	—	—	—	—	—
NE900000	—	—	—	—	—	—	—	—	—	—	—	—	—	—	—
NE900075	—	—	—	—	—	—	—	—	—	—	—	—	—	—	—
NE9001 Series	—	—	—	—	—	—	—	—	—	—	—	—	—	—	—
NE900100	—	—	—	—	—	—	—	—	—	—	—	—	—	—	—
NE900175	—	—	—	—	—	—	—	—	—	—	—	—	—	—	—
NE9002 Series	—	—	—	—	—	—	—	—	—	—	—	—	—	—	—
NE900200	—	—	—	—	—	—	—	—	—	—	—	—	—	—	—
NE900275	—	—	—	—	—	—	—	—	—	—	—	—	—	—	—
NE9004 Series	—	—	—	—	—	—	—	—	—	—	—	—	—	—	—
NE900400	—	—	—	—	—	—	—	—	—	—	—	—	—	—	—
NE900474	—	—	—	—	—	—	—	—	—	—	—	—	—	—	—
NE9008 Series	—	—	—	—	—	—	—	—	—	—	—	—	—	—	—

12 GHz Power-Out 1-dB Compression W	12 GHz Max Gain dB	12 GHz η	18 GHz Power-Out 1-dB Compression W	18 GHz Max Gain dB	18 GHz η	P_O dBm	f GHz	Max Ratings R_{TH} °C/W	Max Ratings T_J	Max Ratings V_{DS}	Max Ratings V_{GS}	V_{DS} nom volts	I_{DSS} nom mA	V_P nom volts	Package Type	Price Quantity 1-100	Price Quantity 1000
1.0	5.5	22	—	—	—	27	12	35	175	10	−8	9	300	6	Chip carrier	—	—
—	—	—	—	—	—	30	12	20	175	10	−8	9	700	6	Chip carrier	—	—
—	—	—	—	—	—	16	15	40	175	10	−8	8	70	6	Chip carrier	—	—
0.04	7.5	25	0.03	5.5	20	20	15	35	175	10	−8	8	120	6	Chip carrier	—	—
0.13	7.0	25	0.10	5.0	20	24	15	29	175	10	−8	8	160	6	Chip carrier	—	—
0.28	5.5	25	0.20	4.0	20	26.5	15	23	175	10	−8	9	325	6	Chip carrier	—	—
0.48	5.5	25	0.40	4.0	20	29.5	15	15	175	10	−8	9	675	6	Chip carrier	—	—
0.95	5.5	25	0.80	3.5	20	20	20	25	175	10	−8	8	90	4	Matched carrier	—	—
—	—	—	—	—	—	27	20	15	175	10	−8	8	300	4	Matched carrier	—	—
—	—	—	—	—	—	37.6	5.9-6.4	4	175	10	−8	9	4500	5	Hermetic	—	—
—	—	—	—	—	—	35	6.4-7.1	6.5	175	10	−8	9	3000	5	Hermetic	—	—
0.2	7	20	—	—	—	0.2	12	—	150	8	−6	6	200	−3	100 mil. metal/ceramic	—	—
0.2	7	20	—	—	—	0.2	12	125	150	8	−6	6	200	−3	100 mil. stripline flange	—	—
0.4	7	20	—	—	—	0.4	12	42	150	11	−9	7	430	−3.5	.130x.420 stripline flange	—	—
0.4	7	20	—	—	—	0.4	12	50	150	11	−9	7	430	−3.5	100 mil. stripline flange	—	—
1.0	6	20	—	—	—	1.0	12	30	150	11	−9	8	650	−3.5	.140x.420 stripline flange	—	—
1.0	6.3	20	—	—	—	1.0	12	32	150	11	−9	8	650	−3.5	.100x.270 chip flange	—	—
1.0	6.3	20	—	—	—	1.0	12	32	150	11	−9	8	650	−3.5	.070x.236 chip flange	—	—
1.6	5	16	—	—	—	1.6	12	15	150	11	−9	8	1300	−3.5	.140x.420 stripline flange	—	—
1.6	5.2	16	—	—	—	1.6	12	16	150	11	−9	8	1300	−3.5	.100x.270 chip flange	—	—
1.6	5.2	16	—	—	—	1.6	12	16	150	11	−9	8	1300	−3.5	.070x.236 chip flange	—	—
—	—	—	—	—	—	2.5	8	10	150	11	−9	9	1950	−3.5	.140x.420 stripline	—	—
—	—	—	—	—	—	3.5	6	10	150	11	−9	8	1300	−4	.173 mil. stripline	—	—
—	—	—	—	—	—	5.0	6	6	150	11	−9	8	1450	−5	.173 mil. stripline flange	—	—
—	—	—	—	—	—	2.3	6	10	150	11	−9	9	2000	−3.5	.500x.827 stripline flange	—	—
—	—	—	—	—	—	2.3	10	10	150	11	−9	9	1950	−3.5	.250x.430 stripline flange	—	—
dBm																	
—	—	—	—	—	—	—	—	—	—	—	—	—	—	—	—	—	—
—	—	—	—	—	—	20	2-10	115	175	10	−10	7	30	−4	Chip	—	—
—	—	—	—	—	—	20	10	188	175	10	−10	7	30	−4	0.08″	—	—
—	—	—	—	—	—	—	—	—	—	—	—	—	—	—	—	—	—
—	—	—	—	—	—	23	2-10	95	175	10	−10	7	75	−4	Chip	—	—
—	—	—	—	—	—	23	10	115	175	10	−10	7	75	−4	0.08″	—	—
—	—	—	—	—	—	—	—	—	—	—	—	—	—	—	—	—	—
—	—	—	—	—	—	23	2-10	—	175	20	−12	9	60	−5.5	Chip	—	—
—	—	—	—	—	—	23	8.4	—	175	20	−12	9	60	−5.5	Hermetic flange	—	—
—	—	—	—	—	—	—	—	—	—	—	—	—	—	—	—	—	—
—	—	—	—	—	—	26	2-10	—	175	20	−12	9	125	−5.5	Chip	—	—
—	—	—	—	—	—	26	7.9	—	175	20	−12	9	125	−5.5	Hermetic flange	—	—
—	—	—	—	—	—	26	8.4	—	175	20	−12	9	125	−5.5	Hermetic flange	—	—
—	—	—	—	—	—	—	—	—	—	—	—	—	—	—	—	—	—
—	—	—	—	—	—	29	2-10	—	175	20	−12	9	275	−5.5	Chip	—	—
—	—	—	—	—	—	29	7.9	—	175	20	−12	9	275	−5.5	Hermetic flange	—	—
—	—	—	—	—	—	29	8.4	—	175	20	−12	9	275	−5.5	Hermetic flange	—	—
—	—	—	—	—	—	—	—	—	—	—	—	—	—	—	—	—	—
—	—	—	—	—	—	32	2-10	17	175	20	−12	9	600	−5.5	Chip	—	—
—	—	—	—	—	—	32	8.5	17	175	20	−12	9	600	−5.5	Hermetic flange	—	—
—	—	—	—	—	—	—	—	—	—	—	—	—	—	—	—	—	—
—	—	—	—	—	—	35	8.5	8	175	20	−12	9	1200	−5.5	Hermetic flange	—	—
—	—	—	—	—	—	—	—	—	—	—	—	—	—	—	—	—	—
—	—	—	—	—	—	20	15.2	—	175	20	−12	8	40	−4	Chip	—	—
—	—	—	—	—	—	20	15.2	—	175	20	−12	8	40	−4	Hermetic flange	—	—
20	8	27	—	—	—	—	—	—	—	—	—	—	—	—	—	—	—
—	—	—	—	—	—	23	14.5	100	175	20	−12	8	80	−4	Chip	—	—
—	—	—	—	—	—	23	14.5	100	175	20	−12	8	80	−4	Hermetic flange	—	—
23	8	27	—	—	—	—	—	—	—	—	—	—	—	—	—	—	—
—	—	—	—	—	—	25	14.5	60	175	20	−12	8	150	−4	Chip	—	—
—	—	—	—	—	—	25	14.5	60	175	20	−12	8	150	−4	Hermetic flange	—	—
25	7	25		—	—	—	—	—	—	—	—	—	—	—	—	—	—
—	—	—	—	—	—	31	15.2	30	175	20	−12	8	340	−4	Chip	—	—
—	—	—	—	—	—	31	15.2	30	175	20	−12	8	340	−4	Hermetic flange	—	—
31	6	25	—	—	—	—	—	—	—	—	—	—	—	—	—	—	—

Power GaAs FETs

FREQUENCY (GHz)

Part Number	2 Power-Out 1-dB Compression W	2 Max Gain dB	2 η	4 Power-Out 1-dB Compression W	4 Max Gain dB	4 η	6 Power-Out 1-dB Compression W	6 Max Gain dB	6 η	8 Power-Out 1-dB Compression W	8 Max Gain dB	8 η	10 Power-Out 1-dB Compression W	10 Max Gain dB	10 η
	dBm			dBm			dBm			dBm					
NE900873	—	—	—	—	—	—	—	—	—	—	—	—	—	—	—
NE3716 Series	—	—	—	37.8	5.5	30	37.8	5.5	30	—	—	—	—	—	—
NE371698	—	—	—	—	—	—	—	—	—	—	—	—	—	—	—
NEZ3742-3	—	—	—	35	11	35	—	—	—	—	—	—	—	—	—
NEZ4450-3	—	—	—	—	—	—	—	—	—	—	—	—	—	—	—
NEZ5055-3	—	—	—	—	—	—	—	—	—	—	—	—	—	—	—
NEZ5459-3	—	—	—	—	—	—	—	—	—	—	—	—	—	—	—
NEZ5964-3	—	—	—	—	—	—	35	9	35	—	—	—	—	—	—
NEZ6472-3	—	—	—	—	—	—	—	—	—	—	—	—	—	—	—
NEZ7178-3	—	—	—	—	—	—	—	—	—	—	—	—	—	—	—
NEZ7984-3	—	—	—	—	—	—	—	—	—	35	7	30	—	—	—
NEZ3742-6	—	—	—	37.8	10	33	—	—	—	—	—	—	—	—	—
NEZ4450-6	—	—	—	—	—	—	—	—	—	—	—	—	—	—	—
NEZ5055-6	—	—	—	—	—	—	—	—	—	—	—	—	—	—	—
NEZ5459-6	—	—	—	—	—	—	—	—	—	—	—	—	—	—	—
NEZ5964-6	—	—	—	—	—	—	37.8	8	33	—	—	—	—	—	—
NEZ6472-6	—	—	—	—	—	—	—	—	—	—	—	—	—	—	—
NEZ7178-6	—	—	—	—	—	—	—	—	—	—	—	—	—	—	—
RAYTHEON CO.															
RPX 2322	—	—	—	.4	12	—	.3	11	—	.25	9	—	.16	8	—
RPX 4328	—	—	—	—	—	—	—	—	—	—	—	—	.5	8	—
RPX 4331	—	—	—	—	—	—	—	—	—	—	—	—	1.0	7	—
RPX 4333	—	—	—	—	—	—	—	—	—	—	—	—	1.5	6	—
RPX 4334	—	—	—	—	—	—	—	—	—	—	—	—	2.0	6	—
RPX 6035	—	—	—	—	—	—	—	—	—	—	—	—	3.0	6	—
RPX 6036	—	—	—	—	—	—	—	—	—	—	—	—	4.0	5	—
RPK 9027	—	—	—	—	—	—	—	—	—	—	—	—	—	—	—
RPK 9030	—	—	—	—	—	—	—	—	—	—	—	—	—	—	—
RIM 3742-3	—	—	—	—	—	—	3	—	—	—	—	—	—	—	—
RIM 5964-3	—	—	—	—	—	—	3	—	—	—	—	—	—	—	—
RIM 6471-3	—	—	—	—	—	—	3	—	—	—	—	—	—	—	—
RIM 7178-3	—	—	—	—	—	—	3	—	—	—	—	—	—	—	—
THOMSON-CSF															
TC 3200	—	—	—	0.05	22.3	—	0.05	21	—	—	—	—	—	—	—
TC 3201	—	—	—	0.1	21.4	—	0.1	20	—	—	—	—	—	—	—
TC 4200	—	—	—	0.2	18	—	0.2	16.4	—	—	—	—	—	—	—
TC 5200	—	—	—	0.5	21.9	—	0.5	20	—	—	—	—	—	—	—
TC 3400	—	—	—	—	—	—	—	—	—	—	—	—	0.05	22	—
TC 3401	—	—	—	—	—	—	—	—	—	—	—	—	0.1	21	—
TC 5501	—	—	—	—	—	—	—	—	—	1	20	—	—	—	—
TC 9301	—	—	—	—	—	—	—	—	—	0.05	—	—	—	—	—
TC 9302	—	—	—	—	—	—	—	—	—	0.1	—	—	—	—	—
TC 9303	—	—	—	—	—	—	—	—	—	—	—	—	—	—	—
TC 9311	—	—	—	—	—	—	—	—	—	—	—	—	0.05	—	—
TC 9312	—	—	—	—	—	—	—	—	—	—	—	—	0.1	—	—
TC 9402	—	—	—	—	—	—	—	—	—	—	—	—	0.05	—	—
TC 9403	—	—	—	—	—	—	—	—	—	—	—	—	0.1	—	—
TC 9501	—	—	—	—	—	—	—	—	—	—	—	—	—	—	—
TC 9502	—	—	—	—	—	—	—	—	—	—	—	—	—	—	—
TOSHIBA CORP.															
S8812	—	—	—	—	—	—	—	—	—	0.05	10	7	—	—	—
S8803	—	—	—	—	—	—	—	—	—	0.2	7	20	—	—	—
S2740	—	—	—	—	—	—	—	—	—	0.5	6	17	—	—	—
S2741	—	—	—	—	—	—	—	—	—	1	5	12	—	—	—
S8820	—	—	—	—	—	—	—	—	—	—	—	—	—	—	—
S8821	—	—	—	—	—	—	—	—	—	—	—	—	—	—	—
S8822	—	—	—	—	—	—	—	—	—	—	—	—	—	—	—
S8823	—	—	—	—	—	—	—	—	—	—	—	—	—	—	—
S8825	—	—	—	—	—	—	—	—	—	—	—	—	—	—	—
S8826	—	—	—	—	—	—	—	—	—	—	—	—	—	—	—
S8827	—	—	—	—	—	—	—	—	—	—	—	—	—	—	—
S8828	—	—	—	—	—	—	—	—	—	—	—	—	—	—	—
VARIAN ASSOCIATES															
VSF9342	—	—	—	—	—	—	.158	15	63	.148	12.5	51	.132	10	—
VSF9343	—	—	—	—	—	—	.158	15	63	.148	12.5	51	.132	10	—

12 Power-Out 1-dB Compression W	12 Max Gain dB	12 η	18 Power-Out 1-dB Compression W	18 Max Gain dB	18 η	P_O dBm	f GHz	Max Ratings R_{TH} °C/W	Max Ratings T_J	Max Ratings V_{DS}	Max Ratings V_{GS}	V_{DS} nom volts	I_{DSS} nom mA	V_P nom volts	Package Type	Price Quantity 1-100	Price Quantity 1000
dBm																	
—	—	—	—	—	—	34	15.2	—	175	20	−12	8	600	−4	Hermetic flange	—	—
34	6	25	—	—	—	—	—	—	—	—	—		—	—	—	—	—
—	—	—	—	—	—	37.8	3.5-8.5	45	175	20	12	9	2400	−5.5	Hermetic flange	—	—
—	—	—	—	—	—	35	4.2	8.0	175	20	−14	9	1200	−3.5	Hermetic Flange	—	—
—	—	—	—	—	—	35	5.0	8.0	175	20	−14	9	1200	−3.5	Hermetic Flange	—	—
—	—	—	—	—	—	35	5.5	8.0	175	20	−14	9	1200	−3.5	Hermetic Flange	—	—
—	—	—	—	—	—	35	5.9	8.0	175	20	−14	9	1200	−3.5	Hermetic Flange	—	—
—	—	—	—	—	—	35	6.4	8.0	175	20	−14	9	1200	−3.5	Hermetic Flange	—	—
—	—	—	—	—	—	35	7.2	8.0	175	20	−14	9	1200	−3.5	Hermetic Flange	—	—
—	—	—	—	—	—	35	7.8	8.0	175	20	−14	9	1200	−3.5	Hermetic Flange	—	—
—	—	—	—	—	—	35	8.4	8.0	175	20	−14	9	1200	−3.5	Hermetic Flange	—	—
—	—	—	—	—	—	37.8	4.2	4.5	175	20	−14	9	1800	−3.5	Hermetic Flange	—	—
—	—	—	—	—	—	37.8	5.0	4.5	175	20	−14	9	1800	−3.5	Hermetic Flange	—	—
—	—	—	—	—	—	37.8	5.5	4.5	175	20	−14	9	1800	−3.5	Hermetic Flange	—	—
—	—	—	—	—	—	37.8	5.9	4.5	175	20	−14	9	1800	−3.5	Hermetic Flange	—	—
—	—	—	—	—	—	37.8	6.4	4.5	175	20	−14	9	1800	−3.5	Hermetic Flange	—	—
—	—	—	—	—	—	37.8	7.2	4.5	175	20	−14	9	1800	−3.5	Hermetic Flange	—	—
—	—	—	—	—	—	37.8	7.8	4.5	175	20	−14	9	1800	−3.5	Hermetic Flange	—	—
—	—	—	—	—	—	22	10	130	175	15	−10	10	140	−4	Various	$ 30	—
—	—	—	—	—	—	27	10	40	175	15	−10	10	250	−4	Various	$100	—
—	—	—	—	—	—	30	10	20	175	15	−10	10	500	−4	Various	$120	—
—	—	—	—	—	—	32	10	15	175	15	−10	10	750	−4	Various	$160	—
—	—	—	—	—	—	33	10	10	175	15	−10	10	1000	−4	Various	$200	—
—	—	—	—	—	—	35	10	7.5	175	15	−10	10	1800	−4	Various	$320	—
—	—	—	—	—	—	36	10	5	175	15	−10	10	2400	−4	Various	$400	—
—	—	—	0.5	6	—	27	18	60	175	12	−10	9	250	−4	Only available on	$200	—
—	—	—	1.0	5	—	30	18	30	175	12	−10	9	500	−4	carriers or as dice	$400	—
—	—	—	—	—	—	—	—	—	—	—	—	10	2400	−3	0.5″ stripline	—	—
—	—	—	—	—	—	—	—	—	—	—	—	10	2400	−3	0.5″ stripline	—	—
—	—	—	—	—	—	—	—	—	—	—	—	10	2400	−3	0.5″ stripline	—	—
—	—	—	—	—	—	—	—	—	—	—	—	10	2400	−3	0.5″ stripline	—	—
—	—	—	—	—	—	17	6	140	170	9	8	7	60	4	BMH 77 P	—	—
—	—	—	—	—	—	20	6	75	170	9	8	7	120	4	BMH 77 P	—	—
—	—	—	—	—	—	23	6	45	170	9	8	8	250	4	BMH 77 P	—	—
—	—	—	—	—	—	27	6	25	170	9	8	8	500	4	BMH 77 P	—	—
—	—	—	—	—	—	17	10	140	170	9	8	7	50	4	BMH 60-BMH 77 P	—	—
—	—	—	—	—	—	20	10	75	170	9	8	7	100	4	BMH 60-BMH 77 P	—	—
0.9	15.4	—	—	—	—	30	11	15	170	10	8	8	1000	4	BMH 60-BMH 77 P	—	—
—	—	—	—	—	—	17	8.5/9.6	140	170	11	—	10	40	—	BMH 60	—	—
—	—	—	—	—	—	20	8.5/9.6	75	170	11	—	10	80	—	BMH 60	—	—
—	—	—	—	—	—	17	9/10.2	140	170	11	—	10	40	—	BMH 60	—	—
—	—	—	—	—	—	20	9/10.2	75	170	11	—	10	80	—	BMH 60	—	—
—	—	—	—	—	—	17	10.2/11.7	140	170	11	—	10	40	—	BMH 60	—	—
—	—	—	—	—	—	20	10.2/11.7	75	170	11	—	10	80	—	BMH 60	—	—
—	—	—	—	—	—	17	11.7/12.5	140	170	11	—	10	40	—	BMH 60	—	—
0.05	—	—	—	—	—	20	11.7/12.5	75	170	11	—	10	80	—	BMH 60	—	—
0.1	—	—	—	—	—	—	—	—	—	—	—	—	—	—	BMH 60	—	—
—	—	—	—	—	—	17	8	100	175	15	−5	10	75	−4	Stripline	—	—
—	—	—	—	—	—	23	8	60	175	15	−5	10	150	−4	Stripline	—	—
—	—	—	—	—	—	27.5	8	30	175	15	−5	10	450	−4	Stripline	—	—
—	—	—	—	—	—	30	8	18	175	15	−5	10	1200	−4	Stripline	—	—
—	—	—	—	—	—	35.5	5.1	7.5	175	15	−5	10	3000	−3.5	Stripline 500 mil	—	—
—	—	—	—	—	—	35.5	6.4	7.5	175	15	−5	10	3000	−3.5	Stripline 500 mil	—	—
—	—	—	—	—	—	35.5	7.2	7.5	175	15	−5	10	3000	−3.5	Stripline 500 mil	—	—
—	—	—	—	—	—	35.5	7.9	7.5	175	15	−5	10	3000	−3.5	Stripline 500 mil	—	—
—	—	—	—	—	—	38	5.1	4	175	15	−5	10	5600	−3.5	Stripline 500 mil	—	—
—	—	—	—	—	—	38	6.4	4	175	15	−5	10	5600	−3.5	Stripline 500 mil	—	—
—	—	—	—	—	—	38	7.2	4	175	15	−5	10	5600	−3.5	Stripline 500 mil	—	—
—	—	—	—	—	—	38	7.9	4	175	15	−5	10	5600	−3.5	Stripline 500 mil	—	—
.120	9	33	.100	5	25	+20	6-18	182	180	7	−6	3	6	5	—	—	—
.120	9	33	.100	5	25	+20	6-18	182	180	7	−6	3	6	3	—	—	—

Thin Film Processing of Hybrid ICs

Hybrid technology will survive and work with emerging MMICs. Process technology is crucial to getting the most from hybrid design.

By Ralph Tramposch, *Materials Research Corporation*

Thin film hybrid technology is crucial to modern, solid-state microwave design. From active seekers for air-to-air missiles to simple but high-volume applications such as front-ends for home direct-broadcast TV receivers, thin film hybrids can provide a practical medium for integrating active and passive components.

In many cases, hybrids offer many advantages that will keep them competitive in the emerging age of monolithics. For instance, good, broadband couplers can only be built cost effectively on thin film hybrid substrates. Also, with hybrids, chips can be tested separately, giving optimum device performance, before they are integrated on the hybrid substrate. In the future, hybrid and monolithic technologies will be used together; small-scale monolithic GaAs and silicon circuits will be combined on hybrid substrates to provide the best of both approaches.

Understanding materials and process technology is central to good thin film hybrid design and manufacture. This technology is reviewed here. In many ways the processes involved in preparation of thin-film hybrid integrated circuits are similar to semiconductor processing. These processes will be described, from metalizing ceramic substrates to forming patterns for thin film hybrid circuits.

Substrate Cleaning

Film growth and adhesion is influenced by the degree of surface cleanliness of the substrate. To achieve reproducible film properties requires thoroughly cleaned surfaces. Knowledge of the type of contaminants involved will generally dictate the method to be used to effect removal. The choice of cleaning techniques will depend on the nature of the substrate and the degree of cleaniness required. In some instances, foreign material may actually aid in promoting adhesion; however, in depositing films on oxide surfaces such as Al_2O_3, a chemical reaction between the film and the surface is considered to be necessary for adhesion. Chromium has a strong affinity for oxygen and chemically bonds to alumina by forming interfacial oxide regions. The substrate surface chemistry may have an important effect on adhesion. Therefore, the surface must be free of contaminants which inhibit the interaction between the atoms of the depositing film and the alumina surface. Alumina surfaces are frequently contaminated with hydrocarbons, alkali halides, and particulates.

Removal of these contaminants can be effected by using, in sequence, organic solvents, hot detergent and water rinses, followed by air firing at very high temperatures. Ultrasonic agitation is used in the solvent and detergent rinses. The surface should be thoroughly rinsed in a de-ionized water cascade after detergent cleaning. Ultrasonic rinsing helps to remove particulates. Air firing avoids the formation of residues from the cleaning solution because organic contaminants are reactively volatilized at high temperatures. Mechanical scrubbing using abrasive cleaners can be more effective than ultrasonic agitation, and a combination of the two would be extremely effective

Other techniques employed to remove oxidizable contaminants include boiling in hydrogen peroxide, hot nitric acid treatment, and UV/O_3 cleaning.[1,2] The latter technique involves subjecting the surface to be cleaned to short UV radiation (1849 Å) from a UV lamp in the presence of oxygen. Ozone is formed, bonds are broken, allowing oxidation of organic surface contaminants. There are many variations in cleaning procedures, all dependent on the degree of surface cleanliness required, and all evolved from basic cleaning processes modified to achieve the desired end results.

Once having established an effective cleaning procedure by experimentation, there should be no deviations in the process, and controls must be instituted to obtain reproducible and consistent results. Figure 1 shows the process steps involved in cleaning alumina substrates contaminated with all types of foreign material. One can apply all or part of the process to a specific cleaning problem. Several important points are to be emphasized:

- Never allow the surface to dry before the final rinse in de-ionized water;
- Rinse the substrate thoroughly in de-ionized water after detergent cleaning;
- The substrates should be placed in the deposition system as soon as possible after removing from the furnace, preferably still hot, to prevent recontamination; and
- Furnaces must be clean and free of particulates which originate from the insulation. Refractories used to hold substrates during firing should have smooth surfaces so as to eliminate the dust from rough, porous surfaces.

Cleaned substrates should be sputtered as soon after cleaning as possible because recontamination begins immediately in normal environments. To overcome this limitation, the substrates are sputter-cleaned or sputter-etched in situ in the deposition process. Sputter etching involves removal of surface atoms on the substrate by applying an RF potential to it, creating a plasma of ions and electrons which bombard the surface. The RF power and gas pressure should be low so as to minimize backscattering of sputtered material to the surface. A light sputter etch is a very effective cleaning method; however, gas incorporated into the surfaces during etching may be released after the sputtered film is deposited, causing

Continued on page 107

Ralph Tramposch was with Materials Research Corporation at the time this article was written. The article is based on materials and technology from MRC.

Continued from page 104

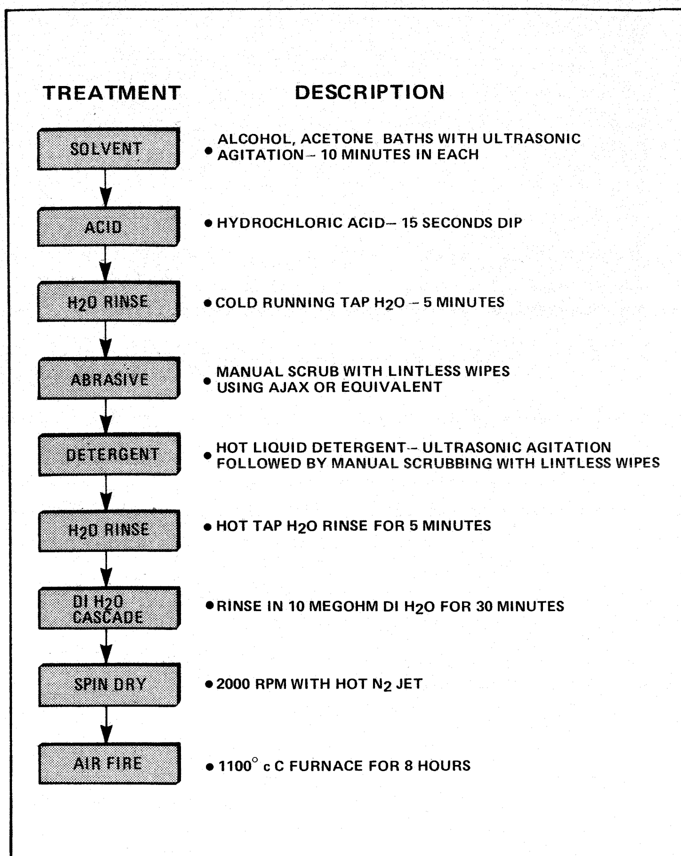

1. Steps involved in cleaning alumina substrates may be applied in part for some cleaning problems.

loss of adhesion. Heating the substrate after sputter etch is recommended to avoid this problem.

Sputtering Parameters for Conductor Films

The sputtering environment is an important consideration in establishing consistent results in film characteristics. The vacuum chamber must be kept as clean as possible and the pressure should be as low as possible, typically in the low to mid 10^{-7} torr range prior to back filling with pure argon at the desired sputtering pressure.

The sputtering parameters which will be defined for Cr/Au and Cr/Cu conductor films were optimized using an MRC 903 inline sputtering system. The three target positions consisted of Marz-grade chromium in an RF diode mode; Marz-grade copper and Marz-grade gold, and INSET target, both in DC magnetron. The target-to-substrate spacing for the chromium target is 5.7 cm; for the INSET targets the spacing is 5.1 cm. The argon gas used is ultra-grade (99.999+% pure) supplied by the Linde Division of Union Carbide.

High vacuum was obtained using a nine-inch diffusion pump with a speed of 1500 1/sec. The sputtering system was also equipped with a sputter etch station and, in general, all substrates received a light sputter etch just prior to deposition so as to promote better adhesion. Substrates are pre-cleaned prior to entering the sputter chamber using procedures already outlined. It is recommended that substrates be sputtered as soon as possible following pre-cleaning. Delays longer than 48 hours should be avoided in order to derive maximum benefits from cleaning. Substrates may be stored indefinitely in hermetically sealed containers or dry boxes with a positive pressure of dry nitrogen.

Substrates are loaded onto clean stainless steel or copper pallets which have been sputter-coated with 500 Å chromium or titanium-tungsten, whichever adhesive layer is to be used. The pre-coating prevents the sides of the substrates from being coated with stainless steel or copper during sputter etching since the surface of the pallet, as well as the substrate, becomes the target during this mode of operation.

The sputter deposition sequence for depositing 200-300Å of either copper or gold is as follows:

1. Pre-coated pallet loaded with substrates is placed into the loadlock and pumped down to 15 microns; it is then back-filled with argon or dry nitrogen and then evacuated again.
2. Pallet is exchanged into main chamber and pressure reduced to 5×10^{-7} torr.
3. Pallet is positioned at the sputter-etch station. The high-vacuum pump is throttled and argon is admitted into the system. System pressure is adjusted by argon flow rate to 9×10^{-3} torr.
4. RF voltage is applied, the power adjusted to 500 W, and automatic timer set for two minutes.
5. Pallet is positioned under shutter adjacent to chromium target. The target is pre-sputtered for one minute using an argon pressure of 9×10^{-3} torr and RF power level of 1.4 kW.
6. The pallet is traversed beneath the target at a rate of seven inches per minute for a deposition rate of 300Å per minute.
7. The pallet is transferred to a position under the shutter adjacent to the copper or gold target. The target is pre-sputtered for ten seconds using an argon pressure of 15 microns. The DC power applied to the copper target is 5.0 kW; for the gold target the power is 2.0 kW. To obtain 3000Å of copper, the pallet is traversed under the target at a speed of 20 inches per minute at a deposition rate of 10,000Å per minute. To obtain 3000Å of gold, the pallet is traversed under the target at a speed of 13 inches per minute at a deposition rate of 6500Å per minute.

The same sputtering conditions and sequences are used to obtain all-sputtered or sputter-to-thickness films. However, multiple passes are used, approximately 100 microinches (2.5 micrometers) per pass.

Typically, Cr/Cu sputtered to 300 microinches is obtained in three passes, each at a scan rate of 2.4 inches/min.

Chromium thickness is determined by measuring the sheet resistance of the film deposited on a glass microscope slide. A plot of sheet resistance as a function of thickness and scan speed for sputtering parameters given above is shown in Figure 2. Sputtering machines are calibrated frequently using this technique. Scan speed is varied slightly to ensure the same chromium sheet resistance from one sputter run to another.

Sputtering Parameters for Resistor Films

The degree of control of the sputtering parameters and environment required in the deposition of resistor films is

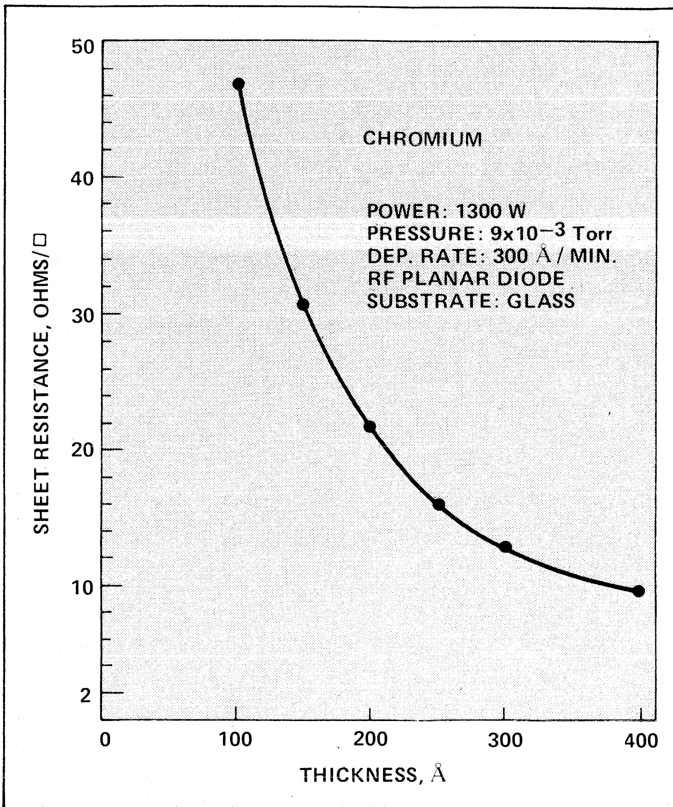

2. Chromium thickness is determined by measuring sheet resistance of the film deposited on a glass microscope slide. Sheet resistance's variance with thickness is plotted here.

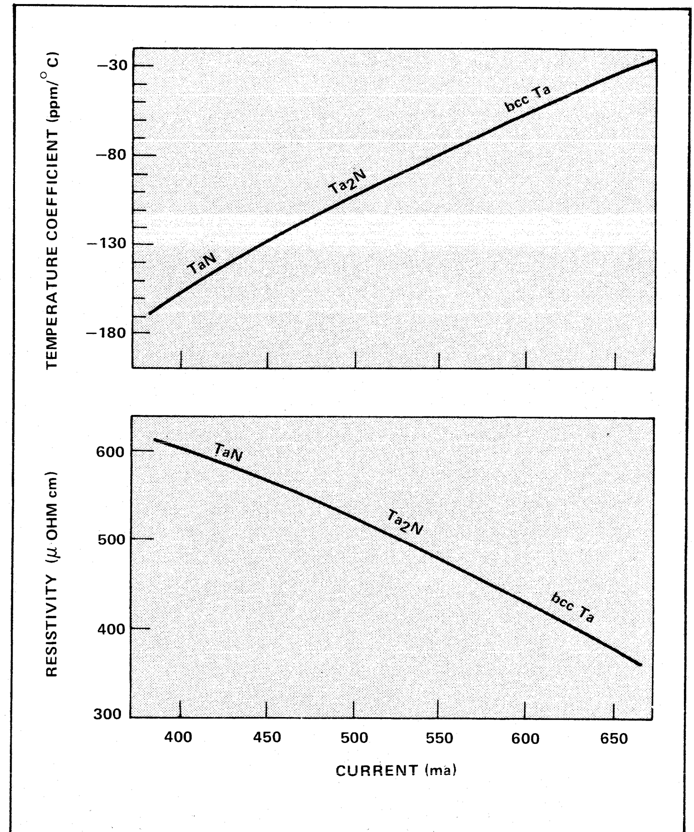

3. Sputtering current also varies film resistance.

significantly greater than is necessary for conductor films. The deposition rate for the latter was somewhat arbitrarily chosen to achieve good adhesion and throughput. Resistor film characteristics are sensitive to deposition rate, gas pressure, residual gas specie, substrate temperatures, and type of substrate. In this section, typical deposition parameters and processing will be covered for the preparation of nickel-chromium and tantalum nitride resistor films.

All that has been stated concerning the requirements for a good sputtering environment applies also to resistor film depositions, but even more so. Targets are pre-sputtered longer and at higher power levels than during film deposition. Film thickness uniformity is very important when making resistor devices. Special shuttering can be used to achieve thickness uniformities better than ±5 percent.

Tantalum nitride is formed by sputtering tantalum in an argon-nitrogen gas mixture. A complete range of compositions may be produced by varying the amount of nitrogen introduced into the system, as discussed. The deposition rate is critical in controlling the properties of the film. For a constant input of nitrogen, changing the deposition rate causes the ratio of nitrogen to tantalum ions arriving at the substrate to change and, therefore, alter film properties. Figure 3 shows the variation in film characteristics as a function of sputtering current for a constant voltage.[3] Sputtering conditions were such that the nitrogen input was kept constant while the argon pressure was increased to increase current. The sputtering voltage was maintained at 5000 V. The sensitivity of film characteristics to deposition rate and nitrogen gas input is quite evident, illustrating the need to maintain tight control on these parameters during reactive sputtering.

To achieve reproducible results and operational control for manufacturing tantalum nitride resistor films, sputtering conditions must be determined so that the operating point is in the "plateau" region where small differences in nitrogen pressure have little effect on film characteristics. In this region, the resistance change due to aging is a minimum, and maximum stability is achieved. The operating point is determined for any sputtering system by maintaining a constant sputtering voltage and gas pressure and varying the partial pressure of nitrogen to define the device characteristics. Subjecting tantalum nitride films deposited at different nitrogen pressures to a 30-minute bake at 425°C changes film resistance as a function of the partial pressure of nitrogen maintaining the sputtering voltage and total gas pressure constant. The minima in the curve occurs at a particular nitrogen pressure which we shall call the operating point. How well these sputtering conditions are maintained will limit the reproducibility in the manufacturing process.

The sputtering sequence for depositing tantalum nitride films on alumina substrates is similar to that described for conductor films, except for the gas mixture and sputter voltage. Data on sheet resistance as a function of scan speed for both as-deposited and stabilized films were obtained for films deposited using a cathode potential of 2 kV peak RF voltage, a total gas pressure of 10×10^{-3} torr, and a partial pressure of nitrogen of 1.5×10^{-4} torr. Films were stabilized at 425°C for 30 minutes in a precision circulating air oven. A stabilization temperature of 300°C is used for tantalum nitride films

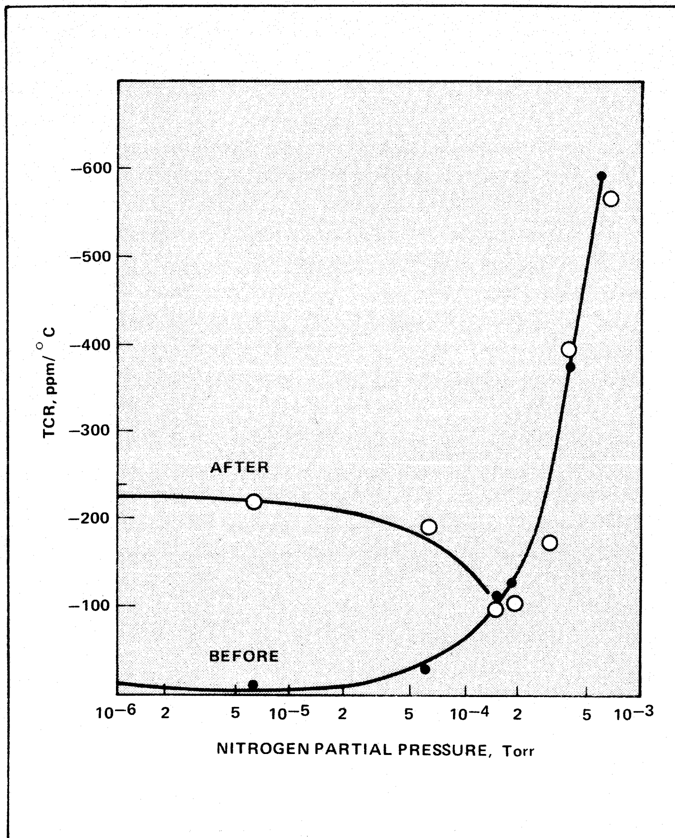

4. Temperature coefficient of resistance (TCR) for tantalum films varies widely with nitrogen partial pressure.

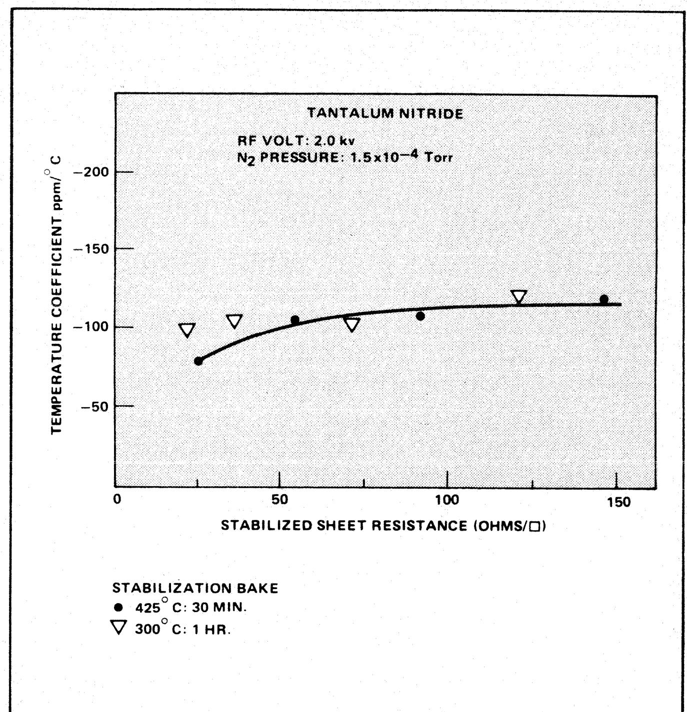

5. TCR is highly linear with sheet resistance and bake temperature.

metalized with chromium-gold for conductor and termination pads.

The stabilization temperature and metalization system chosen will depend on the maximum temperature that the film resistor will be subjected to during processing. Films will obviously be more stable at operational temperatures if stabilized at several hundred degrees higher. This effect shows the aging characteristics of tantalum nitride at 290°C after a stabilization bake. Stabilization temperatures above 400°C provide the best aging characteristics, i.e., smallest change in resistance when subsequently baked at 290°C. Also, it is evident that stabilizing of films at much higher temperatures does not significantly increase stability.

Long-term aging characteristics at 150°C of films doped with different amounts of nitrogen are also important. Films deposited in various partial pressures of nitrogen exhibited a sheet resistance of approximately 50 Ohms per square. Again, it is evident that the optimum concentration of nitrogen in the films occurs when they are deposited in a partial pressure of 1.5×10^{-4} torr. The actual pressure at which this occurs may vary with the type of sputtering system used and sputtering conditions in that system. Variations in the manner in which the reactive gas is admitted into the system will also cause some differences; however, for every sputtering system there will be an operating point which will occur at some partial pressure of nitrogen that will result in films having the maximum stability provided by the optimum nitrogen doping.

The temperature coefficient of resistance (TCR) as a function of nitrogen partial pressure is shown in Figure 4. These data illustrate the metallic behavior of tantalum films, pure and doped with increasing concentrations of nitrogen, before and after baking at 425°C for 30 minutes in air. A large negative change in TCR occurs due to the oxidation of the tantalum. As the nitrogen doping increases, the TCR of as-deposited films also increases, and the change due to oxidation during baking is much less. In the region of the operating point and at higher pressures, there is essentially no change in the TCR due to baking. Figure 5 shows the constancy of TCR as a function of sheet resistance and bake temperature for films deposited at partial pressures of 1.5×10^{-4} torr.

Alloys of nickel-chromium are used as resistor material principally because of their low TCR. To achieve low TCR, alloys having a high chromium content are chosen; i.e., 40 to 60 percent. The chromium oxidizes during a high-temperature stabilization bake in air and causes the TCR to become more negative. Nichrome, which has a chromium content of 20 percent, has relatively high positive TCR.

The TCR of a nickel-chromium film deposited on alumina substrates using a target of 60 percent chromium may be less than +50 ppm/°C depending on deposition conditions and stabilization temperture used. Adding impurity elements to inhibit grain growth, or doping with oxygen, or a combination thereof, has the effect of reducing the TCR to zero ± 20 ppm/°C.

Sputtering and process conditions used to obtain TCRs in the range of +25 to +50 ppm/°C are the following:

- Base pressure in the chamber should be in the mid-seven range before starting sputtering processes;
- Substrates are given a light sputter etch, 500 W RF, 9 microns argon pressure, two-minute duration;

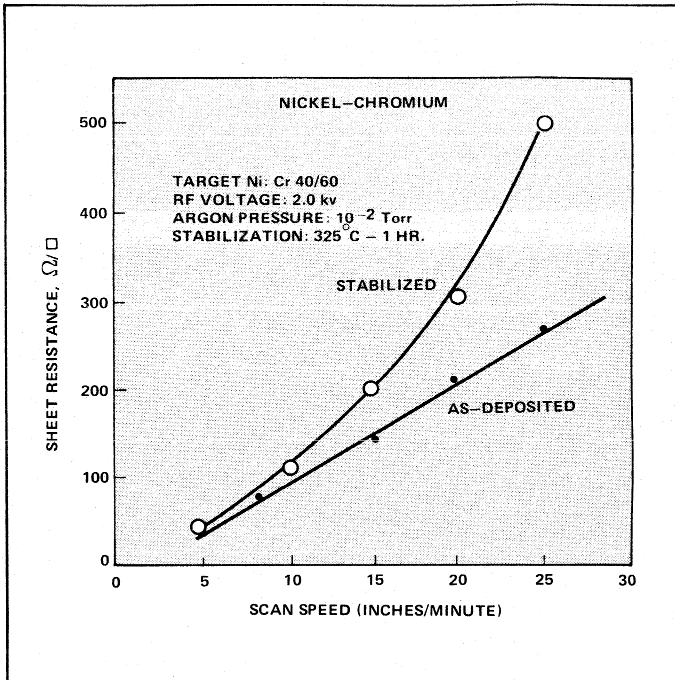

6. Sheet resistance of as-deposited NiCr films is shown before and after stabilization and as a function of scan speed.

- Target is pre-sputtered for two minutes at a power level of 1.5 kW;
- Target voltage is adjusted to 1800 Volts, argon pressure maintained at 9×10^{-3} torr, and the scan speed adjusted to obtain the desired film thickness and sheet resistance. Figure 6 is a plot of sheet resistance of as-deposited NiCr films before and after stabilization as a function of scan speed; and
- After completing the NiCr deposition, a barrier layer of 1500Å of nickel followed by 3000Å of gold is deposited sequentially.

The nickel deposition is made in three passes at a power level and scan speed to minimize the diffusion of nickel into the underlying NiCr. A power level of 1 kW and scan speed of 3.5 in./min. provides a film thickness of 500Å.

Figure 7 shows the effect of stabilization bake temperature on the TCR. As the temperature is increased the TCR becomes more positive, and the rate of change in sheet resistance increases. The bake temperature is optimized to obtain the best trade-off between low TCR and good drift stability at 150°C. Oxygen doping to effect a lowering of the TCR can be accomplished by introducing a small amount of O_2 into the sputtering gas. Reactively sputtered NiCr has a much lower negative TCR initially, which increases in a positive direction

Continued on page 114

7. Stabilization bake temperature affects TCR.

Continued from page 110

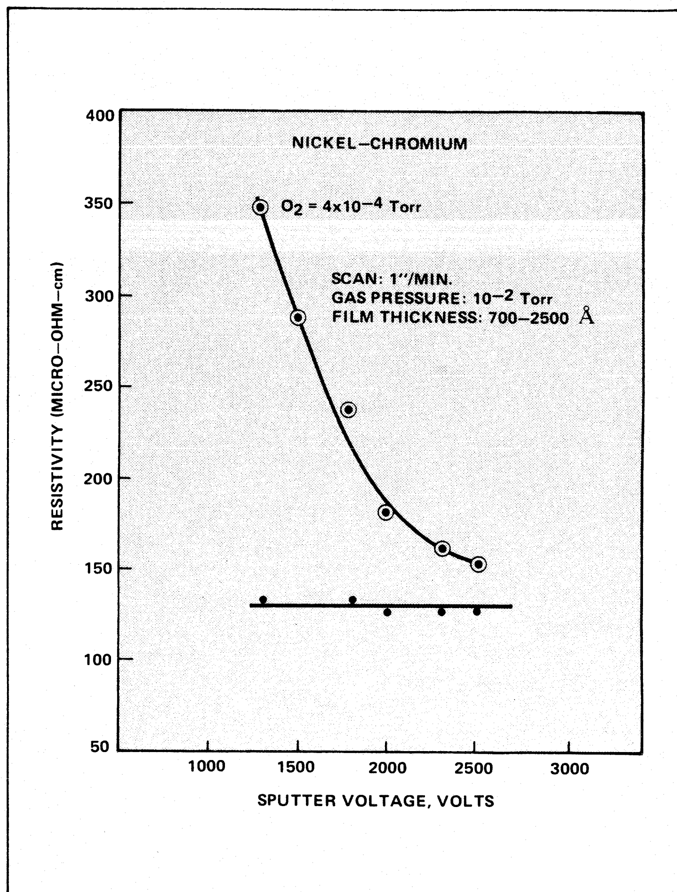

8. Oxygen also alters resistivity of NiCr deposited on alumina.

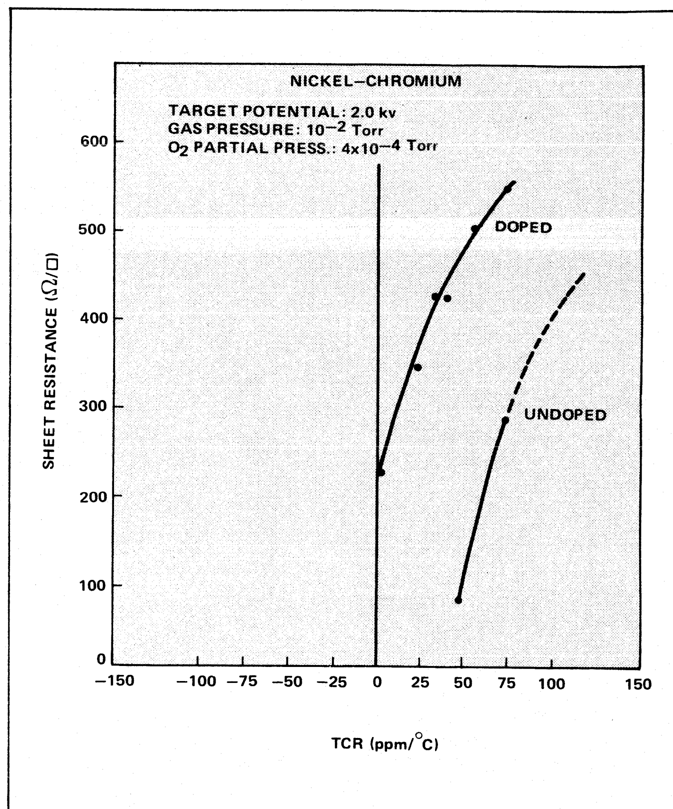

9. Sheet resistance vs. TCR for NiCr films is plotted with and without oxygen doping.

upon annealing during the stabilization bake. The specific resistivity of the oxygen-doped NiCr is much higher than undoped, and the stabilization bake temperature can be increased without a correspondingly large increase in the TCR, as would occur in undoped NiCr.

Figure 8 shows the effect of oxygen on the resistivity of NiCr deposited on alumina at different deposition rates (sputter voltage). As the deposition rate is reduced, the resistivity is increased, because reaction rate is increased. The effect of oxygen doping on the TCR is very evident in Figure 9, which is a plot of sheet resistance vs TCR for NiCr films deposited with and without oxygen doping. All samples were stabilized at 300°C for one hour, and then the TCR was determined. It is clear that oxygen is very effective in lowering the TCR, even in films of relatively high resistivity.

Thin Film Pattern Generation

Early work in generating patterns in thin films involved the use of metal masks and elaborate fixturing. As line widths were reduced to accommodate increasing demands of diminutive circuit dimensions and higher operational frequencies, mechanical masks became impractical, and circuit patterns were delineated by chemical etching using photolithography. Photolithographic techniques have become well established over the years to meet the needs of the semiconductor industry, and processes have been developed far beyond the requirements of present thin film hybrid integrated circuits.

Photolithography—or photoetch, as it is often referred to—makes use of photographic techniques and photosensitive polymers applied as a thin layer to the thin film circuit to be etched. The photosensitive polymer—a photoresist as it is called—is exposed with UV light through a photomask, and an image of the mask pattern is formed in it. After developing the exposed photoresist, the desired pattern is formed on the circuit board with photoresist. Since the photoresist is resistant to most chemical etchants, areas of the thin film which are unprotected are removed by the etchant, leaving the remainder of the film delineated by the photoresist pattern.

There are two types of photoresist. Each differs in response to UV light and the solubility behavior induced toward the developing solvent. Figure 10 shows that behavior schematically. Photoresist material which becomes insoluble when exposed to UV light is referred to as negative photoresist because the pattern formed is the negative of the pattern on the photomask. Positive photoresists are soluble in developing solvents and, therefore, duplicate the pattern on the photomask. There are advantages and disadvantages to both systems. An extensive review of photoresist processing is given elsewhere.[4,5] In hybrid IC processing, positive resists are generally used because they can be applied thicker than negative resists without diminishing line width resolutions. Positive resists also adhere better than negative resists.

Photoresist is applied by spin coating. The substrate is flooded with filtered resist and the excess is removed by revolving on a vacuum chuck at high RPM. A uniformly thin photoresist coating now covers the metalized ceramic. The

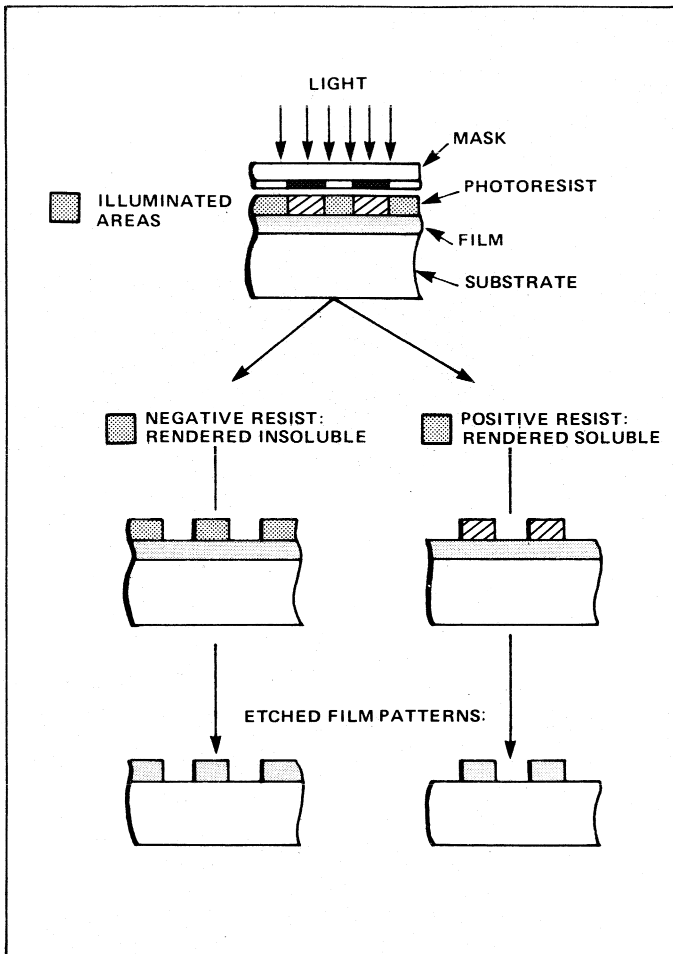

10. Schematic of photoresist process contrasts positive and negative resists.

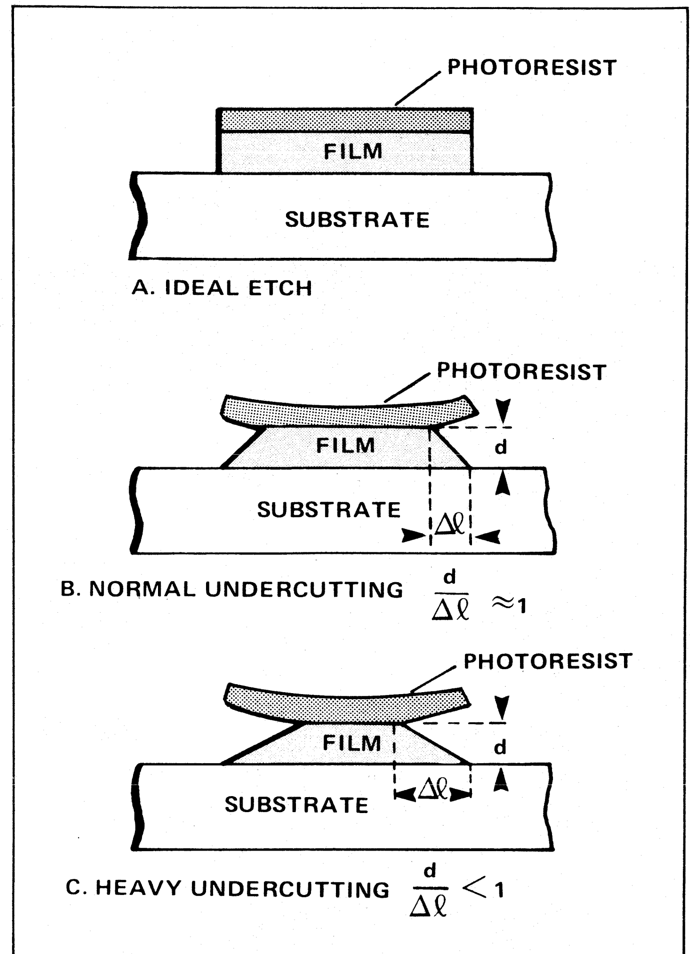

11. Although the ideal etch (a) is straight, undercutting is normal (b) and can be quite heavy (c).

coating is allowed to air dry for 10 to 15 minutes and then is pre-baked at a temperature which will allow the solvent to evaporate without degrading the photosensitivity of the resist. The resist is then exposed to UV light through a contact mask and the pattern developed using the appropriate solvent. A typical photoresist process using the positive resist AZ1350B (product of the Shipley Company, Newton, Mass.) is as follows:

- Metalized substrate is baked at 125°C for 30 minutes;
- Photoresist coating is applied by spinning substrate at 4,000 RPM (coating thickness is 1.5 microns);
- Coated substrate is allowed to air-dry for 15 minutes and then baked at 90°C for 25 minutes in a forced-air oven;
- Expose substrate to UV light ≈300 nanometers wavelength for 10 to 20 seconds depending on lamp intensity;
- Immerse in developer and gently agitate for one minute followed by a D.I. water cascade rinse;
- Spin dry at 2,000 RPM; and
- Post bake at 150°C to improve resist adhesion.

If the exposure time is correct and the developer is reacting properly, the photoresist pattern should replicate the pattern on the photomask.

Assuming all the process parameters were well controlled and the photoresist line widths exactly duplicated the mask, the objective is to achieve the same dimensions in the metal film by chemical etching. Ideally, the etchant should remove only film material not protected by the photoresist. However, chemical etchants react isotropically with polycrystalline and amorphous materials and, therefore, attack the film parallel as well as perpendicular to the surface. Figure 11 illustrates both the ideal and actual behavior in photoetching a thin film.

The ideal behavior as shown in Figure 11a is closely approached in plasma or reactive ion etching. Figure 11b is typical of the profile obtained in etching metal films. The amount of lateral etch is referred to as undercutting, is typically 1, and, therefore, the line width at the surface is narrowed by twice the thickness. Severe undercutting, where the etch factor is considerably less than 1, usually occurs when resist gradually lifts during etching, indicative of poor adhesion.

Another method to delineate a circuit pattern in a thin-film hybrid IC is to pattern-plate. This method is becoming increasingly popular because as an additive technique it offers a number of advantages over subtractive methods:

- Precious metals are deposited only where they are required, i.e., contact pad areas and conductor lines;
- Close dimensional tolerances are easily achieved;
- Thick, narrow lines are possible which would otherwise be unattainable using wet chemical etchants; and

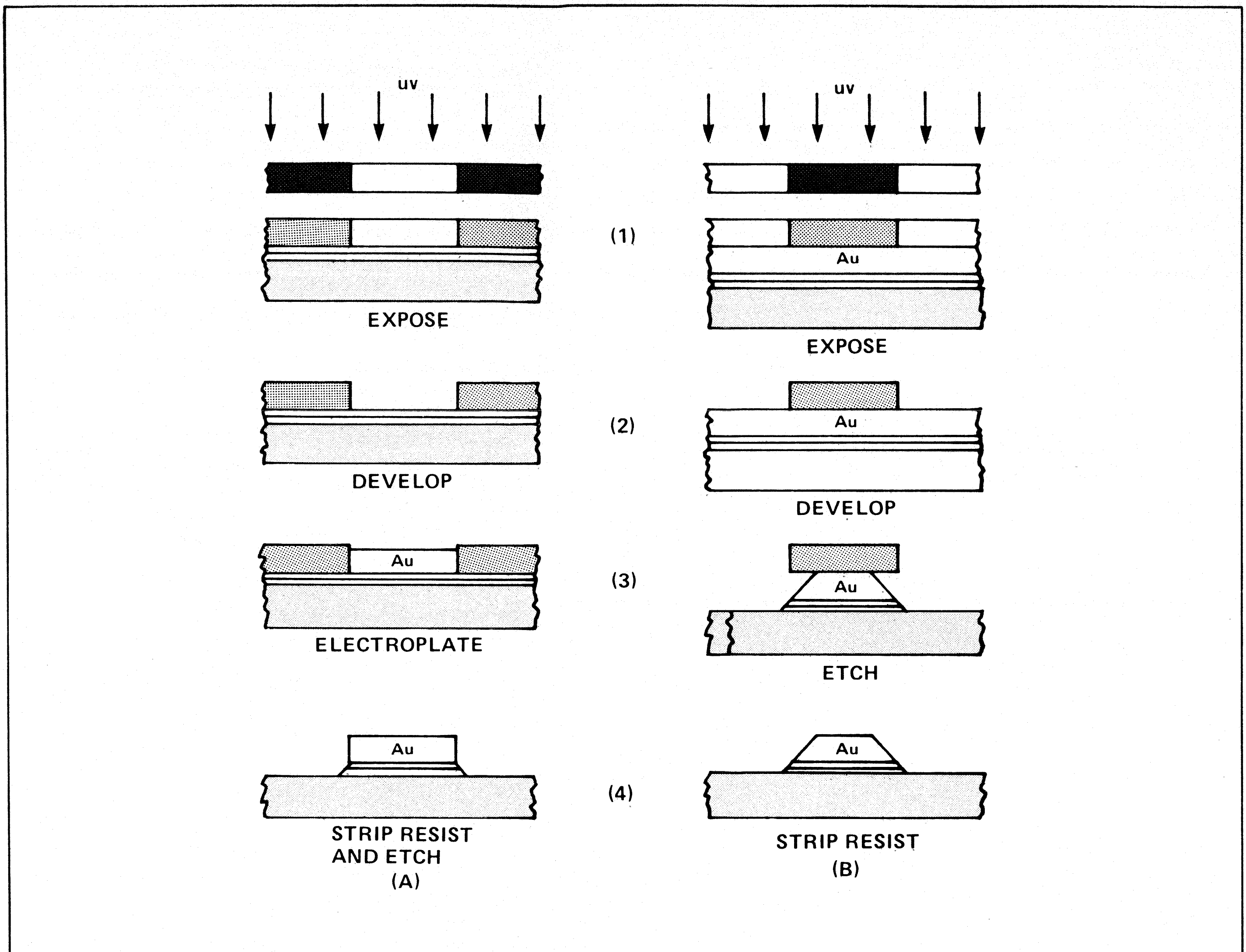

12. Schematic compares pattern plating (a) and photoetch (b) processes.

- The cross section of the line pattern is more nearly rectangular than trapezoidal and more desirable for microwave ICs.

The processes involved in pattern plating are depicted in Figure 12. The subtractive method (photoetch) is also included for a comparison of the two processes. Assume the same pattern is required in each sputtered Cr/Au film. Both processes involve the use of a positive photoresist, electroplating, and etching; however, the sequences are different. In pattern plating, the photoresist is applied to the thin sputtered gold film and exposed to a negative pattern. This permits selective electroplating in areas not protected by the photoresist. The windows in the photoresist correspond to the desired circuit pattern and are plated up to the desired thickness. After plating, the resist is removed and the thin sputtered Au-Cr film is etched away. In the subtractive process, the sputtered gold is first electroplated to desired thickness, then photoresist is applied and exposed through a positive mask pattern, and the unprotected areas etched away. Economically, the other process has a decided advantage in gold usage alone.

The additive process is not without problems, however. The integrity of the resist is critical. The resist must be applied in two or more layers to avoid, or reduce, pinholes. The reaction between the electrolyte and the resist must be minimized to prevent lifting of the resist. Alkaline electrolytes are chosen since positive resists are stabilized in alkaline media. Plating parameters such as temperature, agitation, pH, current density, and conductivity must be carefully controlled and optimized to achieve desired results.

All-Sputtered vs Sputtered and Plated Metalization

Thick conductor films for microwave applications and bonding pads have, until recently, been deposited by sputtering thin films and electroplating them to the required thickness. The availability of DC magnetron sputtering providing high deposition rates and more efficient target utilization has made all-sputtered films an attractive alternative. In this section, a comparison will be made of all-sputtered and sputtered-electroplated Cr/Au and Cr/Cu films on alumina substrates, focusing on such characteristics as adhesion, intrinsic stress, hardness, uniformity, density, and resistivity.

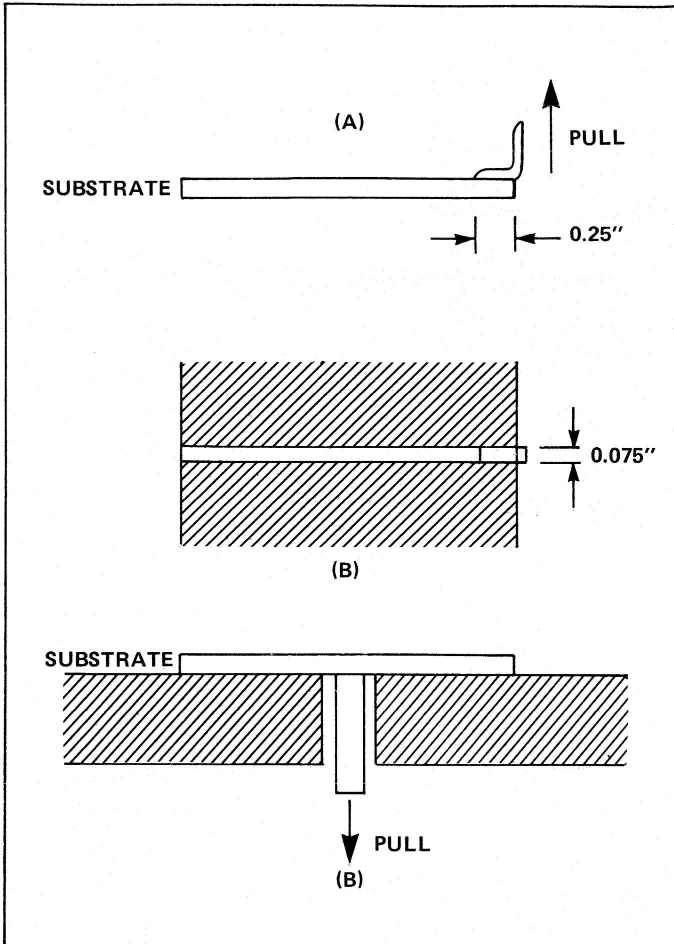

13. Adhesion measurements using a micropull tester can take one of two approaches. (a) Etched strips and copper ribbon are stressed until failure, or (b) a small pin is attached with epoxy and stressed to failure.

All films were prepared by sputtering an adhesive layer of 300Å of Cr onto as-fired 99.6-percent alumina substrates. Immediately following the Cr deposition, 3000Å of either Cu or Au was deposited using an MRC 903 in-line sputtering machine. Prior to film deposition, the substrates were sputter etched for two minutes at an argon pressure of nine microns and an RF power of 500 Watts.

The sputtering conditions for chromium were the same for all films: an RF power of 1.4 kW, an argon pressure of nine microns, and a deposition rate of 350Å/min.

Copper films were sputtered using an INSET target in a DC magnetron mode and the following conditions: 5.0 kW, 15 microns of argon, and 1.33 microns/min. Sputter conditions were the same for gold films except the power was 2 kW and the deposition rate was 0.65 microns/min. Copper and gold films that were not all-sputtered were subsequently plated to 400 microinches in commercial electroplating baths in accordance with recommended procedures.

Adhesion measurements were performed using two techniques as shown in Figure 13. Both techniques employ a micropull tester. In the first method, 0.075-inch–wide strips are etched in the metalization and a tinned copper ribbon, 0.050-in., is attached as shown using Pb/Sn or Au/Sn solder. A dynamic load is applied and the ribbon is pulled until failure. The number of pounds applied when failure occurs is the pull strength. In the second method, a small metal pin is attached perpendicularly with epoxy to a 0.100-inch–diameter pad etched in the metalization. A machine applies an increasing force to the pin until either the metal-substrate or the metal-epoxy bond fails. The results of the adhesion tests are summarized in Table I. There were no failures at the metal-substrate interface; either the solder joint or the epoxy bond failed. The maximum force or stress is tabulated. The minimal acceptable force at which failure occurs using the first test method is five pounds. This translates to approximately 4000 lb./in^2.

Table I.

Summary of Adhesion Test of Electroplated and All-Sputtered Cr/Cu and Cr/Au Films

Cr/Cu Plated	Cr/Cu Sputtered	Cr/Au Plated	Cr/Au Sputtered
FIRST TECHNIQUE			
7.9 lbs.	1.3 lbs.	11.5 lbs.	5.75 lbs.
Sample failed at metal-solder interface			
SECOND TECHNIQUE			
10,520 P.S.I.	10,580 P.S.I.	9,750 P.S.I.	9,410 P.S.I.
Sample failed at metal-epoxy interface			

Since no failures occurred at the film-substrate interface, one cannot draw any conclusions as to the relative strength of the bond. All films, regardless of the method of preparation used, exhibited pull strengths in excess of the minimum acceptable level.

The intrinsic stress in all-sputtered and sputter-and–plated films was determined using thin microscope-slide glass cover slips which were sputter-coated and electroplated on one side under exactly the same conditions as were the alumina substrates. From a measurement of the radius of curvature following metalization, it is possible to calculate the intrinsic stress of the film. It is necessary to determine the film thickness with a Sloan Dektak for use in the calculation. Radius of curvature measurements were made simply by focusing a high-power microscope on the center and edge of the cover slip. The results are presented in Table II. All films were concave after metalization and, therefore, under a compressive-type stress. The stress in copper films is apparently not strongly dependent on the mode of deposition. The stress in gold-plated films, on the other hand, is substantially lower than that in an all-sputtered film. The reasons for these results are not understood; however, thermal expansion mismatch is likely to be a contributing factor.

Continued on page 122

Continued from page 118

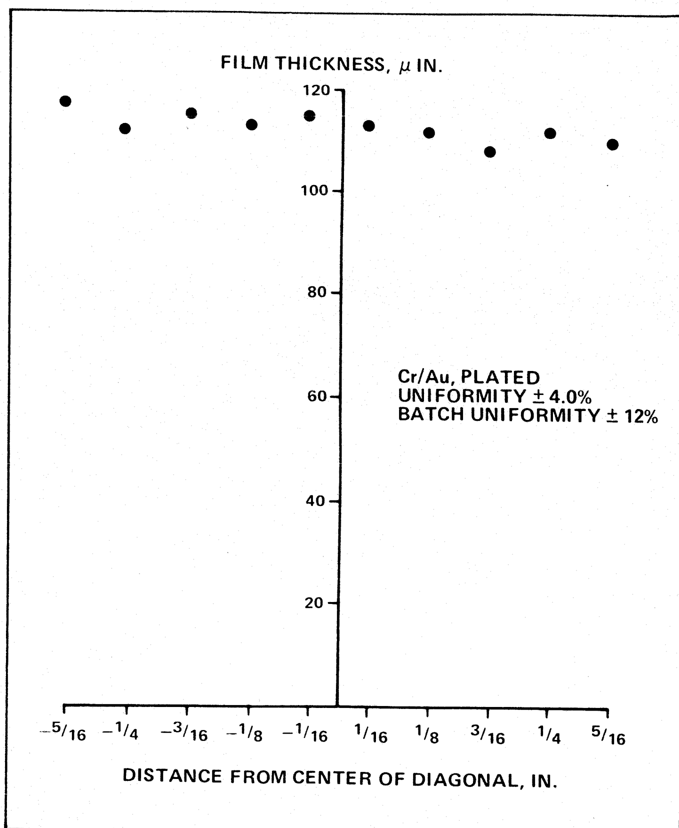

14. Thickness profile of Cr/Au sputtered-electroplated approach compares with . . .

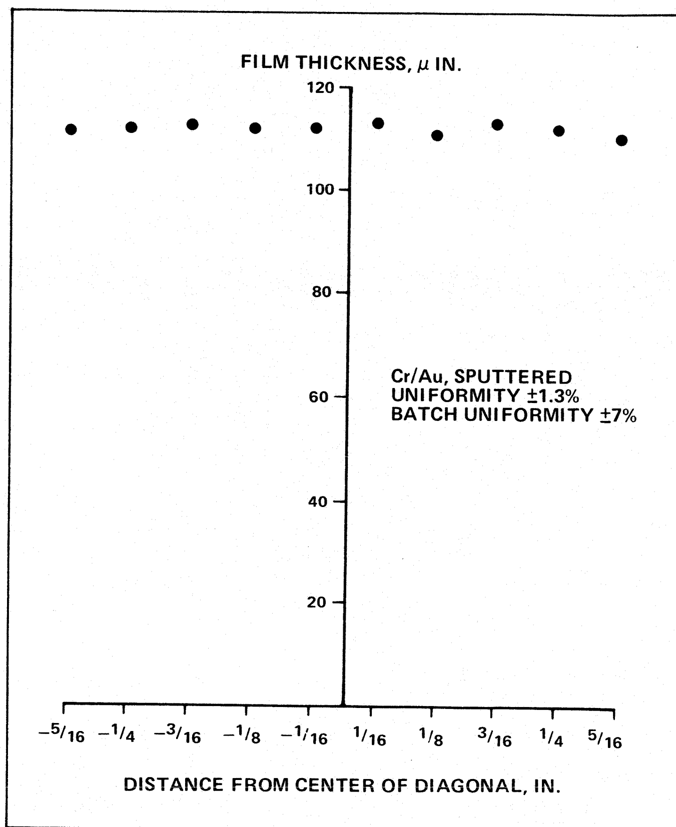

15. . . . **profiles** for the all-sputtered Cr/AU film thickness.

Table II.

Summary of Measurements of Intrinsic Stress In Electroplated and All Sputtered Films

	Cr/Cu Plated	Cr/Cu Sputtered	Cr/Au Plated	Cr/Au Sputtered
Radius, In.	8.76	10.24	17.42	7.03
Thickness, μIn.	339	362	478	448
Stress, P.S.I.	6.88×10^4	5.52×10^4	2.45×10^4	6.48×10^4

Table III.

Measurements of Knoop Hardness in kg/mm² Tabulated For Electroplated and All-Sputtered Cr/Cu and Cr/Au Films

Cr/Cu Plated	Cr/Cu Sputtered	Cr/Au Plated	Cr/Au Sputtered
250	110	90	100

The Knoop hardness for the four types of metalization was determined using a Tukon hardness tester and a five-gram load. Care was exercised in making the measurement to insure that the indentor did not penetrate the metalization through to the substrate. From the data as shown in Table III, the sputtered and plated gold films were of roughly equal hardness, whereas the plated copper films were substantially harder than the all-sputtered copper films. Although the relative hardness values of all-sputtered and plated gold films are as expected, on the basis of the intrinsic stress data, with the plated gold being softer than the all-sputtered gold, one would expect to see a larger difference than is evident here.

The uniformity of film thickness as a function of deposition mode was determined on 1 × 1-inch substrates using a Sloan Dektak. A diagonal line was drawn across the substrates, the film etched off one side of that line, and the thickness measured at points along the diagonal. Typical thickness profiles are shown in Figures 14 and 15, along with the calculated uniformity. As can be seen from the data, the uniformity of film thickness for individual substrates was better than 5 percent in all cases. If batch uniformity is examined, however, we see a large difference between plated and all-sputtered film. Batches of 18 copper-plated films exhibited a uniformity of 15 percent while a batch of 60 gold-plated films exhibited a 12-percent uniformity. Batches of over 100 all-sputtered films were much more uniform in thickness, averaging about 7 percent. The larger spread in film uniformity of plated films is due to the enhanced electric field at the edges and corners of the plating rack.

It is generally recognized that the density of sputtered or electroplated films will be lower than that of the corresponding bulk material. The film density was determined for plated

Table IV.

Film Density in G/cm³ as Determined for Electroplated With All-Sputtered Cr/Cu and Cr/Au Films and Compared With Bulk Values

Cu, Bulk	Cu, Sputtered	Cu, Plated
8.91	8.34	8.18

Au, Bulk	Au, Sputtered	Au, Plated
19.32	18.76	18.65

Table V.

Summary of Resistivity Measurements, in Micro-Ohm-cm, For Electroplated and All-Sputtered Cr/Cu and Cr/Au Films

Cu, Sputtered	Cu, Plated	Au, Sputtered	Au, Plated
2.93	12.4	6.64	3.26

Bulk Cu	Bulk Au	TiW/Au, Sputtered
1.65	2.45	3.0

and all-sputtered films simply by the usual displacement techniques which utilize Archimedes' Principle. In Table IV are shown the values observed and compared with the respective values of bulk density. Although all densities are substantially lower than theoretical density, the densities of both sputtered films are higher than those of electroplated counterparts.

Measurement of film resistivities were performed simply by etching a strip approximately 1.5 mm wide into the metalization, and calculating the resistance of a known volume of material from current voltage data. A four-wire measurement was performed to eliminate the effect of contact resistance as shown in Figure 16. Table V summarizes the results. It can be seen that sputtered copper, although having 1.8 times the resistivity of bulk copper, has a substantially lower resistivity than electroplated copper. The high resistivity of sputtered gold relative to the plated gold is due to the diffusion of chromium into the gold during sputtering. Subsequent removal of the gold revealed that the chromium adhesive layer was, indeed, dissolved by the gold. Resistivity measurements performed on all-sputtered gold with a TiW adhesive layer confirmed that the increase in resistivity is due to chromium diffusion. The resistivity of all-sputtered TiW/Au is 3.0×10^{-6} Ohm-cm. Results of this comparison of all-sputtered to sputtered and electroplated copper and gold films with regard to certain critical parameters may be summarized as follows:

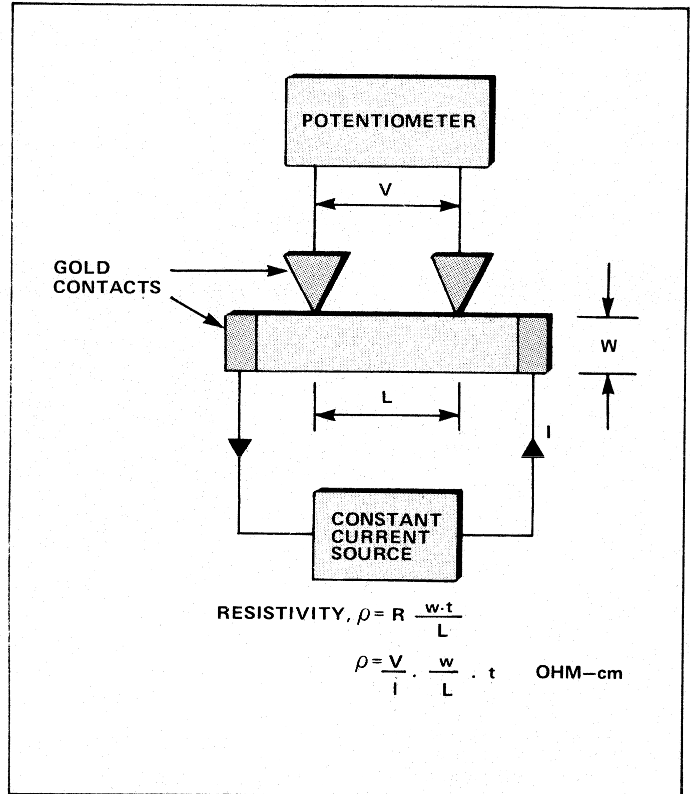

16. Four-wire measurement eliminates the effect of contact resistance when measuring film resistivities.

- The type of deposition has little impact upon film adhesion.
- The intrinsic stress of sputtered copper is lower than that of plated copper films, whereas the reverse is true for gold films.
- Sputtered copper films are much softer than plated films; sputtered gold films are slightly harder than plated gold films.
- Batch uniformity of all-sputtered films is much better than those of plated films.
- Sputtered films have a somewhat higher density than plated films.
- The resistivity of sputtered copper is significantly lower than that of plated copper. If we only consider sputtered gold films with passive adhesive layers, the resisitivity is slightly lower than plated gold. ■

References

1. R. R. Sowell, R. E. Cuthrell, D. M. Mattox, and R. D. Bland, *J. Vac. Sci. Technol.* 11, 1974, p. 274.
2. J. R. Vig and J. W. LeBus, *IEEE Trans. Parts. Hybrids Packag.* 12, 1976, p. 365.
3. R. W. Berry, P. M. Hall, and M. J. Harris, *Thin Film Technology*, Van Nostrand Reinhold Co., 1969, p. 227.
4. L. I. Maissel, and R. Glang, (Editors) *Handbook of Thin Film Technology*, McGaw-Hill, 1970.
5. W. S. DeForest, *Photoresist: Materials and Processes*, McGraw-Hill, 1975.

Tubes Still Vital To Microwave Systems

From ECM to communications, a variety of tubes fills the need for power.

By Robert Espinosa, *Varian Associates*

Many different types of tubes have been invented over the last 40 years to generate and amplify microwave power. The development of most of these has ended due to inherent low energy-conversion efficiency, poor spectrum quality of the output, low gain, or low reliability due to high stress levels inherent in the device.

There are six primary families of microwave tubes in general use today. These six families have survived because their overall performance is adequate and they have some specific features that are exceptional.

Magnetrons, the first of the microwave-generation devices, continue to be the most inexpensive source of microwave power. Crossed-field amplifiers, which evolved from magnetron principles, provide exceptionally efficient high-peak-power sources at frequencies below 10 GHz. Klystron amplifiers provide the user with a friendly, rugged amplifier, which will cover a wide range of applications. Traveling-wave tubes provide amplifications over exceptionally wide bandwidths. The last of the major families to emerge are the gyrotrons, which have assured their continued development and application with the ability to efficiently generate high power at high frequencies.

A summary of the major types of microwave tubes available is presented to provide a quick source of information required to select from among the various device types, and note the power conditioning and other important considerations in tube applications. A general discussion of the available performance and its limits are provided. Power source and connection requirements will also be discussed, providing a guide to future development potential.

Product selection and transmitter design requires muchmore detailed information on these devices than can be presented here, and such information must be obtained directly from the manufacturers. Unfortunately, most manufacturers have discontinued the publication of catalogs because so few of their products are sold as catalog items. The catalogs, however, never contained a complete listing of devices due to restrictions on the release of specific performance parameters for many of their products. Typically, catalogs are used by microwave designers to determine the approximate range of power supply and modulator cooling, and microwave circuit parameters required by devices producing the approximate output power, frequency, and gain required for this application. The information presented here will provide that function as a source of data to make easier that first cut at the design for the purpose of estimating feasibility and ballpark schedule and cost.

Lower-power tube types such as reflex klystrons, O-type backward-wave oscillators, and low-noise and low-power TWTs are not included here because they are being replaced by solid-state devices in nearly all new designs. It is not expected that advances in solid-state performance will continue upward in power and frequency until all microwave tubes are replaced.

In the author's opinion, solid-state sources and amplifiers will not have much impact on future use of high-power microwave tubes. The inherent higher dissipation in the materials used, low device impedance levels, size, operating temperature, and stress limits in the solid-state devices argue against ever successfully building either a discrete device, or by in-circuit combining of several devices, providing output power and efficiency obtainable with the dissipationless, distributed energy conversion processes used in microwave tubes.

Solid-state devices can be used to replace high-power microwave transmitters where large numbers of the low-power devices can be integrated into the antenna aperture to effectively combine power in space. This trend is already evident with the fielding of the Pave Paws all-solid-state phased-array radar. Continuation of this trend to higher frequencies, however, requires technological progress of breakthrough proportions before all-solid-state high-power transmitters will be available, reliable, and affordable.

Traveling-Wave Tubes

Traveling-wave tubes can be divided into many classes according to the interaction circuit used to convert the kinetic energy from the electron beam into microwave energy. Perhaps only four are very significant and only two of them make up over 90 percent of TWTs in use today.

The dominant types are helix and coupled-cavity circuits. TWTs with helix interaction circuits are used universally in ECM and communication transmitters where wide bandwidths are required at CW power levels up to a few hundred Watts, or peak power of less than 5 kW is required. There is a trend toward using more helix TWTs in airborne radar transmitters for smaller aircraft.

Coupled-cavity TWTs use a circuit consisting of a stack of cavities concentric with the electron beam; they are coupled through their end walls to approximate the propagation characteristics of a folded waveguide. Coupled-cavity TWTs are primarily used in coherent

The author wishes to acknowledge the contributions by Bob Berry, Jim Driscoll and Earl McCune of Varian Microwave Tube Division; Bob McMirrough of Hughes, Gerry Karlsruher of the Varian Beverly Division, and Bill Linn of Litton, in gathering material for this article.

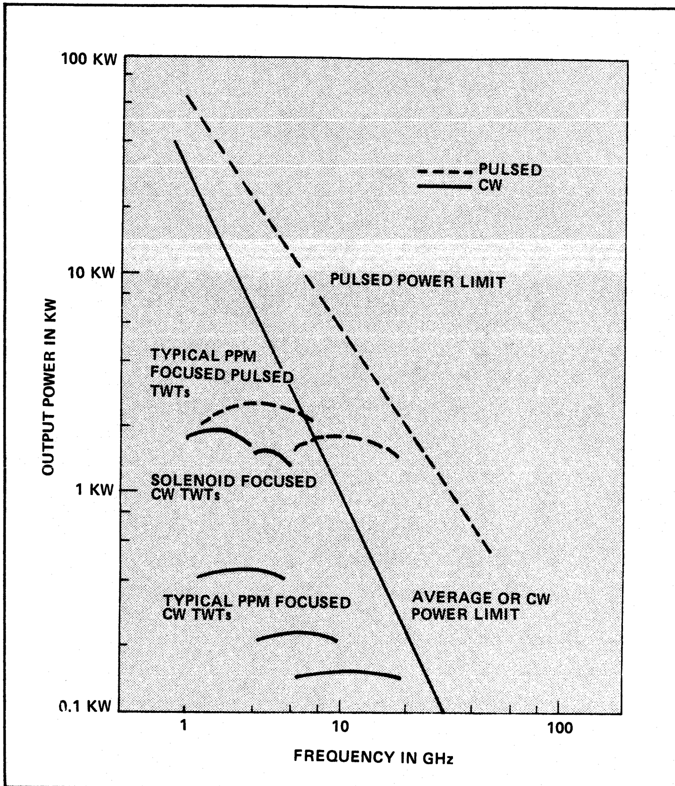

1. **Both typical and limiting** power levels are plotted for helix TWTs.

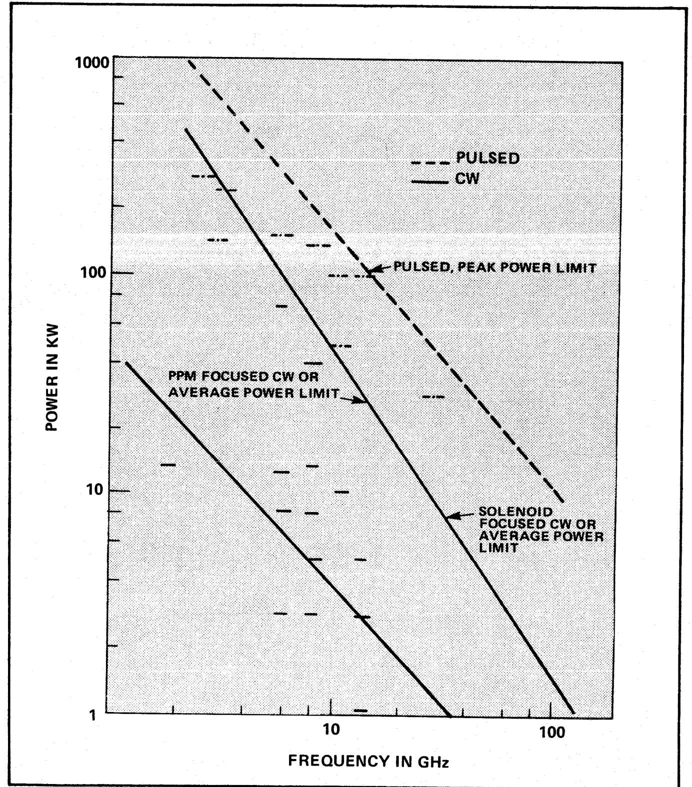

2. **Here, typical and limiting** power levels are given for cavity TWTs.

radar transmitters requiring modest, five to 30 percent bandwidth at power levels up to several hundred kW, and in communications transmitters requiring several kW of CW power. They are used infrequently in ECM transmitters where the platform cross-section is very large, or for stand-off jamming where more than 1 kW of CW or average power is required. The domain in which helix and coupled-cavity tubes perform is shown in Figures 1 and 2.

In that area of the frequency vs power plane between helix and coupled-cavity tubes there are tubes using modified helix and coupled-cavity circuits that provide performance for specialized applications. One of the primary circuit classes used in this intermediate area consist of variations on two contra-wound helices known as ring-bar and ring-loop circuits. TWTs incorporating these circuits provide peak power levels over 5 kW.

Recent interest in developing more equipment operating at millimeter wavelengths has stimulated investigation of modified circuits to provide the high power capacity of coupled-cavity tubes but are more economical to produce, given the precision required in the small sizes appropriate to millimeter wavelength operation. Such circuits include the HIGHTRON, COMB-QUAD, and Karp circuits.

The fourth class of TWTs are forward-wave fundamental coupled-cavity types operating at very high voltages and producing megawatts of peak power over bandwidths up to 10 or 12 percent. They are, of course, used in high-power radars. In general, they are used in only a few radars for which the bandwidth cannot be achieved with a klystron amplifier and coherence is needed which cannot be provided by crossed-field amplifiers.

Aside from the differences between the power and bandwidth provided by helix and coupled-cavity TWTs there are only minor differences in other features of their performance. The modulation, beam focusing, cooling, and efficiency enhancement options are the same for both types. It is therefore appropriate to consider some of these generic TWT features. The only feature unique to a helix TWT is the helix interaction circuit. In TWTs, the electron beam is formed by converging the electrons emitted from a spherical cathode by a Pierce-type electron gun, common to all high-power, linear-beam tubes, including klystrons. The same can be said of the beam-focusing and collection methods.

Modulation Options for TWTs

In microwave tubes, modulation of the electron beam is used as a means of changing the power level of the output signal by some desired value. Frequently, those levels are zero output and the required operating level. Electron beam modulation is not generally used for complex signal waveforms because the relationship of output to beam power is not linear, and due to the fact that other factors—such as beam focusing—will also change at the same time and can depreciate both signal quality and reliability.

There are also many variations in the shapes of electrodes used for modulation or switching the electron beam on and off. The simplest means by which the beam can be switched is turning the HV power supplies on and

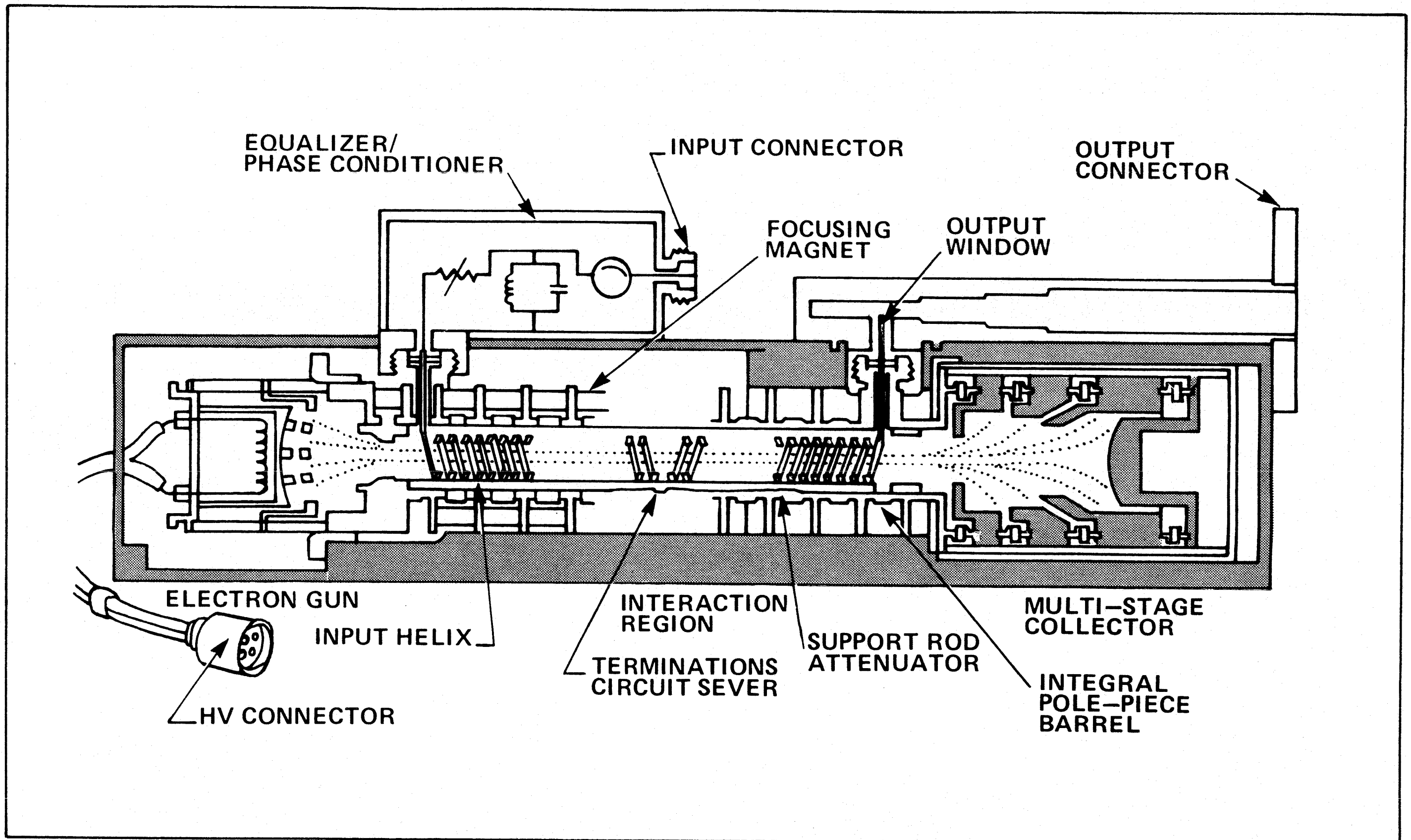

3. Modern PPM-focused TWTs for electronic countermeasures have complex structures to assure high performance over broad bands.

off. This scheme is used in many CW communications and ECM transmitters. The electron gun is only a diode; that is, it consists of a cathode with the attached beam-forming electrode at the same potential, and a hollow anode from which the beam emerges, which is at ground potential. Grids are not present, so the electron gun is rugged and reliable. Diode guns can be used for recurrent pulse modulation because the power supplies and associated capacitance cannot be switched quickly enough. There is also a requirement that the power supply voltages come up rapidly because beam focusing is not optimized for the intermediate value. Current intercepted by the interaction circuit would exceed a safe value during some part of the beam voltage rise time. Figure 3 shows a typical PPM-focused TWT with a non-intercepting gridded gun. Many TWTs do not have grids, and are operated as diodes. The voltage for this tube must rise and fall at a rate such that the intercepted—or a ground—current will not exceed the rated value for more than a few milliseconds.

Poor focusing of the beam during the rise and fall of the beam voltage can be avoided by isolating the electron gun anode, which does not intercept current, and switching the beam with it.

The beam current is zero when the anode is at cathode potential, and at the operating value when the anode is at its operating value, usually at ground. Anode modulation is used where pulse lengths are long relative to the time required to switch the anode voltage supply and associated capacitance.

Most modern ECM and radar transmitters require modulation speeds that can only be achieved when switching over voltage ranges less than 15 percent of the cathode voltage. A method which reduces the modulation voltage to about 15 percent of the cathode voltage isolates the beam-forming electrode, and uses it to switch the beam. Again, grids are not required and the BFE does not intercept current.

With BFE modulation, the beam is at the operating value when the BFE is at or near the cathode potential, and is near zero when the BFE is more negative than the cathode by about 15 percent of the cathode voltage value. In many cases it is not possible to reduce the current to zero and meet the switch speed requirements. The majority of the residual current is intercepted on the tube body and increases ground current. If the intercepted current is appreciable, it will depreciate efficiency and, if not carefully managed, can also reduce tube life and reliability.

Many of the ECM and radar transmitters being designed require modulation rates that can only be achieved with a gridded electron gun. If only the control grid is present, it will be heated by the current intercepted from the beam during the time it is gated on. The duty cycle and pulse width of intercepting grid guns is limited to less than 5 percent and a few microseconds, respectively, when a single grid is used. This limitation is avoided by placing a shadow grid, exactly aligned with the control grid, between the control grid and the cathode. The shadow grid may or may not be attached to the cathode

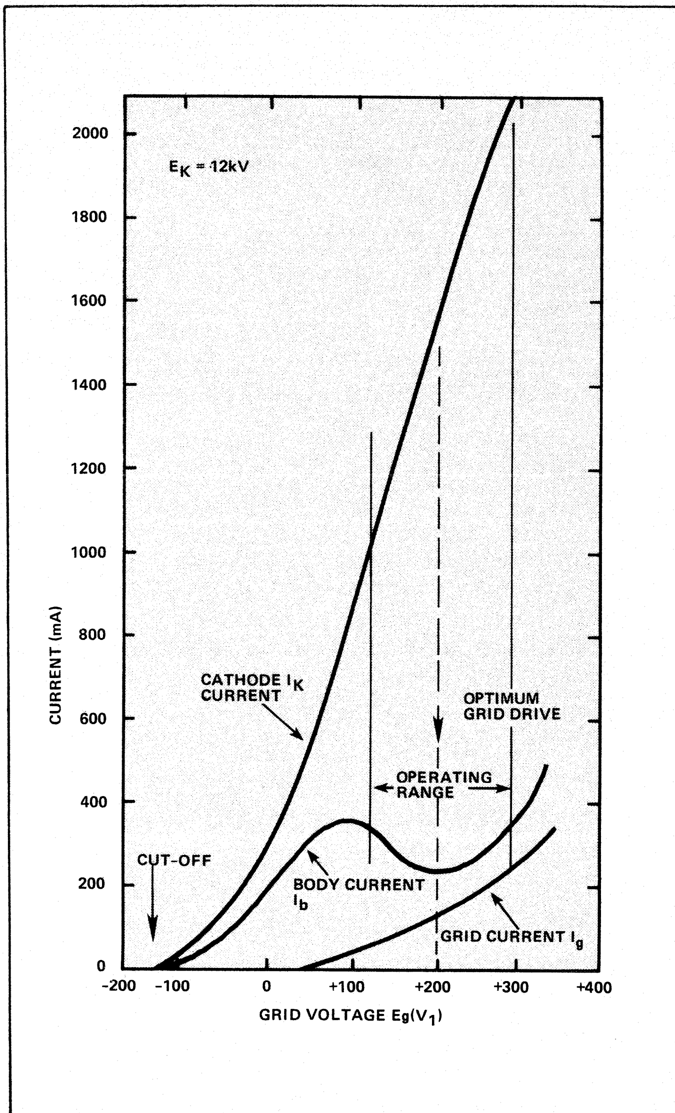

4. Use of a shadow grid overcomes the duty cycle and pulse width limitations of grid guns. Focusing characteristics are shown.

surface but it must be at cathode potential to eliminate interception of the beam current. Typically, grid current is a fraction of one percent of the beam current, and the duty cycle and pulse length are not limited by the electron gun.

With the exception of the value of the control-grid current, the response of both intercepting and non-intercepting grid-controlled tubes is approximately the same. A typical characteristic is shown in Figure 4.

Beam Focusing

All linear beam tubes require a magnetic field to maintain the electron beam in its cylindrical shape through the interaction region. There are three basic ways to provide the magnetic field, with variations on each of them.

A solenoid, which may be wound onto a tube, or may have the tube inserted into it, provides the greatest degree of control over the beam. Solenoid focusing is used for all TWTs designed for operation at high power. Note that in Figures 1 and 2 a solenoid is required for the highest average power tubes.

Permanent magnets can be used to provide the same unidirectional field as a solenoid. Permanent magnet focusing also provides excellent focusing but it is only practical for use in tubes with short interaction lengths because the weight of the magnet increases rapidly as the length of the magentic gap is increased.

Permanent magnet, or PM, focusing is generally not used on TWTs for that reason. PM is used primarily on klystrons and perhaps some millimeter-wave TWTs. PM-focused tubes have strong magnetic fields external to the tube and magnet, which can affect other equipment or components near them. As a result of this lack of shielding, the magnetic field within the tube is also easily perturbed by nearby magnetic material. Contact between the tube and magnetic material or high magnetic fields can permanently change the magnet charge and cause failure of the tube. Extreme care should be taken in designing equipment using PM-focused tubes and in handling of the tubes.

Periodic permanent magnet (PPM) focusing is used on most traveling-wave tubes because it results in the lightest assembly by far. Unlike PM-focused tubes, PPM-focused tubes have little external magnetic field and are generally well-shielded from external influence.

TWT Collectors

Collectors on most tubes are merely cups in which the beam is collected when it emerges from the interaction region. The electrons in the beam have various velocities as a result of the RF interaction in the tube, so they cannot all be collected with minimum energy with a collector at a single potential—although most tubes in service today have only one collector stage.

For applications requiring minimal primary power, multiple stages of collection are required. This arrangement allows the voltage on each of the collector stages to be set to a value which collects the multi-velocity electron beam with minimum power dissipation. Multi-staged depressed collector operation not only reduces the power dissipation within the tube, but it also reduces the power supplied to the tube as the drive power is reduced to bring the TWT into the linear operating range.

In most applications today, collector voltages are set for optimum performance at rated power only. The typical efficiency of such tubes is 30 to 40 percent at rated power. The multi-staged depressed feature can be exploited even further if the power supplies are capable of switching to lower voltages as the drive power is reduced. Figure 5 compares the DC input power required when collector voltages are fixed at rated power, and that required when maintaining the collectors at the optimum value over the drive range. This feature has the potential of providing more efficient operation with multiple simultaneous signals while allowing for limited single-signal operation at full output power.

TWT Amplifier Characteristics

Transfer characteristics for a TWT, one frequency, are shown in Figure 6. These curves should be obtained at

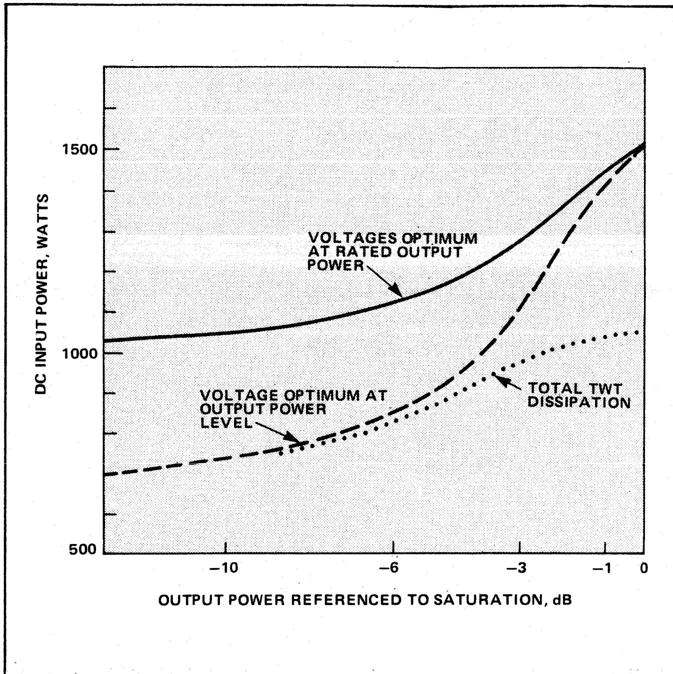

5. Maintaining collector voltage at an optimum value over drive range provides more efficient operation while handling simultaneous signals, yet allows a single signal to operate at full power.

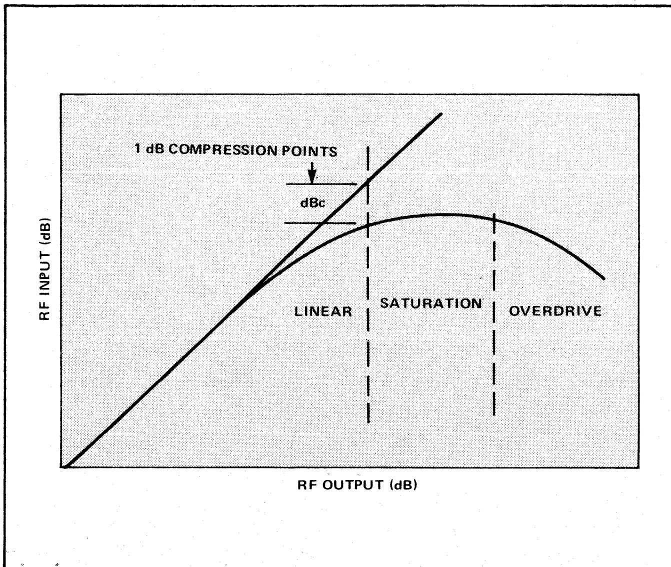

6. A typical TWT exhibits a transfer characteristic of this form.

several frequencies in the band in order to properly characterize the tube.

Dynamic range is defined as that region between the threshold input level and the point at which the gain departs from the small signal value by 1 dB. The gain will continue to decrease, by approximately 6 dB, until the saturation point is reached. The region beyond saturation is called the overdrive region. TWT characteristics differ widely in the overdrive region, so transfer data must also be obtained beyond saturation to properly predict transmitter response to high drive levels.

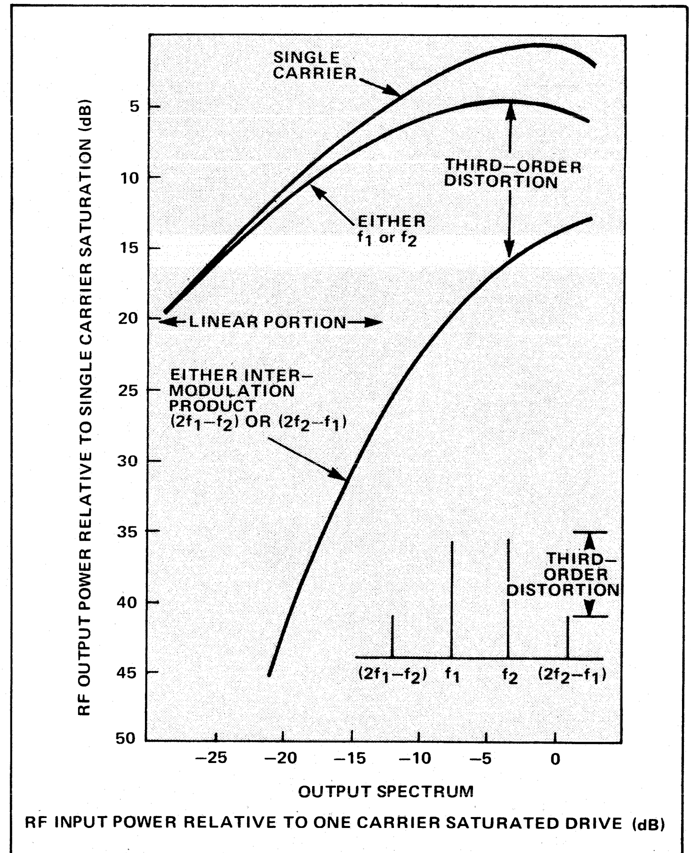

7. Carrier and intermodulation vary with total drive power.

When more than one carrier is introduced at the TWT input, a mixing, or intermodulation (IM) process takes place. This results in intermodulation products which are displaced from the carriers at multiples of the difference frequency.

The power levels of these intermodulation products are dependent on the relative power levels of the carriers and the efficiency of the TWT. In the case of two balanced carriers, Figure 7 shows the variation of carrier and IM product power level with total drive power. The single carrier power curve is also plotted for comparison. As in the case with AM/PM conversion (see below), the IM distortion is significantly reduced in the small-signal (linear) region of the RF drive range. For this reason, communication TWTs are normally operated well below their saturation power level. The system designer must consider the TWT response to the regulation and ripple on power-supply voltages.

Typical values for TWTs are as follows:

- 35 degrees per 1 percent change in cathode voltage,
- 5 degrees per 1 percent change in grid drive,
- 2 degrees per 1 percent change in anode voltage, and
- 0.01 degrees per 1 percent in filament voltage.

These values should be considered as order-of-magnitude since the actual value for any specific tube will be a function of many factors such as type of ciruit, gain, perveance, etc.

The phase-versus-signal frequency characteristics of TWTs are a function of the transit time of the signal

Table I
Primary Suppliers of Microwave Tubes

Supplier Information	Magnetron	Crossed-Field Amplifier	Klystron	Traveling Wave Tubes Helix	Traveling Wave Tubes Coupled Cavity	Gyrotron
AEG-Telefunken, West Germany	●		●	●	●	
Amperex Electronic Company, Hicksville, Long Island, New York	●					
Beam Tube Corporation, Milford, Massachusetts			●			
English Electric Valve Co., Ltd., Chelmsford, Essex, England	●		●	●	●	
EMI Varian, Ltd., Hayes, Middlesex, England	●		●	●	●	
Fujitsu Ltd., Tokyo, Japan	●		●			
Ferranti, Ltd., Dundee, Scotland	●					
General Electric Company, Owensboro, Kentucky			●			
Hughes Aircraft Co., Electron Dynamics Div., Torrance, California			●	●	●	●
Hitachi Ltd., Tokyo, Japan	●					
ITT, Electron Tube Div., Easton, Pennsylvania			●	●		
ITT, Components Group Europe, Paigton, Devon, England			●	●		
Klystronics, Inc., Eatontown, New Jersey			●			
Litton Industries, Tube Division, San Carlos, California	●	●	●	●	●	
LeMateriel Telephonique, Boulogne-Billancourt, France	●					
Teledyne MEC, Palo Alto, California				●		
Microwave Associates, Burlington, Massachusetts	●					
Mictron, Inc., Sarasota, Florida	●					
M-O Valve Co., Ltd., Hammersmith, London, England	●	●	●			
Mullard Ltd., London, England	●	●	●			
Microwave Labs. Inc., Raleigh, North Carolina				●		
Nippon Electric Co., Ltd., Tokyo, Japan	●		●	●	●	●
Aksjeselskapet Nera, Oslo, Norway						
New Japan Radio Co., Ltd., Saitama-Ken, Japan	●		●	●		
Northrop Corp., Des Plaines, Illinois		●		●		
Oki Electric Ind., Ltd., Tokyo, Japan			●			
Omni-Wave Electronics Corp., Gloucester, Massachusetts			●			
RCA Corp., Somerville, New Jersey			●	●		
R.T.C. Laradiotechnique-Compelec Paris, France						
Raytheon Company, Waltham, Massachusetts	●	●	●	●	●	
Signalite, Neptune, New Jersey						
Siemens Corp., Iselin, New Jersey	●		●	●	●	
Sperry Microwave Systems, Gainesville, Florida						
Thomson-CSF Electron Tubes, Inc., Clifton, New Jersey	●	●	●	●	●	●
Toshiba Corp., Japan	●		●			
Varian Associates, Inc., Palo Alto, California	●	●	●	●	●	●
Varian Associates of Canada, Ltd., Ontario, Canada			●	●		
Italtel, Palermo Sicily, Italy	●		●	●	●	

through the tube and of internal and external reflections. Phase linearity is expressed as either group delay or deviation from linear phase in degrees.

The phase shift through the TWT also changes as the drive signal is increased. This is defined as the AM to PM conversion. AM/PM is expressed in degrees/dB and is equal to the slope of the phase shift curve shown in Figure 8. The AM/PM will change with the beam voltage and is usually less at the low-frequency end of the operation band. Typical values for communication TWTs is 5 degrees/dB, but it can be considerably higher.

Noise power output in the absence of a drive signal can be estimated from the following equation with all values expressed in dB:

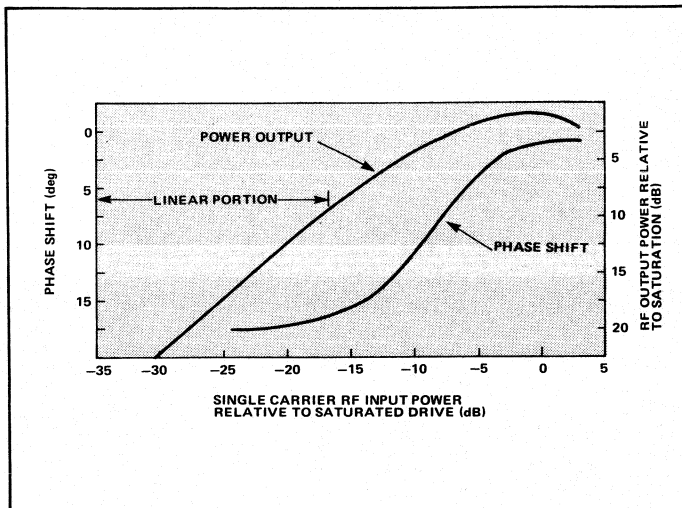

8. Typical power output and phase shift is plotted as a function of RF input power for a communication type TWT. Slope of the phase shift curve is the AM/PM conversion.

$$NP_o = -114 + (BW) + (G_{ss}) + (NF)$$

where:

−114 dBm/MHz thermal noise with input terminated.

BW = system bandwidth and can be determined from the following:

BW (MHz)	dB
1	0
10	10
1000	30
2000	33

G_{ss} = small signal gain
NF = noise figure

Helix TWT Characteristics

Table II lists typical characteristics of CW and pulsed TWTs which can be obtained from several sources. The values listed would not necessarily be met simultaneously by any particular supplier nor do they correspond to any particular tube type. They are listed here to provide a rough estimate of what the operating parameters would be for a tube operating at an octave or more within the indicated frequency band and at the power levels indicated.

Extensive application data and engineering assistance is available from TWT manufacturers. Detailed operating data should, of course, be obtained before commencing a specific equipment design.

State of the Art in Helix TWTs

TWTs used in ECM and communication transmitters have become complex components. In addition to incorporating multi-stage depressed collectors to enhance system efficiency and low-voltage, grid-controlled electron guns for high frequency-modulation rates, they also include several peripheral components to facilitate system interface. Equalizers and phase conditioners are added to the input to compensate for drive-signal amplitude variation and harmonic content. Also added are thermal interlocks and thermisters for cooling-system control, and coding resistors for automatic power supply adjustment.

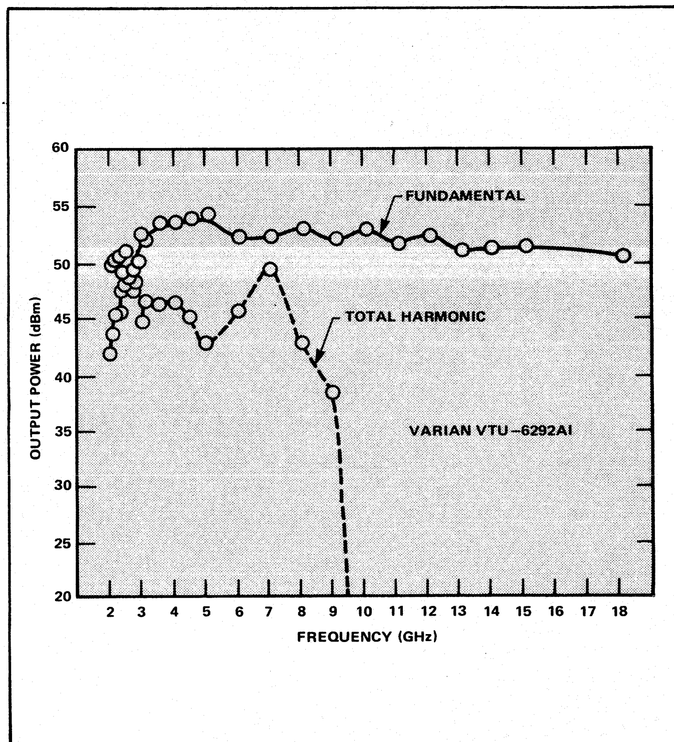

9. Two-octave bandwidths have been achieved through use of anisotropic loading to helix interaction circuits. Electron beam velocity and wave propagation are maintained at a near-optimum extended operating frequency, while simultaneously reducing harmonic output power.

Tube designers have recently extended the bandwidth of helix TWTs to two octaves and more through the use of various anisotropic loading schemes applied to the helix interaction circuits. These techniques keep the velocity of the electron beam and wave propagation on the helix at near the optimum values for energy conversion over a wide frequency band. The result is a considerable extension of the operating frequency band with a simultaneous reduction of 7 dB or more in the associated harmonic output power as shown in Figure 9.

Due to the wide bandwidth of helix TWTs the interaction at the harmonic frequency will result in greater amplification of the harmonic than the fundamental at some frequencies near the lower band edge. These effects can be ameliorated at the expense of additional circuit complexity by the injection of a coherent harmonic signal of the proper phase at the input to the TWT or by properly adjusting the harmonic content of the drive signal.

Klystron Tubes

Since their invention in 1937, by Russell Varian, klystron tubes have been developed to cover the spectrum from UHF to millimeter-waves and from milliwatts to over 100 mW. The lower-power reflex oscillators are being rapidly displaced by solid-state sources, but the amplifiers continue to find new applications as rugged, high gain,

Table II.
Pulsed Helix TWT Characteristics

Frequency Range	Power Watts	Gain dB	Helix Voltage kV	Collector Voltage kV	Cathode Current Amps	Length Inches	Weight Pounds	Focusing Type	Cooling Method
1 to 2.5	100	30	3	3	.33	23	7.5	PPM	C
	200	30	3.5	3.5	.45	23	9	PPM	C
	400	30	4	4	.75	23	14	PPM	C
	1000	25	4.5	4.5	1	23	20	PPM	C/FA
	2000	25	5	5	2	23	35	SOL	L
2 to 6	50	30/50	3	1.7	.15	15	2.5	PPM	C
	100	30/50	3.5	2	.3	16	6.5	PPM	C
	200	30/50	4.4	2.7	.4	20	7.5	PPM	C
	400	30/50	5.7	3.2	.7	22	10	PPM	C
	1000	30/50	7	4	1.2	22	15	PPM	FA
	2000	30/50	8.5	5	1.9	23	40	SOL	L
4 to 10	50	30/50	2.6	1.4	.13	14	2.5	PPM	C
	100	30/50	4.5	2.7	.26	15	6	PPM	C
	200	30/50	8.5	4.4	.3	18.5	7.5	PPM	C
	400	30/50	9.5	4.7	.39	19.5	9.5	PPM	C/FA
	1000	30/50	12	6.5	.6	21	40	SOL	L/FA
7 to 18	50	30/50	4	2.5	.12	13	3	PPM	C
	100	30/50	8.7	4.2	.22	18	5.5	PPM	C
	200	30/50	9.2	4.6	.23	18	6	PPM	C
	300	30/50	9.5	5	.32	20	8	PPM	C/FA

Frequency Range GHz	Power Peak kW	Gain dB	Helix Voltage kV	Cathode Current Pk. Amps	Ground Current Pk. Amps	Collector Voltage kV	Duty Factor	Pulse Length μ Sec	Length Inches	Weight Pounds
1 to 3	1.5	30	7.5	1.25	.3	5	.1	100	20	8
2 to 8	1.5	30	9.1	1.5	.3	6	.05	50	18	7.5
6 to 18	1.5	50	11	15	.35	7	.05	30	16	7

highly efficient and coherent amplifiers are required. These versatile tubes provide everything but wide bandwidth, and some progress has been made in that area with hybrid types such as extended interaction klystrons, (EIK), and twystrons (TM).

Klystron amplifiers are linear-beam tubes, as are TWTs, and have the same modulation options, power supply connection requirements, and generally the same linearity characteristics as TWTs. The exception is that klystrons are not generally available with depressed collectors. Typical operating connections are shown in Figure 10. The collector is usually isolated to permit measurement of body, or ground current, for tube protection and to ease regulation requirements on the high-current supply for pulsed operation.

Limiting and typical power levels for klystrons are shown in Figure 11. The peak power available from klystrons is as great or greater than from magnetron oscillators, but klystrons are capable of much higher average power and the output signal is more coherent. The maximum usable frequency for conventional klystrons is around 40 GHz. Klystron applications fall mostly into five classes. Tubes could certainly be developed to perform in the gaps between these classes, but there appears to be no high-volume requirement for them. The primary classes of klystron applications are the following:

- CW amplifiers for TV transmitters. Television transmitter amplifier tubes are available at 12, 30, 45, and 55 kW of output power and with 8 MHz of instantaneous bandwidth. They are tunable over a 20 to 25 percent frequency band so that the entire UHF-TV band, from 470 MHz to 850 MHz, can be covered with three tubes.
- CW amplifiers for commercial and military communications, and illuminators for semi-active guidance systems. These are very rugged, providing 1 to 50 kW of output power with bandwidths of only a few MHz, but tunable over the applicable communication band.
- CW amplifiers providing very high power, 50 kW to 1 MW, for specialized communication, scientific, and industrial applications.
- Pulsed amplifiers for coherent radar transmitters. They are available with output power of 1 to 200 kW and

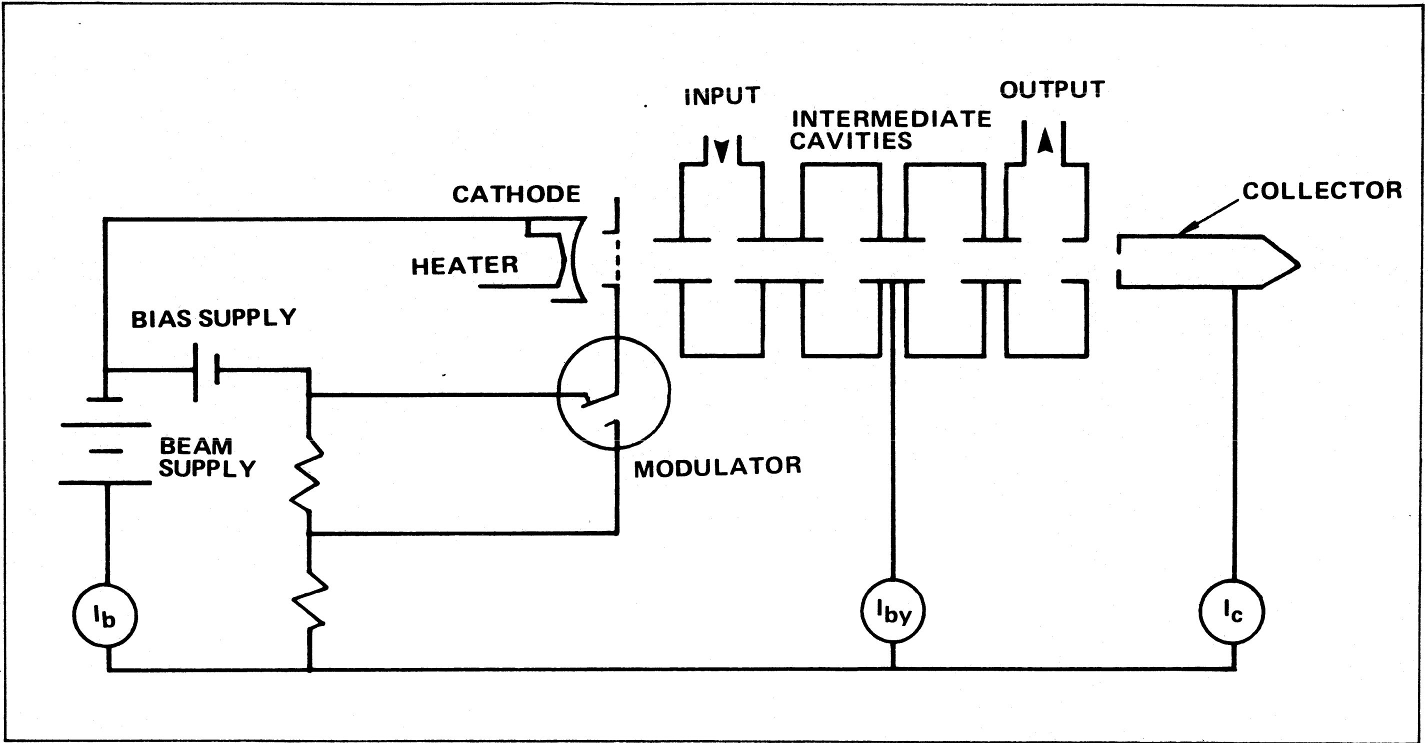

10. Operating connections for a klystron amplifier. Metering is shown for independent collector and body-current measurement.

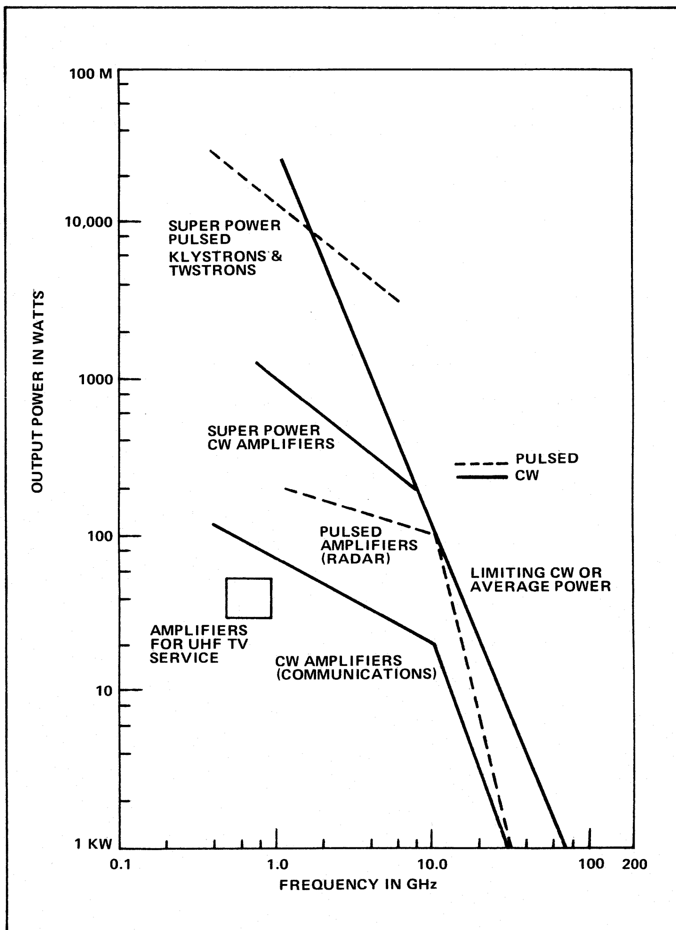

11. Limiting and typical power levels are plotted for klystrons.

with a wide range of duty cycle and pulse width, modulation, and tuning options.

- Pulsed amplifiers with multi-megawatt output for high-power radar transmitters and linear accelerators.

Let's consider performance, operational parameters, and recent advances in CW klystrons.

- *Focusing*. Larger klystrons, operating at frequencies below 1 GHz and power levels above 100 kW at higher frequencies, are focused with solenoid electromagnets. the balance of the tubes are focused with permanent magnets in a C magnet configuration. However, there are some exceptions. The 24-MW, S-band amplifiers used to power the Stanford Linear Accelerator are focused with permanent magnets. Very lightweight electrostatic-focused tubes have also been built to provide power levels of 10 kW at 900 MHz and 1 kW at 2.1 GHz. PPM focusing has also been employed to build light-weight pulsed klystrons.

- *Tuning*. Maximum instantaneous gain is obtained from a klystron by tuning all of the cavities to the same frequency. However, the next-to-the-last cavity is usually tuned above the frequency band because it will increase output power by 0.7 dB to 1 dB even though the gain is reduced as much as 10 dB. Gain may also be traded for bandwidth by stagger-tuning the cavities. Operating data for klystrons usually indicates that the amplifier is broadband or high-efficiency tuned. Figure 12 shows the effect of tuning on the transfer characteristics of a klystron amplifier.

Several options to tuning each of the cavities manually have been developed. Tuners for each of the cavities are ganged together by a system of gears to allow simultaneous tuning from a single knob. Such an arrangement can also be servo-controlled for remote tuning. Recently, tuners

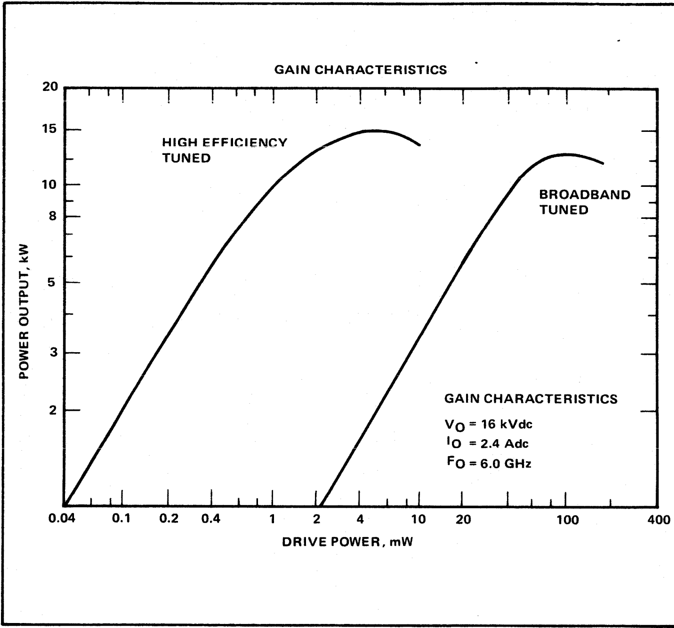

12. Tuning changes the transfer characteristics of the klystron in this manner.

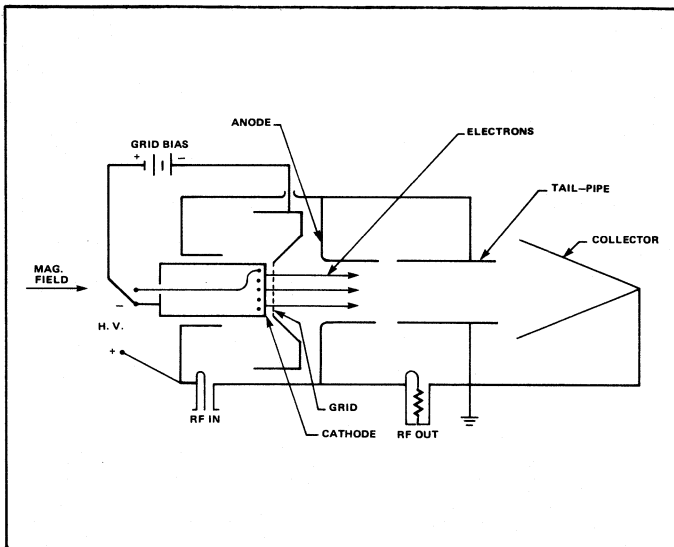

13. A klystrode is a hybrid tube combining the features of power-grid tubes and klystrons. Klystrodes are smaller and provide more efficient, Class A operation.

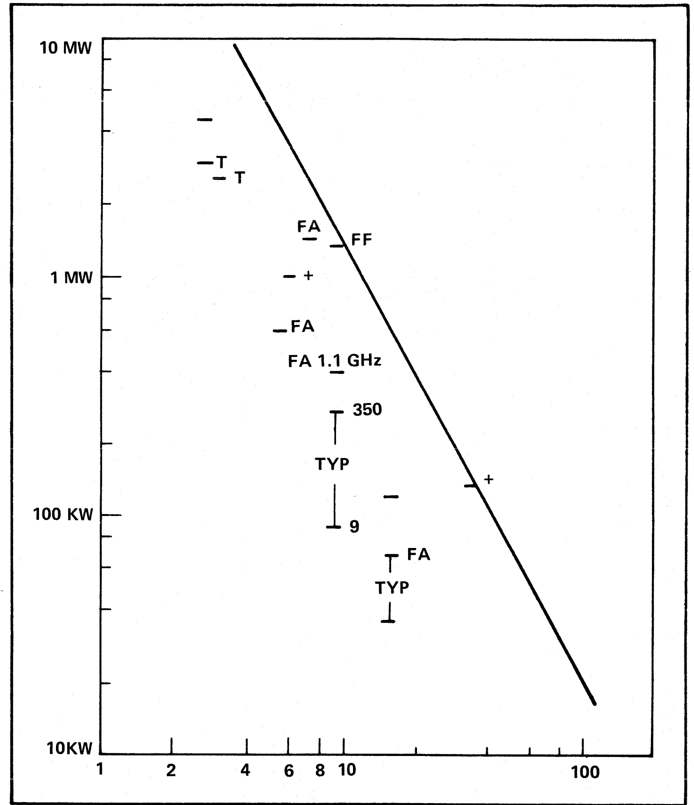

14. Typical and limiting peak power levels are plotted for magnetrons. Typical duty cycles are less than 0.001 and average power is below 1 kW at 10 GHz.

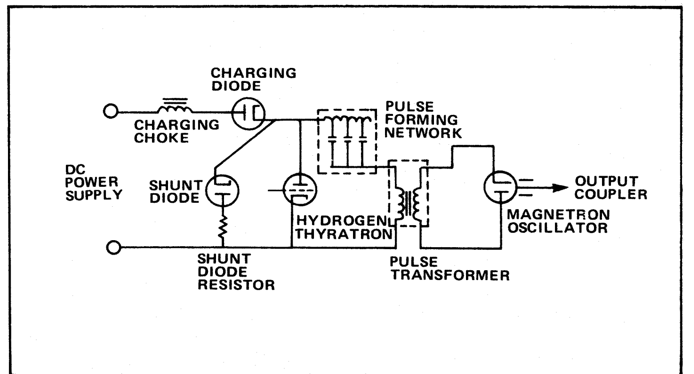

15. This operating diagram shows a magnetron connected to a line-type modulator.

have been equipped with step mechanisms and the appropriate digital electronics to provide a digital interface for remote tuning.

- *Efficiency*. Progress in klystron development and design has produced tubes operating at 60 to 70 percent efficiency optimization of cavity geometry, spacing, and resonant frequency. The efficiency is also a function of the operating voltage which allows the output power to be adjusted over a considerable range as long as the electron beam focusing is well-behaved.

The use of depressed collector potentials to enhance efficiency, as is done in TWTs, has not been widely applied to klystrons. Klystron interaction, and their characteristic high conversion efficiency, results in a much wider distribution of electron velocity in the spent beam of a klystron compared to a TWT. The feasibility of increasing efficiency with multiple-stage depressed collector has been shown, and efforts are currently underway to apply the concept to TV broadcast transmitter klystrons.

- *Recent Developments*. Klystrons have been hybridized by adding a TWT output section to make multi-megawatt amplifiers called twystrons (TM). More recently, considerable progress has been made by using cavities with multiple coupled gaps, similar to coupled-cavity circuits, to extend the bandwidth and power output. These extended-interaction klystrons, EIKs, have extended the frequency range of

klystron oscillators and amplifiers to over 200 GHz. EIK oscillators provide economical sources of pulsed and CW power in narrow bands in the 30 to 220 GHz range. A low voltage, 1 to 3 kV, electrode is available for applications requiring short pulses and high PRF.

On the other end of the frequency range, the klystrode has been introduced for UHF-TV audio service and is expected to find additional applications. The klystrode is another hybrid combining features of power grid tubes and klystrons as shown schematically in Figure 13. The input (grid) circuit is driven from a cavity as is an RF tetrode, and the output is taken from a coaxial cavity as a klystron. Higher power gain, 8 to 10 dB, and higher frequency operation is provided compared to a tetrode. Compared to a klystron, it is likely to be smaller and provide higher efficiency in Class A operation.

Magnetrons

Magnetron oscillators have been the primary source of power for radar transmitters since 1940, and are still being designed into systems today. The longevity of the magnetron is due to the fact that it is the most efficient and lowest-cost source of microwave power. Clever magnetron and transmitter designers have continued to increase tuning speed and bandwidth, to improve frequency stability, and to reduce weight to meet the more demanding requirements of many modern radar applications. The available power from magnetrons and from typical tubes in some popular bands is shown in Figure 14.

The low cost of magnetrons and their associated transmitters is due to their simplicity. A magnetron is a diode containing both the beam formation and microwave interaction in a small space closely coupled to its power supply and output circuit, as shown in Figure 15. The interaction between the tube, modulator, and output circuit, and the statistical processes involved in starting the oscillator, gives understanding to some terms which are used to specify magnetron performance.

- *Pushing.* Pushing is a measure of the change in frequency as the current through the magnetron is changed. The magnetron should be operated from as near a constant current source as possible, if frequency changes are to be minimized. Magnetron operating data are most frequently given as a function of the current as shown in Figure 16.
- *Pulling.* The pulling figure is a measure of the change in frequency of the tube caused by change in the phase or magnitude of the reflection coefficient of the antenna or load.

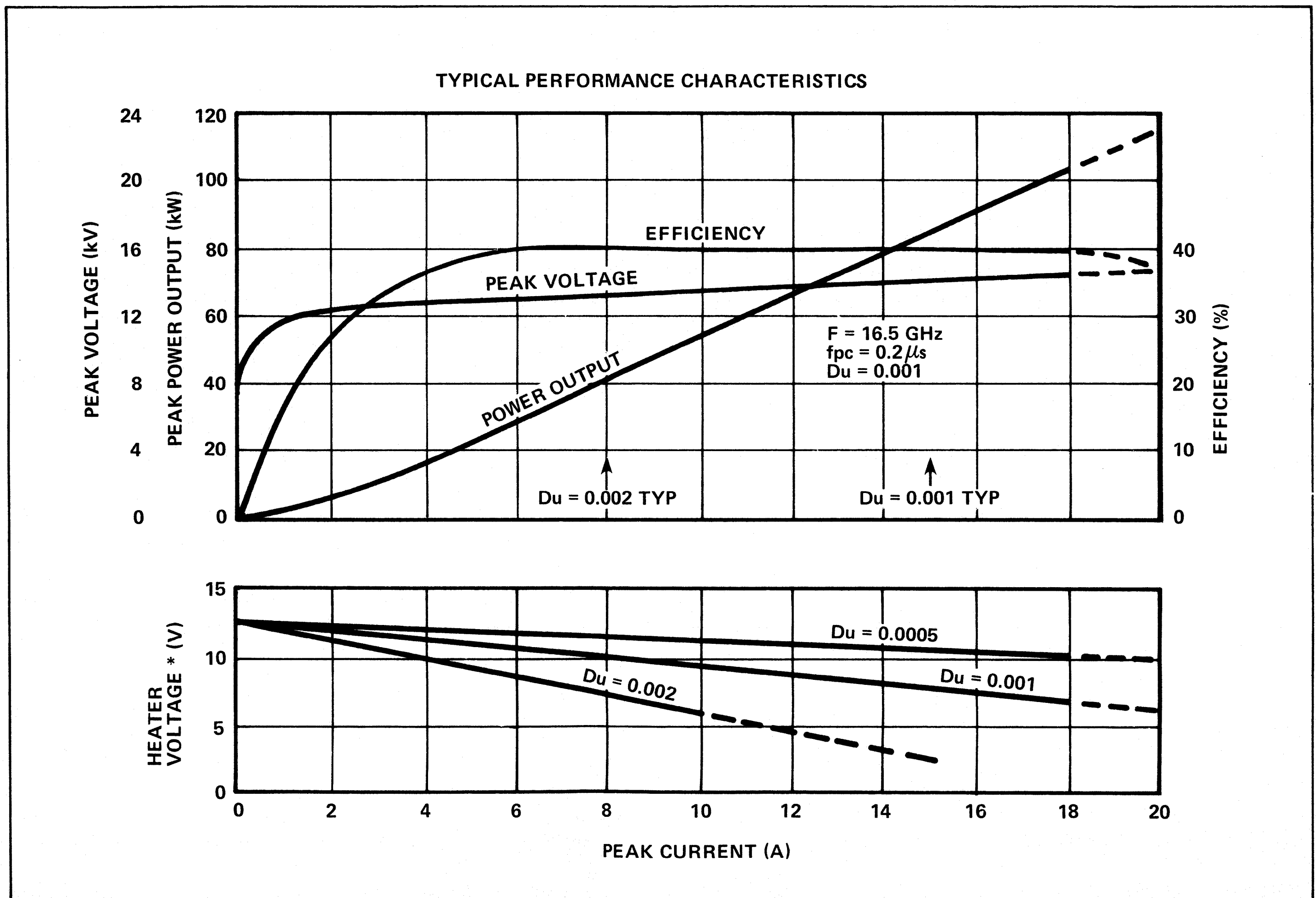

16. Typical performance is shown for a Ku-band, 60-kW, tunable coaxial magnetron.

Continued from page 125

Table III.
Typical Magnetron Operating Parameters

Frequency Range GHz	Peak Power kW	Pulse Width m Sec.	Duty Cycle	Anode Voltage kV	Anode Current Amps	Heater Power Watts	Tuning Range MHz	Tuning Rate Hz
1.1 - 1.4								
2.7 - 3.4	500	5	.002	28	45	200	200	
	1000	4	.0015	38	80	220	200	
	2000	3	.0012	50	50	220	200	
	4000	2.5	.0005	65	90	220	200	
5.4 - 5.9	100	3.5	.0015	18	18	100	500	10
	250	3.5	.0012	25	25	100	500	10
	500	3	.001	32	36	100	500	10
	1000	3.5	.001	36	60	100	500	10
8.5 - 10.0	50	6	.001	12	12	45	1000	20
	100	5	.001	17	20	50	1000	20
	200	5	.001	25	27	100	1000	20
	500	4	.0012	35	30	125	1000	20
14 - 17.0	35	1.5	.002	15	14	35	500	
	75	1.5	.0012	18	18	40	650	
	125	1.2	.001	17	20	50	800	
	250	.5	.0008	20	20	50	1000	
31 - 36.0	25	1	.001	15	12	35		
	50	.8	.007	20	18	45		
	100	.6	.006	23	23	50		
	200	.5	.005	25	27	80		

- *Time Jitter.* Jitter is the variation in time, in nanoseconds, for the magnetron to start or stop in relation to the applied modulation pulse.
- *RRV.* The maximum rate of rise of the applied voltage pulse which will allow the magnetron to make a smooth transition into oscillation at the desired frequency. Usually given in kV per microsecond.
- *Heater Voltage Change.* The cathode of the magnetron is heated by electron bombardment during operation, so it is necessary to change the power supplied to the filament as a function of both peak current and duty cycle as shown in Figure 16.

Four classes or types of magnetrons have been developed to improve specific performance qualities of these tubes for specific radar applications. Using the defined terms, it is easy to express differences between the primary types.

The strapped-vane magnetron is usually referred to as the conventional magnetron, which has been the workhorse of the radar world at frequencies up through X band. Other magnetrons are usually described in terms of how they compare with tubes using this basic vane and strap circuit.

A variation on the vane and strap circuit, known as the rising sun structure, is easier to fabricate for frequencies above X band. Rising sun structures have been used to provide magnetrons for very short pulse operation at frequencies to 100 GHz.

The coaxial magnetron was developed in the early 1960s to significantly improve pushing and pulling figures for applications requiring greater frequency stability. A resonator that is coaxial with the cathode and anode is placed between the anode structure and output coupler. The high-Q cavity both isolates the interaction region of the magnetron from the load and provides a stabilizing cavity for the oscillator. Frequency stability is increased by a factor of 4 to 10, but at the expense of making the tube larger and heavier by a factor of 20 to 50 percent. Coaxial geometry also permits production of practical magnetrons for operation at frequencies to 70 GHz.

Voltage–tuned magnetrons (VTMs) contain an anode that is used to control the current through the tube. The voltage applied to the current-control electrode tunes the magnetron frequency. VTMs provide a light-weight, low-cost, tunable power source with efficiency up to 50 percent and bandwidth greater than 10 percent. The upper frequency limit for VTMs is in the 10 to 12 GHz range, although experimental models have been built as high as 16 GHz.

All magnetron types are tunable and available with a variety of mechanisms providing manual frequency settings, swept, or either frequency tuning, servo-controlled, or combinations of these. An output voltage can also be provided for remote frequency indication. Operating parameters are shown in Table III; these are typical of magnetrons with operating frequencies and power levels indicated.

Crossed-Field Amplifiers

Crossed-field amplifiers evolved from attempts to build a microwave amplifier with magnetrontype interaction. Early attempts in the 1940s used an electron beam injected

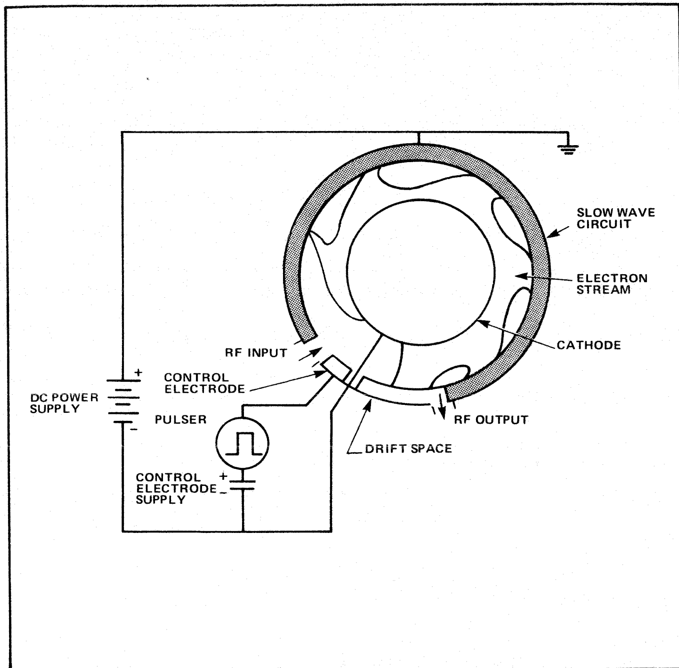

17. An injected-beam crossed-field amplifier debuted in the 1940s, but in the 1950s were built using a format more like the magnetron, incorporating a cathode as the primary source of current through secondary emission.

into a crossed-field interaction space coupled to a slow-wave circuit. This class of amplifier is referred to as an injected-beam, crossed-field amplifier.

The most successful developments started in the 1950s when tubes were built in a format more closely resembling the magnetron, with current supplied primarily by secondary emission from the negative electrode or cathode (Fig. 17). A cathode or sole electrode limits the electron current which is distributed along the entire length of the interaction space. This class of CFA is referred to as a distributed-emission tube. Distribution CFAs developed rapidly, and are in wide use as high-peak-power amplifiers for many of today's transportable and shipborne radars.

Distributed-emission CFAs are characterized by high efficiency, in the order of 40 to 70 percent, moderate gain of 8 to 12 dB, very small size and weight relative to their high peak output power, and bandwidths of up to 25 percent.

Injected-beam CFAs have found limited use as high-average-power CW amplifiers with a few kilowatts of peak power. They have, however, been built with bandwidths exceeding one octave, and are exceptional as compact, high-average-power amplifiers in specialized applications.

Both the injected-beam and distributed-emission CFAs can be built in linear format or circular format shown in Figure 17, strongly resembling that of the magnetron. In the circular format, the electron stream from a distributed-emission CFA can also be allowed to reenter, or recirculate, through the interaction region to enhance efficiency with some attendant depreciation in noise performance.

The close similarity between the interaction principles and physical configuration of the CFAs and magnetrons strongly suggests that the peak and average power capabilities of the CFAs would be approximately the same as magnetrons. Because of the relatively small size of the interaction space and the intensity of the beam wave interaction, nearly all of the unradiated power from the crossed-field amplifier must be dissipated on the interaction, or slow-wave, circuit which comprises the major part of the anode area. The limits of available peak power for CFAs is very close to that for magnetrons which are shown in Figure 14.

As might be expected, the similarities to the magnetron also extend to the operating characteristics of a distributed-emission CFA. The electron current is supplied entirely by secondary emission from the cathode. A secondary emission is initiated (by the bombardment of the cathode) of electrons which are accelerated by the DC and RF fields. It is not necessary to heat the cathode in a distributed-emission CFA, but only to assure that it is coated with a material having a high secondary emission yield. In many of the high-power amplifiers it is necessary to cool the cathode to maintain stable and reliable operation. Because of the statistical process by which the emission is initiated, some time-jitter at the leading and trailing edges of the pulse is experienced, but it is less than observed in magnetrons. Unlike the magnetron, in which the RF fields must be built up to fill the high-Q cavity, the level of residual noise causes the high RF drive signal to the CFA to initiate the required level of emission very quickly. Typical jitter times in crossed-field amplifiers are less than one nanosecond, about one-fifty that of the typical coaxial magnetron.

The emission buildup requires that both the RF drive signal and the applied cathode/anode DC voltage must be present. It is necessary to apply the RF drive prior to the DC operating voltage from the modulator. As a general rule, it is desired that the RF drive level should have reached 90 percent of its final value by the time the applied voltage pulse has reached 50 percent value on turn-off. If the RF drive is absent when the DC is applied, the resultant output may be either an out-of-band oscillation or broadband noise. This will also be the result if the drive power is removed prior to the end of the pulse. Distributed emission tubes are, therefore, restricted to use as saturated amplifiers, which find ideal application in high-power radars and cannot be used in applications requiring linear amplification.

Two other features related to the stability on the rise and fall of the pulse are shown in Figure 17. The first of these is the drift region between the output and the input, which is necessary to allow the re-entrant electron beam to be demodulated to inhibit feedback oscillations. In a non-re-entrant amplifier, the drift region can be configured to collect the balance of the spent electron stream. There is also a control electrode (Figure 17). The control electrode is used in DC-operated, re-entrant beam amplifiers to assure rapid turn-off. With the DC voltage continuously applied, the noise built up during the pulse may be sufficient to maintain the secondary emission even after the RF drive signal is removed. In order to inhibit the resulting slow decay of the pulse trailing edge, a positive voltage with respect to the cathode is applied to the control electrode to collect the space charge remaining in

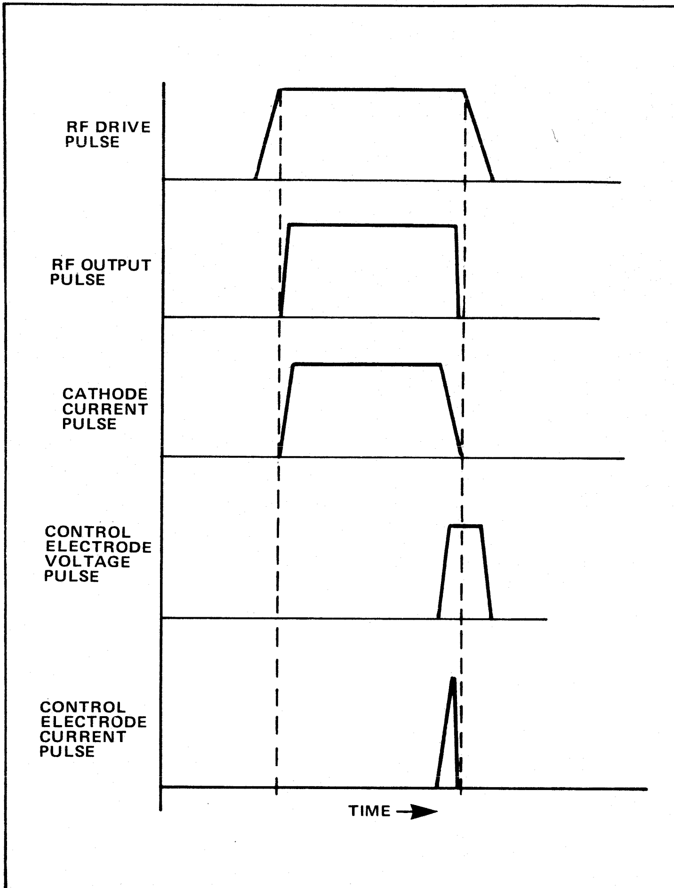

18. Pulse timing and nesting for a DC-operated CFA. It is necessary for the RF drive pulse to encompass the output pulse regardless of the type of modulation.

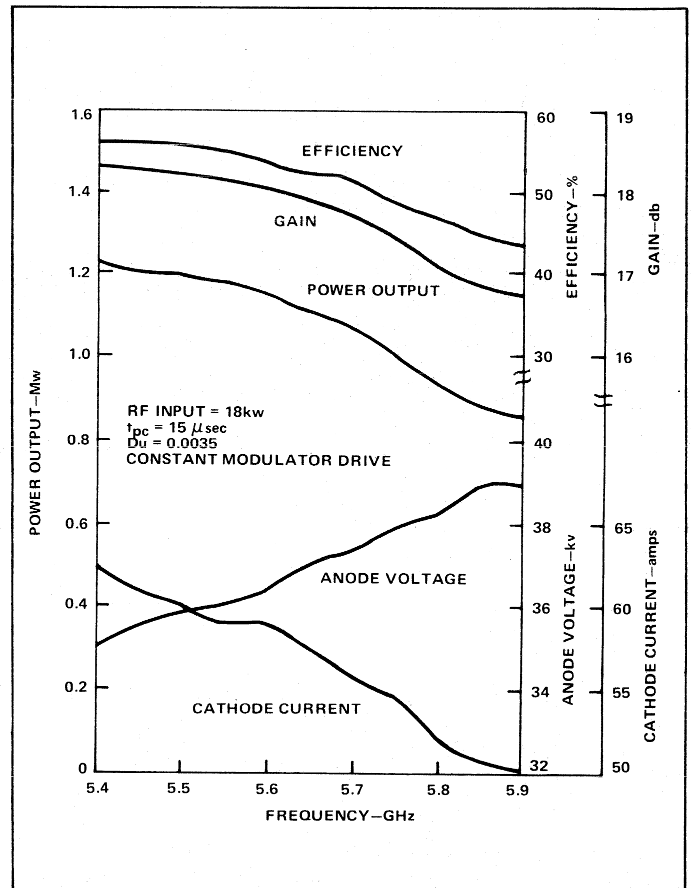

19. Typical performance for the SFD 231 CFA; the variation of anode voltage and cathode current are shown vs. frequency.

the amplifier. Correct pulse timing for a DC-operated, distributed-emission CFA is shown in Figure 18.

Typical operation of a broadband, forward wave, crossed-field amplifier is shown in Figure 19. Note that in addition to the gain, output power, and efficiency, which are shown for most RF amplifiers, anode voltage and current are also shown as a function of frequency. In noting the similarities between the CFA and magnetron operation, recall that the magnetron oscillator frequency is a strong function of the magnetron current.

Since the frequency of the crossed-field amplifier is controlled by a strong input drive signal, the beam impedance is caused to change with frequency. The applied voltage and current measured at the tube will then vary with frequency as functions of the modulator and beam impedance. If the peak current to the amplifier is held constant, the crossed-field amplifier will deliver its broadest-band operation. In general, the line type modulator is a good approximation to a constant current source, while operation from a DC power supply or from a hard tube modulator approach can be used to achieve nearly constant voltage operation.

Since the gain of crossed-field amplifiers is relatively low, they are usually used with klystron or traveling-wave tube-drivers or with other CFAs to provide the required gain for a transmitter amplifier chain. This combination provides both high efficiency and excellent phase stability for coherent radar applications. The phase sensitivity with voltage for a crossed-field amplifier is typically 4 to 10 degrees per percent change in voltage compared to more than 30 degrees per one-percent change for TWTs. The AM-PM sensitivity for CFAs is 1 to 2 degrees per dB compared with 4 to 10 degrees for TWTs operating at saturation. Recently, both injected-beam and distributed-emission tubes have been developed that achieve 27 to 30 dB of gain. Introduction of these high-gain CFAs into systems will considerably diminish the driver tube requirement and increase output to input isolation in the tubes to the 30- to 40-dB level compared to that of 1 to 6 dB for the conventional low-gain tubes.

Crossed-field amplifiers have been built in frequencies ranging from UHF to Ka band. At the lower frequencies, they are extremely attractive because of their ability to provide high peak power more efficiently and from devices a fraction of the size of all alternative amplifier tubes. The compact nature of these amplifiers makes them very difficult to fabricate at the higher frequencies. The operating data from typical CFAs is shown in Table IV. The values shown are less "typical" than those shown for other tube types in this article because of wide variations in the way various suppliers design and fabricate their tubes.

Table IV. Typical CFA Operating Parameters

Frequency Range GHz	Band-Width MHz	Peak Power kW	Duty Cycle	Pulse Width Micro S	Anode Voltage kV	Peak Current Amps	Effic-iency %	Gain dB	Weight Lbs
1.0 - 2.0	500	5	.4	1000	6.5	2	40	20	25
	700	5000	.007	10	100	95	55	11	120
2.5 - 3.5	1000	5	.5	500	7.5	1.5	40	15	12
	200	50	.004	50	25	3.5	70	13	60
	200	750	.002	25	35	38	55	10	110
	200	2500	.0006	10	55	65	70	8	125
5.4 - 6.0	1500	5	.2	500	8	1.5	35	15	15
	500	50	.005	15	10	12.5	40	14	25
	500	500	.001	30	25	40	50	14	60
	500	1000	.001	15	40	50	50	13	75
9.0 - 10	1000	5	.1	500	10	1	25	28	12
	600	250	.01	5	30	22	40	18	30
	600	500	.005	4	32	35	40	14	32
	500	1000	.001	2	38	60	45	14	40

Gyrotron Tubes

The gyrotron is a microwave vacuum tube based on the interaction between an electron beam and microwave fields where coupling is achieved by the cyclotron resonance condition. This type of coupling allows the beam- and microwave-circuit dimensions to be large compared to a wavelength. Thus, the power-density problems encountered in conventional traveling-wave tubes and klystrons at millimeter wavelengths are avoided in the gyrotron. Figure 20 illustrates the power-handling capability of the gyrotron compared to conventional devices.

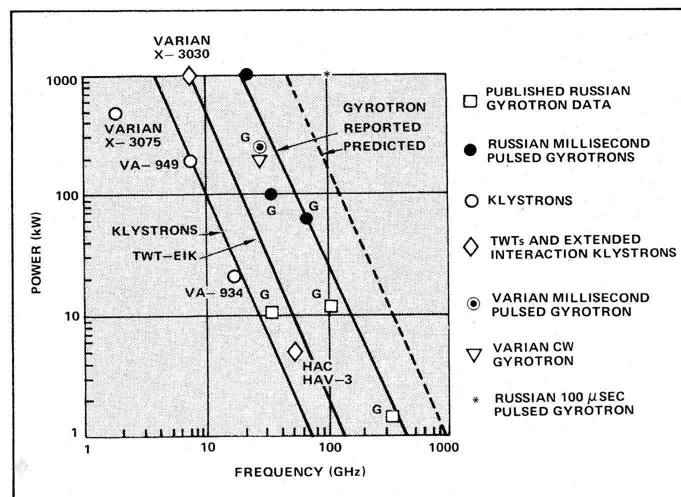

20. Long pulse or CW microwave sources have produced powers of over 100 kW at over 100 GHz.

The name "gyrotron" has been used to describe microwave oscillators based on the interaction of electrons orbiting in a DC magnetic field under the conditions of cyclotron resonance, where the magnitude of the DC magnetic field and the microwave frequency are specifically related. These devices were single-cavity oscillators where the entire interaction took place in a single microwave cavity. It should be recognized that the same basic interaction can be used with different variations, such as amplifiers, using several resonant cavities or traveling-wave circuits. These variations can be called gyroklystrons, gyro-TWTs, etc. Also the term "cyclotron resonance maser" has been frequently used in the literature to describe the same basic interaction, which emphasizes that the interaction can be described using either classical or quantum mechanics.

Gyro-devices require an electron beam where most of the electron energy is transverse to the axis of the tube, unlike linear beam tubes such as klystrons and TWTs where energy parallel to the axis is all that can be used. This has required the development of a series of new electron guns for these devices. These are called "magnetron injection guns" because of the similarity to the electron trajectory in a magnetron. The beam of electrons with their cyclonic motion is injected into the interaction region where the energy exchange between the electrons and the RF wave takes place.

An important characteristic of the gyrotron is that it requires the application of a DC magnetic field which is specifically related to the operating frequency by the cyclotron resonance condition. This relationship is given by the equation

$$\omega = n\omega_c \tag{1}$$

where ω is the operating fequency, n is an integer, and ω_c is the cyclotron frequency or angular velocity of the electron given by

$$\omega_c = \frac{eB}{\gamma m_o} \tag{2}$$

B is the DC magnetic field, e is the electron charge, m_o is the rest mass, and γ is the relativistic mass factor.

Effective interaction occurs only for magnetic fields where n is near integer values. For most microwave field shapes, such as encountered in conventional waveguides and resonators, the fundamental resonance condition with n = 1 has the strongest interaction. With certain special

microwave field shapes, useful interaction can take place with larger integer values of n. These harmonic interactions have the advantage that the magnitude of the DC magnetic field for a given frequency can be reduced by 1/n. The salient gyro-device characteristics and their implications are shown in Table V.

Table V.
Gyro-Devices

Characteristics	Implications
1. Large area for beam and microwave circuit 100 times area in klystron or conventional TWT	100 times power output of conventional tubes
2. Applied magnetic field proportional to frequency $B(kG) \sim 0.35\ f(GHz) \times \frac{\gamma}{n}$ γ = Relativistic mass factor n = harmonic number	Superconducting magnets for 60 GHz or higher

The frequency of the single-cavity gyrotron oscillator is influenced by both the cavity resonance and the value of the DC magnetic field. In general, the output frequency is approximately linearly related to the DC magnetic field over the half-power bandwidth of the cavity. Practical cavity Qs are in the range of 500 to 5000. higher frequency stability requires tighter control on magnetic field.

In the gyroklystron, an input cavity is used to modulate the beam and subsequent cavities are used for further amplification or energy removal. In the gyroklystron, instantaneous bandwidths of one percent are practical.

Another variation which has a larger bandwidth is the gyro-TWT. In this case, a propagating waveguide is used for continuous interaction with the beam. An instantaneous bandwidth of five to ten percent is achievable, and magnetic tuning should double the available bandwidth. Gyro TWT power gain of 20 to 30 dB and an efficiency of 15 to 25 percent have been achieved in early Varian experiments.

The requirements for operation of the gyrotron, whether oscillator or amplifier, are similar to those for any linear-beam tube such as a high-power klystron or TWT. However, differences exist, and as the designs evolve and become more sophisticated, some changes in method of operation can be expected. Shown in Table VI are the operating parameters for a typical 200-kilowatt pulsed oscillator.

Most gyrotrons currently use a temperature–limited cathode to control the beam current. Beam current is controlled by changing the cathode emission/temperature. This is accomplished by variations in the heater voltage. Table VII gives tyical sensitivities to these critical parameters.

In pulsing the gyrotron, the preferred method is to hold the cathode voltage constant and to pulse the gun anode from 1 to 1.5 kV below cathode voltage up to the operating voltage of approximately 25 kV above the cathode. Since the gun anode intercepts very little current, less than 20 milliamps, this does not require switching high energy. If it is desired to cathode-pulse the tube, then some provision must be made to keep the gun anode at a voltage less than the proportional cathode operating voltage during the rise and fall of the cathode voltage pulse. This can be done with a voltage divider if proper precautions are taken.

Table VI.
Operating Parameters

Frequency	28 GHz
Beam Voltage	80 kV
Beam Current	8 A
Gun Anode Voltage	25 kV
Magnet Coil Current	
Main Coil #1	480 A
Main Coil #2	472 A
Main Coil #3	480 A
Main Coil #4	480 A
Gun Coil #1	10.2 A
Gun Coil #2	10.0 A
Heater Voltage	8.1 V
Heater Current	4.6 A
Body and Collector Water Flow	15 gpm
Normal Tube Pressure (with Heater Voltage)	$<10^{-8}$ Torr
Maximum Duty Factor	5%
Rated Pulse Length	20 ms

Table VII.
Sensitivities

Parameter	Typical Value	Sensitivity (dB %)
Gun Coil	10 A	0.11
Heater Voltage	12 V	0.32
Gun Anode Voltage	25 kV	0.39
Beam Voltage	80 kV	0.54
Main Magnet	500 A	1.21

The collector will be off ground by enough to allow monitoring the body current. Some protection must be provided to limit the energy which can be discharged in the tube in the event of an arc. This is normally provided by a crowbar which fires within five microseconds in the event of an arc or high body current, and limits the energy discharged into the tube. Additional protection must be provided against failure of the magnetic field, coolant flow failure in either the tube or magnet, and arcing in the output waveguide. The latter will require an arc detector which looks directly at the output window.

In the case of pulsed tubes, some protection must be provided against long pulses or CW operation. A small Vac-Ion pump is provided which, as a minimum, should be energized during operation. This may be monitored visually or may be connected to protection circuitry to remove beam voltage from the tube in case of excessive Vac-Ion pump pressure. ■

Ferrites Control Microwave Energy

Ferrite components are widely used by system designers for the particular microwave transmission properties exhibited by the materials of which they are composed.

By Fred J. Rosenbaum, *Central Microwave Company*

Today's microwave systems employ large numbers of devices that use the properties of ferrite materials to control the transmission of microwave energy. Devices such as circulators, isolators, phase shifters, limiters, and tunable filters are readily assembled to perform a variety of functions needed by the component, subsystem, and system designer. It is not an exaggeration to say that without ferrite components, today's systems would be configured quite differently and would not perform at present levels. Indeed, many systems would not be possible at all. The unique feature of ferrite devices is their non-reciprocal nature. That is, signal transmission between a pair of terminals is dependent on the direction of signal flow. For example, an isolator provides a low-loss path from A to B (Fig. 1), but a high-loss path for transmission from B to A.

Ferrite components may be realized in waveguide, coaxial, stripline, or microstrip geometries. The many different functions that can be obtained from them can be understood in terms of three common elements: the ferrite medium, a circuit to interact with the ferrite, and a magnetic bias field. This article describes the principles of operation of a number of ferrite components, the performance that can be expected from them, and some design data which may be useful in specifying components for system application.

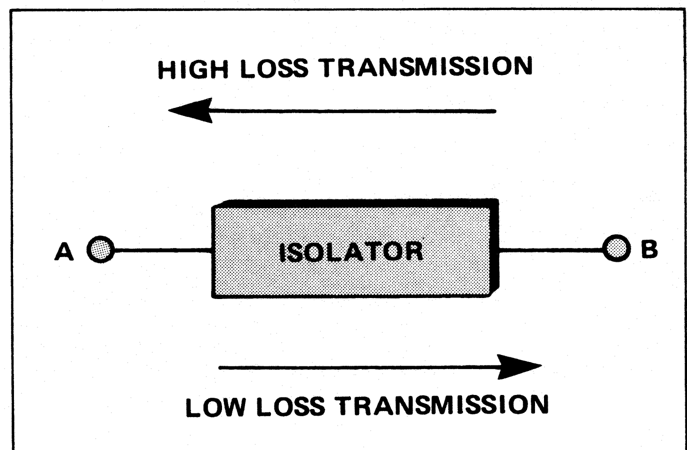

1. Isolators simply provide a low-loss path in one direction and a high-loss path in the opposite direction.

Material Properties

• *Ferrite* is a generic term for the ferromagnetic oxides, including the garnets. Most microwave ferrites are polycrystalline. In their manufacture, small (micron-sized) particles of singlecrystal material are sintered with a binder to form the desired shape, such as planar substrates, rods, and bars. Each particle is a single magnetic domain with a net magnetic moment, like an infinitesimal bar magnet. The resultant material is a hard, brittle ceramic with two important properties. First, the permeability of the ferrite can be varied with the application of an external magnetic bias field. Second, its electrical conductivity is very low; ferrites are ceramic dielectrics. Being good insulators, they are easily penetrated by microwave-frequency electromagnetic waves which can propagate in them with low dielectric loss. Their permittivity is given by

$$\epsilon = \epsilon_o (\epsilon' - j\epsilon'') \quad (1)$$

where $\epsilon_o = 8.85$ M 10^{-12} f/m, the permittivity of free space. The dielectric loss tangent is

$$\tan \delta_e = \frac{\epsilon''}{\epsilon'} \quad (2)$$

For most ferrites the relative permittivity, ϵ', is between 9 and 16. Typically, loss tangents are less then 10^{-3}.

• *Saturation Magnetization.* In addition to their dielectric properties, ferrites are characterized by their saturation magnetization ($4\pi M_s$), Curie temperature (T_c), resonance line width (ΔH), and spin wave linewidth (ΔH_k). The saturation magnetization measures the net magnetic moment per unit volume of the material when all the individual single-crystal magnetic domains are aligned in an external magnetizing field. The saturation moment depends on the specific formulation of the ferromagnetic oxide obtained when metal ions are appropriately substituted in the crystal lattice making up the single crystal domains. Typical ions are Al, Fe, Ga, Mg, Mn, Ni, and Zn. The ions do not necessarily have to be magnetic to influence the saturation magnetization. By varying the formulation, values of $4\pi M_s$ ranging from 200 to 5000 G can be obtained.

Since the magnetization results from the particular ordering of magnetic ions on specific sites of the ferrite crystal lattice, disturbing the ordering changes the magnetization. Thus, the magnetic properties of ferrites will be temperature dependant. In fact, the net magnetization vanishes at a characteristic temperature known as the Curie point (T_c). Depending on the formulation, Curie temperatures of particular ferrites range from 85°C to 600°C.

• *Magnetic Loss.* In addition to their dielectric loss, ferrites also exhibit magnetic loss resulting from the interaction between the microwave magnetic field and the system of magnetic dipoles making up the magnetic domains. Energy extracted from the field is lost to the lattice as heat.[5,8] The energy is carried by spin-waves which are modes or characteristic motions of the magnetic dipoles of the medium.[22,23] Since adjacent dipoles are coupled to one another by their

Fred J. Rosenbaum is chief scientist with Central Microwave Company, Maryland Heights, Missouri 63043.

magnetic fields, a disturbance in the motion of one dipole will be transmitted to surrounding ones, so fluctuations in the magnetization which travel throughout the ferrite can be induced. Energy is lost due to the drag introduced by impurity atoms whose response to the microwave magnetic field is strongly damped. A measure of the loss associated with spin wave propagation is given by the spin-wave line width, ΔH_k. Non-uniformities in the ferrite medium, such as variations in the volume density of the magnetic ions, pores, non-magnetic inclusions, cracks, or surface roughness, all contribute to scatter the energy of the spin-waves more effectively. The total energy loss to the lattice due to magnetic interactions is characterized by the magnetic linewidth measured at ferromagnetic resonance ΔH. Note that $\Delta H > \Delta H_k$, since ΔH_k is due primarily to the magnetic damping of the material while ΔH includes all the magnetic loss processes.

- *Non-Linear Loss.* The microwave power lost to the ferrite is linear with input power up to some critical power level, beyond which the losses change non-linearly. This threshold phenomenon is connected to the existence of a critical microwave magnetic field, h_c. The spin-waves responsible for resonance loss can also be excited by large microwave magnetic fields at frequencies far from resonance. The critical field is given by[23]

$$h_c = C \frac{\omega}{\omega_m} \Delta H_k \quad \text{Oe.} \qquad (3)$$

where ω is the microwave radian frequency: $\omega_m \alpha 4\pi M_s$. The factor C is a function of factors such as the ferrite shape, the polarization of the microwave magnetic field, and the applied biasing magnetic field. Both ΔH_k and C are determined experimentally; C is of order unity and ΔH_k is in the range 1-20 Oe.[25] The fact that a critical microwave magnetic field intensity for non-linear loss exists places a limit on the power handling capability of particular ferrite devices. Furthermore, it suggests that to increase the critical power the impedance level of the device should be made high.

Figure 2 represents the relative power loss in a ferrite as a function of applied DC magnetic bias field. The parameter is the microwave magnetic field h, relative to h_c. At low drive levels, the loss is high in the vicinity of ferromagnetic resonance. For $h / h_c \simeq 1$, the resonance linewidth broadens, the peak loss drops, and the loss increases everywhere else. For $h / h_c > 1$, a subsidiary resonance appears around $H_{dc} = H_o/2$. In addition to an increase in insertion loss at high power levels, other undesirable phenomena can be observed due to this non-linear effect. For example, harmonic generation is possible and, at much lower power levels,[26] ferrite components can be a source of intermodulation distortion.[27]

To increase the power handling capacity of ferrite devices, the material chosen for the application should have low saturation magnetization and high spin-wave or resonance linewidth. Furthermore, if an external bias field is used, it should be chosen, if possible, to remove the subsidiary resonance far from the operating frequency. A device which employs this non-linearity is the ferrite limiter.[5] These components are designed for use as part of transmit-receive (TR) protection. The ferrite medium, geometry, and bias field are chosen so as to introduce the subsidiary resonance at a desired level of h_c.

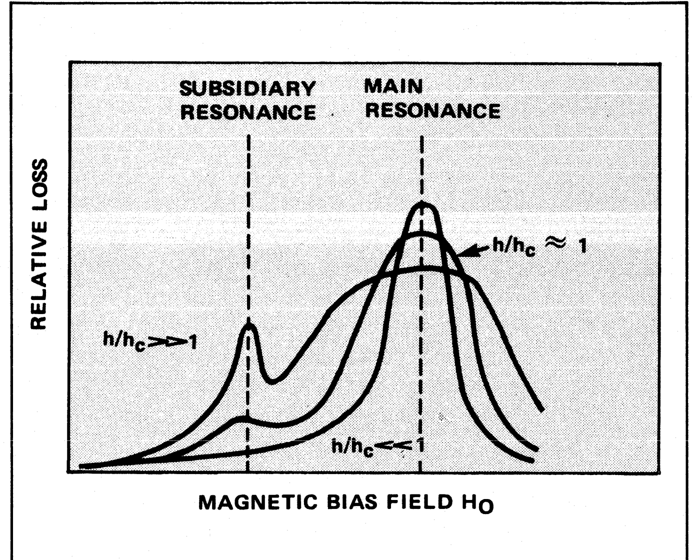

2. Power loss varies as applied, DC magnetic bias.

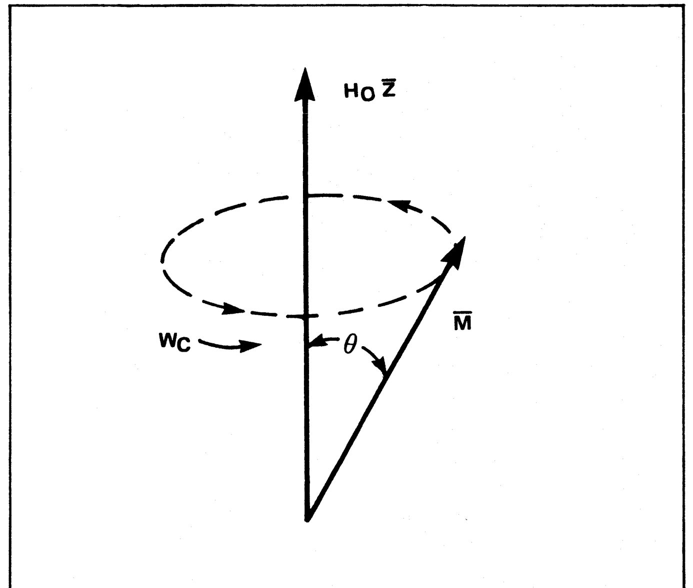

3. Magnetic dipole moment precesses about the bias magnetic field.

- *Microwave–Ferrite Interaction.* The fundamental interaction in ferrites involves the coupling of their electron spin system to electromagnetic waves. The magnetic dipole moment of the spinning electron precesses about the direction of the bias magnetic field H_o (Fig. 3), with a radian frequency $\omega_o = 2\pi(\gamma H_o)$, where γ is the gyromagnetic ratio. It has the value of 2.8 MHz/Oe for most ferrites.

If a circularly polarized (CP) microwave magnetic field of frequency ω is applied in the plane normal to H_o, energy transfer from the microwave field to the spin system occurs when $\omega \approx \omega_o$ (resonance) provided that the sense of CP is the same as the sense of precession; that is, the angle between H_o and the magnetization reaches 90°. The opposite sense of CP will not couple to the spin system and will propagate through the medium unattenuated.

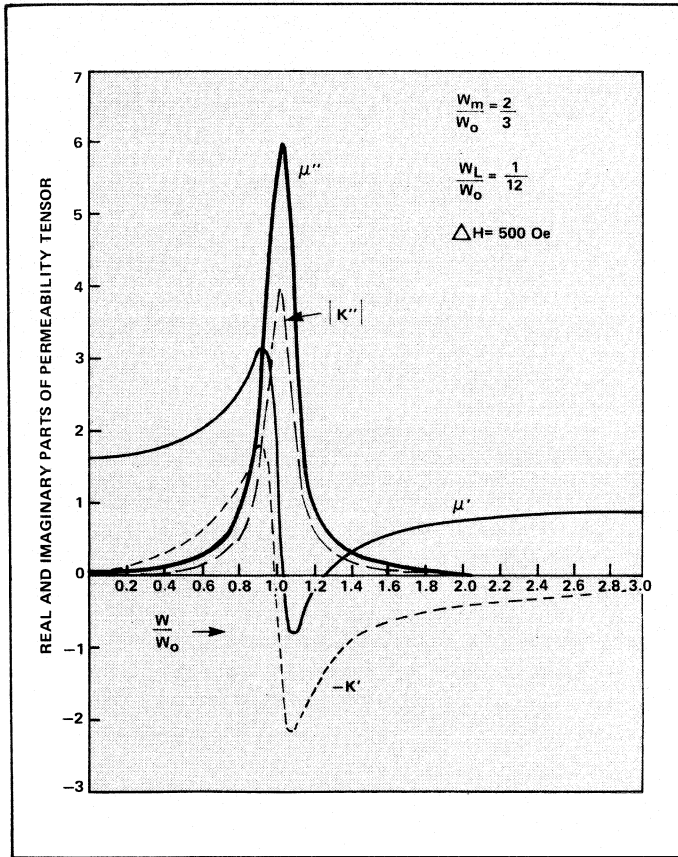

4. If the internal magnetic field is held constant, then this can represent the frequency dependence of μ and K.

The microwave properties of the ferrite are described by the Polder tensor[28] which relates the microwave induction B to the microwave magnetic field intensity $\overline{H}$;

$$\overline{B} = \overline{\overline{\mu}} \cdot \overline{H} \tag{4}$$

A ferrite is said to be magnetically saturated in an external bias field when all the magnetic domains are aligned along the direction of H_o, i.e. the magnetization of the sample is at its saturation value $4\pi M_s$. For a magnetically saturated ferrite, magnetized in the z direction with a microwave field propagating in this direction, the Polder tensor is

$$\overline{\overline{\mu}} = \mu_o \begin{bmatrix} \mu & -j\chi & 0 \\ j\chi & \mu & 0 \\ 0 & 0 & \mu_z \end{bmatrix} \tag{5}$$

where, for the case of small magnetic losses the elements are given by

$$\mu = 1 + \frac{\omega_m [\omega_o + j\omega_L]}{[\omega_o + j\omega_L]^2 - \omega^2} = \mu' - j\mu'' \tag{6a}$$

$$\kappa = \frac{-\omega_m \omega}{[\omega_o + j\omega_L]^2 - \omega^2} = \kappa' - j\kappa'' \tag{6b}$$

$$\mu_Z = 1 \tag{6c}$$

with

$\mu_o = 4\pi \times 10^{-7}$ h/m = permeability of free space
$\omega_o = 2\pi\gamma H_o$ = resonant radian frequency
$\omega = 2\pi f$ = microwave radian frequency
$\omega_m = 2\pi\gamma(4\pi M_s)$
$4\pi M_s$ = saturation magnetization of the ferrite
$\gamma = 2.8$ MHz/Oe
$\omega_L = \frac{1}{T} = \frac{2\pi(\gamma\Delta H)}{2}$
T = macroscopic relaxation time which includes spin-spin and spin-lattice damping[29]
ΔH = resonance line width.

The permeability tensor elements of Equation (5) are plotted in Figure 4 for the parameter ratios shown. If the internal magnetic field, H_o, is held constant, then the figure represents the frequency dependence of μ and k. Their real parts are zero near $\omega/\omega_o = 1$; their imaginary parts peak there. This frequency is called the ferromagnetic resonance frequency. Conventionally, the frequency region $\omega/\omega_o > 1$ is called "above resonance." It should be noted that the horizontal axis could also be interpreted as a magnetic field axis for fixed frequency. The resonance line width, ΔH, is defined as the internal magnetic field difference measured between the points where the imaginary parts of the permeability tensor decrease to one-half their resonance values. Typical values for ΔH in ferrites and garnets range from 40 to 900 Oe.

The shape of the ferrite in a particular component influences the internal field. An unbounded ferrite medium would remain saturated down to zero bias field. However, a sample with finite dimensions exhibits demagnetization which results from the discontinuity of the normal components of the magnetic field at the boundary between the external medium (e.g. free space) and the ferrite. Demagnetizing factors for an ellipsoidal sample and its limiting shapes (sphere, rod, and plane) in a uniform magnetic field are given in Figure 5 and in the table below.[30]

	N_x	N_y	N_z
Sphere	$\frac{1}{3}$	$\frac{1}{3}$	$\frac{1}{3}$
Rod	$\frac{1}{2}$	$\frac{1}{2}$	0
Plane	0	0	1

For a bounded piece of material, the ferrimagnetic resonance frequency is given by Kittel's equation[31]

$$\omega_r = \{[2\pi\gamma H_a + (n_y - N_z)\omega_m][2\pi\gamma H_a + (N_y - N_z)\omega_m]\}^{1/2} \tag{7}$$

where N_x, N_y, and N_z are the appropriate demagnetizing factors for the shape of the sample. They are related by $N_x \times N_y \times N_z = 1$.

Many microwave devices operate with internal fields below what would be needed to saturate the ferrite. In this condition the ferrite is said to be partially magnetized, and the permeability tensor elements are approximately given by[25, 32-34]

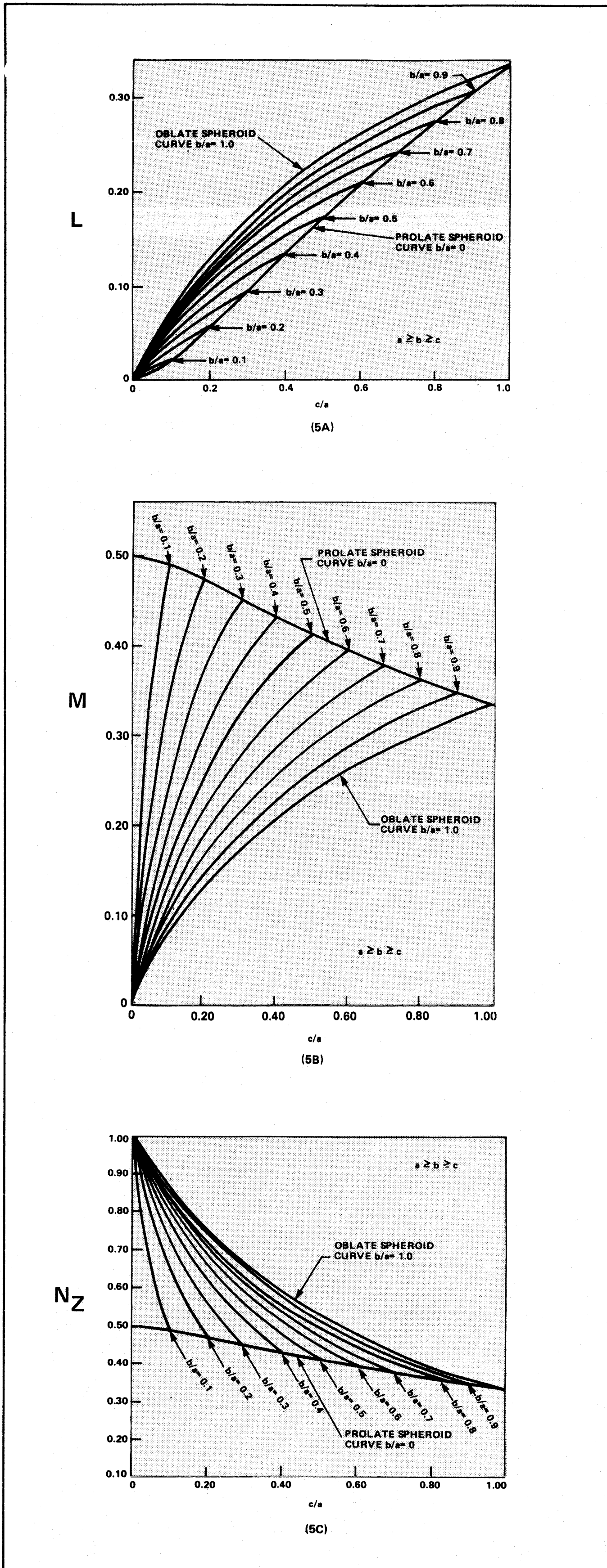

5. Demagnetizing factors can be read for an ellipsoidal sample and its limiting shapes.

$$\mu = \mu_{dem} + (1-\mu_{dem}) \left(\frac{4\pi M}{4\pi M_s}\right)^{3/2} \quad (8a)$$

$$\kappa = \frac{\gamma(4\pi M)}{\omega} \quad (8b)$$

$$\mu_z = \mu^{dem} \quad (8c)$$

$$\mu_{dem} = \frac{1}{3} + \frac{2}{3}\sqrt{1 - (\frac{\omega_m}{\omega})^2} \quad (8d)$$

where $4\pi M$ is the average magnetization of the ferrite. For this example, the loss free case has been assumed. In latched or remanent operation, $4\pi M$ may be varied as described in the next section.

In partially magnetized ferrites, magnetic loss occurs for $\omega \leqq \omega_m$. This effect, termed "low field loss," is a consequence of resonances of the non-aligned domains in the sample.[35] It may be avoided by choosing $\omega/\omega_m < 1$ over the desired operating frequency range. Low field loss vanishes when the ferrite is saturated.

The Hysteresis Loop and Remanent Operation

An unmagnetized ferrite can be thought of as being composed of randomly oriented microscopic domains, each fully saturated internally. If a magnetizing field is applied to the ferrite, these domains orient along the applied field direction. The process occurs first through the growth of those domains most favorably aligned initially. For very small applied fields, domain wall motion is reversible. At higher applied fields, new, larger domains form. Now the motion is irreversible: if the field is removed, a net *remanent* magnetization persists; the magnetic induction relaxes to its maximum remanent value B_r. The ferrite sample is now established on its major B-H (hysteresis) loop (as shown schematically in Figure 6 for a toroidal shape). Application of a static field in excess of $-H_c$, the coercive force, will cause the induction to traverse the loop in the direction of the arrows. Returning this field to zero produces a remanent induction of $-B_r$. The magnetization ratio $4\pi M_r/4\pi M_s$ in a useful figure of merit for latching devices. It is important that $4\pi \overline{M} = \overline{B} - \overline{H}$.

Microwave propagation in devices using partially magnetized ferrites can be controlled by adjusting the internal magnetization ($4\pi M$), and thereby the permeability (as indicated in Eqs. 8). A useful property of the hysteresis loop is that the magnetization can be "latched" at the desired value without the need of maintaining a continuous holding field.[36] Several methods exist for setting the desired magnetization.[16] For example, a low-reluctance magnetic circuit such as a toroid can be switched from $-B_r$ to B_r by driving a pulse of current through a latching wire threading the toroid. The current must be large enough to produce $H >> H_c$. Numerous latching ferrite phase shifters[37,38] and circulators employ this switching technique.[39-41] Different phase states are obtained by cascading toroids of different lengths.

The internal magnetization can be conveniently latched to any value between $\pm 4\pi M_r$ by partially switching the toroid. This "flux drive" method operates by first establishing the toroid in a reference state, say $-B_r$, by applying a large negative pulsed field. The ferrite is then driven up the major B-H loop to a point B′ (Fig. 6). If the drive is now removed (H=O), the ferrite will relax to some remanent state $4\pi M'$

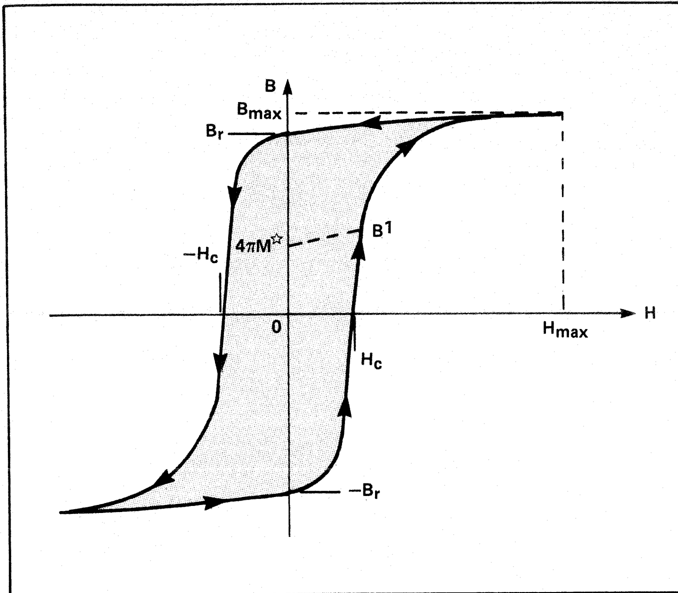

6. This hysteresis loop is followed in the direction of the arrows if a static field in excess of $-H_c$ is applied.

along a minor hysteresis loop. The flux density, which must be supplied to drive the toroid from $-4\pi M_r$ to $4\pi M'$, is $|B'+B_r|$.

According to Faraday's law, the voltage V developed at the terminals of the latching wire is

$$V = -\frac{d\phi}{dt} \tag{9}$$

when the flux, ϕ, is the toroid change at a rate $-d\phi/dt$. The net flux change is

$$-\Delta\phi \quad \int_{o}^{t'} V\,dt \tag{9a}$$

Thus, if the toroid latching wire is driven with a voltage V(t) for a time t′ the flux in the toroid must change by $-\Delta\phi$. This change in flux is related to the change in flux density, so by controlling the volt-time integral one may meter out precisely the necessary flux change to establish the required magnetization state.

In a flux drive device, a low impedance electronic driver provides a voltage pulse of fixed characteristics for a prescribed length of time. If a square wave is used, then either its amplitude or duration can be adjusted to obtain the desired magnetic state. Since the source ideally has zero impedance, the current needed to magnetize the ferrite adjusts itself to changes in the B–H loop due to temperature, stress, etc., to give the particular characteristic for the forced flux change. In practice, the toroid is reset to one of the major-loop remanence points, then driven to the required state.

Figure 7 shows the result of an analysis[42] relating the pulse duration τ_m and voltage amplitide needed to switch a toroid from $-B_r$ to $+B_r$ in m-pulses. The switching circuit assumes a 5Ω source impedance and a 100 turn coil. The analysis gives

$$\tau_m = \frac{2}{m} \quad \frac{n\Phi}{V-RI} \quad V > IR \tag{10}$$

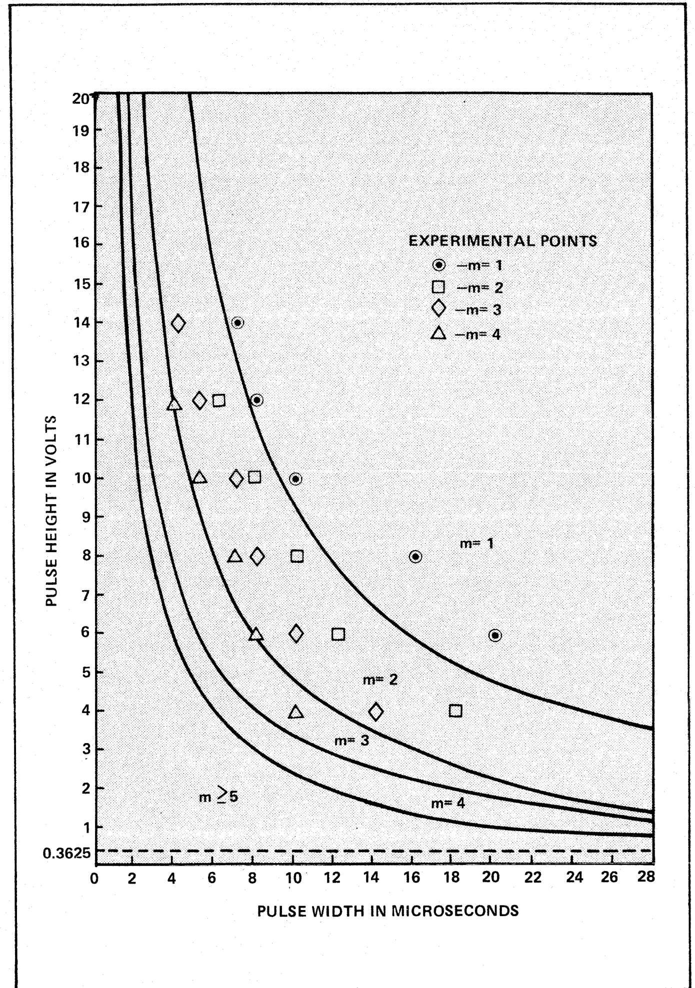

7. Boundary curves show the limits of pulse height and width needed to switch a toroid with 'm' pulses.

where V is the applied pulse height, N the number of turns on the switching coil and R the source resistance. The quantity I is the current needed to produce a field $H=H_c$ in the coil and Φ is the remanent flux in the latched toroid. These quantities can be determined experimentally for a given latching device. For the data shown here, I=72.5 mA and $\Phi = 45 \times 10^{-8}$ Webers. The areas between the curves, indicated by m=1, 2, etc., represent the voltage and pulse width combinations for which m-pulses are needed to switch from $-\Phi$ to Φ. Low voltages of long duration can be used, as well as high voltages of short duration. The boundary curves asymptotically approach V=0.3625 Volts, the minimum value for latching the toroid to Φ, i.e., V=IR (Eq. 10). Also shown in the figure are experimental results for a 1″ × 1″ × 0.025″ rectangular toroid of TT1–390 ferrite material. These curves can be used to aid in latching device design.[42]

The volt-time integral (Eq. 9) is independent of the shape of the B-H loop, its temperature dependence, linearity, etc. This relative temperature insensitivity is significant in the application of latching phase shifters.[43] Figure 8 shows manufacturers' data on the temperature variation of the hysteresis loop properties of TTI-390. Its ferrimagnetic properties vanish at T_c=320°C and change significantly over a normal

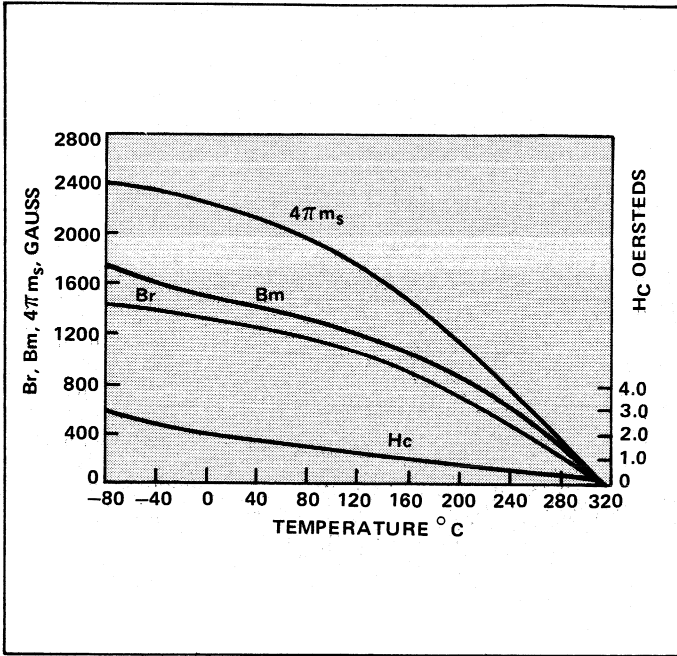

8. Skewed hysteresis shows the effect of an air gap in the magnetic circuit. (Hord, Boy, and Rosenbaum)

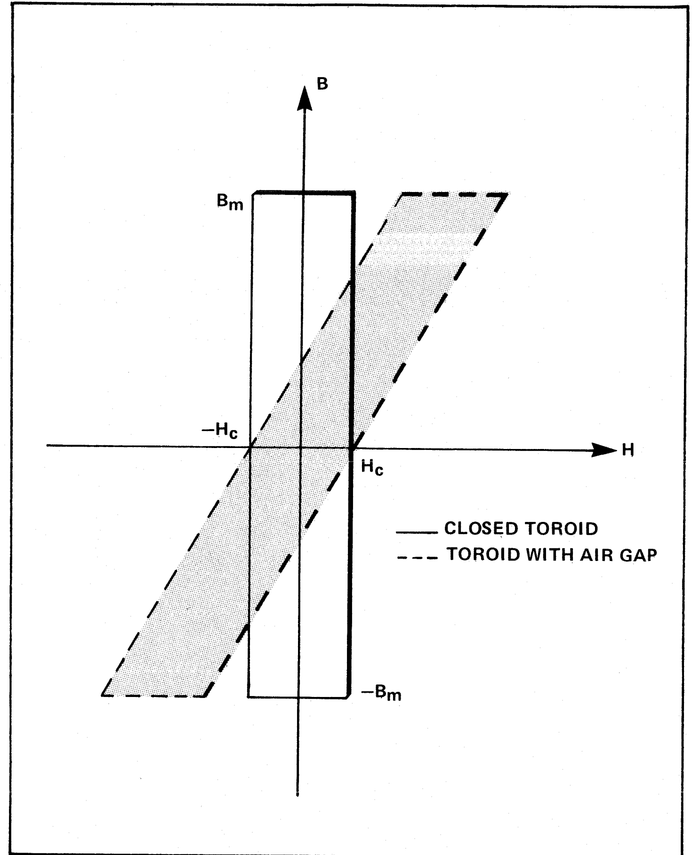

9. Demagnetizing factors of the general ellipsoid along each semiaxis show the ellipsoid semiaxes are a≥b≥c. (J.A. Osborn, Phys. Rev., vol. 67, p. 351, 1945.)

operating temperature range of −40°C to 80°C. Materials with higher Curie temperatures exhibit less temperature dependence over this range.

Stresses in the ferrite produced by magnetostriction reduce the remanence ratio. For latching applications, materials with low magnetostriction are preferred. Stresses also may be introduced in the machining of ferrite parts, by mechanical pressure in device fabrication, and by thermal effects.[16]

The energy per unit volume expended to switch a ferrite between its remanent states is

$$\frac{W}{Vol.} = \int_{-B_r}^{B_r} H\, dB \quad \text{Joules} - m^{-3} \qquad (11)$$

For an idealized square loop material depicted in Figure 8 the maximum energy is

$$\frac{W_{max}}{Vol.} = 2H_c B_m \qquad \text{Joules} - m^{-3} \qquad (12)$$

where the magnetic quantities are expressed in MKS units. For commonly used microwave ferrites, switching energies are in the 50-100 $\mu J/m^3$ range.

The shape of the B-H loop depends on the magnetic circuit.[43] If the ferrite shape forms a closed magnetic flux path, then a vertical B-H loop is obtained. If there is an air gap, the hysteresis loop will be skewed to the right of the idealized loop (Fig. 9). The area under the loop, however, remains constant. The ferrite can be latched at the major loop remanent flux level provided that

$$H_c l_f > H_{air} l_{air} \qquad (13)$$

where H_c = coercive force of ferrite
l_f = equivalent path length of ferrite
H_{air} = magnetic field intensity in air gap
l_{air} = equivalent path length of air gap

If this condition is not satisfied, the ferrite can still be latched, but at a lower remanent flux level.

For a toroid with an idealized B-H loop—assuming a single turn latching wire—the approximate drive current and voltage are given by

$$I = H_c l_f \quad \text{Amps} \qquad (14a)$$

$$V = \frac{2 B_m A}{T_s} \quad \text{Volts} \qquad (14b)$$

where A is the cross-sectional area of the toroid and T_s is the switching time. The ferrite volume is Al_f. If it is assumed that the current remains constant during switching ($H \approx H_c$), then the instantaneous impedance of the switching circuit that must be driven is principally resistive and is given by

$$R = \frac{V}{1} = \frac{2 B_m A}{T_s H_c l_f} \qquad (14c)$$

This effective resistance is quite low. It depends on the geometry of the ferrite toroid, its magnetic parameters, and the switching time. If N turns are used, R increases by N^2.

For major-loop switching, the time it takes for the toroid induction to change from $-B_r$ to $+B_r$ is given, empirically, by

$$T_s = \frac{S_w}{H - H_t} \qquad (15)$$

where S_w is the switching coefficient in Oe-μsec, H is the driving field and H_t is the threshold field needed for switching.[44] It is slightly larger than the coercive force H_c. The switching time is measured between the 10% and 90% points on the magnetic flux waveform detected by integrating the voltage induced in a secondary winding on the toroid.

The switching coefficient can be interpreted as the field strength in excess of H_t needed to switch the toroid from $-B_r$ to $+B_r$ in 1 μsec. Both H_t and S_w are constants for a given material, although they will vary with temperature. T_s can be made arbitrarily small by driving the magnetic circuit hard enough, i.e., $H >> H_c$ (Eq. 15). For major loop switching, H must be greater than 5–10 times H_c. Practical drivers, however, will limit the maximum drive that can be applied, other factors notwithstanding, since the terminal voltage the driver must tolerate is inversely proportional to T_s (Eq. 14b) and the peak current required is $I_p \approx H_{max} 1_f$. With present ferrites and transistor drivers, switching times on the order of 0.1–1 μsec are achievable. Switching times for practical devices, including a reset-set cycle, are around 10 μsec.[45]

The maximum energy given by Equation 12 is the energy dissipated in hysteresis loss. There are additional losses which must also be supplied when the ferrite is switched. These include circuit losses and eddy current losses, particularly the shorted turn effect which is present whenever other conductors thread the magnetic circuit. This situation is often encountered in the construction of latching waveguide phase shifters.[46,47]

Circulators and Isolators

Scattering Matrix and Applications

The most commonly encountered ferrite device is the circulator or isolator. Circulators typically are three-port devices while isolators are two-port ones. Figure 10 shows the schematic representation for these components. An ideal circulator transmits energy incident at port (1) to port (2) while port (3) is isolated. Likewise a signal at (2) is transmitted to (3) with (1) isolated, and so forth.

The scattering matrix for a circulator is given by[48]

$$[S] = \begin{bmatrix} S_{11} & S_{21} & S_{31} \\ S_{31} & S_{11} & S_{21} \\ S_{21} & S_{31} & S_{11} \end{bmatrix} \qquad (17)$$

where S_{11} is the input reflection coefficient at each port, S_{21} is the transmission coefficient from (1)→(2), and S_{31} from (1)→(3). Notice the cyclic symmetry of S_{ij}. The [S] matrix for an ideal, loss-less circulator can have two forms; the first signifies circulation (3)→(2)→(1)→(3)

$$\begin{matrix} 0 & 1 & 0 \\ 0 & 0 & 1 \\ 1 & 0 & 0 \end{matrix} \quad \text{or} \quad \begin{matrix} 0 & 0 & 1 \\ 1 & 0 & 0 \\ 0 & 1 & 0 \end{matrix} \qquad (18)$$

while the second represents the transmission (1)→(2)→

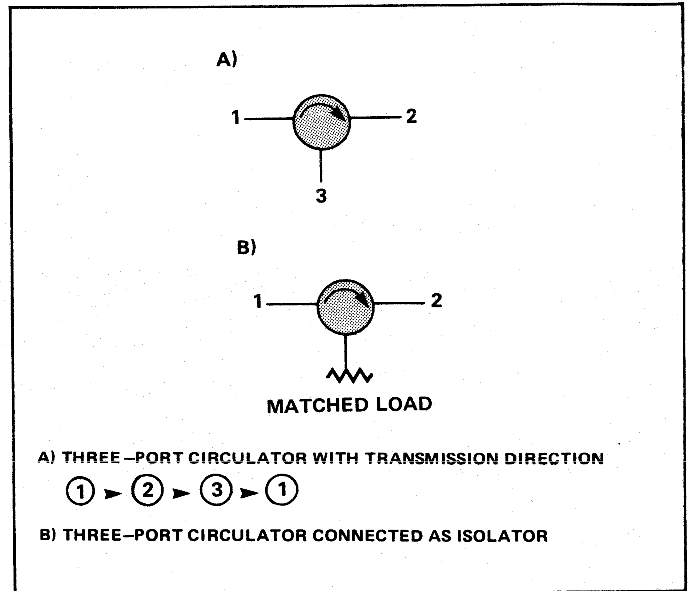

10. Schematic representation for circulators and isolators: a) three-port circulator with transmission direction (1) — (2) — (3) — (1).

(3)→(1). Thus, the ideal circulator is a matched three-port junction with infinite isolation. If the circulator is loss-free but not ideal, then the unitary property of the scattering matrix requires

$$|S_{11}|^2 + |S_{31}|^2 + |S_{21}|^2 = 1 \qquad (19a)$$

and

$$S_{11}S_{21}^{*} + S_{31}S_{11}^{*} + S_{21}S_{31}^{*} = 0 \qquad (19b)$$

For nearly ideal behavior, one desires good transmission ($S_{21} \approx 1$), a well-matched input ($S_{11} \approx 0$) and high isolation ($S_{31} \approx 0$). In Equation 19b, since S_{11} and S_{31} are small, their product $S_{31}S_{11}^{*}$ will be much smaller than either of the other terms and can be neglected. This leads to the result

$$|S_{11}| \approx |S_{21}| \qquad (20a)$$

Thus, for a well-matched low-loss circulator the input reflection coefficient is a good measure of the isolation, i.e.,

$$\text{Isolation}\Big|_{dB} \approx 20 \log |S_{11}| \qquad (20b)$$

Substituting Equation 20a into 19a leads to:

$$|S_{21}| \approx 1 - 2|S_{11}|^2 \qquad (21a)$$

or

$$|S_{21}| \approx 1 - |S_{11}|^2 \qquad (21b)$$

Thus, the insertion loss also depends on the input match:

$$\text{Insertion loss}\Big|_{dB} \approx 20 \log |S_{21}| \qquad (21c)$$

Continued on page 163

Continued from page 140

Table I
Typical Properties of Some Commercial Microwave Ferrites.

Composition	Saturation Magnetization $4\pi M_s$ (Gauss)	Curie Temperature T_c (°C)	Dielectric Constant ϵ	Loss Tangent Tan δ_e	Resonance Linewidth ΔH (Oe)	Spin-Wave Linewidth ΔH_k (Oe)	Remanent Induction B_r (Gauss)	Coercive Force H_c (Oe)
Mg Mn	2150	320	13	<.0003	540	2.5	1290	1.8
Mg Mn Al	750 - 2000	90 - 290	11.3 - 12.4	<.0003	100 - 250	2.1 - 5.2	540 - 1400	.5 - 1.6
Mg Mn Zn	250 - 3000	225 - 275	12.4 - 13.1	<.0005	190 - 520	2.3 -3.3	1400 - 2000	.85 - 1.4
Ni Al	500 -1000	120 - 400	9 - 12	<.001	150 - 320	-	140 - 450	2 - 5
Ni Co	3000	585	12.8	<.003	350	12.4	1853	5.7
Ni Zn	4000 - 5000	375	12.5	<.003	160 - 340	-	1800 - 1950	.96 - 3
Ni Co Al	1400 - 2500	425 - 570	9 - 12.7	<.002	250 - 900	6.1 - 33	440 - 1490	4.1 - 26
Ni Mg Ti	1800	500	10	<.002	700	>45	-	-
Li	3750	640	15	<.003	<650	-	2580	2.4
Li Ti	1000 - 2900	300 - 600	15.2 - 18	<.003	300 - 500	1.5	670 - 2000	1 - 2.5
Li Zn	4100 - 4800	400 - 570	14.5 - 14.8	<.003	240 - 550	-	2840 - 3050	.89 - 2.6
Li Ti Co	600	235	18.1	<.003	350	3.9	300	1.9
Li Ti Zn	900 - 3000	150 - 210	15 - 18	<.003	90 - 150	2.1	590 - 1580	.55 - .69
YIG	1780	280	15	<.0002	45	1.43	1280	.45
YIG Al	175 - 1200	85 - 220	13.8 - 14.8	<.0002	40 - 50	1.4 - 2.1	40 - 790	.55 - .9
YIG Gd	725 - 1600	280	15.1 - 15.4	<.0002	50 - 200	3.8 - 7.6	360 - 990	.83 - 1.5
YIG Ho	550 - 1600	180 - 280	14.4 - 15.4	<.0002	70 - 120	5.4 - 8.5	280 - 990	.8 - 1
YIG Gd Al	400 - 1400	150 - 280	14.2 - 15.2	<.0002	50 - 90	3.2 - 5.2	190 - 920	.7 - 1

Practical circulators usually have insertion loss <0.5dB (0.3 dB typical) including circuit, ferrite and mismatch loss, with isolation greater than 20 dB. The usable bandwidth of a circulator is often specified in terms of its 20 dB isolation bandwidth. Figure 11 depicts the behavior of a typical microwave frequency circulator.

If the output ports of the circulator are terminated in loads with a reflection coefficient S_2 at (2) and S_3 at (3), respectively, then the reflection coefficient at the input, (1), becomes

$$S_{11}^{1} = S_{11} + \frac{S_{13}S_{12}S_3}{1-S_{11}S_3} + \frac{N}{O} \quad (22)$$

where

$$N = S_{21}(1-S_{11}S_{13}) + S_3 S_{31}^2$$

and

$$D = (1-S_{11}S_2)(1-S_{11}S_3) - S_2 S_3 S_{21} S_{31}$$

The transmission coefficient from (1)→(2) is given by

$$S_{21}^{1} = \frac{N}{D} \quad (23)$$

and isolation from (1)→(3) by

$$S_{31}^{1} = \frac{S_{31}}{1-S_{11}S_3} + \frac{S_2 S_{21} N}{(1-S_{11}S_3)D} \quad (24)$$

The performance of the circulator depends on the properties of the load reflection coefficients.

Consider S_{11}^{1} if (3) is terminated in a matched load (S_3=0), and (2) in an arbitrary load: see Fig. 10b. Then, Equation 22 yields

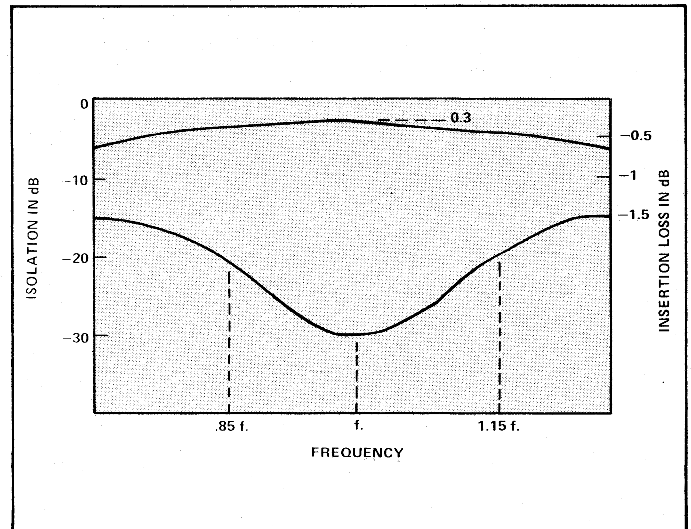

11. Typical circulator performance reaches minimum at some f_0.

$$S_{11}^{1} = S_{11} + \frac{S_{21}S_{12}S_3}{1-S_{11}S_2} \quad (25a)$$

Using the approximations of Equations 20a and 21b, one obtains

$$S_{11}^{1} = S_{11} + \frac{S_{11}\left[1-\left|S_{11}\right|^2\right]S_2 e^{j(\theta_{21}+\theta_{31})}}{1-S_{11}S_2} \quad (26)$$

where θij are the phase angles of the respective quantities. This result represents the relationship between the VSWR at the input to the circulator, the isolation of the circulator, and the load VSWR. It is expressed by means of a nomogram in Figure 12.

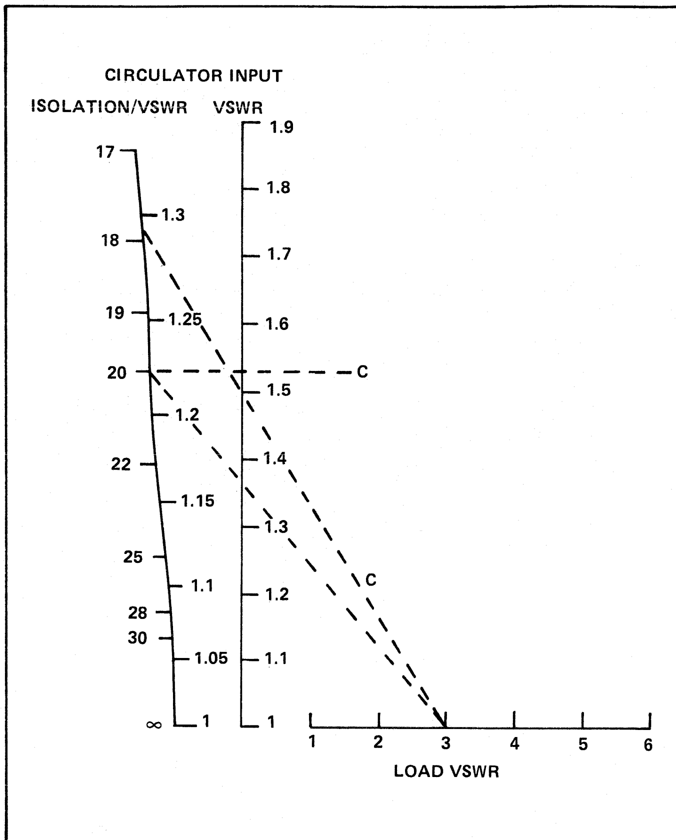

12. A nomogram can be used to determine circulator performance by relating input VSWR, isolation, and load VSWR.

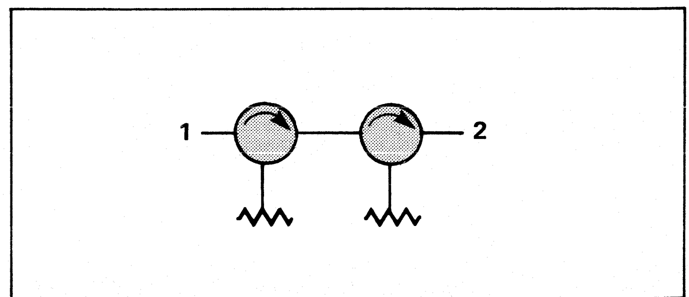

13. High-isolation connection couples a pair of devices.

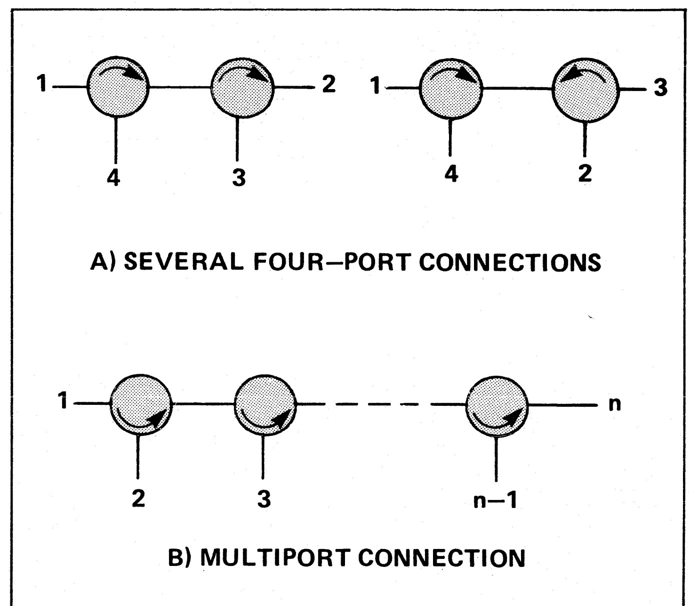

14. Three examples show how multiple circulators can be connected in different configurations.

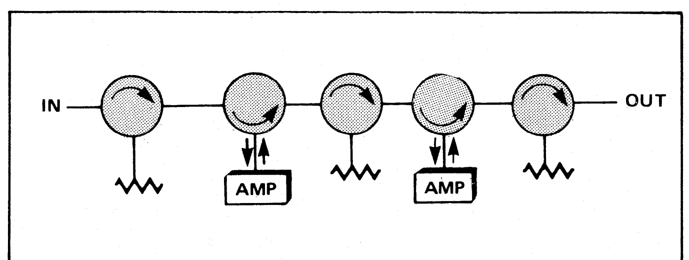

15. Two-stage reflection amplifier uses five junction circulators.

Several examples of the use of the nomogram are given here.

a.) Supposing that one wants the input VSWR that will be obtained with a 20 dB circulator terminated by a 3:1 VSWR (see line A). The result is 1.36:1. The circulator itself will have a VSWR of 1.22:1 if both ports are terminated in matched loads. The VSWR produced by a short circuit is 1.53:1. A horizontal line B through the isolation describes the case of infinite VSWR.

b.) What circulation performance is needed to ensure an input VSWR of less than 1.5 with load VSWR up to 3:1? Line C shows that an 18 dB isolator (VSWR 1.29:1) is adequate. Equation 26 can be used to calculate cases not displayed in Figure 12.

The assumptions made in constructing Fig. 12 are that the circulator is loss-less and well-matched (Isolation > 15dB); losses will improve the isolation. Furthermore, these results are for the worst case, where all the quantities in Equation 26 are taken as purely real. If (3) is mismatched, the input VSWR of the circulator will be larger than the value predicted from the nomogram. In this case, a worst-case VSWR can be obtained by applying Equation 22.

Isolators provide a two-port non-reciprocal transmission line in which propagation from (1)→(2) occurs with low insertion loss while (2)→(1) is the high isolation path. Isolators are frequently employed to control VSWR in various microwave components (such as amplifiers), and to provide protection from high VSWR. They also are used to stabilize microwave generators from frequency changes due to load variations. Isolators can be derived from circulators or can be constructed directly, based on the properties of ferrite loaded non-reciprocal transmission lines. Figure 10b shows a circulator connected as an isolator by the addition of a matched load at port (3). This case is described by Equation 26 and Figure 12.

A circulator with port (3) matched has a significant advantage over other isolator realizations in that an external load can be used. This is particularly helpful in high-power isolators where the power rating is set by the average power that can be dissipated in the load. (See also non-linear loss.)

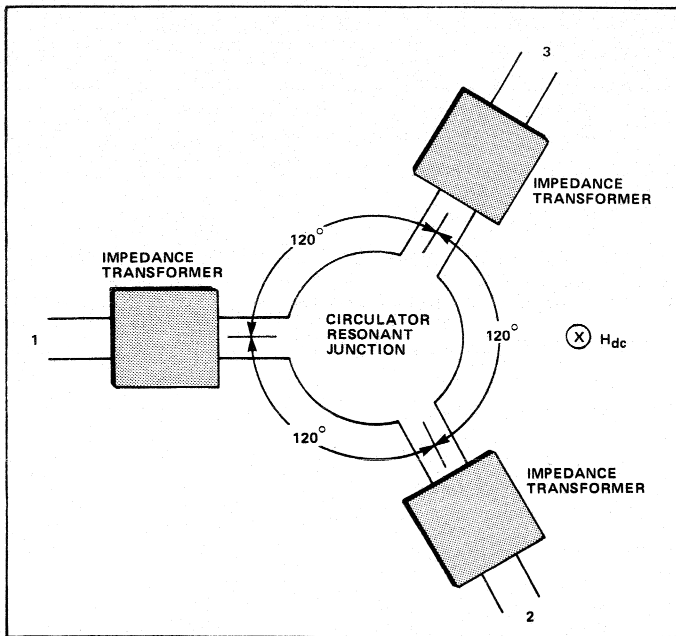

16. Center conductor pattern is used for a stripline or microstrip junction circulator.

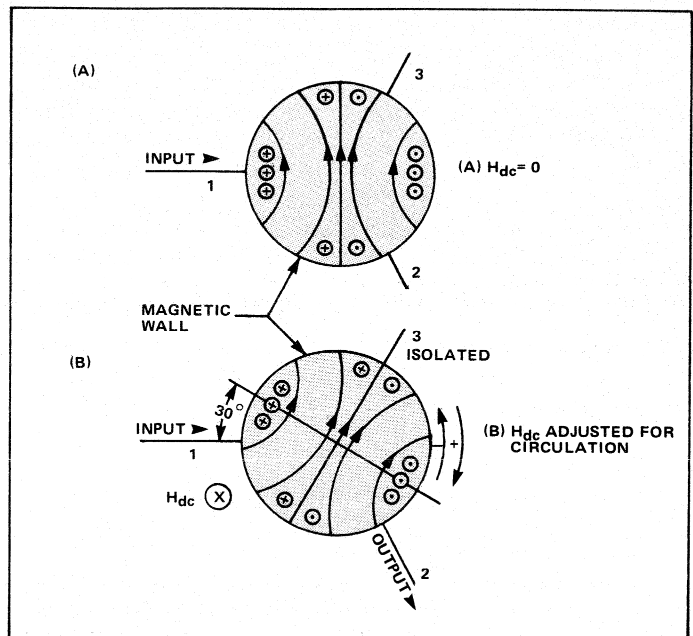

17. These standing-wave patterns are representative of Y-junction circulators. (Fay and Comstock)

Due to the fact that the isolation and input reflection coefficient are related (Eq. 20), there is a trade-off between isolation and bandwidth. High isolation requires a small reflection coefficient which can be provided over only limited bandwidths. Thus, if high isolation and wide bandwidth are both required, moderate isolation (20 dB) circulators (isolators) can be cascaded. The circuit for a wideband, high-isolation isolator is shown schematically in Figure 13. Multiport circulators can also be realized by cascades of three-port devices (Fig. 14). The location of a particular port can be chosen by controlling the sense of circulation (Fig. 13). The penalties incurred in employing multi-junction circulators are greater size, weight, cost, and increased insertion loss. Figure 15 shows a typical application of a multiport circulator in a microwave reflection Gunn or IMPATT amplifier. The input and output circulators are connected as isolators to control input VSWR and to prevent high VSWR instabilities. The third circulator provides interstage isolation.

Operating Principles

Circulators can be realized in rectangular waveguide, stripline, or microstrip geometries. Common to all is a junction region where three transmission lines meet, an appropriately shaped ferrite piece loading the junction, and external bias magnets. The operating principles will be discussed in terms of the Y-junction circulator in stripline or microstrip. The center conductor pattern is indicated in Figure 16. Here three conductors meet the disk resonator at angles of 120° to one another. The junction conductor (and/or ferrite piece) may be circular, triangular or have a three-fold symmetry pattern with respect to 120°.

Two conditions must be satisfied to obtain circulator action: **i**) the junction must be resonant, and **ii**) each port must be impedance-matched. A free-standing ferrite-loaded junction will resonate at an infinite number of frequencies (modes) depending on its shape and the imposed boundary conditions, and many of these modes are degenerate (have the same resonant frequency). However, if a magnetic bias field is applied normal to the plane of the junction, these degenerate modes will split due to the bias field dependent anisotropy of the ferrite. (See Eq. 8 for μ and κ.)

The presence of the transmission lines modifies the boundary conditions and acts to couple the resonator modes. Furthermore, since energy can be extracted from the resonator by the transmission lines, its loaded Q is affected by the width of the lines. A complex standing wave structure results in the resonator whose energy distribution can be controlled by the magnitude of the external magnetic bias field.[49] It is possible to position the field pattern so that energy incident on (1) is coupled to (2) with a minimum coupling to (3). Figure 15 shows a simplified representation for a single pair of unperturbed modes ($n=\pm1$). In Figure 17a, no bias field is applied and so the field distribution is symmetric with respect to (1). The solid curves represent the microwave magnetic field lines, while the circles show the electric field direction. Energy is transmitted equally from (1) to (2) and (3). When an appropriate bias field is applied, the pattern is rotated 30° and port (3) is isolated as shown in Figure 17b. Note the null in the electric field at (3). In this case, the field amplitudes at (1) and (2) are equal, but a 180° phase shift has occurred. Reversing the bias field direction would rotate the pattern to –30° and isolate (2). In this way switchable circulators can be realized.

Permanent magnets located under (and over) the Y-junction resonator provide the bias field. Most circulators are operated just in the vicinity of saturation, with an internal field near zero (Fig. 6). For a flat disk geometry such as encountered in stripline or microstrip circulators, the demagnetizing factors are $N_x=0$, $N_y=0$, and $N_z=1$ (Fig. 5). From Equation 7, the ferromagnetic resonance frequency is $\omega_r = 2\pi\alpha[H_a-4\pi M_s]$ and the internal field is $H_a-4\pi M_s$. This means that an external field about equal to the saturation

magnetization must be applied to the ferrite disk to produce an internal field to saturate the disk.

Once this resonance condition is established at the frequency of interest, the junction must be impedance-matched to obtain $S_{11}=0$. This is the purpose of the networks shown in Figure 16.[50] The isolation bandwidth that can be obtained depends on the frequency difference between the degenerate modes, the variation with frequency of the input impedance on each line at the junction, and the response of the matching networks. A low-Q resonance lends itself to broadband operation. Circulators with 25 percent bandwidths are common, and octave bandwidths can be obtained on microstrip and stripline with proper design.[51] Waveguide designs have yet to yield good performance over full waveguide bands.

Limitations

As the temperature of the ferrite is increased, the saturation magnetization decreases and so does the anisotropy ratio, k/μ. Thus, junction performance will decline as the operating temperature is raised. Likewise the junction resonance will shift lower in frequency. The performance of circulators can be controlled by choosing a material whose $4\pi M_s$ changes slowly over the range of operating temperatures and by designing for adequate bandwidth to accommodate the change in impedance and resonant frequency.

Circulators will exhibit excess insertion-loss characteristics at high power levels as noted previously. Likewise, intermodulation distortion can occur.[27] These undesirable effects can be controlled by use of rare-earth doped garnet materials and by circuit design to minimize the magnitude of the microwave magnetic field.

The anisotropy ratio of the ferrite is given by $\kappa/\mu=\omega_m/\omega$. This indicates that as the frequency increases the ferrite becomes more isotropic in nature; its non-reciprocal properties diminish. The highest value of $4\pi M_s$, (5000 G) and hence ω_4 is obtained with NiZn ferrites (See Table 1); $f_m=\gamma(4\pi M_s)=$ 14 GHz. At 50 GHz $\kappa/\mu=0.28$ and at 100 GHz $\kappa/\mu=0.14$. Wideband components with good performance become difficult to design at high, millimeter frequencies because of the small anisotropy.[52,53]

Phase Shifters

Types of Devices and Applications

Ferrite phase shifters provide a means of adjusting the electrical phase length of a section of transmission line without changing the physical length. In fact, the phase is controlled by the application of an external magnetic field or control current. Ferrite phase shifters are characterized by a large insertion phase, ϕ_0, and a differential phase shift, $\Delta\phi$ which can easily exceed 360°:

$$\Delta\phi = \phi_0 + \phi_2 - (\phi_0 + \phi_1) \tag{27}$$

$$\Delta\phi = \phi_2 - \phi_1 \tag{28}$$

Where ϕ_1 and ϕ_2 are different phase states of the phase shifter.

Insertion phase values at several thousand degrees are not unusual. Ferrite phase shifters typically have low insertion loss, ≤1dB, over moderate bandwidths, >10 percent, and can handle high power levels. Phase control may be either analog or digital. However, in either case the phase is continuously variable with the magnetic field. Ferrite phase shifters also tend to be relatively large and somewhat heavy. Furthermore, since they are controlled magnetically, changing the phase requires changing the applied magnetic field. This tends to be a slower process than can be achieved with the electrically switchable, diode phase shifter. Ferrite phase shifters also may exhibit a phase hysteresis related to the low frequency B-H loop (Section 1).

The devices can be characterized as reciprocal or nonreciprocal, analog or digital, latching or non-latching. The scattering matrices of ideal (loss-free) phase shifters are given by

$$\text{Reciprocal: } [S]_{rec} = \begin{bmatrix} 0 & e^{-J\phi} \\ e^{-J\phi} & 0 \end{bmatrix}$$

$$\text{Non-Reciprocal: } [S]_{non} = \begin{bmatrix} 0 & e^{-J\phi_1} \\ e^{-J\phi_2} & 0 \end{bmatrix} \tag{29a}$$

Reciprocal phase shifters add the same phase to waves traveling in either direction through the device. The nonreciprocal phase shifter adds different phase shifts to waves traveling in opposite directions.

The desired phase state can be achieved either by applying the appropriate field (analog) or by switching fixed phase length or phase bits. Some phase shifters can be designed to use the low-frequency hysteresis loop to obtain remanent (latching) operation, while others require the application of a continuous holding field (nonlatching). The differential phase shift may be either positive or negative.

The differential phase shift depends on the propagation constants of the ferrite loaded transmission line and the physical length, l;

$$\Delta\phi = l(\beta_2 - \beta_1)$$

Or, in normalized form (29b)

$$\Delta\phi = \beta_0 l \left(\frac{\beta_2}{\beta_0} - \frac{\beta_1}{\beta_0} \right) = \frac{2\pi l}{\lambda_0} \left(\widetilde{\beta}_2 - \widetilde{\beta}_1 \right)$$

where β_0 is the insertion phase constant and λ_0 is the guided wavelength in that state. Because of the existence of loss in practical devices, the propagation constant is complex $(\gamma=\alpha+j\beta)$, so phase shifters exhibit insertion loss.

$$\begin{aligned} \text{I.L.} &= \alpha l \\ &= \beta_0 l \frac{\alpha}{\beta_0} \\ &= \frac{2\pi l}{\lambda_0} \widetilde{\alpha} \text{ or, in dB,} \\ \text{I.L.} \Big|_{dB} &= 8.68 \frac{2\pi l \widetilde{\alpha}}{\lambda_0} \end{aligned} \tag{29c}$$

Now γ changes with applied field, so that the insertion loss will depend on the phase state and will be modulated as the phase is varied. A useful figure of merit is the ratio of the differential phase shift that can be obtained compared to the loss:

$$FM = \Delta \frac{\phi_{max}}{I.L.} = \text{degrees/dB} \qquad (29d)$$

One other observation regarding phase shifters can also be made. The impedance in any transmission medium is inversely proportional to the phase constant, i.e.

$$Z_{\omega} \; \alpha \; 1/\beta \qquad (29e)$$

The characteristic impedance is just an apometrical factor times Z_{oo}. So

$$Z_c \; \alpha \; \frac{G}{\beta} \qquad (29f)$$

Thus, as the phase state of the phase shifter is varied the characteristic impedance changes and so the input impedance match, and hence, the input VSWR will also be modulated. The usable bandwidth of any type of phase shifter will depend on the worst case VSWR that can be tolerated in a particular application. ■

References

1. J. Smit and H.P.J. Wign, *Ferrites*, Wiley, New York, 1959
2. R.F. Soohoo, *Theory and Application of Ferrites*, Prentice Hall, Inc., Englewood Cliffs, N. J., 1960
3. P.J.B. Clarricoats, *Microwave Ferrites*, Wiley & Son, N.Y., 1961
4. R.A. Waldron, *Ferrites*, D. Van Nostrand, New York, 1961
5. B. Bax and K.J. Button, *Microwave Ferrites and Ferromagnetics*, McGraw-Hill, New York, 1962
6. A.G. Gurevich, *Ferrites at Microwave Frequencies*, Consultants Bureau, New York, 1963
7. L. Thourel, *The Use of Ferrites at Microwave Frequencies*, Pergamon Press, Oxford, 1964
8. W.H. von Aulock, ed., *Handbook of Microwave Ferrite Materials*, Academic Press, New York, 1965
9. W.H. von Aulock and C.E. Fay, *Linear Ferrite Devices for Microwave Applications*, Advances in Electronics and Electron Physics, Supp. 5, Academic Press, 1965
10. L. Thourel, *Dispositifs a Ferrites Pour Micro-ondes*, Massen & Cie, Paris, 1969
11. J. Helszazn, *Principals of Microwave Ferrite Engineering*, Wiley-Interscience, New York, 1969
12. I. Wolff, *Felder und Wellan in Gyrotropen Microwellenstruturen*, F. Vieweg & Sohn, Braunschunerg, 1973
13. J. Helszazn, *Non-Reciprocal Microwave Junctions and Circulators*, Wiley-Interscience, New York, 1975
14. M. S. Sodah, and N. C. Srivastava, *Microwave Propagation in Ferromagnetics*, Plenum Press, New York 1981
15. "Ferrites Issue," *Proc. IRE*, vol. 44, October 1956
16. W.J. Ince and D.H. Temme, "Phases and Time Delay Elements," *Advances in Microwaves*, Vol. 4, L. Young, Ed., Academic Press, New York, 1969
17. H. Bosma, "Junction Circulators," *Advances in Microwaves*, Vol. 6, L. Young, Ed., Academic Press, New York, 1971
18. F.J. Rosenboum, "Integrated Ferromagnetic Devices," *Advances in Microwaves*, vol. 8, L. Young & H. Sobol, Ed., Academic Press, New York, 1974
19. Reference deleted
20. R.C. Kumar, "Ferrite Junction Circulator Bibliography," *IEEE Trans Microwave Theory Tech.*, vol. MTT-18, pp. 524–530, September 1970
21. R. Knerr, "An Annotated Bibliography of Microwave Circulators and Isolators 1968–1975," *IEEE Transactions on Microwave Theory and Techniques*, vol. MTT-18, pp. 818–825, October 1975.
22. P.E. Tannenwald, "Spin Waves," *Microwave Journal*, vol. 2, pp 25–28, July 1959
23. H. Suhl, "The Nonlinear Behavior of Ferrites at High Microwave Levels," *Proc. IRE*, vol. 44, pp. 1210–1214, October 1944
24. W.H. von Aulock, "Selection of Ferrite Materials for Microwave Device Applications," *IEEE Trans On Magnetics*, vol. 2, p. 251–255, September 1966
25. J.J. Green, F. Sandy, and C.E. Patton, "Microwave Properties of Partially Magnetized Ferrites," Final Report RADC-TR-68-312. Rome Air Development Center, Griffiss Air Force Base, Rome, New York, 1968
26. J.L. Melchor, W.P. Ayres, and P.H. Vartanian, "Microwave Frequency Doubling from 9 to 18 GHz in Ferrites," *Proc. IRE*, vol. 45, p. 643, 1957
27. J.E. Erickson, Y.S. Wu, and W.H. Ku, "Intermodulation Reduction in Communication Systems Using Circulators," Final Report RADC-TR-73-404, Rome Air Development Center, Griffiss Air Force Base, New York, March 1974
28. D. Polder, "On the Theory of Ferromagnetic Resonance," *Phi. Mag.*, vol. 40, pp. 99–115, 1949
29. L. Landon and E. Lifshitz, "On the Theory of Dispersion of Magnetic Permeability in Ferromagnetic Bodies," *Physik Z. Souzetunion*, vol. 8, p. 153, 1935 (in English)
30. J.A. Osborne, "Demagnetizing Factors of the General Ellipsoid," *Phys. Rev.*, vol. 67, p. 351, 1945
31. C. Kittel, "On the Theory of Ferromagnetic Resonance Absorption," *Phys. Rev.*, vol. 71, p. 270, 1947
32. G.T. Rado, "Theory of the Microwave Permeability Tensor and Faraday Effect in Nonsaturated Ferromagnetic Materials," *Phys. Rev.*, vol. 89, p. 529, 1953
33. E. Schlomann, "Microwave Behavior of Partially Magnetized Ferrites," *J. Appl. Phys.*, vol. 41, pp. 204–214, 1970
34. J.J. Green and F. Sandy, "Microwave Characterization of Partially Magnetized Ferrites, and a Catalogue of Low Power Loss Parameters and High Power Thresholds for Partially Magnetized Ferrites," *IEEE Trans. Microwave Theory and Techniques*, vol. 22, pp. 641–645, and 645–651, 1974
35. D. Polder and J. Smit, "Resonance Phenomena in Ferrites," *Rev. Mod. Phys.*, vol. 25, p. 89, 1953
36. M.A. Trenhaft and L.M. Silber, "Use of Microwave Ferrite Toroides to Eliminate External Magnets and Reduce Switching Power," *Proc. IRE*, vol. 46, p. 1538, August 1958
37. L.R. Whicker and R.R. Jones, "A Digital Latching Ferrite Strip Transmission Line Phase Shifter," *IEEE Trans. on Microwave Theory and Techniques*, vol. MTT-13, pp. 781–784, November 1965
38. W.J. Ince and E. Stern, "Nonreciprocal Remanence Phase Shifters Rectangular Waveguide," *IEEE Trans. On Microwave Theory and Techniques*, vol. MTT-15, pp. 87–95, 1967
39. B. Hershenov, "Microstrip Junction Circulator for Microwave Integrated Circuits," *IEEE Trans. on Microwave Theory and Techniques*, vol. MTT-15, pp. 748–750, December 1967
40. J.L. Allen and D.R. Taft, "Ferrite Elements for Hybrid Microwave Integrated Systems," *IEEE Trans. on Microwave Theory and Techniques*, vol. MTT-16, pp. 405–411, July 1968
41. G.R. Harrison, G.H. Robinson, B.R. Savage, and D. R. Taft, "Ferromagnetic Parts for Microwave Integrated Circuits," *IEEE Trans. on Microwave Theory and Techniques*, vol. MTT-19, pp. 577–588, July 1971
42. R.S. Mueller and F.J. Rosenbaum, "On the Latching of Ferrite Microwave Devices," *IEEE Trans. on Microwave Theory and Techniques*, vol. MTT-24, pp. 522–525, August 1976
43. W.E. Hord, C.R. Boyd, Jr., and F.J. Rosenbaum, "Application of Reciprocal Latching Ferrite Phase Shifter to Lightweight Electronic Scanning Phased Arrays," *Proc. IEEE*, vol. 56, pp. 1931–1939, November 1968
44. A.J. Meyerhoff, *Digital Applications of Magnetic Devices*, p. 46, Wiley and Son, New York, 1960
45. R. R. Jones and J. A. Kempic, "Switching Energy of a Microwave Polycrystalline Ferromagnetic Toroid," *Proc. National Electronic Conference*, vol. 21, pp. 56–60, December 1965
46. C.R. Boyd, Jr., "A Dual-Mode Latching Reciprocal Phase Shifter," *1970 G-MTT International Microwave Symposium Digest*, pp. 337–340, May 1970, IEEE Cat. No. 70C10 MTT
47. R.G. Roberts, "An X-Band Reciprocal Latching Faraday Rotator Phase Shifter," *1970 G-MTT International Microwave Symposium Digest*, pp. 341–345, May 1970, IEEE Cat. No. 70C10-MTT
48. H. Bosma, "On Stripline Y-Circulation at UHF," *IEEE Trans on Microwave Theory and Techniques*, vol. MTT-12, pp. 61–72, January 1964
49. C.E. Fay and R.L. Comstock, "Operator of the Ferrite Junction Circulator," *IEEE Trans on Microwave Theory and Techniques*, vol. MTT-13, pp. 15–27, January 1965
50. L.K. Anderson, "An analysis of Broadband Circulators with External Tuning Elements," *IEEE Trans. on Microwave Theory and Techniques*, vol. MTT-22, pp. 849–856, October 1974
51. Reference deleted
52. B. Owen and C.E. Barnes, "The Compact Turnstile Circulator," *IEEE Trans. on Microwave Theory and Techniques*, vol. MTT-18, pp. 1096–1100, December 1970
53. E.J. Dunlinger, "Design of Partial Height Ferrite Waveguide Circulators," *IEEE Trans. on Microwave Theory and Techniques*, vol. MTT-22, pp. 810–813, August 1974
54. J. Helszajn and F.C. Tan, "Design Data for Radial-Waveguide Circulators Using Partial Height Ferrite Resonators," *IEEE Trans. on Microwave Theory and Techniques*, vol. MTT-23, pp. 288–298, March 1975

Understanding Filters And Multiplexers

Microwave multiplexers and their primary components—mixers—are examined, highlighting their practical applications in microwave systems.

By Harold L. Schumacher, *Microphase Corporation*

The microwave filter is a reciprocal two-port device that can be realized as a lumped- or distributed-element network. These lumped- and distributed-element realizations will be discussed with particular emphasis on practical utilization in present microwave systems applications.

Although several physical microwave configurations are discussed, emphasis is given to the lumped-component bandpass filter, interdigital and combline-distributed–element bandpass filters, and the elliptic-function type lowpass and highpass filter designs. Other design methods are also mentioned, complete with references. The Chebychev response shape, because of its widespread use, is considered in detail. A complete set of design curves for the low ripple 0.025-dB condition is included.

Consideration is given to the dissipation-loss relationship for response shapes that can be described in terms of normalized element values, and how bandwidth variation affects the loss for filters with different numbers of resonant circuits. The practical problem of edge-of-band roll-off that usually accompanies sharp-rise filters is also considered.

Attention is focused upon the asymmetry that can be expected from medium- to wide-bandwidth filters of the interdigital, combline and lumped-element varieties and the practical limitations to the use of the Chebychev design curves.

Since the filters that are discussed are the main components of multiplexers, a comprehensive view of non-contiguous and contiguous multiplexers is included. This discussion starts with the non-contiguous multiplexer and ties the two types of multiplexers together by presenting a 24-channel contiguous channelizer constructed of six non-contiguous quadruplexers.

The lowpass/highpass class of multiplexers is considered next. Performance criteria are given in the form of a triplexer. A single diplexer is extracted from the triplexer and used as a model to explain the principle of power splitting, which is present in all direct contiguous multiplexers. The design approach for a complementary pair of Chebychev filters is given using singly terminated, normalized models. Graphs indicate the susceptance cancellation and give the final multiplexed insertion loss and VSWR performance. Finally, performance data are presented for an extremely fast-rise diplexer constructed in coaxial stub configuration.

A comb-line bandpass filter diplexer is used to illustrate partially complementary use of multiplexers, utilizing a susceptance-annulling network. Doubly terminated models are used by eliminating the input sections at the multiplexed input terminals. Graphs are presented showing the input admittance before and after the parallel connection of the two filters and the final input VSWR performance.

Photographs, a block diagram, and actual performance data are included to illustrate the practical realization of microwave multiplexers.

Filters

Entering the maze-like world of electrical filters and selecting the "continuous wave" class of filters, one is led to a group of common "passive" filters. It is these passive filters and groups of filters called multiplexers that constitute the heart of many microwave systems. The mathematical origin of the passive filter is a "lossless reciprocal" four-terminal network. For microwave applications, the networks can either be lumped component, distributed component, or a hybrid combination of the two.

The lumped-element filter has progressively improved over the years by virtue of the consistent improvement in capacitors. The limitations on capacitors for high-frequency microwave filter applications have been the capacitor self-resonant frequency and its unloaded Q. The small ceramic chip capacitors presently available have extended the usable filter frequency range through and beyond X band. Even though the unloaded Qs have improved, they do represent serious dissipation loss limitations at the higher microwave frequencies. Consequently, these miniature lumped-element filters are limited to relatively wide bandwidth applications with low to medium filter selectivity.

The distributed-element microwave filter structure has widespread applications. Since most of these filters use the dominant quarter-wavelength mode, the size of the filter diminishes with increasing frequency. Filters in the lower microwave portion of the spectrum can be miniaturized by use of foreshortening techniques, applicable mainly to the comb-line, loaded-interdigital and loaded-coaxial structures. The interdigital and comb-line configurations usually appear in a thick stripline structure utilizing either round rods or rectangular bars. The unloaded Qs of these structures are high, and consequently losses are relatively low.

Higher-Q filters can be realized in waveguide structures. These filters have become highly specialized because of the advances made in coaxial, strip-line, and lumped-element configurations. Use of waveguide filters is usually limited to extremely low-loss, narrow-bandwidth applications, and/or in pure waveguide systems.

Even though the majority of filters used in military microwave applications are bandpass filters, the lowpass and highpass filters are finding increased application in the current trend towards broadband systems. These uses are more

Continued on page 171

Harold L. Schumacher is head of the Engineering Department at Microphase Corporation, Norwalk, Connecticut.

Continued from page 168

Table I.
A_m = 0.025 dB RIPPLE

N	Ratio Of BW(1 dB)/BW (0.025 dB)	Ratio Of BW (3 dB)/BW(0.025 dB)	Summation Of G Coefficients G(1) to G(N)
2	1.961769	2.658012	1.0646
3	1.396142	1.653751	2.5743
4	1.216916	1.352408	4.2978
5	1.137102	1.221113	6.1796
6	1.094564	1.151901	8.0750
7	1.069191	1.110875	10.0471
8	1.052833	1.084529	11.9915
9	1.041669	1.066595	13.9936
10	1.033707	1.053829	15.9562
11	1.027830	1.044419	17.9707
12	1.023368	1.037280	19.9414
13	1.019900	1.031737	21.9619
14	1.017151	1.027345	23.9368
15	1.014935	1.023806	25.9606
16	1.013122	1.020914	27.9378
17	1.011621	1.018518	29.9634
18	1.010363	1.016512	31.9420
19	1.009300	1.014816	33.9688
20	1.008392	1.013368	35.9482
21	1.007611	1.012123	37.9758
22	1.006934	1.011044	39.9558
23	1.006343	1.010103	41.9840
24	1.005825	1.009277	43.9644
25	1.005368	1.008549	45.9929

directed to multiplexer and multioctave bandpass filter applications than individual components. Even though the common coaxial varying-impedance-type lowpass filter will always find extensive use in microwave systems, the modern broadband applications have exceptionally sharp selectivity requirements. This usually means an elliptic-function-type filter response. As a distributed network, lowpass and highpass filters with series-lumped or distributed elements and shunt-distributed resonate networks have successfully supplied the industry's needs for many years. These exceptionally small coaxial structures are being manufactured to operate at frequencies up to 40 GHz.

Hybrid techniques are used in many applications for the design of all types of filters (lowpass, highpass, bandpass and bandreject). This usually involves the combination of lumped and distributed elements in a single filter. Hybrid techniques can be applied to coaxial structures as well as stripline devices. The resultant filter usually is smaller in size with little or no deterioration in overall performance characteristics.

Filters constructed as microwave integrated circuits are limited to relatively wide-band devices, where the higher insertion losses of the low-Q MIC structure can be tolerated. This restricts the application of filter designs to certain types of low selectivity lowpass, highpass, and bandpass filters. The MIC structure is also susceptible to higher-order modes, which can seriously affect the filter's stopband performance.

The majority of microwave filters are designed to one of the Chebychev response characteristics. There are a multitude of published design techniques that are dependent upon the element values of a lowpass prototype filter.[1] Since element values are available for other response characteristics, such as the maximally flat attenuation or Butterworth condition or the linear phase and Gaussian conditions, appropriate filters can be constructed to provide these response shapes. These polynomial designs have all their poles of attenuation (frequencies of zero transmission) at either DC or infinite frequency. Equation (1)[2] is used to determine the response characteristics of the lowpass prototype Chebychev filter.

$$\text{Attenuation (dB)} = 10 \operatorname{Log}_{10} \left\{1 + \epsilon \cosh^2 \left[N \cosh^{-1} \left(\frac{\omega}{\omega_1} \right) \right] \right\} \quad \omega \geqq \omega_1 \qquad (1)$$

Where $\epsilon = (10^{A_m/10} - 1)$

A_m = Maximum dB ripple in passband

N = Numbers of reactive elements in filter circuit

ω_1 = Edge of passband where the insertion loss is equal to A_m dB

ω/ω_1 = Ratio of radian frequency where the attenuation is desired to the edge of band radian frequency.

Because of the widespread use of the low-ripple Chebychev conditions, Figure 1 is presented as a comprehensive reference for the 0.025-dB ripple condition VSWR = 1.164) for N=2 through 25. This condition should have widespread application for most low-VSWR designs used in any of the physical filter configurations. In those instances where it is

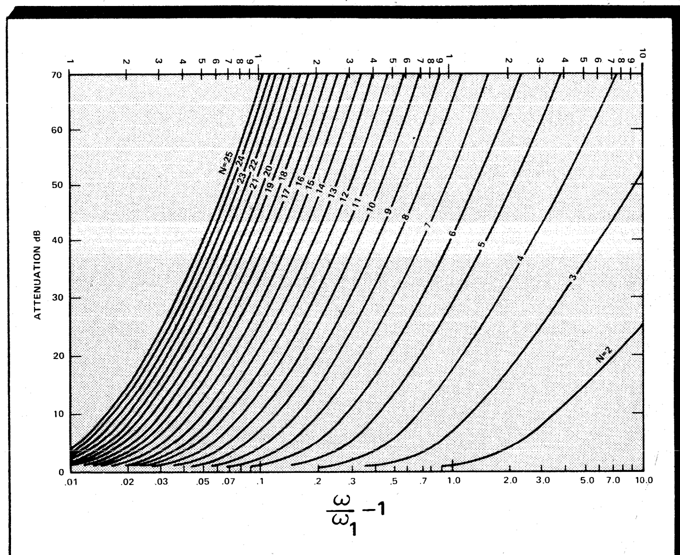

1. Attenuation vs ω/ω_1 - 1 for N = 2 through N = 25 with a ripple bandwidth of A_m = 0.025 dB.

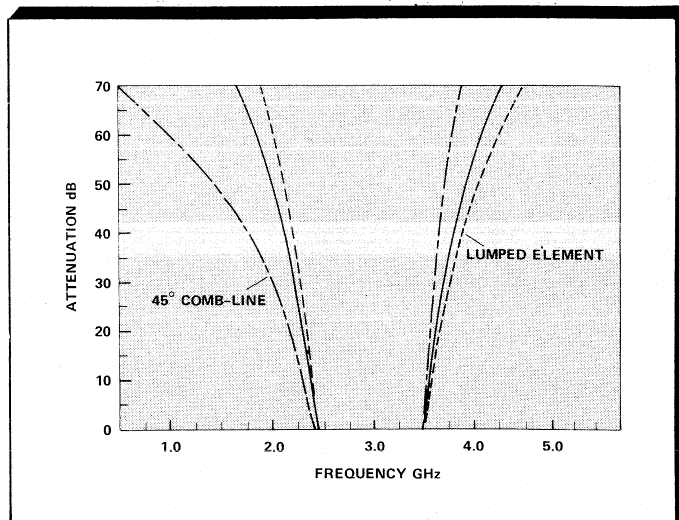

2. Computer generated response characteristics, N = 7, A_m = 0.025, f_o = 3.0 GHz and W (fractional bandwidth) = 0.3333 for a lumped constant and a 45° comb-line bandpass filter, compared with a theoretical symmetrical filter from data of figure 1 (solid curve).

desirable to know the 1-dB or 3-dB bandwidths relative to the design 0.025-dB–ripple bandwidth, Table I gives a tabulation of this ratio for filters with two to 25 resonators. The summation of the G coefficients from G(1) to G(N) for each value of N from two to 25 is also included in the table.

Care should be taken in the use of Figure 1. Note that for ease of presentation on 3-cycle semi-logarithmic paper, the abscissa is plotted as $\omega/\omega_1 -1$. For bandpass filters, utilizing an appropriate transformation, the curves are applicable to filters with symmetric response shapes. The curves are therefore useful for most types of narrow-band filters with bandwidths up to approximately 10 percent. Bandpass filter response shapes are usually asymmetric for wider bandwidths. The interdigital bandpass filter is an exception, with reasonably symmetric response shapes up to and beyond an octave in bandwidth.

To illustrate this asymmetry we will consider two common bandpass filter types:

- The lumped constant design, and
- The comb-line design (45° loading).

Both filters will have the same design parameters, f_o = 3.0 GHz, W = 0.3333 (1-GHz bandwidth), N = 7, and A_m = 0.025 dB. For comparison, the lossless condition is computer analyzed and plotted in Figure 2. The solid curve in Figure 2 is the symmetric condition taken from Figure 1. The interdigital-type filter would closely follow the response of the solid curve.

Although some filter structures are practical with up to 25 resonators (stripline and coaxial applications) other response shapes are required for extremely-sharp-rise, wide-bandwidth applications. These designs can be provided by use of the elliptic-function–type response and the older image parameter theory of design. Both approaches have provisions for the inclusion of resonant circuits between DC and infinite frequency (finite frequencies of zero transmission). Tables of coefficients for various lowpass prototype filters are available for the elliptic function or Cauer type design.[3] A brief explanation, complete with references, of the image parameter theory of design is also available.[4]

The design methods given above will provide complete coverage for most applications. There are, however, those situations that could require a special design, tailored to one specific application; possibly a bandpass filter with drastically different rejection levels for the two skirts, used in an application where the excess filtering derived from a symmetrical design is undesirable. A filter tailored to the specific requirements can be synthesized directly from an appropriate transfer function by use of a digital computer.[5] Although not as versatile as the direct-synthesis method, the image-parameter design technique also gives complete freedom to the placement of finite transmission zeros.

It should be noted that not all of the filter-characteristic designs can be realized as distributed-element microwave structures. Even in lumped-element applications, certain circuit values become impractical, thereby limiting the feasibility of constructing certain circuit types. Even if a microwave structure is feasible, manufacturing and/or cost problems can preclude its use in preference to proven cost-effective designs. An example of this is the digital elliptic filter,[6] an adaptation of the elliptic-function design to the digital-type structure; it has not experienced widespread use in microwave systems, compared with the interdigital- and comb-line-type filters.

The passband insertion loss of microwave filters is of considerable importance in most applications.

The dissipation loss at the center of the passband of small-ripple Chebychev bandpass filters can be determined from[7]

$$L_o(\text{dB}) = \frac{4.343}{WQ_u} \sum_{i=1}^{N} g_i \qquad (2)$$

Continued on page 174

Continued from page 172

Where L_o = Passband frequency dissipation loss

W = Fractional bandwidth = $\frac{\text{ripple bandwidth}}{f_0}$

F_0 = Center frequency

Q_u = Unloaded Q

g_i = Element values of prototype filter

The summation of the g coefficients for the 0.025-dB Chebychev condition for N = 2 to N = 25 is included in Table I.

One important aspect of bandpass filter design is the use of an expanded ripple passband to help decrease the magnitude of the dissipation loss at the passband center and especially at the edges of the ripple bandwidth. The significance of this is most prevalent when N is less than seven resonators as indicated in Figure 3 for a round-rod, interdigital strip-line filter at 12 GHz, with a 60-dB bandwidth of ± 2.0 GHz. When N = 5, A_m = 0.025, the ripple bandwidth is 1000 MHz, and dissipation loss is 0.43 dB for a ground-plane spacing of 0.180 (a practical value of Q_u for this silver-plated filter would be 750). If we now increase N and expand the ripple bandwidth to maintain the same 60-dB rejection at f_o ± 2.0 GHz the insertion loss per equation (2) will give the results indicated in Figure 3. The only assumption made in these calculations is that the Q_u = 750 remains constant as the ripple bandwidth is increased for each value of N. Therefore, for small values of N, filter performance can be improved by increasing the ripple bandwidth and adding one or two more resonators. As N increases this situation changes and an increase in the number of resonators not only causes the center-band dissipation loss to rise but creates a sharp rise in the loss at the edges of the ripple bandwidth.

If we now consider a bandpass filter, N = 17, A_m = 0.025 dB and computer-analyze its passband insertion loss and group-delay performance for two conditions of unloaded Q,[8]

(1) A normal average lossy coaxial filter (WQ_u = 186).
(2) The same filter as (1) reduced in size by using a smaller ground plane spacing (WQ_u = 117).

Both of these filters are centered at 12 GHz with a 1000-MHz equal-ripple bandwidth. The passband edge results are plotted in normalized fashion in Figure 4, expanded to show the behavior over the last 125 MHz of the actual edge of the band. The group-delay plot indicates the slight decrease in peak group delay as the dissipation loss of the filter increases.

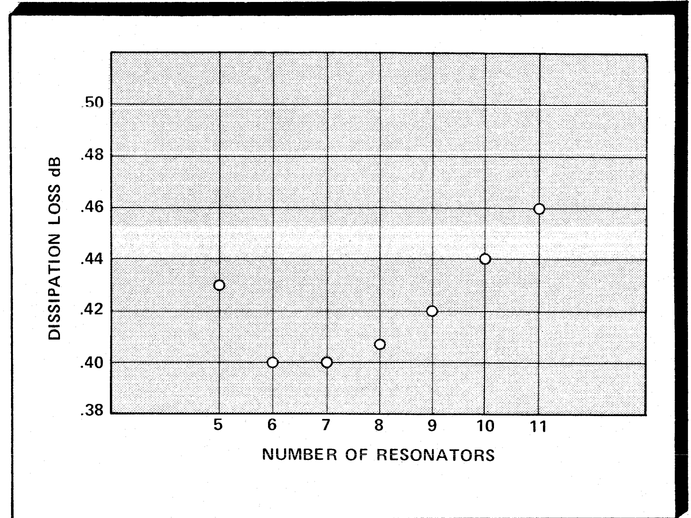

3. Dissipation loss for interdigital filters with 5 to 11 resonators at A_m = 0.025 dB, a varying ripple bandwidth, Q_u = 750, and a 60-dB attenuation at 10.0 and 14.0 GHz using equation (2).

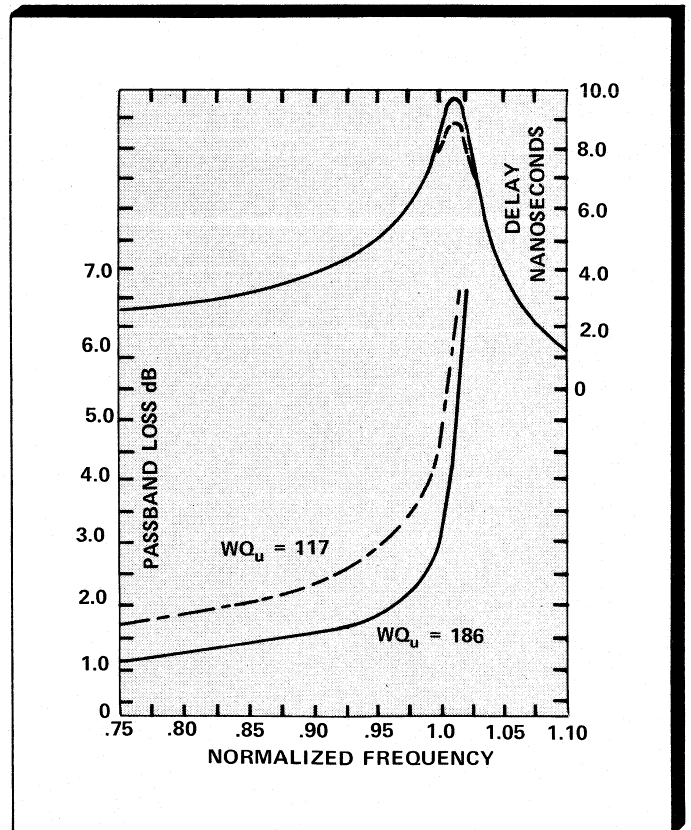

4. Computer generated passband loss vs normalized frequency for an average lossy interdigital filter (WQ_u = 186) and a smaller filter with 37 percent reduction in Q_u(WQ_u = 117).

Multiplexers

When two or more filters are combined at a common input or conversely are combined for a common output, the filtering device is termed a multiplexer. If two adjacent filters share a common crossover frequency (each filter has 3-dB branching loss), the multiplexer is termed a contiguous multiplexer. All other multiplexers that do not share a common crossover frequency can be called non-contiguous multiplexers.

The design of the non-contiguous multiplexer is relatively straightforward because all the filters of the multiplexer are designed as if they would operate as individual filters (the real part of the input admittance is matched to the external circuitry and the imaginary part is zero). The common junction of the non-contiguous multiplexer is therefore designed

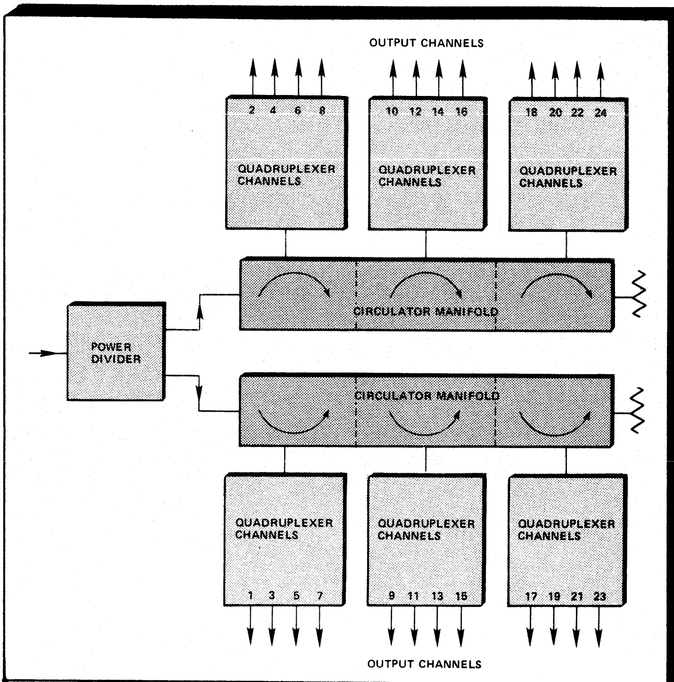

5. Block diagram of Microphase model R3814 24 channel-channelizer.

such that, at the operating frequencies of each individual filter, all other filters present an open circuit at the common junction.

A typical frequency channelizer following this multiplexing principle has been built. The channelizer has a single input port covering a 1.0-GHz bandwidth from 2.5 to 3.5 GHz. The outputs consist of 24 equal and contiguous narrowband channels. Although the outputs are contiguous, the basic component of the subsystem is a non-contiguous quadruplexer. As shown in Figure 5, a power divider splits the input into two equal paths, each of which feeds a circulator manifold (three cascaded circulators). One manifold is used to multiplex the even channels while the other manifold is used to multiplex the odd channels. Consequently, the outputs of each quadruplexer are non-adjacent channels. Each individual filter used in the six quadruplexers is a four-resonator combline design. Each quadruplexer is constructed in a cluster configuration fed through a common junction at the input connector. All the quadruplexers are designed to be identical in size, leading to the compact symmetrical packaging of this multiplexer. The 1-dB bandwidth of each comb-filter is 40 MHz; all channels of the channelizer cross over at the nominal 1-dB points. The use of a power divider with the accompanying sacrifice of 3 dB in power allows for the overlap at the crossover frequency. The same configuration can be used for

6. Ideal 1.0 to 8.0 GHz triplexer showing extent of cross-over region and resultant branching losses. Response of end-of-band highpass and lowpass filters are shown dotted.

different output combinations. If all the quadruplexers were replaced by triplexers, we would have an 18-channel channelizer. Combinations of quadruplexers, triplexers, and diplexers can result in any combination of outputs.

Contiguous multiplexing can best be illustrated with the use of lowpass and highpass filtering; Figure 6 is a 1.0-to-8.0-GHz triplexer.[9] In this figure the band-end response characteristics and their respective highpass and lowpass filters are shown dotted. Without these filters, the low-frequency passband will extend to DC, and the high-frequency passband will extend to an upper frequency defined by the multplexer specification. Analyzing this response even further, Figure 7 shows the lowpass and highpass filters which have been extracted from the triplexer of Figure 6. Figure 7 represents a diplexer, which is the basic building block of the lowpass-highpass multiplexer (the multiplexer consists of cascaded diplexers). The individual filters complement each other and, consequently, when properly diplexed, present a constant resistive input impedance throughout the cross-over region.

The passband insertion loss of these multiplexers is typically less than 1 dB, exclusive of the cross-over region. Referring to Figure 7, energy is split between two physical channels in the cross-over region and, as a result, the multiplexer is subject to branching losses. These losses cause a gradual transition from the in-band insertion loss to the steep-rise portion of each of the filter skirts. After the 16-dB skirt rejection level (0.1-dB branching loss), each filter resumes its nominal rejection characteristics. This transition must be present in all direct contiguous multiplexers. Note in Figure 7, at frequency f, the energy is unequally split between the low- and high-frequency channels. If the low-frequency channel has a loss of 5 dB, excluding dissipation loss, the branching loss of the high-frequency channel is 1.65 dB (similar to the feed-through loss of a 5.0-dB directional coupler). As shown in

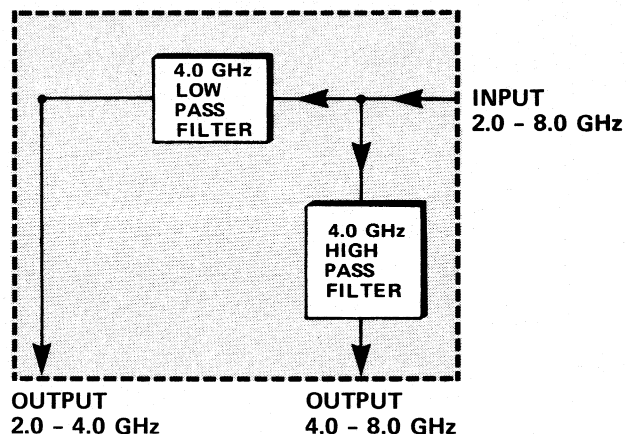

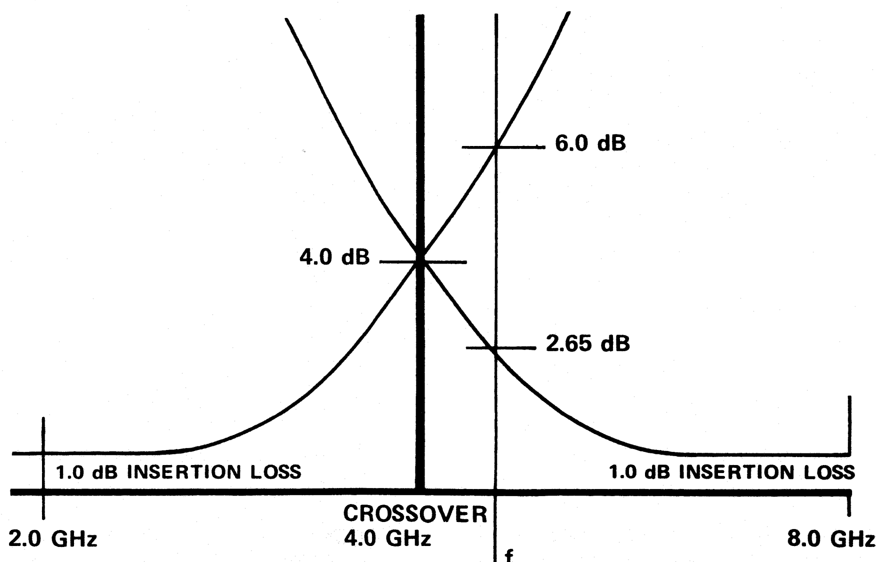

7. Response of a single diplexer extracted from triplexer of Figure 7 shows cross-over point and the unequal power splits that result between the low and high frequency channels at frequency f.

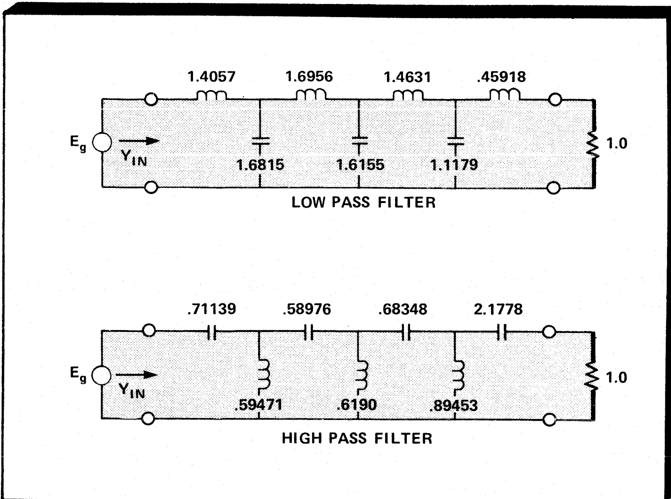

8. Normalized N = 7, A_m = 0.025 dB singly terminated lowpass and highpass filters.

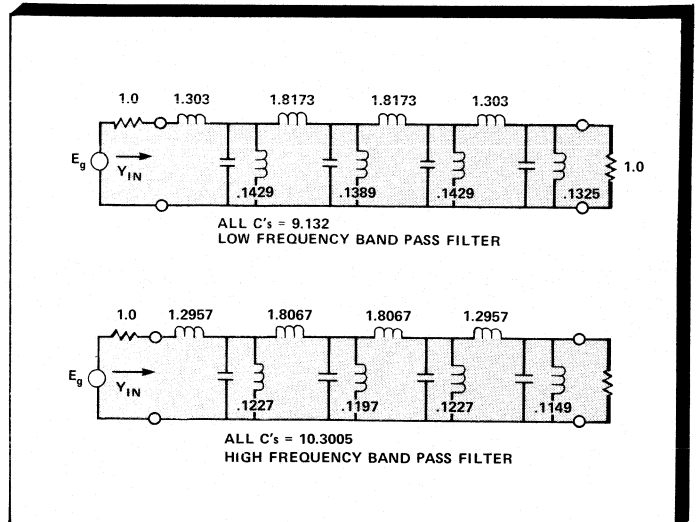

10. Normalized N = 5, A_m = 0.025 doubly terminated lumped-element comb-line type bandpass filters with first resonator removed.

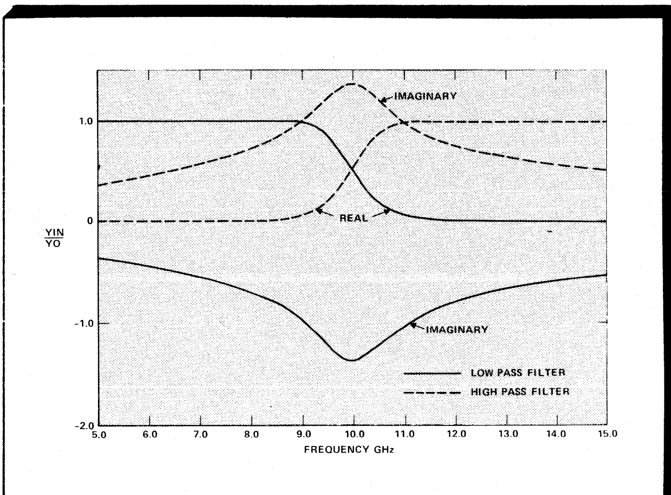

9. Computer generated Y_{IN}/Y_O vs frequency for each filter of figure 8, showing the real and imaginary parts of both filters.

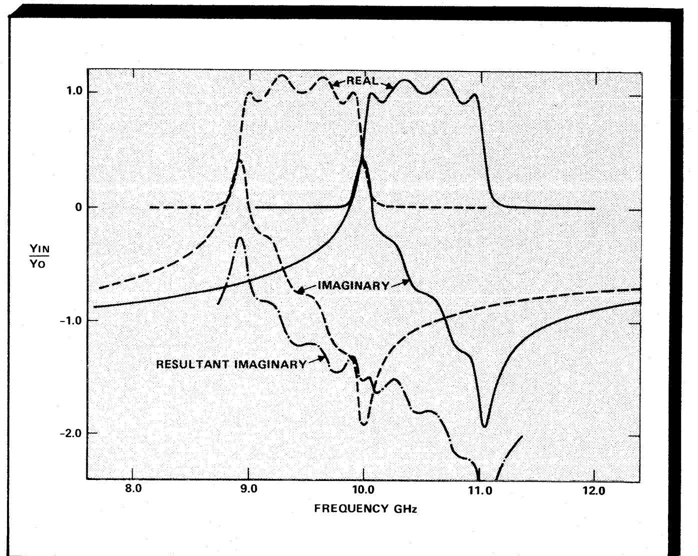

11. Computer generated Y_{IN}/Y_O vs frequency for each filter of Figure 10 showing the real and imaginary parts of both filters. The resultant addition of the two imaginary parts is also shown.

Figure 6, the cross-over region extends up to the cross-over frequency. The insertion loss in this region increases from the highest loss in the passband (which occurs at the edges of the band) to the actual cross-over loss. This loss includes a 3-dB branch loss because of the equal disribution of energy between two adjacent channels at this frequency.

A lowpass and a highpass filter can be contiguously diplexed if each filter is a minimum-susceptance network as seen looking into the common junction diplexed terminals.[10] When properly diplexed, the input admittance at the common terminal will be matched to the external source. To illustrate this, consider the computer analysis of a Chebychev lowpass and highpass filter, both N=7, A_m = 0.025. Two singly terminated filter networks will meet the criteria of the minimum-susceptance network. These circuits are shown in Figure 8 and the real and imaginary parts of their respective input admittances are shown in Figure 9. Proper design requires that the cutoff frequencies of each filter be adjusted such that the real part of the input admittance is approximately 0.5 mhos (normalized) for each filter.

It is evident from the VSWR/attenuation response of the filter when combined in parallel to form a diplexer that the imaginary part of Y_{in} of the filters is of such value that their addition will result in an approximate zero value when the two filters are combined. The two filters tend to complement each other. Contiguous diplexers constructed of lowpass and highpass filters are therefore called complementary diplexers.

Actual multiplexers designed to meet systems specifications require high degrees of isolation between channels. Broadband filters, such as Chebychev lowpass and highpass filters, usually cannot physically meet these steep skirt requirements, because their poles of attenuation are either located at DC (highpass) or infinite frequency (lowpass). Filters that can meet these steep requirements are those that exhibit poles of

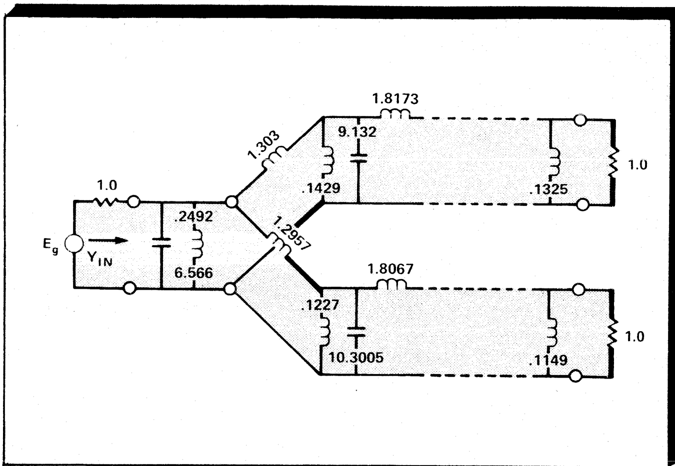

12. Parallel connection of two filters of figure 10 and the addition of the susceptance-annulling network at the input terminals of the diplexer.

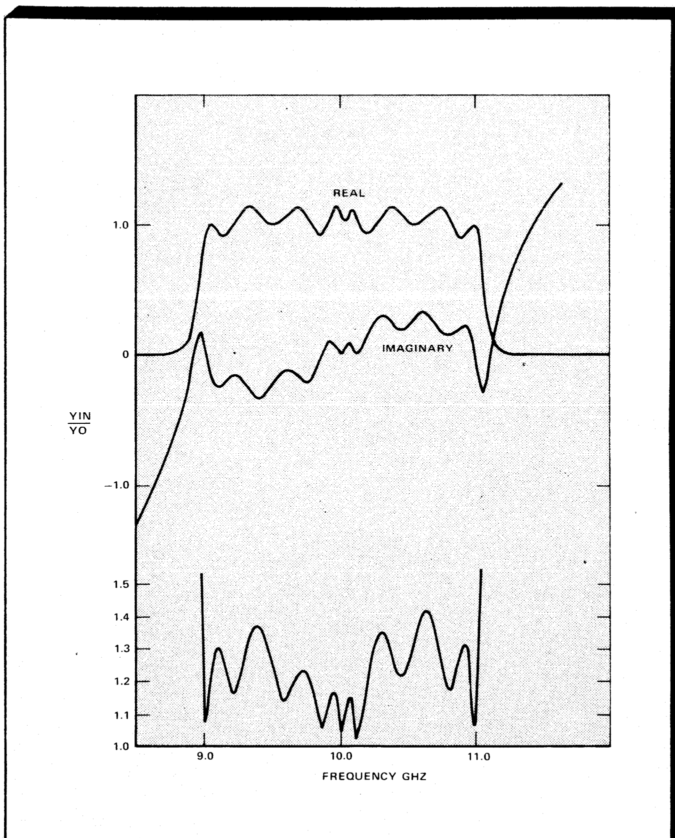

13. Computer generated Y_{IN}/Y_O and VSWR vs frequency for the parallel-connected diplexer of figure 12.

attenuation at finite frequencies located close to the edge of the passband. In a coaxial configuration, these stub-type filters utilize shunt elements, which are distributed resonant networks producing elliptic-function–type stopbands. A plot of the actual data for an extremely sharp-rise diplexer of the coaxial stub type shows that this diplexer has a 3.2 percent selectivity on the highpass skirt and a 3.6 percent selectivity on the lowpass skirt measured between the cross-over frequency and the first 60-dB frequency.

Two bandpass filters can also be multiplexed if each filter is a minimum-susceptance network at the input terminals. To illustrate this we will consider the computer analysis of two normalized circuits using the lumped constant equivalency of a comb-line–type filter.[11] In this design approach, two doubly-terminated circuits are chosen and then the first resonator from each filter is eliminated, thereby converting the circuit to the minimum input susceptance requirement. Both filters will be $N = 5$, $A_m = 0.025$ designs with an approximate cross-over frequency of 10 GHz. Figure 10 illustrates the two foreshortened band-pass filter circuits and Figure 11, shows the real and imaginary part of the input admittance, of the individual filters. As can be seen from Figure 11, the imaginary part of the input admittance does not cancel when the two circuits are connected in parallel. The approximate resultant susceptance is also sketched in Figure 11.

This resultant susceptance can be approximately cancelled by the positive portion of the susceptance of a parallel resonant circuit connected at the common diplexer terminals. Figure 12 is the final circuit with the parallel resonant circuit at the input terminals; Figure 13 is a graph of the overall input admittance, and the diplexer input VSWR.

Because the susceptance of two bandpass filters does not completely cancel when contiguously multiplexed, the multiplexer is called a partially complimentary multiplexer. The resonant circuit added to the input terminals is called a susceptance annulling network. ■

References

1. G. L. Matthaei, Leo Young, and E. M. T. Jones, *Microwave Filters, Impedance-Matching Networks, and Coupling Structures*, McGraw Hill Book Co., Inc., New York, N.Y., 1964, Ch. 4.
2. G. L. Matthaei, Leo Young and E. M. T. Jones, *Microwave Filters, Impedance-Matching Networks, and Coupling Structures*, McGraw Hill Book Co., New York, N.Y., 1964, page 86.
3. Anatol I. Zverev, *Handbook of Filter Synthesis*, John Wiley and Sons, Inc., New York, N.Y., 1967.
4. G. L. Matthaei, Leo Young and E. M. T. Jones, *Microwave Filters, Impedance-Matching Networks, and Coupling Structures*, McGraw Hill Book, Co., Inc., New York, N.Y., 1964, Ch. 3.
5. George Szentirmai, "FILSYN-A General Purpose Filter Synthesis Program," *Proc. of IEEE* Vol. 65 No. 10, October 1977, pp 1443-1458.
6. M. C. Horton, and R. J. Wenzel, "The Digital Elliptic Filter—A Compact Sharp-Cutoff Design for Wide Bandstop or Bandpass Requirements," *IEEE Transactions on MTT*, Vol MTT-15, No. 5, May 1967, pp 307-314.
7. Harold L. Schumacher, "Dissipation Loss of Chebychev Band Pass Filters," *Microwave Journal*, August 1967, pp 41-43.
8. Robert L. Sleven, "Pseudo-Exact Band Pass Filter Design Saves Time," *Microwaves*, August 1968, pp 38-47.
9. Harold L. Schumacher, "Coax Multiplexers: Key to EW Signal Sorting," *Microwave Systems News*, August/September 1976, pp 89-93.
10. L. Young, *Advances in Microwaves*, Academic Press, New York, N.Y. 1967, pp 237-326.
11. P. La Tourrette, "Combline Filter Multiplexers," *Microwave Journal*, August 1977, pp 55-59.

Designing a Synthesized Signal Generator

YIG oscillators are crucial to design of modern instrumentation. This article progresses step-by-step through the design of a real-world product based on YIG-tuned oscillators: a synthesized signal generator.

By Howard W. Mette, Giga-tronics, Inc.

The requirements for designing, testing, maintaining, and calibrating today's sophisticated radar, EW, and telecommunications systems have created a demand for microwave signal sources that have the combined frequency precision, signal controllability, and spectral purity found only in a synthesized signal generator. These sources are in demand for general-purpose design and testing of components and subsystems, as well as in ATE applications for system production test, field maintenance, and calibration.

This article describes a microprocessor-controlled, synthesized signal generator design that allows one to easily configure specific instruments in order to most economically accommodate applications for single or multi-band coverage in the frequency range of 50 MHz to 26 GHz. It provides high powered, exceptionally clean and stable, leveled outputs which can be swept, attenuated, and modulated to meet the most exacting test requirements.

Two-Loop Indirect Synthesis With Downconversion

The technique employed to generate frequencies in the 2- to 26-GHz range is known as two-loop indirect synthesis because, as we shall see, it uses two closed loops—the reference loop and the output loop—to establish precise, stable output frequencies. Output frequencies below 2 GHz are established by a downconversion technique using two of the output YIG-tuned oscillators.

Before discussing two-loop indirect synthesis and downconversion, it is important to understand the operation of two basic circuits that are used repeatedly: the phase-lock loop and the sampling mixer.

- *The Phase Lock Loop* (PLL). A PLL provides a means of phase locking a variable oscillator (VCXO or YIG) to a fixed frequency oscillator (master reference), thereby imparting the accuracy and stability of the master reference to the output of the variable oscillator.

A simple example (Fig. 1) shows a 100-MHz VCXO, which we want to control so that its output has a stability of 1 part in 10^{-6}/year. It is phase locked to a master reference that has that stability.

The VCXO is operating at some frequency, 100 MHz $\pm x$, and its output is divided by 10 to obtain an input to the phase detector of 10 MHz $\pm x/10$. The other input to the phase detector is from the 10-MHz master reference. The outputs from the phase detector are pulses the width of which are proportional to the time difference in the zero crossing of its input signals. If the divide-by-10 signal leads the master reference, pulses will be present at one output. If the divide-by-10 signal lags the master reference, pulses will be present on the other output. In either case, the pulse width will be proportional to the amount of lead or lag.

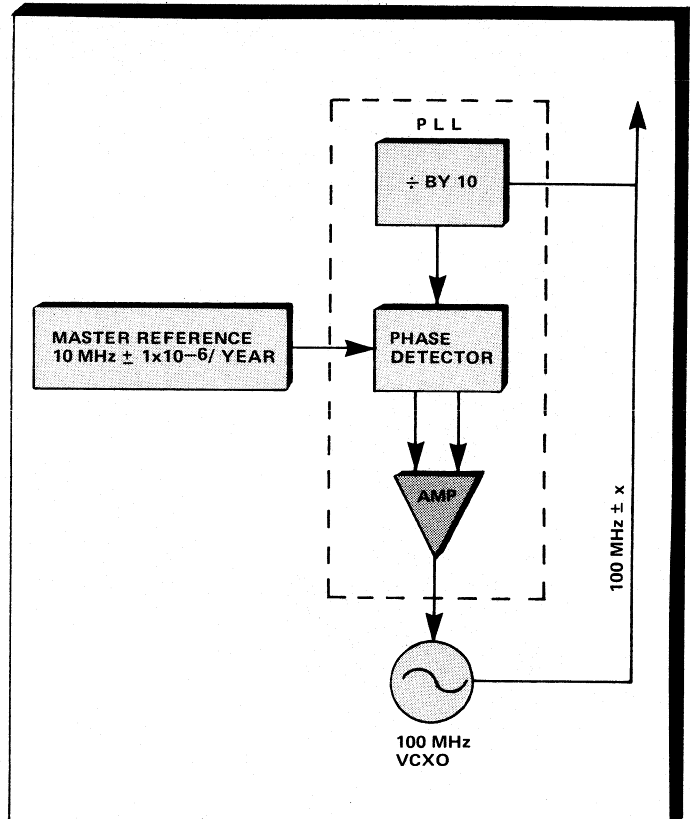

1. Phase-lock loops impose the stability of a master reference on the output of a variable oscillator.

The amplifier acts as a low-pass filter with gain so that its output amplitude is a DC signal (voltage or current, depending on oscillator requirements) proportional to the phase (zero crossing time) difference of the two phase-detector inputs. Note that if the signals at the two phase-detector inputs are slightly different in frequency, their phase (zero crossing time) difference will continue to increase (Fig. 2). The negative feedback within the PLL will correct for this changing phase difference. Since the feedback causes the phase difference to remain constant, the frequency difference must be zero. Thus, the amplifier's output signal controls the frequency of the VCXO, tuning it to reduce the error

Howard W. Mette is the marketing manager for Giga-tronics, Inc., 2495 Estand Way, Pleasant Hill, Calif.

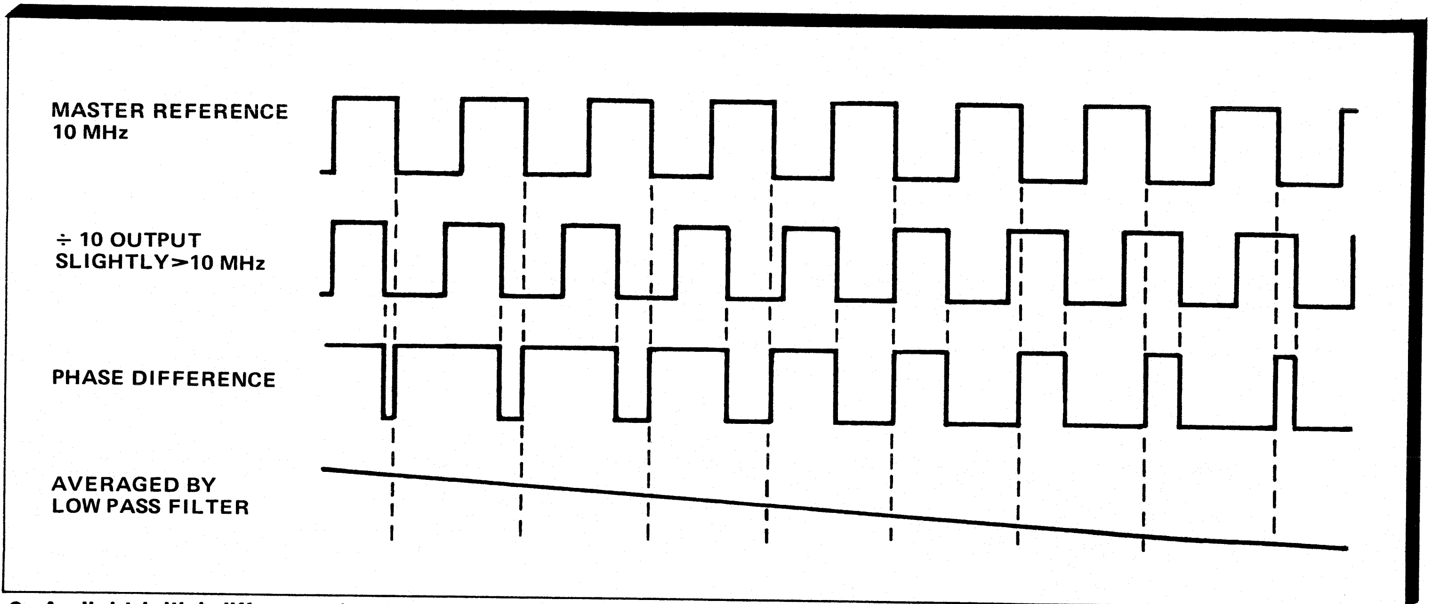

2. A slight initial difference in phase will increase, unless the negative feedback from a phase-lock loop corrects for the difference.

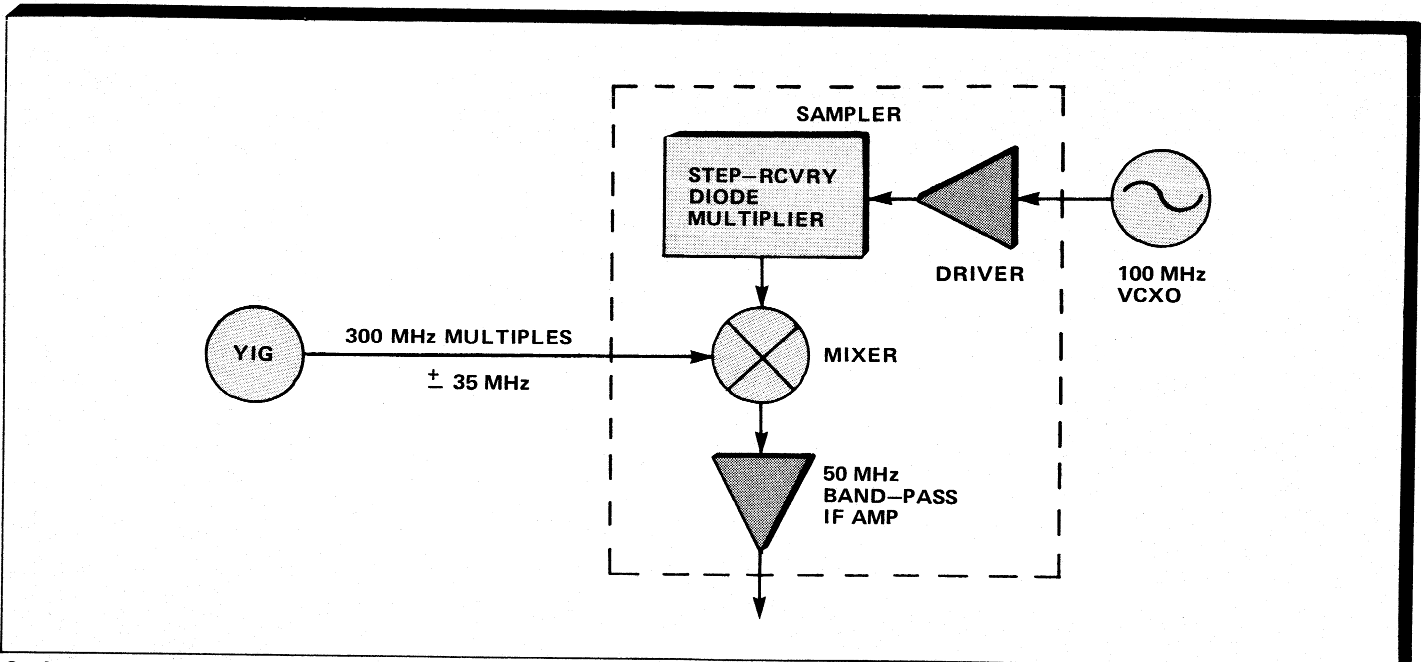

3. A sampler mixer selects the proper IF, generated as the difference betweeen a YIG-output and a multiplied VCXO at a lower frequency.

(x), until its frequency is exactly 10 times the frequency of the master reference.

• *The Sampling Mixer (Sampler).* The samplers used in the design generate a properly selected intermediate frequency (IF), which is the difference between a YIG-generated microwave frequency and the proper multiple of a second, lower frequency.

A simple example (Fig. 3) of this could be a YIG-tuned oscillator that can be coarse-tuned to within ±35 MHz of multiples of 300 MHz, and it is necessary to generate an IF that will show how far from the 300-MHz multiple it is and in which direction. The step-recovery diode multiplier produces harmonic multiples of 100 MHz and inputs them to the mixer. The other input to the mixer is the YIG frequency, which is known to be within ±35 MHz of a 300-MHz multiple. Of all the possible beat frequencies, only one will be less than 50 MHz; it is the only one that will pass through the 50-MHz bandpass IF amplifier. The output frequency of that amplifier will tell how far from the 300-MHz multiple the YIG frequency is and in which direction from it.

For the sake of simplicity, in the following discussion of two-loop indirect synthesis and downconversion, the phase-lock loop and the sampling mixer will be denoted by the block diagram symbols:

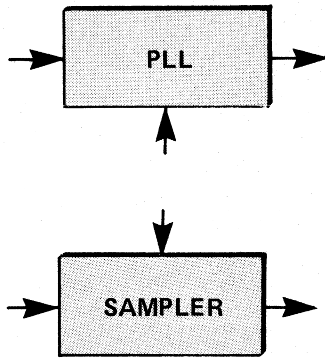

As noted previously, frequencies between 2 and 26 GHz are generated by the use of two closed loops, the reference loop and the output loop.

• *The Reference Loop.* The purpose of the reference loop is to produce a series of precise frequencies in 300-MHz steps from 2 to 26 GHz, select the proper one as reference for a desired output frequency, and lock it to the master reference.

First, the following algorithm:

$$\mathrm{INT}\,[(f_{out} - 100)/300] \times 300 + 5 = f_{ref}$$

where f is in MHz.

The reference frequencies (f_{ref}) produced by this algorithm are in steps of 300 MHz. That is, the output frequency (f_{out}) can change by 300 MHz before the reference changes, as may be seen in the table.

If the signal generator is asked (via front panel control or remote programming) for an output frequency of 5.678 GHz, the microprocessor immediately calculates the proper reference frequency:

$$\begin{aligned} f_{ref} &= \mathrm{INT}\,[(5{,}678 - 100)/300] \times 300 + 5 \\ &= 1\ \mathrm{INT}\,[5{,}578/300] \times 300 + 5 \\ &= \mathrm{INT}\,[18.59333333] \times 300 + 5 \\ &= 18 \times 300 + 5 = 5{,}405\ \mathrm{MHz} = 5.405\ \mathrm{GHz} \end{aligned}$$

Using this calculated f_{ref} (Fig. 4), the microprocessor supplies the proper digital input to the digital-to-analog converter (DAC) to coarse-tune the reference YIG, through

Continued on page 190

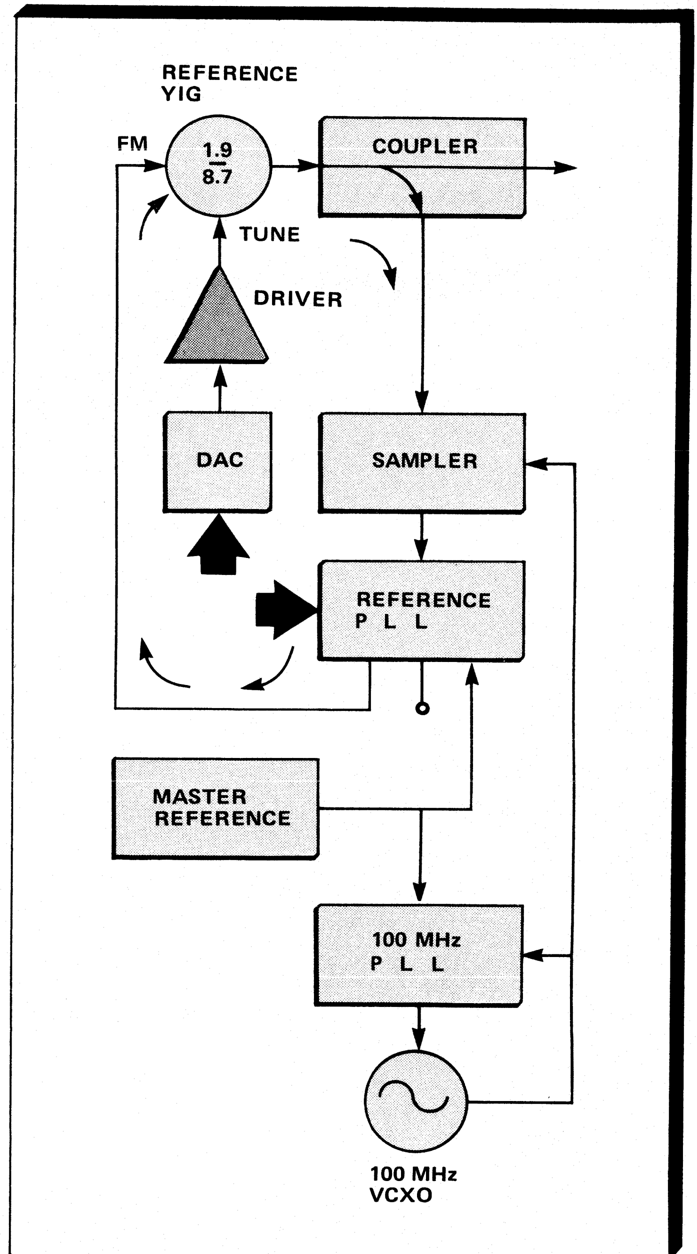

4. Coarse tuning of the YIG is achieved with a microprocessor signal sent through a digital-to-analog converter.

Table I.
For f_{out} of: $(f_{out} - 100)/300$ is: & INT $[(f_{out} - 100)/300] \times 300 + 4 = f_{ref}$

For f_{out} of:	$(f_{out} - 100)/300$ is:	&	INT	$\times 300 + 5 = f_{ref}$
2499 MHz	7.996666667	&	7	× 300 + 5 = 2105 MHz
2500 MHz	8.000000000	&	8	× 300 + 5 = 2405 MHz
•	•	•	•	• •
•	•	•	•	• •
2799 MHz	8.996666667	&	8	× 300 + 5 = 2405 MHz
2800 MHz	9.000000000	&	9	× 300 + 5 = 2705 MHz
•	•	•	•	• •
•	•	•	•	• •
3099 MHz	9.996666667	&	9	× 300 + 5 = 2705 MHz
•	•	•	•	• •
•	•	•	•	• •

Continued from page 186

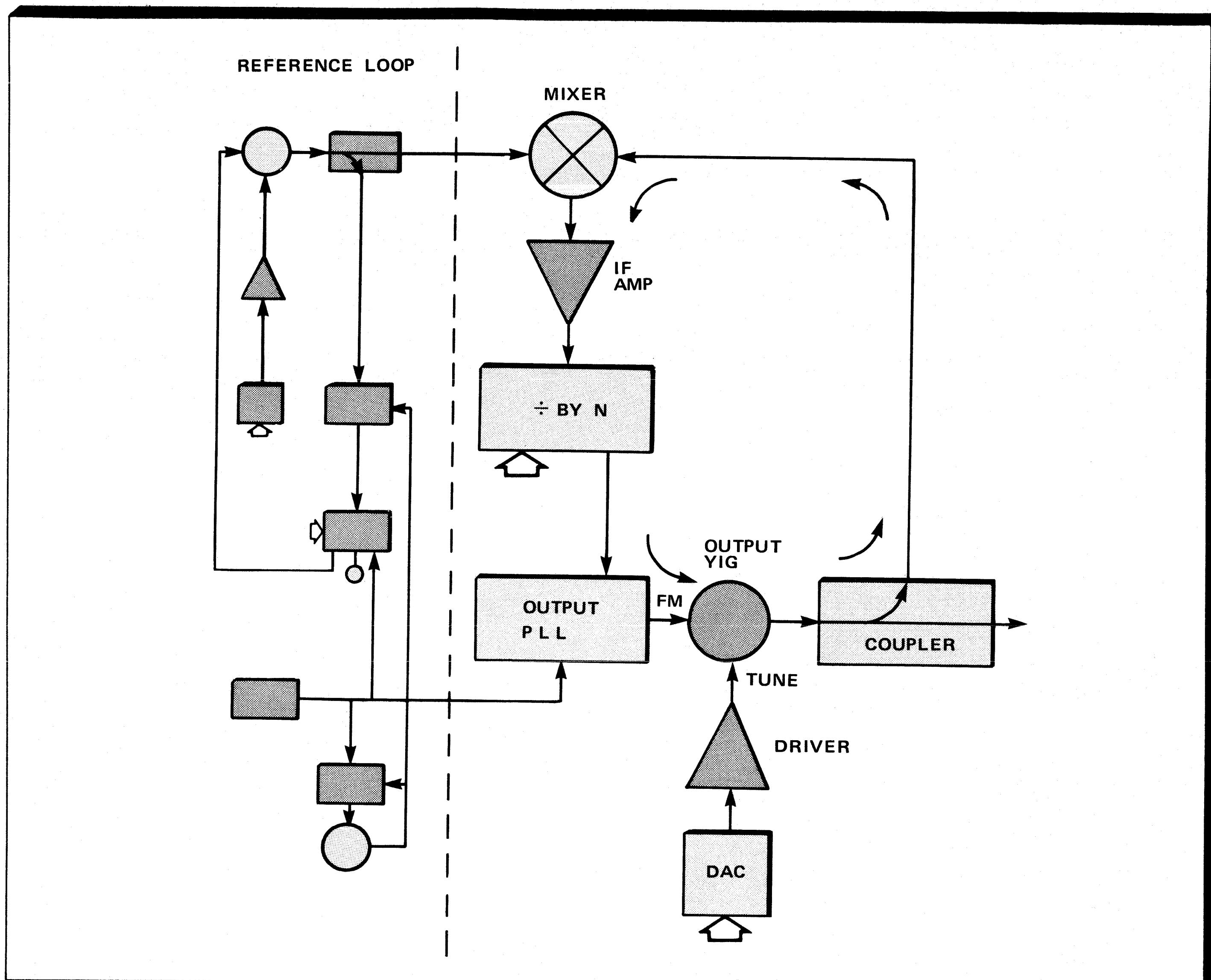

5. In the output loop, a microprocessor again controls the output YIG, tuning it until the phase detector output is balanced and the output YIG is locked to the master reference.

the YIG driver, to 5.405 GHz. Accuracies and linearities of the DAC, driver, and YIG are such that this coarse tuning will bring the YIG to within ±35 MHz of the desired f_{ref}. A portion of the YIG output is coupled to the sampler. This coupler incorporates two switched filters to reduce oscillator harmonics in the sampler path, preventing the possibility of false locks. The sampler mixes the YIG frequency with multiples of 100 MHz (which are phase-locked to the master reference) to produce IFs. Since the YIG is at 5.405 GHz ±35 MHz, the 54th harmonic will produce an IF that is less than 40 MHz (−30 to +40 MHz), which will pass through the 50-MHz band-pass IF amplifier to the reference PLL. The reference PLL compares this IF to 5 MHz (the 10-MHz master reference divided by 2) in its phase detector, and sends a correction signal to the YIG FM coil in a direction to reduce the error. When the IF is 5 MHz, the output of the reference PLL is balanced and the YIG is at 5.405 GHz, phase locked to the master reference.

The generation of reference frequencies for other desired signal generator outputs are established in a similar manner, except for two obvious areas that do not fit the foregoing explanation: outputs below 2.199 GHz and above 7.999 GHz. For output frequencies from 2.000 to 2.199 GHz, the algorithm yields an f_{ref} of 1.805 GHz. This is below the lower frequency limit of the reference YIG (1.9 GHz). So, for output frequencies below 2.200 GHz, the microprocessor system automatically establishes an f_{ref} of 1.905 GHz and subsequently compensates for it in the divide-by-N circuit of the output loop.

For output frequencies above 7.999 GHz, the required reference frequencies will soon exceed the upper frequency limit of the reference YIG (8.7 GHz) and cannot be operated on a 1:1 basis with the output. Therefore, for output frequencies of 8 to 26 GHz, the reference YIG is operated on a 1:3 basis with the output, and its third harmonic is used in subsequent circuitry. This allows a much smaller tuning

range for the reference and permits a single oscillator to be used. For output frequencies above 7.999 GHz, the sampler phase detector's reference is also changed from 5 MHz to 1.667 MHz (5/3).

- *The Output Loop*. The function of the output loop is to complete the generation of the final output frequency. The output loop and its relationship to the reference loop are illustrated in Figure 5. In a manner similar to that which we saw in the reference loop, the microprocessor provides a digital input to the output YIG DAC. The DAC converts this digital input to an analog signal which coarse-tunes the output YIG to 5.678 GHz (the desired output frequency for this example) within about ±35 MHz. A coupler delivers a portion of the YIG output to a mixer. The other input to the mixer is the 5.405 GHz to which the reference loop is locked. If the output YIG is at exactly 5.678 GHz, the IF from the mixer will be 5.678 GHz – 5.405 GHz, or 273 MHz.

While the action described above is taking place, the microprocessor calculates the difference between the desired output frequency and the selected reference frequency. It then sets an N of 273 into the divide-by-N circuit. Thus, it can be seen that if the IF from the mixer is 273 MHz, the output of the divide-by-N circuit will be 1 MHz. The phase detector in the output PLL compares the output of the divide-by-N circuit with 1 MHz (the 10-MHz master reference frequency divided by 10). If the output of the divide-by-N circuit is something other than 1 MHz (i.e., the output YIG is not at exactly 5.678 GHz and, thus, the IF from the mixer is not exactly 273 MHz), the output PLL creates a signal to drive the FM coil of the output YIG in a direction to reduce the error. This action continues until the phase detector output is balanced (i.e., both of its inputs are at 1 MHz). The output YIG is then at exactly 5.678 GHz and it is phase-locked to the master reference.

Every instrument contains the 1.9- to 8.7-GHz reference loop YIG-tuned oscillator, and may contain from one to four output YIG-tuned oscillators, depending on the output frequencies required for a particular application. YIG-tuned oscillators covering the 2 to 8, 8 to 12, 12 to 18 and 18 to 26 GHz bands are used as required. Depending on the specific output frequency called for, the microprocessor automatically selects the proper YIG-tuned output oscillator to be used.

Some Notes of Interest

There are several things that should be noted before continuing to study the remainder of the design. The master reference discussed previously the one to which all other oscillators are phase locked for accuracy and stability, is built into the synthesizer. There are master references available which provide appreciably higher stabilities than the one built into the instrument. Since it is neither economically feasible nor necessary to build higher stability into each and every instrument, an external reference input is provided for those applications that do require the higher degree of stability.

Actually, the master-reference oscillator is directly connected only to the 100-MHz PLL. Once the 100-MHz VCXO is locked to the master reference, attaining the stability of the master reference, all other 10-MHz references required in the instrument are derived from the master by dividing it by 10. This takes advantage of the superior phase-noise characteristics of the VXCO, transferring them to the remainder of the instrument.

It was mentioned in the reference-loop discussion that for output frequencies from 2.000 to 2.199 GHz the reference-frequency algorithm required a frequency below the lower limits of the reference oscillator. So, for that band of frequencies, the microprocessor automatically sets the reference frequency to 1.905 GHz instead of 1.805 GHz. The microprocessor automatically compensates for this in the divide-by-N circuit in the output loop by subtracting 100 from the N that it would normally set. The divide-by-N circuit is capable of accepting inputs from the mixer of 95 to 395 MHz and dividing them by the appropriate predetermined number. Reference-frequency step separations of 300 MHz were chosen to eliminate the possibility of the instrument output locking to the wrong reference frequency and producing an output frequency which is different from that selected by the operator. In instruments utilizing reference frequencies that are too closely spaced, this often occurs even though the instrument indicates a locked condition.

In a synthesizer application, the tuning coil of the YIG-tuned oscillator is normally paralleled with a capacitor to quiet any noise that might be contributed by the driver. This capacitor, however, greatly slows the time it takes to slew the oscillator from one frequency to another. This synthesizer design incorporates a patented circuit which, under microprocessor control, electronically removes the capacitor from across the tuning coil when changing frequencies. It automatically charges the capacitor to the potential across the coil at the new frequency and replaces it when the new frequency has been attained, without disturbing the new frequency setting.

Finally, the microprocessor can also control the instrument in either of two sweep modes: digitally controlled continuous sweep or a step-and-dwell mode whereby the instrument attains a frequency lock at each step before proceeding to the next. This allows the synthesizer to be used in applications requiring a swept frequency source.

- *The Downconverter*. A downconversion mixing technique is used to produce outputs from 50 MHz to 2 GHz. When output frequencies below 2 GHz are required, the system automatically utilizes the 2 to 8 and the 8 to 12 GHz fundamental-output oscillators to generate them. Figure 6 illustrates the downconverter and shows its relationship to the reference and output loops.

The function of the 2- to 8-GHz oscillator is that of a fixed-frequency local oscillator (LO) for the downconverter mixer. For downconverter operation, the 2- to 8-GHz oscillator is controlled in a loop of exactly the same configuration as the reference loop discussed earlier, and its operation is exactly the same. The YIG is coarse tuned to a predetermined LO frequency. A sample of its output is coupled to the sampler which mixes it with harmonics of 100 MHz to produce an IF of less than 50 MHz. This IF is compared with 5 MHz derived from the master reference in the fixed LO PLL's phase detector to produce a correction signal to move the YIG to its proper frequency and lock it. The LO frequency used is either 7.005 GHz or 8.005 GHz, selected to best

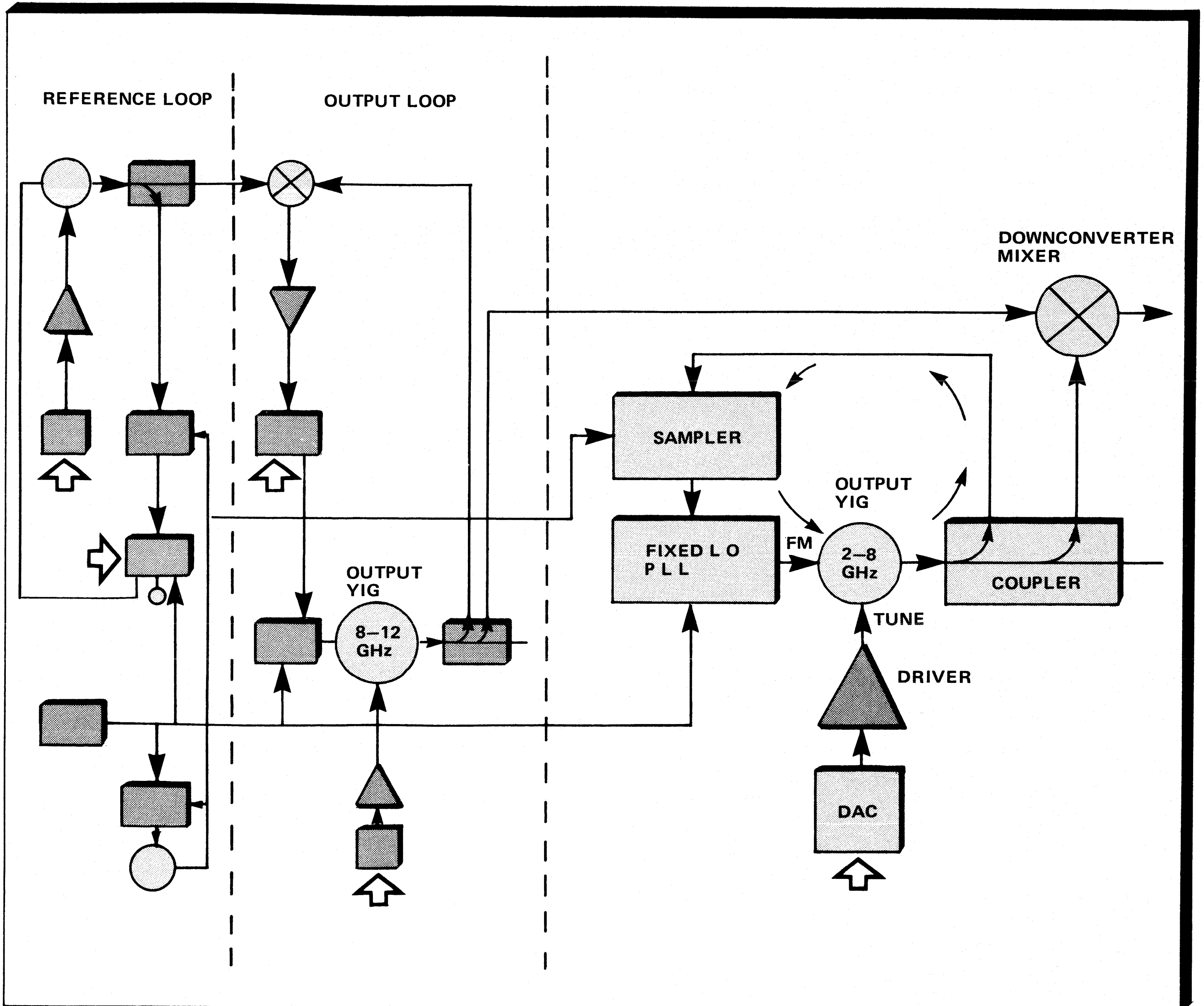

6. From 50 MHz to 2 GHz, downconversion mixing provides outputs, based on 2 to 8 and 8 to 12 GHz output oscillators.

reduce the production of high-order spurious signals when mixed with the output of the 8- to 12-GHz output oscillator.

The 8- to 12-GHz oscillator is operated as it normally would in the output loop which we previously discussed. Its output, over the range of 8.005 to 10.004 GHz, mixed with the LO frequency, produces downconverter mixer outputs from 0 to 1.999 GHz. This output is amplified and directed to a set of switched filters to attenuate harmonics. Since the 2- to 8-GHz YIG serves two purposes, there are two inputs to its FM coil. These inputs are automatically switched as required.

• *The RF Path.* Two-loop indirect synthesis and downconversion have provided a means of setting the YIG-tuned oscillator to provide output power at precise, stable frequencies from 50 MHz to 26 GHz. Now, the output power from the YIG-tuned output oscillators must be delivered to the device to be tested in a form that is compatible with that device's signal input requirements. This normally includes output power leveling and precision attenuation, harmonic filtering, and modulation of the output waveform.

Using the YIG-tuned oscillators available on the market today, this design is capable of producing outputs in the area of +10 dBm to 18 GHz and to +5 dBm at 26 GHz. Additionally, its microprocessor control and built-in memory capability allow it to store correction factors to compensate for variations in the level coupler, detector, and attenuator to provide leveled output accuracy within ±1 dB to 18 GHz and ±2 dB to 26 GHz at any attenuator setting.

The combination of today's YIG-tuned oscillator technology, two loop indirect synthesis techniques, and a very carefully planned and designed RF path have produced an indispensable tool for the testing, maintenance, and calibration of radar, EW, and microwave telecommunications components and systems. ■

Diode Switching

Diode switch types are growing to meet diverging uses.

By Robert V. Garver

Basics of diode switches are reviewed for radar and communications applications, and the various types of switches described, including device sketches and performance curves.

Diode switches have become one of the basic building blocks of modern microwave systems. They are easily designed into hybrid integrated circuits simplifying their widespread use and have broad applications from test and measurements to communication to radar.

For instance, multiple-throw diode switches are used in making wideband frequency sources as the device that switches the several sources to the one output for each frequency band. One form of diode switch is the gate for sampling oscilloscopes and network analyzers.

Radar has made use of diode switches in a number of ways. A high-speed diode switch has been used as modulator for a relatively low-power source to make very short pulses. The low-power radar can resolve targets very close together and at very close range. High-power diode switches have been used in normal long-range radars to protect the receiver from saturation or the mixer from damage due to transmitter leak-through. They have been used in coherent pulse Doppler systems to prevent outside signal sources from cohering the oscillator. In general, a switch can time-gate out undesired signals. Switches are used extensively in radar systems that time-share expensive components such as the antenna.

Communication systems make broad use of diode switches. The three tuning circuits for the antenna of the 30-to-88–MHz manpack FM radio are switched in by PIN diode switches. Long haul line-of-sight microwave communication systems must have a standby channel available to accomodate transmission-path fades or system failures. These standby channels are easily handled by diode switches. While frequency-division multiplex is handled by channel-dropping filters, time-division multiplex is handled by diode switches.

Basic Applications

One of the first diode switches was found to provide high insertion loss at high powers. It was equivalent to a diode across the line. The output tended to be fixed as incident power increased. This important discovery yielded the first microwave diode limiter; it was very fast. It was so fast that it was used after a ferrite limiter to clean up spike leakage. Now diode limiters can handle high power as well as low power, so high-power PIN-diode limiters are used first to handle high power and are backed up by low-power varactor-type limiters that clean up the leakage past the big diodes. Now it is known that any diode switch that provides high isolation in the conduction state performs as a limiter when the bias port is short-circuited.

Diode switches go gradually from the low loss (ON) state to the high loss (OFF) state. They are therefore inherently variable attenuators, however, an attenuator normally absorbs power rather than reflect it as an ideal diode switch does. A diode switch then serves as a variable attenuator by varying the control current. If an input match is required, special designs must be used as indicated herein.

A frequent application of diode switches is to move between different lengths of transmission line making up a switched-line phase shifter. This type of phase shifter has the advantage when it is used for control of a phased-array radar that covers a broad band. (Note that the bits switched in are not phase bits, but time-delay bits.) When put on the two normal output ports of a 90-degree 3-dB coupler, the diode can switch between two different impedance states performing different modulation functions. When the diodes exhibit high VSWRs in both bias states, the device serves as a low-loss phase shifter. The diode in this configuration provides the basic 180-degree phase shifter used in most digital diode phase shifters. Use of phase shift bits of varying size is possible by controlling the diode impedances. The third type of phase shifter uses diodes loading a transmission line approximately a quarter wavelength apart. In this application the diodes must switch between two admittance states.

Basic Switching

Having touched briefly on diodes' use as phase shifters, limiters, and variable attenuators, let's first examine the basic operation of diodes and then their performance tradeoffs.

A. *Diode equivalent circuit.* Since the tiny junction of a diode is too small to practically handle, the diode is placed in a cartridge. This cartridge has parasitic inductances and capacitances adding to the equivalent circuit of the diode and these must be taken into account when designing microwave diode switches. As shown in Figure 1, the basic diode has a junction capacitance C_j due the depleted junction (I-region for PIN diode), a series resistance R_s due to the bulk semiconductor resistance to the metal ends of the cartridge. When the diode is forward-biased the switch closes causing C_j to be shorted out. L_w is the inductance of the whisker (taken from the olden days when diodes were made by finding a sensitive spot on a galena crystal with a cat's whisker). In glass-packaged diodes this whisker is a fine wire

Robert V. Garver is author of Microwave Diode Control Devices, *published by Artech House, Inc.*

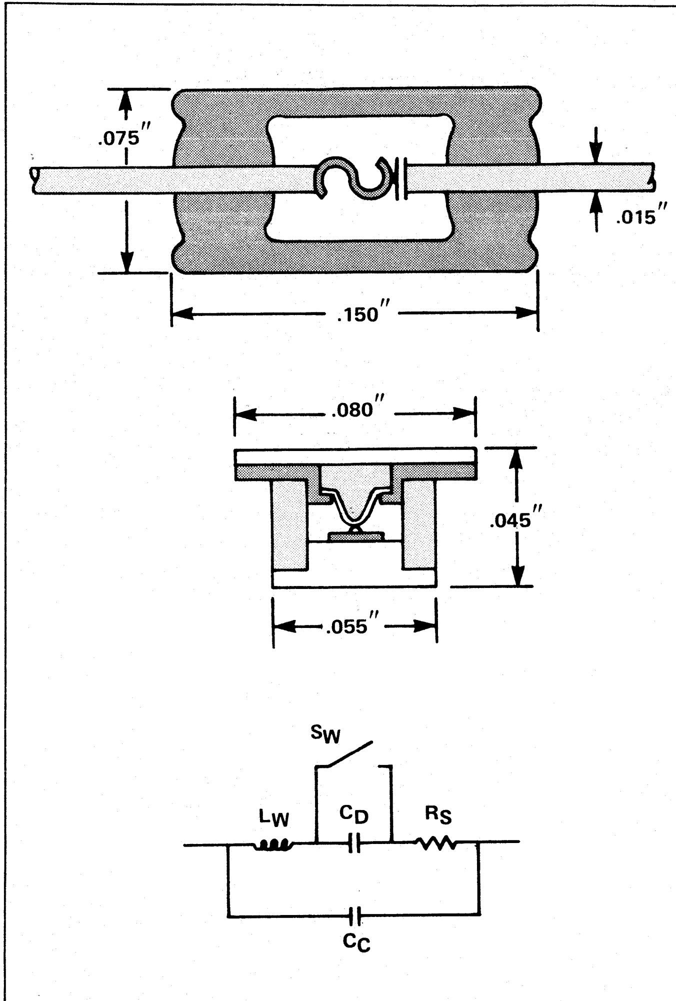

1. Basic equivalent circuit for a diode switch is shown along with typical packages.

and in pill-packaged diodes or chips for integrated circuits it is the gold bonding wire. C_c is the capacitance of the cartridge. This is the capacitance that would be measured if the diode die were removed.

Typical values for these elments are:

- R_s: 0.2 – 5 Ohms,
- C_d: 0.01 – 1 pF,
- L_w: 0.1 – 5 nH, and
- C_c: 0.05 – 0.1 pF.

They can begin to contribute to resonances as low as 1 GHz. In calculating the attenuation of a diode switch, the impedance of this circuit is calculated for each frequency and bias state using the attenuation equation.

B. *The attenuation equation.* The attenuation equation, basic to understanding and working with diode switches, is most easily derived using ABCD matrices. For a series diode, Z = R + jX is used for the series (B) element and attenuation α is given by

$$\alpha = 20\log\left|\frac{1}{S_{21}}\right|$$

$$\alpha = 10\log\left\{\left(\frac{R}{2Z_o}+1\right)^2+\left(\frac{X}{2Z_o}\right)^2\right\}$$

where Z_o is the characteristic impedance of the transmission line in which the diode is being mounted. For shunt diodes, substitute Y for Z, G for R, and B for X.

C. *Basic bandwidth curves.* By using one element for the diode in each bias state—L_w or C_t (= $C_c + C_d$)—it is possible to calculate the baseband frequency capability of the switch using the attenuation equation. The baseband responses of these elements are shown in Figure 2. If we wanted to make a series switch working up to 2 GHz providing more than 20 dB isolation and less than 1 dB insertion loss, we should select a diode with no more than 0.08 pF and 4 nH. Or if we wanted to use a shunt diode, the elements should be no more than 0.2 nH and 1.5 pF. A conventional glass-packaged diode in series in stripline will provide the necessary low parasitics. In order to make a good design, the exact parasitics of the diode should be used to calculate the insertion loss and isolation over the frequency range of interest. As the resonance of the diode is approached, insertion loss increases and isolation decreases faster than indicated by the curves.

The curves in Figure 2 are more broadly applicable than just giving the performance of a baseband switch. When a single diode is tuned to any frequency to optimize performance, the chart gives the bandwidth of the switch.

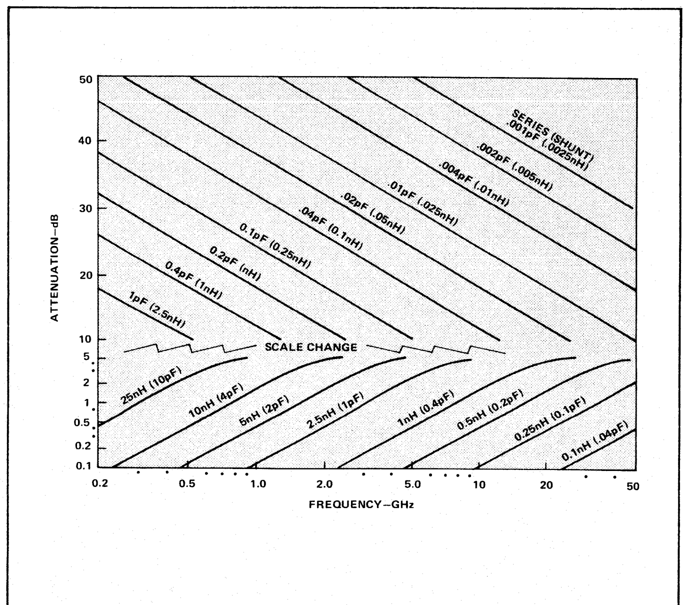

2. Baseband responses for diode switches can be used to calculate performance or determine the bandwidth of a switch.

D. *TEM transmission line bias circuits.* A bias circuit for a diode switch should not increase the insertion loss significantly, and it should not permit RF to leak out into the bias circuit and other parts of the system. The basic elements for TEM transmission-line bias circuits are shown in Figure 3. Discrete components, as shown, may be used at frequencies

Continued on page 200

Continued from page 196

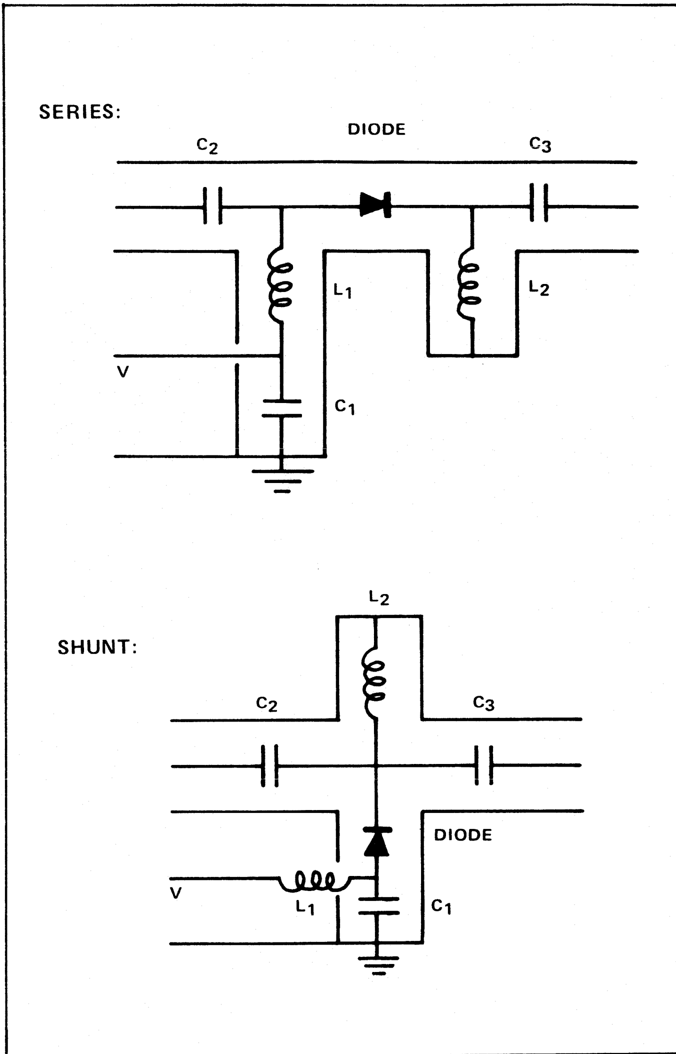

3. Discrete components, as shown, are used only below 100 MHz, but are replaced by transmission-line equivalents at microwave frequencies.

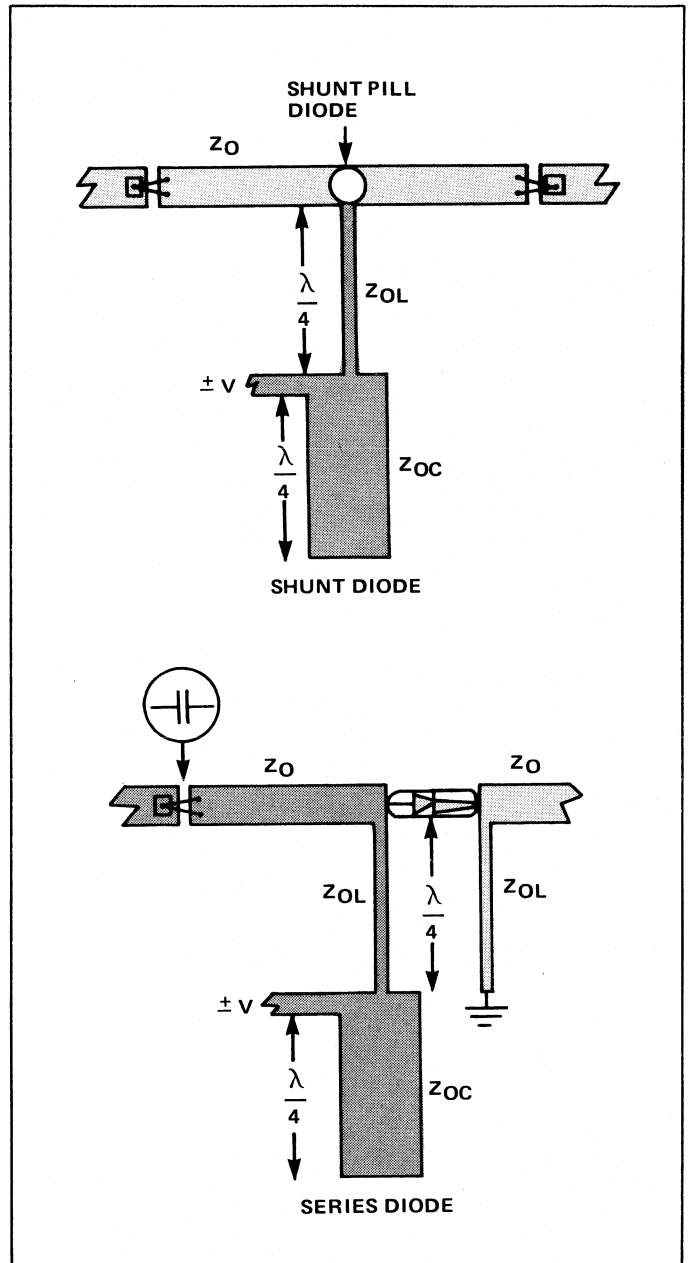

4. TEM diode switches and bias circuits do not have to be laid out in a straight line as shown, but can be wrapped to save space.

below 100 MHz, but at microwave frequencies, transmission-line elements are normally used for most of the elements. The inductors are usually high-impedance ($Z_o > 100$ Ohms) quarter-wave length transmission lines, and C1 is frequently a low-impedance ($Z_o < 25$ Ohms) quarter-wavelength transmission line. A bias tee with these paraeters will provide less than 0.1 dB insertion loss over an octave bandwidth. The series capacitors are normally chip capacitors, the kind used for hybrid integrated circuits. When a fine wire one-quarter-wavelength long is used for the inductors and other tricks (ref. 1, chap. 3) are used to lower the Z_o of the capacitor, several octaves of bandwidth are provided by the bias tee.

E. *Layout of TEM switches.* The layout of typical TEM diode switches with their bias circuits is shown in Figure 4. The inductors are provided by Z_{ol} while the bias stub capacitors are provided by Z_{oc}. If chip capacitors were to be used for the bias stub, then ground would have to be provided at their location. This could be accomplished by wrapping the bottom ground plane to the capacitor point or by drilling a hole through the substrate. Only when substrate surface area is at a premium are these alternatives exercised. To get the highest Z_{ol}, the circuit pattern can be etched without a conductor printed, and bonding wire (for hybrid integrated circuits) or 44-gauge transformer wire (for conventional stripline) can be attached to the end points in assembly. The components do not have to be laid out in straight lines as shown, but can be wrapped to save space. Normal care should be taken to prevent coupling between lines that are close together.

Wide-Band Low-VSWR Switches

A. *Low-pass filter.* When the design of a diode switch is based on filter theory, very low VSWRs can be obtained over substantial bandwidths. A low-pass filter is shown in Figure

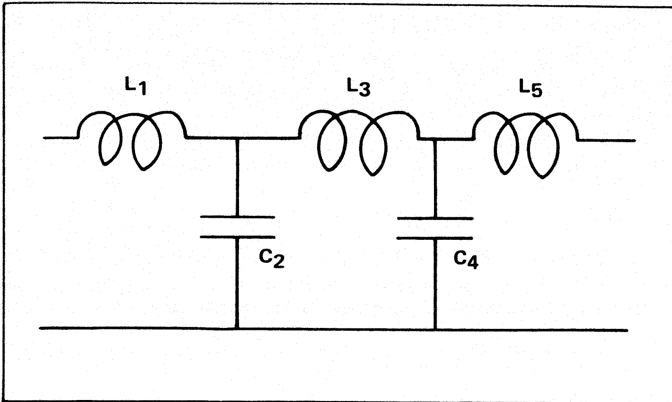

5. Low VSWRs can be obtained over substantial bandwidths through the use of filter theory.

5. Diodes and bias circuits can be integrated into the filter to become elements of the filter and therefore provide the response dictated by the theory. A series forward-biased diode is inductive and becomes a series element in the filter, whereas a shunt reverse-biased diode is capacitive and becomes a shunt element in the filter.

B. *Insertion loss response of a low-pass filter.* The responses of two 1-pF diodes shunting a 50-Ohm line are shown in Figure 6. The worst VSWR occurs when they are in the same plane and there are no other filter elements in the structure. In the next curve they are elements 1 and 3 of a pi filter circuit. In the lowest bandwidth curve they are elements 2 and 4 of the circuit shown in Figure 5. Bandwidth is much improved by using the filter structures. In order to include the bias circuit in the filter structure, bandpass filter structures must be used involving more sophisticated filter theory relationships (Richard's Equation and Kuroda's Identity, ref. 1, chap. 3).

C. *Layout of a wide-band TEM switch.* The switch as derived using filter theory and illustrated in Figures 5 and 6 could be laid out on a substrate as shown in Figure 7. Since the series inductors are made of fine wire and are really high-impedance transmission line of finite length, their parasitic capacitance must be taken into account. The capacitance per unit length C of a short length of transmission line is given by

$$C = \frac{1}{cZ_o} \qquad \text{(a)}$$

where c is the speed of light in the medium of the TEM transmission line (wave propagation velocity). The inductance per unit length L is given by

$$L = \frac{Z_o}{c} \qquad \text{(b)}$$

In the equivalent circuit of the switch (Fig. 5), half of the capacitance is added to the circuit at each end of the inductors and that by the diodes is merged with it. To a fair first approximation the extra capacitances at the ends of the filter can be ignored.

Pushing the Power Limit

The power limits on a diode switch are fixed by the diode's reverse-bias breakdown voltage E_b, and its dissipation rating P_d, its series resistance R_s, and the characteristic

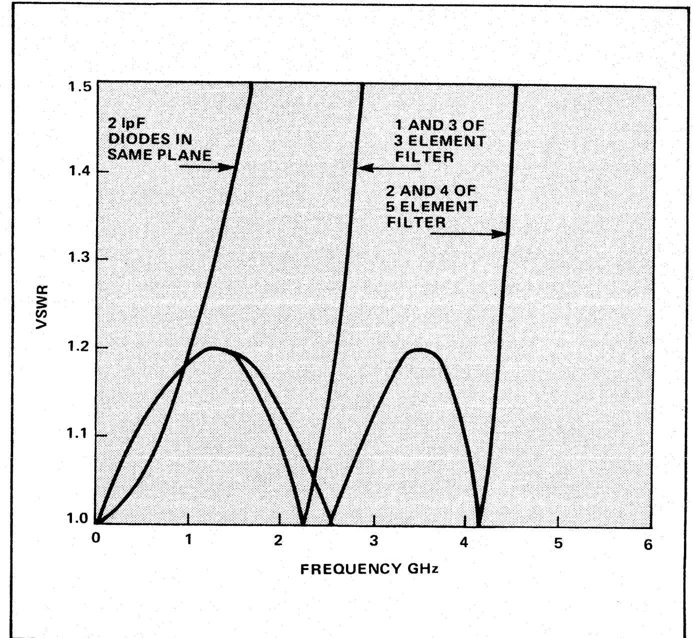

6. Worst VSWR for this case, a pair of diodes shunting a 50-Ohm line, occurs when the diodes are in the same plane and there are no other filter elements.

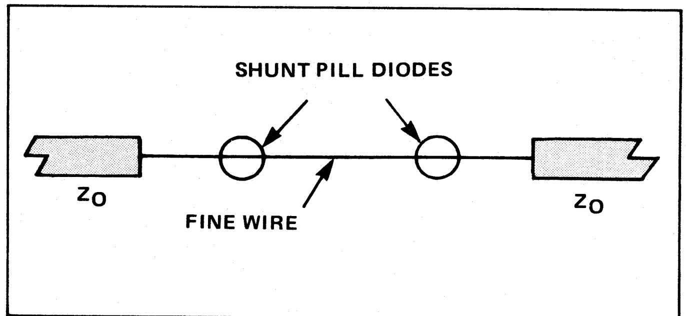

7. Laying the switch out on a substrate requires taking into account the parasitic capacitance of the fine wires used as series inductors.

impedance of the transmission line in which it is mounted. These limits are given by the following equations:

	series diode	shunt diode
peak power	$\frac{(E_b)^2}{32 Z_o}$	$\frac{(E_b)^2}{8 Z_o}$
avg. power	$\frac{P_d Z_o}{R_s}$	$\frac{P_d Z_o}{4 R_s}$

(c)

A. *Power vs characteristic impedance.* The power limits are functions of Z_o, indicating that the power rating of a diode switch can be tailored by altering the characteristic impedance of the structure in which the diode is moutned. The power ratings of two diodes have been plotted in Figure 8 to demonstrate this Z_o dependence. The above equations were based on the off diode being biased to half the breakdown voltage, a practice which reduces intermodulation products and the generation of harmonics to a minimum. In many applications these factors are not

important, and high bias voltages are difficult to obtain. When it can be tolerated, the diode need only be biased slightly into reverse (approx. 10 V), expanding the peak-power limit by a factor of 4 as shown in Figure 8.

Practical factors limit the range of characteristic impedances that can be made in TEM transmission lines. When a strip is much wider than required for 10 Ohms, it becomes wider than it is long and difficult to make it a quarter-wavelength long. When a Z_o gets above 100 Ohms, it is no longer practical to etch it with the rest of the printed circuit because the edge imperfections could cause a break in the line. The standard solution is to leave a gap for the center conductor and solder a fine wire in the gap. The characteristic impedance can be controlled by using the formula for slab line when making stripline. Different-diameter wires give different characteristic impedances, and there is a wide selection of transformer wire readily available, the smallest being 44-gauge which is 0.002 in. in diameter. This wire in stripline using 1/16-in. boards will give 160 Ohms. When a quarter wavelength of this line is placed in front of and after a diode, the diode is transformed into an environment of 520 Ohms. In the same way, surrounding a diode by 10-Ohm quarter-wavelength lines places it in an environment of 2 Ohms. (The above transformations are based on the main transmission line being 50 Ohms.) These transformers will allow diodes to be placed in environments that take full advantage of their power-handling capacity. Care must be exercised in designing these switches: All insertion loss, isolation, and bandwidth calculations must take into account the new characteristic impedance and the finite bandwidth of the transforming structure. For wider bandwidth (but less transforming range), multiple-section quarter-wavelength transformers may be used.

B. *Layout of power TEM switch.* A sample shunt diode switch in a transforming structure is shown in Figure 9. Z_{ol} is 35 Ohms and Z_q is 55 Ohms. This switch provides a VSWR less than 1.4 over a 2-octave bandwidth.[1] The diode is transformed into an environment of 25 Ohms. When the 1-kV diode of Figure 8 is used, the switch can control 20 kW peak and 700 W average (at the center frequency).

Double-Throw Switches

Double-throw switches can be made using reflection devices or lumped-element circuits. In conjunction with a

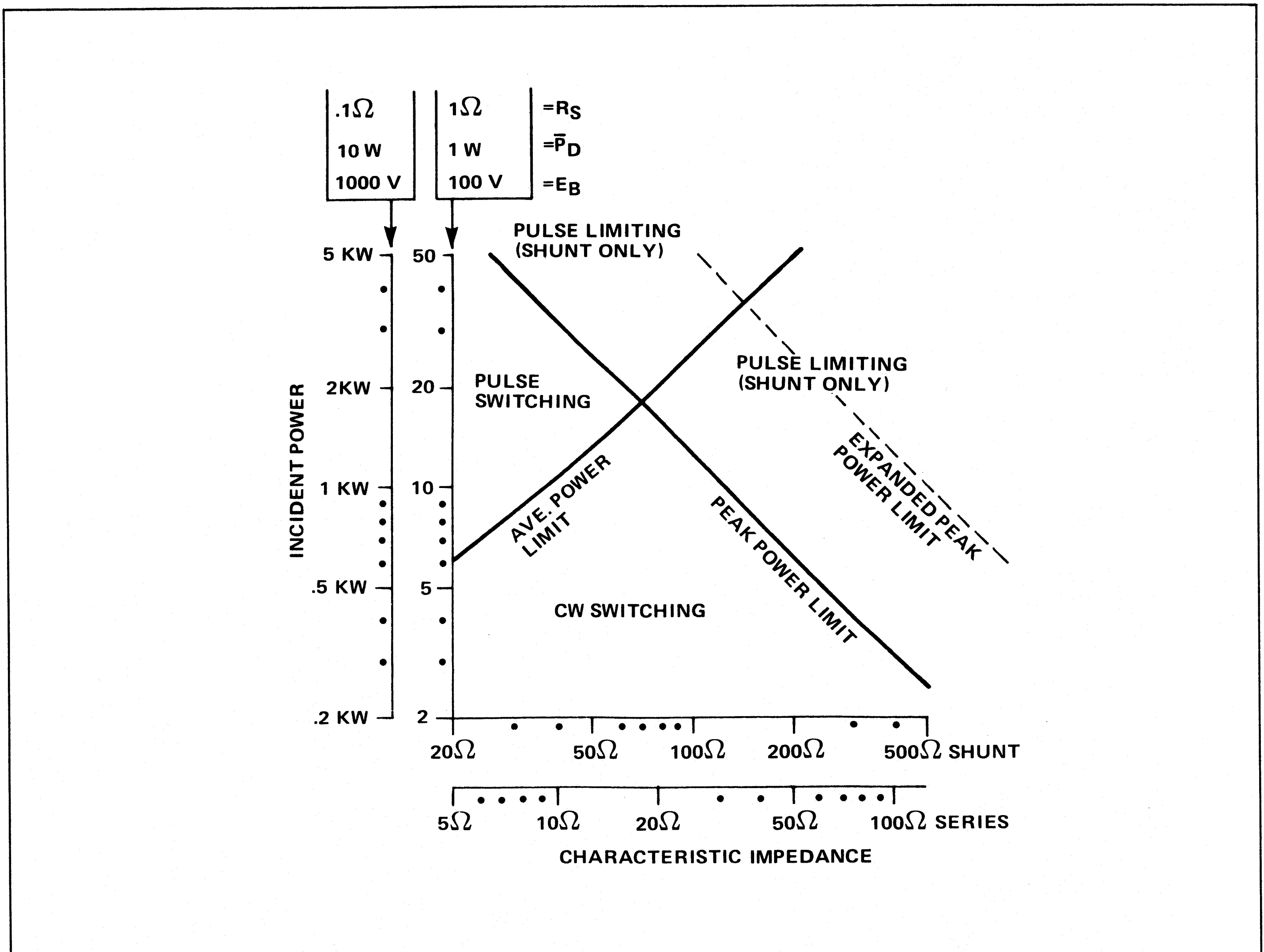

8. Power ratings show dependence on the impedance Z_o.

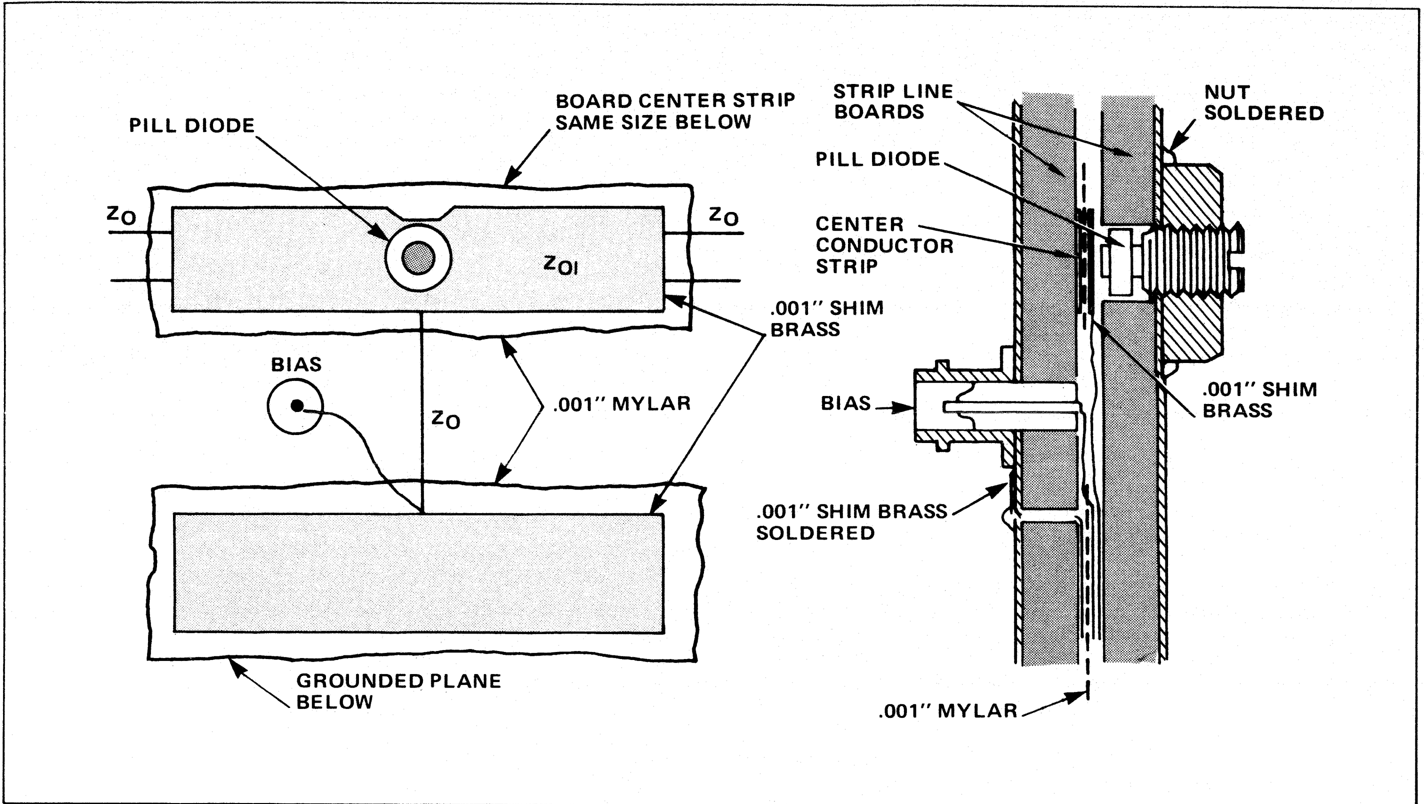

9. This shunt diode switch provides a VSWR of less than 1.4 over a 2-octave bandwidth. With a 1000-Volt diode the switch can control 20 kW peak and 700 Watts average.

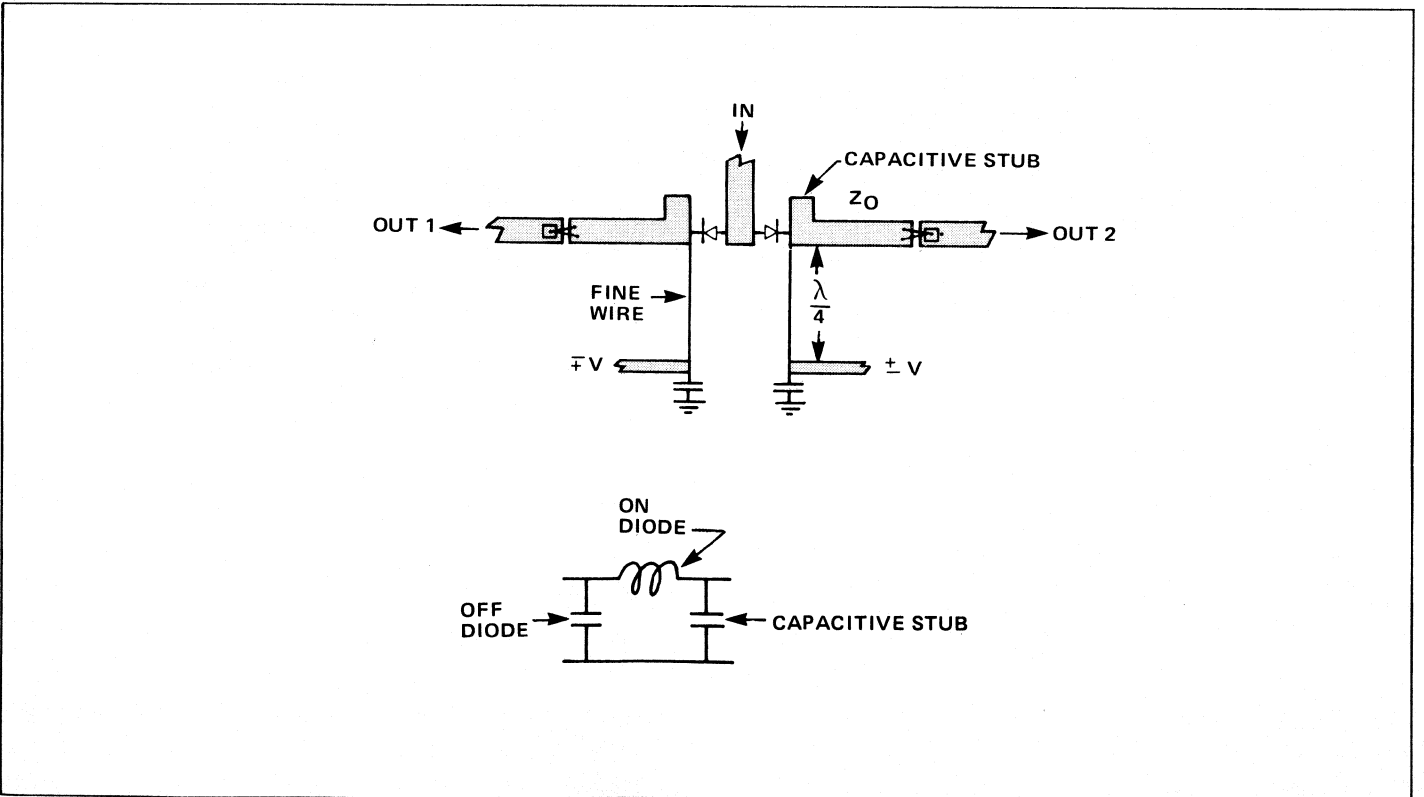

10. In this double-throw switch, when one diode is biased into conduction the other is reverse biased.

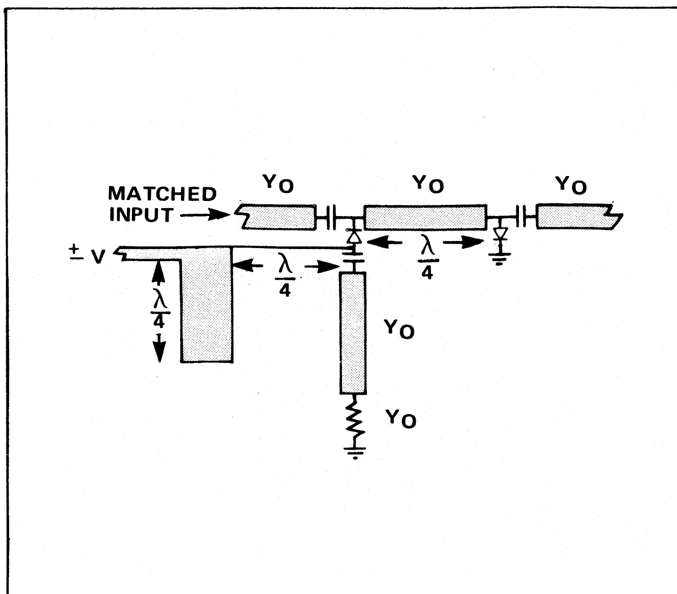

11. Matching problems can be taken care of by using this circuit; either diodes in series or shunt configurations can be used with varying degrees of control.

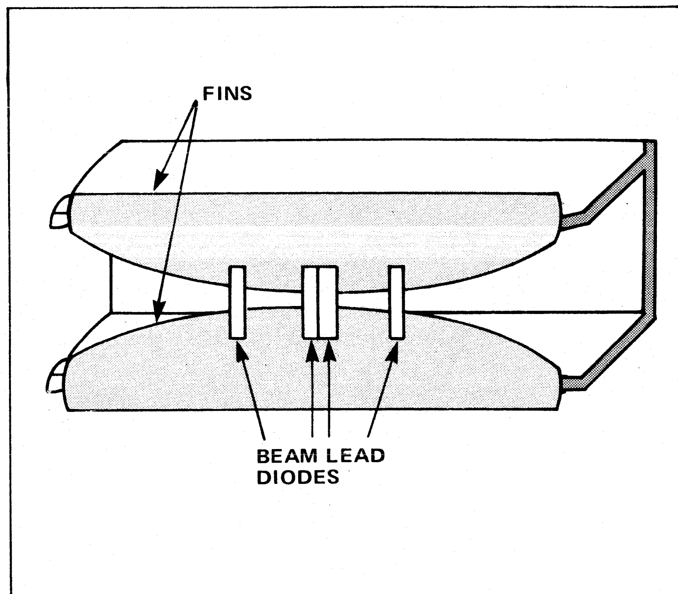

12. Finline diode structures such as this make switching possible at millimeter frequencies.

circulator or a pair of 3-dB couplers, the normal output of the switch becomes one output and the reflected power becomes the other. More bandwidth, however, is achievable by using lumped circuits. A lumped-circuit-element, double-throw switch is shown in Figure 10. When one diode is biased into conduction, the other is reverse-biased. The biased diodes can be represented by the pi equivalent circuit shown in Figure 10.

Assuming that the bias circuits can be made more wideband than the diodes, then the equivalent circuit showing only the diodes can be used to optimize the low VSWR of the switch. The ON diode is inductive and the OFF diode is capacitive. All of the parameters in the equivalent circuit can be adjusted to derive the desired low-pass filter response. The capacitance of the OFF diode can be added to by extending the input line beyond the junction with the diodes. This will be a short capacitive stub. The inductance of the diode can be added to by allowing the leads to be longer than the minimum. (The additional capacitance of this line should be added to the capacitors as before.) The final element is the shunt capacitor which is a capacitive stub added at the output end of each diode.

Matched Switching (and Variable Attenuator)

Matched switches can be made by using any of the above double-throw switches and putting a matched load on one of the ports. In order to make the switches matched between switching states (and thus make a matched variable attenuator), the bias currents on the diodes would have to be controlled in a nonlinear way. A circuit that takes care of the matching problem (over a limited bandwidth) is shown in Figure 11. Identical diodes are used and the same bias current is passed through both diodes in series.[2] If one configuration (diode in series or diode in shunt) gives a greater range of control, the dummy load should be placed on the other diode.

Mm-Wave Switching

With the advent of finline, wideband diode switching at mm-wave frequencies has become possible.[3] The structure as shown in Figure 12 is much like ridged waveguide but the ridges are printed on a circuit board; very small and precise patterns can be printed on it. The board is placed vertically along the center of the waveguide in the E-field maximum plane. Very small gaps are possible without creating unusually low characteristic impedances and the matching taper is included on the board. The structure is ideal for diode switches because the two halves of the board can be biased outside of the waveguide, and beam-lead diodes can be mounted across the gap using conventional hybrid integrated circuit techniques. These switches typically provide 15 dB isolation per diode up to about 100 GHz. (Note that the diodes are mounted a quarter-wavelength apart.) It is difficult to get much more than 30 dB with this structure because evanescent waves propagate around the OFF diodes in the waveguides beyond cutoff caused by cutting the waveguide in half with the circuit board. More isolation can be obtained by having more diodes and making the waveguide below cutoff longer (at the cost of increased insertion loss). ■

References

1. R. V. Garver, *Microwave Diode Control Devices*, Artech House, 1976, Dedham, MA
2. J. C. Hoover, "A Mono-Control Microwave Semiconductor Switch," 1964 *IEEE PTGMTT International Symposium Digest*, May 1964, pp. 204-207
3. P.J. Meier, "Integrated Fin-Line Millimeter Components," *IEEE Trans. on Microwave Theory and Techniques*, vol. MTT-22, pp. 1209-1216, Dec. 1974

YIG-Tuned Oscillator Fundamentals

Our technical chapter on oscillators focuses on YIG-tuned devices, with one article on their fundamentals and a complementary feature on YIG-oscillator-based synthesizers.

By Northe K. Osbrink and the Oscillator Engineering staff, MIC *Division, Avantek, Inc.*

In general, YIG-tuned oscillators have several special advantages: low phase noise; wide operating frequency range; and excellent tuning linearity, typically 0.08 percent. YIG-tuned microwave transistor oscillators are widely used in military and commercial systems because of their unique performance characteristics combined with their reliability, which is enhanced by the low failure rate of the silicon bipolar and GaAs field-effect transistors from which they are built.

Microwave oscillator transistors, mounted in an unpackaged chip form on a thin-film hybrid microwave integrated circuit (MIC) can cover more than two octaves in the frequency range from 1 to 40 GHz, when tuned by yttrium-iron-garnet (YIG) resonators.

Bipolar transistor oscillators operating between 1 and 12.4 GHz have been available since 1978, and this upper limit will be at least 20 GHz by 1984. GaAs FET oscillators are currently available operating between 7 and 40 GHz.

The major advantage of the bipolar transistor oscillator compared to the GaAs FET oscillators is its 10 to 15 dB lower phase noise, and a much wider tuning range. The major advantage of the GaAs FET oscillator is its higher operating frequency. YIG-tuned transistor oscillators normally include a buffer amplifier to increase output power and to provide excellent frequency pulling performance.

The three essential parts of any YIG oscillator are: a means of storing energy (the YIG resonator); a dynamic negative resistance; and a magnetic structure to produce a variable DC magnetic field across the YIG-sphere resonator so that frequency tuning can be achieved.

Although other configurations may be used, some YIG tuning magnets are electromagnets with a single air gap. Figure 1 shows a simple sketch of the main oscillator elements. The DC current through the main tuning coil provides the required DC magnetic field across the pole gap. The YIG sphere, FM coil, and MIC oscillator substrate are located in the gap of the electromagnet.

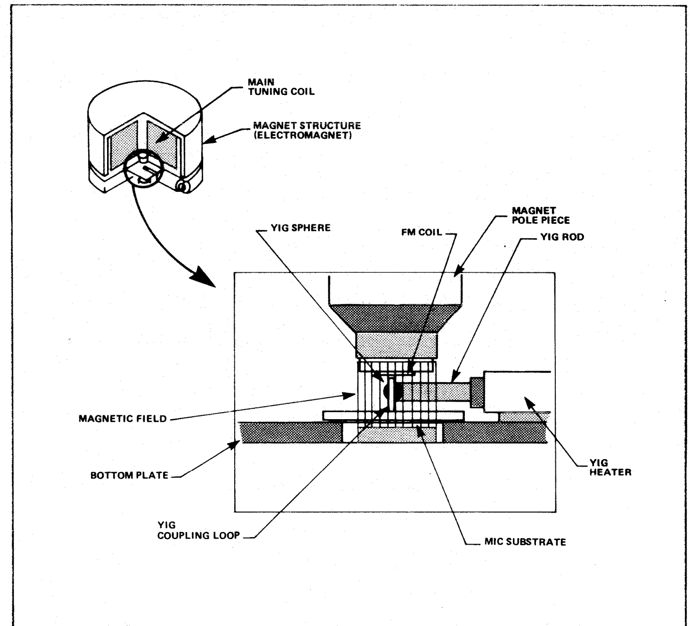

1. YIG oscillators have three essential parts: a YIG resonator to store energy; a dynamic negative resistance; and a variable magnetic field for tuning.

The Resonant Frequency

Single crystal yttrium-iron-garnet (YIG) and gallium-doped YIG (Ga YIG) are part of a family of ferrites that resonate at microwave frequencies when immersed in a magnetic field. This resonance is directly proportional to the applied magnetic field, and, therefore, very linear tuning is achieved by changing the magnetic field with an electric current. Hence, the resonator consists of a YIG (or Ga YIG) sphere, the electromagnet, and the coupling loop.

The physical phenomena utilized for the resonance of YIG material is associated with the motion of magnetic dipoles in the presence of a constant magnetic field and a superimposed RF magnetic field.

The spinning electron may be considered as a spinning mass with precessional motion about a DC magnetic field, which is charged electrically and is similar in many respects to the classical mechanical gyroscope. The DC magnetic forces acting on the magnetic dipole are comparable to the gravitational force acting on a mechanical top. The RF magnetic field will be applied perpendicular to the DC field and will exert a periodic sidewise thrust or torque.[1] The resonant frequency, f_o, of an isotropic YIG sphere in a uniform magnetic field, H_o, is given by

$$f_o = \gamma H_o, \tag{1}$$

where:

γ = 2.8 MHz/(sec.) (Oersted), gyromagnetic ratio,
H_o = DC magnetic field in Oersteds.

The Equivalent Circuit

In order to make the discussion of the YIG crystal properties more meaningful, it is worthwhile to examine the equivalent circuit of the YIG and its relation to the functioning of a microwave resonator. Figure 2 illustrates the important

Northe K. Osbrink is manager of publications editing at Avantek, Inc., Santa Clara, California. All credit for the contents of this article must be given to many current and former members of the Oscillator Engineering staff, MIC Division, Avantek, Inc.

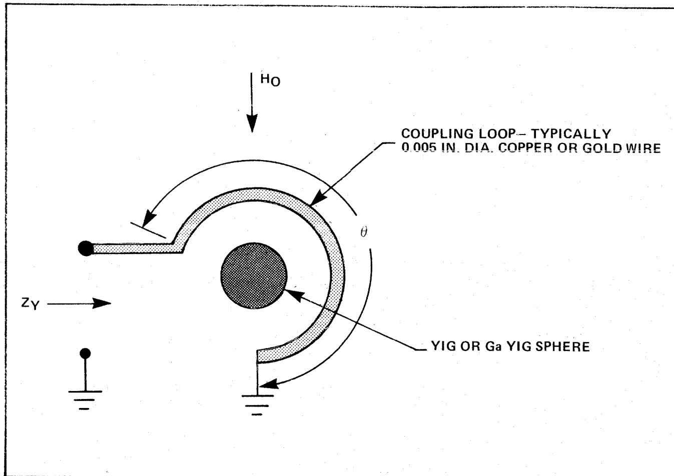

2. Loop coupling circuit provides DC magnetic bias for tuning.

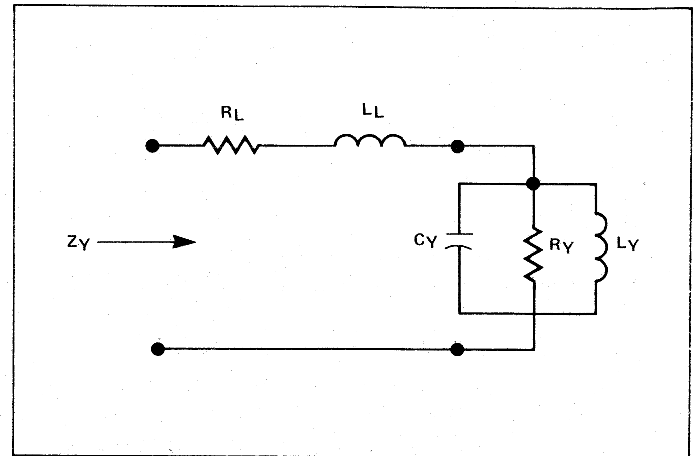

3. In this equivalent circuit of a loop-coupled YIG resonator, the resonant circuit is induced in series with the loop impedance.

parameters of the loop-coupled YIG, and Figure 3, the equivalent circuit.

In Figure 2, the YIG is located at the center of a loop of wire. The loop angle θ may be a full 360 degrees or, as suggested in Figure 2, less. It can also be greater than 360 degrees in cases where especially tight coupling is required.

The DC magnetic bias field, H_o, is also shown in Figure 2. H_o may be applied in any direction which is perpendicular to the RF field of the loop, i.e., in the plane of the loop.

Figure 3 is the equivalent circuit corresponding to Figure 2. The parallel resonant circuit is induced in series with the loop impedance by the coupling of the YIG; L_L and R_L are the inductance and resistance, respective, of the coupling loop.

The input impedance of this circuit is given by:

$$Z_y = R_L + jWL_L + \frac{jW^3L_y}{W_o^2 - W^2 + j\,\frac{WW_o^1}{Qu}} \quad (2)$$

where:

$W = 2\pi f$ frequency in radians;
$W_o = 2\pi f_o$ resonant frequency of YIG in radians;
$Q_u = R_y/W_oL_y = H_o/\Delta H$ unloaded Q of the YIG sphere.

The equivalent circuit parameters are related to the basic YIG resonator and loop parameters as follows:

$$L_y = \mu_o V_y K^2 W_m \quad (3)$$

$$R_y = W_o W_m \mu_o V_y K^2 Q_u = W_o L_y Q_u \quad (4)$$

$$C_y = 1/W_o^2 L_y \quad (5)$$

where:

μ_o = permeability of free space
$V_y = 4\pi/3\ dy^3$ volume of YIG sphere in cm^3
d_y = diameter of YIG sphere in cm
K = coupling coefficient between YIG sphere and coupling loop in cm^{-1}
$W_m = \gamma\,(4\pi M_s)$
$4\pi M_s$ = saturation magnetization in Gauss

The coupling coefficient K is a geometric coupling factor and is related to loop angle, θ, and loop diameter, d_l, as follows:

$$K = \frac{I}{d_l} \times \frac{\theta}{360} \quad (6)$$

The unloaded Q (Q_u) can also be expressed in terms of the resonance linewidth ΔH and the DC bias field H_o as follows:

$$Q_u = \frac{H_o}{\Delta H} \quad (7)$$

The convenience of this formulation lies in the fact that the quality of YIG spheres is usually specified by the manufacturer in terms of ΔH rather than Q_u. It is almost always given in cgs units, i.e., Oersteds.

The tightness of coupling between the loop and the YIG can also be expressed as the external Q (Q_e) of the resonator. If an external resistance R_o is connected to the terminals of the loop, then Q_e is defined as:

$$Q_e = \frac{R_o}{\omega_o L_y} \quad (8)$$

Since:

$$R_y = \omega_o L_y Q_u \quad (9)$$

$$= R_o \times \frac{Q_u}{Q_e} \quad (9a)$$

Thus, the impedance level R_y of the parallel resonant circuit at resonance is proportional to two quantities which are easily obtained from a single bandwidth measurement.[2]

Similarly, the inductance L_y is related to calculated, or measured, Q_e as follows:

$$L_y = \frac{R_o}{\omega_o Q_e} \quad (10)$$

YIG equivalent circuit parameters can thus be estimated quite easily and quickly from a knowledge of the external Q, or Q_e. Figure 4 shows theoretical values of Q_e as a function of YIG-sphere diameter with loop diameter as a parameter for the 360-degree-loop case, and for a pure YIG ($4\ \pi M_s = 1780$ Gauss) sphere.

The unloaded Q (Q_u) of the YIG resonator also varies with frequency, producing corresponding variations of Z_{in} (see Equation 9). Q_u varies with frequency of a pure YIG

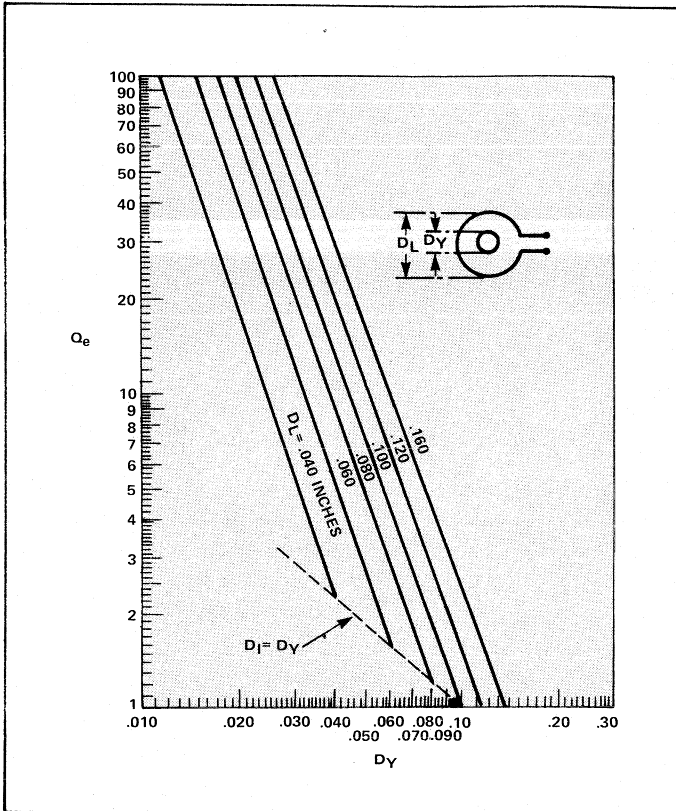

4. External Q for a YIG sphere varies with diameter.

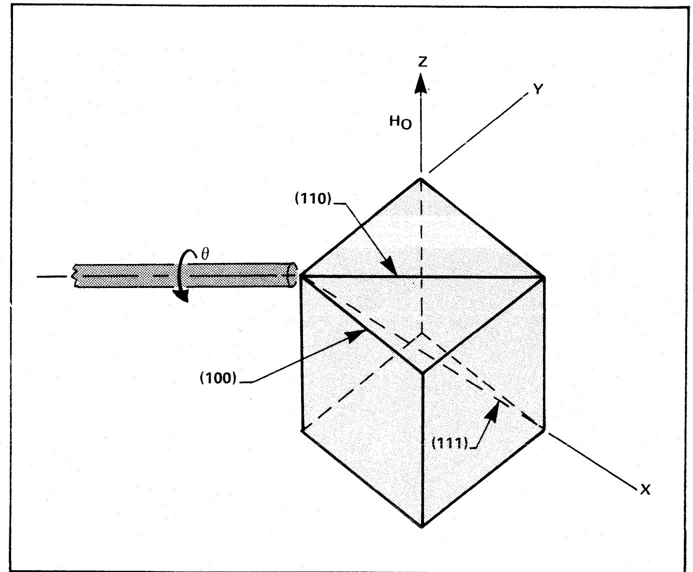

5. Orientation of the crystal axis with the BeO rod can be used for temperature compensation.

sphere in a strip transmission-line-coupling circuit.[3] Q_u decreases rapidly as f_o approaches $(4\pi M_s)/3$, where $4\pi M_s$ becomes unsaturated. A higher Q_u is achieved at the lower frequencies by using gallium-substituted YIG (Ga YIG), which has lower values of $4\pi M_s$.

The premature decline phenomenon[4] inside the YIG sphere limits its use as a high Q resonator to frequencies above f_{min}

where: $$f_{min} = \frac{2}{3}\,\Upsilon(4\pi M_s) \tag{11}$$

The YIG resonator is now electrically characterized; later, the requirment for oscillations will be examined. These results will be necessary to determine the oscillator frequency range of oscillations using computer-aided-design (CAD) techniques.

Frequency Sensitivity

The resonator frequency varies with temperature. Several different physical mechanisms contribute to the frequency drift as follows:[5]

- magnetic anisotrophy,
- propagation scattering,
- frequency pulling due to proximity effect of conducting surfaces, and
- Inductive circuit coupling.

The largest of these effects is magnetic anisotropy, i.e., the variation of the resonant frequency as the orientation of the crystal axis is varied with respect to the DC bias field. This effect is quite complex and varies with the bias field H_o as well as temperature.

One simple approach to the compensation of the effects is as follows: The YIG is mounted on a ceramic rod, usually beryllium oxide (BeO) for good thermal conductivity. An orientation procedure is used by means of which the mounting rod axis is caused to coincide with the [110] axis of the YIG crystal.[6] This orientation is illustrated in Figure 5 which also illustrates the principal crystal axis. Rotation of the rod produces a variation of the resonant frequency. Using simple theory, which does not include variations with respect to H_o, the resonant frequency f_o is given by [7]

$$f_o = 2.8 \times 10^6 H_o + 2.8 \times 10^6 \left(\frac{K_1}{4\pi M_s}\right) \times \left\{2 - \frac{5}{2}\sin^2\theta - \frac{15}{8}\sin^2 2\theta\right\} \tag{12}$$

where θ is the angle between the DC field H_o and a cube edge [100]. At room temperature where, for pure YIG, $(K_1/4\pi M_s) = -43$ Oersteds, the deviation term is –240 MHz.

$(K_1/4\pi M_s)$ is a function of temperature varying from 200 θe at 50°K to 4 θe at 500°K, so oscillator frequency will vary with temperature by an amount which depends on the angle θ. Conventionally, an angle $\theta = 29.7°$ (the [225] direction) is chosen at which the anisotropy term in Equation 4 is zero. This is called the thermal compensation axis.

Tokheim and Johnson have shown[5] that the [225] direction is not the optimum one; the theory upon which the [225] axis is based does not include variation of the anisotropy term with H_o, i.e., with center frequency f_o. They have concluded that better compensation is achieved when the DC field is in the {100} plane with $\theta \approx 32°$, i.e., the [0, 8, 13] direction.

Figure 6 shows a surface of resonance frequency at constant H_o as a function of crystal orientation near one of the [100] directions. The optimum thermal compensation direction according to Tokheim and Johnson is with $H \simeq 32°$ and $\theta = 0°$, i.e., the {100} plane. It is obvious that if the direction

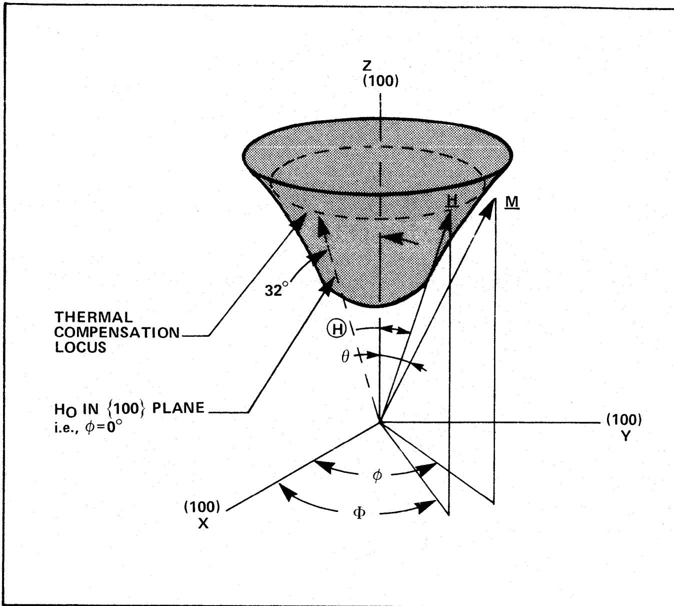

6. Surface resonance is shown of a ferromagnetic resonance frequency at constant H_0 as a function of crystal orientation near a [100°] direction.

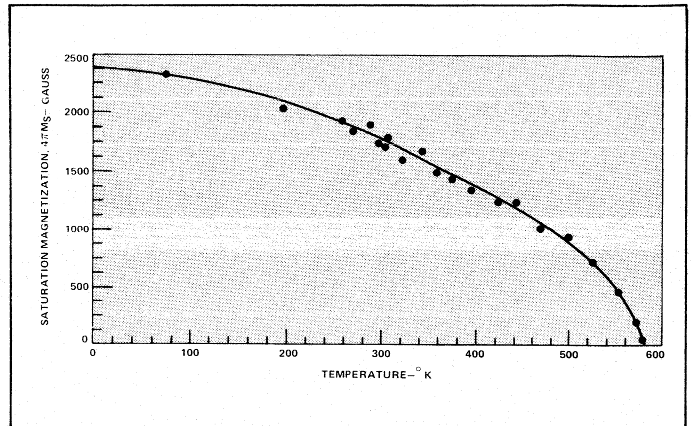

7. Saturation magnetization is plotted vs. temperature of pure YIG.

of H_o is rotated through 360° in the {100} plane, it will intercept the thermal compensation locus eight times as compared with four if rotated in the {110} plane.

A shift, Δf, in f_o is produced[8] when a conducting wall is close to the YIG sphere. For the case where the conducting plane is perpendicular to the DC field H_o[5],

$$\Delta f = 2.8 \times 10^6 \left(\frac{4\pi M_s}{24}\right)\left(\frac{r_y}{d}\right)^3 \qquad (13)$$

where r_y is the radius of the YIG and d the distance from the center of the sphere to the conducting wall. Δf is a function of temperature. Figure 7 shows a plot of $4\pi M_s$ vs. temperature of pure YIG. Application of equation 13 together with data in Figure 6 shows that a drift of around −4 MHz over a temperature range of −54°C to +100°C would be produced if $r_y/d = 0.5$.

In addition to the effects of magnetic anisotropy and conducting-surface proximity, there are frequency shifts due to propagation effects within the YIG[9] and pulling due to the coupling loop due to load impedance variations. As a practical matter, then, temperature compensation must be optimized and verified experimentally, varying the ambient temperature over the specified range and adjusting the orientation of the crystal axes to obtain the smallest frequency drift. As suggested above, better compensation will be achievable with the YIG mounted on a rod along a [100] axis so that H_o is in the {100} plane. It is also important to minimize the range of variation of the YIG-sphere temperature. This is done conventionally by using a self-regulating positive-temperature-coefficient heater.

The thermal coefficient of expansion of the magnet material also affects the resonant frequency. This is due to the variation of the magnet pole gap with temperature, which affects the magnetic field density and results in a variation of H_o, the magnetic field, since $B = \mu_o H_o$.

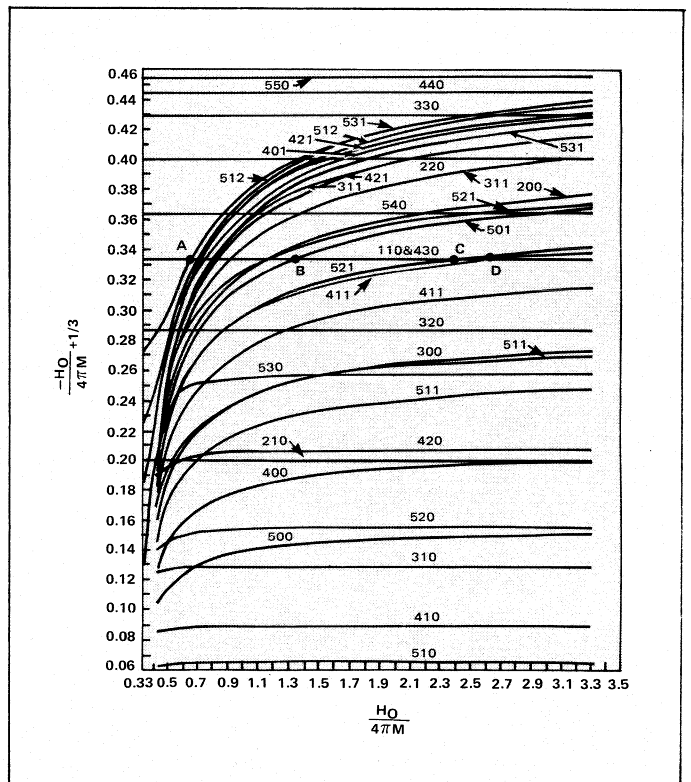

8. A normalized chart displays the magnetostatic modes of a ferromagnetic sphere. From "Ferromagnetic Resonance Modes in Spheres" by P. D. Fletcher and R. O. Bell, J. App. Phys., Vol. 30 (1959), No. 5, pp. 687-698.

The Magnetostatic Modes

One of the most important practical problems in YIG oscillator manufacture is the elimination of unwanted spurious oscillations and spectral-line-broadening effects due to the YIG. It is generally accepted that most of these spurious effects result from the presence of other resonances, due to magnetostatic modes.[10, 11]

The YIG resonance which is used to tune the oscillator is called the free precession or 110 mode. The RF magnetization associated with this mode is uniform throughout the sphere. There are higher-order modes of resonance called magnetostatic modes for which the RF magnetization is

nonuniform. These modes arise from the interaction of the magnetization with itself.

Figure 8 is a normalized mode chart for the magnetostatic modes of a ferromagnetic sphere.[11] The modes are classified by a three-index (n, m, r) scheme. The first index is the periodicity in θ, the angle measured from the direction of H_o; m refers to the periodicity in the azimuth angle θ; and r refers to the number of roots required to satisfy boundary conditions.

Some of the modes, e.g., 320 and 210, tune at the same rate as the fundamental 110 mode. The 210 mode is one of these for which the distribution of RF magnetization can easily be illustrated as is done in Figure 9. The intensity of the RF magnetization is maximum at the "north" pole of the sphere, decreasing linearly to a maximum at the "south" pole. The RF magnetization vectors m_{rf} can be pictured as rotating at an RF rate in the x-y plane. It is obvious that the 210 mode can be excited by an RF field which has a gradient in the z direction.

The sloping curves represent higher-order modes which do not tune linearly with H_o. Where they cross the horizontal line representing the uniform precession, 110 mode, the higher-order-mode resonant frequency coincides with that of the uniform precession. Table 1 shows some of the fields and frequencies at which resonances of the uniform precession and higher order modes coincide. Pure YIG ($4\pi M_s$ = 1780 Gauss) has many magnetostatic mode coincidences in the C-band range. It is therefore desirable to use a lower-saturation-magnetization Ga YIG to minimize spurious oscillations.

Table I.

Higher-Order Mode Coincidence Frequencies

Mode Index (n, m, r)	Coincidence Frequency (with 110 Mode) $4\pi M_S$ = 1780 Gauss	$4\pi M_S$ = 500 Gauss
421	4257.3 MHz	1182.6 MHz
311	4699.8	1305.5
521	5881.7	1633.8
200	5886.7	1635.2
501	6340.7	1761.2
521	11254.3	3126.2
411	1344.7	3733.8

In addition to spurious oscillations, magnetostatic resonances can cause detuning effects. When the higher order magnetostatic resonance is close to the uniform precession resonance, it will cause the uniform precession frequency to be "pushed" upward if the higher order mode frequency is the lower frequency. If the higher order mode frequency is on the high side of the uniform precession frequency, it will "push" the uniform precession frequency downward.

In an oscillator application, the method and magnitude of coupling, the circuit design, and the YIG selection will prevent many modes that are within the band of interest to have little or no effect on performance. However, the best YIG selection for an application is to avoid all modes by operating between points B and C on the 110 mode.

The MIC Negative Resistance

In order to have a condition of potential instability which can lead to oscillations, a negative real part of the input

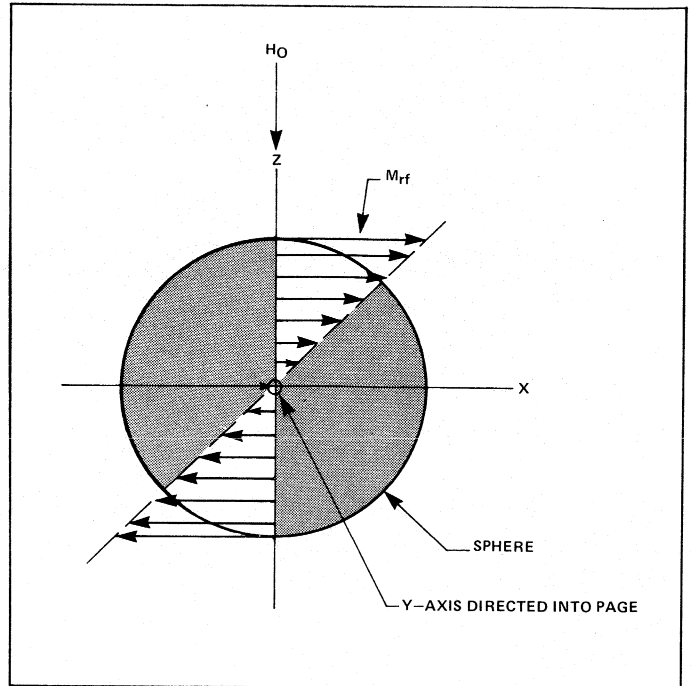

9. Distribution of RF magnetization is plotted for the 210 mode in a sphere.

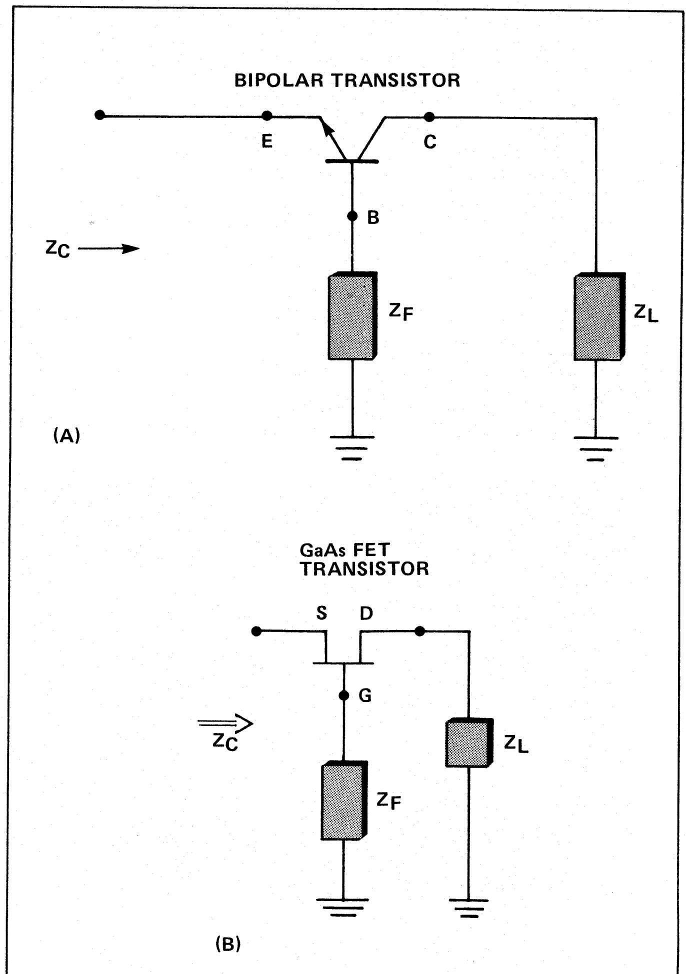

10. Negative resistance is obtained with these circuits, one for a bipolar transistor (a) and the other for a GaAs FET (b).

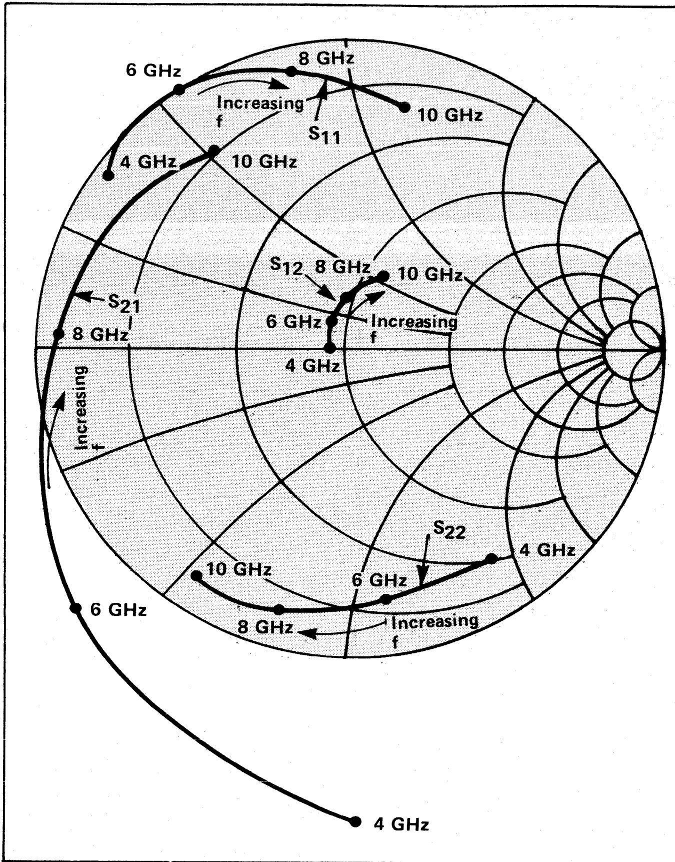

11. S-parameter data is plotted for a bipolar transistor in common base configuration.

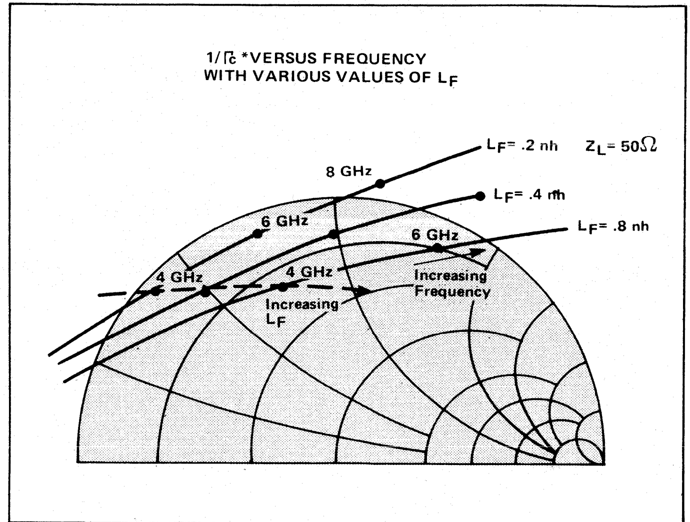

12. Inverse of the reflection coefficient is plotted versus frequency for various values of L_f. The inverse is dependent on feedback inductance; as L_f is increased, the upper frequency limit of the negative R also decreases.

impedance Z_c is required at the port of the transistor circuit which connects to the YIG resonator circuit. Figure 10 shows two of several configurations used to obtain a negative resistance (real part). The DC bias circuit has been eliminated from this diagram for clarity. Three basic two-port elements are required; the elements are:

- Transistor,
- Z_F, base or gate feedback impedance, and
- Z_L, load impedance.

The transistor is the basic active element needed to produce the negative resistance. It can be completely characterized by using S parameters over the frequency range of interest. (For information on S parameters, see the bipolar chapter.) Figure 11 shows typical S parameters of a common-base chip transistor. Similar data can be obtained when using the GaAs FET transistor. We will later cover in greater detail the important considerations that are required to produce a transistor for oscillator applications in these frequency ranges.

The feedback impedance, Z_F, is a small length of bonding wire and can be considered as a pure inductance of 1/2 to 2 nH. Therefore, $Z_F = jw\, L_F$ where L_F is feedback inductance.

The load impedance Z_L is a shunt capacitance element of about 0.5 pF optimized for best RF power, and the 50-Ohm-output microstrip or coaxial line. However, the element Z_1 for this application will include a buffer amplifier to isolate oscillator performance from load impedance variations external to the oscillator output port.

It is convenient to transform this Z_c to a reflection coefficient, Γ_c (which is also the S_{11} of the S-parameters) assuming a characteristic impedance of Z_o (typically 50 Ohms), by the equation:

$$\Gamma_c = \frac{Z_c - Z_0}{Z_c + Z_0} \quad \text{or} \quad \frac{z_c - 1}{z_c + 1} \qquad (14)$$

where $z_c = \dfrac{Z_c}{Z_0}$ Normalized input impedance.

This transform allows a more meaningful analysis for the conditions for oscillation, as will be discussed in the next section. This also makes the analysis compatible with many CAD techniques. The S parameters of the basic transistor are measured, this data is stored in the computer data files, and then fed into a computer program that performs the network analysis calculation of the transistor in the chosen circuit. Figure 12 shows typical Smith-chart plot of this data as a function of frequency. The data is plotted in the form $1/\Gamma_c^*$. Plotting the inverse of Γ_c maps all the negative resistance region inside the normal Smith-chart circle, since negative R implies $\Gamma_c > 1$. The conjugate then converts us back to the true phase of Γ_c. From this plot one can see that $1/\Gamma_c^*$ is dependent on the feedback inductance L_F. Generally, as L_F is increased, the lowest frequency where negative resistance occurs decreases, hence the oscillator starting frequency and the upper frequency limit of the negative R also decrease.

Increasing L_F will also increase the magnitude of the negative R; $1/|\Gamma_c^*|$ becomes smaller in the midband region, which means the oscillator will oscillate stronger. This could drive the transistor into a non-linear saturation region. When that happens, the harmonic-signal levels produced in the oscillator increase. If the oscillations become too strong, a parametric conversion effect can take place in the transistor, and subharmonic power is generated—that is, power at one half the fundamental operating frequency. These factors imply a design tradeoff between having enough L_F to obtain

the lowest frequency of oscillation desired, and having a minimum L_F to minimize harmonic problems.

The negative resistance is also a function of the load impedance, Z_L, or load reflection coefficient, Γ_L. Figure 13 is a plot of CAD data of $1/\Gamma_c^*$ for a single frequency for all values of Γ_L. Essentially, this is a mapping of the Γ_L Smith-chart plane onto the $1/\Gamma_c^*$ plane. From this, it is clear that the value of the load impedance is a valuable oscillator design parameter.

A mapping of Z_L onto $1/\Gamma_c^*$ is also shown in Figure 13 for the case when a buffer amplifier is inserted between the oscillator output and the load. The advantages of a buffer amplifier are clearly shown. The mapping circle becomes much smaller than the unbuffered case, and the load sensitivity of $1/\Gamma_c^*$ is substantially reduced.

It should be noted that the transistor S parameter data mentioned here is small-signal data. As the oscillations build up in the transistor, a large-signal condition is reached very quickly where this data is no longer valid. The large-signal case does not have an easy closed form solution, but considering the small-signal case, does tell us when the conditions for potential instability and thus oscillation have been met. The use of CAD provides a strong analytical and design tool, and the MIC thin-film circuit technology provides accurate and repeatable production fabrication of these designs.

Conditions for Oscillations

Once the YIG resonator circuit and negative resistance circuit are realized, one must know the conditions for oscillation in order to merge these into a controlled and well-defined oscillator. Figure 14 shows a block diagram of the major components of the oscillator. In order to understand the conditions for oscillation, the stability criteria for the system must be examined. This is done by examining the characteristic equation obtained from the network analysis.

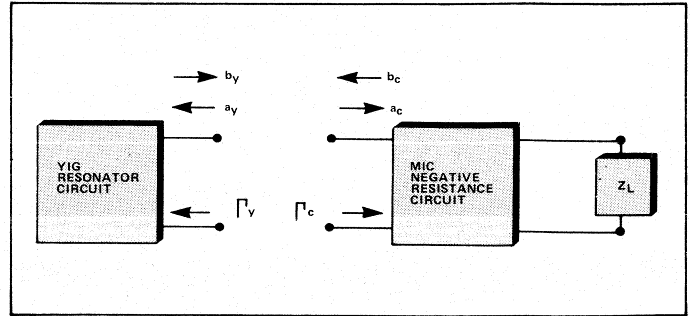

14. Major components of the YIG oscillator are the resonator circuit, the negative resistance circuit, and the load impedance.

The development of this equation is shown below:

$$S_{11}^{y} = \frac{by}{ay} \quad \text{and} \quad S_{11}^{c} = \frac{bc}{ac} \qquad (15)$$

where: $\Gamma_y = S_{11}^{y}$, reflection coefficient of the YIG resonator circuit,

$\Gamma_c = S_{11}^{c}$ reflection coefficient of the MIC negative-resistance circuit,

ay, ac, by, and bc are incidence and reflective waves related to power flow for their respective two-port.

Continued on page 222

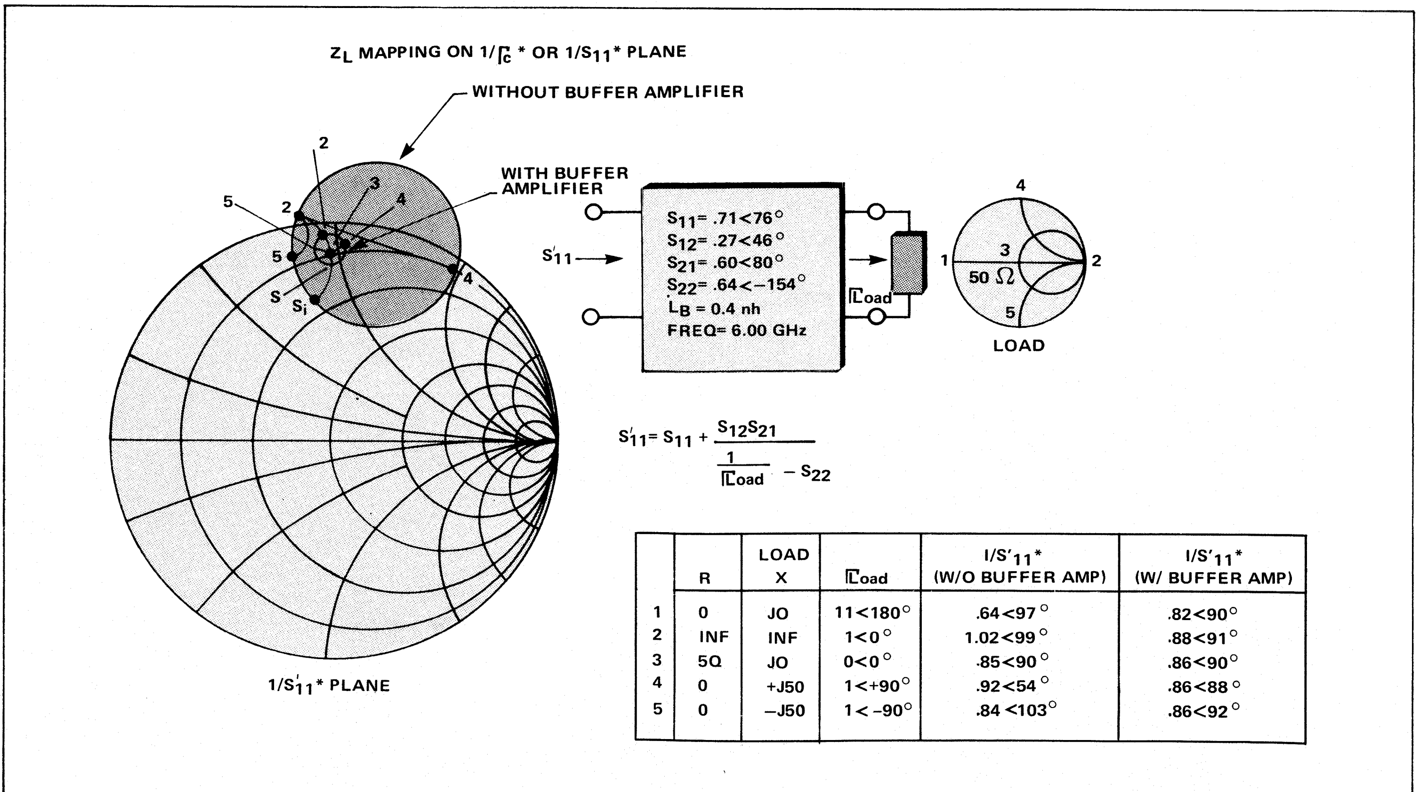

	R	LOAD X	ΓLoad	I/S'11* (W/O BUFFER AMP)	I/S'11* (W/ BUFFER AMP)
1	0	JO	11<180°	.64<97°	.82<90°
2	INF	INF	1<0°	1.02<99°	.88<91°
3	5Ω	JO	0<0°	.85<90°	.86<90°
4	0	+J50	1<+90°	.92<54°	.86<88°
5	0	–J50	1< -90°	.84 <103°	.86<92°

13. CAD data indicates that value of the load impedance is a valuable design parameter.

Continued from page 218

However, at steady-state oscillations:

$$by = ac \text{ and } bc = ay \quad (16)$$

because of conservation of power flow. Therefore,

$$by = S_{11}^{y}\ ay = S_{11}^{y}\ bc = S_{11}^{y} S_{11}^{c}\ ac = by \quad (17)$$

This requires:

$$S_{11}^{y} S_{11}^{c} - 1 = 0, \text{ or } \Gamma_y \Gamma_c - 1 = 0, \quad (18)$$

where Γ_c, as mentioned in the last section, represents the small signal case. Solving this equation:

$$\Gamma_y = \frac{1}{\Gamma_c} \quad (19)$$

thus it becomes clear why this form was plotted as such in the last section.

In order for this system to be potentially unstable, there must be one or more zeros of the characteristic equation in the right half plane (RHP) of the impedance plane. Since the Smith chart is a bilinear transformation of the impedance plane, and if we consider the inside area of the Smith chart to be the negative resistance region, then the zeros of the characteristic equation must lie inside the Smith chart. If we assume that Γ_c is a slowly varying function of frequency compared to the Γ_y such that it could be considered constant, then applying Nyquist's stability criteria to the characteristic equation implies Γ_y must encircle the point $1/\Gamma_c$ at least once to have a pole(s) in the RHP and thus be potentially unstable.

Note that it is reasonably accurate to assume Γ_c varies slowly in relation to Γ_y in this case since the YIG resonator circuit is a high Q resonator. A typical plot of Z_y or Γ_y takes the form of a circle near the circumference of the Smith chart. Recall that this input impedance Z_y was described earlier. If this is compared with Figure 12, we can see that the Nyquist criteria are satisfied; thus the conditions for oscillation are satisfied. Figure 15 shows both plots of Γ_c and $1/\Gamma_y{}^*$. One may note that it is also possible to predict approximately over what frequency range the oscillator will oscillate by seeing where $1/\Gamma_c{}^*$ enters and leaves the Γ_y coupling circle.

The above analysis considers only the small signal case. As oscillations build up, the transistor very quickly changes from a small-signal to a large-signal case. When this occurs, the measured S parameters and $1/\Gamma_c{}^*$ values change significantly. The oscillations will grow and change the characteristics of the transistor such that the pole(s) in the RHP move toward the LHP until they reach the imaginary axis, under stable oscillating conditions. If this did not happen, the transistor would quickly destroy itself in a runaway condition. At this point of stable oscillations, the negative real part of the MIC input impedance equals the positive real part of the YIG resonator impedance, and the imaginary parts of the two impedances are conjugately matched. Since $1/\Gamma_c{}^*$ is inductive, the YIG resonator circuit resonates the transistor circuit on the high side of its self-resonance.

The conjugate matching of the two impedances allows an understanding of the effect that load variations have on the oscillator parameters. It was shown in the last section that the $1/\Gamma_c{}^*$ is a strong function of load impedance, Z_L. If Z_L is changed, i.e. a change of phase and/or magnitude of the load VSWR, $1/\Gamma_c{}^*$, Z_c, will change. In order to continue to satisfy the conditions for stable oscillations, the imaginary part of Z_y must change. If the magnet current and coupling remain

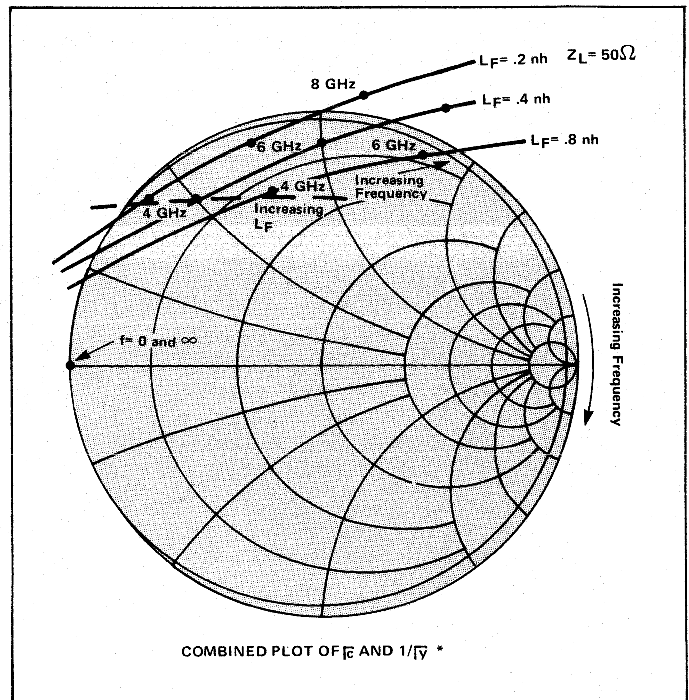

15. Plots of both the reflection coefficient and its inverse are useful in predicting the range of oscillation.

constant, then the element values do not vary. The only way for the reactance of Z_y to change is for the frequency to shift, which causes frequency pulling in the oscillator. The effect is minimized when a buffer amplifier is used. The same argument can be used to explain frequency pushing. As the operating voltage of the transistor varies, Z_c changes, the operating frequency changes.

The conditions for oscillation are dictated by the Nyquist stability criteria which says the coupling circle of the YIG-resonator-circuit reflection coefficient must encircle the transistor reflection coefficient for any given frequency, and the frequency bandwidth is roughly determined by that range of frequencies for which the $1/\Gamma_c{}^*$ is encircled by the coupling circle of Γ_y. Stable oscillations are realized when the magnitude of the real parts Z_c and Z_y are equal and the reactances are conjugately matched.

Oscillator Transistors

A transistor intended for use as a microwave oscillator must satisfy several requirements simultaneously:

- high f_{max} to insure reasonable efficiency,
- area adequate to give enough power, and
- thermal resistance low enough to insure thermal stability.

In general, the value of f_{max} can be made larger for smaller-area devices; conversely, larger-area devices yield higher output power at lower frequencies. Thus a power/efficiency tradeoff is encountered. The maximum frequency of oscillation f_{max}, is the most reliable index of the ability of a transistor to produce useful power; f_{max} is dependent in a rather complex way on a number of internal transistor parameters.

A good insight into the parameters of a bipolar transistor can be obtained by looking at a somewhat expanded expression for f_{max}.

$$f_{max} \cong \left\{ \frac{f_t}{8\pi \left[r_{con} C_{ct} + \frac{R_{sb} S_{BE} C_s}{2 L_e N_b} + r_{bi} C_{ci} \right]} \right\}^{1/2} \quad (20)$$

Figure 16 shows the physical location of the values given above and listed below.

r_{con} = base contact resistance
C_{ct} = total collector capacitance
R_{sb} = sheet resistance, active base
S_{BE} = space emitter to base stripe
C_s = capacitance base register between stripes to coil
L_e = length of emitters stripe
N_b = number of base stripes
r_{bi} = base resistance under emitter stripe
C_{ci} = collector base capacitance under emitter stripe

Each of the terms can now be analyzed in detail to see how f_{max} can be maximized. First of all, we can derive f_t:

$$\frac{1}{2\pi f_t} \cong \frac{26}{I_E} (C_{TE} + C_c + C_x) + \frac{W_b^2}{2.43 D_B} + \frac{K}{2V} \left(\frac{V_{cb}}{N_c} \right)^{1/2} \quad (21)$$

f_t = frequency when $|h_{fe}|$ is one
I_E = emitter current in mW
C_{TE} = emitter transition capacitance
C_c = collector capacitance
C_x = external e–b capacitance
W_b = base width
D_B = diffusion constant for minority carriers in base
K = constant
V = scattering limit of velocity of carriers
V_{cb} = collector voltage
N_c = carrier concentration in epitaxial layer

To increase f_t, the following real options are available:
- reduce C_{TE} by making emitter narrower,
- reduce W_b (shallow diffusion), or
- increase N_c (heavier-doped epitaxial layers).

The next parameter (from Eq. 20) is base contact resistance r_{con}. To reduce it we can:
- increase base doping in P^+ region,
- increase number of base contacts,
- increase length of base contacts, or
- use a lower-contact–resistance metal system.

Reducing C_{ct} is accomplished by reducing the overall device size. This could only be done at the expense of higher contact resistance and less current capability. Therefore, C_{ct} will not be considered as a variable parameter.

The base sheet resistance, R_{sb}, can be decreased up to the point where the reduction in r_{bi} is offset by the reduction in mobility. Spacing between base and emitter, S_{BE}, can be decreased to the point where production yields suffer. This dimension is in the 1-to-2-micron range. C_S will also be reduced by making S_{BE} smaller and is therefore also limited by yield considerations.

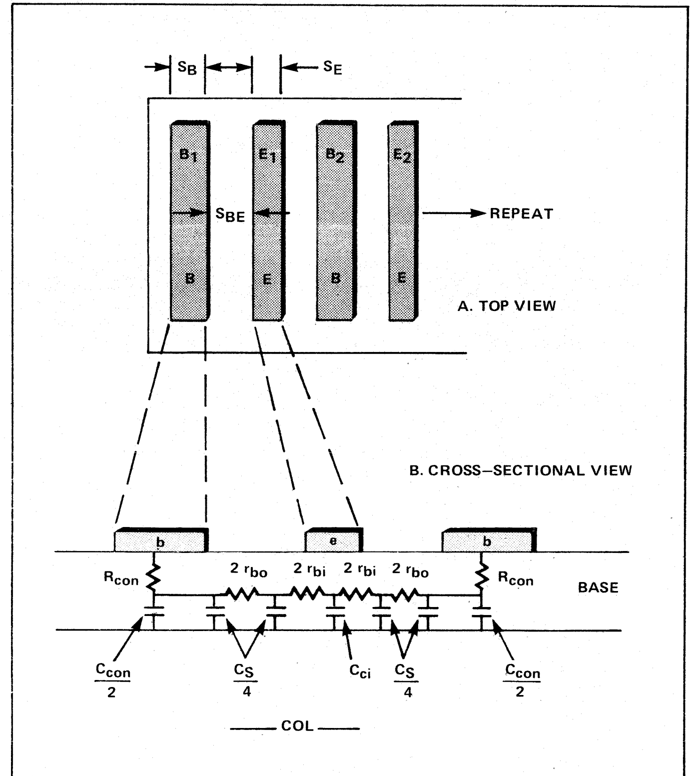

16. Location of base parameters is plotted for a bipolar transistor.

Increasing both the emitter's length, L_e, and the number of base fingers, n_b, will reduce base resistance, but will increase capacitance.

The base resistance under the emitter r_{bi} can be decreased by increasing the doping level in the base, N_B, and by making the emitters narrower (reduce S_e). The latter is a very powerful tool for increasing f_{max} since it also reduces C_{ci}.

The device parameter's tradeoff for the GaAs transistor is different. However, the goal of maximizing f_{max} and optimizing the useful power output within thermal limits are basically the same.

Mechanical, electrical, and thermal properties must be carefully selected when choosing the basic material to build a YIG oscillator that will perform reliably within rigid electrical specifications over stringent environmental conditions. Also, manufacturability of an oscillator product over many years requires batch-to-batch consistency of the properties of the material used. The material selected must be capable of being fabricated and processed with relatively high yields.

Mechanical Structure

The magnet material is selected to provide the required magnetic field density, linearity, and hysteresis over the temperature and frequency range specified. Equally important is the temperature coefficient of expansion and the thermal sensitivity of permeability since these coefficients directly affect frequency drift with temperature. The material must be rigid because it is the mechanical structure of the oscillator, and variation of the magnet gap must be kept within

0.000050 inches to meet reasonable stability specification. The other environmental requirements also have an impact on the choice of the material because of the mechanical integrity required for shock, pressure/altitude, explosive atmosphere, and acoustic noise. The oscillator requires RF connectors and a mounting method in the system; consideration of mounting is very important for best thermal performance. After all these considerations the material must be chosen for ease of fabrication and be capable of being the hermetic enclosure. The material chosen is 48 percent nickel, and 52 percent iron.

• *MIC Substrate Assembly.* This assembly consists of BeO and alumina; attached to it are the transistor, chip capacitors, and gold bonding wires. The choice of materials and assembly procedures are the basis of Avantek MIC oscillator techniques. All materials used are non-magnetic to preserve the magnetic-field uniformity within the magnetic-pole gap and have proven reliability and repeatability from batch to batch. The materials chosen are capable of metallization in large quantities with high yields.

The metallized beryllium oxide (BeO) is used as a thermal heat conductor, DC and RF ground, and a rigid circuit carrier. The electrical insulating properties are necessary to reduce eddy-current losses and provide better FM coil modulation performance. The thermal conductivity of BeO provides a low thermal impedance from the alumina circuit to the mechanical structure, insuring high-temperature performance to electrical specifications and improved MTBF. The YIG coupling loop is mounted on a bypass MOS capacitor and to the alumina RF substrate, both of which are die-attached to the metallized BeO. It is very important that the coupling loop be rigid and fixed with respect to the YIG sphere for operation under vibration requirements.

Alumina ceramic, Al_2O_3, material is consistent, non-varying in dielectric constant from lot to lot; and the surface finish available is excellent and provides low-loss, uniform RF transmission lines and repeatable resistor values. The repeatability of the electrical specification over the temperature extremes together with the special oscillator transistor provides the consistency required for manufacturability.

• *YIG Sphere Assembly.* The YIG sphere is a unique material requirement; it is the microwave resonator when immersed in the necessary magnetic field. These spheres are processed in batches of thousands. Manufacturing techniques for YIG spheres are well established and the technology has matured for the past twenty years. The other materials in this assembly are BeO to provide electrical isolation, and aluminum. These materials are selected on the basis of mechanical strength and thermal heat conductivity such that YIG spheres' displacement under environmental conditions in the coupling loop is invariant and maintained at the temperature of the YIG heater.

The YIG sphere is a single-crystal garnet prepared with a $4\pi M_s$ of 200 to 1,780 Gauss. These are guaranteed to fall within ±5% or better for a stated $4\pi M_s$ value. Uniformity of material properties is generally ±2 percent. Spheres are processed in diameters of 0.2 to 2 mm with tolerance of ±5 μm.

Pure YIG spheres have a $4\pi M_s$ of 1,780 Gauss and are normally 0.018 ±0.001 inch in diameter. Sphericity is less than 0.5 percent deviation. The resonance line width is specified to be less than 0.4 Oersted at 25°C and this measurement is made at 5.1 GHz. The crystal batch is sampled and it must qualify in an oscillator circuit so that the electric specifications will be realizable with yields greater than 80% before it is acceptable.

• *FM Coil Assembly.* The FM coil assembly consists of about 16 turns of #40 wire mounted on the magnet pole face.

• *Other Purchased and Required Parts.* Various miscellaneous parts are grouped in this category. The two most important ones are the YIG heater assembly and the main coils.

The YIG heater is composed of a positive-temperature-coefficient semiconductor resistor, mounted on two rigid plastic ears with the means to grip the YIG rod assembly in a coaxial fashion. The positive TC resistor is a commercially available part. The control temperature is +105°±5°C and the required DC resistance is 35 to 100 Ohms at +25°C. The YIG heater reduces the temperature variation of the YIG sphere by a factor of about 1/7 relative to the case temperature variation of the oscillator. This improves the thermal drift, reduces possibilities of moding, and improves electrical performance over temperature.

The main coil is made of copper wire because of its low DC resistance. The wire is wrapped in high-temperature epoxy for good mechanical strength at the maximum temperature. Wire size and turns are selected to meet the specifications of DC resistance, inductance, and main coil sensitivity. ■

References

1. B. Lax and K. J. Button, *Microwave Ferrites and Ferromagnetics,* McGraw-Hill Book Co, 1962, pp 145–196.
2. P. S. Carter, "Orthogonal-Loop-Coupled Magnetic Resonance Filters and Bandwidth Narrowing Due to Coupling Inductance," *IEEE Trans,* MTT, Vol. MTT-18, No. 2, February 1970.
3. P. S. Carter Jr. and C. Flammer, "Unloaded Q of Single Crystal Yttrium-Iron-Garnet Resonator as a Function of Frequency," *IRE Trans MTT (corres.)* Vol. MTT-8, Sept. 1960, pp 570–571.
4. Lax, *ibid.* p 673.
5. R. E. Tokheim and G. F. Johnson, "Optimum Thermal Compensation Axes in YIG and GaYIG Ferromagnetic Spheres," 1970 Inter Mag. Conference; paper 10.8.
6. Y. Sato and P. S. Carter, "A Device for Rapidly Aligning and Mounting Ferromagnetic Single Crystals Along and Desired Axis," *IRE Trans MTT (Corres.)* Vol. MTT-10, pp 611- 612, November 1962.
7. J. E. Artman, "Microwave Resonance Relations in Anisotropic Single Crystal Ferrites," *Proc. IRE,* Vol. 44, pp 1284–1293, October 1956.
8. L. K. Anderson, "Coupling of Small Ferromagnetic Ellipsoids to Microwave Circuits," *Microwave Lab. Report No. 880,* Hansen Laboratories of Physics, Stanford University, Stanford, Calif.
9. J. Mercereau, "Ferromagnetic Resonance of Factor to Order $(kR)^2$," *J. Appl. Phys. 30* 1845, April 1959.
10. L. P. Walker, "Magnetostatic Modes in Ferromagnetic Resonance," *Physical Review,* Vol. 105, No. 2, January 1957.
11. P. C. Fletcher and R. O. Bell, "Ferromagnetic Resonance Modes in Sphere," *J. Appl. Phys.,* Vol. 30, No. 5, May 1959.

Cost-for-Performance Criteria for Mixers

Because there is no universally appropriate mixer, the extensive variety of models must be evaluated for the type best suited to its application.

By FERENC MARKI, *Western Microwave, Inc.*

Microwave mixers covering the 1.0- to 18-GHz band will be discussed in this article, written for the "bench engineer" and the "hardware" designer. It is a basic reference guide with some information detailing the most popular definitions of mixer performance parameters.

Microwave mixers are offered by a number of manufacturers, each claiming to have the best line of mixers in the industry. In the last decade numerous new types of microwave mixers have been introduced, from low-noise to wide-band, while no significant changes have taken place on the device itself—at the mixer diode level. New packaging types were introduced, adding to the abundance of styles, performance, and price. To some engineers this represented a welcome evolutionary change, but to others it only added to the difficulty and confusion of mixer selection. This section, Guide to Mixer Selection, should be helpful in making your choice. A universal mixer circuit, if there were such a thing, would eliminate the difficulty of choosing. Meanwhile, we have a large selection of good mixers offered by the industry.

Mixer Evolution, The Balanced Mixer Family Circle

The balanced mixer family is made up of mixers that use the in-phase and the 180 degree out-of-phase power dividers in some combination. A balanced mixer out-phases or cancels certain intermodulation products between the LO and the RF signal inputs. These are the mixers most commonly offered by the mixer manfuacturers.

The first member of the mixer family is the one-diode or single ended mixer. This mixer or diode is present in all mixers and provides the basic mixing process, which is simply the spreading of the input signal's energy in the frequency domain, all non-linear elements will do the same to some degree. The non-linear element used in most mixers is the Schottky-barrier mixer diode.

The subsequent members of the family are balanced mixers. Balancing is the same as out-phasing signals to create a reactive cancellation. This is accomplished with a channelization technique using phase-correlating power dividers of zero and 180-degree type. Consequently *all* multiple-diode-type mixers are channelized mixers. The number of diodes alone does not determine if the mixer is balanced, single balanced or double balanced. Mixer balance is the measure of cancellation of single tone intermodulation products between the LO and RF signals. If the single diode mixer generates 100 percent of the intermodulation products, the single balanced mixer will reduce this to 50 percent, and the double balanced mixer will further reduce it to a 25 percent intermodulation content as viewed at the mixer's output (IF port).

There are two ways to make the simplest single-balanced mixers. Both involve the use of baluns, the 180-degree

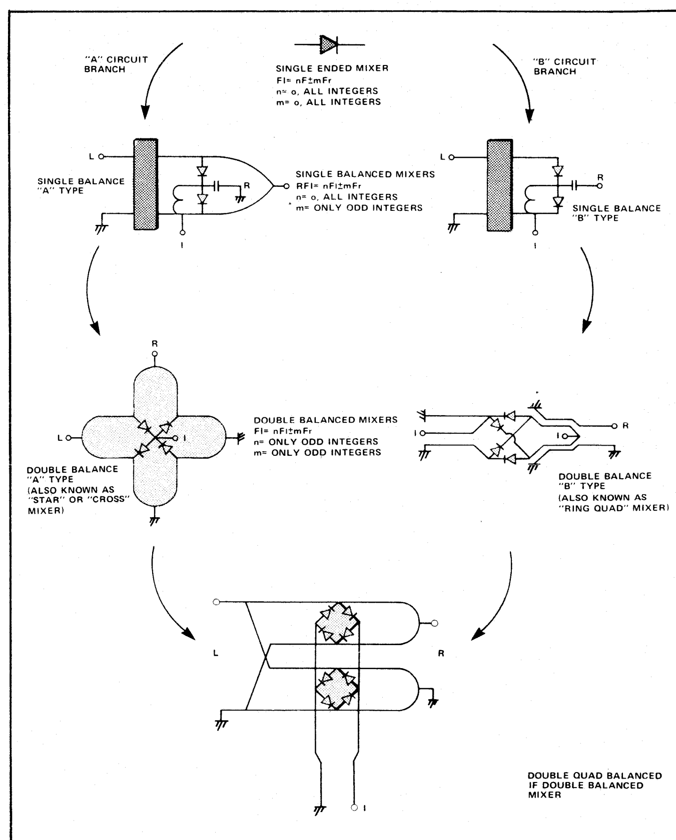

1. Balanced mixer family circle.

reactive (no isolation between the two output ports) power dividers. Both involve the use of some form of an in-phase reactive power divider. The only significant difference between these two single balanced mixers is the way in-phase power division is accomplished. These single-balanced mixers are the basic building blocks of the double-balanced mixers. The difference between the two basic branches of the family of single/double-balanced mixers is the way the in-phase power division is provided. Branch "A" of the family (Fig. 1), uses an in-phase power divider that first divides the signal input into two channels and then recombines the signals at the junction of the two diodes. Branch "B" of the family guides the signal input directly into the junction of the two diodes and provides two separate ground return paths for the signal. No significant performance difference will result from using the "A" type

Ferenc Marki is manager of the Microwave Integrated Circuit Division at Western Microwave, Inc., Santa Clara, Calif.

Double Balanced Microwave Mixer 8.0 to 14.0 GHz

- DC to 4.0 GHz IF Band
- 6 dB Conversion Loss Typ.
- 25 dB Isolation Typ.

PARAMETER	FREQUENCY RANGE		SPECIFICATION[2]	
SSB Conversion Loss or SSB Noise Figure[1]	F_R, F_L	8.0 to 14.0 GHz	5.5 dB typ	7.5 dB max
	F_I	DC to 1.0 GHz		
	F_R, F_L	8.0 to 14.0 GHz	6.5 dB typ	8.0 dB max
	F_I	DC to 3.0 GHz		
	F_R, F_L	8.0 to 14.0 GHz	7.0 dB typ	8.5 dB max
	F_I	DC to 4.0 GHz		
Isolation				
L-R, R-L, L-I	F	8.0 to 14.0 GHz	30 dB typ	22 dB min
R-I	F_R	8.0 to 14.0 GHz	25 dB typ	
VSWR				
L Port	F_L	8.0 to 14.0 GHz	1.7:1 typ	
R Port	F_R	8.0 to 14.0 GHz	1.7:1 typ	
I Port	F_I	.01 to 4.0 GHz	1.5:1 typ	
Conversion Compression 1.0 dB max	F_R, F_L	8.0 to 14.0 GHz	RF +4 dBm min, L version	
	F_I	.01 to 4.0 GHz	RF +5 dBm min, M version	
Third Order Two Tone Input Intercept Point	F_R, F_L	8.0 to 14.0 GHz	+15 dBm typ[3], L version	
	F_I	.01 to 4.0 GHz	+20 dBm typ[3], M version	

2a. Tabulated typical performance of a "B" type "ring quad" double-balanced mixer.

single balanced mixer or the "B" type single balanced mixer. Only the physical construction will dictate the use of one or the other type. The physical construction, then, is an important element in determining the total mixer performance, for it contains filter networks that basically provide the frequency domain boundry conditions for the diodes.

The branch "A" double balanced mixer is made by taking two "A" type single balanced mixers and connecting them at the junction of their respective diodes, forming a four-diode junction, two diodes pointing into and two diodes pointing out of the junction. This type of double-balanced mixer is also known as the "star" or "cross" mixer.

The branch "B" double balanced mixer is built by taking two "B" type single-balanced mixers and connecting them at the diode ends where the baluns are found. The two baluns become one which serves both diode pairs. However, to make the mixer double balanced, one pair of diodes must be rotated so that the four diodes form a ring (Fig. 1). This is the well-known ring quad. If one pair of diodes is not rotated, a bridge quad is formed which is also known as a full wave rectifier quad. The mixer thus created is a single-balanced mixer having two channels and a balanced IF port. This bridge mixer has many useful applications that include a biasable wideband mixer. A new balun is created in the construction of both "A" and "B" type double-balanced mixers. The minimum number of baluns necessary to make a double-balanced mixer is two. Note that the bridge-type mixer actually has three baluns, but it is no more than a single balanced mixer. There are no significant differences between the "A" and "B" type double-balanced mixers.

Physical construction, ease of assembly, and availability of monolithically created diode quads guide the selection of a mixer circuit for construction and mass production. Excellent mixer performance resulted in the massive use of the "B" circuit (ring quads) by major mixer manufacturers. The "A" circuit is used by some manufacturers mostly in narrow band, high-performance applications.

In recent years, a new type of double-balanced mixer emerged and is being produced in large quantities by mixer manufacturers. This mixer has two quads, or a total of eight diodes, and can be considered as both an "A" type circuit and a "B" type circuit. In fact, the mixer circuit is the result

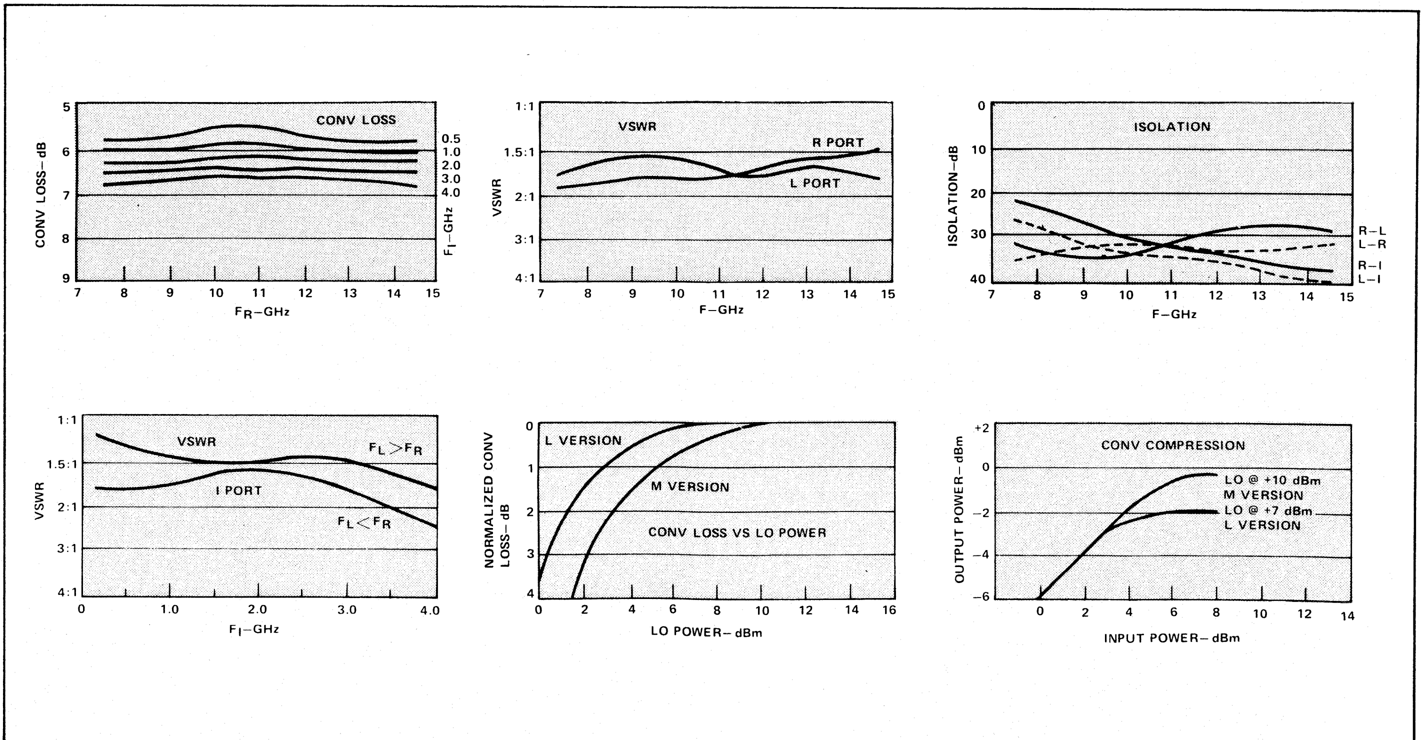

2b. Typical performance curves of a "B" type "ring quad" double balanced mixer.

Double Balanced Microwave Mixer 2.0 to 18.0 GHz

- 0.005 to 4.0 GHz IF Band
- 6.5 dB Conversion Loss Typ.
- 30 dB Isolation Typ.

PARAMETER	FREQUENCY RANGE		SPECIFICATION[2]	
SSB Conversion Loss or SSB Noise Figure[1]	F_R, F_L	2.0 to 18.0 GHz	6.5 dB typ	8.5 dB max
	F_I	0.005 to 1.5 GHz		
	F_R, F_L	2.0 to 18.0 GHz	7.0 dB typ	9.0 dB max
	F_I	0.005 to 2.5 GHz		
	F_R, F_L	2.0 to 18.0 GHz	7.5 dB typ	9.5 dB max
	F_I	0.005 to 4.0 GHz		
Isolation				
L-R	F_L	2.0 to 4.0 GHz	20 dB typ	16 dB min
		4.0 to 18.0 GHz	25 dB typ	20 dB min
L-I	F_L	2.0 to 18.0 GHz	30 dB typ	20 dB min
R-L, R-I	F_R	2.0 to 18.0 GHz	25 dB typ	
VSWR				
L Port	F_L	2.0 to 18.0 GHz	2.0:1 typ	
R Port	F_R	2.0 to 18.0 GHz	2.5:1 typ	
I Port	F_I	0.005 to 4.0 GHz	1.5:1 typ	
Conversion Compression 1.0 dB max	F_R, F_L	2.0 to 18.0 GHz	RF 6 dBm min, M version	
	F_I	0.005 to 4.0 GHz	RF 8 dBm min, H version	
Third Order Two Tone Input Intercept Point	F_R, F_L	2.0 to 18.0 GHz	20 dBm typ[3], M version	
	F_I	0.005 to 4.0 GHz	22 dBm typ[3], H version	

3a. Tabulated typical performance of a double quad IF type double-balanced mixer.

of doubling either "A" or "B" type double-balanced mixers in a parallel construction that creates a balanced IF port. A balun is constructed on the IF port which combines the output of each of the two double-balanced mixers. The most significant performance improvement of this mixer over the simple four-diode double-balanced mixers is the wide IF frequency coverage independent of the LO and RF port frequency range. The balanced mixer family is mostly complete. There are some circuits that are related to this mixer family but which will not be discussed in this article. A complete pictorial presentation is shown in Figure 1.

Mixer Performance

The typical performance of a "B" type four-diode double-balanced mixer is given in Figures 2a and 2b, and a typical performance of the two quad balanced IF type double balanced mixer is given in Figures 3a and 3b.

- *Conversion loss* is the most fundamental performance specification of a mixer; it is the ratio of converted IF output to the small signal IF input power expressed as a dB loss. The small signal input level should be used for the conversion loss calculation and should be the lowest level input regardless of what port the signal is injected into. A typical conversion loss for a mixer is six to seven dB for downconversion and seven to eight dB for upconversion. Typically, only the downconversion conversion loss is specified by most manufacturers.
- *Isolation* is the second most common specification. The LO to RF isolation and the LO to IF isolation is specified by virtually all of the manufacturers. Isolation is the ratio of output power to input power in dB.
- *VSWR* of the three ports of a mixer are generally not specified, but performance curves are provided by most manufacturers. Most modern mixers have VSWR's better than 2:1 at all three ports.
- *One-dB compression point* is measured and specified as an input compression. The LO drive level should always be stated in conjunction with this specification. At the one-dB compression point the conversion loss increases by one dB over the conversion loss measured in the linear range.
- *LO drive level specification* is generally stated as a minimum and maximum level. Mixer performance remains essentially the same at this specified range. The optimum LO drive level reflects the type of diode being used. Diode

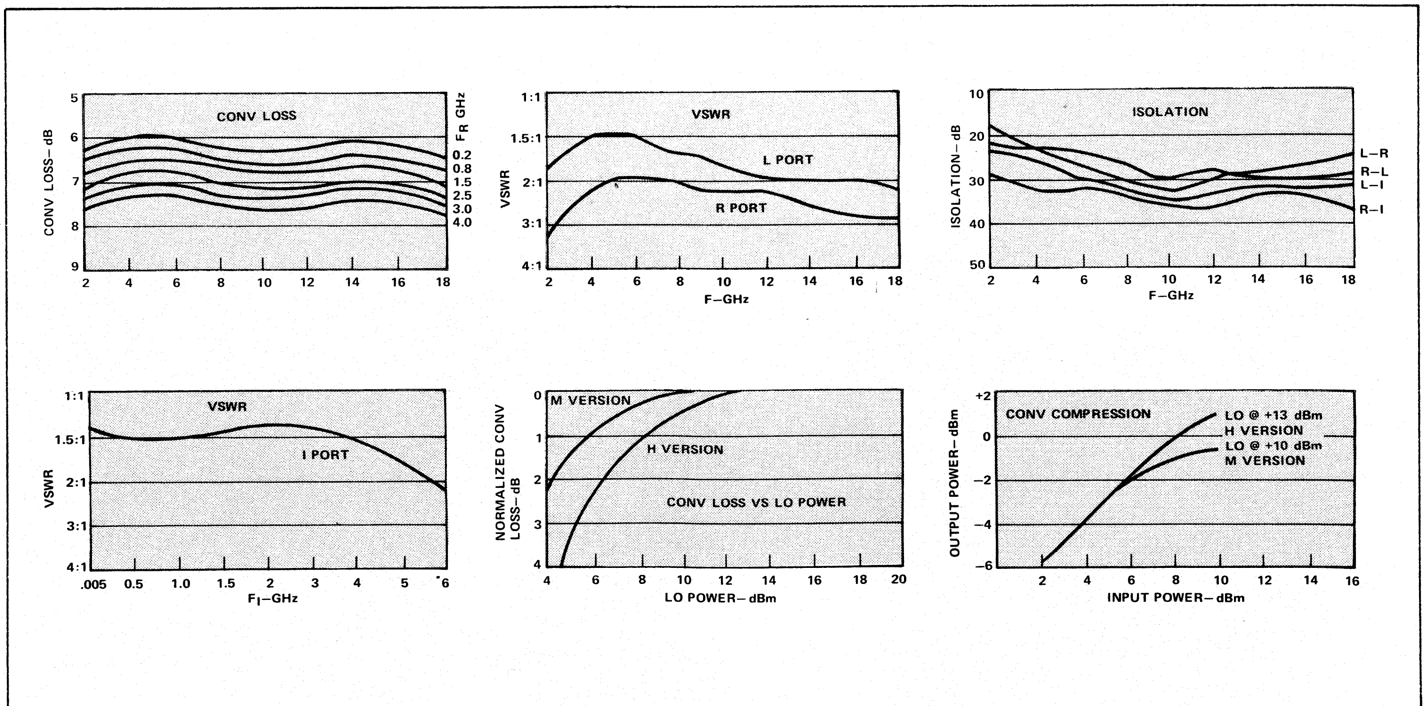

3b. Typical performance curves of a double quad balanced IF type double-balanced mixer.

quads are now available with barrier potentials ranging from low to very high levels. Monolithic multiple junction quads are now available from some manufacturers.

- *Noise figure* of a mixer is most often specified as a single sideband noise figure. The conversion loss of a mixer and its noise figure are almost the same due to the fact that in most commercially available diodes the intrinsic noise temperature ratio is *one*.
- *Single-tone intermodulation products* result from the mixing of the LO and RF signals. Double balanced mixers suppress most of these products. Unit-to-unit variation of a particular mixer type can be as much as 10 dB. Figure 4 shows a typical microwave mixer performance.

TYPICAL SINGLE TONE INTERMODULATION SUPPRESSION (dBc) FOR −10 dBm INPUT

HARMONICS OF F_R (m) \ HARMONICS OF F_L (n)	1	2	3	4	5	6
6	>70	>70	>70	>70	>70	>70
5	>70	>70	>70	>70	>70	>70
4	>70	>70	>70	>70	>70	>70
3	65	>70	>70	>70	64	>70
2	55	56	55	57	55	60
1	0	30	19	39	36	45

4. Typical single-tone intermodulation suppression (dBc) for -10 dBm input.

- *Two-tone intermodulation suppression*, (2FR1-FR2)-FL, should always be specified with the LO drive. Diodes with large barrier potentials are often used to improve the two tone performance. Another method uses a resistor in the path of the rectified current that is generated by the LO drive. The voltage drop across the small resistor back biases the diode and increases the forward voltage potential. This self-biasing or self-back-biasing method assures that the best two-tone performance for a given LO drive is obtained. Input intercept points as high as 30 dBm can be achieved with both types of circuit constructions. The two-tone performance of a mixer should not be confused with the single-tone intermodulation performance. A well-constructed, well-balanced double balanced mixer that has excellent single-tone intermodulation performance may or may not have a good two-tone performance. However, a good two-tone performance and a good single-tone intermodulation suppression can be obtained in the same mixer. Generally if a good two-tone performance is required, be prepared to supply the necessary LO drive level.

Image Rejection In a Mixer

An ordinary double or single balanced mixer will convert from either sidebands, upper or lower, with equal efficiency. Consequently, this mixer downconverts the non-correlated noise from both sidebands and adds the two powers, resulting in a 3 dB increase in noise power output at the I port. It is important to note that if the image noise of an RF amplifier placed in front of a mixer is allowed to be downconverted into the I port, no amount of RF gain will remove the added 3 dB in noise figure.

Image reject mixers will take care of the problem of added noise figure. There are two types of image reject mixers. One type has an image filter at the RF input and will either reflect the image noise back into the source or will reactively terminate it. In either case, the mixer does not downconvert the image noise. The other type of image reject mixer is a channelized mixer that will downconvert the image noise into one of the two IF ports and will downconvert the real signal and noise into the other IF port. The channelized image reject mixer is very common for low IF frequency applications. Noise contribution vs. image rejection is shown in Figure 5.

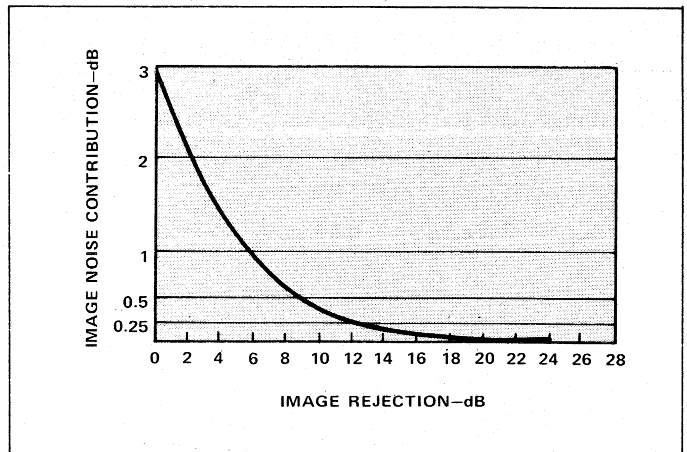

5. Noise contribution versus image rejection.

Mixer Package Styles

There is no standard mixer size. Mixer package styles are numerous, but they fall into two general categories—connectorized and unconnectorized. The connectorized mixers range in size from as small as 0.5″ by 0.5″ to as much as two to three inches square. The most common size is about one inch long and one inch wide and a half inch thick. The unconnectorized type of mixers are either the microstrip terminated flatpacks or the pin terminated, generally hermetically sealed pin packages. A number of pin package type mixers can be made connectorized by simply sliding a connector onto the pin. These connectors are also field replaceable. The average thickness of the pin packages is 0.2 inches. Some have mounting holes, others do not.

Guide To Mixer Selection

Mixers should be selected on the basis of application/performance and price/availability. There are numerous

mixers on the market with varied performance, but the best mixer is one that does the job for the lowest price and can be easily obtained.

The first question then is this: What is the job; what is the application? A set of questions about the application can establish the minimum specification of a mixer.

1. *What is the LO drive level available for the mixer?*
   The answer to this question will help to identify the type of mixer as being high level, low level, biasable etc. The tone performance and one dB compression point is thus established. If the performance is not satisfactory, the LO drive may have to be increased.

2. *What is the LO input frequency?*
   It is assumed at this point that the LO drive signal is the largest signal level of the two inputs injected into the mixer. Any of the three ports L, R, and I of the mixer can become the LO large signal input port. The L, R, and I port designation is historical and has no other significance. A more appropriate designation should be J1, J2, and J3 ports.

3. *What is the small signal maximum input power and what is its frequency?*
   The maximum input power will indicate if the mixer is operated in the linear region and which port will be the small signal input port.

4. *What is the output frequency?*
   Once this frequency is known, the frequency relationship of the two input signals and the one output signal is established. Whether one calls this relationship an upconversion or a downconversion is not important. For any combination of two input ports, the third port will be the output port.

5. *How good should the mixer port VSWRs be?*
   Mixers in general have poor VSWR's. Even when the ports are well matched at the input and output frequencies, the mixer behavior in a system environment cannot be totally predicted. Single-tone intermodulation products are presented at all three ports of the mixer. The most troublesome of these products is the (2FL-FR) pseudo-image that comes out of the mixer's R port. If this product is not well-terminated, it will reflect back into the mixer for further re-mixing with the LO. The resultant product (2FL-FR-FL) will be in phase correlation with the primary mixing product, the intermediate frequency FI. As much as ±3.0 dB ripple can result when a mixer R port is connected to a narrow bandpass filter. An attenuator or isolator can eliminate this problem when placed between the filter and the mixer.

6. *Is carrier suppression desirable?*
   Carrier suppression is specified for upconversion, and LO to RF isolation is specified for downconversion. To achieve the best carrier suppression, the low frequency IF input signal level must be the largest of the two input signal levels. In this way the carrier suppression is always equal to LO to RF isolation minus the conversion loss.

7. *What about intermodulation suppression, spurs, etc?*
   Single- and two-tone intermodulation products are suppressed by different mechanisms. If good two-tone suppression is needed, be prepared to supply the mixer with large LO drives. If good single-tone intermodulation product suppression is needed, select a mixer with good balance. If a mixer cancels a product, it will do so with two of its diodes. There is no difference between the performance of a single balanced mixer and a double balanced mixer when both cancel the product in question. However, higher order products of the small signal are better suppressed in a double or multichannel mixer because the signal level at the diodes is lowered by the power division between the channels. The dual-quad double balanced mixer, especially in the upconverter mode, will add (m-l) times 3 dB to the suppression over the single quad double balanced mixer for products of the (nFL ± mFR) type, where FR is the small signal frequency.

8. *What package style should be selected?*
   This is your choice. Package styles are many and should be selected on the basis of application.

Bibliography

Richard T. Davis, "Front End Designs - Assaulting The Old Noise Barriers," *MicroWaves*, Vol. 10, No. 4, pp. 32-36, (April 1971).

Dr. E. James Crescenzi, Jr., Richard W. Oglesbee, Roger A. Chapell, "Integrating Components For New Front End Designs," *MicroWaves*, Vol. 13, No. 8, pp. 35-47, (August 1974).

Robert B. Wilds, "Microwave Two-Phase Converters For Imageless Receivers," *Microwave Journal*, Vol. 4, No. 9, pp. 84-87, (September 1961).

Dr. E. James Croscenzi, Jr. and Ferenc A. Marki, "Fused Silica: A Better Substrate for Mixers?" *MicroWaves*, Vol. 15, No. 1, pp. 34-3, (January 1976).

D. L. Cheadle, "Selecting Mixer For Best Intermod Performance Parts I and II," *MicroWaves*, Vol. 12, Nos. 11 and 12, pp. 48-52 and pp. 58-62, (November 1973 and December 1973).

Lawrence E. Dicksons and Douglas W. Maki, "An Integrated-Circuit Balanced Mixer Image and Sum Enhanced," *IEEE Transactions, Microwave Theory and Techniques*, pp. 276-281, (March 1975).

James B. Cochrane and Ferenc A. Marki, "Thin-Film Mixers Team Up To Block Out Image Noise," *MicroWaves*, Vol. 16, No. 3, pp. 34-40 & p. 84, (March 1977).

Ferenc Marki, "Miniature Image Reject Mixers and Their Use in Low-Noise Front-Ends In Conjunction with GaAs FET Amplifers, Conference Record, Circuits, Systems and Computers", *IEEE Catalog* No. 77CH1315-1 C/CAS, Nov. 7-9, 1977.

Antenna Design Tradeoffs Examined

Handy nomograms and basic equations apply to antennas from printed circuits to large phased arrays.

By J. R. Forrest, *University College London*

A wide variety of microwave antennas is in common use. Reflector antennas using a parabolic dish and a single waveguide feed predominate. However, greater control of the radiation pattern is possible with a phased-array aperture made up of many individual radiating elements, each with phase and amplitude response that can be separately defined. Printed circuit antennas, either individually or in phase-array form, are also becoming more common, particularly for applications where a flat or conformal antenna is required.

Some of the basic design principles relating the important antenna parameters such as directivity, gain, beamwidth, sidelobe level, and bandwidth will be discussed here. It is impossible to give very detailed design data for such a wide topic, but a major aim will be to identify references where the reader may find that detailed design information.

Basic Definitions

An antenna is simply a component for the conversion of an electrical signal into an electromagnetic wave or vice-versa. It is a reciprocal component and may be thought of as an aperture of defined dimensions that can support electric currents and associated electric fields.

The radiation pattern of an antenna is a plot of the relative strength of the radiation field as a function of the angles θ and ϕ for a given distance r from the antenna in spherical geometry. Unless otherwise specified, the field is taken to be that in the so-called "far-field" region at distances greater than $2D^2/\lambda$ from the antenna (where D is the aperture dimension in the plane of measurement and λ is the radiation wavelength).

For some purposes, isotropic (i.e., omnidirectional) radiators are required. Most antennas, however, have a capability for increased response in a given direction, the radiation pattern comprising a main lobe and several sidelobes of lesser amplitude. The antenna beamwidth, θ_B, is usually specified as the angular separation of the −3-dB points of the main lobe.

A directional antenna has a concentrating effect when emitting power or receiving signals. There frequently is confusion between the terms "directivity" and "gain." The directivity $G_D(\theta,\phi)$ in a given direction θ,ϕ is given by:

$$G_D(\theta,\phi) = 4\pi \times \frac{\text{Power radiated per unit solid angle in direction } \theta,\phi}{\text{total radiated power}} \tag{1}$$

It is the power density in that direction, relative to that which an isotropic radiator would produce. The maximum directivity G_{DM}, frequently abbreviated just as directivity, is strictly the value of the directivity in the direction corresponding to the peak of the main lobe.

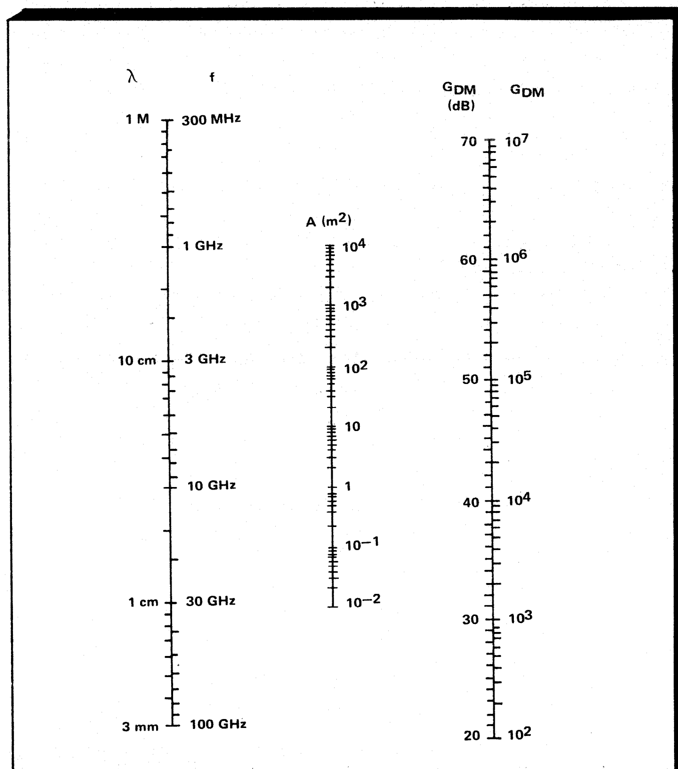

1. This nomograph can be used to calculate the maximum directivity of a uniformly illuminated aperture. Here, maximum directivity is G_{DM}.

The maximum directivity of any antenna aperture of area A, which has a uniform aperture field (a so-called uniform aperture illumination function) is given by

$$G_{DM} = \frac{4\pi A}{\lambda^2} \tag{2}$$

The nomograph of Figure 1 enables the maximum theoretical directivity of such an antenna to be evaluated. However, obtaining a practical value of maximum directivity for a given antenna involves pattern integration in three dimensions to obtain a true value of the denominator in Equation (1).

The gain, or power gain, $G(\theta,\phi)$ differs from the directivity in that it takes into account the inefficiencies of the

Dr. John R. Forrest is with the University College London. He will also be the technical chairman of the upcoming Military Microwaves Conference.

antenna through dissipative losses in conductors and dielectrics.

$$G(\theta,\phi) = 4\pi \times \frac{\text{Power density radiated per unit solid angle in direction } \theta,\phi}{\text{total input power to the antenna}} \quad (3)$$

The usual method of measuring directive gain is to compare the directive gain of a given antenna with that of a standard antenna (standard gain horn, for example). It is assumed that both the antenna under test and the standard gain antenna are impedance-matched to the generator or load. If the antenna under test is mismatched, its full gain will not be realized, the shortfall being the mismatch loss. The maximum gain G_M, often abbreviated simply as gain, is the value of the gain in the direction corresponding to the peak of the main lobe. Thus,

$$G(\theta,\phi) = \eta\, G_D(\theta,\phi) \quad (4)$$

where η represents the antenna efficiency (sometimes called the antenna loss factor).

For any antenna aperture, the antenna radiation pattern is obtained by taking the Fourier transform of the field distribution across the aperture. In the simple case of a uniformly illuminated rectangular aperture with dimensions d_1 and d_2, the far-field pattern as in Figure 2 is of the familiar (sin u)/u form in angle θ with $u = (\pi d_1/\lambda) \sin\theta$ for the measurement plane containing the aperture dimension d_1, and likewise with d_2 for the orthogonal plane. The beamwidths θ_{B1} and θ_{B2} in the orthogonal planes are given by:

$$\theta_{B1,2} = \frac{0.88\lambda}{d_{1,2}} \text{ or } \theta^{o}_{B1,2} \approx \frac{50\lambda}{d_{1,2}} \quad (5)$$

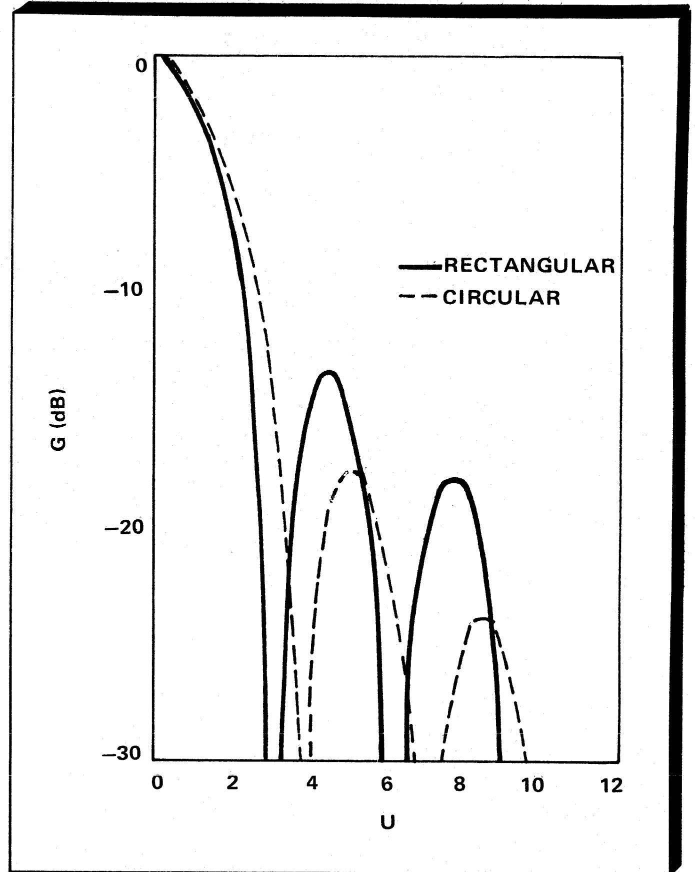

2. Shape of the aperture has a significant effect on the far field pattern, as seen by comparing patterns for rectangular and circular apertures.

Table I

Far Field Radiation Pattern Characteristics of Various Aperture Illumination Functions

Aperture Illumination Function With Axis z	Relative Maximum Directivity	Half-Power Beamwidth, Deg. (λ/d)	Intensity of First Sidelobe, dB Below Maximum Intensity
Uniform; A(z) = 1	1	51	13.2
Cosine; A(z) = $\cos^n(\pi z/2)$:			
n = 0	1	51	13.2
n = 1	0.810	69	23
n = 2	0.667	83	32
n = 3	0.575	95	40
n = 4	0.515	111	48
Parabolic; A(z) = $1 - (1-\Delta)z^2$:			
Δ = 1.0	1	51	13.2
Δ = 0.8	0.994	53	15.8
Δ = 0.5	0.970	56	17.1
Δ = 0	0.833	66	20.6
Triangular; A(z) = $1 - \lvert z \rvert$	0.75	73	26.4
Circular; A(z) = $\sqrt{1-z^2}$	0.865	58.5	17.6

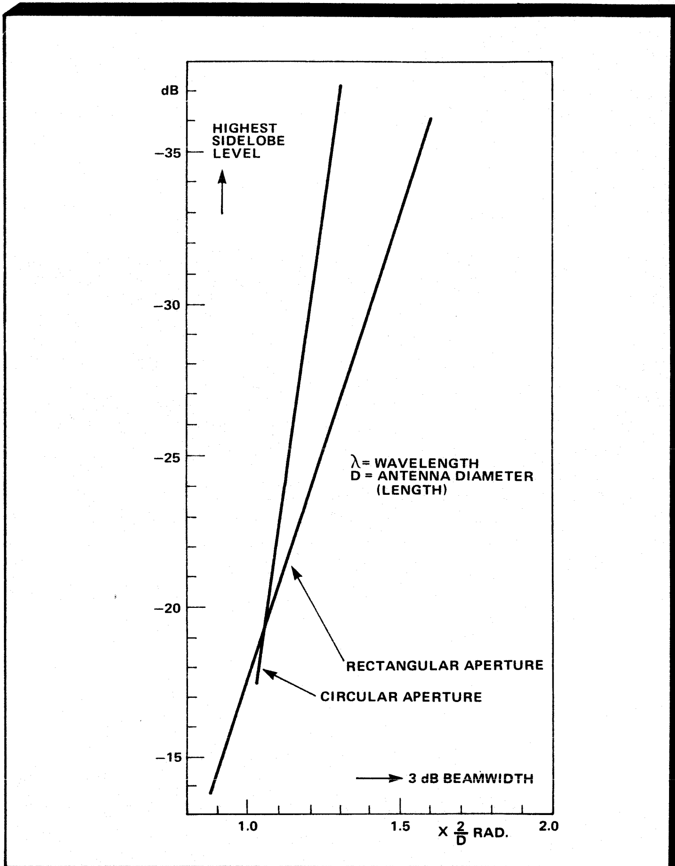

3. These approximations show how sidelobe level varies as a function of the 3-dB beamwidth.

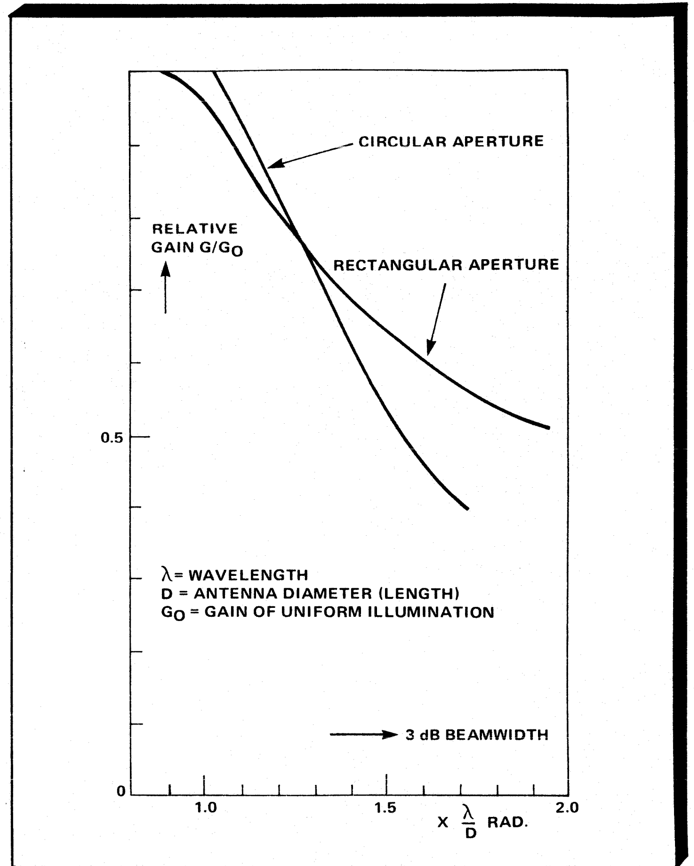

4. Relative gain is plotted as a function of the 3-dB beamwidth for both circular and rectangular apertures.

and the maximum directivity of such a uniformly illuminated aperture, from Equations (2) and (5) is:

$$G_{DM} = \frac{4\pi(0.88)^2}{\theta_{B1}\,\theta_{B2}} \approx \frac{32{,}000}{\theta^o_{B1}\,\theta^o_{B2}} \tag{6}$$

The shape of the aperture has a significant effect on the beamwidth. For arbitrary shapes, no simple relationships exist and the Fourier transform must be applied. However, in the case of a circular aperture with diameter D, the far-field radiation pattern is of first-order Bessel function form $J_1(u)/u$ with $u = (\pi D/\lambda)\sin\theta$. The beamwidth is then

$$\theta_B = \frac{1.03\lambda}{D} \text{ or } \theta^o_B \approx \frac{60\lambda}{D} \tag{7}$$

A departure from a uniform illumination function brings changes in directivity, gain, beamwidth, and sidelobe level. An amplitude taper with weaker field strength at the aperture edges reduces sidelobe levels, but also reduces directivity and gain together with an increase in beamwidth. A range of common tapering functions[2] is given in Table I. Another commonly used aperture illumination function is that due to Taylor[3]; useful design tables have been compiled by Hansen.[4]

A tapered aperture illumination does not use the aperture as efficiently as a uniform illumination, and the maximum gain is often put in the form:

$$G_M = \eta_l\,\eta_a\,G_{DM} \tag{8}$$

where the total efficiency η is expressed as a part η_l representing losses, as before, and a part η_a representing the inefficient use of the aperture ($\eta_a = 1$ for uniform illumination).

Figures 3 and 4 give approximate guidelines for the relationships between gain, sidelobe level, and beamwidth, which are similar for a wide variety of taper functions.

The effect of errors in the amplitude and phase of the aperture illumination produces characteristic features in the far-field radiation pattern[5] as shown in Figure 5. An understanding of these effects is often useful in aiding pattern-error diagnostics in antennas.

Phased Array Antennas

A special case of an antenna aperture is that where the aperture comprises a number (ranging from a few to many thousands) of individual radiating elements. A principal advantage of dividing the aperture in this way is that the aperture illumination can be easily controlled in amplitude and phase. Electric control is straightforward and permits rapid beam steering or pattern adaptivity to null interference, without the need for antenna motion.

The spacing, s, of the individual radiating elements is usually on the order of a half wavelength. Closer spacing can give rise to an increase in maximum directivity (superdirectivity or supergain), but the benefits are usually small

ERROR	APERTURE ILLUMINATION		RADIATION PATTERN
	AMPLITUDE DISTRIBUTION f (x)	PHASE DISTRIBUTION ψ (x)	
(a) NONE	f(x), x	ψ(z), x	θ
PATTERN SYMMETRICAL IN AMPLITUDE PHASE OF PATTERN IS CONSTANT MINIMA CLEARLY DEFINED			
(b) ASYMMETRICAL AMPLITUDE			
PATTERN SYMMETRICAL IN AMPLITUDE PHASE OF PATTERN IS ASYMMETRICAL MINIMA FILLED IN AND SIDE LOBES RAISED			
(c) EVEN PHASE CURVATURE			
PATTERN SYMMETRICAL IN BOTH AMPLITUDE AND PHASE MINIMA FILLED IN AND SIDE LOBES RAISED			
(d) ODD PHASE CURVATURE			
PATTERN IS ASYMMETRICAL, BUT PHASE IS CONSTANT BEAM TILTS MINIMA CLEARLY DEFINED			
(e) AMPLITUDE MODULATION			
SUBSIDIARY BEAMS PRODUCED AT SIN $\theta = \pm \frac{\lambda}{d}$			
(f) PHASE MODULATION			
SUBSIDIARY BEAMS IN TIME PHASE QUADRATURE			
(g) EVEN ORDER DISCONTINUOUS PHASE ERROR			
CAN BE CONSIDERED AS A CONTINUOUS PHASE CURVATURE AS IN (C), TOGETHER WITH A NON–PERIODIC PHASE MODULATION			
(h) ODD ORDER DISCONTINUOUS PHASE ERROR			
CAN BE CONSIDERED AS A CONTINUOUS PHASE CURVATURE AS IN (D), TOGETHER WITH A NON–PERIODIC PHASE MODULATION			

5. Errors in amplitude and phase distort the far-field radiation pattern in ways that can be used in diagnosing the pattern errors.

because of the difficulties in impedance matching caused by the increased mutual coupling.[6] Increasing the spacing beyond half a wavelength gives a slight progressive decrease in maximum directivity; as the spacing approaches one wavelength, λ, the maximum directivity drops suddenly as large secondary maxima in the radiation pattern (grating lobes) appear at angles given by:

$$\theta = \sin^{-1}(\pm m \lambda / s) \qquad (8a)$$

with m an integer.

The appearance of a grating lobe occurs for spacings less than one wavelength if the array is electronically steered. The maximum element spacing suitable for an array to be electronically steered to an angle θ_{max} is:

$$s < \frac{\lambda}{1 + |\sin\theta_{max}|} \qquad (9)$$

As the beam of a phased array is scanned, the presented aperture in the direction of the beam decreases by a factor $\cos\theta_s$, where θ_s is the beam steering angle away from the normal to the array. Thus, the maximum directivity falls and the beamwidth increases by this same $\cos\theta_s$ factor. The $\cos\theta_s$ factor is only an approximation to practice because the elements themselves usually have some directive properties and also there may be directivity loss due to impedance mismatches as the scan angle increases.[7]

A difficulty with phased arrays is the large number of individual elements required. Inspection of Equation (2) shows that for $s = \lambda/2$,

$$G_{DM} \approx \pi N \qquad (10)$$

and for a pencil beam of beamwidth θ_B,

$$\theta_B \approx 10^4/N \qquad (11)$$

Errors in amplitude and phase across an array from element to element give differences in radiation pattern, notably as increases in sidelobe level, from that due to a continuous aperture. An approximate guide to the mean square error, $\overline{\epsilon^2}$, allowable for an array of maximum gain G_M to achieve fan-out relative sidelobe levels of G_S is given by:[8]

$$\overline{\epsilon^2} \lesssim G_M \cdot G_S/10\pi \qquad (12)$$

Which implies about a 10-degree RMS error when the random sidelobe level is numerically equal to the gain.

In beam-steering, the phase-front steps from element to element and this gives rise to so-called quantization sidelobes with an RMS value:[9]

$$(\overline{G_S^2})^{1/2} \approx \frac{5}{(2)^{2p} N} \qquad (13)$$

and a loss in gain

$$\Delta G \approx \frac{\pi^2}{3(2)^{2p}} \qquad (14)$$

where p is the number of control bits for the phase shifter (phase step $= 2\pi/2^n$) and N is the number of elements in the array.

When the gain of phased arrays is being considered, it should be remembered that allowance needs to be made for losses in the network linking all the elements to a common port, and also for any losses in amplitude or phase control components. Active arrays, in which each element has an active microwave circuit to define the noise figure or to generate the required transmitted power close to the aperture, overcome this problem. Thus they are inherently attractive for use with monolithic microwave integrated circuits where large numbers of active circuits present less of a cost penalty.

Printed-Circuit Antennas

The attraction of a printed-circuit antenna is that it may be mass-produced easily. Arrays, together with their signal distribution networks, are easy to fabricate in a single process. Moreover, such antennas are easily adapted to non-planar surfaces and require negligible penetration depth into the surface.

Printed circuit antennas may take many forms,[10,11] but the simplest is based on the microstrip transmission line. Discontinuities in such lines (sharp bends or open-circuit sections) radiate energy easily as a result of the fringing electric field at the edge of the line and associated with the discontinuity. A simple picture[12] indicates that the discontinuity behaves in similar manner to a slot radiator or its equivalent dipole representation.

The microstrip line is characterized in terms of its impedance Z_m and guide wavelength λ_m for a given line width w, substrate thickness h, and substrate relative permittivity ϵ_r. Many different relationships have been given,[10,11] but a relatively simple one[10] yields:

$$Z_m = Z_o/(\epsilon_{eff})^{1/2} \qquad \lambda_m = \lambda/(\epsilon_{eff})^{1/2} \qquad (15)$$

with an effective relative permittivity:

$$\epsilon_{eff} = \tfrac{1}{2}\left[\epsilon_r + 1 + (\epsilon_r - 1)\,(1 + 10h/w)^{-1/2}\right] \qquad (16)$$

where $Z_0 = 377\Omega$, λ = free-space wavelength $= 2\pi c/\omega$, with ω the operating angular frequency.

Line losses are characterized in terms of a dielectric loss factor:[10]

$$\alpha_d \approx 27.3\,\frac{\epsilon_r}{\epsilon_{eff}} \cdot \frac{(\epsilon_{eff} - 1)\tan\delta}{(\epsilon_r - 1)\lambda_m}\ \text{dB/cm} \qquad (17)$$

and a conductor loss factor

$$\alpha_c \approx \frac{8.68}{w Z_m}\left(\frac{\omega\mu_o}{2\sigma_c}\right)^{1/2}\ \text{dB/cm} \qquad (18)$$

where $\tan\delta$ is the dielectric loss tangent, μ_0 is the permeability of free space, and σ_c is the microstrip metal conductivity. Such equations are useful in the calculation of the properties of the network linking the elements in an array, as well as for the radiating elements themselves.

The simplest radiating element is the open circuit end of a section of line. In order to calculate the power transfer to the radiated field, a value for the radiation conductance, G_R, is required. This is given by:[10]

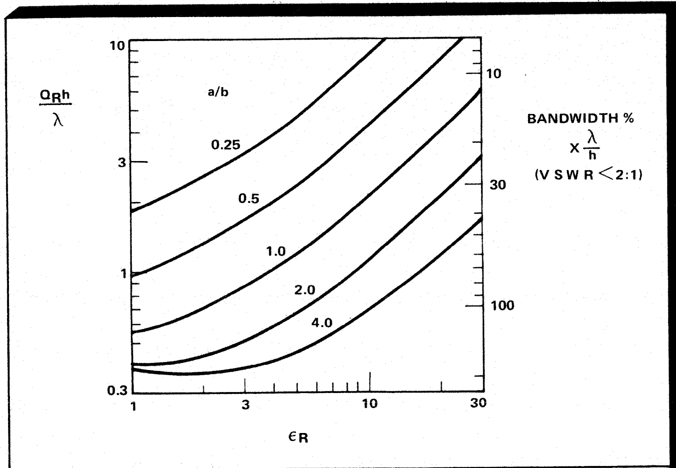

6. Theoretical radiation Q factor and bandwidth are plotted for a rectangular patch antenna. (Path dimensions are a and b and the curves are presented in terms of the aspect ratio a/b.)

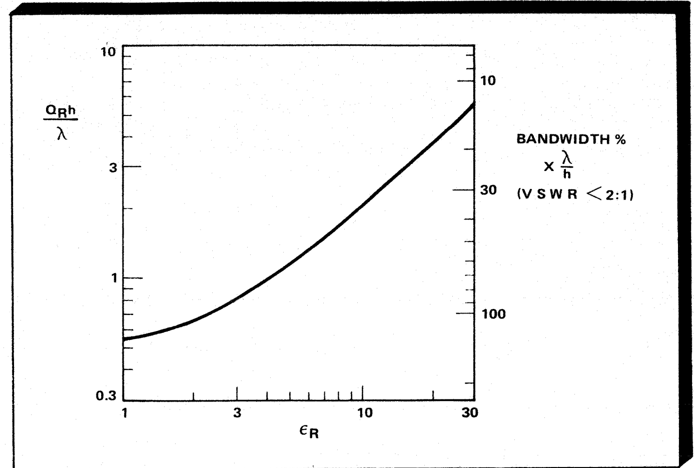

7. Theoretical radiation Q factor and bandwidth are similarly plotted for a circular path in dominant excitation mode.

$$G_R = \frac{1}{120\pi^2} F_2 \left(\frac{240\pi^2 h}{\lambda Z_m \epsilon_{eff}^{1/2}} \right) \tag{19}$$

with $F_2(x) = x\ Si(x) - 2\sin^2(x/2) - 1 + \sin(x)/x$

The proportion of power radiated can thus be controlled by the relative values of the radiation conductance at the discontinuity and the characteristic impedance of the line itself.

Resonant elements usually make the most efficient radiating elements and can easily be formed by a section of line $n\lambda_m/2$ long, open-circuited at either end: the so-called microstrip patch antenna. Coupling to such a resonant element is either by a probe through the substrate or by a thin feed line connecting with the resonator or close to it.

The total Q factor of a resonant element is given as the parallel combination of the Q factors due to radiation, dielectric, and conductor loss:

$$\frac{1}{Q_T} = \frac{1}{Q_R} + \frac{1}{Q_D} + \frac{1}{Q_C} \tag{20}$$

where $Q_D = 1/\tan\delta$ (21)

$Q_C = h(\mu_o \pi f_r \sigma_c)^{1/2}$ and f_r is the resonant frequency

$Q_R = \frac{\pi}{4 G_R Z_m}$ provided the reactance of the radiating discontinuity is negligible

Since conductor loss usually dominates over dielectric loss, the antenna efficiency

$$\eta \approx \frac{Q_C}{Q_C + Q_R} \times 100\% \tag{22}$$

and the bandwidth

$$B = \frac{100(S-1)}{Q_T \cdot S^{1/2}} \% \tag{23}$$

usually quoted as that to a value of VSWR, S = 2.

Circular patches are often also used as resonant elements, the patch radius being given for the dominant mode by:

$$a \approx \frac{0.29\lambda}{\epsilon_r^{1/2}} \tag{24}$$

Figures 6 and 7 show typical values of theoretical radiation Q factor for rectangular and circular patches.[10]

Microstrip resonant patch radiators can be broadbanded to a limited extent by careful impedance matching over the required operating frequency range.[13] ■

References

1. "IEEE Standard Definitions of Terms for Antennas." *IEEE Trans AP-17*, pp. 264–269 (1969).
2. S. Silver, *Microwave Antenna Theory and Design*, MIT Rad Lab Series, McGraw-Hill Book Co., Inc., New York, Vol. 12 (1949).
3. T.T. Taylor, "Design of Circular Apertures for Narrow Beamwidth and Low Sidelobes," *IRE Trans AP-8*, pp. 17–22 (1960).
4. R.C. Hansen, "Tables of Taylor Distribution for Circular Aperture Antennas," *IRE Trans AP-8*, pp. 23–26 (1960).
5. Table provided by Professor K. Milne.
6. R.S. Elliott, *Antenna Theory and Design*, Prentice-Hall, New Jersey (1981).
7. M. Skolnik, *Radar Handbook*, McGraw-Hill Book Co., New York, Ch. 11, (1970).
8. J.L. Allen, "The Theory of Array Antennas," *MIT Lincoln Laboratory Technical Report No. 323* (1963).
9. R.J. Mailloux, "Phased Array Theory and Technology," *Proc. IEEEE, 70*, pp. 246–291 (1982).
10. J.R. James, P. S. Hall, and C. Wood, *Microstrip Antenna Theory and Design*, IEE/Peter Peregrinus Ltd., U.K. (1981).
11. I.J. Bahl and P. Bhartia, *Microstrip Antennas*, Artech House, U.S.A. (1980).
12. J.R. Forrest, "Assessing Antennas for Small Satcom Terminals." *Microwave System News*, pp. 77–100 (Oct. 1981).
13. J.M. Griffin and J.R. Forrest, "Broadband Circular Disk Microstrip Antennas," *Electronics Letters, 18*, No. 6, pp. 266–269 (1982).

Microwave System Testing

Systems needs are surveyed from a general overview of the problems and today's answers to specific examples of how complete, active subassemblies are tested.

By Alan W. Carlson, M/A-COM Components, Inc.

Testing plays a major role in the design, development, and production of modern microwave systems. Demand for high reliability and dependable performance calls for using automated testing to the greatest extent possible.

But the level of automation must be dictated by the economics of cost-effective production. Automatic testing is generally capable of maintaining high product quality with little or no added costs in part because skilled technicians' labor is expensive and in short supply. Automatic testing that is properly designed allows an operator with lower skills to test microwave products. Many systems require automatic testing for technical reasons since certain tests are impossible to perform manually. Microwave systems testing and automation are therefore inseparable.

The following sections discuss the various classes of test equipment needed for microwave systems. Design considerations and general needs of each type of test equipment are highlighted. Several specific examples of test systems are given with the major emphasis put on factory-floor test equipment, since the other classes can be viewed as a subset of this type.

Factory Test Equipment

Factory-floor test equipment for a microwave system consists of a number of individual test stations with a collective mission of assuring reliable and proper system performance. The specifications of individual parts are interlocked at a lower level to make sure that higher-level system specifications are met. The individual test stations can be isolated units or linked via a computer network. A computer network linking the various stations is a major requirement for automatic factories and shop floor control.

The factory test equipment can be divided into the following categories:

- *Device Testing.* Device testers are stations that test individual discrete devices and digital or analog integrated circuits. The integrated circuits can be either monolithic or hybrid. Most microwave systems use hybrid integrated circuits for specialized applications for which available monolithic circuits cannot be used. If the devices being tested are purchased from other vendors, the test equipment involved would be considered part of incoming inspection. Commercial automatic test equipment is available for most lower frequency needs in device testing. For testing microwave devices and hybrid ICs, either special test equipment must be designed or the testing must be performed at the vendor's facilities.
- *Component Testing.* Test equipment in this area consists primarily of custom stations for microwave components and commercially available stations for printed-circuit board and harness testing. With the large variety of test equipment offered for both printed-circuit board and harness testing, it is impractical to build custom stations for most low-frequency component testing needs. But for high-frequency circuit boards, microwave components, and cables, custom-made test stations are usually required. The selection of complete automatic test stations for such components is very limited but, fortunately, a large selection of bus-controlled instruments is available. Such instruments can be configured into versatile automatic stations with the addition of suitable controllers.
- *System and Subsystem Testing.* The system and subsystem test equipment is usually the most complex and requires the largest amount of custom-built equipment. The test stations must simulate the interaction of the subsystem or system with its operating environment. Tests at this level range from simple prime power consumption tests to complex-use tests in the presence of interfering signals. Most modern systems contain embedded computers or microprocessors which can only be tested effectively with another computer.
- *Environmental Testing.* The individual components and complete systems must be tested under a variety of environmental conditions such as temperature, vibration, altitude, and acceleration. The systems which perform such tests must combine conventional electronic instrumentation with environmental chambers and mechanical tables. The transient nature of such testing often requires that the test system be automated. The design of such systems is very challenging since the electrical and mechanical environment is often hostile. Usually the final acceptance of complete systems involves extensive environmental testing.

On the factory floor, each unit must be tested several times at various stages of the production and reliability assurance process. Testing speed must be maximized by proper instrument choices so that a proper production testing rate can be obtained with a minimum number of test stations. The UUT (unit under test) must be capable of being connected to the test station in a minimum amount of time.

The interface with the test operator must be designed to be simple and clear in order to minimize the required skill of test operators. The station must be designed with a definite purpose in mind. It is difficult to make a fast acceptance tester and a powerful fault isolation station out of the same test station. Clear and complete calibration procedures must be developed to assure test accuracy with a maximum interval between system calibrations by the standards department.

Many microwave test stations must be certified as acceptable by the military. The certification process is greatly

Alan W. Carlson is a vice president at M/A-COM Components, Inc., Burlington, Mass.

simplified if the station is initially designed for demonstrating the necessary test accuracy. Many components and subassemblies require a large volume of test data and reports. The automatic test stations should be capable of providing for the output, storage, and statistical analysis of all data in the proper form.

Field Test Equipment

The purpose of field test equipment is to verify system performance at the sites where that system is used. Such locations are usually far-removed from sources of sophisticated electronic instruments. The field test equipment usually performs a small number of higher level system or subsystem tests. In most cases, the test station is a small, custom made, portable unit that is brought to the system. The tests performed by the field equipment must be sufficient to predict confidently that the system will perform to its full specification. Specific fault diagnosis for repair purposes is usually not available from field test equipment.

Design of field test equipment should emphasize gross operational tests as opposed to detailed parameter tests. Field test equipment must be easy to use. The skill levels of the operators and the conditions under which they must use the equipment do not permit complicated and confusing test sequences. In many cases, an embedded microprocessor will be used to automate the test sequence and make the station easy to use.

Rugged construction and small size are essential. Many field test units are built directly into a suitcase-like carrying case. Since laboratory prime power sources are not available for field testing, the test unit must have a portable source of prime power. This prime power must be self-contained in the tester or obtained from the system under test. Any field test unit must be capable of being calibrated at the factory or a local standards lab, but the time between calibrations should be as long as possible to maximize test equipment availability and minimize maintenance. A self-test routine is also desirable.

Repair Facility Test Equipment

For many systems, the factory serves as a repair facility. For other systems, one or more repair sites are supported. Wherever the repairs are made, the requirements for test equipment are the same: The repair facility test equipment must perform a series of tests sufficient to isolate and identify the defective components of the system. After the repair is completed, the full operation of the system must be verified by the same or additional equipment.

Test equipment design must emphasize fault diagnosis. Specific test sequences must be executed to systematically check the various parts of the system and isolate the problem to the lowest-level component that is practical to replace. For microwave systems, the lowest-level replacement parts would be a microwave component or subsystem. In order to facilitate troubleshooting, a large selection of test options should be available; ideally, they should be menu driven since the skill level of repair facility operators will not be much greater than that of factory test operators.

It is desirable to support a microwave system repair facility with a minimum number of test stations. For this reason, any given station should be capable of testing as much of the system as possible. One of the repair facility stations must have acceptance-testing capability for the full system. This is necessary to verify system performance after the repair is made. Each of the test stations must be capable of being calibrated and certified for proper operation, ideally as seldom as possible.

Testing Problems

Many problems commonly occur in automatic test stations for microwave subsystems and systems (see Table I). Measurement of state-of-the-art components and subassemblies becomes more difficult and challenges the state-of-the-art in instrumentation. Novel measurement techniques must be developed *simultaneously* with component and subassembly development. In many cases, engineering cannot test the product being developed without proper automatic techniques developed for that product. The test equipment designer is often faced with integrating conflicting measurements into a common test stand. Actions that enhance measurement of a specific parameter can be detrimental to the measurement of another parameter. For instance, the clocks in microprocessor-controlled instruments often jam delicate noise or T_{ss} measurements.

Table I.

General Testing Problems for Microwave Systems and Subsystems
• State-of-the-art measurements
• Integration of "conflicting" measurements
• Production environment
• Interface with environmental equipment

Test equipment must be designed for a production atmosphere. Stations must be capable of producing accurate test data with minimum downtime. The test fixtures must be rugged enough to withstand hundreds of insertions without damage. Each station should be able to produce excellent test data when operated by a minimally skilled test operator.

Many times the UUT must be tested at extreme temperatures, or under acceleration or vibration, adding another level of challenge to the designer of automated microwave test equipment. Testing problems for several types of subassemblies are discussed and examples given of appropriate automatic test systems.

Multiport Passive Networks

A typical multiport passive network will serve as our first example for automatic test systems (Fig. 1). This class of subsystem occurs in most microwave systems. A typical unit will have multiple RF inputs which may be coaxial or waveguide. In addition, each unit will have several RF outputs which are usually coaxial. Additional inputs are needed to control switches or attenuators which may be present in the assembly. Each unit will contain a variety of power dividers, hybrid couplers, and other passive microwave circuitry. All of the passive circuitry (which can include switches and attenuators) preserves the frequency of the input signal; the output frequency will always equal the

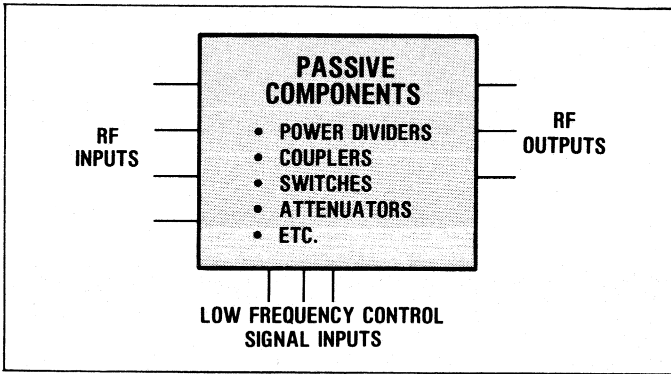

1. A multiport, passive network subassembly contains a variety of passive components such as power dividers, couplers, switches, and attenuators. Control signals must be provided as well as measurements for RF inputs and outputs.

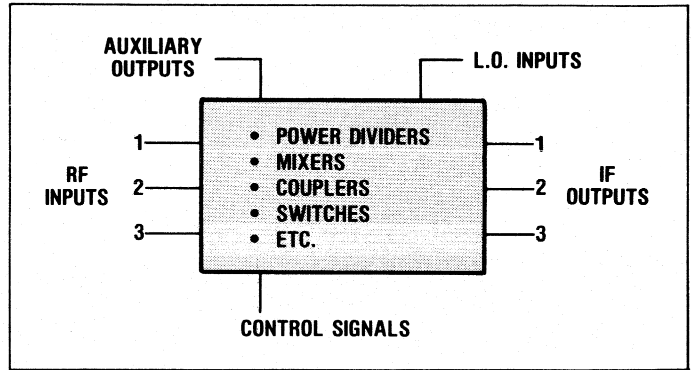

3. Multichannel receivers provide a somewhat more difficult testing challenge; several inputs lead to mixers within the assembly, LOs and built-in test functions must be considered.

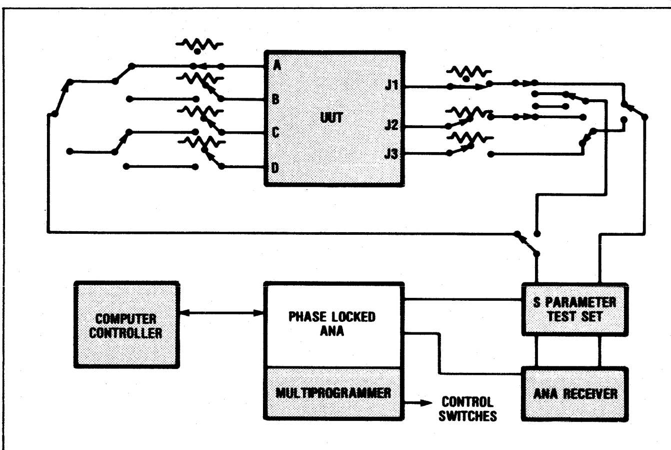

2. An automated test station for a passive network typically has a phase-locked ANA under control of one of a variety of computers, from desk-tops to minis.

input frequency. The tests commonly needed in order to completely test such a multiport passive network are listed in Table II. It is usually necessary to measure the VSWR of each RF port over a range of frequencies. The insertion loss between various combinations of input and output ports must be verified.

Table II.

Tests Needed for Multiport Passive Networks
• VSWR
• Insertion loss (isolation)
• Phase matching or tracking
• Amplitude matching or tracking
• Control functions

Many times there are precise specifications of the output signal's phase relative to excitation at a specific input port. Often there are phase matching or tracking specifications between the various output ports. Similar specifications are usually present for amplitude matching and tracking between various ports. In addition, the proper operation of all control functions must be verified. The necessity for both amplitude and phase data forces one to use a phase-sensitive receiver in the microwave test system. These data are usually obtained from an automatic network analyzer (ANA) or similar instrument. Test sequences using automated measurements with manual port and path switching are long, tedious, and subject to error. An ideal test system is one which automates all port and path switching as well as the instrumentation.

Figure 2 shows a block diagram of an automatic test system designed to test a multiport passive network with a single insertion. A phase-locked ANA is used to maximize the test system accuracy and repeatability. The total test system is controlled by a computer controller. The computer controller can be a desktop computer, a minicomputer, or even a personal computer with an IEEE-488 output port for instrument control. A multiprogrammer is used to control the various switches and to exercise the control functions of the UUT. Broadband coaxial switches are used to terminate the unused ports and to direct the proper signals to the ANA receiver. The test port and path switching is accomplished via a combination of the coaxial switches and the S-parameter test box. This system is capable of completely testing a multiport passive network within 10 minutes or less. Special adapters are designed for daily system calibration. Such a system will provide fast and reliable microwave testing in a production atmosphere. In many cases, multiport networks can be tuned directly on the test system.

Care must be taken to minimize the VSWR of all the components and cables in the switching matrices. This specific test system does not require the dedication of an ANA to a specific test station. If production schedules do not require complete 24-hour use of the system, the switching matrix and test fixture can be easily disconnected to allow the ANA to be used for other purposes.

Multichannel Receivers

A microwave multichannel receiver subassembly represents a slightly more difficult testing challenge. A typical unit will have several RF inputs to the mixers contained in the assembly (Fig. 3). The various mixers are often driven from a common local oscillator input. In some cases, multiple local oscillator inputs are present. Many times there are auxiliary outputs to provide BIT functions or to

Continued on page 251

Continued from page 248

carry the LO signal to other parts of the system. Each RF input will have a corresponding IF output port. Typical subassemblies contain a variety of power dividers, mixers, couplers, switches, and other microwave components. Components such as switches and attenuators will need corresponding control inputs for their operation. The subsystem is complicated by different freqeuncy signals simultaneously present in the unit.

The testing requirements for multichannel receiver subassemblies are listed in Table III. Noise figure and conversion loss of each mixer must be tested over a range of input frequencies and local oscillator drive levels.

Table III.

Testing Requirements for Multichannel Receivers
• Noise figure
• VSWR (often hot)
• Isolation
• Conversion loss
• Control functions

The VSWR of all ports must be measured with the receive ports measured in a hot state. That is, the RF port VSWR must be measured over a frequency range with local oscillator power applied. The measurement system must contend with a certain amount of local oscillator power coming out of the RF input ports. Port-to-port isolation must be measured and compared to specifications. All control functions present in the unit must be exercised and tested for proper operation.

To achieve this, a scalar network analyzer is used to measure the VSWR of the RF and local oscillator ports (see block diagram, Fig. 4). The use of a scalar network analyzer makes the problem of obtaining accurate VSWR readings more difficult. With the scalar analyzer, vector error corrections for coupler directivity and connection interfaces cannot be made. For this reason, it is important to locate the directional couplers used in the VSWR measurement as close as possible to the port being tested. Switches and long cables between the couplers and the test ports should be avoided.

If the UUT has built-in circulators on the receive ports, either a CW or modulated scalar analyzer can be used for the measurement. If the unit does not have a circulator built into each receive port, a scalar analyzer with a modulated test signal will not provide accurate VSWR measurements. In this case, the radiated local oscillator signal is reflected into the mixer again, and provides error signals in the detection band of the modulated scalar analyzer. For such cases, a spectrum analyzer is the best choice for measuring VSWR. It can measure the power at a specific test frequency without errors due to the presence of signals at other frequencies.

A solid-state noise source with an automated noise-figure meter is used to determine the noise figure of the various mixers in the unit. Two sweepers, each with programmable power level, are used for the RF and LO sources, respectively. A counter and power meter are used to measure the frequency and power of the various test signals.

Continued on page 254

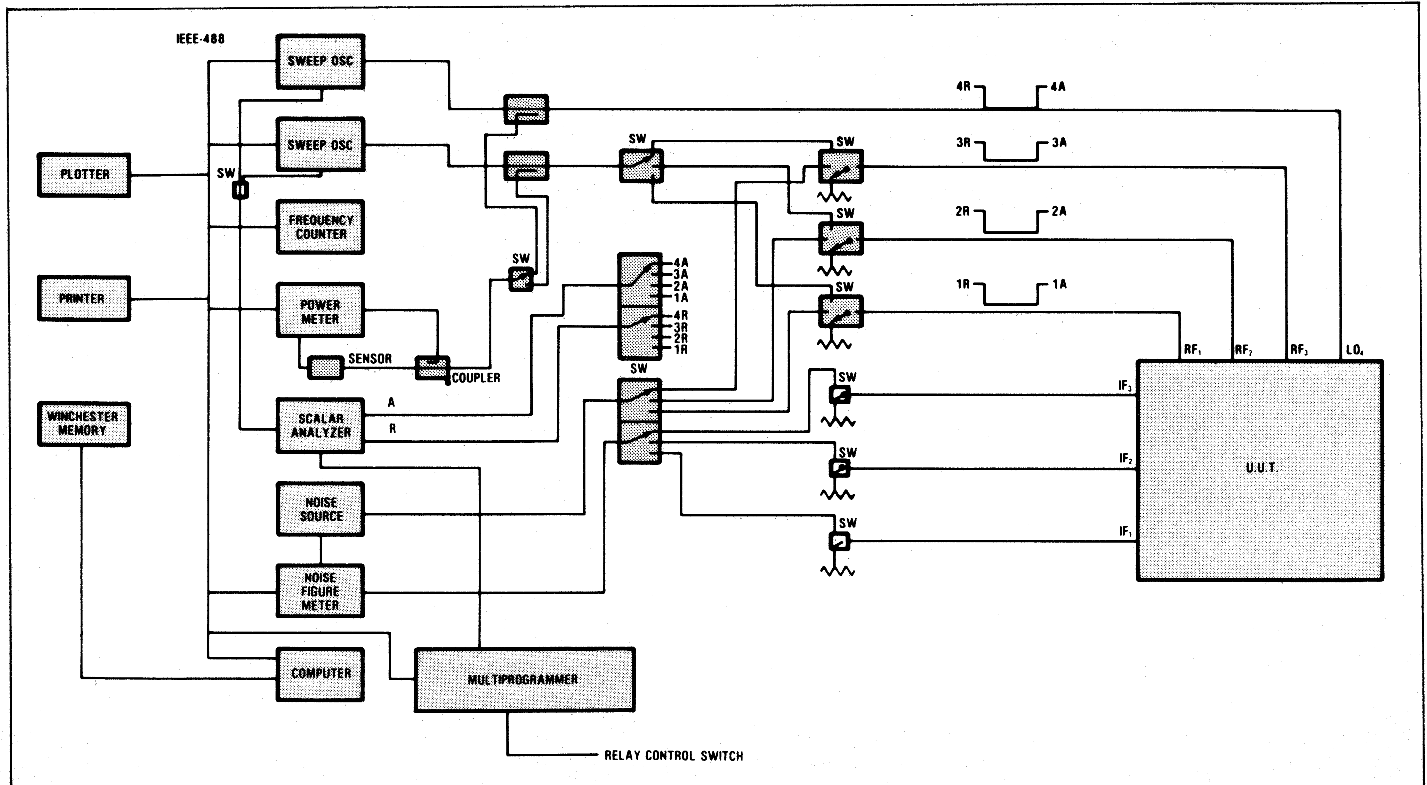

4. **A scalar network analyzer** is necessary to measure VSWR, but complicates measurement necessitating careful location of directional couplers.

Continued from page 251

All the instruments are under computer control via an IEEE-488 bus. The controller has a standard set of computer peripherals: a printer, plotter, and Winchester disk for data storage. Quick disconnects are used to permit rapid connection and disconnection of the UUT. Such quick disconnects have been used at frequencies as high as 13 GHz. This test system will completely test a multichannel mixer in less than five minutes.

Subassembly with an Active Source

Another large class of microwave subassemblies contain active microwave sources (Fig. 5). The subassembly can contain a variety of solid-state oscillators, VCOs and amplifiers, as well as passive components such as switches, attenuators, and limiters. Many units contain multiple RF inputs and outputs which can be used for additional purposes within a microwave system. If there is a VCO in the subassembly, there will be an input port for the tuning signal. Switches and attenuators, if present, require control signals for their operation. The testing of such subassemblies automatically requires the use of instrumentation such as spectrum analyzers and digital oscilloscopes.

This category of subassemblies has a variety of requirements (Table IV). Power output as a function of DC and RF drive level must be measured. If a VCO is present, the output power and frequency must be measured as a function of the applied tuning voltage. These data must be compared to the tuning linearity requirements of the unit. Often it is necessary to measure the AM and FM noise as well as the spurious responses of the various active outputs. Transient behavior of the unit such as turn-on time or post-tuning drift is often among the required measurements. In many cases, the modulation characteristics of the RF sources must be measured and compared to specifications. Also, the normal microwave tests such as isolation and VSWR are usually needed.

Table IV.

Testing Requirements for Subassemblies with Active Sources
• Power output
• Tuning characteristics
• AM and FM noise
• Transient behavior
• Modulation characteristics
• Normal microwave tests

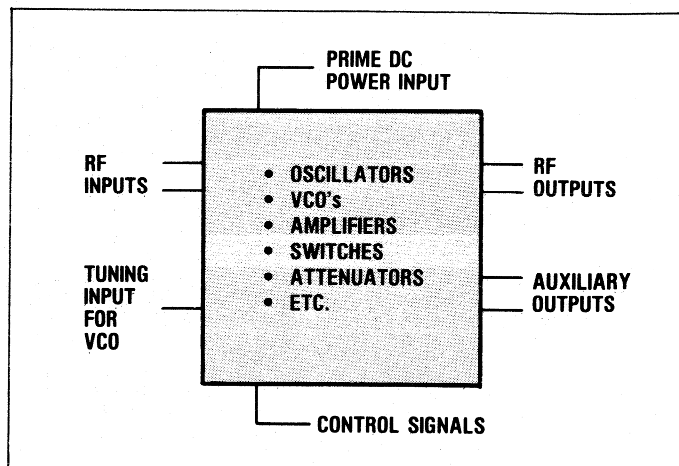

5. In addition to VSWR and isolation, such parameters as post-tuning drift must be determined for active sources.

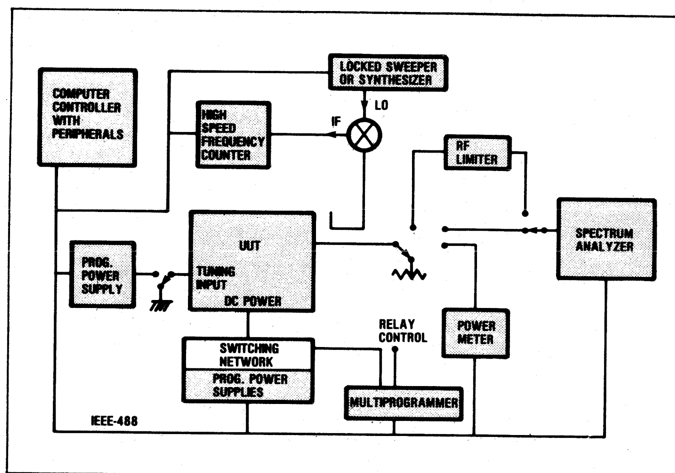

6. Spectrum analyzers determine AM noise and spurious responses, while use of programmable power supplies and frequency counters is necessary to characterize a VCO, as shown in this test system for VCO characterization.

In an automatic test system for characterizing a VCO, programmable power supplies and a switching network provide the DC power input to the UUT (Fig. 6). An additional programmable power supply provides the necessary tuning voltage to the VCO. A power meter and frequency counter are used to measure the tuning characteristics of the VCO. A programmable spectrum analyzer is used to measure the AM noise and spurious responses of the oscillator. With a limiter, the same spectrum analyzer is used to measure the FM and phase noise of the oscillator. Alternate techniques for phase-noise measurements may require a delay line discriminator or RF bridge. High-speed counters are available up to frequencies of 500 MHz. By using a mixer to downconvert the VCO output to within this range, a variety of transient and post-tuning-drift measurements can be made directly with the counter. The test system is controlled by a computer with the standard peripherals via the IEEE-488 bus.

This test system is capable of providing complete characterization, including full graphical output, on a wide range of VCOs. Many VCO parameters cannot be measured manually with conventional instrumentation in any reasonable amount of time. Such a system is vital to successful microwave VCO development and subassembly engineering, as well as for production testing.

Active Seeker Assemblies

In a microwave missile, an active seeker assembly is usually the highest-level subsystem that must be tested before the entire guidance section is tested (Fig. 7). While, in an actual system, the RF input and output ports are terminated with antennas, the units are generally first tested without the antennas. Testing a unit with the antennas

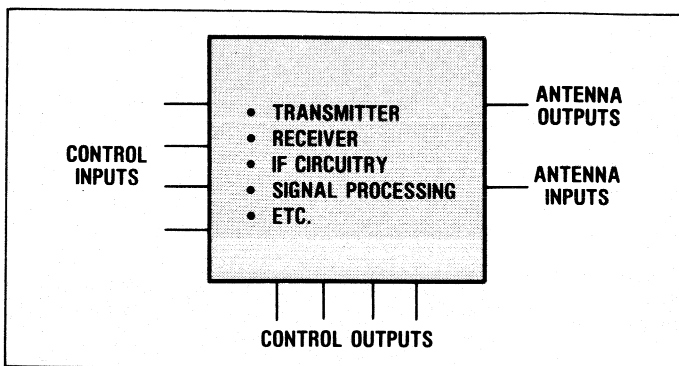

7. One of the most complex test challenges is an active seeker assembly, which contains full transmitter, receiver, IF, and signal processing circuitry.

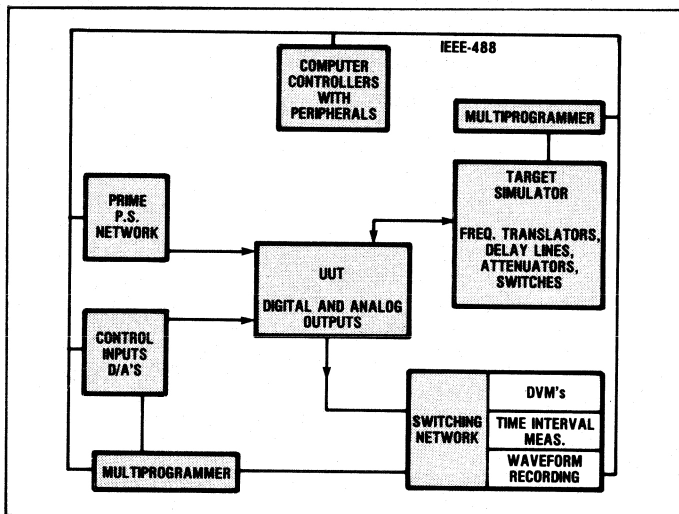

8. A test that requires four hours of manual, and expensive, labor can be reduced to fifteen minutes on an automated test system. Computer controls for programmable power supplies, digital voltmeters, frequency translators, delay lines, and the like, are provided over IEEE-488 buses.

mounted requires special provisions such as an anechoic chamber. In most cases a wide variety of both digital and analog control inputs as well as DC power supplies are needed. The operation of the unit generates a large number of both digital and analog output signals. Inside the active seeker one finds a transmitter and a receiver as well as various IF and signal processing circuitry. The test procedure for such an assembly consists of exercising all of its functions in a series of operational tests.

Test requirements for active seekers are substantially different from the earlier examples (Table V). At this level of

Table V.

Requirements for Active Seekers
• Operational testing
• Target simulation
• Power output
• Full function tests
• Timing and transients

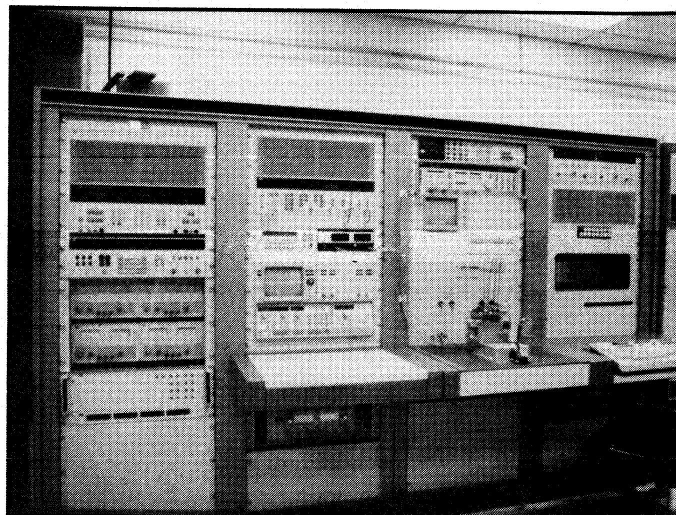

9. The complexity of some automated test systems can be seen in this hardware realization of the prior schematic.

integration, a series of operational tests must be performed in sequence to test the proper functioning of the active seeker. Proper target simulation is a challenging aspect of test system design for this type of subassembly.

The RF power output of the transmitter must be measured and compared to specifications. Certain tests require measuring the timing between various inputs and outputs and the characterization of various output transients in response to specific inputs. Many of the tests simulate full functional tests of the seeker. They are very different from the classical microwave measurements previously discussed. A proper test system must sequence through the entire acceptance test with a single insertion of the unit in the test system, as shown in the block diagram (Fig. 8). The target simulator is a major portion of the test station. The target simulator may contain various combinations of frequency translators, delay lines, attenuators, and switches to generate the necessary microwave test signals. A network of programmable or fixed power supplies provides the DC power to the UUT. A multiprogrammer is used to generate and sequence the various control inputs to the seeker. The output signals are characterized by a measurement system consisting of digital voltmeters, time-interval measuring equipment, and digital oscilloscopes or waveform recorders. As before, the system is controlled by a computer controller with a standard set of peripherals. This test system is necessary to reduce a long, involved test sequence to one that is consistent with high-volume production. The actual test system is shown in Figure 9. Such a system reduces the test time for seeker assembly from a four-hour manual sequence to a fifteen-minute automatic sequence. The actual seeker can be connected or disconnected from the test station in approximately thirty seconds.

Automatic test stations are vital for cost-effective production, support, and repair of microwave systems. The stations that test the microwave components, subsystems, and systems generally must be custom-designed and fabricated. The design, construction, and software generation for these test stations provide a challenge for the microwave engineering community. ■

Semiconductor Thermal Considerations In System Design

Junction temperature has ramifications all the way up to systems performance and reliability.

By Bernard S. Siegal, *Sage Enterprises, Inc.*

Microwave system designers must contend with three trends in the industry that necessitate a new look at semiconductor thermal considerations. First is a greater requirement for device and circuit reliability to ensure long-term operation in harsh environments. Second is a need for improved performance and quality in all aspects of the system, from the component level on up. Lastly, the first two requirements are made more difficult by a combination of the increased complexity, greater physical density, and higher operating frequencies of current and future microwave systems.

Common to each of these three trends is that each directly impacts, or is impacted by, the operating junction temperature of the semiconductor devices used in the system. Designing for a junction temperature (T_J) of 70°C for a critical semiconductor device, such as a GaAs FET power amplifier stage, is one thing, but achieving it is something else. If the actual T_J is 80°C, then that device will probably fail in half the expected operating lifetime. The environmental temperature extremes that avionic and space systems are often subjected to accelerate the problem of maintaining acceptable junction temperatures. The impact of junction temperature variation on long-term reliability can be quickly determined by using the Acceleration Factor relationship described in the Appendix.

While the subject of semiconductor thermal considerations is complex and lengthy, the system designer must be aware of the basics in order to properly design, manufacture, and test his microwave systems. Toward this end, following is a concise discussion of semiconductor heat flow characteristics, junction temperature measurement techniques, use of measurement results, and applications of thermal testing in device design, manufacturing, selection, and use.

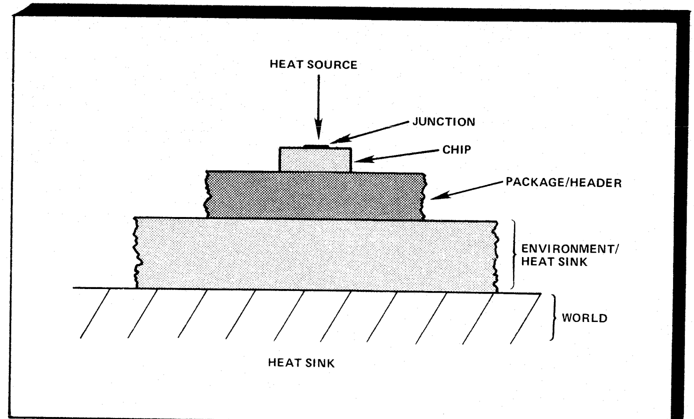

1. Typical generalized mounting structure for just about any microwave semiconductor device. Transistor devices will usually have another layer, a ceramic substrate, between the chip and the package/header in order to provide collector (or drain) isolation.

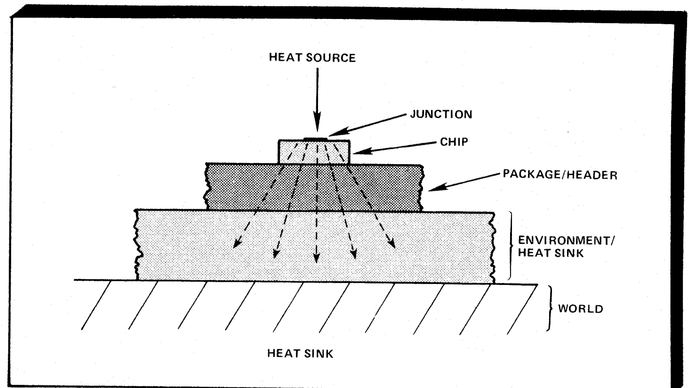

2. Heat flow from the junction to the outside world usually occurs through the chip to whatever the chip is mounted on; heat flow via other means or paths is very small and can be neglected in most cases. A linear flow configuration is usually used for manual modeling.

Heat Flow Characteristics

Before starting any discussion of semiconductor thermal properties, one must keep in mind that until the semiconductor chip is mounted in some way, it really has only minimal thermal capacity. Besides the need to make electrical connections to the chip, the chip thermal mass is insufficient to handle anything other than an extremely short-duration power pulse. Thus, the type of mounting (conventional, flip chip, etc.), attachment technology (eutectic, solder, epoxy, etc.), and physical definition of the mount material (package and/or substrate size, environment, etc.) all enter into any discussion of semiconductor heat-flow characteristics.

Consider the generalized case of a chip mounted as shown in Figure 1. The chip is mounted on an alumina substrate, which is mounted in an MIC package; the package in turn is mounted to a system heatsink. In most cases, the leads used to make electrical connection to the top of the chip are assumed to be sufficiently small in cross sectional area so as to have limited heat removal ability. This forces all the heat generated in the chip to flow to the outside world through the chip-mounting surface interface, commonly referred to as the die bond or chip attach. Exceptions

Bernard S. Siegal is president of Sage Enterpries, Inc., Mountain View, Calif.

to this assumption are usually found in beam lead devices—the beams are the only physical connection to the outside world—and devices with plated heatsink, top contacts or special heat-conducting top-contact material.

The actual form of the heat flow is dependent on the heat source shape and flow configuration. Listed below are some common heat source shapes and examples of the devices in which they may be found:

Shape	Device Type
circular	mesa diode
square	transistor
rectangular (long, thin line)	GaAs FET
point	point contact

Heat flow configurations fall into two categories: columar or spreading. The former occurs when the heat source cross-sectional area is large compared to the cross-sectional area of the material through which the heat must travel. The latter configuration occurs when the heat source cross-sectional area is small compared to the cross-sectional area of the material through which the heat must flow. The complex three-dimensional Laplace equation can be used to determine exact spreading shape for specific cases; the usual approach is to assume linear spreading at a 26 or 45 degree angle, as shown in the example of Figure 2.

While this approach provides a relatively simple method for calculating an approximate value of the steady-state thermal resistance, more accurate calculations can be obtained using the latest computer modeling programs. Even sophisticated computer programs, however, cannot monitor normal manufacturing process variations; modeling is best suited to device design applications.

The structure shown in Figure 1 can be modeled in an electrical analog by using the transmission line circuit of Figure 3. Each element in the heat flow path from the junction outward has a thermal resistance and a thermal capacitance, the product of which yields a thermal time constant. From the transmission line analogy, it is easy to see how the heat generated at the junction propagates through each element to the "world." A plot of junction temperature as a function of time after power is first applied to the device as shown in Figure 4. The near-horizontal regions of the plot represent heat propagation through significant thermal masses while the more-vertical regions are indicative of the interfaces between thermal masses, such as the die-attachment material.

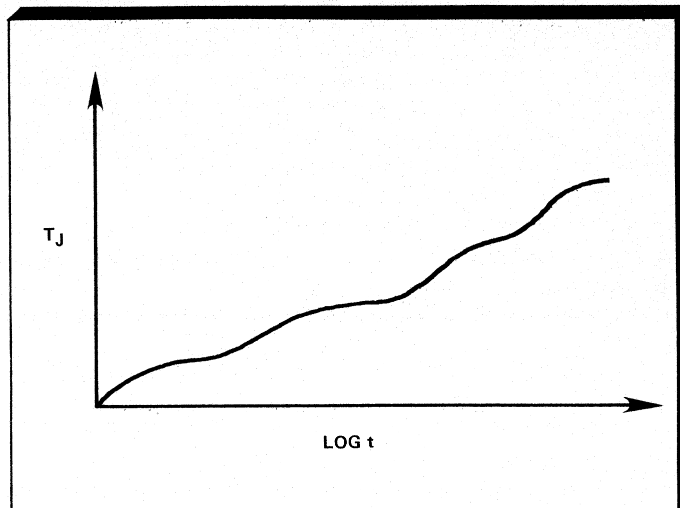

4. When power is supplied to the heat source of Figure 3, the junction temperature (T_J) will vary with time as the heat propagates from the source to the heat sink. Every component in the heat flow path has a B, C_B, and t_B with the latter increasing as heat flows away from the junction. The plateaus are the result of thermal masses while the steeper portions are the interfaces between the masses.

Measurement Techniques

While there are several available techniques used for junction temperature measurement, only two are commonly accepted. These are the infrared measurement (IRM) and electrical test measurement (ETM) techniques. Each has

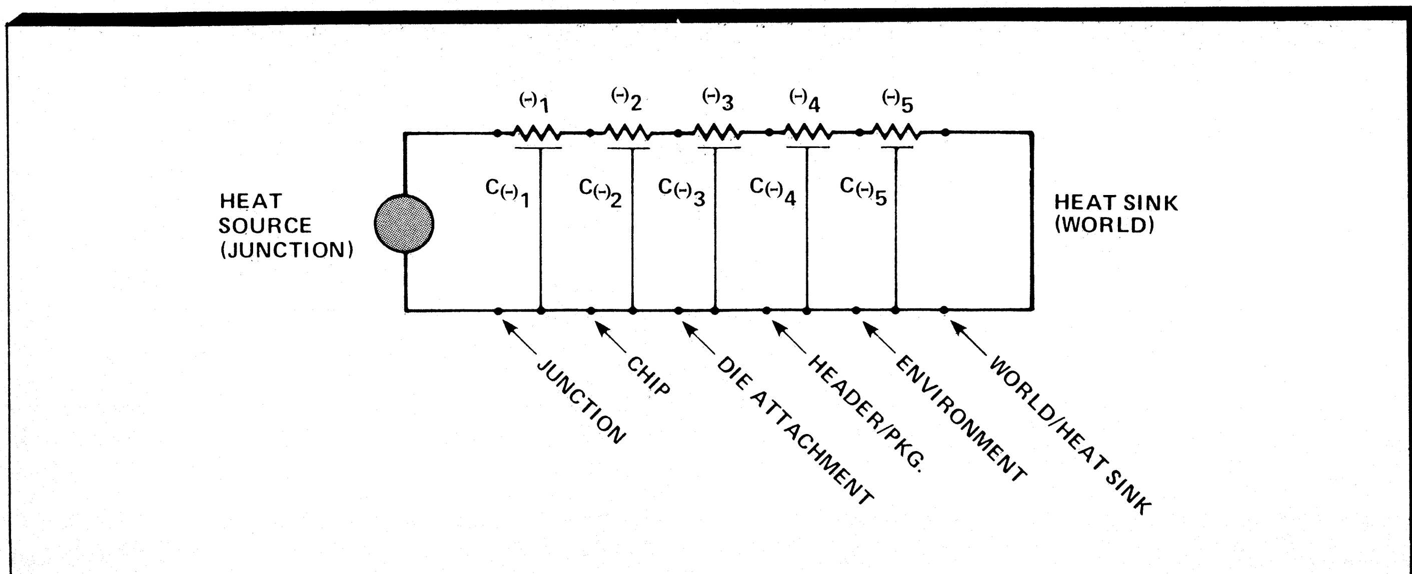

3. A transmission line analogy can be made for the simple heat flow configuration of Figure 2. Each element in the heat flow path has thermal resistance (B) and capacitance (C_B).

certain advantages and disadvantages and must be carefully selected to satisfy the measurement requirements.

The IRM technique is usually implemented using an IR detector coupled to an optical microscope, as shown in Figure 5. The chip surface is viewed directly while the device is powered up; this requires a suitable test fixture with clear access to the chip surface. By changing the X-Y position of the DUT (device under test), it is possible to scan the chip surface for temperature profiles or fix on the highest temperature point. While capable of supplying a great deal of thermal information, the IRM technique does have some severe difficulties and limitations. Foremost of these is the fact that the DUT must be unencapsulated. This is a handicap both for manufacturers during the production cycle because of potential chip contamination, and users during incoming inspection and component evaluation, as the package would have to be opened. The DUT surface also must either be coated with a material of known, constant emissivity or carefully calibrated to determine the emissivity of the various surface materials. The viewing angle also impacts the emissivity, as does the materials being viewed—some materials are transparent to IR. Only the most sophisticated IR microscopes are capable of temperature measurements during fast-pulse conditions. Also, consideration must be given to the IR microscope's spot size. Latest versions of these microscopes have spot sizes down to a diameter of approximately 0.001 inch, a seemingly small size but actually quite large compared to the junction dimensions of the latest microwave devices. This causes the temperature readings taken with this technique to be averaged over the spot size.

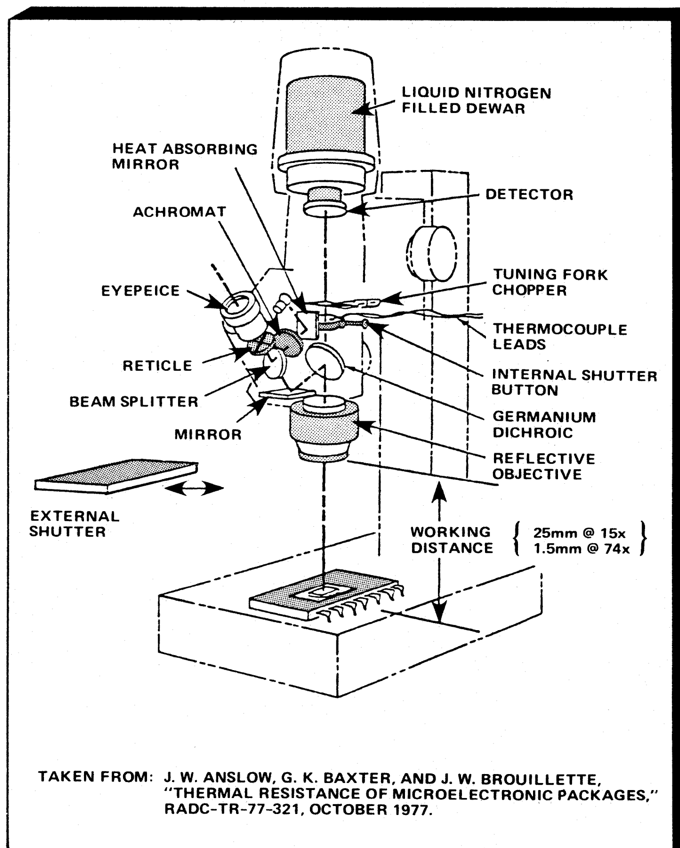

5. A typical setup for a high-resolution infrared microscope. The DUT is moved in the X-Y plane in order to scan for the DUT's peak temperature or to determine temperature profiles. Newer microscopes have sophisticated controls and motorized stages to simplify operation and automate scanning.

Table I

ETM Temperature-Sensitive Parameters

Device Type	TSPs		
Bipolar transistor	V_{BE}	V_{CB}	
Junction FET	V_{GSF}	R_{DS} (ON)	
MOS FET	V_{BCF}	R_{RDS} (ON)	V_{TH}
PIN diode	V_F	V_{BR}	
Schottky diode	V_F	V_{BR}	
LED and laser diode	V_F	V_{BR}	
PIN diode	V_F	V_{BR}	
Varactor diode	V_F	V_{BR}	
Gunn diode	V_{LF}		
IMPATT diode	V_{BR}	V_F	
Thyristor (SCR, triac, etc.)	V_{AK}		
Integrated circuit	V_F (substrate diode)		

The ETM method relies on the fact that every semiconductor device has at least one electrical parameter that is linearly related to junction temperature. In GaAs FETs, for instance, the forward biased gate-source Schottky junction voltage (V_{GSf}) under constant current conditions is just such a parameter. Table 1 lists the most commonly used temperature-sensitive parameters (TSPs) for microwave devices. The ETM is basically a two-step procedure. The DUT's TSP must first be calibrated against junction temperature. The appropriate conditions are applied, and the TSP is measured at two or more externally applied temperature conditions; the reciprocal of the resultant TSP-T_J slope yields the K Factor in degrees C/mV. The measurement conditions are chosen to be low enough in DUT power dissipation so as not to cause significant self-heating, but high enough to ensure reliable and repeatable measurements. The next step is the actual thermal measurement. The DUT is subjected to three sets of pulses: TSP measurement pulses; heating pulses; and then another set of TSP measurement pulses. The difference between the two TSP voltage measurements is directly related to the change in T_J through the calibration factor K.

Figure 6 demonstrates how the ETM is implemented for the GaAs FET; other devices are handled in a very similar way. The ETM has many pluses going for it: No special handling is required; calibration of the device is relatively simple and may not need to be done on other than a sample basis if the devices are similar enough. ETM also lends itself to automation which greatly reduces operator skill-level requirements, equally applicable by both device manufacturer and user. The approach easily provides thermal transient information, and can be implemented right after chip attachment and before wire bonding. On the minus side, the ETM can indicate the presence of hot spots but not their precise physical location. Individual device calibration may be necessary if the processing technology is not sufficiently advanced. Care is required to eliminate potential switching and/or oscillation problems, and the test circuit must be

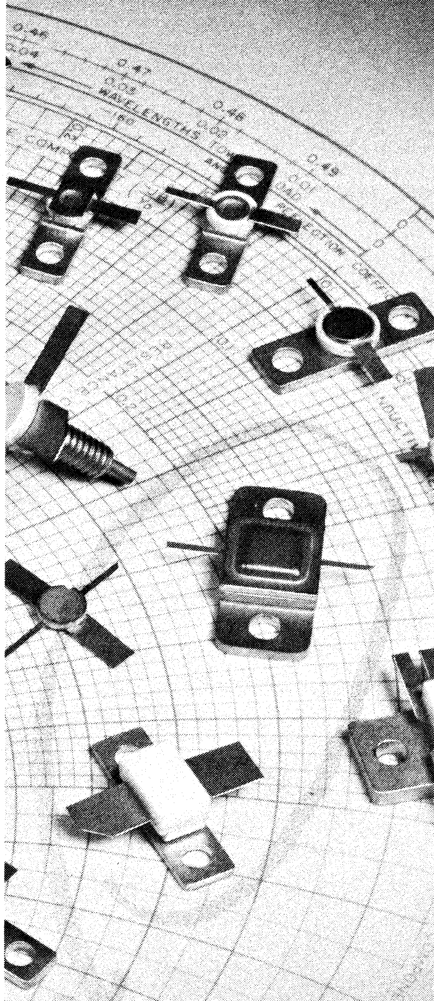

LET'S TALK IFF/DME

To meet your needs in commercial, general aviation and military IFF equipment, we offer a full range of short pulse (10 μsec, 1%) high power transistors. We can supply fully characterized devices in glued top or solder sealed packages — in either single or balanced formats, up to 1100 watts — including high power (30W) oscillators.

Let's talk about your requirements — we would like to be your Power House. Write for more information to Amperex, 230 Duffy Avenue, Hicksville, NY 11802. Telephone 516-931-6200.

Amperex

A NORTH AMERICAN PHILIPS COMPANY

new products

MOBILE COMMUNICATIONS

RF Transistors from 900 MHz down to 1 MHz for reliable Mobile Communcations

The new range of Amperex Mobile Transistors delivers the power you need to be successful in cellular communications. The Amperex transistors are measured and characterized at 900 MHz and 12.5 volts. Now you can take advantage of the entire 900 MHz mobile band. These transistors are manufactured in large quantity to give you the benefit of low cost coupled with high performance. The BLV93 is input matched for broadband applications and is supplied as a common emitter transistor for stability in your circuits. The BLV91 is an excellent driver for the BLV93. And the BLU98, which is manufactured on an automated assembly line, is perfect as the input stage in cellular radio power amplifiers. Write for full specs including recommended circuits.

•BLU 98

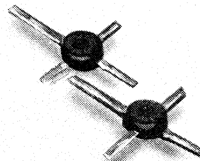

SOT 103/E1 900 MHz

Application: 900 MHz Radio Telephone; **Power:** 0.5W; **Freq.:**900 MHz; **Gain:**≥9.0dB; V_{CE}: 12.5V; **Efficiency:**≥50%

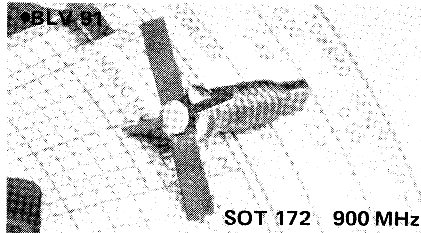

Application: 900 MHz Radio Telephone; **Power:** 2W; **Freq.:** 900 MHz; **Gain:**≥6.5dB; V_{CE}: 12.5V; **Efficiency:**≥50%

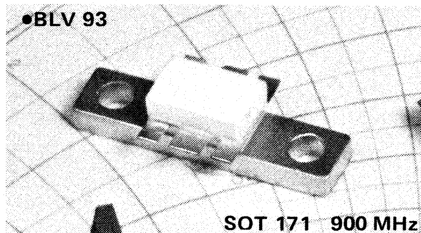

Application: 900 MHz Radio Telephone: **Power:** 8W; **Freq.:**900 MHz; **Gain:**≥6dB; V_{CE}: 12.5V; **Efficiency:**≥50%.

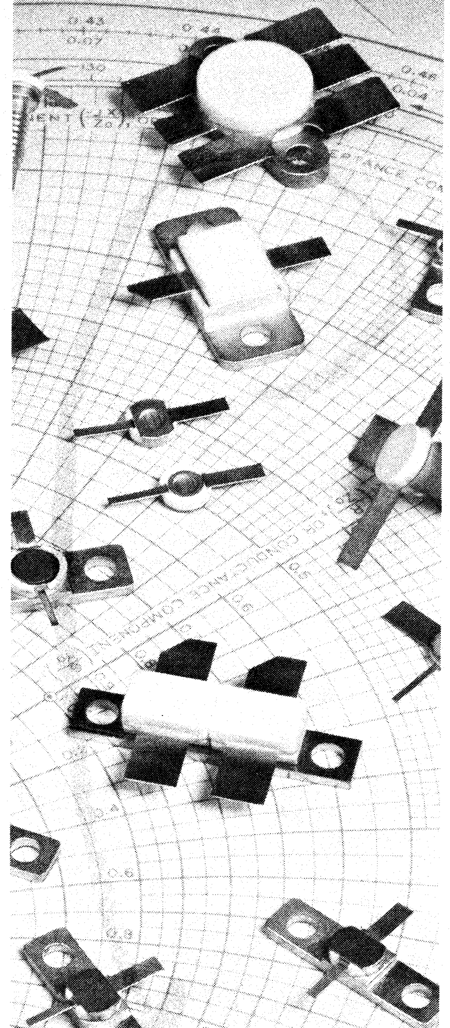

LET'S TALK TACAN

The Amperex medium short pulse (10 μsec, 10%) transistors are especially suited for the 960 to 1215 MHz Tacan band. Types with input prematching or with both input and output prematching make our line of TACAN transistors the most complete available.

Single ended or balanced, Amperex can deliver up to 300W types now and our 600W types are being developed to give you the power you need ... we would like to be your Power House.

Write for complete information. Amperex, 230 Duffy Avenue, Hicksville, NY 11802. Call 516-931-6200.

Amperex

A NORTH AMERICAN PHILIPS COMPANY

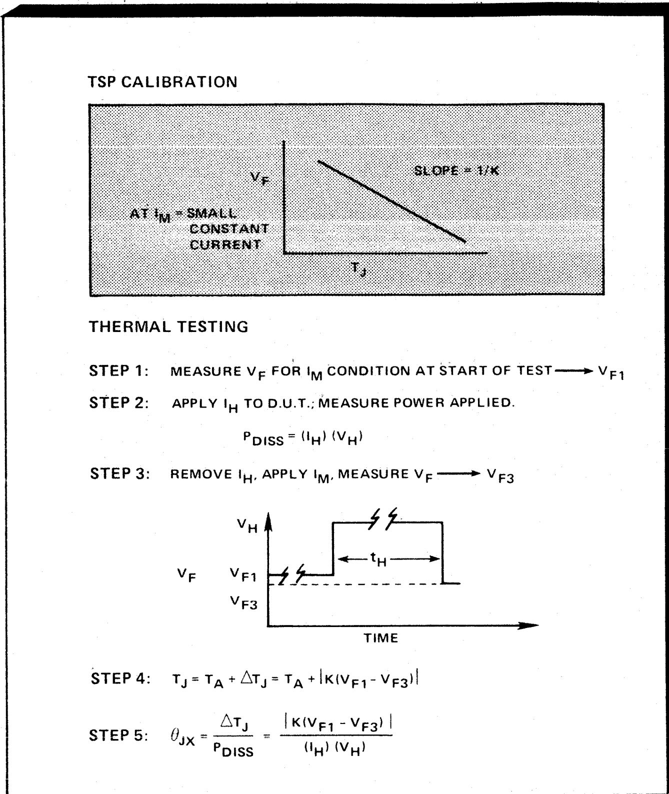

6. The ETM consists of a calibration step to determine the TSP-temperature relation and then the application of a series of electrical pulses to the DUT, as shown above for the simplest case—a pn diode. Depending on the device type and manfuacturing process control, the calibration can be performed on a sample basis.

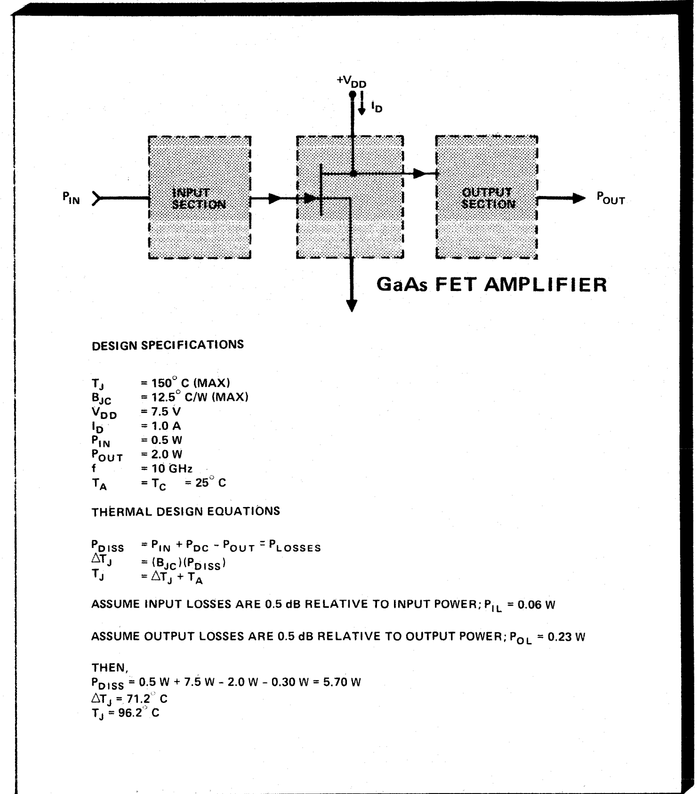

7. A simple set of calculations can determine if the device's T_J is within acceptable limits. Increasing the ambient or case temperature by 54°C will cause the device to be operating at maximum allowable T_J. Under short duration pulse conditions, the thermal impedance would be less than B_{JC} with a resultant reduction in T_J.

carefully implanted to get the proper results and avoid potential damage to the DUT.

Using Measurement Results

The measurement results from either method yield a specific junction temperature for a given set of operating conditions. A more meaningful piece of information that is applicable to any operating condition is the thermal resistance parameter, usually shown as B_{JX}. The subscripts show from where to where the thermal resistance is measured; J stands for junction and X indicates an undefined reference condition. If the thermal resistance were being specified for conditions of thermal equilibrium with the device package well-heatsunk, then the X would replaced with C and the parameter would be shown as B_{JC}. Similarly, A would be used for a non-heatsunk device operating in ambient air and L would be used for a liquid environment. Transient conditions would more correctly be stated as thermal impedance, but the more common practice is to use thermal resistance with the X subscript and the test conditions clearly stated.

Thermal resistance is easily calculated from the above described measurement methods using the following equations:

$$B_{JX} = \frac{(T_{J2} - T_{J1})}{(P_{Diss})} = \frac{|\,K\,(V_{GSf1} - V_{GSf2})\,|}{(V_H)\,(H)}$$

where

T_{J2} and T_{J1} are the hot and cold junction temperatures, respectively, as measured by the IRM,

P_{Diss} is the power dissipation in the device during the IRM measurement,

K is the ETM calibration factor described previously,

V_{GSf1} and V_{GSf2} are the before and after voltage measurements of the ETM, and

V_H and I_H are the power dissipation conditions applied during the ETM measurement.

Once the thermal resistance is known for a given device, the actual junction temperature for any given power dissipation and ambient temperature conditions can be found using this simple equation:

$$T_J = T_A + (P_{Diss})\,(B_{JX})$$

This deceptively simple equation must be used with some caution, however. Thermal resistance cannot be assumed to be a fixed value for a specific device-package combination; both power dissipation level and junction temperature will cause a variation in B_{JX}. The change is usually fairly small

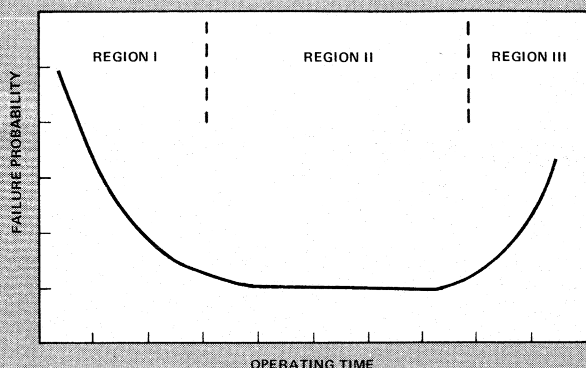

A-1. The generalized curve of semiconductor device failure probability for a large number of devices plotted as a function of operating time. High-reliability systems require devices fitting in the Region II category.

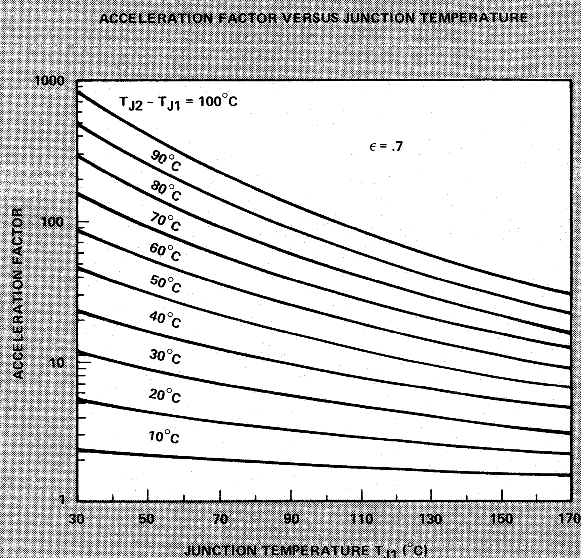

A-2. This graph is a useful tool for estimating the MTTF of a device or devices operating at different junction temperatures. The effects of junction temperature variation on electrical performance is not considered by this curve.

Acceleration Factor Relates Junction Temperature to Reliability

The traditional "bathtub" curve, as shown in Figure A-1, describes the probability of semiconductor device failure as a function of operating life. Region I deals with infant mortality associated with manufacturing problems. Region II relates the low probability of failure that occurs after the Region I failures have occurred. Device failures occurring in this region are usually from external conditions—exceeding breakdown voltage, overcurrent surges, etc. Region III comes about because of the natural wearout mechanism within the device, a chemical reaction effect described by the Arrhenius equation. This equation can be used to derive an acceleration factor that relates time to failure at one junction temperature (T_{J1}) to that for a different junction temperature (T_{J2}) for either the same or different devices. The A.F. is shown as a function of the cooler junction temperature, with contours for the difference in the two junction temperatures, in Figure A-2. From this figure, note that a temperature difference of only 10°C, at T_{J1} at 70°C, is enough to cause a 2:1 difference in mean-time-to-failure; if the cooler device has a MTTF of five years, it is probable that the hotter device will fail in only two and a half years.

(maybe ±10%), and little information is supplied to make suitable corrections. Figure 7 shows how T_J can be calculated for actual circuit applications. Note that the actual power dissipation must not only consider the DC power but the RF power as well.

Applying Thermal Testing

Besides being used for junction temperature measurements, the IRM and ETM techniques are useful in device design, product characterization, production testing, and component evaluation. Thus, thermal testing is applicable to both the device manufacturer and user. The following are specific thermal testing applications.

- *Device Design.* The nature of microwave semiconductor devices is that power dissipation occurs in very small areas, thus giving rise to high power densities. Poor device layout design and/or processing variations can cause troublesome hot spots. Temperatures within these areas can reach levels several times higher than the rest of the device junction. The IRM can be used to locate these areas and provide the device designer information to properly redesign the device layout, and/or guidance towards improving the device processing.
- *Product Characterization.* Once the device layout and processing steps have been sufficiently developed, the mounted device is characterized to determine conformance with the design specifications and to provide applications information to potential users. The heating curve, such as the one shown in Figure 8, not only provides the thermal equilibrium characteristic, but also shows how devices behave under thermal transient conditions. The thermal impedance for a heating pulse of any length can be calculated in the same manner as for B_{JX} shown previously. Since many microwave devices operate under pulse conditions,

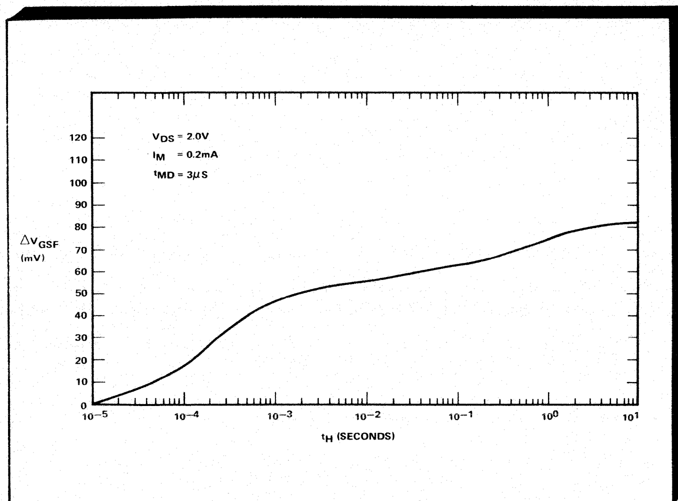

8. A typical heating curve for a GaAs FET in a flange-type package mounted on a good heat sink. The TSP for the FET is the forward biased gate-source junction voltage (V_{GSf}). As the heating time (t_H) is increased, the junction temperature also increases as the heat propagates from the junction. Ultimately the curve flattens out, in the 6 to 10 second region, as the package reaches equilibrium with the heat sink.

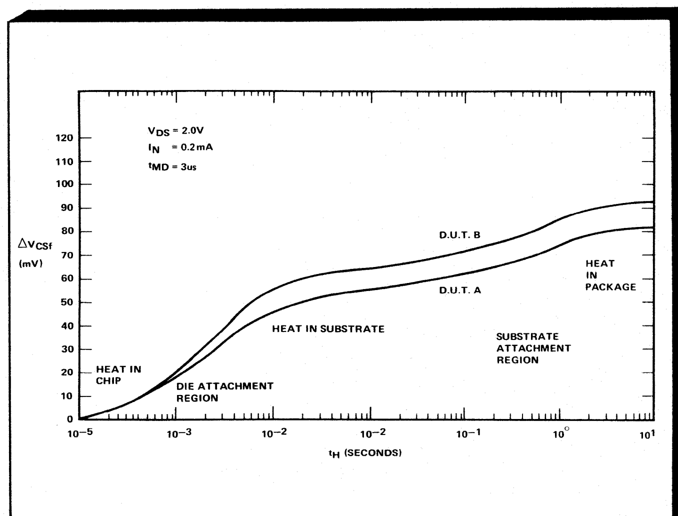

9. The heating curve of Figure 8 is repeated with the addition of a similar curve for a device of the same part number and electrical characteristics. Note that for very short t_H values the curves come together, indicating the chips are thermally the same. Increasing t_H to values sufficient to overcome the chip thermal time constant shows a distinct difference in the die attachment integrity of the two devices. The constant offset between the two curves after the die attachment region shows that the devices have similar package thermal characteristics.

thermal impedance is the more appropriate parameter and, if applied properly, can be used to get greater performance out of the device.

• *Production Testing.* To guarantee device performance, the manufacturer usually has to make a thermal measurement as part of final test. The IRM measurement would require the test before the device is encapsulated and, hence, subject the device to potential contamination. The device would have to be inserted carefully into a heatsink-type test fixture, be tested, and be removed from the fixture—all of which takes considerable time. The ETM can overcome these problems by making use of the device thermal transient response. As shown in Figure 9, the heating curves for two devices of the same chip design and specification, but with different levels of die attachment integrity, are distinctly different once the heating-power pulse width is sufficiently greater than the chip thermal time constant. Note that the curves have a constant offset after the die attachment region, as the devices have thermally identical packages. Assuming a high confidence in the packages' thermal consistency, a very short thermal transient test can easily be implemented in final test to assure device thermal conformance—the test fixture does not require heatsinking because the heat does not have time to propagate to the package.

• *Component Evaluation.* The enlightened microwave system designer will want to use components in which he has confidence, especially such key elements as the semiconductor devices. Thus, the component selection process requires careful thermal evaluation in addition to the more common DC and RF evaluations. Not only will thermal evaluation of a potential vendor's devices provide a measure of manufacturing consistency, but it can also determine which of several vendors supplying a given part-number device is doing a better job from a thermal point of view. The system designer gains added benefit from doing his own thermal testing in that he can evaluate the device under conditions peculiar to his system's environment, such as ambient temperature, various cooling methods, pulse conditions, and so on.

The importance of junction temperature on microwave semiconductor device performance cannot be overlooked. The complex nature of semiconductor thermal characteristics is beyond the scope of this article. However, whether for a device manufacturer or user, this article provides a basic understanding of appropriate measurement methods, how to implement them, and how to make use of the information obtained from them to improve device/system performance, quality, and reliability. ■

References

Dr. G.G. Cohen, "Infrared Microscopy For Evaluation of Silicon Devices and Die-Attach Bonds," *Multidisciplinary Microscopy, SPIE Vol. 104,* 1977, pp. 125-131.

D. Epstein, "Application and Use of Acceleration Factors in Microelectronics Testing," *Solid State Technology,* Nov. 1982, pp. 116-122.

B. Johnsen, "When Will Your RF Power Transistor Really Fail?" *R.F. Design,* Nov./Dec. 1978, pp. 40-49.

C.A. Lidback, "Scanning I. R. Microscopy Techniques For Semiconductor Thermal Analysis," 17th Annual Proceedings Reliabiity Physics, IEEE Catalog No. 78CH1425-8 Phy., 1979.

G. Owen, "Thermal Management Techniques Keep Semiconductors Cool," *Electronics,* Sept. 1980, pp. 135-142.

B.S. Siegal, "Use Electrical Tests For Thermal Measurements," *Microwaves,* June 1976.

B.S. Siegal,"Electrical Thermal Testing Puts Quality in GaAs FET Systems," *Microwave System News,* August 1981, p. 108.

L.G. Walshak and W.E. Poole, "Thermal Resistance Measurement By IR Scanning," *Microwaves,* February 1976, pp. 54-59.

Testing Oscillators, Amplifiers, and Mixers

Tests are presented to provide the microwave engineer with the capability to characterize several kinds of performance for those three component classes. The test techniques included permit the required measurements without costly or elaborate instrumentation.

By Charles E. Foster, Courtney E. Krehbiel, *and* Kurt Zublin, *Wavetek*

The system engineer who specifies microwave components for integration into his system must often characterize these components to ensure proper operation not only during development but also during the production phase. For the characterization, he has two basic choices:

- *Accept test data as given to him by the component manufacturers, or*
- *Repeat some of the critical measurements himself and supplement the manufacturer's test data with additional measurements necessitated by unusual system performance or component interface requirements.*

This is written for those who select the latter of these two choices, but who are not experienced component engineers.

In an attempt to provide meaningful information in limited space, several decisions and assumptions had to be made. Discussions are limited to oscillators, amplifiers, and mixers; tests include only the most critical ones. These selections are based on the authors' experiences and should be useful to the system engineer in specifying and performing additional test parameters for future requirements.

Oscillators

Oscillators are available in large variety. Historically, microwave-tube oscillators were of the cavity-type resonator, either fixed or mechanically tuned. When semiconductor oscillators became available, tuning range increased substantially and wideband electronic tuning became possible. These advancements caused more complex testing methods to be required.

Three areas of tests will be described:

- output load related,
- tuning characteristics, and
- spectral signal purity.

The system engineer doing component integration in the system often has limited access to sophisticated test instruments such as spectrum and network analyzers. These pieces of test equipment might be used to check overall system performance. It may be difficult to justify the purchase of a second analyzer, which could cost up to two orders of magnitude more than the oscillator under test. Test methods described here make use of lower-cost instruments, thus allowing a test setup to be composed of instruments and components that are readily available to the microwave engineer. For more complicated tests the reader is referred to the application notes of various manufacturers.

- *Load-Related Tests.* Since the oscillator is a signal source creating its own microwave signal, it can be influenced in various degrees by the type of load that dissipates its power output. Some kind of isolation has to be provided such that the oscillator power output and its frequency are independent or remain within specified limits when the load impedance varies over a given range. The isolation can be created by decoupling the output, by establishing a weaker coupling to the resonator with a sacrifice in power output, or by providing a buffer amplifier with sufficient forward gain and reverse attenuation. In cases where the tuning range is not excessive, a simple ferrite isolator can be utilized, also.

There are two main methods for creating a known, variable load mismatch (Fig. 1). One can use a standard calibrated mismatch, e.g., VSWR 2:1, connected to a line stretcher which is in the form of an adjustable air-coaxial line. Changing the stretcher length will change the phase of the mismatch from zero to 180 degrees for a half-wavelength change in line length. However, a good low-loss and constant-impedance–type line stretcher with small, residual connector mismatches is expensive and difficult to find.

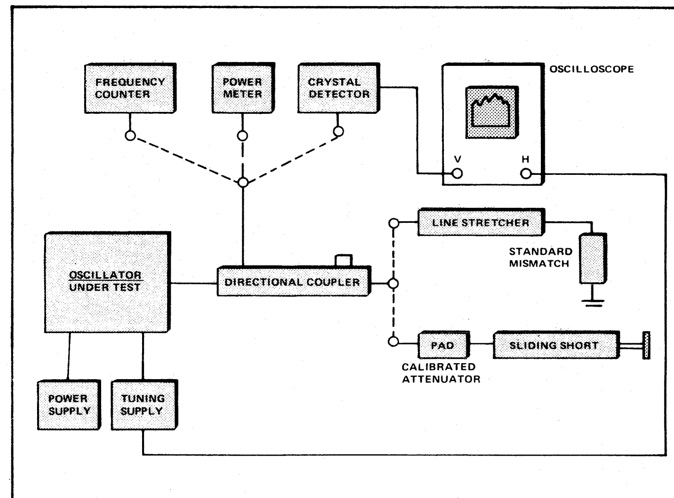

1. Test-setups are shown for frequency pulling and power output variation with load mismatch.

An easier approach is to use a sliding short with a calibrated attenuator pad. The sliding short establishes a movable short circuit in shunt with the line rather than in series like the line stretcher, where contact losses are more difficult to minimize. The actual mismatch at the oscillator

Charles E. Foster, Courtney E. Krehbiel, and Kurt Zublin, are manager, engineering manager, and senior project engineer, respectively, at the Microwave Business Unit, Wavetek San Diego, San Diego, Calif. *Two of the authors would like to express special thanks to the third author, Kurt Zublin, for his untiring efforts and special insight which have made this chapter possible.*

is either magnified or reduced by the residual VSWRs of the calibrated pad and directional coupler. The total VSWR of two mismatches can range from $VSWR_1 \times VSWR_2$ to $VSWR_1/VSWR_2$ depending upon the phase relationships between the mismatches. Of course, $VSWR_1/VSWR_2$ must be greater than or equal to one.

An additional source of error is caused by the insertion loss of the directional coupler which reduces the calculated mismatch. This error has been plotted in Figure 2. For example, a 2:1 load mismatch will be reduced to 1.72:1 with a lossy line of 1-dB attenuation. The importance of a good directional coupler with residual VSWRs of less than 1.1:1 and insertion loss of less than 0.5 dB becomes evident. Two types of measurements can now be performed as a function of load mismatch: power output variation and frequency pulling.

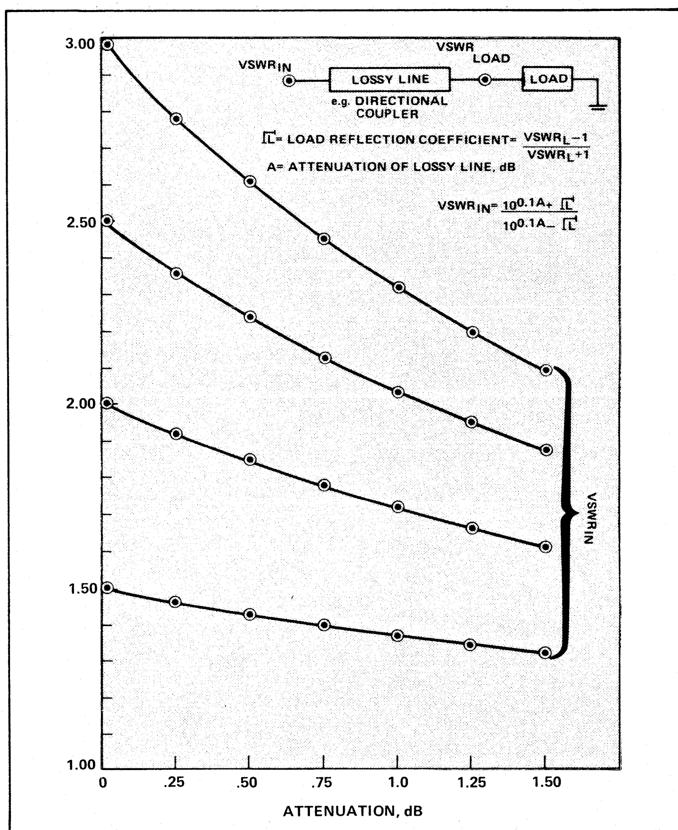

2. Load mismatch error is caused by line losses.

In the case of a fixed-frequency oscillator, one can replace the crystal detector with a power meter and measure the output-power variations as a function of variable phase (sliding short) for a given mismatch magnitude. Switching over to a frequency counter, the frequency pushing can be measured directly for the same mismatch condition.

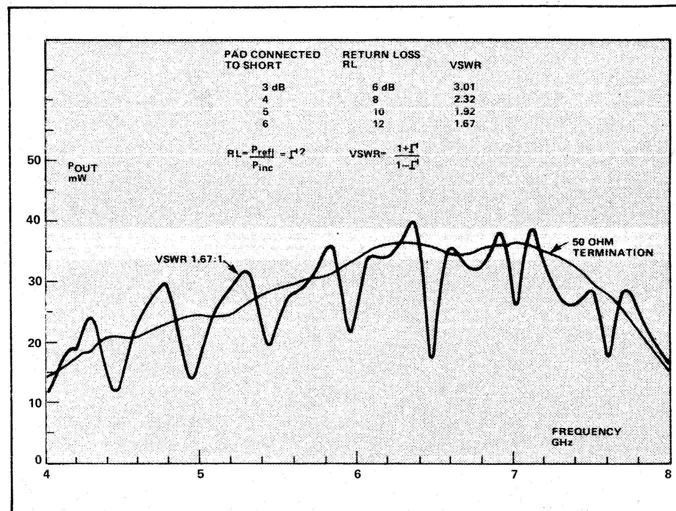

3. Typical power output variation of unbuffered oscillator includes return loss 12 dB, VSWR 1.67:1.

Tunable oscillators, especially broadband, can show the power output variation vs mismatch on a swept display by using a crystal detector and oscilloscope. The directional coupler is in most cases several half-wavelengths long. The sliding short is then not necessary and the calibrated pad is terminated with a short. A typical power output variation over a 2:1 frequency range is shown in Figure 3 for an oscillator which has no buffer stage. A short-circuited 6-dB pad was chosen (12-dB return loss) representing a load VSWR of 1.67:1. By tuning the oscillator manually, one can determine the frequency-pulling figure by recording the frequency difference from a linearly changing frequency for a perfect load since the phase at the line input will vary with frequency.

- *Tuning Characteristics.* The tuning characteristics of an oscillator can be, broadly speaking, divided into two areas: static and dynamic. In the first case, tuning is accomplished manually, that is, at a slow rate. Tuning range and tuning linearity can be determined by simple measurements. At higher tuning speed, this could be a ramp or step tuning; the measurement techniques have to be more refined.

Oscillators that are tuned by a change in magnetic field—e.g., YIG resonators—are slow by nature since the induced eddy-current field in the magnetic circuit opposes the tuning field. The tuning field is established by a solenoid of large inductance and follows an exponential rise with an applied current step. It is for this very reason that YIG-tuned oscillators have a secondary tuning port. This so-called FM coil allows tuning rates as high as 10 MHz but with limited frequency deviation of perhaps ±100 MHz. Another advantage of a separate tuning coil is the capability of phase locking the oscillator for better frequency stability. YIG-tuned oscillators are inherently linear (±0.1 percent) and cover several frequency octaves.

The varactor-tuned oscillator does not have this tuning-speed limitation. Tuning is achieved by a capacitance change which is voltage controlled, and the amount of charge current is very small compared with a magnetically tuned oscillator. The voltage-tuned oscillator has a non-linear tuning characteristic and the tuning range is usually limited to an octave. Many tests can be described which are related to the tuning characteristics of an oscillator. Tuning linearity and tuning speed are probably the most important ones.

- *Tuning Linearity.* Tuning linearity is normally specified when the oscillator is operating into a perfect load. This situation does not exist when the oscillator is incorporated in a system where other component mismatches exist. Depending on the amount of frequency pulling as was

described in the previous test, the tuning linearity can be substantially degraded. For example, a 4-GHz oscillator that has a 0.1-percent deviation from linear tuning—that is, 4 MHz—and a pulling figure of 2 MHz with a load mismatch of 1.67:1 (12-dB return loss) will show a 50-percent tuning linearity degradation. Frequency pulling quite often is not specified for the second harmonic. This harmonic signal can be as large as −10 dBc for broadband oscillators. In applications where incremental tuning linearity is critical, one should recognize that tests with an actual system load, rather than a 50-Ohm termination, are essential. Manual test setups consisting of a frequency counter, oscillator tuning supply, and biasing power supply can provide the necessary information; however, the measurement and data-recording time for the many small frequency increments often dictates the need for an automated test setup.

- *Tuning Speed.* Oscillator parameters influenced by the tuning rate are: tuning range, tuning linearity, and frequency settling time. The tuning range of a manually tuned oscillator can be quite different when swept at a fast rate. This can be caused by a delay in the drive circuit or by the oscillator itself. On the other hand, a linearizer circuit can have a tuning-rate limitation which adversely changes the tuning linearity. Testing an oscillator to these criteria is relatively simple.

A frequency response-time test can require expensive instrumentation using a pulse counter or discriminator with a waveform recorder.[2,3] Figure 4 shows a test setup that uses a beat-frequency method providing the advantage of requiring only low-cost instrumentation. This measurement technique has been used extensively with YIG-tuned oscillators, and gives accurate results.

The frequency of the oscillator under test changes as a function of time during the step inteval. A known frequency of a signal generator with good short-term stability is mixed with the oscillator output in a crystal detector and a beat note is created when the two frequencies coincide. This beat note can be observed on a dual-trace oscilloscope and referenced to the time base. The response of the step pulse is shown simultaneously on the second trace. Start and stop frequency can be easily determined where the beat note expands horizontally (zero beat). The oscilloscope amplifier for the beat note should have a narrow bandwidth for good resolution since the blip is essentially twice the amplifier bandwidth. A switchable (mercury relay) stable DC voltage source is preferred over a long pulse from a function generator since the voltage droop should be less than 100 microvolts. When a variable-frequency signal generator is not available, a second oscillator under test could be substituted.

The change in frequency during the step is measured as follows: The frequency of the signal generator is gradually changed, its frequency monitored on a frequency counter. A succession of beat notes can be observed and the time interval after the step occurrence measured for various frequency offsets from the final frequency. A typical step frequency response is shown in Figure 5 for a YIG-tuned oscillator. As can be seen, settling time is extensive. The frequency error is, for this reason, quite often specified as a percentage of the actual frequency step. The aperiodic shape of the settling curve is typical for a tuning-current driver which has a smooth frequency roll-off characteristic. Oscillators with different compensation in the drive circuit can show an overshoot and ringing. This test setup measures settling times as long as several seconds. The mercury relay is the limiting element for faster switching speed measurements. It can be eliminated and the output pulse from the function generator can be directly connected to the tuning circuit. A flat top is still essential for accurate measurements.

Post-tuning drift can occur for a large frequency excursion and long dwell times before the next step is applied. It is more pronounced in a YIG-tuned oscillator where it is caused by the large thermal time constant of the magnetic circuit. Post-tuning drift can extend over several minutes and should be specified separately from the settling time. A

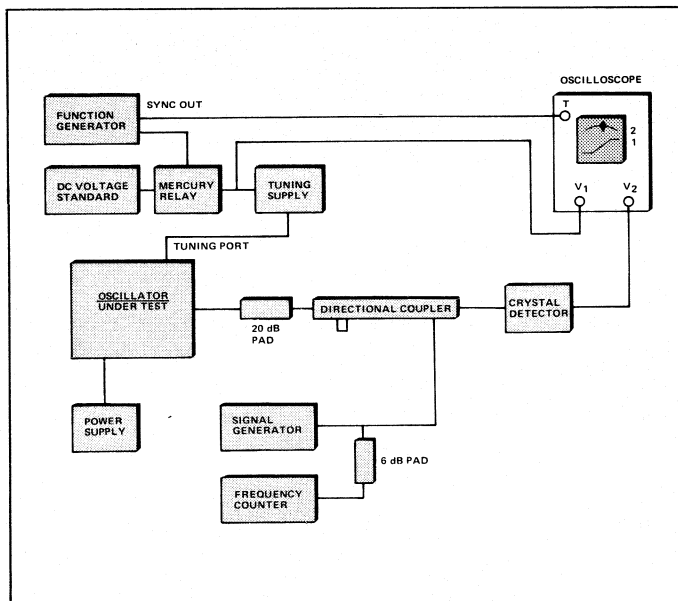

4. Test-setup for switching speed measurements makes use of the beat frequency method.

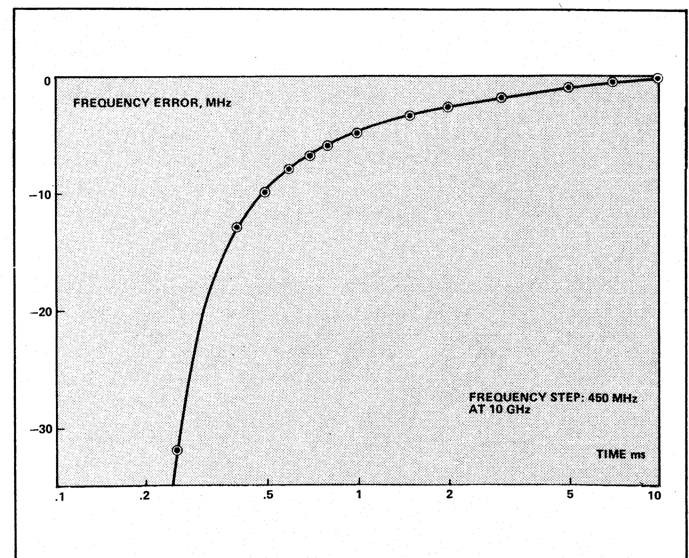

5. Typical frequency response time of a YIG-tuned oscillator reveals an extensive settling time. Frequency step: 450 MHz.

varactor-tuned oscillator dissipates much less power and a frequency change after a step can be associated with losses in the varactor rather than the oscillator itself.

- *Spectral Signal Purity.* The carrier signal of any oscillator is built up from the noise level of an active device by its signal gain. A tunable high-Q resonator which is loosely coupled provides the frequency selection and determines the noise sideband level. These noise sidebands can be either inherent in the oscillator, or are system-contributed by less-than-ideal tuning or biasing conditions. The first case can be described by a phase noise measurement; it requires good short-term stability of the carrier. In the second case, when the carrier is modulated by external signals which influence the frequency to a higher degree than its amplitude, one speaks of residual frequency modulation.

Signal-purity specifications should also include spurious signal levels. These can be harmonically related or can occur at random, and most likely are measured with an amplitude-calibrated spectrum analyzer.

We limit our discussion to two types of measurements: a. residual FM, and b. phase noise. The test-setup shown in Figure 6 makes use of a delay-line discriminator which is used for both measurement types.

- *Residual FM.* Oscillators which have a short term stability comparable to the residual FM level are much easier to measure with a discriminator than with a spectrum analyzer. With the discriminator, slow frequency drift can be eliminated from the oscilloscope presentation by switching the amplifier input from DC- to AC-coupled. the peak-to-peak frequency deviation can then easily be measured with a high-sensitivity amplifier. An oscilloscope amplifier with selectable upper and lower 3-dB bandwidth is ideally suited for the measurement since the residual FM is normally specified in a given post-detection bandwidth.[4,5]

The delay line discriminator is composed of the following components: in phase 3-dB power divider, mixer, delay line, and isolators. Frequency coverage is determined by the bandwidth of the individual components. Although multi-octave coverage is possible, a more sensitive discriminator can be built for a narrower frequency range.

The mixer should be of a double-balanced kind with DC-coupled IF output. A good, balanced design is essential in order to achieve a linear discriminator characteristic independent of power input variation. In application, the mixer is a phase detector since the RF signal is divided into a reference and a delay path. The differential delay, which can be expressed as a phase difference between the two signals, creates an output signal at the IF port which is a linear function of frequency. The periodic zero crossing can be calculated from the equation shown in Figure 6.

Deviation from linearity can be kept under one percent provided the frequency deviation to be measured is less than 10 percent of ΔF, the zero-frequency crossing separation. Since the slope of the discriminator is a function of input power level as well as of frequency, accurate calibration of the tuning sensitivity is essential.

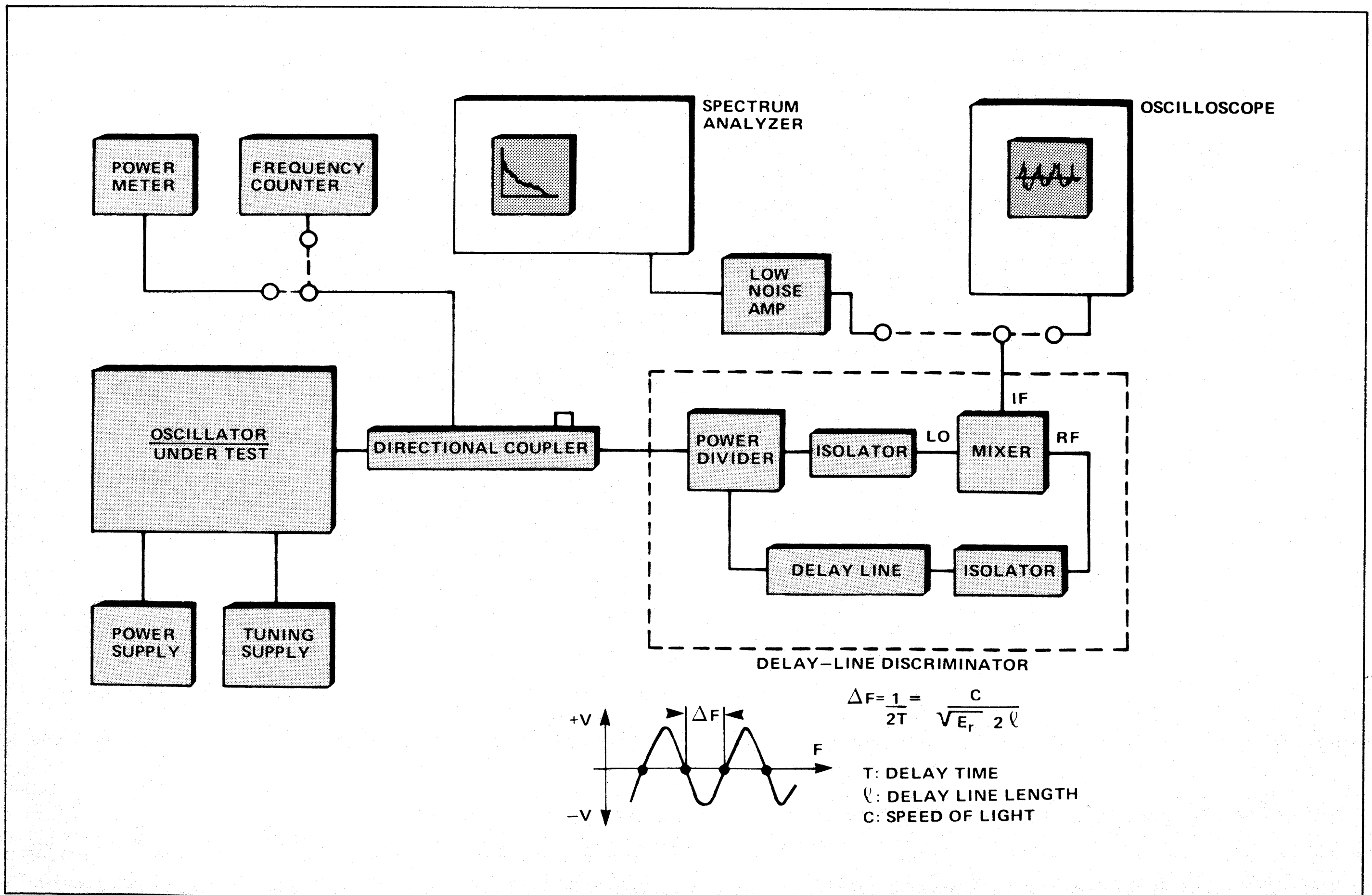

6. Test-setup for residual FM and phase noise measurements replaces the earlier oscillator with a spectrum analyzer.

The delay line can be made with several feet of semi-rigid coaxial cable. The larger the diameter, the lower the insertion loss. A practical example for X band is the following:

Delay Line	**Discriminator**
Cable 0.085 in. OD	Sensitivity: 300 kHz/mV
Length: 5 ft.	Input power: 0 dBm
Insertion loss: 4 dB	Crossover separation, ΔF: 68 MHz

The fact that measurements can only be performed at the zero crossover frequencies can be overcome with a phase trimmer in one of the lines.

- *Phase Noise.* Of all the microwave measurements in the field, the accurate determination of phase noise of an oscillator is the most difficult to make. Automated phase-noise-measurement systems have been introduced lately which are of great help in this task. However, one should not overlook a manual system which might not have the absolute accuracy but which provides the operator with sufficient comparative information. In many cases, a quick relative measurement is all that is needed. For example, is there a difference in noise performance when the second harmonic is terminated or reflected from an unmatched component? How will noise on the bias supply lines degrade the phase-noise performance? The measurement system as described is an expansion of the previous one for residual FM.

In order to detect phase noise, a more sensitive test setup is needed (Fig. 6). The oscilloscope is replaced with a low-frequency spectrum analyzer and a 60-dB–gain, low-noise amplifier is added. The necessary frequency range of the spectrum analyzer is determined by how far away from the carrier the phase noise has to be measured. The amplifier bandwidth must be optimized for the measurement frequency range. It is mandatory that the analyzer's noise floor be low, better than –150 $\text{dBV}/\sqrt{\text{Hz}}$. This can be obtained with a fast Fourier transform (FFT) spectrum analyzer available from several instrumentation manufacturers. Discriminator sensitivity can also be increased by suppressing the carrier from the phase detector.

The measurement procedure is as follows: Discriminator sensitivity is determined at a crossover point with a known small frequency deviation in order to stay within the linear range. The measured voltage on the analyzer at a given separation from the carrier is expressed in $\mu\text{V}/\sqrt{\text{Hz}}$ and can be converted to an equivalent ΔF_{RMS} with the known discriminator sensitivity. Single-sideband phase noise can also be measured in dBc/Hz at a given frequency offset from the carrier. The chart in Figure 7 will be helpful to convert from one expression to the other. In cases where either frequency drift or short-term stability of the oscillator is a problem, one can stabilize the carrier with a simple automatic frequency-control circuit by using an identical delay line provided the oscillator has a phase-lock input.

Generally speaking, AM noise is 10 to 20 dB smaller than phase noise and can be neglected in many applications. If a measurement becomes necessary, one can use the same test setup. The oscillator is tuned to a peak of the discriminator curve and the AM noise is determined from the analyzer reading. However, better sensitivity can be achieved with a low noise tunable detector.

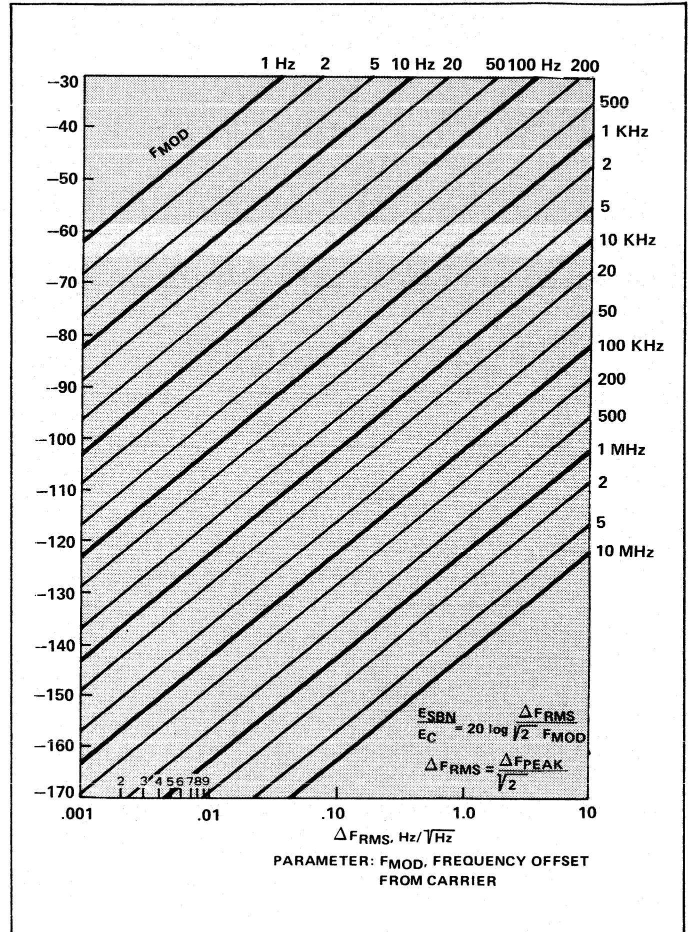

7. Phase noise conversion chart enables conversion of parameters.

Amplifiers

Microwave amplifiers are probably the broadest single component category the system designer has to deal with. The many different types can indeed be overwhelming to the novice. However, they can be classified according to three distinct parameters: noise figure, gain, and power output. A further grouping related to the application of the amplifier is shown in Table I.

Table I
Classifying Amplifiers

Application	Noise Figure	Gain	Power Output
Small signal amplifier for receiver	Low	30 dB min	Approx. 10 mW
Buffer amplifier for oscillator	Medium	10 dB	Approx. 100 mW
Driver for power amplifier	High	5 dB	Approx. 1 W

In addition, there are other amplifiers available for special applications, such as variable gain and limiting types. Amplifiers that require good gain flatness over a wide temperature

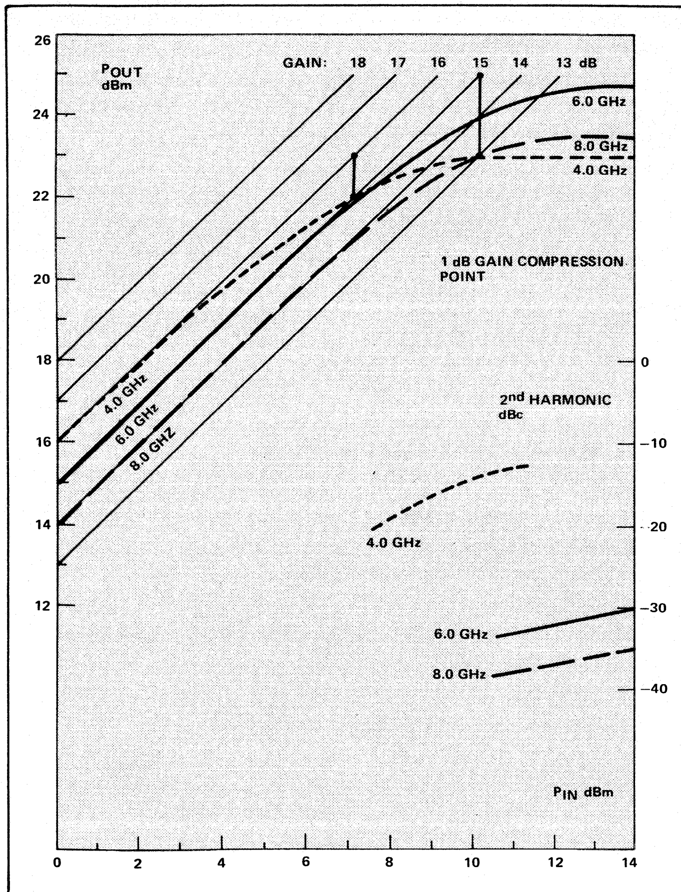

8. Gain and gain compression characteristics are plotted for a medium-power C-Band amplifier.

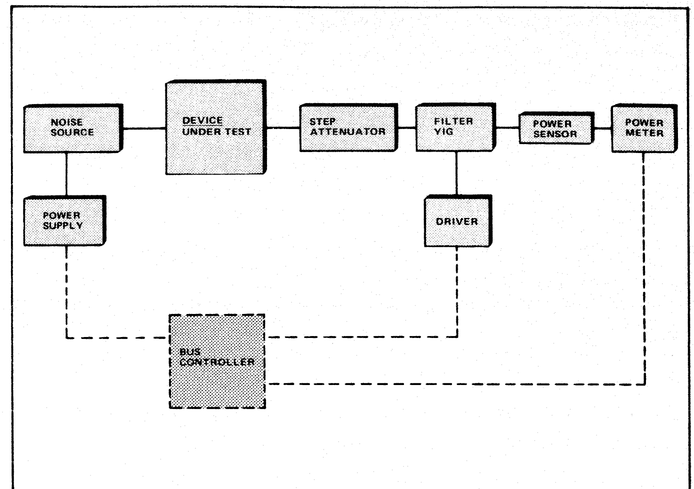

9. Test-setup allows direct noise figure measurements.

range are internally compensated either by adjustable bias voltage or with a PIN-diode attenuator for tighter control.

Many more tests can be performed on an amplifier than on an oscillator because an amplifier is a two-port device. Whereas an oscillator creates its own test signal, an external signal has to be applied to the input port of the amplifier. This signal must be variable in frequency and amplitude.

How an amplifier's specifications are written depends a great deal on its application in the system. Many parameters are temperature sensitive and most manufacturers guarantee performance at room temperature only. Typical variations with temperature are sometimes given. There are at least a dozen tests which can be carried out on an amplifier. Only three—gain, noise figure, and harmonic distortion—will be discussed in more detail.

- *Gain.* Gain is expressed as the ratio of output power to the applied input power at the amplifier. As long as gain is independent of input level, one speaks in terms of linear or small-signal gain. With increasing input signal-level power, output saturation will occur and gain compression shows up. This point has to be defined for an accurate measurement and is determined where the gain has decreased by one decibel. Power output at this input level is expressed in dBm at 1-dB gain compression. The ideal broadband amplifier would have a 1-dB–gain compression point independent of frequency and occurring at the same input level. What one measures in reality is illustrated in Figure 8. The gain of a C-band buffer-amplifier was measured at three discrete frequencies by increasing the input level in 1-dB steps.

Significant information can be read off the graph: Small-signal gain is highest at 4 GHz. Small-signal gain variations amount to 2 dB total. In spite of the fact that the small-signal power output is higher at 4 GHz, the 1-dB gain compression point occurs earlier compared with 6 GHz and saturated power output is therefore lower. Rather than making these measurements point by point, a direct plot of this graph is possible by means of a programmable signal generator and power meter.

In applications which require tight gain flatness tolerances one should also specify gain ripple. These fine gain variations occur over small frequency intervals when the amplifier operates between mismatched source and load impedances.[7] The reflected power can either be added or subtracted depending on the phase of the mismatch. A graph similar to that shown for an oscillator in Figure 3 can also be recorded for an amplifier. An amplifier with an output mismatch of 2:1 and operating into a 2:1 load mismatch can have a ±0.5-dB gain variation.

- *Noise Figure.* The noise figure of an amplifier tells the design engineer by how much the overall system performance degrades, e.g., loss in sensitivity. He is therefore concerned with the noise figure of the component he purchases as well as the overall system noise figure. Noise figure is a figure of merit in the true sense of the word, expressing the electrical noise introduced by the amplifier compared to thermal noise at a given temperature.[8]

The basic definition for noise figure, F, is the ratio between the input signal-to-noise ratio and the output signal-to-noise ratio. Another derived expression is $F = 1 + T_e/T_s$ which is based on the assumption that the amplifier noise can be expressed by a "noise" resistor at an equivalent noise temperature T_e. The amplifier is now considered noiseless. One further assumes a perfect match between source and device for maximum power transfer. The source noise is considered thermal from a resistor at a temperature T_s. Strictly speaking, the noise generated from the amplifier is not thermal but a series of randomly distributed current pulses caused by the moving charges of the carriers in the transistor, and is called "shot noise." by varying the source

temperature between hot and cold and measuring the power ratio, expressed as the Y factor, one can determine:

$$T_e = \frac{T_H - YT_C}{Y-1}$$

$$Y = \frac{P_H}{P_c}$$

This is the classical measurement method. It has been superseded with the advent of solid-state noise generators although it is still used for very accurate measurements or for calibrating other noise sources. Since the noise figure is a function of temperature, it is referred to a source temperature T_s of 290K. The noise figure can be written as:

$$F = 1 + \frac{T_H + YT_C}{290\,(Y-1)}$$

$$F = \frac{(T_H/290-1)\ -Y(T_C/290-1)}{Y-1}$$

Making the cold-temperature measurement at 290K simplifies the expression to:

$$F = \frac{(T_H/290-1)}{Y-1}$$

$$F_{dB} = 10 \log (T_H/290-1) - 10 \log (Y-1)$$

The first term is called the Excess Noise Ratio (ENR) of the noise sources and is the difference in noise with the source on and off. A correct ENR is important for accurate noise figure measurement. Solid-state noise sources must be calibrated over the frequency range of interest. The Y factor is a power ratio and can be determined quite accurately.

Automated noise-measurement systems have become available lately. They have the advantage of higher accuracy since error corrections can be applied, e.g., ENR variations with frequency, actual T_C rather than 290K, RF correction losses, and others.[9]

Basically, two measurement methods are possible; both can be automated. The first one makes use of a downconverter and the noise measurement is performed at an IF frequency. With the availability of more accurate microwave test equipment, direct measurements became possible. Such a system is shown in Figure 9. Broadband frequency coverage is determined by the individual components: noise source and power meter. The tunable YIG filter allows the selection of a particular measurement frequency. An average noise figure is measured over the bandwidth of the tunable filter which can be an order of magnitude wider than for a downconverter test system.[10]

An approximate noise figure can be calculated from the overall measured noise output power of an amplifier when a noise generator is not available since:

$$P_{N_{out}} = KT_S BGF$$

An absolute power measurement becomes necessary. The noise floor of a broadband, high-gain microwave amplifier is quite high and an accurate measurement is possible. The other two unknowns, bandwidth (B) and gain (G) however, cannot be copied form the data sheet. Most amplifiers have an unspecified roll-off characteristic at the frequency band edges and an actual gain plot versus frequency has to be taken. A practical example is shown in Figure 10, of an instrumentation X-band amplifier, which has an excess low-frequency bandwidth of over 2 GHz as well as two high-gain peaks. Since the measured noise output power represents the total integrated noise over this bandwidth, a substantial error—too large a noise figure—would be made by relying on the specified bandwidth only.

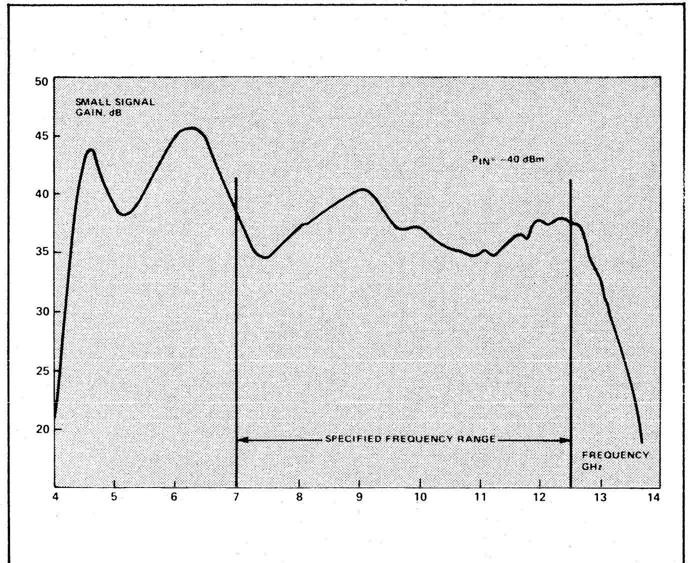

10. Small-signal gain of an X-band instrumentation amplifier shows typical problems because of gain peaks.

• *Harmonic Distortion.* Different kinds of distortion can be defined depending on amplifier types and their applications. The largest unwanted signal in most amplifiers is the second harmonic. Higher-order intermodulation products, which are the result of mixing products of two or more simultaneously applied signals, are important in amplifiers which are operated over the full dynamic range. Dynamic range can be defined as the ratio of the maximum signal, usually measured at the 1-dB gain compression point, and the minimum discernable signal, which lies 3 dB above the amplifier noise level.

The appropriate test instrument for the measurement of spurious signal levels is the spectrum analyzer. The analyzer allows direct observation and simple measurement of the spurious signal levels with respect to the desired signal. However, when the second harmonic falls in the millimeter-wavelength range, external mixers are required. Sensitivity is degraded and the display must be calibrated. A different approach using a direct-reading power meter and highpass filter is possible, provided the harmonic level is in the order of -20 dBm or greater.

Harmonic distortion can occur in the amplifier when the signal level exceeds the constant gain range. This is shown in Figure 8 for a medium-power C-band amplifier for three different frequencies and as a function of input power level. The worst case occurs at 4 GHz; the second harmonic falls

in the frequency range where the amplifier still has appreciable gain. Gain compression of the fundamental signal also occurs at a smaller input signal level at 4 GHz than at other frequencies—7 dBm at 4 GHz compared with 10 dBm at 6 and 8 GHz—emphasizing the second harmonic level.

Another form of harmonic distortion can occur when the input signal already has a large second harmonic, e.g., an oscillator driving a buffer amplifier. Figure 11 is an illustration of what can happen in a practical case. Amplifiers from two different manufacturers were evaluated. Both met the +20-dBm power output and 14-dB small-signal gain specifications. A frequency range of 3.6 to 7.6 GHz had to be covered, and a standard off-the-shelf amplifier was considered for price reasons.

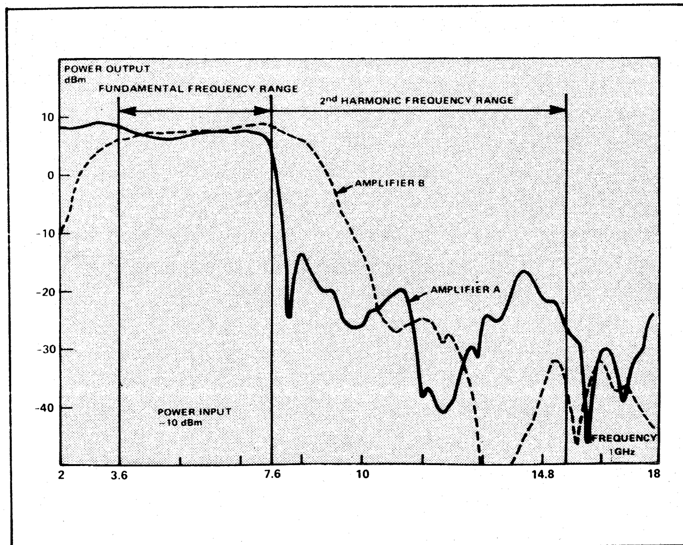

11. Amplifier gain response at second harmonic demonstrates typical problems.

The small signal gain is plotted for −10 dBm input power over the 2-to-18–GHz frequency range. As can be seen, amplifier A is of a basic 2-to-8–GHz design with a steep gain roll-off above 7.6 GHz. Amplifier B, however, was designed for 4-to-8–GHz coverage and still shows substantial gain at 9 GHz. The second harmonic from the oscillator will therefore be at a higher level. Another fact which should not be overlooked is the peak at 14 GHz of amplifier A, which increases the second harmonic. When either amplifier is driven to saturation, an enhancement of the oscillator's second harmonic level of at least 3 dB can be expected, caused by gain compression over the fundamental frequency range. In addition, at this input level the amplifier creates its own second harmonic which can be either in or out of phase with the oscillator's spurious response.

The maximum second-harmonic levels of −20 dBm are sufficient for many applications. Stricter requirements can be satisfied with additional filtering, especially where an octave frequency range is covered. A lowpass filter with switchable cutoff frequencies, or a tracking filter, are some of the possibilities.

There are a number of additional tests that can be performed on an amplifier. Which ones are chosen is really determined by the application of an amplifier in the system; previously discussed parameters—gain, output power and noise figure—are temperature-sensitive and degrade with increasing temperature. Input VSWR should be specified at the actual drive level. The phase characteristics are related to phase shift, linearity, and group delay. The damage level or RF burn-out could be important where pulse spikes from a transmitter occur. Overdrive recovery and settling time determine the amplifier response for large-signal applications. Operating into a load mismatch can cause amplifier instabilities. Spurious signals associated with low frequency oscillators, and which originate in the built-in regulator circuit, are sometimes overlooked. They appear as very small modulation sidebands, e.g., −50 dBc. All of these considerations may require additional tests to determine acceptable performance levels of purchased amplifiers.

Mixers

This discussion on component testing began with the one-port oscillator, followed by the two-port amplifier. The mixer is a three-port device. The three ports are usually designated by the frequency of the corresponding signals, RF, LO, and IF. The combination of the RF and LO signal in a non-linear device such as a diode creates mixing products, one of which is the desired down- or up-converted IF signal. All others should be rejected in the ideal case.

The development of mixers has kept pace with the advancement of semiconductor technology. The early point-contact diode was superseded by the beam-lead Schottky-barrier diode. However, mixer configurations have not changed substantially with time. The single balanced mixer circuit of forty years ago, such as the X-band waveguide magic-T mixer, has been gradually replaced with more-compact stripline and microstrip designs. At millimeter wavelengths, one finds coplanar and finline configurations. In the majority of applications, the double-balanced mixer is still the preferred one. Image-rejection mixers are also available, and more recent developments encompass the active mixer, e.g., dual gate FET.[13]

The task of choosing an optimum mixer for a specific application is probably the most difficult job the design engineer has to undertake when compared with the selection of an oscillator or amplifier. Although the specifications for bandwidth, conversion loss, noise figure, isolation, and VSWR appear to be simple, remember we are dealing with three distinct signals of different frequencies and amplitudes. A multitude of unwanted higher-order mixing products, mLO ± nRF (where m and n are integers), can degrade the mixer performance substantially.[14,15]

Mixer performance tests must be carried out with at least two microwave signals, RF and LO, which can be varied in frequency and amplitude. The downconverted signal which might also be in the microwave frequency range normally must be measured with a spectrum analyzer. An additional RF signal will be required for two-tone intermodulation distortion measurements.

The overall performance of the mixer is determined mainly by the hybrid coupler configuration and, to a lesser extent, by the diode type. Either 90-deg. or 180-deg. couplers in a single- or double-balanced configuration are possible combinations. Table II summarizes some of the important characteristics of typical X-band mixers with Schottky barrier

Table II

Performance Comparison of Typical X-Band Mixer Types

Parameters (Typical)	Balanced		Double Balanced	
	90° Hybrid	180° Hybrid	90° Hybrid	180° Hybrid
Number of diodes	2	2	4	4
LO power, mW	+ 7	+ 7	+10	+10
Conversion loss, dB	6	7	8	8
Isolation, dB LO/RF	10	18	25	23
VSWR	1.6	2.0	1.4	2.0
Intercept point, dBm	+15	+15	+18	+18
Single tone spurious suppression	Poor	Poor	Good	Good
Harmonic rejection	Poor	Good	Fair	Very Good
IF bandwidth, GHz	DC to 1	DC to 0.4	DC to 0.4	DC to 4.0
Biasable	Yes	Yes	No	No

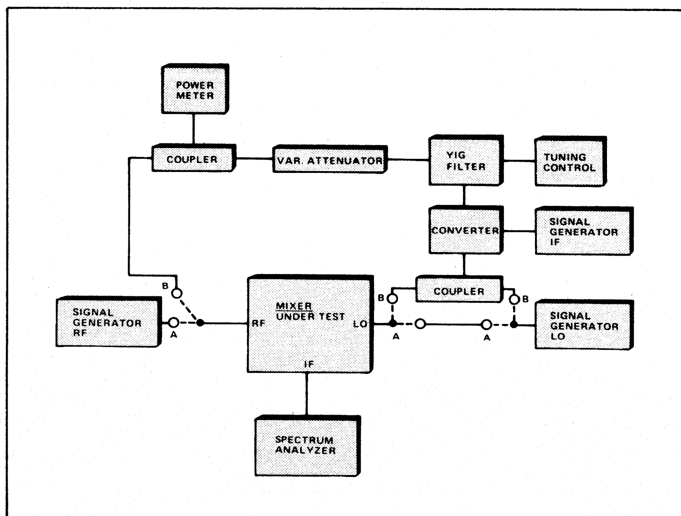

12. Test-setup measures conversion loss, the ratio of IF output power/RF input power expressed in dB for a given LO power level.

diodes. In applications where insufficient LO power is available, the mixer can be DC biased in order to overcome the increased conversion loss. Special kinds of mixers such as the image rejection mixer, quadrature IF mixer, and others fall outside this general discussion.[16]

• *Conversion Loss.* The conversion loss of a mixer can be measured with a test set-up as shown in Figure 12. Conversion loss is the ratio of IF output power to RF input power expressed in dB for a given LO power level. The IF level can be determined with a power meter, or the difference between the two signals can be read directly off a spectrum analyzer.

Making the measurements with two signal generators (channel A) requires at least one with sufficient output power to drive the LO port, typically +10 dBm. If only one signal generator is available, a conversion approach becomes necessary in order to create the RF signal (channel B). The YIG filter allows the selection of the upper or lower sideband for the RF port. The variable attenuator, coupler, and power meter were added to monitor the signal level when the mixer is tested over a large frequency range. A YIG filter has to be selected with appropriate bandwidth to get sufficient rejection of the unwanted sideband. When measuring mixers over a wide frequency range, the downconversion approach is preferable, since a fixed IF offset is maintained and tracking between two signal generators is eliminated.

A graph similar to Figure 8 can be plotted for a mixer by varying the RF signal (P_{in}) and recording the IF signal (P_{out}) for a given LO level. A 1-dB conversion compression point can be defined as the input signal level which causes a 1-dB increase in conversion loss, similar to the gain compression point of an amplifier. This point also determines the upper signal level for dynamic range measurements, the lower being set by the noise figure of the mixer.

• *Noise Figure.* In most cases, the noise figure of a mixer is specified with the inclusion of the IF noise figure. Subtracting the IF noise figure from the overall noise figure does not necessarily determine the mixer noise figure. The reverse is also true when the two noise figures are added. Only when mismatch losses between the mixer IF port and the following amplifier, as well as the conversion loss of the mixer, are known and taken into account is this a valid approach. Whenever possible, buying the mixer with a built-in preamplifier will eliminate this uncertainty. The manufacturer can optimize the overall noise figure which does not have to coincide with best input impedance match.

Quite often, mixer noise figure is equated with its conversion loss since a mixer can be looked upon as an

attenuator. This simplified comparison can give erroneous results caused by the excess noise of the mixer diodes.[17] High-level mixers, which are driven with large peak currents, are vulnerable to excess noise. Mixers that are used as phase detectors are especially sensitive to 1/f noise since they operate at zero IF. Flicker noise contribution is normally not included in the noise figure since the IF is specified above a minimum frequency, e.g., 500 kHz.

The preferred method for performing mixer noise figure measurements is with automated test equipment.[9] Precautions have to be taken in order to account for all sources of errors. A broadband, solid-state noise source can leak noise signals directly into the IF band in mixers with low RF-to-IF isolation. Another noise contribution can be the LO signal when its noise sidebands are downconverted to the IF band. The spectral purity of the LO signal should, therefore, be checked with a spectrum analyzer.

Automated noise-figure–measurement systems sometimes have the limitation that a low-enough IF cannot be covered. A direct measurement with a power meter and high-gain, low-noise amplifier can give accurate results.[17]

The noise figure of a mixer influences the system sensitivity directly. A reliable and accurate value is important. However, in most cases, a verification of the noise figure by the system designer cannot be performed due to the complexity and cost of the test instrumentation.

• *Distortion.* There is only one downconverted signal which is of interest; all the other mixing products can be classified as distortion. A spectrum analyzer with an accurately calibrated display allows relative measurements of the unwanted signals with respect to the desired one.

Harmonic distortion is caused by mixer-generated harmonics of the LO and RF signals. It can be expressed as $mf_{LO} \pm nf_{RF}$, where m and n are the harmonic numbers of the corresponding signals. In most cases, the second harmonic of the LO signal itself is small enough (i.e., ≤xxdBc) and will not create mixing products.

Intermodulation distortion or two-tone distortion occurs when two RF signals are present. The so-called third-order product which is defined as $(2 f_{RF2} - f_{RF1}) \pm f_{LO}$ can easily fall in the IF band. The prediction of third-order signal suppression of a mixer is determined by its intercept point. This is the point where the signal level of the desired output coincides with the third-order–product signal level. The higher the intercept point, the better the suppression.

A third form of distortion is in the form of cross modulation. It occurs when modulation sidebands from one RF signal are transferred to an unmodulated second RF signal when both signals are applied to the mixer RF port. A high intercept point is also beneficial to the suppression.

The image signal cannot be called a distortion product since it occurs at the same frequency as the IF signal. It can be suppressed by special mixers[16] or filtered with a preselector ahead of the mixer.

While by no means all-inclusive, the tests presented in this chapter provide both the beginning and experienced microwave engineer with capability to verify many types of performance for three different classes of components.

This chapter provides test techniques capable of making the required measurements without excessively elaborate or expensive test instrumentation. The test set-up used by the reader should be modified where appropriate to take advantage of the equipment available. In many instances, the addition of a spectrum analyzer will provide more insight into the test results. In general, this instrument was not included in tests except where necessary.

In most cases, it is possible to automate the test set-up. For other component testing requirements, there are datasheeted systems available to perform the desired measurement on a semi-automatic basis. The latter is obviously preferable where the operator is faced with a large quantity of testing, such as a production final-test station. ■

References

Oscillators

1. A.W. Vemis, "Specifying Isolation To Limit Frequency Pulling," *Microwaves*, May 1976, pp 55-57.
2. EIP Application Note 101, "A New Approach To Frequency Measurement In The Time Domain," May 1978.
3. Hewlett-Packard Application Note 313-3, "Using The 5180A Waveform Recorder To Measure Microwave VCO Settling Time And Post Tuning Drift."
4. R.S. Brozovich, "A Unified Analysis of Transmission Line Discriminators For F.M. Noise Measurements," *IEEE MTT-S Digest*, June 1983, pp 369-371.
5. F. Labaar, "New Discriminator Boosts Phase-Noise Testing," *Microwaves*, March 1982, pp 65-69.
6. B. Prouty and J. Gibbs, "Using Phase Noise Measurements To Improve Performance," *Microwave Journal*, December 1981, pp 47-56.

Amplifiers

7. R. Waugh, "Use Simple Guidelines To Predict Gain Ripple," *Microwaves*, December 1978, pp 81-82.
8. W.E. Pastori, "A Review of Noise Figure Instrumentation," *Microwave Journal*, April 1983, pp 113-122.
9. N. Kuhn, "Getting Started With Automatic Noise Figure Measurements," *Microwave Systems News*, January 1983, pp 120-136.
10. Integra Application Note, "Low Cost and Accurate Noise Figure Measurements, 2-18 GHz."
11. P.M. White, "Improved IMD Measurements For GaAs Power FETs," *Microwaves & RF*, February 1983, pp 80-82.
12. K.E. Zublin and B. Moeen-Ziai, "Band-Reject Filters Suppress Second Harmonics," *Microwaves & RF*, March 1983, pp 131-134.

Mixers

13. C. Tsironis et al., "Modeling and Evaluation of Dual Gate MESFETs as Low Noise, Self-oscillating and Image-rejection Mixers," *IEEE MTT-S Digest*, 1983, pp 443-445.
14. D. Neuf and D. Brown, "What To Look For In Mixer Specs," *Microwaves*, November 1974, pp 48-60.
15. D. Cheadle, "Selecting Mixers For Best Intermod Performance" Parts I and II, *Microwaves*, November 1973, pp 48-52, and December 1973, pp 58-62.
16. D. Neuf and S. Spohrer, "Conventional and New Applications For The Quadrature IF Microwave Mixer," *Microwave Journal*, January 1983, pp 99-109.
17. D. Cheadle, "Measure Mixer Noise With Your Power Meter," *Microwaves*, March 1975, pp 42-49.

Special Section
Millimeter-Wave Technology

This special section was organized by Dr. H. J. Kuno, associate manager of the solid-state microwave product line at Hughes Aircraft Company's Electron Dynamics Division, Torrance, California, and written by his associates at Hughes' EDD. Kuno is a member of MSN's editorial review board.

Device and Components Surveyed

By Dr. H.J. Kuno *Hughes Aircraft Company*

Introduction

This special section describes design considerations and trade-offs for the key elements of millimeter-wave systems through a trio of complementary articles: solid state millimeter-wave power sources; millimeter-wave receivers; and millimeter-wave filters.

In the first paper, R. S. Ying presents an overview of the current state of the art of solid-state millimeter-wave devices for transmitter applications. Typical performance characteristics of IMPATT *and Gunn devices are discussed. A comparison of stabilized amplifiers and injection-locked oscillators as used for millimeter-wave power amplification is presented. Techniques for achieving coherent transmitters and examples of coherent and noncoherent millimeter-wave radar systems are described. A survey of the commercial availability of solid-state millimeter-wave sources is also presented.*

The second paper, written by J. A. Paul, describes various parameters that affect the performance of millimeter-wave receiver downconverters. The amount each factor contributes to the receiver noise is graphically presented as design data.

In the third paper, D. W. Ball and L. Q. Bui discuss various design trade-offs among parameters such as insertion loss, rejection, and bandwidth for millimeter-wave bandpass filters. Design data are graphically presented with an example of an E-plane filter design.

Solid-State Sources Power Millimeter Transmitters

By R. S. Ying, *Hughes Aircraft Company*

Of the many solid-state active devices that are developed or under development, the two most commonly used in millimeter-wave systems are the IMPATT and Gunn diodes (Fig. 1). These two-terminal devices are usually operated in the fundamental-frequency mode. While both silicon and GaAs are used in IMPATT fabrication, silicon IMPATTs have demonstrated far-superior frequency performance and reliability as shown in Figure 2 for pulsed-diode and Figure 3 for CW-diode performance as a function of frequency. However, the Read structure GaAs IMPATT diodes have demonstrated a higher efficiency than the more conventional flat profile silicon IMPATT diodes for frequencies below 40 GHz. For example, efficiency of 20 percent has been reported[1] for GaAs double-drift Read diodes at 35 GHz compared to the 13 percent for flat-profile double-drift silicon IMPATT diodes.[2] The high efficiency advantage of GaAs IMPATTs, however, is not so clear at higher frequencies. Recent results with GaAs IMPATT diodes included an 8-percent efficiency at 56 GHz and 4 percent at 66 GHz.[3] These values are comparable to the more routinely achieved 8-to-9–percent efficiency of silicon diodes at the same frequency.

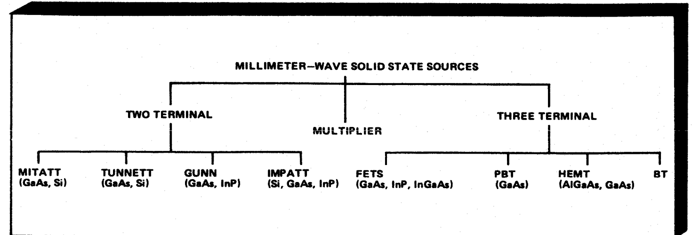

1. Of all the solid-state active devices available or under development, the two most commonly used in millimeter-wave systems are IMPATT and Gunn diodes.

At the present time, IMPATT diodes are the only available high-power, fundamental-mode sources at millimeter-wave frequencies. They are mostly used as transmitters in

R. S. Ying is manager of the millimeter-wave/microwave circuits department at the Hughes Aircraft Company's Electron Dynamics Division.

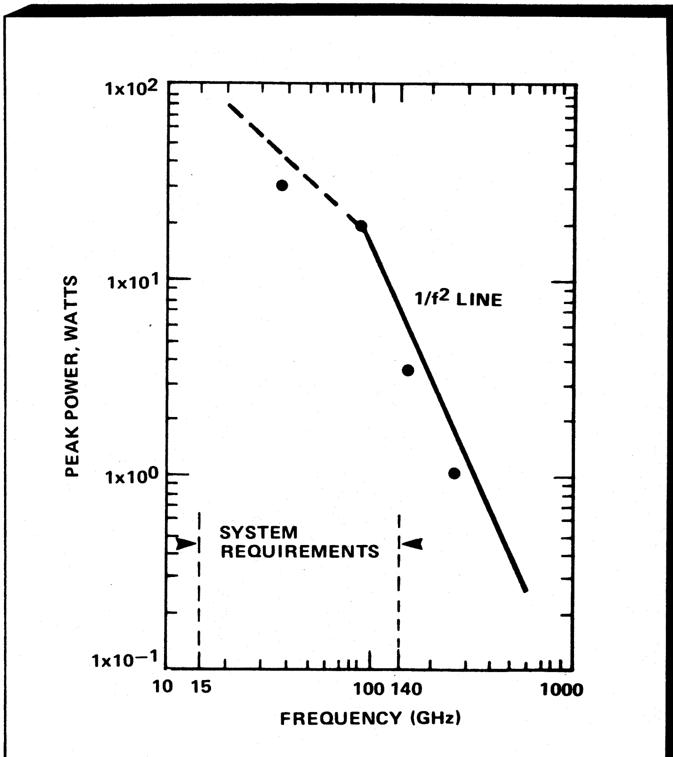

2. Silicon IMPATTs have exhibited superior frequency performance and reliability (compared with GaAs) for pulsed-diode performance as a function of frequency.

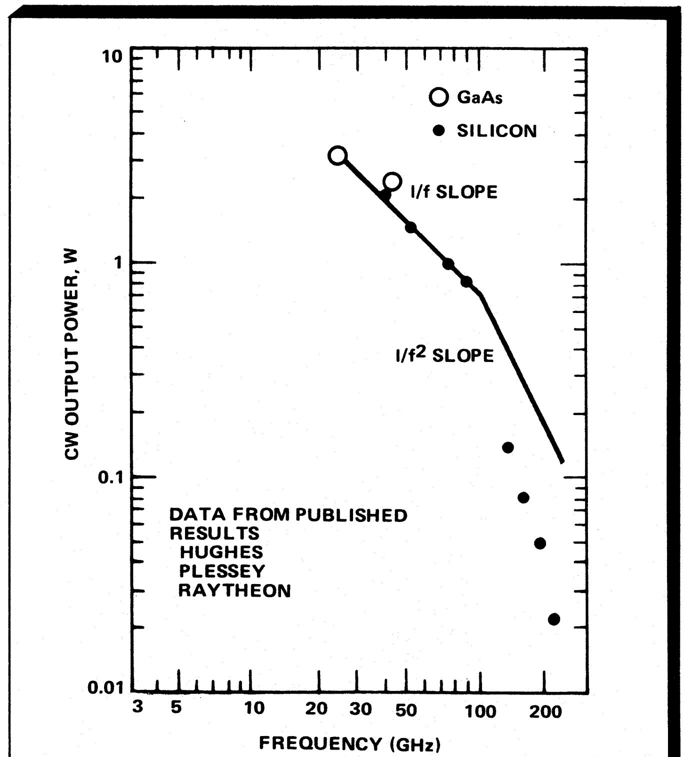

3. Superior performance has also been demonstrated for silicon IMPATTs for CW diodes.

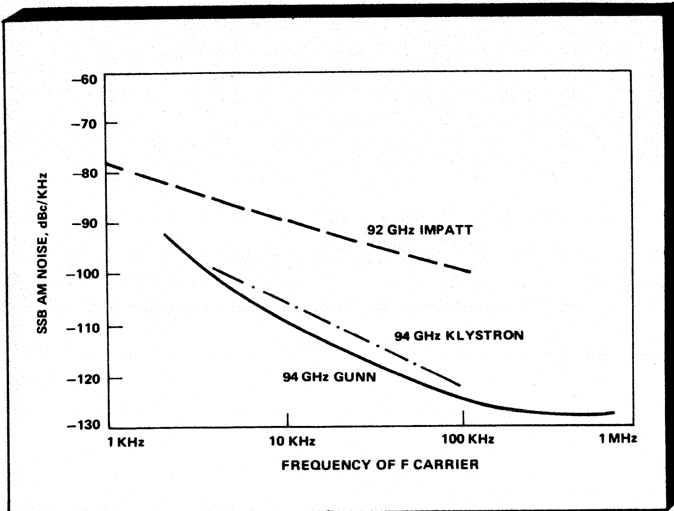

4. Due to their low-noise properties — typically 10 to 20 dB lower than IMPATTs — Gunns are often used as local oscillators for receivers.

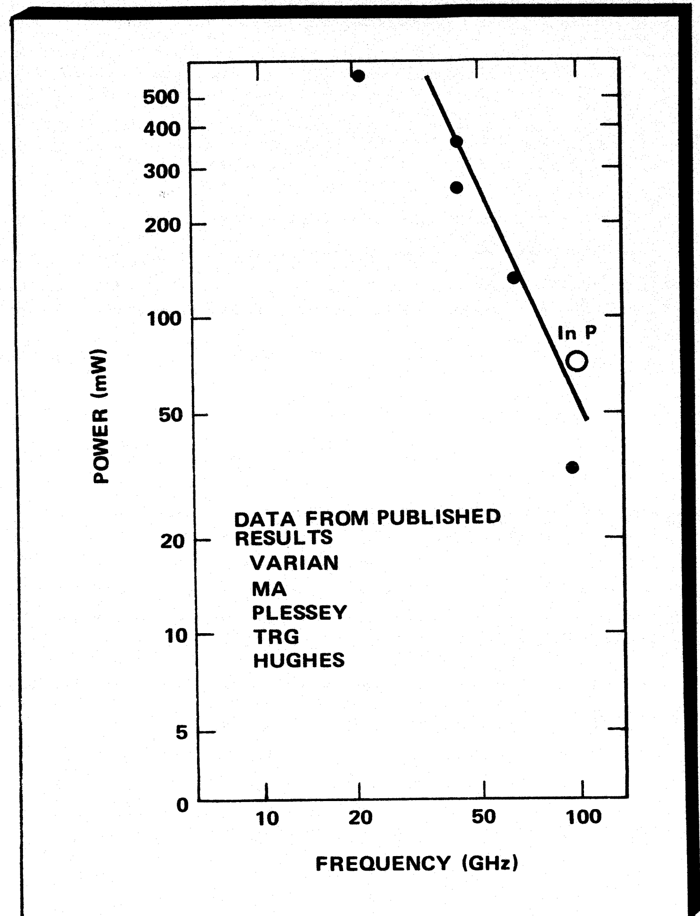

5. Advances in InP Gunn diodes may extend the usefulness of Gunn devices beyond 100 GHz.

applications such as missile guidance, fuses, sensors, and smart projectiles. Only in rare occasions, and only with the aid of filters, are they used on local oscillators in receiver applications, because of their high noise performance compared to the Gunn devices.

Gunn diodes are lower-power devices than IMPATT diodes. However, because of their low-noise properties, typically 10 to 20 dB lower than IMPATTs, as shown in Figure 4 of the AM noise comparison of IMPATTs, Gunns and klystrons, they are often used as local oscillators for receivers or sometimes in FMCW systems up to 94 GHz. Beyond that frequency, the output power of GaAs Gunn diodes becomes insignificant. Recent advances in InP Gunn diodes may extend the usefulness of Gunn devices beyond 100 GHz, as shown by Gunn diode performance over the frequency ranges in Figure 5.

While three-terminal FET devices also have limited power output at millimeter-wave frequencies,[4] results such as 10 dBm at Ka band and 7 dBm at 70 GHz have made FET devices attractive in local-oscillator and phased-array module applications. Other three-terminal devices, although theoretically having high-frequency potential, are still in early developmental phases.

Power Combiner

The output power from a single solid-state device is generally either thermally or impedance-limited as shown by the $1/f$ and $1/f^2$ relationship in Figures 2, 3, and 5. To achieve higher output power than is possible from a single device, power combiners must be used. Two basic types of power combiners have been developed: the narrowband resonant cavity and the broadband non-resonant power accumulator. Figure 6 shows the two basic types of combiners and their variations. The cylindrical resonant combiner shown in Figure 6a has been demonstrated for frequencies up to 40 GHz. Output power of 10 Watts CW at Ka band has been achieved. The waveguide Kurokawa combiner shown in Figure 6b in principle can be broadband. However, because of the close coupling, the bandwidth is again limited. Using this

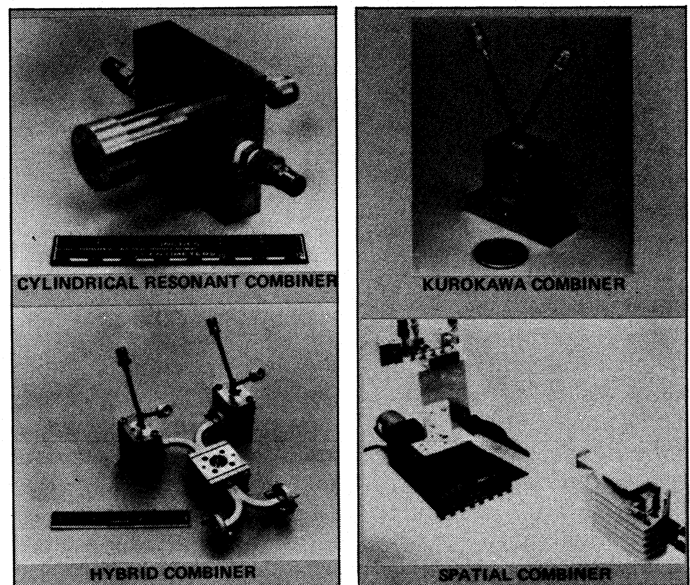

6. Two basic types of power combiners have been developed: the narrowband resonant cavity and the broadband non-resonant power accumulator. Among the variations of these are a), the cylindrical resonant combiner, which has been demonstrated up to 40 GHz; b), the waveguide Kurokawa combiner; c), the hybrid coupled combiner made up of two Kurokawa combiners; and d), a three-element, linear array, prototype spatial combiner.

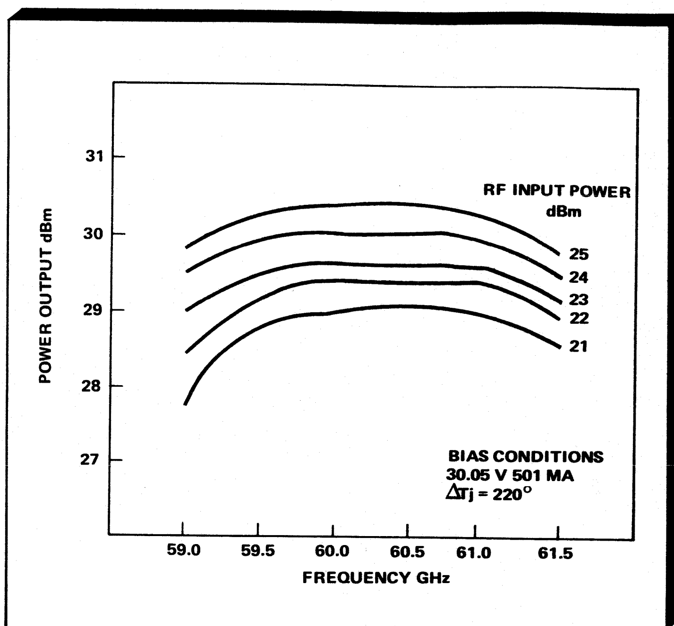

7. Typical performance of single-diode IMPATT modules at V band.

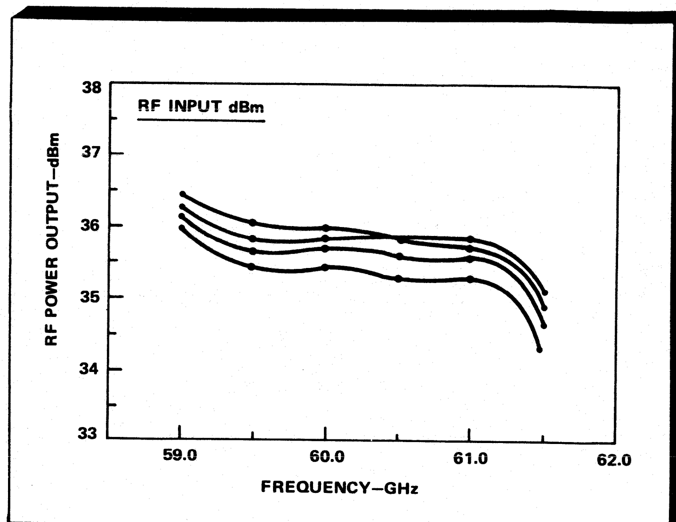

8. Typical combiner performance using four single-diode IMPATT modules.

approach, a 4-diode combiner has produced over 40 Watts of peak power at 94 GHz. Both the cylindrical and Kurokawa combiners can be further combined at a higher level. The hybrid coupled combiner shown in Figure 6c combines two of the 2-diode Kurokawa combiners. In actual experiment, four of the 2-diode Kurokawa combines were combined to achieve over 63 Watts of peak power at 94 GHz. In Figure 6d, a 3-element, linear array, prototype spatial combiner is shown That combiner has an efficiency as high as 85 to 90 percent. For broadband combiners, 4.6 Watts and 4 Watts CW output power have been achieved at Q and V bands, respectively, over a 2.5-GHz bandwidth. The combiners consists of four single-diode IMPATT modules combined via three hybrid magic tees. Figure 7 shows the typical performance of the single-diode IMPATT modules at V band, while Figure 8 shows the combiner performance using four of these modules. Figure 9 is a picture of the complete combiner assembly.

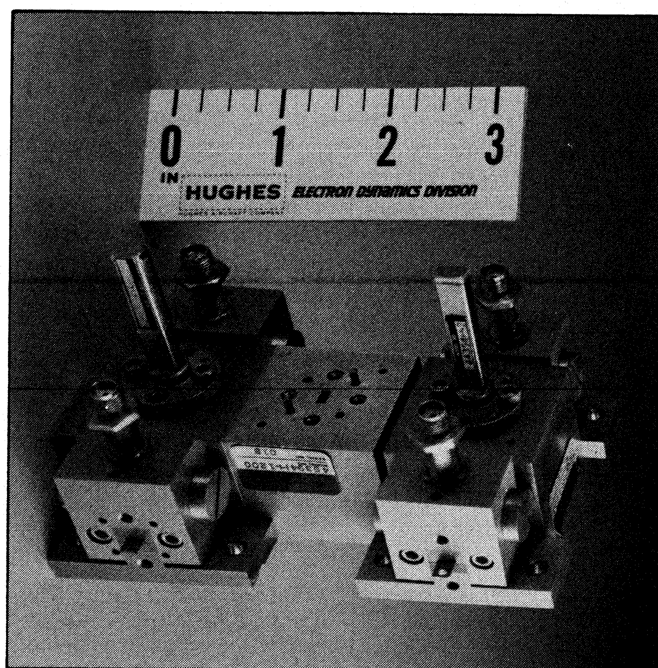

9. A complete "broadband" four-IMPATT-diode V-band combiner.

Stable Amplifier Operation vs. ILO Operation

IMPATT diodes are one-port negative-resistance devices. Each IMPATT diode in a complex power amplifier acts as a reflection amplifier which may be operated in a stable amplifier mode or an injection-locked oscillator mode. The circuit hardware required to operate a given diode in either mode is essentially the same. The mode of operation is determined by the circuit impedance presented to the diode, and normally there are only minor differences in the tuning of the passive circuitry between amplifiers operating in the two modes.

The negative resistance of a silicon double-drift IMPATT diode is in the 2-Ohm range. The negative resistance exists over a very wide frequency range, typically an octave or more. As long as the circuit impedance presented to the diode at any frequency is greater than the negative resistance of the diode at that frequency, the diode operates as a stable amplifier. Gain and output power are found as follows:

$$G = \frac{R_L + |R_D|}{R_L - |R_D|}, R_L > |R_D| \qquad (1)$$

$$P = \frac{1}{2}\frac{V_S^2}{R_L} \qquad (2)$$

where
G = gain
R_L = effective load impedance
$|R_D|$ = magnitude of the (negative) diode resistance
P = output power
V_S = output signal amplitude

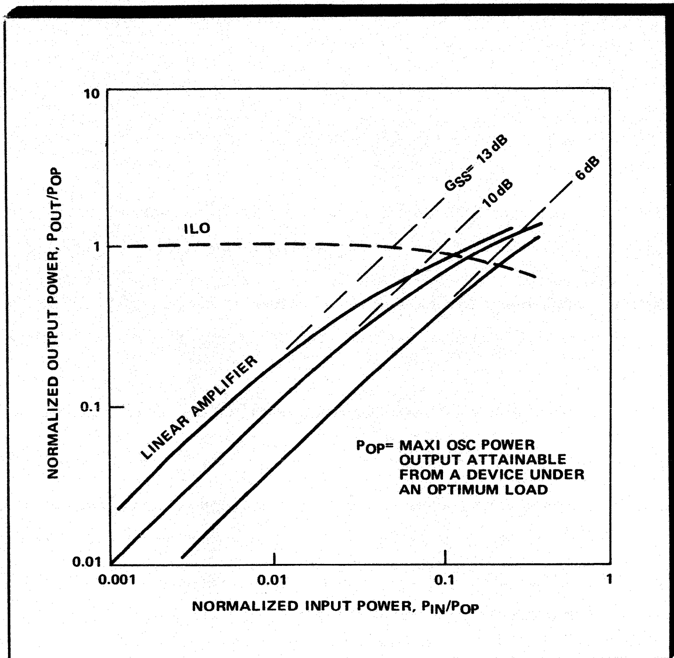

10. Power-gain saturation characteristics show theoretically calculated output vs. input power-transfer characteristics of stabilized amplifiers and injection-locked oscillators.

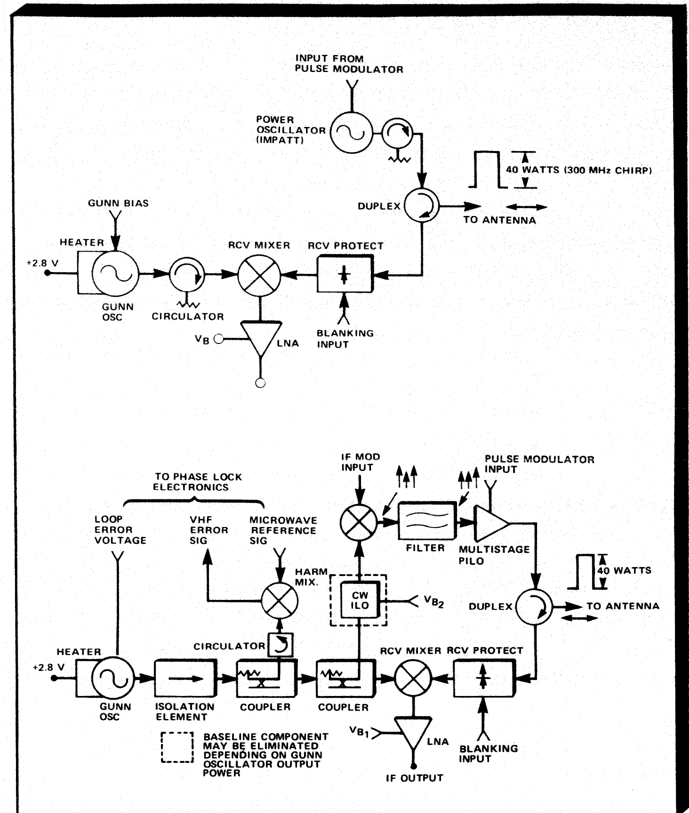

11. Most active pulsed systems fall into one of two categories: a), simple non-coherent systems and b), more-sophisticated coherent systems. Coherent systems have the advantage of being able to achieve higher average power without sacrificing the range solutions.

As R_L decreases and becomes equal to R_D, gain goes to infinity and the diode begins to oscillate. The frequency of oscillation depends upon the diode and circuit reactances, which are not considered here.

A further reduction in R_L will cause the oscillations to grow until the nonlinear nature of the IMPATT diode causes the diode negative resistance to decrease in magnitude to match the circuit impedance. The power output of the oscillator is determined by the circuit impedance R_L and the impedance-vs-amplitude characteristics of the diode. Higher power is associated with low circuit impedance.

The maximum achievable value of the signal amplitude, V_S, is fixed by the IMPATT diode physics and is approximately one third of the avalanche voltages of the diode. Once the diode is optimized for operation in a particular frequency band, the maximum value of V_S is fixed. The diode negative-impedance R_D is fixed by diode physics and bias current. The mode of operation, either stable or injection locked, and the available power are determined by R_L.

To illustrate the minor differences in the tuning of amplifiers for the stable- and the injection-locking mode, extensive experiments at V band have been performed. A single diode amplifier was tuned in the stable amplifier mode. Output power of over 1 Watt with 3- to 4-dB gain was obtained in a 2.5-GHz band as shown in Figure 7. The same ampliifer, when tuned for injection-locked mode, provided the same output power over the 2.5-GHz band, but with a higher gain of 8 to 10 dB.

This is also illustrated by the power-gain saturation characteristics shown in Figure 10 where theoretically calculated output vs input power-transfer characteristics of stabilized amplifiers and injection-locked oscillators is shown. Both input and output power levels are normalized to the maximum oscillation power attainable from a device when the lead impedance is tuned for an optimum value.

Systems Applications

Systems using solid state sources generally have operational ranges between three and 10 km: three km in adverse weather and greater than five km in clear weather. These systems can be classified as missile seekers, radars, fuses and sensors, EW, and communications; some active and some passive.

There are two basic schemes for most active pulsed systems: the simple non-coherent system shown in Figure 11a and more-sophisticated coherent systems shown in Figure 11b. The coherent system has the advantage of its ability to obtain higher average power without sacrificing the range solutions, and may also provide better target and clutter resolution. The coherent systems are generally achieved by injection-locking the pulsed IMPATT oscillator from a stable source such as a phase-locked Gunn source.

Linear chirp is achieved by injecting a low-frequency linearly chirped frequency (SAW filter) to the coherent signal through an upconverter. The output linearly chirped signal is again used to injection-lock a high-power IMPATT pulsed source. Normally, a 500-MHz injection-locked bandwidth can be achieved. The return signal is detected in matched SAW filters to obtain better SNR.

Examples of the non-coherent transceiver is shown (Fig. 12) for a W-band prototype missile seeker. This seeker uses a 5-Watt pulsed chirp IMPATT source as the transmitter for clutter smoothing. It is mounted on a pod next to an IR seeker and below a television monitor to compare tracking accuracy and facilitate visual monitoring. This prototype seeker has been the baseline design for many missile-seeker programs since then. Figure 13 shows a 94-GHz FMCW Doppler radar for tracking ship movements. The radar utilizes a 100 mW CW IMPATT oscillator. Figure 14 is a breadboard transceiver aimed at fuse sensor application. The unit has a 60-GHz self-mixing Gunn oscillator to perform both the transmit and receiver functions. The range of the sensor is limited to less than 100 feet, but the resolution can be less than an inch. Figure 15 is a photograph of a dual-frequency (94 and 140 GHz) coherent/non-coherent beamrider radar for missile guidance. This radar has three antennas: a standard gain horn and two 3-ft. antennas. The operations of the radar starts off with a non-coherent transmitted signal using the gain horn to track the target at the centroid of the beam while at the same time the missile is fired. Because of the broad beamwidth, the missile can also be tracked and guided towards the centroid. Midway through

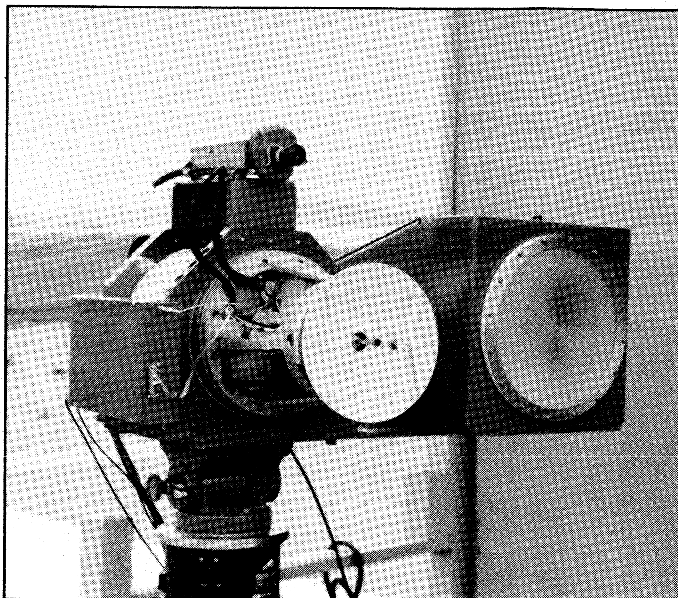

12. This prototype transceiver for a missile seeker has an IR seeker mounted next to a millimeter-wave seeker to compare tracking accuracy. The mm-wave seeker has a 5-Watt, non-coherent, pulsed chirp IMPATT transmitter.

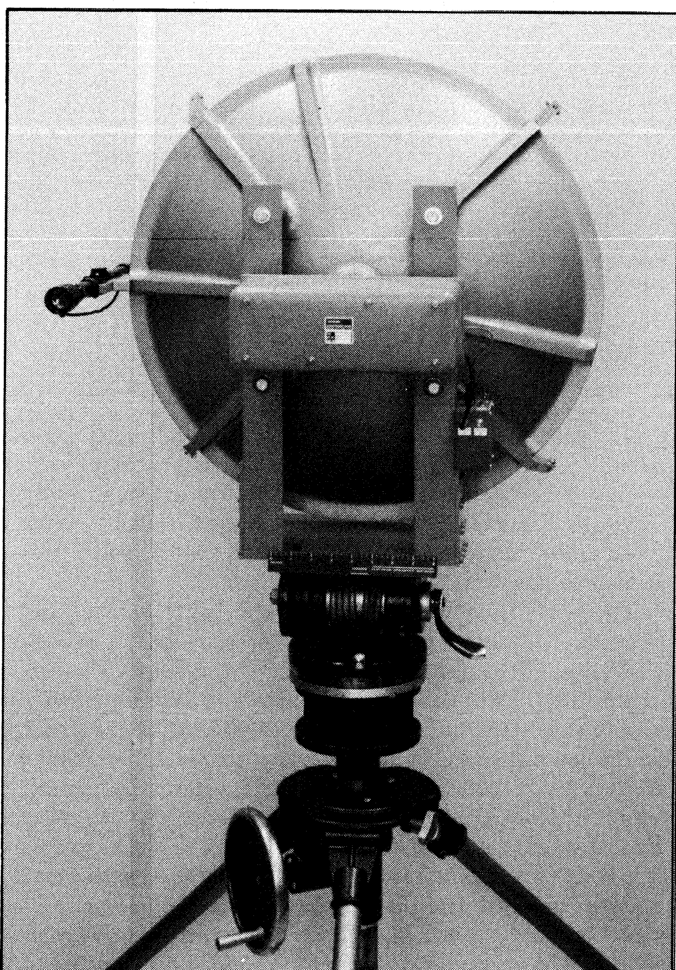

13. This 94-GHz FMCW Doppler radar for tracking ship movements uses a 100-mW CW IMPATT oscillator.

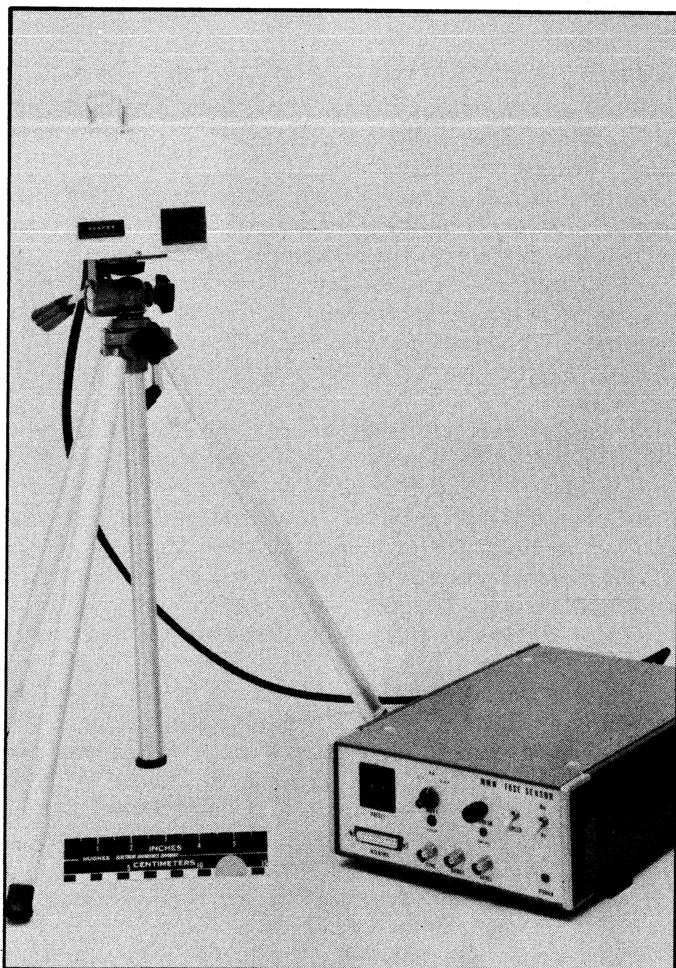

14. A broadband transceiver aimed at fuse sensor applications, contains a 60-GHz self-mixing Gunn oscillator to perform both the transmit and receive functions.

Table I

Commercial Suppliers for Millimeter-Wave Power Sources

Manufacturer	Devices/Components (Up to 140 GHz)				
	Silicon IMPATTs	Gunn Diodes	Oscillators	Amplifiers	Transmitters
Hughes Electron Dynamics Division	X	X	X	X	X
Varian		X	X	X(1)	
Central Microwave		X	X		
Plessey	X		X		
Alpha-TRG		X	X		
M/A-Com	X(2)	X	X		
Thomson CSF	X		X		
NEC	X		X	X	

(1) For frequencies lower than 60 GHz.
(2) For frequencies lower than 40 GHz.

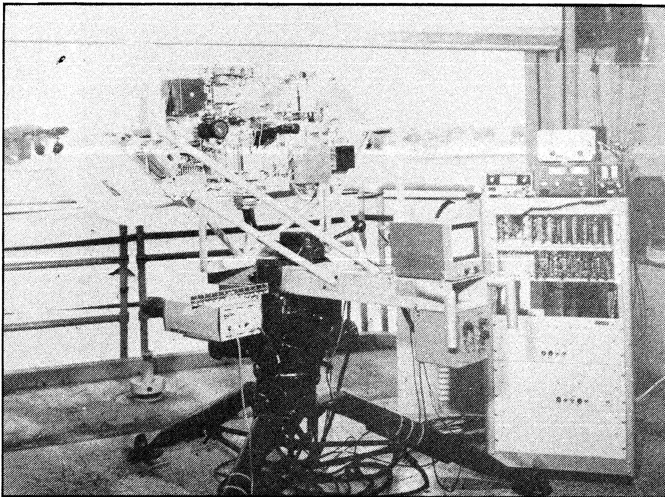

15. This dual frequency (94 and 140 GHz) coherent/non-coherent beamrider radar for missile guidance has three antennas; a standard gain horn and two 3-ft. antennas.

the missile flight, the radar is switched to a 94-GHz coherent signal transmitted through a 3-ft. antenna to give better resolution. During the terminal flight, the radar is then switched to the 140-GHz non-coherent signal using the other 3-ft. antenna to improve further the tracking and targeting accuracy. For both the 94- and 140-GHz systems, pulsed IMPATT transmitters were used. The output power of these transmitters are 6 Watts at 94 GHz and 1 Watt at 140 GHz, respectively.

Commercial Availability

State-of-the-art devices with the performance shown in Figures 2, 3, and 5 can generally be obtained from companies, such as Hughes, Raytheon, and Varian, that are prime developers in silicon, GaAs IMPATT, and Gunn diodes; and from Texas Instruments, Raytheon, Hughes, and RCA for FET-type devices. These devices typically have output powers 3 dB higher than those that are commercially available. For Silicon IMPATT diodes, Hughes has a complete diode catalog for devices up to frequencies of 140 GHz, while NEC and Thomson CSF have commercial devices up through 94 GHz. Typically, the quoted power output is at a junction operating temperature of 250°C or less at an ambient of 25°C. At this temperture, the MTBF of the IMPATT devices can be as high as 20,000 hours or 10 years. There is as yet no commercial supplier for millimeter-wave high-efficiency GaAs IMPATT diodes, primarily because of reproducibility concerns.

GaAs Gunn diodes are available commercially from companies such as Varian, Central Microwave, M/A-Com, Hughes, Alpha-TRG, and Plessey. In general, the output power of available Gunn diodes from most vendors is approximately the same. Higher-power InP Gunn diodes are not available commercially, but can be obtained on a special basis from Varian.

For millimeter-wave transmitter and receiver components, the two major suppliers are Hughes and Alpha-TRG, with Hughes being the major supplier for both types of components and TRG mostly for receiver components. Table I is a summary of the commercial suppliers and the products which they carry. ■

References

1. "EHF GaAs Double-Drift IMPATT Diodes," *Air Force Avionics Lab Report* AFAL-TR-79-1204.
2. "EHF Silicon IMPATT Diodes," *Air Force Avionics Lab Report* AFWAL-TR-80-1178.
3. R. Blumgold, AFAL private communication
4. J.C. Rosenberg, "GaAs FET Amplifiers Reach Millimeter-Wave," *Microwaves*, June 1982, pp. 67–87.

Specifying Millimeter Downconverters

By Jeffrey A. Paul, *Hughes Aircraft Company*

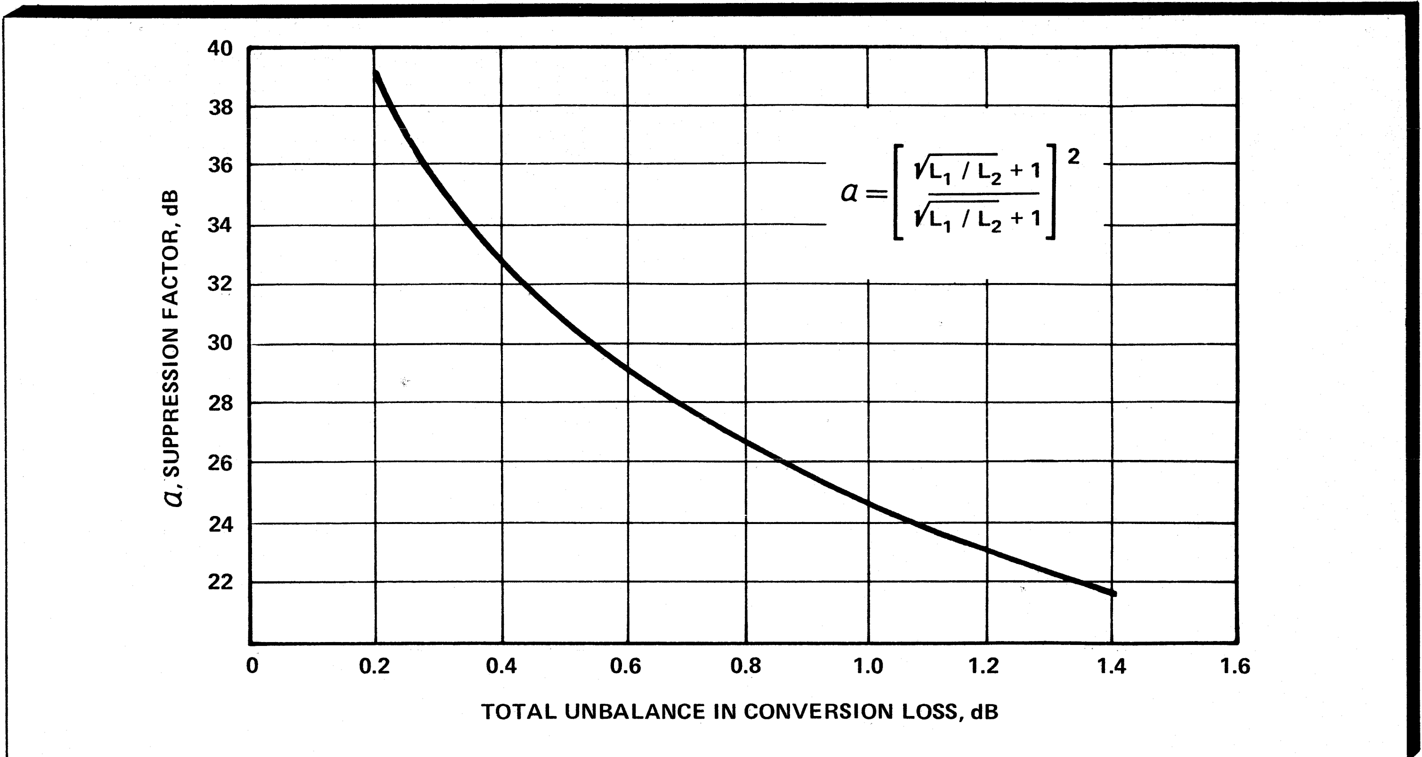

1. AM Supression Factor vs Imbalance

There are numerous requirements for millimeter-wave receivers which can be met by a wide variety of mixer types and designs. However, by and large, most millimeter-wave receiver applictions require the use of balanced mixer structures for reasons of low noise figure, high AM suppression, and good LO-RF isolation. A number of critical parameters that will aid in specifying, designing, and measuring receivers for noise performance are given in Figures 1 through 6.

Some of the key factors which contribute to the noise figure of a receiver are front-end losses, conversion loss, mismatch, diode noise temperature, local-oscillator AM noise, and IF amplifier noise figure. For most room-temperature applications the diode noise temperature may be ignored as a significant contributor to receiver noise figure. However, front-end losses and IF amplifier noise figure will contribute directly to the overall receiver noise figure and need to be minimized for best performance. Minimizing conversion loss may not necessarily produce the lowest noise figure because of the need to balance both the amplitude and phase of the two mixer diodes in order to provide local oscillator AM noise suppression. Without good AM suppression, the local oscillator will introduce additional noise in the IF circuit and

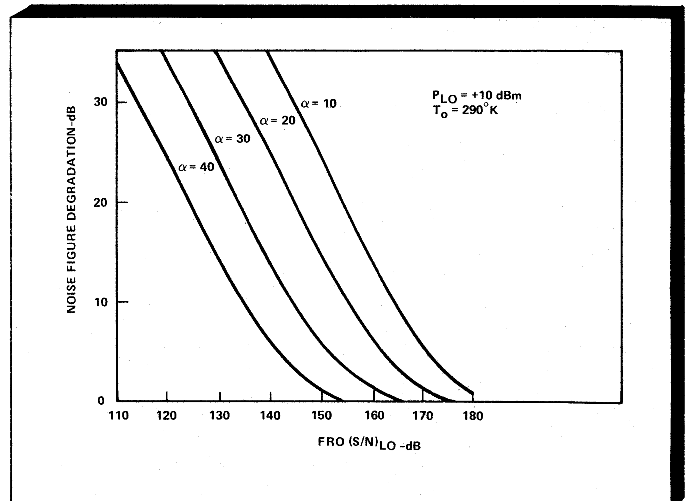

2. Noise Figure Degradation vs $(S/N)_{LO}$

Jeffrey A. Paul is assistant department manager of the millimeter-wave/microwave circuits department at the Hughes Aircraft Company's Electron Dynamics Division.

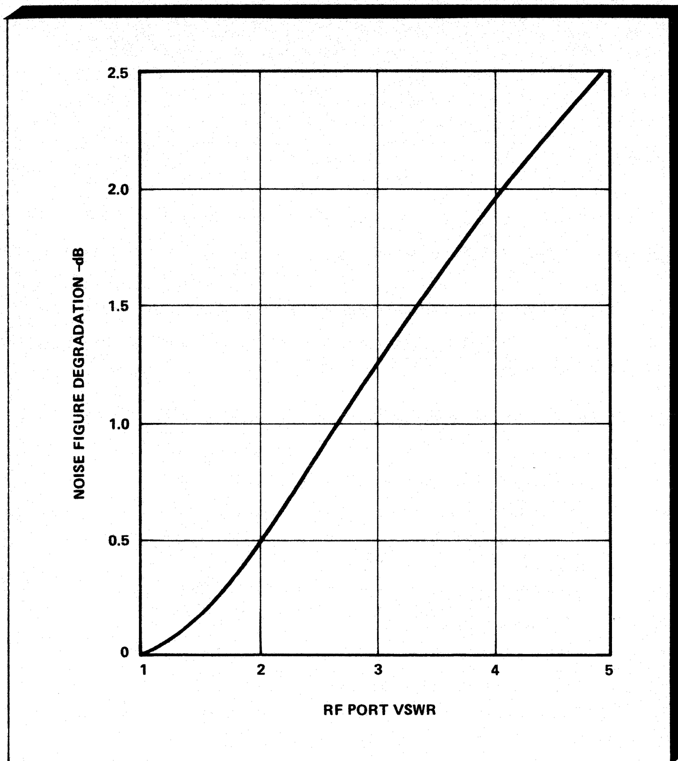

3. Noise Figure Degradation vs VSWR

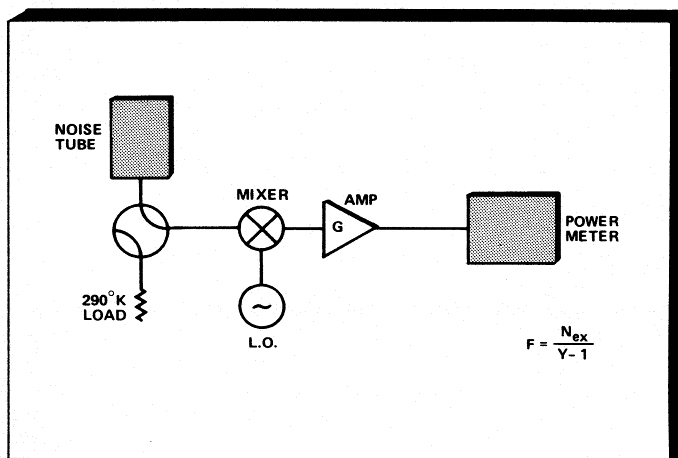

4. Noise Figure Test Setup

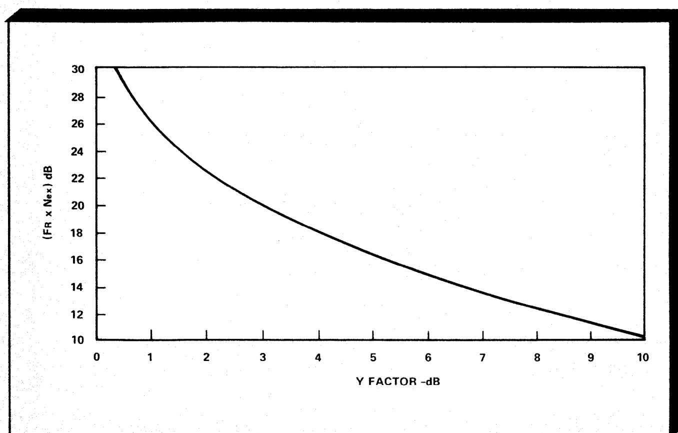

5. Noise Figure vs Y-Factor

degrade the mixer noise figure. Figure 1 shows how an imbalance in the conversion loss (L_1 and L_2) of the two individual diodes in a balanced mixer affects the AM suppression factor. Figure 2 shows how the overall receiver noise figure, F_R, is affected by the AM suppression factor and the LO S/N ratio. F_{RO} represents the receiver noise figure for a noise-free LO.

Mismatch at the RF port of a mixer will also degrade overall receiver noise figure since the available power is not totally delivered to the mixer. Figure 3 plots the degradation as a function of VSWR. LO port mismatch will not degrade noise figure provided that sufficient drive to the mixer diodes is supplied.

Noise figure may be measured by several techniques, but the use of a broadband noise source is often the easiest. Figure 4 illustrates the test setup for noise figure measurement. The change in IF noise power is measured as the RF input to the mixer is switched from the noise source to a reference load. The ratio of the IF power measurements is called the Y-factor and N_{EX} is equal to the noise source output power divided by KTB. The double-sideband noise figure (F_{DSB}) is just the ratio of N_{EX} to Y-1, provided the noise source bandwidth covers both sidebands of the mixer. Figure 5 plots the noise figures vs Y-factor and N_{EX}.

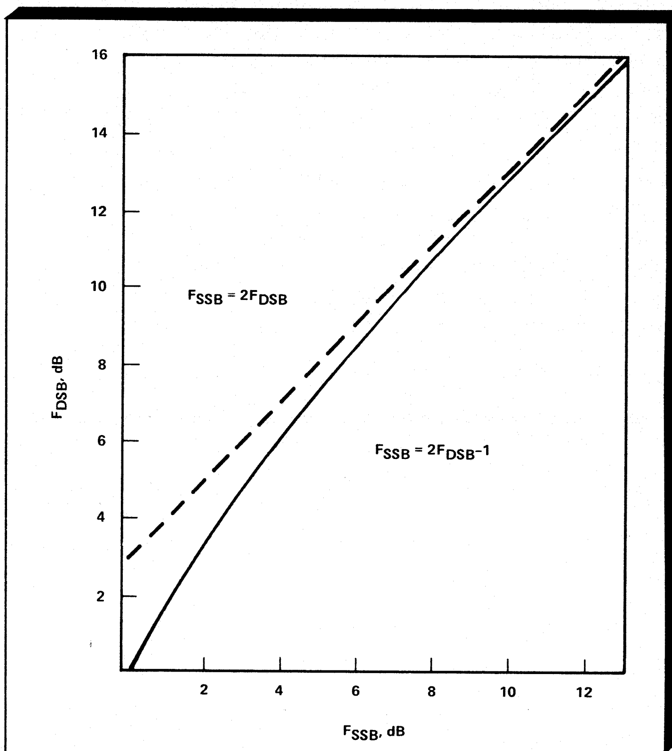

6. F_{SSB} vs F_{DSB}

It is often necessary to specify the single-sideband noise figure (F_{SSB}) of a receiver rather than F_{DSB}. The relationship between F_{SSB} and F_{DSB} is simply $F_{SSB} = 2F_{DSB} - 1$. Figure 6 shows the true conversion from F_{DSB} to F_{SSB} (solid line) as well as the asymptotic value for large noise figures (broken line). For high-noise-figure receivers, F_{SSB} and F_{DSB} are conveniently about 3 dB different, but the exact expression must be used when converting a low noise figure value. ■

E-Plane Filters Designed For Millimeter Use

By D. W. Ball and L. Q. Bui, *Hughes Aircraft Company*

Given the need for low cost, highly reproducible filters at millimeter-wave frequencies, this article describes a simple design procedure for realizing a high-performance bandpass filter using E-Plane printed circuit technology. Filters with bandpass responses up to 20 percent bandwidth have been designed using this technique with very good repeatability at center frequencies exceeding 150 GHz. The filter design is based on curves developed for specific waveguide bands that allow the designer to quickly yield a working device without considerable machine-shop delays and costs normally incurred using iris or post-coupled waveguide structures.

The basic filter structure allows simplicity of the housing and the E-Plane resonator circuits. Only three parts comprise the filter, a pair of split-block housing parts and the inductive coupled resonators which are fabricated by using precision photo-lithography and etching techniques.

The design procedure is based on the low-pass to bandpass transformation outlined by Matthaei, et al[1], to derive the K inverters and subsequent inductive discontinuities having the appropriate shunt reactances $X_{j,j+n}$ for the classical shunt-inductance coupled, waveguide filters.

Figure 1 shows the design curves that determine the equivalent series parasitic inductance which must be accounted for within the resonator and the septum width required for the calculated shunt inductance. As an example of the design procedure, let us take a typical filter specification as shown below:

Specifications	Values
Center Frequency	30 GHz
Bandwidth	2 GHz
Insertion Loss	≤ 1.0 dB
Rejection at 28 GHz	≥ 35 dB
Rejection at 32 GHz	≥ 25 dB
In-band VSWR	≤ 1.4:1
Response	Chebychev

According to the mapping, a 5-section 0.1 dB ripple design will satisfy the rejection criteria and VSWR.

The prototype design parameters for this filter are:

$$g_1 = 1.1468 = g_5$$
$$g_2 = 1.3712 = g_4$$
$$g_3 = 1.9750$$

From these values we derive the K inverters, $K_{I,I+1}$

D.W. Ball and L.Q. Bui are staff members with Hughes Aircraft Company's Electron Dynamics Division.

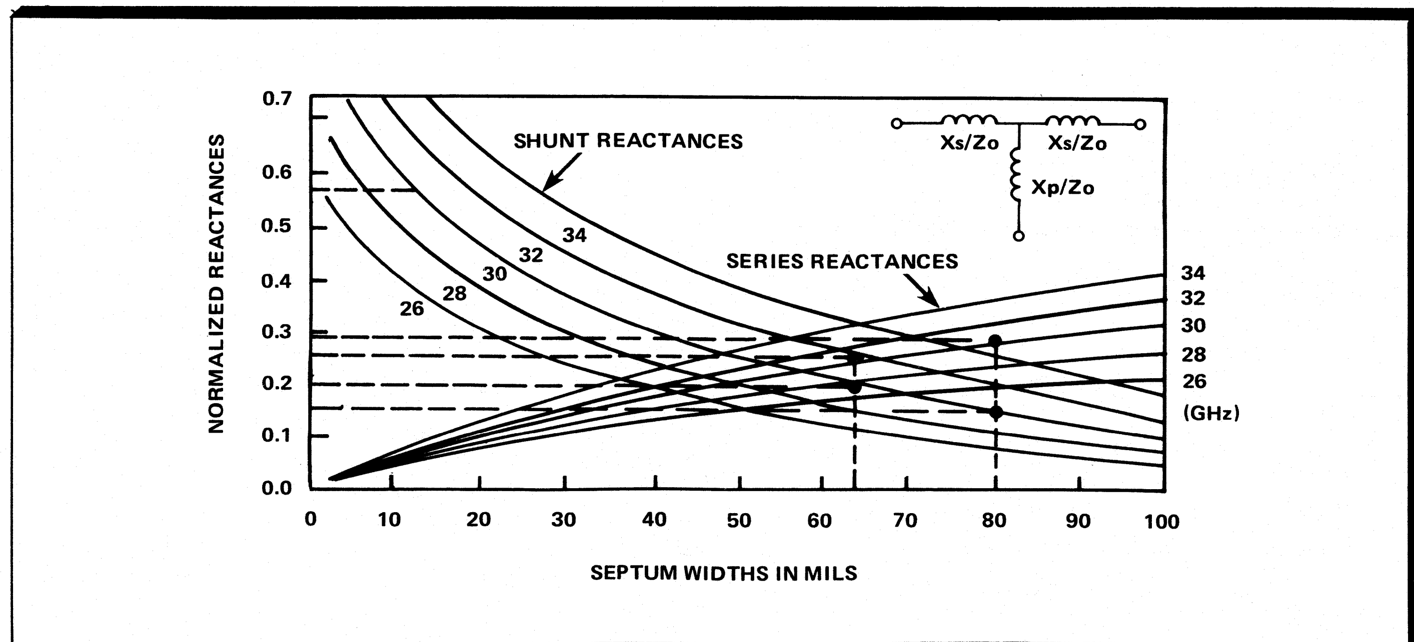

1. Septum width vs. X_p and X_s is plotted with frequency as a parameter.

N	KN(I, I+1)
1	.423
2	.166
3	.127
4	.127
5	.166
6	.423

From the K inverters we calculate the normalized shunt reactance X_{p/Z_o}.

N	K_{p/Z_o}
1, 6	.5615
2, 5	.2014
3, 4	.1539

Using Figure 1, which is a graph of normalized series reactance (X_s) and parallel reactance (X) with frequency as a parameter, we find the width of the E-plane septum at 30 GHz which yields the value of X_p. We also find the value of the parasitic series reactance X_s. All three values are tabulated below:

Normalized Reactances

N	X_p (Ohms)	X_s (Ohms)	$W_{SEPT.}$ (inches)
1, 6	.5615	.0716	0.0126
2, 5	.2014	.1678	0.0642
3, 4	.1539	.1290	0.0126

To determine the septum spacing ($0_{I,\ I+1}$), we must account for the normalized series reactance X_s. From the general model of the inverter we find:

$$0_{I,\ I+1} = \pi - \tan^{-1}(2 \times X_p + X_s) - \tan^{-1} X_s, \text{ in Radians}$$

From this equation we calculate the distance from each resonator center and its equivalent length in mils. Again, this is tabulated below for 30 GHz center frequency.

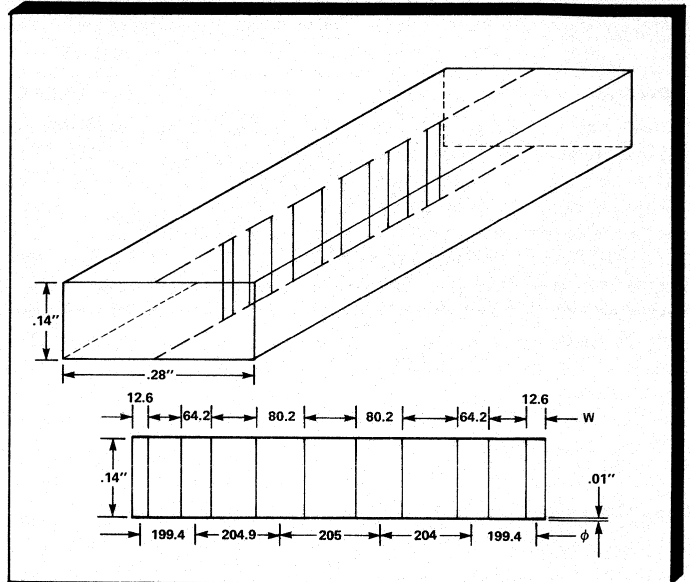

2. Completed filter uses the layout shown.

$0_{1,\ I=1}$ (Radians)	l (inches)
2.254	0.1994
2.315	0.2049
2.320	0.2053

The filter design is now complete with its layout shown in Figure 2. Shown in Figure 3 are the calculated and measured responses which show very good agreement. ■

Reference

1. Matthaei, et al, *Microwave Filters, Impedance Matching Networks, and Coupling Structures*, McGraw-Hill, 1964.

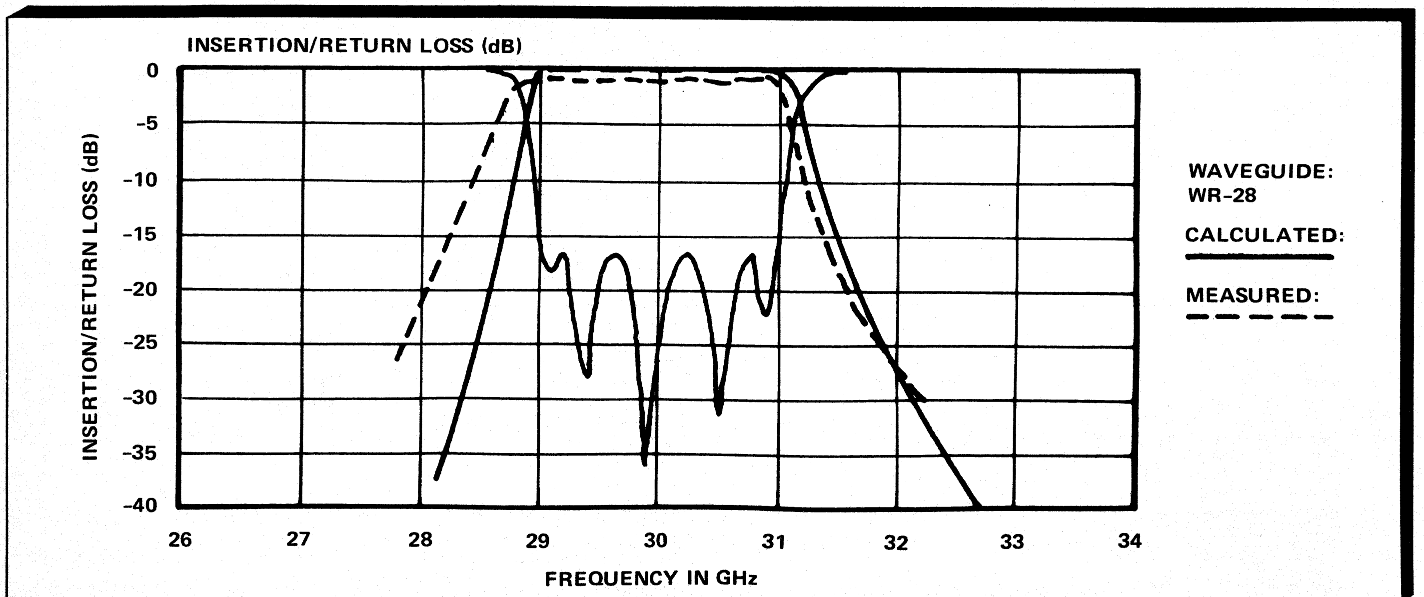

3. Measured and calculated response of E-plane filter is as indicated; measured return loss is not shown.

The Microwave System Designer's Handbook

Advertiser	Page #
Acrian, Inc.	Cover 3
Adams-Russell Co., Anzac Division	106, 229
Advanced Control Components, Inc.	105
Airtron, Division of Litton Industries	188–189
Alpha Industries, Inc.	285
American Electronic Laboratories, Inc.	27
Amperex, Inc.	261
Andersen Laboratories, Inc.	169, 209
Andrew Corp.	239
Applied Microwave Dynamics, Inc.	181
Astrolab, Inc.	185, 217
Avantek, Inc.	18–19
California Amplifier	250
California Eastern Laboratories, Inc.	33, 73
Com Dev Ltd.	135
Communications Techniques, Inc.	206
Comstron Corp.	151
Comtech Microwave	12
Custom Components, Inc.	211
Daico Industries, Inc.	205
Dow Key, Division of Kilovac Corp.	215
EEV, Inc.	129
Engelmann Microwave Co.	121
E.W. Communications, Inc.	257
Harris Corp., Microwave Division	75
Hartman Systems, Inc.	187
Honeywell, Inc., Spacekom Microwave Center	252–253
Hughes Aircraft Company	263
Innowave	152
JFW Industries, Inc.	42
Johanson Manufacturing Corp.	173
KDI Pyrofilm Corp.	120
Keltec Florida, Division of Amstar	119
KW Engineering, Inc.	170
M/A-COM Baytron, Inc.	85, 161
M/A-COM Components Marketing Inc.	123
M/A-COM Microwave Circuits, Inc.	255
M/A-COM Microwave Components, Inc.	159
Magnum Microwave	227
Megiddo Corp.	21
Merrimac Industries, Inc.	112–113, 220–221
Microlab/FXR	125
Micronetics, Inc.	16
Microwave Semiconductor Corp.	39
Millitech	219
Miteq, Inc.	179
Mitsubishi Electronics America, Inc.	80–81
Narda Microwave Corp.	193, 213, 231
Northern Scientific Laboratories, Inc.	155
Olektron Corp.	24
Peninsula Publishing	287
Planar Microwave	266
Programmed Test Sources, Inc.	233
Raytheon Microwave Tube Operation	127
RFD, Inc.	111
RHG Electronics Laboratory, Inc.	Cover 2
Sanders Associates, Inc., Microwave Division	31
Scientific-Atlanta, Inc.	137–140
SDI	162
Struthers Electronics Corp.	197, 198, 199
Synergy Microwave Corp.	235
Systron Donner Microwave Division	247
Trak Microwave Corp.	175
Transco Products, Inc.	10, 236
TRW Microwave, Inc.	249
Uniform Tubes, Inc.	143
UTE Microwave, Inc.	223
Varian Associates	279
Watkins-Johnson Company	4, 6, 195, 245
Wavetek San Diego, Inc.	183
Weinschel Engineering, Inc.	133, 269
Western Microwave	2–3

EDITOR
Bert Berson

MANAGING EDITOR
Alexander E. Braun

ASSOCIATE EDITORS
Cedric R. Braun
Robert M. Vanderheiden

CONTRIBUTING EDITORS
D.W. Ball
Joseph S. Barrera
L.Q. Bui
Alan W. Carlson
Robert J. Espinosa
John R. Forrest
C.E. Foster
Robert V. Garver
C.E. Krehbiel
John Kuno
Ferenc Marki
Howard W. Mette
Northe K. Osbrink
Jeffrey A. Paul
Fred J. Rosenbaum
Harold L. Schumacher
Bernard S. Siegal
Kenneth J. Sleger
Craig P. Snapp
Ralph Tramposch
Alan Walker
R.S. Ying
K. Zublin

EDITORIAL ASSISTANT
Rachel Crutchfield

EDITORIAL REVIEW BOARD
Prof. J.H. Collins (Chairman)
Chuck Abronson
Dr. David Adams
Bert Berson
James K. Fitzpatrick
Dr. Michael Howes
Dr. W. Keith Kennedy
John Kuno
Ralph Levy
Joel Naidus
John M. Owens
Dr. D. Howard Phillips
Allen E. Rosenzweig
Dr. Gerry Schaffner
Bernard S. Siegal
Harold Sobol
Dr. Kunihiro Suetake
Dr. Bruno O. Weinschel

ASIAN CORRESPONDENT
S. Kazama
6-2-3, Hirayama, Hino-shi
Tokyo, Japan T 191
0 425-91-2477

PRODUCTION DIRECTOR
Jacalyn S. Toorenaar

ADVERTISING TRAFFIC COORDINATORS
Dyan L. Feil
Russell C. Pike

ART DIRECTOR
Richard San Miguel

DESIGN COORDINATOR
Claire Dacko

DESIGN GROUP
John Campanaro
Frank Fletcher
Charline Greco
Susan D. Hill
Cynthia Milligan

CIRCULATION MANAGER
Katherine A. Sund

CIRCULATION ASSISTANTS
Carol J. Polster
Anna Teach

MARKETING/SALES DIRECTOR
Ruth Breashears

MARKETING SERVICES MANAGER
Burt Sakai

SPECIAL PROJECTS/ MARKETING SERVICES
Jenifer Jacobs
Nancy E. Goyette
Susan Thrasher

ADVERTISING SALES COORDINATOR
Annette A. Hoshida

SALES ASSISTANT
Gail L. Perkins

ADMINISTRATION

PRESIDENT
Anthony Yaconetti

VICE PRESIDENT FINANCE
Cora M. McKinley